Importance of TRPV4 channel in the mitochondrial structure-function relationship: Implication in pain and other pathophysiology

By
ASHUTOSH KUMAR
LIFE07201004001
National Institute of Science Education and Research,
Bhubaneswar

A thesis submitted to the
Board of Studies in Life Sciences
In partial fulfillment of the requirements
For the Degree of

DOCTOR OF PHILOSOPHY
Of
HOMI BHABHA NATIONAL INSTITUTE

September, 2016

Homi Bhabha National Institute

Recommendations of the Viva Voce Board

As members of the Viva Voce Board, we certify that we have read the dissertation prepared by Ashutosh Kumar entitled **"Importance of TRPV4 channel in the mitochondrial structure-function relationship: Implication in pain and other pathophysiology"** and recommend that it may be accepted as fulfilling the dissertation requirement for the Degree of Doctor of Philosophy.

---**Date:** 15/09/16

Chairman
Prof. Parimal C. Sen

---**Date:**

Convener:
Dr. Chandan Goswami Chandan Goswami 15/09/16

---**Date:** 15/09/16

External examiner:
Prof. Parimal C. Sen

---**Date:** 15-9-16

Member 1:
Dr. Praful Singru

---**Date:**

Member 2:
Dr. Abdur Rahaman 15-9-16

---**Date:**

Member 3:

Final approval and acceptance of this dissertation is contingent upon the candidate's submission of the final copies of the dissertation to HBNI.

I hereby certify that I have read this dissertation prepared under my direction and recommend that it may be accepted as fulfilling the dissertation requirement.

Date: 15-9-2016

Place: NISER, Bhubaneswar

Chandan Goswami

(Dr. Chandan Goswami)

STATEMENT BY AUTHOR

This dissertation has been submitted in partial fulfilment of requirements for an advanced degree at Homi Bhabha National Institute (HBNI) and is deposited in the Library to be made available to borrowers under rules of the HBNI.

Brief quotations from this dissertation are allowable without special permission, provided that accurate acknowledgement of source is made. Requests for permission for extended quotation from or reproduction of this manuscript in whole or in part may be granted by the Competent Authority of HBNI when in his or her judgment the proposed use of the material is in the interests of scholarship. In all other instances, however, permission must be obtained from the author.

Ashutosh Kumar

DECLARATION

I, hereby declare that the investigation presented in the thesis has been carried out by me. The work is original and has not been submitted earlier as a whole or in part for a degree / diploma at this or any other Institution / University.

NISER, Bhubaneswar

15 Sept, 2016

Ashutosh Kumar

Publications in Refereed Journal

A. <u>Published (Pertaining in thesis):</u>

1. ‡ *****Verma P, **Kumar A**, Goswami C. (2010) TRPV4-mediated channelopathies. *Channels (Austin)*. **4**, 319-328
2. **Kumar A**, Goswami L, Goswami C. (2013) Importance of TRP channels in pain: implications for stress. *Frontiers in Bioscience*. (*Schol Ed*) **5**, 19-38
3. ***Kumar A**, Majhi R, Yadav M, Szallasi A, Goswami C. (2013) TRPV1 activators ("vanilloids") as neurotoxins. Book chapter (Springer), pp 611-636
4. ‡ *****Majhi RK, **Kumar A**, Yadav M, Swain N, Kumari S, Saha A, Pradhan A, Goswami L, Saha S, Samanta L, Maity A, Nayak TK, Chattopadhyay S, Rajakuberan C, Kumar A, Goswami C. (2013) Thermosensitive ion channel TRPV1 is endogenously expressed in the sperm of a fresh water teleost fish (*Labeo rohita*) and regulates sperm motility. *Channels* **7,** 1-10
5. **Kumar A**, Kumari S, Majhi RK, Swain N, Yadav M, Goswami C. (2015) Regulation of TRP channels by steroids: Implications in physiology and diseases. *General and Comparative Endocrinology* **220**:23-32
6. *Kumari S, ***Kumar A**, *Sardar P, Yadav M, Majhi RK, Kumar A, Goswami C. (2015) Influence of membrane cholesterol in the molecular evolution and functional regulation of TRPV4. *Biochem Biophys Res Commun*. **456**, 312-9
7. Majhi R K, **Kumar A**, Yadav M, Kumar P, Maiti A, Giri S.C., Goswami C. (2015) Light and electron microscopic study of mature spermatozoa from white pekin duck (*Anas platyrhynchos*): An ultrastructural and molecular analysis. ***Andrology*** doi: 10.1111/andr.12130
8. **Kumar A,** Majhi RK, Swain N, Giri SC, Kar S, Samanta L, Goswami C. (2016) TRPV4 is endogenously expressed in vertebrate spermatozoa and regulates intracellular calcium in human sperm. *Biochem Biophys Res Commun.* **473** (4):781-8.

B. <u>Other Publications:</u>

1. Sanyasi S, **Kumar A**, Goswami C, Bandyopadhyay A, Goswami L. (2014) A carboxy methyl tamarind polysaccharide matrix for adhesion and growth of osteoclast-precursor cells. *Carbohydrate Polymers*, **101**, 1033-1042

2. Kumar A, Sahu SK, Mohanty S, Chakrabarti S, Maji S, Reddy RR, **Jha AK**, Goswami C, Kundu CN, Rajasubramaniam S, Verma SC, Choudhuri T. (2014) Kaposi sarcoma herpes virus latency associated nuclear antigen protein release the G2/M cell cycle blocks by modulating ATM/ATR mediated checkpoint pathway. *PLoS One* **9**(6):e100228.

3. Pradhan N, Pratheek BM, Garai A, **Kumar A**, Meena VS, Ghosh S, Singh S, Kumari S, Chandrashekar TK, Goswami C, Chattopadhyay S, Kar S, Maiti PK. (2014) Induction of apoptosis by Fe(salen)Cl through caspase-dependent pathway specifically in tumor cells. *Cell Biol Int.* **38**(10):1118-31.

4. Majhi RK, Saha S, **Kumar A**, Swain N, Goswami L, Mohapatra P, Maity AA, Kumar Sahoo V, Kumar A, Goswami C. (2014) Sperm specific expression of temperature-sensitive ion channel TRPM8 correlates with vertebrate evolution. *PeerJ* DOI: 10.7287/peerj.preprints

C. <u>Manuscript in preparation:</u>

1. Ashutosh Kumar and Chandan Goswami (2015) TRPV4 interacts with mitochondrial proteins and regulates mitochondrial structure – function relationship by acting as a mitochondrial Ca^{2+}-importer

(‡ = Cover Page; * = Equal contribution)

2010 **2013**

<u>Conferences:</u>

<u>Abstracts and posters (Presenting author):</u>

1. Presented poster and abstract in an International conference: "Cell signaling and Disease" in Kalinga Institute of Technology, Bhubaneswar, India (29-30th Oct, 2010)
Title: "*Understanding the molecular mechanisms and structure –function relationship of TRPV4*"

2. Presented poster and abstract in Bangalore Microscopy Course (BMC-2011) at NCBS, Bangalore, India (18-25th Sept. 2011)
Title: "*Dissecting TRPV4-mediated mitochondrial regulation and function*"

3. Presented poster and abstract in an international Conference on Repromics – Omics in reproduction and development: RGCB, Trivandrum, India (7-9th Feb, 2013)
Title: "*Endogenous expression and functional characterization of TRPV4 in the sperm cells*".

4. Presented poster and abstract in an international Conference on International Conference on neuroscience-Brain plasticity and neurological disorders: Ravenshaw University, Cuttack (9-11th Nov, 2013)
Title: "*Importance of membrane cholesterol in the possible development of TRPV4-mediated channelopathies*".
(Received 1st prize in Poster presentation)

Conference attended:

5. Participated in SERB School in Neuroscience - VIth Edition, from Dec 10th- 23rd 2012 at NISER, Bhubaneswar, Orissa

6. XXXV All India Cell Biology Conference, Bhubaneswar, 16-18th Dec 2011

7. Indian Immunology Society - Odisha Chapter, Aug 11, 2012, NISER, Bhubaneswar

8. 83rd Annual meeting of Society of Biological Chemists (India) and symposium on 'Evolution: Molecules to Life', from Dec 18 - 21, 2014

Invited talks:

1. 2nd National Conference of Indian Society of Assisted Reproduction. 8-9th August 2015. Bhubaneswar

Title: "Thermosensitive TRP channels are endogenously expressed in human sperm and regulate progesterone mediated sperm activation". **(Received oral presentation award)**

Ashutosh kumar

Dedicated to……

My Parents

ACKNOWLEDGEMENTS

This thesis would have been a seemingly impossible task had I not received the guidance and cooperation from several individuals who in one way or other contributed and extended their valuable assistance in fulfilment of this study.

It gives me immense pleasure to extend my cordial gratitude to my supervisor Dr. Chandan Goswami for his scientific assistance and continuous support throughout the course of this work. His comprehensive knowledge in this field and enthusiasm for science has always instilled in me the urge to learn and work more. I will always be indebted towards him for the scientific skills that I have acquired from him. I would also like to acknowledge his patience that he has exhibited while critically correcting this thesis.

I would also like to express my gratitude towards my thesis committee members Prof. P. V. Satyam (IOP, Bhubaneswar), Dr. Praful Singru (NISER, Bhubaneswar) and Dr. Abdur Rahaman (NISER, Bhubaneswar) for their support and scientific suggestions during the course of my research work. I am highly obliged to current and former Chairpersons, School of Biological Sciences, NISER, as well as all the faculty and staff members of School of Biological Sciences for their constant help and support. Support from Imaging facility, NMR facility, Flow cytometry facility, Animal house facility of NISER and people involved in these facilities are greatly acknowledged.

My sincere appreciation to all the scientists and researchers who provided the constructs and samples (collected from Frozen Semen Bank, Cuttack; Central Institute for Fisheries and Aquaculture, Bhubaneswar; Central Avian Research Institute, Bhubaneswar; Kar Clinic, Bhubaneswar), required during my thesis work without which it would have been impossible to continue my work further. My special thanks to Prof. Eckart D. Gundelfinger and Dr. Karl-Heinz Smalla (Magdeburg, Germany) who provided synaptosomal fractions of rat fore brain for some critical experiments. I am thankful to Prof. H. H. Ropers, Dr. Tim Hucho, Dr. Rudi Lurz and other lab members (Max Planck Institute of Molecular Genetics, Berlin) for sending cell lines, technical supports and some critical reagents. I am thankful to Dr. Ansgar Santel (Berlin, Germany) for antibodies and constructs.

I also owe the success to all my teachers of Utkal University, Bhubaneswar (Biotechnology Department). I am thankful to Dr. Luna Goswami (KIIT University, Bhubaneswar), Prof. Luna Samanta (Ravenshaw University, Cuttack), Dr. Sujata Kar (Kar Clinic, Bhubaneswar), Dr. Apratim Maity (OUAT, Bhubaneswar), Dr. Ashish Saha (CIFA,

Bhubaneswar), Dr. P Routray (CIFA, Bhubaneswar) Dr. Sunil Chandra Giri (CARI, Bhubaneswar) and Dr. Pratush Mohapatra (RPRC, Bhubaneswar) for providing samples. I thank Dr. Abhishek Kumar (Heidelberg, Germany) for his help. I would like to give my sincere appreciation for technical and scientific input from Dr. Arindam Ghosh (NMR facility, NISER). I thank team members of Zeiss India, GE healthcare Life sciences and Prof. Jason Swedlow (University of Dundee, UK) and Dr. Markus Posch (University of Dundee, UK) for extending their super resolution facilities respectively. I would also like to thank all funding agencies (DAE, DST, DBT, ICMR) for extending their financial support during my PhD tenure.

My labmates Manoj, Rakesh, Nirlipta, Somdatta, Rashmita, Shikha, Arijit, Anurag and Nikhil had been constantly supportive and had made my journey in this lab enjoyable. Special mention in this regard involves all the members of Lab 8 (NISER campus) who have not only helped me with their research inputs but have also made my stay a memorable one.

I cherish the light moments that I spent with my batch mates and my beloved juniors for their support during my tough times in this tenure. I would like to express my sincere gratitude to a number of people to whom I am really indebted for their help, support and motivation in all my endeavours.

I owe my heartfelt gratitude to my parents who have always encouraged me throughout my life. Their constant sacrifices were indispensable without which this work could not have been accomplished. I appreciate the efforts of my younger brothers for taking over my responsibilities during this period. It would have been impossible to reach here without the support, love and affection of my family.

Ashutosh Kumar

INDEX

Homi Bhabha National Institute
Ph. D. PROGRAMME
SYNOPSIS

1. **Name of the Student: Ashutosh Kumar**

2. **Name of the Constituent Institution: National Institute of Science Education and Research (NISER)**

3. **Enrolment No. : LIFE07201004001**

4. **Title of the Thesis: Importance of TRPV4 channel in the mitochondrial structure-function relationship: Implication in pain and other pathophysiology**

5. **Board of Studies: Life Science**

Preamble

INTRODUCTION:

Based on amino acid sequence and homology; Transient Receptor Potential (TRP) ion channels are classified into 7 subfamilies namely TRPC (Canonical), TRPM (Melastatin), TRPV (Vanilloid), TRPA (Ankyrin), TRPML (Mucolipin), and TRPP (Polycystin). TRP channels conduct influx of different monovalent and divalent cations down their electrochemical gradients [1-3]. These channels are present in most of the tissue and cell types especially in sensory organs where these are involved in critical functions such as vision, taste, touch, auditory, olfactory and temperature sensation. TRP channel was first discovered in *Drosophila* photoreceptor (as *trp* mutant) where response against light was defective [4]. Like voltage-gated Na^+ channels; TRP channels also contain six transmembrane (6TM) helices and the pore domain is present between the 5^{th} (S5) and 6^{th} (S6) transmembrane region. Both N- and C-termini are located at the intracellular sides [1]. TRP channels form homo- or heterotetramer and only such tetramers act as functional ion channels. Most of the TRP channels contain a conserved sequence of 25 amino acids located immediately after the 6^{th} transmembrane segment (S6) commonly known as "TRP-box", a typical structural signature, characteristic of several TRP channels.

Among all TRP channels, TRPV represents a subfamily belonging to TRP super family of ion channels and consists of 6 members (TRPV1-6). TRPV1-V4 are thermosensitive in nature and thus can be activated at different temperatures, ranging from 30°C to 52°C. Other two members of this subfamily, namely TRPV5 and TRPV6 are not thermosensitive but are highly selective for Ca^{2+} ion [5]. Transient Receptor Potential Vanniloid sub-type 4 (TRPV4) is a non-selective cationic channel and is expressed in nervous and sensory systems such as in brain, spinal cord, peripheral and sensory neurons, and also in a broad range of non-neuronal tissues including lung, spleen, kidney, testis, adipose tissue, cochlea, skin, smooth muscle, liver, bone, cartilage and vascular endothelium where it regulates diverse cellular physiology [6-11]. In case of sensory neurons, TRPV4 is localized in free nerve endings of A- and C-fibers where it is involved in mechano-transduction and detection of different noxious painful stimuli (hyperalgesia) [12]. Among TRPV family of ion channels, TRPV4 is a unique channel as so far a large number of point mutations that have been reported in human population, and all these mutations correlate well with the development of several pathophysiological conditions including *Brachyolmia*, *Charcot-Marie-Tooth disease type 2C* (CMT2C) and *skeletal dysplasia* [13-15]. TRPV4 act as a polymodal receptor, and thus can be activated by various chemical and physical stimuli.

Different compounds such as 4α-phorbol 12,13-didecanoate (4α-PDD; a phorbol ester derivative), endogenous ligands such as endocannabinoids and arachidonic acid (AA) metabolites, diverse physical stimuli such as temperature (>27°C), mechanical force, low pH, and also by changes in osmotic pressure; all can activate TRPV4 [16]. So far expression of TRPV4 is reported from both neuronal as well as non-neuronal cells and tissues. Abnormality in TRPV4 expression and function also correlate well with the development of pathophysiological disorders. In case of neuronal cell, TRPV4 is present at the nerve terminals where it plays important role in regulation of Ca^{2+}-signalling, microtubule dynamics and several downstream signalling pathways. It is well known that mitochondrial dysfunction in cells correlate well with the production of ROS, NOS, translocation of PKCε and excesses of Ca^{2+}-influx which in turn leads to several pathophysiological disorders including neurodegeneration and neuropathic pain [17-21]. Both mitochondrial number and distribution are random in most cells but are very specific in case of differentiated cells like neuron and muscles [22]. In neuronal cells mitochondrial number and its position are higher in high energy demanding area such as in pre-synaptic and post-synaptic areas, growth cones, axonal branches, nodes-of-Ranvier and in dendritic spines which maintain the plasticity of neuron [22]. In this context, abnormality in TRPV4 functions as well as mitochondrial dysfunction, both shows the same symptoms of neuropathic pain or chronic pain. However, if these two aspects are interrelated or not and the underlying mechanism governing these dysfunctions are still elusive.

In last few decades, intracellular localization of TRP channels was investigated. Such studies have unravelled the intracellular localization of TRP ion channels and have also partly characterized their functions within these subcellular organelles [23]. For example, TRPV1 and TRPV3 are physically and functionally present in ER and regulate ER functions [24, 25]. Similarly, surface expression and localization of TRPV4 depends on several key factors such as correct folding within ER, glycosylation, tetramer assembly, recycling and proteasomal degradation [26, 14]. Apart from membrane localization, subcellular localization of TRPV4 in nucleus and ER was also reported recently, though no functional significance was attributed in these cases [27]. The surface expression of TRPV4 is largely reduced in case of its point mutations and different point mutants localize in the cytoplasm as relatively big spots [28]. However, the exact identity and characterizations of different TRPV4 mutants has not been done yet. Based on the literature describing genetic interaction and regulation of biochemical pathway/s by TRPV4, presence of TRPV4 in mitochondria can be speculated. However, so far no systematic studies have been conducted to explore if TRPV4 is physically

present in mitochondria and if it regulates mitochondrial function/s. This thesis work explored TRPV4 in the context of mitochondrial localization and functional regulation. This work demonstrates that TRPV4 not only localizes into mitochondria but also regulates its critical functions in different manner. This work confirms that TRPV4 is endogenously present in the mitochondria of different cellular systems. *In vivo, in vitro* and *in silico* results indicate that mitochondrial localization and its functional regulation by TRPV4 are common aspects in many cellular systems from vertebrate origin.

AIMS OF THE PRESENT STUDY:

1. Characterization of TRPV4 in the context of different intracellular organelles

2. Exploring whether TRPV4 interacts with mitochondria and with mitochondrial proteins

3. Regulation of mitochondrial morphology, calcium homeostasis, potentiality, metabolite and other functional parameters by TRPV4

4. Characterization of the Mitochondrial Targeting Signal (MTS) present in TRPV4

5. Characterization of TRPV4 in sperm cells and its functional association with mitochondria

ORGANISATION OF THE THESIS:

The work reported in the thesis is embodied into five chapters. Chapter 1 deals with general introduction and review of literature in details with latest scientific information related to the concerned work and aim of the studies. Chapter 2 contains all the results obtained to justify the above mentioned objectives. Furthermore, result section was subdivided into 5 sub-sections based on the specific objectives. Chapter 3 is the part which includes extensive discussion on the results obtained in this work in the light of pre-existing literature and also proposes new hypothetical models and pathways involving TRPV4 and mitochondria. Chapter 4 provides a comprehensive idea about the entire work done, conclusions and future direction of the present study. Chapter 5 includes materials and methodologies employed for the current study. Chapter 6 includes all the bibliographic information mentioned in this study.

Results:

1. Characterization of TRPV4 in the context of different intracellular organelles

To achieve this objective, TRPV4 was expressed transiently by over expression or by stable selection in selected neuronal and in multiple non-neuronal cells (F11, a DRG neuron-derived cell line; HaCaT, CHOK1, HeLa, Cos7 cell line and in HUVEC as primary cell). Both, immunostaining of fixed cells and confocal imaging of live cells were performed to visualize the distribution of TRPV4 in different sub-cellular organelles. Colocalization studies of TRPV4 with different mitochondrial markers such as Hsp60, Cyt C, mitoDsRed and Mitotracker Red suggest that TRPV4 primarily localizes in mitochondria. Along with the plasma membrane, TRPV4 is also present in the mitochondrial structures located at the perinuclear regions. Live cell experiments with Mitotracker-Red labelled cells as well as with mitoDsRed expressing cells indicate that TRPV4 localizes in mitochondria in live HaCaT cells and such colocalization are prominent when TRPV4 expression is at the lower levels. Furthermore endogenous presence of TRPV4 in mitochondria was validated by biochemical fractionation followed by Western Blot analysis using highly specific anti-TRPV4 antibody and mitochondria purified from Goat brain, Goat adipose, Rat fore brain as well as from CHOK1-TRPV4 stable cell lines.

2. Exploring whether TRPV4 interacts with mitochondria and with mitochondrial proteins

Transfection based experiments in HaCaT cells suggest that only C-terminal fragment of TRPV4 (718-871 aa) can localize to mitochondria while the N-terminal fragment or the transmembrane region do not localise to mitochondria. Experiments with purified protein confirm that the C-terminal fragment of TRPV4 also interacts with intact mitochondria. Further pull down experiment identified mitochondrial dynamics regulatory proteins Mfn2 and Mfn1 as well as matrix chaperone protein Hsp60 as TRPV4 interacting proteins. Interaction of TRPV4-Ct with Mfn2 and Mfn1 is direct and independent of Ca^{2+}, GTP and/or ATP. Interaction of TRPV4 with these mitochondrial markers strongly suggests that TRPV4 is involved in the regulation of mitochondrial fission and fusion.

3. Regulation of mitochondrial morphology, calcium homeostasis, potentiality, metabolite and other functional parameters by TRPV4

TRPV4 act as a non-selective cation channel conducting influx of Ca^{2+} and other divalent cations inside the cell. Mitochondria plays an important role in Ca^{2+}-buffering by sequestering excess of intracellular Ca^{2+} and then releasing them in extracellular fluid through uniporter pump/s [29]. It has been reported that excess Ca^{2+}-load within mitochondria leads to mitochondrial dysfunction and altered mitochondrial morphology which correlate well with several diseases and the development of pathophysiological conditions [30]. Results described in previous section confirmed that TRPV4 is physically present in mitochondria and interacts with mitochondrial proteins. Work described in this chapter explores the functional significance of TRPV4 inside mitochondria. Most of the functional and biochemical characterization were performed using mitochondria isolated from Goat brain, or using HaCat cells expressing TRPV4 transiently, or CHOK1 cells expressing TRPV4 after stable selection. Results indicate that presence of TRPV4 activator alters mitochondrial morphology significantly and becomes circular or round-shaped as compared to normal elongated mitochondria in control conditions. It was also observed that TRPV4 activator increases and inhibitor decreases the level of Ca^{2+} within mitochondria. Furthermore, mitochondrial potentiality decreases significantly in presence of TRPV4 activator and increases in presence of TRPV4 inhibitor. Mitochondrial Ca^{2+} regulation is crucial for several metabolic enzymes and is equally important for the proper activity of mitochondrial electron transport chain and thus for ATP production. In this context, results suggest that both TRPV4 activation and inhibition affects the enzymatic activities involved in electron transport chain.

Ca^{2+}-influx inside mitochondria is known to regulate mitochondrial metabolism in several ways. Mitochondria serve as an important organelle for synthesis and transportation of different lipids, sterols/cholesterol and different lipid derivatives (such as different steroids) or their precursors and derivatives. Therefore abnormality in mitochondrial energetics results in abnormalities in the synthesis of several small molecules such as lipid derivatives, cholesterol and its derivatives, NAD+/NADH, ADP/ATP and other bio-metabolites. In this notion, the results obtained in this work also suggest that TRPV4 can serve as a regulator for mitochondrial metabolism. Such involvement of TRPV4 in metabolic functions seem to be largely conserved throughout the vertebrate evolution as suggested by conserved synteny organization where TRPV4 gene loci is flanked by two important metabolic pathway precursor genes on both sides, namely by glycolipid transfer protein (GLTP) on one side and by mevalonate kinase (MVK) on the other side. Physical interaction of TRPV4 with mevalonate, cholesterol and its derivatives such as different steroids to the

conserved intracellular Loop4 region suggest that TRPV4 is involved in such metabolism *per se* and such interactions are also highly significant for several physiological functions.

4. Characterization of the Mitochondrial Targeting Signal (MTS) present in TRPV4

Most of the mitochondrial proteins are encoded by nuclear genome and possesses conventional pre-sequences called Mitochondrial Targeting Signal (MTS) which are essential for translocation of these proteins into the mitochondria. Mitochondrial pre-sequences are typically 15-40 amino acid long enriched with positively charged residues and is present at the N-terminus of the protein [31]. Previous results described that the C-terminus of TRPV4 localizes inside the mitochondria. However bioinformatics approach including MitoProt and TargetP1.1 analysis assigns very low score to this fragment. Based on *in silico* prediction for mitochondrial targeting signal (MTS), a novel stretch of TRPV4 protein sequence (592-630 aa) was found which has higher score for mitochondrial signal peptide. Notably, in human population, a large number of point mutations have been reported to be present in this region. *In silico* analysis suggest that this predicted TRPV4-MTS sequence is conserved throughout the vertebrate evolution and has potential amphipathic stretch sequence which can help in mitochondrial import. *In vitro* experiments confirmed that this TRPV4-MTS indeed localizes inside the mitochondria in HaCaT cell and colocalizes with different mitochondrial markers such as mitoDsRed and Hsp60. Analysis different point mutants located within this region suggest that mutations in this region affect mitochondrial localization. Further biochemical pull down study also confirms that this short sequence can interact with Cytochrome C directly in a Ca^{2+}-sensitive manner.

5. Characterization of TRPV4 in sperm cells and its functional association with mitochondria

The previous chapters described the physical presence of TRPV4 in mitochondria and its importance in the regulation of mitochondrial structure and function in different cell lines and in primary cells. To explore if TRPV4 can regulate mitochondrial structure-function, mature sperm/spermatozoa from different species were used as model systems. Mature sperm cells are extremely sensitive to different temperatures and represent transcriptionally as well as translationally silenced cellular systems. Therefore, sperm cells rely mainly on the Ca^{2+}-signaling events. In addition, mature sperm cells have high number of mitochondria precisely located at neck regions. Therefore, sperm cell offers a unique model system to study the effect of TRPV4-mediated changes in mitochondrial organization and functions. Indeed, our

experiments confirm that endogenous expression of TRPV4 in sperm cell is conserved throughout vertebrate evolution. TRPV4 also colocalizes with mitochondria of sperm cell obtained from different vertebrates such as fish, duck and human. The work described in this chapter characterizes the qualitative and quantitative changes in the mitochondrial morphology and intracellular Ca^{2+} -levels in mature sperm from different vertebrates.

Using high-end imaging methodologies, work described in this chapter confirms that mitochondrial morphology is altered upon activation of TRPV4. Super-Resolution images of Bull sperm indicate that TRPV4 activation alters mitochondrial coiling within the neck region of sperm to a large extent. In case of human sperm, TRPV4 activator and inhibitors significantly altered capacitation, acrosomal reaction, calcium-dynamics and sperm-motility. Inhibition of TRPV4 by specific inhibitor not only reduces progesterone-mediated hyperacivation but also reduces the Ca^{2+}-wave propagated through the mitochondrial coiling region. Collectively, results obtained in this work confirm the involvement of TRPV4 in Progesterone-signaling. *In vitro* results also suggest that TRPV4 can act as an alternative "Progesterone receptor" as progesterone can directly bind to the intracellular loop 4 region, demonstrating that TRP channels are important in the context of steroid-mediated signalling events.

Discussion and conclusion:

Precise response against minute changes in temperature is a hall mark and common sensory function in many biological systems. A handful number of reports suggest that mitochondria alone is involved in cellular thermo-sensation and also responds to slight changes in temperature, though the exact molecular mechanisms and players involved in such functions are not known (32). Mitochondria is known to contain different types of Ca^{2+} channels and uniporters which can potentially modulate cell signalling events, inter-organeller communication, ageing, cell proliferation, cell death and thus involved in development of pathophysiological diseases. For example, Voltage Dependent Anion Channel (VDAC) is present on the outer mitochondrial membrane and regulates mitochondrial Ca^{2+}-level and thereby controls mitochondrial metabolites and energetics [33]. Presence of TRPV4 in the plasma membrane is well established. In this study we have investigated the presence of TRPV4 in specific intracellular organelles. Localization of TRPV4 in intracellular organelles has been reported in different cellular system which mainly correlates well with different pathophysiological conditions including faulty protein trafficking, impaired protein folding and/or tetramerization, and ER stress [26, 34].

So far a few studies on TRPV4 have described its regulation in the context of surface expression and subcellular distribution. Both N-and C-terminus are important for several functions attributed to TRPV4. The C-terminus of TRPV4 interacts with different cytoskeletal elements [35]. A small fragment of TRPV4 present at the C-terminus is important for tetramerization and cell surface expression as deletion of this 16 aa fragment leads to accumulation of non-functional TRPV4 in ER [27]. It has also been demonstrated that interaction of PACSIN3, a cytoskeletal protein with the N-terminal region of TRPV4 enhances its membrane localization [36]. Though all these studies characterized the trafficking of TRPV4 to a large extent, the understanding of surface expression as well as intracellular distribution of TRPV4 and actual regulation/s underlying this is still fragmented.

The work described in this thesis confirms the physical presence of TRPV4 in the mitochondria and also establishes physical interaction of TRPV4 with different mitochondrial proteins, namely Mfn1, Mfn2, Hsp60 and Cytochrome C. These interactions are largely indicative of the importance of TRPV4 in mitochondrial fission and fusion events and therefore involve mitochondrial structure and function in details. The obtained data also suggest that TRPV4-Mfn2 complex is relevant for the specialized region that forms close contacts between ER and mitochondria commonly termed as mitochondria-associated membrane (abbreviated as "MAM"). Although Mfn2 is an outer mitochondrial membrane protein, but its amount is 14-fold higher in the MAM region which helps in transient tethering of ER with mitochondria [37]. MAM is also the specialized region through which communication between ER and mitochondria for the transport of lipid and/or lipid derivatives, metabolite and Ca^{2+} exchange takes place [38]. The TRPV4-Mfn2 complex at MAM is also important for the mitochondrial dynamics involving Mfn2 and Mfn1 [39, 40]. It seems that after or during tetrameric assembly of TRPV4 in ER, a fraction of TRPV4 translocates to the mitochondria through MAM.

In agreement with the physical interaction of TRPV4 with Mfn2 and Mfn1, TRPV4-positive mitochondria have altered morphology and Hsp60 level. This is also in line with the fact that TRPV4 activation or inhibition largely regulates mitochondrial structure and functions. This induces further alteration in mitochondrial shape which becomes spherical or round-shaped and leads to mitochondrial aggregation. These results also suggest for a possible function of endogenous TRPV4-mediated regulation of the cristae curvature where both activation as well as inhibition can alter cristae organization. Recent research indicates that mitochondrial morphology largely depends on the actual lipid composition or lipid signalling molecules present within mitochondria [41]. Certain regulatory enzymes and

different specific lipids such as cardiolipin, phosphatidic acid, lysophosphatidic acid, diacylglycerol, phosphatidylethanolamine etc. regulate mitochondrial morphology and such functions are conserved from yeast to higher mammals [41]. As most cases, the mitochondrial lipids are synthesized in the MAM region and subsequently transported into the mitochondria. Therefore, it is most likely that TRPV4 regulates lipid composition or synthesis within the mitochondria resulting alteration in mitochondrial morphology. Interaction of diverse sterols and steroids including cholesterol and progesterone, with the conserved Loop4 region of TRPV4, indicates its importance in complex signalling events.

Diverse effects of TRPV4 on the regulation of function and morphology of mitochondria is conserved in several cell lines and primary cells tested in this work. Since sperm cells are highly mobile and show extreme response against a large number of variable factors such as slight changes in temperature, pH, osmolality, presence of salts, and other factors at very low concentrations, presence of different TRP channels including TRPV4 is highly significant [42, 43]. Indeed TRPV4-mediated regulation of mitochondria is also relevant in mature sperm cells from different species which are actually devoid of many cellular machineries and are transcriptionally and translationally silent. In mature sperm cell, TRPV4 has a role in Ca^{2+}-influx and Ca^{2+}-buffering. Precise localization of TRPV4 also correlates well with the motility of mature sperm cells from human.

In conclusion, this work established physical presence of TRPV4 in mitochondria in diverse cells including mature sperm and in all cases TRPV4 not only regulates mitochondrial morphology but also regulates the mitochondrial calcium homeostasis, oxidative potentiality and metabolism. Such findings have broad implications in the molecular understanding of several pathophysiological disorders where TRPV4 and/or mitochondrial abnormalities are involved. This in turn has several bio-medical applications too.

References:

1. Clapham, D. E., Montell, C., Schultz, G. and Julius, D. (2003). International Union of Pharmacology. XLIII. Compendium of Voltage-Gated Ion Channels : Transient Receptor Potential Channels. Pharmacol. Rev. 55, 591–596.

2. Clapham, D. E., Runnels, L. W. and Strübing, C. (2001). The TRP ion channel family. Nat. Rev. Neurosci. 2, 387–396.

3. Ramsey, I. S., Delling, M. and Clapham, D. E. (2006). An introduction to TRP channels. Annu. Rev. Physiol. 68, 619–647.

4. Minke, B. (1977). Drosophila mutant with a transducer defect. Biophys. Struct. Mech. 3, 59–64.

5. Voets, T., Talavera, K., Owsianik, G. and Nilius, B. (2005). Sensing with TRP channels. Nat. Chem. Biol. 1, 85–92.

6. Chung, M.-K., Lee, H. and Caterina, M. J. (2003). Warm temperatures activate TRPV4 in mouse 308 keratinocytes. J. Biol. Chem. 278, 32037–46.

7. Fernández-Fernández, J. M., Nobles, M., Currid, A., Vázquez, E. and Valverde, M. a (2002). Maxi K+ channel mediates regulatory volume decrease response in a human bronchial epithelial cell line. Am. J. Physiol. Cell Physiol. 283, C1705–C1714.

8. Jia, Y., McLeod, R. L., Wang, X., Parra, L. E., Egan, R. W. and Hey, J. A. (2002). Anandamide induces cough in conscious guinea-pigs through VR1 receptors. Br. J. Pharmacol. 137, 831–836.

9. Liedtke, W., Choe, Y., Marti-Renom, M. A., Bell, A. M., Denis, C. S., Sali, A., Hudspeth, A. J., Friedman, J. M. and Heller, S. (2000). Vanilloid receptor-related osmotically activated channel (VR-OAC), a candidate vertebrate osmoreceptor. Cell 103, 35.

10. Strotmann, R., Harteneck, C., Nunnenmacher, K., Schultz, G. and Plant, T. D. (2000). OTRPC4, a nonselective cation channel that confers sensitivity to extracellular osmolarity. Nat. Cell Biol. 2, 695–702.

11. Wissenbach, U., Bödding, M., Freichel, M. and Flockerzi, V. (2000). Trp12, a novel Trp related protein from kidney. FEBS Lett. 485, 127–134.

12. Suzuki, M., Watanabe, Y., Oyama, Y., Mizuno, A., Kusano, E., Hirao, A. and Ookawara, S. (2003). Localization of mechanosensitive channel TRPV4 in mouse skin. Neurosci. Lett. 353, 189–192.

13. Rock MJ, Prenen J, Funari VA, Funari TL, Merriman B, Nelson SF, et al. (2008) Gain-of-function mutations in TRPV4 cause autosomal dominant brachyolmia. Nat Genet. 40:999-1003.

14. Verma P, Kumar A, Goswami C. (2010) TRPV4-mediated channelopathies. Channels (Austin). 4, 4.

15. Bernd Nilius and Thomas Voets (2013). The puzzle of TRPV4 channelopathies. EMBO reports. 14, 152–163.

16. Watanabe, H., Davis, J. B., Smart, D., Jerman, J. C., Smith, G. D., Hayes, P., Vriens, J., Cairns, W., Wissenbach, U., Prenen, J., et al. (2002). Activation of TRPV4 Channels (hVRL-2/mTRP12) by Phorbol Derivatives. J. Biol. Chem. 277, 13569–13577.

17. Yowtak, J., Lee, K. Y., Kim, H. Y., Wang, J., Kim, H. K., Chung, K. and Chung, J. M. (2011). Reactive oxygen species contribute to neuropathic pain by reducing spinal GABA release. Pain 152, 844–852.

18. Barrière, D. A., Rieusset, J., Chanteranne, D., Busserolles, J., Chauvin, M.-A., Chapuis, L., Salles, J., Dubray, C. and Morio, B. (2012). Paclitaxel therapy potentiates cold hyperalgesia in streptozotocin-induced diabetic rats through enhanced mitochondrial reactive oxygen species production and TRPA1 sensitization. Pain 153, 553–61.

19. Li, Z., Ji, G., Neugebauer, V. (2011). Mitochondrial reactive oxygen species are activated by mGluR5 through IP3 and activate ERK and PKA to increase excitability of amygdala neurons and pain behavior. J. Neurosci. 31, 1114–1127.

20. Joseph, E. K. and Levine, J. D. (2010). Multiple PKCε-dependent mechanisms mediating mechanical hyperalgesia. Pain 150, 17–21.

21. Xiao, W. H. and Bennett, G. J. (2012). Effects of mitochondrial poisons on the neuropathic pain produced by the chemotherapeutic agents, paclitaxel and oxaliplatin. Pain 153, 704–709.

22. Hollenbeck, P. J. (2005). The axonal transport of mitochondria. J. Cell Sci. 118, 5411–5419.

23. Dong, X. P., X. Wang & H. Xu. (2010) TRP channels of intracellular membranes. J Neurochem, 113, 313-28.

24. Gallego-Sandín, S., Rodríguez-García, A., Alonso, M. T. and García-Sancho, J. (2009). The endoplasmic reticulum of dorsal root ganglion neurons contains functional TRPV1 channels. J. Biol. Chem. 284, 32591–32601.

25. Lo IC, Chan HC, Qi Z1, Ng KL, So C, Tsang SY (2015) TRPV3 Channel Negatively Regulates Cell Cycle Progression and Safeguards the Pluripotency of Embryonic Stem Cells. J Cell Physiol. 2015 Jun 30.

26. Xu H, Fu Y, Tian W, Cohen DM. (2006) Glycosylation of the osmoresponsive transient receptor potential channel TRPV4 on Asn-651 influences membrane trafficking. Am J Physiol Renal Physiol. 290:1103-9.

27. Becker D, Müller M, Leuner K, Jendrach M. (2008) The C-terminal domain of TRPV4 is essential for plasma membrane localization. Mol Membr Biol. 25:139-51.

28. Auer-Grumbach, M., Olschewski, A., Papić, L., Kremer, H., McEntagart, M. E., Uhrig, S., Fischer, C., Fröhlich, E., Bálint, Z., Tang, B., et al. (2010). Alterations in the ankyrin domain of TRPV4 cause congenital distal SMA, scapuloperoneal SMA and HMSN2C. Nat. Genet. 42, 160–164.

29. De Stefani, D., Raffaello, A., Teardo, E., Szabo`, I., and Rizzuto, R. (2011). A forty-kilodalton protein of the inner membrane is the mitochondrial calcium uniporter. Nature 476, 336–340.

30. Szabadkai G, Simoni AM, Bianchi K, De Stefani D, Leo S, Wieckowski MR, Rizzuto R. (2006). Mitochondrial dynamics and Ca2+ signaling. Biochim Biophys Acta. 1763(5-6):442-9.

31. Omura, T. (1998). Mitochondria-targeting sequence, a multi-role sorting sequence recognized at all steps of protein import into mitochondria. J. Biochem. 123, 1010–1016.

32. Gambert, S., and D. Ricquier. 2007. Mitochondrial thermogenesis and obesity. Curr. Opin. Clin. Nutr. Metab. Care. 10:664–670.

33. Shoshan-Barmatz, V., De Pinto, V., Zweckstetter, M., Raviv, Z., Keinan, N. and Arbel, N. (2010). VDAC, a multi-functional mitochondrial protein regulating cell life and death. Mol. Aspects Med. 31, 227–285.

34. Arniges, M., Fernández-Fernández, J. M., Albrecht, N., Schaefer, M. and Valverde, M. A. (2006). Human TRPV4 channel splice variants revealed a key role of ankyrin domains in multimerization and trafficking. J. Biol. Chem. 281, 1580–1586.

35. Goswami C, Julia Kuhn, Paul A. Heppenstall, Tim Hucho. (2010) Importance of Non-Selective Cation Channel TRPV4 Interaction with Cytoskeleton and Their Reciprocal Regulations in Cultured Cells. PLOS one. 5 e11654.

36. D'Hoedt, D., Owsianik, G., Prenen, J., Cuajungco, M. P., Grimm, C., Heller, S., Voets, T. and Nilius, B. (2008). Stimulus-specific modulation of the cation channel TRPV4 by PACSIN 3. J. Biol. Chem. 283, 6272–6280.

37. De Brito, O. M. and Scorrano, L. (2008). Mitofusin 2 tethers endoplasmic reticulum to mitochondria. Nature 456, 605–610.

38. Vance, J. E. (2014). MAM (mitochondria-associated membranes) in mammalian cells: Lipids and beyond. Biochim. Biophys. Acta - Mol. Cell Biol. Lipids 1841, 595–609.

39. Nunnari, J. and Suomalainen, A. (2012). Mitochondria: In sickness and in health. Cell 148, 1145–1159.

40. Chen, H., Detmer, S. A., Ewald, A. J., Griffin, E. E., Fraser, S. E. and Chan, D. C. (2003). Mitofusins Mfn1 and Mfn2 coordinately regulate mitochondrial fusion and are essential for embryonic development. J. Cell Biol. 160, 189–200.

41. Ha, E. E.-J. and Frohman, M. A. (2014). Regulation of mitochondrial morphology by lipids. Biofactors 1–6.

42. Bahat, A., Tur-Kaspa, I., Gakamsky, A., Giojalas, L. C., Breitbart, H. and Eisenbach, M. (2003). Thermotaxis of mammalian sperm cells: A potential navigation mechanism in the female genital tract. Nat. Med. 9, 149–150.

43. Hamamah, S. and Gatti, J. L. (1998). Role of the ionic environment and internal pH on sperm activity. Hum. Reprod. 13 Suppl 4, 20–30.

List of table: **Page no.**

List of figure: **Page no.**

List of abbreviations:

4αPDD	4α-Phorbol 12,13-didecanoate
5-HT	5-hydroxytryptamine
Amp	Ampicillin
APS	Ammonium persulphate
ATP	Adenosine triphosphate
Bp	Base pair
BSA	Bovine serum albumin
CBB	Coomassie Brilliant Blue G250
CCCP	Carbonyl cyanide m-chlorophenyl hydrazine
CHOK1-Mock	Chinese Hamster Ovary K1-Mock
CHOK1-V4	Chinese Hamster Ovary K1-TRPV4
Cyt C	Cytochrome C
DAPI	4',6-diamidino-2-phenylindole
DCPIP	2,6-Dichlorophenolindophenol
DMSO	Dimethyl Sulfoxide
DNA	Deoxyribonucleic acid
dNTP	deoxy Nucleotide Tri Phosphate
DRG	Dorsal root ganglion
DTT	Dithiothreitol
DU	Decylubiquinone
ECL	Enhanced Chemiluminescent
EDTA	Ethylenediaminetetraacetic acid
EGTA	Ethylene glycol bis(2-aminoethyl ether)tetraacetic acid
EM	Electron Microscopy
Endo H	Endoglycosidase H
ER	Endoplasmic Reticulam
EtBr	Ethidium Bromide
FBS	Fetal calf serum
Fluo-4 AM	Non-fluorescent acetoxymethyl ester
PI	Complete protease inhibitor
PFA	Paraformaldehyde
GFP	Green Fluorescence Protein
GTP	Guanosine 5′-triphosphate
H	hour (Time unit)
HCl	Hydrogen Chloride
$HClO_4$	Perchloric acid
HEPES	4-(2-Hydroxyethyl)piperazine-1-ethanesulfonic acid
HRP	Horseradish Peroxidase

Hz	Hertz
IPTG	Isopropyl thiogalactose
IRTX	5'-iodoresiniferatoxin
JC-1	5,5′,6,6′-tetrachloro-1,1′,3,3′-tetraethylbenzimidazolocarbocyanine iodide
Kan	Kanamycin
Kb	Kilo base
kDa	Kilo Dalton
KO	Knock out
KOH	Potassium Hydroxide
L	Litre (volume unit)
L4	Loop4
LB	Luria-Bertani
MAM	Mitochondria-associated membrane
MBP	Maltose Binding Protein
MFI	Mean Fluorescence Intensity
Min	Minutes (Time unit)
MitoTracker Red	MitoTracker Red FM
NA	Numerical aperture
$NaBH_4$	Sodium borohydride
NaCl	Sodium Chloride
NaOH	Sodium Hydroxide
NADH	Nicotinamide adenine dinucleotide (reduced form)
NOS	Nitric oxide synthase
NOX	NADPH oxidase
PAGE	Poly Acrylamide Gel Electrophoresis
PBS	Phosphate buffer saline
PCR	Polymerase Chain Reaction
PGE2	Prostaglandin E2
PMSF	Phenylmethanesulfonyl fluoride
PNGase F	Peptide -N-Glycosidase F
PIPES	1,4-Piperazinediethanesulfonic acid
PKA	Protein Kinase A
PKC	Protein Kinase C
PPM	Parts per million
PSD	Post synaptic density
PVDF membrane	Polyvinylidene difluoride membrane
ROS	Reactive oxygen species
RPM	Revolution-Per-Minute
RT	Room temperature
RTX	Resiniferatoxin

Sd	Swim-down
SDS	Sodium Dodecyl Sulphate
Su	Swim-up
TAE	Tris-Acetic Acid-EDTA
TEMED	N,N,N′,N′-Tetramethylethylenediamine
TG	Trigeminal
TM	Transmembrane
Tris	Tris Hydroxymethylaminoethane
TRP	Transient Receptor Potential
v/v	Volume per volume
w/v	Weight per volume

Chapter 1

Introduction and Review of Literature

1.1. General introduction TRP family ion channels

1.1.1 Initial history of TRP channels discovery

The Transient Receptor Potential (TRP) ion channels are non-selective cation channels which mediate the influx of mono- and divalent-cations down their electrochemical gradients. TRP channel was first discovered in *Drosophila* photoreceptor (as *trp* mutant) where response against light was defective [1]. In 1969, for the first time *Drosophila trp* mutant was isolated and characterized based on their visual pigment impairment and this mutant shows transient response with light [2]. It was observed that during prolonged illumination on *Drosophila* photoreceptors, these *trp*-mutant flies transiently go blind and which can be rescued by removing light illumination from photoreceptor for at least 1 minute. Because of this electrophysiological phenotype due to the defects in photoreceptor, this mutant was named as *"transient receptor potential" or trp* mutants [3]. After the discovery of *trp* gene, over 20 years till 1989, it was not confirmed if *trp* protein acts as a channel or not. The cloning of trp gene and its amino acid sequence provided strong indication that *trp* gene may actually act as an ion channel [4-5]. A more definitive nature of TRP was suggested by the hydrophobicity plot of TRP protein. Such analysis reveals that TRP protein have 6-8 transmembrane domain and it was proposed that *"TRP protein is an ion channel"* by Craig Montell and his associates [6]. After several months work confirmed that TRP channel actually act as a calcium ion channel and cause Ca^{2+}-influx inside the cell [7]. Since its discovery, so far several TRP channels have been identified in all animals and these channels are involved in a plethora of sensory and physiological functions.

TRPV1 is the first founding member of TRPV sub family of ion channels. Rat TRPV1 was identified in a cDNA screening where response against capsaicin was tested [8]. Most of the mammalian TRPV1 respond against capsaicin in different heterologous systems and cause robust Ca^{2+}-influx. Identification of TRPV1 has been considered as a mile stone in

pain research. Recently TRP channels have been identified from several fungal systems also [9-10]. However, so far TRP channels have not been detected in plants, though some other ion channels namely cyclic nucleotide gated calcium channels have been proposed as the functional homologues of TRP channels in plants [11-12].

1.1.2 Evolution of TRP channels

TRP channels regulate critical physiological and cellular functions in cells and these functions are mostly conserved from yeast to higher mammals. Expression of functional TRP channels has been reported in invertebrates such as worms, mosquito, fruit fly, as well as in vertebrates such as zebrafish, birds, mice and human [13]. TRP channels are also present in fungi, such as TrpY1 in yeast (*Saccharomyces cerevisiae*) where it regulates mechanosensation property of vacuolar osmotic pressure [9-10]. TrpY1 is a yeast vacuolar protein and it is specifically evolved in yeast which is distinct from other metazoan ancestors [14]. Previous study suggested that in Protista such as *Thecamonas trahens* has TRPP and TRPV ion channels and it was believed that this could be the most ancient form of metazoan TRP channels [14]. Moreover in choanoflagellates (*Monosiga brevicollis* and *Salpingoeca rosetta*) contain five different TRP channels namely TRPA, TRPC, TRPM, TRPML, and TRPV which indicates that most of the TRP family ion channels emerged from unicellular metazoan. Identification of these channels in choanoflagellates indicates that these five channels evolved before emergence of any multicellular higher animals. Though neurons are not present in choanoflagellates and sponges but both organisms respond to environmental stimuli which suggest that theses stimuli may be perceived by TRP channel [15-16]. Phylogenetic analysis reveals that sponges (oldest metazoan, 600 MYA) have two subfamily of ion channel namely TRPA and TRPML [17]. *Cnidaria* (evolved 540 MYA) have TRPA, TRPC, TRPM, TRPML, TRPP and TRPV family of ion channels [17]. Arthropod includes

largest classes of animal group which is present in freshwater, seawater and terrestrial places and phylogenetic analysis suggests that this phylum have almost all type of TRP family ion channels [17]. Analysis of the molecular evolution of TRP channels shows evolutionary plasticity. In many cases, such plasticity is accompanied by gene duplication and multiplication events as well. In certain cases, some of the TRP channels are absent in one phylum and again re-appear in next higher phylum suggesting mostly gene-loss events. In general, several factors such as interaction with specific ligands, presence of specific lipid components in membrane, environmental cues, body temperature etc. have played important roles in the molecular evolution of TRP channels.

1.1.3 Classification of TRP channels

Based on amino acid sequence and homology; Transient Receptor Potential (TRP) ion channels are classified into 7 subfamilies namely TRPC (Canonical), TRPM (Melastatin), TRPV (Vanilloid), TRPA (Ankyrin), TRPML (Mucolipin), TRPN (No mechanoreceptor potential C) and TRPP (Polycystin) [18-20] **(Fig. 1)**. The eighth subfamily, TRPY, known as yeast TRPs, is distantly related to these classical 7 subfamily members and is responsible for sensing hypertonicity [14]. The presence of TRPs in yeast indicates that TRP channels precede the emergence of metazoan organisms [9-10]. The TRPN channels are not present in mammals but they are expressed in some vertebrates such as in zebrafish. Till now 7 mammalian TRPC have been described (TRPC1-7) but TRPC2 is absent in human. All other TRPCs are present in different cellular system. Mammalian TRPM consist of 8 members of subfamily. The TRPV family contains 6 members and some of these channels have thermosensitive properties. In most animals, TRPVs are present as a single copy gene. However, in amphibians, multiple copies of TRPV4 are present. TRPA1 is the only member present in this family and it was previously known as ANKTM1 because this protein has

several N-terminal ankyrin repeats [21]. The mammalian TRPM subfamily contains eight members (TRPM1-8). TRPM1 is the first protein in mammalian TRPM which was initially named as "melastatin", as its expression level correlates inversely with the melanomic cell lines [22]. TRPML1 (mucolipin-1) is the founding member of TRPML superfamily ion channel. TRPML1 and TRPML2 have lysosomal targeting signals and localizes with lysosomal membrane [13, 23]. Accordingly, mutation in TRPML1 leads to lysosomal disorders namely mucolipidosis IV which results in severe neurodegeneration. TRPP family represents the most primitive subfamily of TRPs as TRPP2 is archetype (a homolog of microbes) and it is also present in yeast cell. TRPP2 was first discovered as a protein disruptor relevant in Autosomal dominant polycystic kidney disease (ADPKD) [10, 24].

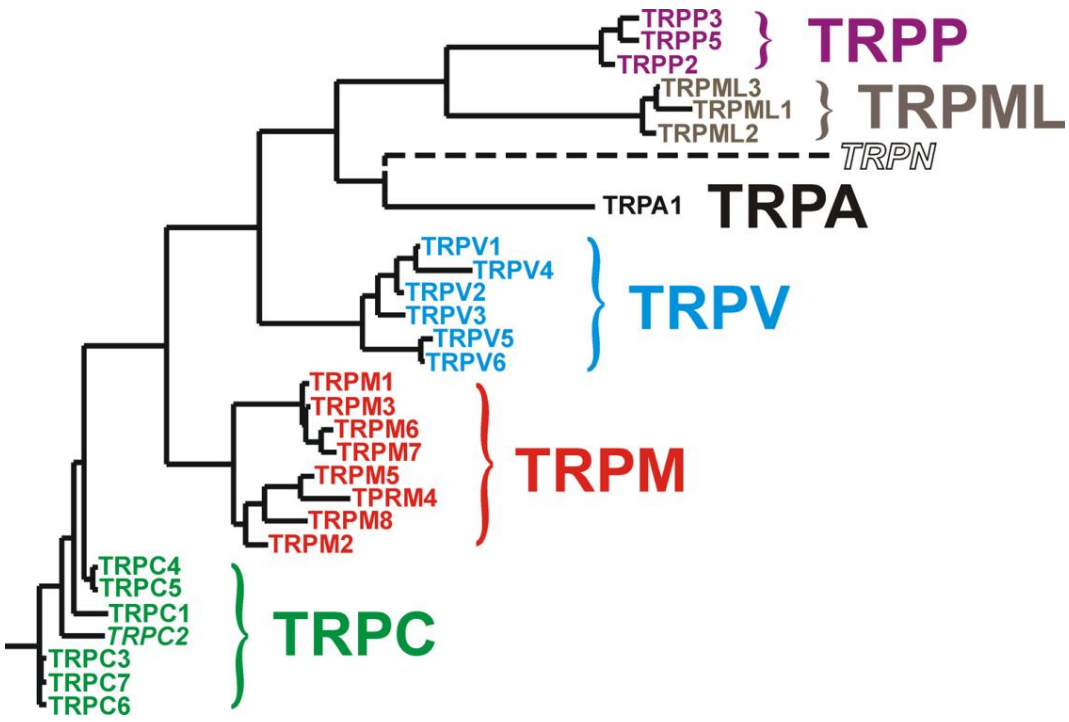

Fig 1: Family tree of TRPs channels. TRP members are divided into 7 sub family: TRPC (Canonical), TRPM (Melastatin), TRPV (Vanilloid), TRPA (ANKTM1), TRPML (Mucolipin), TRPN (No mechanoreceptor potential C) and TRPP (Polycystin). Image taken from Clapham D.E.; 2003 [18].

1.1.4. General domain and motif structures of TRP channels

Like voltage-gated Na^+ channels, TRP channels also contain six transmembrane (6TM) helices and the pore domain is present between the 5^{th} (S5) and 6^{th} (S6)

transmembrane region. Both N- and C-termini are located at the intracellular sides [18]. The N-terminal cytoplasmic domain of the TRPV and the TRPC channels contain single to multiple ankyrin repeats. The C-terminal cytoplasmic domain contains a TRP-box (in many TRP channels), which is well conserved in members of the TRPC subfamily, but is less conserved in members belonging to TRPM and TRPV subfamilies. TRP channels form homo- or heterotetramer and such tetramers act as functional ion channels. Most of the TRP channels contain a conserved sequence of 25 amino acids located immediately after the 6th transmembrane segment (S6) commonly known as "TRP-box", a typical structural signature characteristic of several TRP channels. "TRP-box" is well conserved in members of the TRPC subfamily, but is less conserved within TRPM and TRPV subfamilies. Most of the TRP channels contain a Ca^{2+}-sensing EF-hand motif, different phosphorylation sites, PIP_2 and Calmodulin-binding sites.

1.1.5. Function of TRP channels

TRP channels are mostly associated with the neuronal and/or sensory functions. However, in recent time, involvement of TRP channels in functions mediated by non-neuronal cells has also been reported. Most of the TRPs channels act as non-selective cation channels with very high to modest permeability towards Ca^{2+} ions. In addition, TRP channels are modulated by Ca^{2+} itself, which generate positive or negative feedback loop mechanism to regulate intracellular Ca^{2+} levels [25]. TRPs channels are involved in the regulation of intracellular Ca^{2+}-homeostasis and thus regulate the plasticity on Ca^{2+}-signalling. TRP-mediated Ca^{2+}-influx regulates important physiological functions, such as fertilization, cell differentiation and proliferation, cell death, neurotransmitter release, muscles contraction and transcription factor activation, etc [26]. In most conditions, Ca^{2+}-influx inside the cells occurs through TRPs present in cell membrane and/or in intracellular organelles and cause changes

in the membrane potential which creates driving force for Ca^{2+} uptake [27]. Though all TRP channels allow the entry of several divalent or monovalent cations inside the cell, the selectivity for Ca^{2+} over the Na^{+} is higher in the case of TRPV5 and TRPV6 [28, 29]. The variance in the selection of divalent cation (Ca^{2+}) depends on the selectivity filter of pore and dynamic nature of pore behaviour of the TRPV5 and TRPV6 channels [30, 31].

In case of TRPV5 and TRPV6, homo or hetero teteramerization results in the formation of the specific "selective filter" by negatively charged amino acids [32-33]. For example, tetrameric structure of TRPV5 and TRPV6 forms a tetrameric ring made of D^{542} and D^{541} acidic amino acids, which act as the "selective filter" and specifically allow only Ca^{2+} ions from extracellular sides towards the inside [34]. The mammalian TRPC family is subdivided into 4 other sub-families (such as TRPC1, TRPC2, TRPC3/6/7 and TRPC4/5) based on their functional significance and sequence alignment. TRPC channels are in general non selective cationic channel and their selectivity for Ca^{2+} ion differs among all these members **(Fig 2)**.

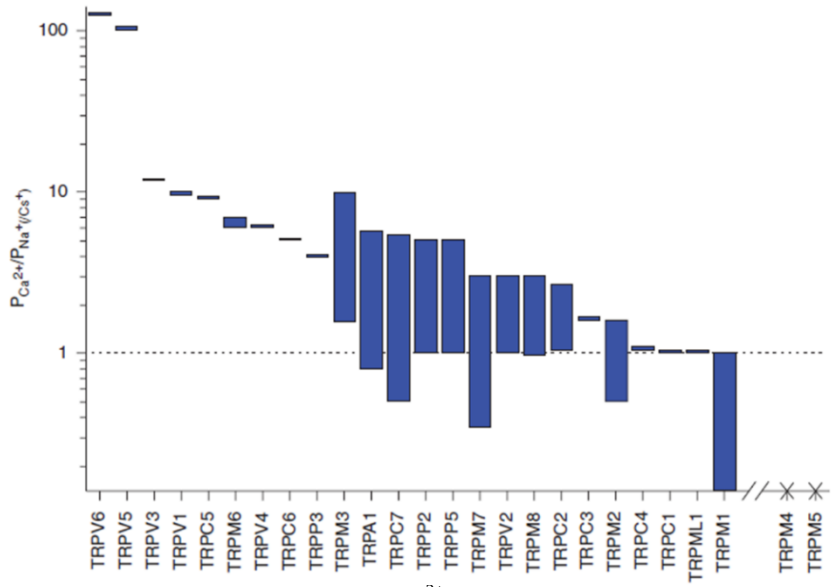

Fig 2: Ca^{2+}-selectivity of different TRP channels. Ca^{2+}-selectivity of different TRP channels indicating that TRPV5 and TRPV6 have highest affinity for calcium and TRPM1 has the lowest. TRPM4 and TRPM5 are impermeable for calcium. (Image taken from Grees et al., 2010) [35].

1.1.6 Structure of TRP channels

The topological architecture of TRP channels is composed of six transmembrane segments (S1–S6), intracellular N- and C-terminal domains, and a pore-forming loop between S5 and S6 [36]. The N- and C-terminal domains of TRP channels are located towards the cytoplasmic side which allow TRP channels to interact with diverse cytoplasmic proteins. The length of the cytosolic tails (both N- and C-terminus) varies in different TRP channel subfamilies mainly due to their different structural and functional domains [37].

TRPP and TRPML channels seem to possess an extended extracellular loop between S1 and S2, but experimental evidence for this structural model is lacking [20]. TRP channels contain a conserved sequence of 25 amino acids located immediately after the 6th transmembrane segment (S6) commonly known as "TRP-box", a typical structural signature, characteristic of all TRP channels (except TRPA and TRPP members) [18, 21]. In case of TRPC ion channel, a highly conserved 6 amino acid sequence is present which is similar to TRP-box containing "EWKFAR" sequence [21]. It has been also reported that sequence within the TRP-box is responsible for PIP_2-binding and regulates the gating property of TRP channels, at least such importance has been documented in case of TRPM8 and TRPV5 channels [38, 39]. In general, TRPV and TRPC channels contain 3-5 ankyrin repeats in the N- terminal cytoplasmic domain. However as high as 17 ankyrin repeats are present in TRPA members [36]. So far, X-ray diffraction structures of TRP channels are not available or limited to certain fragments only, though high resolution structure is available for selected few TRP channels (discussed later). Most of the TRP channels form homo- or heterotetramer and the tetrameric structures only can form the functional ion channel. TRP channels are believed to have similar transmembrane topology and subunit organization as reported for the voltage-gated potassium (Kv) or sodium (Nav) ion channels [20]. So far only few TRP channels have been crystallized and 3-D cryo-EM structure has been reported. For example,

initially full-length TRPV1 structure has been solved by single-particle electron cryomicroscopy (cryo-EM) in 19-Å resolution [40]. This structures indicated that only one third of this ion channel is present in membrane and the other two third portion is hanging towards the cytoplasmic area and such structure is termed as ‘‘hanging gondola’’ [40-42]. Very recently, single-particle electron cryomicroscopy revealed structure of tetrameric TRPV1 at 3.4-Å resolution, both in open- and closed-conformation (**Fig 3**) [43, 44]. These structural details provide useful information regarding structure-function relationship of TRPVs. The tetrameric structure of TRP channels confirmed that the S5 and S6 region is important for the pore formation and also provides the selectivity filter which selectively allows certain ions only to cross plasma membrane (**Fig 5**) [44]. In comparison to TRPV1-V4, TRPV5 and TRPV6 have distinct amino acid sequences and in TRPV5/6 the selective filters is more specific for Ca^{2+} ions only. However recent Cryo-EM structure (4Å) of TRPV2 suggest that it has 6 TM region and TM-6 largely involved in gating regulation or pore opening through rearrangements in the secondary structure of S6 (**Fig 4**) [45].

1.1.7 Structure of TRPV4 ion channel

On the basis of structural and functional properties, TRPV family divided into four groups: TRPV1/TRPV2, TRPV3, TRPV4 and TRPV5/6 [46, 47]. TRPV1-4 are polymodal, thermosensitive and non-selective cation channels and mostly allows Ca^{2+} as well as other ions inside the cell upon activation. The human TRPV4 gene is present on chromosome 12q23-q24.1 and consists of 15 exons which codes for 5 different splice variants.

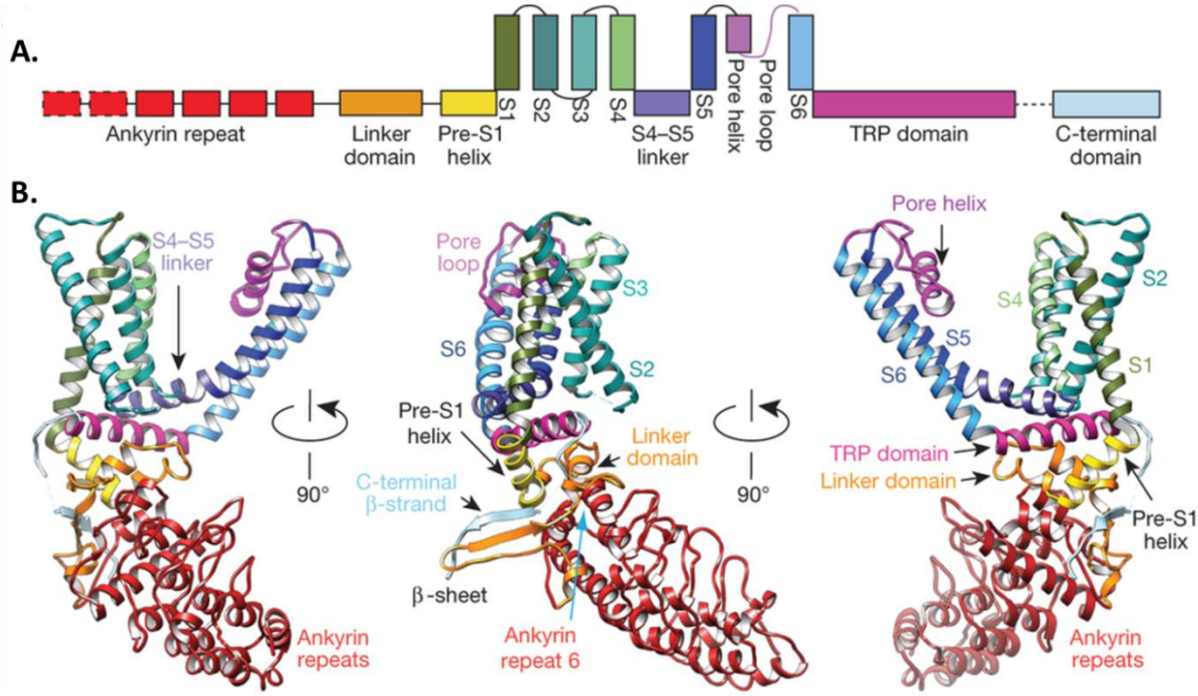

Fig 3: Molecular structure of TRPV1. A. Linear graphical representation of monomeric TRPV1 structure indicating the different domain, pore region, transmembrane and loop region. B. Representing the ribbon like structure and three different views of TRPV1 tetrameric structure and pore region in closed state. (Image taken from Liao et al., 2013)[44].

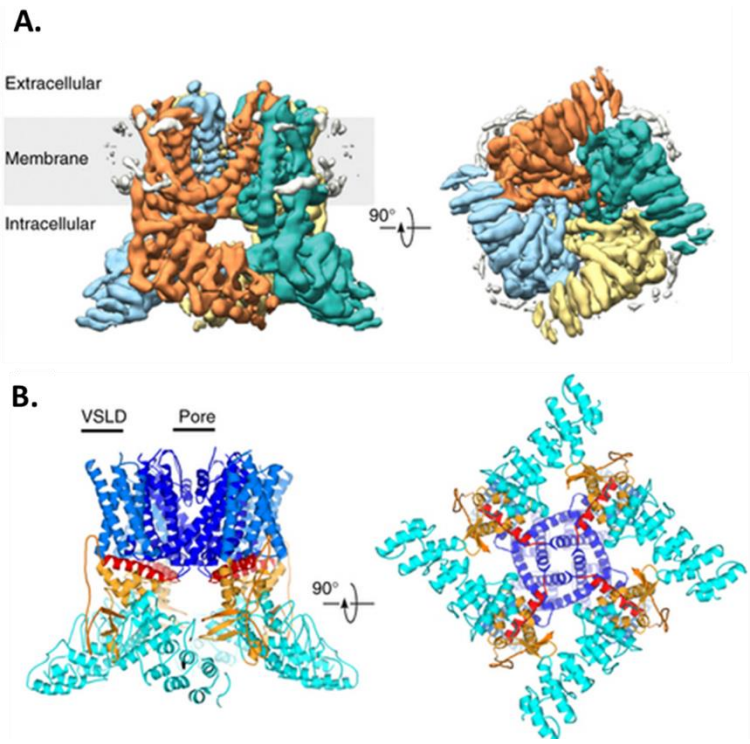

Fig 4: Topological structure of TRPV2. A. Cryo-EM reconstruction, showing the four-fold-symmetric TRPV2 homotetramer. Each promoter is coloured differently. B. The atomic model of TRPV2 built from the EM density, with the domain architecture delineated by different colours. (Image taken from Lejla et al., 2016) [45].

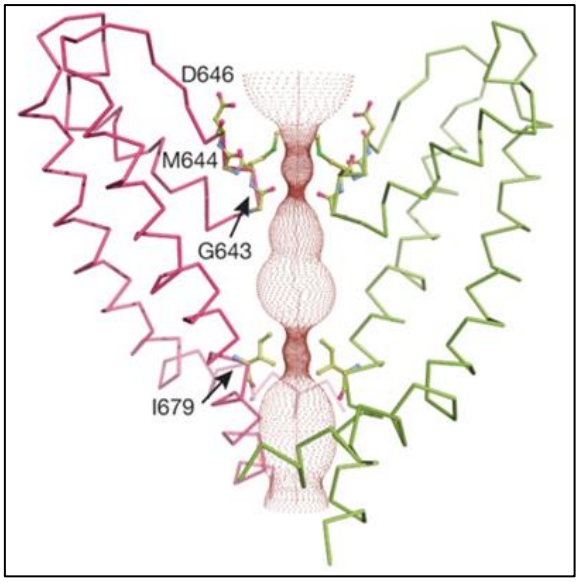

Fig 5: Selectivity filter of TRPV1 ion channel. Representing image shows the selectivity filter of TRPV1 and specific amino acid residue lies in this region which forms a lower gate for passing divalent cations (Image taken from Liao et al., 2013) [44].

Human TRPV4 consists of 871 amino acids (full length), and has five splice variants including TRPV4-A (full length), TRPV4-B (lacking exon 7), TRPV4-C (lacking exon 5), TRPV4-D (short deletion inside exon 2) and TRPV4-E (lacking D237-284 and D384-444 amino acids) [48]. Similar to other TRPVs, TRPV4 has 6 ankyrin (ANK) repeats, 33-amino acid motifs which involved in protein–protein interactions and also helps in tetrameric assembly of TRPV4 channel [36, 49, 50]. Apparently, the C-terminal cytoplasmic region of TRPV4 does not have any specific domain or motifs that can impart some especial structure-function prediction related to TRPV4. However, the C-terminal cytoplasmic domain of TRPV4 contains a conserved TRP-box motif, which is a specific characteristic signature present in many other TRP channels. The C-terminus of TRPV4 also contains a tubulin-binding motif sequence where positively charged amino acids are conserved in several species [51].

At present, no crystallographic or nuclear magnetic resonance (NMR) data is available that can shed light on the fine atomic structure of functional TRPV4. However, recently, structure of Rat TRPV4 was analysed at a resolution of 3.5 nm by cryo-electron

microscopy [52]. This electron microscopic (EM) study was conducted on His-tagged TRPV4 expressed in Baculovirus infected Sf9 cells, solubilized with detergents and further purified by several chromatography columns. As TRPV1 and TRPV4 share a high-degree (~41%) of sequence identity and functional TRPV4 also forms a similar "hanging gondola"-like structure. Cryo-EM structure of TRPV4 shows length 130 Å (from top to bottom) and width 85 Å. Volume analysis (3D construction) of TRPV4 indicated that approximately 30% volume of the functional channel lies in the plasma membrane and 70% of the total volume remains hanging from the plasma membrane (**Fig 6**).

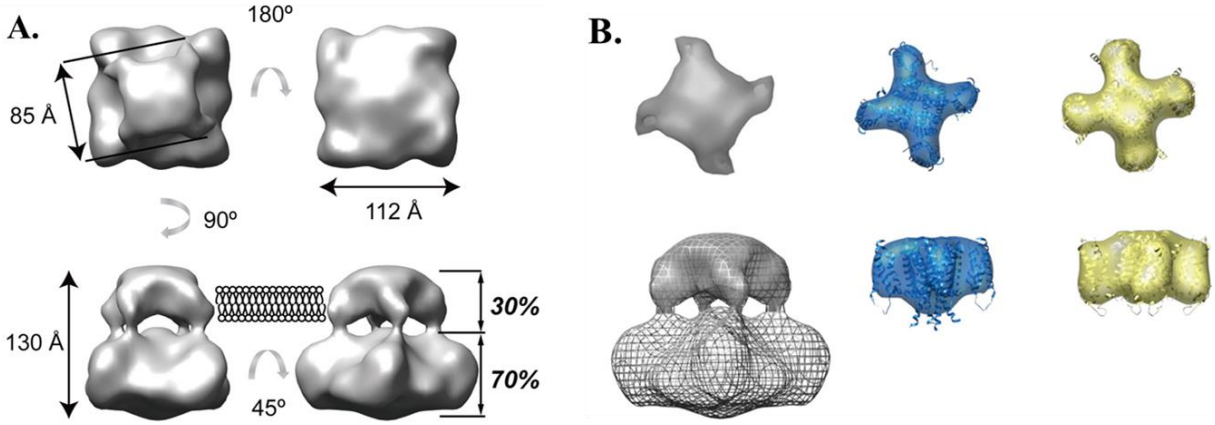

Fig 6: Cryo-EM structure of TRPV4. A. Shown are the surface expressed rTRPV4 and views from four different angles. Dimensions and estimated volume analysis are indicated accordingly. B. Shown are surface view of 6 transmembrane region of tetrameric, TRPV4 (grey), cyclic nucleotide-modulated potassium channel from *Mesorhizobium loti* (MlotiK1, blue) and voltage-gated potassium channel (Kv1.2, yellow). Surface representations were calculated from atomic coordinates that are shown at 3 nm resolution. (Image taken Shigematsu et al., 2010) [52].

1.1.8 Expression, function and distribution of TRPV4

TRPV4 is expressed in a broad range of tissues (neuronal and non-neuronal), including lung, spleen, kidney, testis, fat (Adipose tissue), brain, cochlea, skin, smooth muscle, liver, bone, cartilage and vascular endothelium where it regulates the physiology of these systems [53-58]. TRPV4 not only functions as the "cellular osmosensor", but also act as the "cellular mechanosensor" and is involved in the -transduction of sensory information in

A- and C-fibres (in case of DRG neurons). It is reported that TRPV4 plays an important role in thermoregulation through epidermal keratinocytes [53, 59]. TRPV4 is expressed in osteoblasts and osteoclasts and such expression has been correlated with the bone formation and remodelling functions [60, 61]. In case of chondrocytes, it is shown to regulate the chondrocyte polarity and differentiation and in endochondral ossification [62].

In agreement with its functions, TRPV4 knockout mice exhibit reduced pressure and osmotic sensitivity, altered thermal selection, and hearing loss [63-67]. TRPV4 is abundantly expressed in urothelial cells of renal pelvis, ureters, urinary bladder and urethra and regulates the water permeability in nephron [63, 68]. In respiratory system, TRPV4 is predominantly expressed in cilia of bronchial epithelium and lungs where it regulates ciliary beating frequency and mucociliary transport [69]. Moreover TRPV4 is also present in ciliated epithelia of the bile ducts and the Fallopian tube where it might have an important role in regulation of bile flow and oocyte transport respectively [70, 71]. TRPV4 is expressed in smooth muscle cells lining the pulmonary artery, aorta and cerebral arteries and more abundantly present in vascular endothelium [72-74]. In mouse nervous tissue, TRPV4 is distinctly present in the different regions of brain and its associated tissues such as in cortical astrocytes, sympathetic ganglia, parasympathetic and sympathetic nerves trigeminal neurons, ependymal cells of the lateral ventricles, median preoptic areas, vascular organ of the lamina terminalis and in subfornical organ where it is involved in different sensory functions [56, 57, 75, 76]. In the inner ear, TRPV4 is expressed in multiple sites such as inner hair cells, outer hair cells, spinal ganglion neurons and in the epithelial cells of the stria vascularis. It is also expressed in the apical membrane of the mitochondria-rich epithelial cells in the endolymphatic sac [77, 78]. Recently expression of TRPV4 in T cells has also been demonstrated [79]. TRPV4 seem to play important role in the T cell activation process, possibly by complex Ca^{2+}-signalling events.

1.2. Regulation of TRPV4 by different signalling pathways

1.2.1 Ca^{2+}-based signalling cues

TRPV4 is endogenously expressed in a wide range of tissues and cells where it regulates broad range of function/s and in most cases such involvement is due to its importance in the context of calcium signalling events. Unlike other TRP channels, TRPV4 is involved in the major regulation of Ca^{2+}-signalling by influencing both Ca^{2+}-currents as well as the magnitude of such currents. Typical outward current (OW) rectifying currents are due to a Ca^{2+} block around 0 mV and the magnitudes of inward (IW) currents depend on the extracellular Ca^{2+} concentrations indicating a Ca^{2+}-mediated inhibition. In the absence of extracellular Ca^{2+}, 4αPDD-mediated TRPV4 currents show a weaker OW rectification, and the currents also reverse at less positive potentials [80]. Apart from different Ca^{2+}-selective ion channels, TRPV4 plays a pivotal role in regulating the cellular Ca^{2+}-homeostasis and signalling. Notably, Ca^{2+} is one of the very important ubiquitous intracellular secondary messengers which are involved in many signalling pathways critical for physiological functions. It regulates crucial cellular functions such as fertilization, cell proliferation, apoptosis and cell necrosis. It also regulates functional responses including muscle contraction, cell migration, secretion, metabolic pathways, gene expression and cell differentiation. TRPV4 activation causes reabsorption of bone tissue by increasing the number of osteoclast cells. TRPV4-mediated Ca^{2+}-influx regulates differentiation of osteoclast cells which is critical for bone cell remodelling [81]. TRPV4 mutants, namely R616Q and V620I (Gain-of-function mutants) were introduced in TRPV4 KO mice and TRPV4 (R616Q/V620I) transgenic animals were produced [81]. As expected, in these transgenic lines, higher Ca^{2+}-level is observed in osteoclast cells and results in reduction in bone mass [81]. It was also reported that TRPV4-mediated Ca^{2+}-influx evoked intracellular Ca^{2+}-oscillations, which trigger nuclear factor-activated T cells (NFAT) c1-responsive gene

transcription and that change is critical for osteoclast differentiations [60]. Ca^{2+}-homeostasis in endothelial cells (EC) is still unclear. It was suggested that apart from other transporter (SERCA, NCX) endogenous TRPV4 presents in EC plays important role in Ca^{2+}-dependent endothelial nitric oxide synthase-induction and regulation of Ca^{2+}-homeostasis [74].

1.2.2 Role of different kinases

In addition to various physical and chemical stimuli that activate TRPV4, phosphorylation at various positions also modulated its activity. TRPV4 phosphorylation regulates either its channel activity or trafficking or localization into the membrane. TRPV4 has been proposed to play a key role in the mechanical hyperalgesia which is primarily caused by inflammation or tissue damage. As a downstream effect, several inflammatory molecules are known to be released during tissue damage. These inflammatory molecules include bradykinin, PGE2, 5-HT and histamine which directly sensitize primary afferent neurons, and results in hyperalgesia. These inflammatory molecules indirectly activate downstream signalling molecules which includes protein kinase C (PKC) and cyclic AMP-dependent protein kinase (PKA) [82-84]. It has been reported that transiently expressed TRPV4 in HEK293 cells, after treatment with phorbol 12-myristate 13-acetate (PMA, PKC activator) increases the serine and/or threonine phosphorylation in the N-terminus region (S162, T175 and S189) of TRPV4 and regulates its swelling property against hypotonic solutions. The adenylate cyclase activator forskolin (FSK) induces phosphorylation at the serine residue (S824) located in the C-terminal region of TRPV4 and regulates the activation properties. It has been reported that the phosphorylation (PKC or PKA mediated) rate is significantly increased in presence of scaffolding protein AKAP79 which helps in the assembly of PKC and PKA protein and formed signalling complex with TRPV4. It is still not known whether AKAP79 directly binds with TRPV4 or not, but it is essential for the

recruitment of PKC and PKA which forms signalling complex with TRPV4 at the sub-membranous regions [85, 86]. In arterial myocytes cells, anchoring protein AKAP150 and protein kinase C (PKC) play critical roles in the regulation of TRPV4 channels during angiotensin II (AngII) signalling [87]. Another report suggests that Src family tyrosine kinases (SFKs) induce tyrosine phosphorylation at Tyr253, Tyr110 and Tyr805 of TRPV4. These phosphorylations regulate the TRPV4 channel activity as well [88, 89]. However, the surface expression of TRPV4 is not altered or reduced in case of tyrosine phosphorylation [88].

It was demonstrated that hyperalgesia (a pathophysiological situation where mild sensory cues become painful) activates downstream Protein Kinase A (PKA), Protein Kinase C (PKCε), and Protein Lipase C (PLCβ) pathways and different inflammatory molecules which in turn activate TRPV4 and results in TRPV4-mediated hyperalgesia [90, 91]. Recent study suggests that in case of mechanical hyperalgesia, PKCε, a cytoplasmic kinase is translocated to the mitochondria and phosphorylates several mitochondria proteins [92]. Pull down experiments also indicate that PKCε directly interacts with C-terminus of TRPV4 but how it regulates the channel function is not known [51].

1.2.3 MAP kinase and immune cell associated interleukins

Mitogen-activated protein kinase (MAP kinase) pathway is an important signalling pathway for cellular function which can be modulated by changes in the osmolarity of the surroundings or osmotic stress conditions [93]. TRPV4 is responsible for osmotic alterations and cell volume regulation in cells. Exposure of articular chondrocytes cells, to hypo-osmotic condition induces the expression of TRPV4 and an increase in the phosphorylation of ERK1/2 (MAP kinase). However in hyper-osmotic condition, p38 MAPK phosphorylation increases drastically [94]. It was also observed that inhibitor of MAP kinase significantly

reduces the TRPV4 expression [94]. In tumour endothelial cells, TRPV4 activation reduces ERK1/2 phosphorylation significantly and that correlates with reduced endothelial cell proliferation *in vivo* [95]. TRPV4 is abundantly expressed in trigeminal ganglion (TG) sensory neurons and senses nociceptive stimuli there. It was observed that TRPV4 activation causes massive Ca^{2+}-influx in TG and as downstream signalling events, it activates MEK-ERK MAP kinase signalling pathway [96]. Thus TRPV4 acts as an important candidate relevant in trigeminal nerve associated pain. Therefore, application of TRPV4 antagonist in the TG neuron is a potential pain management strategy which can prevent TG-induced long-term pain such as pain involved in migraine, headaches, temporomandibular joint, facial and dental pain- etc [96].

TRP ion channels are major transduction molecules of nociception. Especially TRPV4 is involved in sensation of noxious mechanical stimuli during the tissue inflammation [97, 98]. The inflammatory molecules such as cytokines and interleukins attenuate thermal hyperalgesia which indirectly regulates the expression and activation of TRPV4 in rat DRG neurons, interleukin 17A (IL-17A, a nocieceptor molecule involved in mechanical stimuli) is expressed in the membrane and it increases the expression of TRPV4 channel. IL-17A-deficient mice exhibited a reduction of mechanical hyperalgesia but not of thermal hyperalgesia, suggesting that IL-17 is particularly involved in mechanical but not in thermal hyperalgesia [99]. TRPV4 is present in the articular chondrocytes where it regulates osmotic stress through Ca^{2+}-homeostasis. In chondrocytes, it regulates the expression of interleukin-1 (IL-1) and prostaglandin E2 (PGE2), especially in response to osmotic stress [100].

1.2.4 Mitochondrial free radicals (ROS & NOS)

It is known that excess of intracellular Ca^{2+} leads to increase in mitochondrial ROS and NOS production. Elevated ROS production due to excessive Ca^{2+}-influx leads to several

neurological disorder and abnormalities in the Ca^{2+} signalling pathway, especially in neuronal tissues [101] **(Fig 7**). TRPV4 activation increases mitochondrial ROS production in coronary endothelial cells (ECs) and induces ROS-dependent vasodilation in coronary arterioles. In coronary ECs, TRPV4 channel-mediated Ca^{2+}-influx inside the cell is mechanistically linked with the flow signal and mitochondrial ROS production [102]. It was speculated that TRPV4 present in plasma membrane are in close juxtaposition with mitochondria in ECs, and this association facilitated by the cytoskeleton, therefore TRPV4-mediated Ca^{2+}-influx may be selectively targeted to mitochondria, leading to subsequent mitochondrial ROS production [102]. However the detailed molecular mechanism behind TRPV4-mediated Ca^{2+}-influx and mitochondrial ROS production remains unclear. TRPV4 activation in ECs increased the production of mitochondrial H_2O_2. It was hypothesized that TPPV4-dependent Ca^{2+}-influx induces mitochondrial H_2O_2 formation and results in vasodilatation in ECs [102].

It has been shown that TRPV4 activation increases intracellular Ca^{2+} in the mouse cortical collecting duct that results in flow-induced nitric oxide (NO) production in kidney [103]. TRPV4-induced NO production is blocked in presence of TRPV4-antagonists, namely ruthenium red and RN1734 and luminal flow do not increase NO production in the absence of extracellular Ca^{2+}. A similar result was also observed in ECs cells where it regulates flow-induced vasodilation in mesenteric artery through TRPV4 mediated NO production [104]. TRPV4 contributed to mechanical allodynia and neuropathic hyperalgesia in neuronal system that is also mediated through NO–cGMP–PKG pathway [105]. TRPV4 induces NO production through the activation of the NF-κB pathway in the DRG neurones but exact molecular mechanisms remain unclear [106].

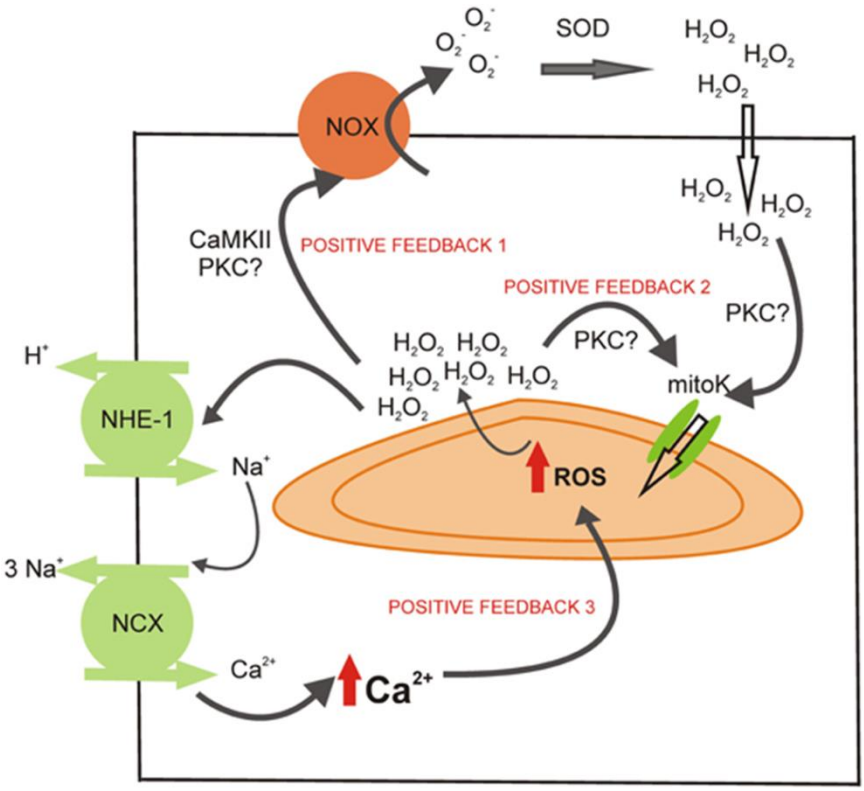

Fig 7: Schematic diagram of Ca^{2+}-mediated free radical production in mitochondria. Represented hypothetical model shows mitochondrial ROS, NOS and H_2O_2 production after excess Ca^{2+}-load. Free radical generated through ROS pathway regulates different PKCs and NOX pathway. (Image taken from Giusti et al., 2013) [107].

1.3. Different activator of TRPV4 channels: Endogenous and Exogenous ligand

1.3.1 Physical stimuli-mediated activation of TRPV4

TRPV4 is a classic example of polymodal channels regulated by diverse physical and chemical stimuli, implicating modes of regulation of TRPV4. Detection of osmotic stimuli or osmosensation is important in all organisms. TRPV4 channel was initially cloned based on its sensitivity to hypo-osmotic cell swelling, suggesting that TRPV4 is a mechanosensitive ion channel [56-58]. Indeed, the mechanosensitive nature of TRPV4 was previously demonstrated in a study where mechanosensory defects observed in osm-9 mutant of *C. elegans* was rescued by human TRPV4 [108]. This experiment suggests that TRPV4 functions as an osmosensitive and mechanosensitive channel involved in sensory functions and the mechanosensory function of TRPV4 is conserved in almost all animals [108]. Indeed,

TRPV4 plays important role in sensing "cell swelling" and "mechanosensation", two important cellular functions relevant in several tissues such as inner ear, sensory neurons, renal tubular epithelial cells, cilia of oviductal epithelial cells and in endothelial cells [56, 109]. In TRPV4-expressing HEK293 cells and M-1 renal collecting duct cells, application of shear stress (or fluid flow) across the apical surface confirmed the mechanosensitive nature of TRPV4 [110, 111]. However mechanical stimulation of TRPV4 is highly sensitive to changes in the temperature which indicates the temperature-induced sensitization to mechanical stimuli [56, 110].

Furthermore it has been reported that TRPV4-deficient animals (*trpv4*$^{-/-}$ mice) reveal defective ability for sensing plasma osmolarity by the sensory circumventricular organs of the hypothalamus, which in turn regulates secretion of antidiuretic hormone (ADH) and therefore controls osmolarity of the extracellular fluid [66, 112]. TRPV4 KO mice have impaired sensation of tail pressure recognized by sensory DRG neurons. TRPV4 KO animals also have impaired regulation of cell volume (especially of aortic endothelial cells) against hypotonic solution, indicating that TRPV4 act as a high threshold mechanoreceptor [64, 113]. TRPV4 KO mice preferred warmer footpad temperatures as compare to WT, indicating that TRPV4 is involved in thermal hyperalgesia [114].

The mechanisms involved in body temperature regulation and sensation are extremely important as it influences different physiological and pathophysiologic functions. Warm-blooded animals have complex abilities to sense different temperatures and respond to changes in surrounding temperatures. The discovery of the temperature sensitive TRP channels (TRPV1-V4, also known as "thermo-TRPs") allowed great advancements on the understanding of the mechanisms involved in thermosensation. The TRPV channels are known to be activated at defined temperature thresholds: TRPV1 at 42°C; TRPV2 at 52°C; TRPV3 at 31°C; and TRPV4 at nearly 27–35°C [8, 115-121]. In case of heat-sensitive

TRPVs channels, changes in the temperature from warm to hot range results in the left-shift of the voltage sensitivity. In contrast, for cold-activated TRPs channels, changes from cool to very cold results in right-shift in the voltage sensitivity and thereby activates these channels. However TRPV4 does not show any voltage sensitivity in patch-clamp studies where the membrane was detached from the cell suggesting that other intracellular factor/s is/are involved in the regulations of temperature dependent regulation of TRPV4 channels [29]. The physiological relevance of TRPV4 in thermosensation is still unclear, however it has been reported that TRPV4 expression in skin keratinocytes can act as a sensor of "warm" temperature [29, 53, 122].

1.3.2 Pharmacological activators and inhibitors of TRPV4

TRPV4 agonist: The potent activator of TRPV4 is a synthetic phorbol ester, 4α-phorbol 12,13-didecanoate (4αPDD) which can activate TRPV4 even at relatively modest concentration (<1 μM) [121]. So far it is the most potent known activator of TRPV4 with an EC50 (Effective concentration at half of the maximum) of 200–400 nM. In addition, 4αPDD is relatively more specific for TRPV4 because it remains neutral to other TRPV family members. It binds to the TM3 and TM4 region of TRPV4 (Leu584 and Trp586) [123]. The 4αPDD is a non-protein kinase C–activating phorphol ester and is not metabolized quickly. TRPV4-currents generated by application of 4αPDD is transient and repetitive applications of this activator results in decreased responses and channel becomes desensitized [80, 124]. In addition to 4α- form of PDD, its 4β-form can activate the TRPV4 channel at almost similar concentration suggesting that both stereoisomers can activate TRPV4 (**Fig 8**).

The classical PKC activator phorbol 12-myristate 13-acetate (PMA), which is structurally similar to 4αPDD, shows 50-fold low potency than 4αPDD in case of TRPV4

activation. This data strongly suggest that 4αPDD binding site is completely different as compared to PMA binding site (phorbol ester/ diacylglycerol-type receptor target) [121].

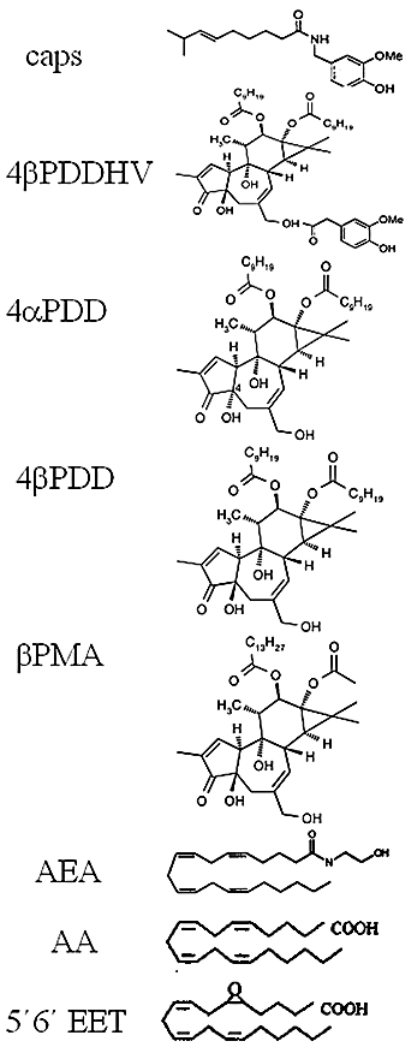

	TRPV1	TRPV4
caps	340nM	none
4βPDDHV	60nM	400nM, cleavage to PDD
4αPDD	none	185 - 400nM
4βPDD	none	340-500nM
βPMA	sensitize PKC	3 μM
AEA	1 – 10 μM	2 μM
AA	none	1.8 μM
5′6′ EET	none	150nM

Fig 8: Comparison of the pharmacology of activation of TRPV1 and TRPV4 by phorbols and endogenous fatty acids. (Image taken from Nilus et al., 2004) [125].

Apart from 4αPDD, TRPV4 can also be activated by different endogenous lipid derivatives and lipid metabolites. Endocannabinoids are endogenous lipids which include amides and esters of long-chain polyunsaturated fatty acids and these compounds generally activate metabotropic cannabinoid receptors (CB1). Recent reports suggest that endocannabinoid anandamide (AEA) and its metabolite arachidonic acid (AA) can cause

significant increase in intracellular Ca^{2+} and increase whole cell currents in TRPV4-expressing HEK cell but not in TRPV4-negative cells [80].

It was also suggested that a nonmetabolizable analogue of AEA (e.g., methanandamide), an inhibitor of fatty acid amidohydrolase, phenylmethylsulfonyl fluoride cannot induce TRPV4 activation. Subsequently it has been shown that synthesis of EET metabolites of AA via the cytochrome P450 epoxygenase pathway (5,6-EET and 8,9-EET) could also activate TRPV4 [113, 126]. Furthermore, activation by endogenous ligands (such as by AA metabolites) appears to be distinct from the 4αPDD-mediated activation because mutation in 4αPDD binding site cannot alter the activation by lipid derivatives [126]. Other studies have shown that the 11,12-EET may similarly activate TRPV4 [72]. Accumulating evidence suggesting that AA pathway and the epoxygenase metabolites play key roles in regulating TRPV4 activity in the endogenous settings.

TRPV4 is also able to sense sun-burn induced pain and is able to sense UV radiation. It has been shown that skin epithelial cells of mice containing TRPV4 can transmit UV-B signal to sensory neurons and is responsible for sunburn-associated pain [127].

TRPV4 antagonist: A major problem of TRPV4 antagonists is their lack of specificity. Three (ruthenium red, gadolinium and La^{3+}) have been classically used to study TRPV4-mediated cationic currents, although none of them is specific, and all three have similar actions on other TRPV channels, i.e. inhibiting inward currents but not outward currents [57, 125]. Citral, a bioactive component of lemon and commonly used as a taste enhancer or an insect repellent, was also found to be a transient antagonist for TRPV4 [128]. This compound modulates several TRPs and can induce versatile responses depending on the nature of the biological systems. Recently, HC-067047 has been reported as a new potent TRPV4 inhibitor that reversibly abolishes TRPV4 activity independent of the stimulus used for activation

[129]. Another set of antagonists, namely RN1747 and RN1734, a pair of structurally related compounds were also discovered which completely inhibit both ligand- and hypotonicity-activated TRPV4 currents and these compounds are widely used as TRPV4-specific antagonist [130]. However it was not known how and where it binds within TRPV4. Their activities against human, rat and mouse TRPV4 were characterized using electrophysiology and intracellular Ca^{2+}-influx [130].

1.4. Subcellular distribution and trafficking of TRPV4-Wt and mutants

In most of the ion channels, the overall activity of channels is controlled by trafficking of channel containing vesicles to the plasma membrane. Generally a pool of ion channels are maintained within intact vesicles within the cytoplasm and these pools are recycled to the plasma membrane whereas other pool may be targeted for degradation [131]. TRP channels present in the membrane are activated and/or regulated by protein kinases, lipid signalling events and or other factors. However, it is not clear whether intracellular localized TRP channels can also be regulated by the same signalling mechanisms or not. Surface expression of TRPV4 is regulated by various factors such as by protein folding, protein tetramerization, post translational modification, Ubiquitin-mediated degradation, lysosomal degradation, etc.

1.4.1 Sub-cellular localization of TRPV4 in different systems

While a number of studies have confirmed the localization of TRP channels in plasma membrane and also in ER, the sub-cellular localization of these ion channels remain poorly established. In particularly, the sub-cellular localization of TRPV4 and its precise localization in intra-cellular compartments have not been characterized. In addition, apart from the ER, so far no sub-cellular organelles have been specifically probed for the presence of TRPV4

either. However, several cell biological and biochemical characterization studies indicate the presence of TRPV4 in ER. For example, TRPV4 has also an N-linked glycosylation motif within the pore-forming loop. In this case, the glycosylation is on the Asparagine residue located at position 651 and glycosylation at this position promotes the retention of TRPV4 in the ER [132]. It has also been demonstrated that interaction of PACSIN 3 (a cytoskeletal protein) to the N-terminal region of TRPV4 enhances the membrane localization [133]. Previously it has been reported that deletion of extreme C-terminal 16 amino acid residues of TRPV4 does not alter the surface expression, as truncated TRPV4 (1–855 aa) can be exported to the membrane and this surface expression is equivalent to that of the wild type TRPV4 (1–871 aa) [134]. However, the same study revealed that the deletion of upstream 16 amino acids at the region of C-terminus of TRPV4 (828–844) results in accumulation of ion channel in the ER. Another report demonstrates that deletion of amino acid residue 132–144 (located at the N-terminal cytoplasmic domain), i.e., deletion of Proline-rich domain (PRD) resulted in loss of channel function despite having proper trafficking at the membrane [135]. As both N- and C-terminal regions seems to be important, the reported self-interaction between N- and C-terminal of TRPV4 mediated by Calmodulin and Ca^{2+} might play an important role here [136].

Within the N-terminus, the ARD regions (amino acid residues 132–383) seem to be important for assembly and maturation of TRPV4 [137, 138]. This conclusion is drawn on the basis of the fact that TRPV4 splice variants namely B-, C- and E-isotypes cannot assemble into functional channel [137]. These isotypes lack regions located at the N-terminal region, are sequestered in endoplasmic reticulum and thus cannot reach to the plasma membrane. In contrast, A- and D-isotypes are transported to the membrane and can form functional channels. Thus cells expressing A- and D-isotypes can responded to TRPV4-specific stimuli [137]. Though all these studies characterized the trafficking of TRPV4 to a large extent, the

understanding of surface expression of TRPV4 and actual regulation/s underlying this is still fragmented.

1.4.2 Surface expression and recycling of TRPV4

Generally, surface expression of TRP channels is an important and complex aspect regulated by multiple factors. Depending on the signalling events, new functional channels are recruited to the plasmamembrane when required [134, 139, 140]. The pre-existing channels are either recycled by endocytosis and exocytosis or internalized and degraded by 26S proteasomal pathway if not required [140]. These regulations are essential and form the basis of channel homeostasis at the plasma membrane. In that context, multi vesicular body (MVB) pathway is important as it regulates the level of surface expression by degrading the internalized transmembrane proteins at lysosome [141]. Surface expression of transmembrane proteins can also be regulated by Ubiquitin, a 76 amino acid long chain that serves as a degradation signal in Ubiquitin-mediated Proteasomal degradation pathway [142]. However, recent studies demonstrated that Ubiquitin can also be used as a sorting signal for MVB pathway for intracellular pool of TRPV4 [143-145]. These internalized TRPV4 containing vesicles efficiently recycles to the plasma membrane. However, it has been observed that in spite of being tagged with Ubiquitin, some of the TRPV4 do not get degraded, but become accumulated beneath plasma membrane [139]. Thus, AIP4 seems to plays a role which is not only relevant in the context of Ubiquitination of the TRPV4 but also can direct the TRPV4 under regulation by MVB pathway. As AIP4 binds to the N-terminal region of the TRPV4, mutations in this region can lead to altered Ubiquitination [139]. This altered Ubiquitination might affect the surface expression of TRPV4 and that may altered its cellular function.

TRPV4-R269H mutant mostly accumulated in the cytoplasm, indicating that amino acid R269 located at the 3rd ARD is important for the surface expression, at least in case of

HeLa cells [146]. However, using a different cellular system, namely HEK cell, another group has reported that the same TRPV4-R269H mutant has proper cell surface expression [147]. A similar study revealed that a different mutation at the same position, i.e., TRPV4-R269C does not have an altered surface expression in HeLa cells [146]. In contrast, R316C mutant reveals a loss of function (compared to the wild type) when expressed in HeLa cells while the same mutation reveals a gain of function in HEK cells [147].

Sequence analysis of TRPV4 also revealed differential distribution of the wild type and mutant TRPV4. Both carboxyl-terminal dilysine KKXX motif which interacts with coat protein I (CopI complex) and the internally positioned RXR motif regulate the retention of any protein within endoplasmic reticulum [148]. Apparently, TRPV4 polypeptide contains four RXR motifs, two on the N-terminal region (122RWR and 269RGR) and two at the C-terminal (816RLR and 819RDR) cytoplasmic domain. Interestingly, different mutations at R269 position (R269C and R269H) can destroy the function of one RXR motif located at the N-terminal domain and thus regulate the surface expression significantly.

1.5. Regulation of TRPV4 by interacting proteins and lipids

TRPV4 is involved in diverse cellular functions and its N- and C-terminal domains face towards the cytoplasmic region. Therefore these domains interact with diverse type of proteins and regulate channel functions. Since TRPV4 is physically present in lipid bilayer; therefor it is also regulated by various membrane components such as cholesterol, lipid and its derivatives, as well as by other transmembrane proteins including other ion channels.

1.5. 1 TRPV4 interacting proteins and its regulations

a. MAP7: The cell shape or morphology is regulated by microfilament and microtubules and their associated proteins. The C-terminus of TRPV4 has been reported to interact with tubulin

and actin cytoskeleton and such interactions are involved in regulation of microtubule dynamics and intracellular signalling [51]. Recent study also suggested that microtubule associated protein7 (MAP7) functionally interacts with the C-terminus of TRPV4 (785-808 aa), a region which is next to the CaM-binding domain and enhances its surface expression [149].

This finding for the first time describes the characteristics of this channel in relation to the cytoskeleton. It was reported that MAP7 enhances the channels' expression in cellular plasma membranes and therefore enhances the response against TRPV4-specific stimuli. Membrane localization of TRPV4 significantly decreased in cell lines that do not express MAP7. It was reported that osmotic activation of TRPV4 with MAP7 requires both actin microfilaments as well as microtubules as pharmacological modification of actin and microtubule dynamics (by Phalloidin, Cytochalasin-B and Taxol) can alter the TRPV4-induced currents [149]. It was speculated that MAP7 is important in the regulation of the osmotic stimuli to the channel.

b. PACSIN3: PACSIN3 is a cytoplasmic adaptor protein that belongs to Fes-Cip4 homology-Bin-Amphiphysin-Rvs (FBAR) protein superfamily [150]. Members of this superfamily participate in many cellular processes such as endocytosis, regulation of cell morphology, motility, neurotransmission or connecting cell membrane with submembranous cytoskeleton [151]. It was found that PACSIN3 could modulate TRPV4 function by a direct binding. All three members, namely PACSIN1-3 were able to bind to TRPV4, but only PACSIN3 regulated its activity and cellular localization [152]. While TRPV4 membrane expression is enhanced in the presence of PACSIN3, the channels' activity is widely reduced. Coimmunoprecipitation studies demonstrated that PACSIN3 binds to the N-terminal proline-rich domain (PRD) of the channel via its SH3 domain [152]. A similar regulation has been

demonstrated between PACSIN3 and glucose transporter GLUT1 where PACSIN3 enhances the expression of the transporter in the membrane [153].

c. OS-9: OS-9 is a ubiquitous protein found in the cytoplasmic site of the ER that plays a role in selecting substrates for degradation. It interacts with the N-terminal tail of TRPV4 (amino acids 438- 468) and reduces the amount of TRPV4 expression in the membrane. It preferably binds to TRPV4 monomers and it is thought to prevent the channel polyubiquitination. This would hold and protect monomers in the ER against premature Proteasomal degradation. OS-9 would act as an auxiliary protein not only for TRPV4 but also for TRPV1 maturation. OS-9 can rescue the adverse effects of TRPV4 overexpression during zebrafish development [154].

d. Aquaporins: Aquaporins (AQP) are proteins embedded in the cell membrane that regulate water flow. These are essential players in water regulation. Considering the role of TRPV4 in maintenance of cellular osmoregulation, it is in full agreement that TRPV4 and Aquaporins interact, both at the physical as well as functional level. Indeed, at least two Aquaporins; namely AQP4 and AQP5 functionally interact with TRPV4. It is reported that reduction in AQP5 membrane protein depends on the expression and activity of TRPV4 [155]. This reduction was counterbalanced by inhibiting TRPV4 activity by ruthenium red. In contrast, hypotonicity increased the surface expression of both AQP5 and TRPV4. Notably, AQP5 is required for activating TRPV4 by hypotonicity rather than cell swelling *per se* [156]. It is not clear whether these differences could be due to different cell models, but these findings point to a functional complex formed by AQP5 and TRPV4 in the context of cell volume homeostasis. In astrocytes also this functional complex is composed of TRPV4 and AQP4. Co-immunoprecipitation assays demonstrated direct binding between these and presence of both proteins are important for the cell volume homeostasis. Silencing of either TRPV4 or

AQP4 inhibited regulatory volume decrease (RVD) and altered cell volume homeostasis in astrocytes [157].

e. Actin and tubulin: TRPV4 interacts directly with actin and tubulin [51, 149, 158]. It was observed that the interaction between the channel and F-actin was essential for the maintenance of the cell volume homeostasis and that when actin was destabilized with Latrunculin; TRPV4 is no longer capable of responding to cell swelling [159]. It was suggested that actin microfilaments interacting with TRPV4 can act as the mechanotransducers rendering TRPV4 as a mechanosensitive ion channels [160]. For tubulin, competition was observed between actin and tubulin binding, and TRPV4 was able to modulate cytoskeleton functions [51]. Like TRPV1, TRPV4 activation also regulates both actin and tubulin cytoskeleton and regulates cell morphology [51, 161]. The exact site where tubulin or actin interacts with TRPV4 is not elucidated, but it seems that the C-terminal region is sufficient for these two interactions and both tubulin and actin competes for the same binding sites [51]. Stabilization of microtubules by Taxol(R) also results in altered desensitization of TRPV4 and reduced influx of Ca^{2+} within cells [51].

f. Caveolin-1: Caveolin-1 is a scaffolding protein present in lipid rafts. It clusters lipids and signalling molecules within the caveolae and may regulate the activity of the proteins found in these structures. TRPV4 is also found in lipid rafts and interacts with caveolin-1 [162-164]. Caveolin-1 KO mice results in reduced TRPV4 activity, showing that importance of the TRPV4 clusters in endothelial cells. This interaction may help to explain the role of TRPV4 in vasodilatation or in the endothelium-derived hyperpolarizing factor-mediated relaxation [163].

g. β-catenin and E-cadherin: Tight junctions (TJ) and adherens junctions (AJ) have been proven to be essential in the preservation of the skin barrier function. Cell-cell junctions in keratinocytes depend on the interaction of TJ and AJ with the actin cytoskeleton. Notably, β-catenin and E-cadherin are the major components of the TJ and a recent report shows that both interact with TRPV4 [165]. This interaction plays an important role in maintaining the integrity of the skin barrier. TRPV3, also a TRP present in keratinocytes did not show interaction with β-catenin or E-cadherin. The first segment of the N-terminal tail until the beginning of the ankyrin repeats of TRPV4 is enough to retain this interaction [165].

1.5.2 Regulation of TRPV4 by cytoskeletal and scaffold proteins

TRPV4 forms supramolecular complexes with cytoskeletal proteins and regulatory kinases, which potentially regulates various cellular signalling pathways [51]. TRPV4 and actin association was first revealed in live cell using Time- and space-correlated single photon counting (TSCSPC) using different cellular systems [160]. Later, colocalization of TRPV4 and actin was also observed in highly dynamic membrane structures, such as microvilli, filopodia and lamellipodia of different cellular systems [51, 159]. It was observed that TRPV4 and actin interaction decreases significantly in presence of actin-destabilizing reagent Latrunculin A [159]. TRPV4 C-terminus is sufficient to interact with actin and tubulin. More specifically, phosphorylation of TRPV4 by serum glucocorticoid-induced protein kinase1 (SGK1) on the Ser 824 residue is required for its interaction with F-actin [166].

1.5.3 Regulation of TRPV4 by another receptors and ion channels

Functional complex formation between TRPV4 and the angiotensin receptor (AT1aR) and the ligase adaptor β-arrestin has recently been described in vascular smooth muscle cells

[167]. Notably, β-arrestin controls internalization of the G protein-coupled receptors and therefore controls their activity [168]. This indicates the existence of a trimeric protein complex formed by G protein-coupled angiotensin receptor, β-arrestin and TRPV4. Upon angiotensin stimulation, β-arrestin leads to an Ubiquitination and further internalization of TRPV4. Detail molecular analysis revealed that β-arrestin acts as an adaptor between the already described AIP4 and TRPV4 leading to the channel Ubiquitination. This process is dependent on the presence of β-arrestin and on the angiotensin stimulation. With no stimulation, β-arrestin does not bind the channel and there is no internalization. With no β-arrestin, AIP4 does not internalize TRPV4 [167]. Angiotensin-mediated signalling pathways are critical in vasoconstriction regulation or other vascular effects and TRPV4 also appears to influence vascular tone [113, 169, 170].

Among TRPV family ion channels, homo-oligomeric tetramers are preferentially selected during channel assembly. Experimental observations suggest that trans-membrane domain, as well as N- and C- terminal regions of TRPV channel plays critical role in channel homo- or hetero-tetramerization [171]. TRPV4 interacts with TRPP2 channel physically and functionally and this heteromeric complex regulates thermosensor property *in vivo* [172]. TRPV4 also forms heteromeric complex with TRPC1 and this complex may mediate flow-induced Ca^{2+}-influx in vascular endothelial cells [173]. Moreover some reports suggest the formation of heteromeric TRP channels by more than two types of TRP channels. For example formation of a heteromeric TRPV4-TRPC1-TRPP2 complex in primary cultured rat mesenteric artery endothelial cells (MAECs) and HEK293 cells shows that this heteromeric complex has much diversity of function and structural features [174].

1.5.4 Regulation of TRPV4 by vesicular proteins

So far few reports have confirmed that TRPV4 interacts with different vesicular proteins and such interactions have importance in the context of physiological functions. For example, blood flow through vascular endothelium exerts shear stress on walls of blood vessels. Shear stress alters localization of TRPV4 in these cells and also induces its activation. This sensitization of TRPV4 in vascular endothelial cells was attributed to the transport of intracellular pools of TRPV4 to the plasma membrane via Dynamin- and Clathrin-mediated exocytosis (**Fig 9**). This translocation involved key proteins like Integrins, ILK, Akt and involves release of Ca^{2+} from intracellular stores as well as phosphorylation of TRPV4 at Tyrosine 110 residue [175]. In HeLa cells, TRPV4 has been found to colocalize with a t-SNARE protein, namely with Syntaxin 4 that is present at the plasma membrane [139].

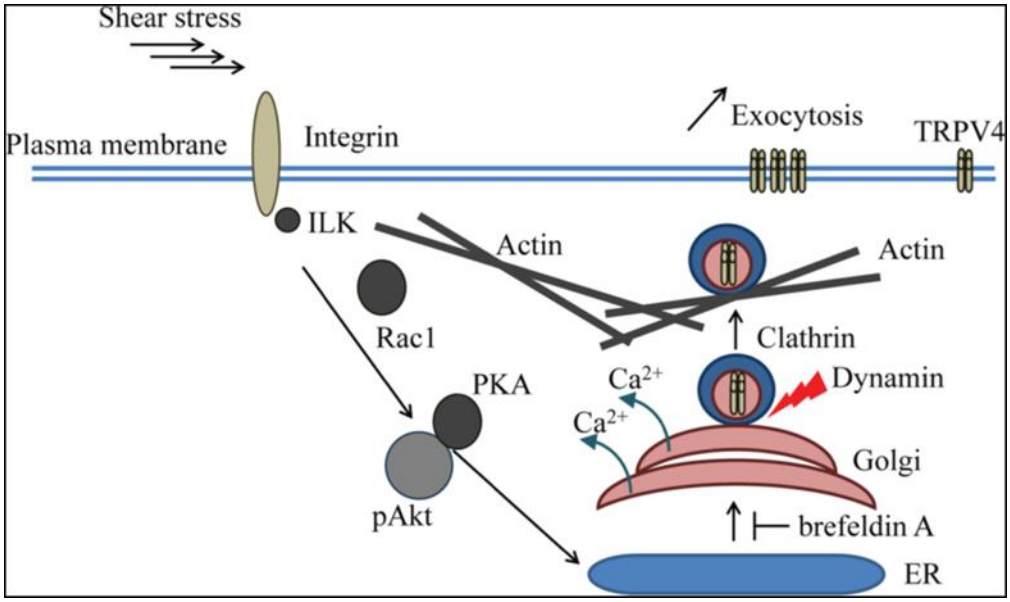

Fig 9: Integrins play role in the surface expression of TRPV4. Integrins localized on plasma membrane sense increase in shear stress and this in turn causes the release of TRPV4 ion channel from intracellular organelles to the plasma membrane via clathrin-coated vesicles and this translocation is dependent upon the presence of an intact actin cytoskeleton as well as on the release of calcium from intracellular stores. (Image taken from Baratchi et al., 2015) [175].

1.6 Importance of TRPV4 in human physiology and TRPV4 mediated channelopathies

Though initially thought to be expressed in peripheral neurons only, later reports confirmed that TRPV4 is expressed in almost all tissue. Also, in comparison to other TRP channels, TRPV4 represents one of the few TRP channels which are characterized extensively in the context of several physiological conditions. Initially TRPV4 channels was identified in several osmo- and mechanosensory cells such as inner-ear hair cells, sensory neurons, and Merkel cells, etc. where its expression was correlated with the osmosensory function of this cells. [56]. However, later on, based on their presence in different tissues and cells diverse cellular function of TRPV4 was elucidated (**Fig 10**). In agreement with that, mutations in TRPV4 results in several developmental disorders. Notably, most of these mutations are deleterious but not always lethal or embryonic lethal and in some cases even transmit too in few generations. In the following sections, some of these functions and its importance in diseases are described in details.

1.6.1 TRPV4 mutants and genetic disorders

During the course of evolution TRPV4 remained conserved in all vertebrates, yet in human population a large number of mutations have been reported that cause malfunctions [177, 178]. In most cases, these mutations in TRPV4 results in either "gain-of-functions" number of diseases and pathophysiology, commonly known as "TRPV4-induced channelopathies" (**Table 1**). Recently, a few naturally occurring TRPV4 mutants have been identified. Interestingly, most of these missense and nonsense point mutations are linked with the development of genetic disorders in human and a detailed list of naturally occurring TRPV4 mutations and related disease is documented (**Table 1**). Here we briefly discuss some of these mutations gained importance in terms of genetic disease.

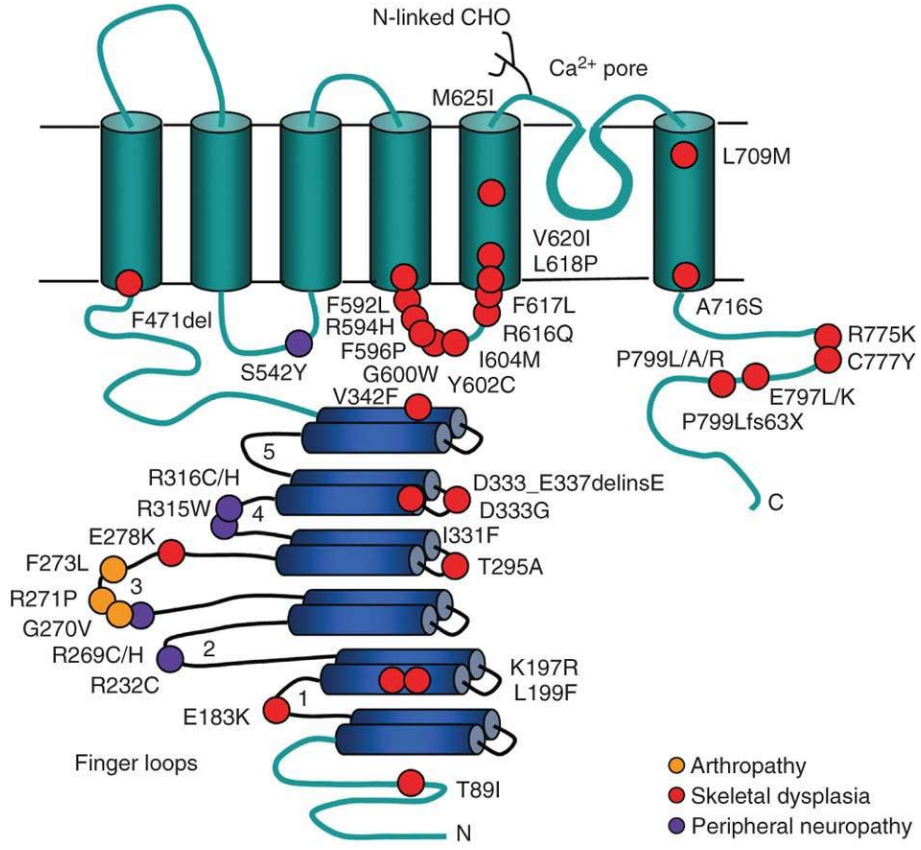

Fig 10: Schematic diagram of the natural occurring hTRPV4 mutations. Representing TRPV4 image shows six transmembrane domains, a pore loop region between the 5th and 6th transmembrane region, intracellular N- and C-terminal domains. Six ankyrin repeat domains are present on the N-terminal domains. Several naturally occurring mutants have been reported for TRPV4 which are associated with various pathological conditions (Image taken from Lamande et. al, 2011) [176].

a. Brachyolmia: Using a linkage analysis and candidate gene sequencing, it was reported that some patients affected with brachylomia have missense mutation in TRPV4, specifically at position R616Q or V620I respectively [179]. These mutations are located at the loop region connecting 4th and 5th TM as well as in the 5th-TM region which forms the functional pore. Each of these two mutations increases basal level of Ca^{2+} as compared to the TRPV4-Wt. Also the response against 4αPDD (TRPV4-specific agonist) is more in these mutants when compared to the TRPV4-Wt. This result also indicates that these two mutations preferably stabilize TRPV4 in its "open stage" resulting in constitutive activity of the channel.

b. Spinal muscular atrophy (SMA): SMA is a heterogeneous disorder of peripheral nervous system. Patients with SMA have been reported to have single missense mutations in different positions in TRPV4, such as at the position R316C, R269H and R315W [146]. These mutations are primarily located at the ARD of TRPV4. These mutants (R316C, R269H and R315W) reveal "loss-of-function" when challenged by hypo-osmotic solution and 4αPDD [146].

c. Hereditary motor and sensory neuropathy type 2 (HMSN2C): Charcot Marie Tooth disease type 2C (CMT2C) and Scapuloperoneal Spinal Muscular Atrophy (SPSMA) are also known as HMSN2C. SPSMA patients are characterized by weakness of scapular muscle and bone abnormalities. CMT2C leads to weakness of distal limbs, vocal cords and often impairs hearing and vision. Genetic analyses of these patients have shown the presence of missense mutations at the TRPV4, especially at the R269H, R315W and R316C positions [146].

d. Spondylometaphyseal dysplasias (SMDK) and metatropic dysplasia:

SMDK is an autosomal dominant dysplasia. Genetic mapping of the patients affected with this disease have shown the presence of missense mutation in TRPV4, either at R594H, D333G or at A716S [180]. Any of these mutations seems to alter the basal level activity. In addition, I331F and P799L mutations are known to induce metatropic dysplasia (**Represented in Table 1**) [180].

Table1: List of naturally occurring TRPV4 mutations and disease (Verma et al., 2010) [177]

	Mutation	Residue	Change in charge	Domain/ motif effected	Effects on ion conductivity	Genetic disorder
1	-	P19S	Nonpolar to polar	N-terminal	Less conductivity	Hyponatermia
2	C366T (exon 2)	T89I	Polar (uncharged) to nonpolar	N-terminal	Not done	Metatropic dysplasia
3	G547A (exon 3)	E183K	Negative to plus	ARD1	Not done	SEDM-PM2
4	A590G (exon 4)	K197R	Plus to plus	ARD2	Not done	Metatropic dysplasia
5	-	L199F	Nonpolar to aromatic	ARD2	Not done	Metatropic dysplasia
6	G806A (exon 5)	R269H	Plus to plus	ARD3	Less conductivity	SMA
7	G806A (exon 5)	R269H	Plus to plus	ARD3	More conductivity	CMT2C, SPSMA
8	G806A (exon 5)	R269H	Plus to plus	ARD3	More conductivity	CMT2C
9	G806A (exon 5	R269C	Plus to polar un charged	ARD3	More conductivity	CMT2C
10	-	E278K	Negative to plus	ARD3	Not done	SMDK
11	-	T295A	Polar (uncharged) to nonpolar	ARD4	Not done	Metatropic dysplasia
12	C 943T (exon 6)	R315W	Plus to aromatic	ARD4	Less conductivity	HMSN2C
13	C946T (exon 6)	R316C	Plus to polar (uncharged)	ARD4	Less conductivity	HMSN2C
14	A1080T (exon 6)	I331F	Nonpolar to aromatic	ARD5	Not done	Metatropic dysplasia
15	-	I331T	Nonpolar to polar (uncharged)	ARD5	Not done	Metatropic dysplasia
16	A992G (exon 6)	D333G	Negative to nonploar	ARD4	More conductivity	SMDK
17	-	V342F	Nonpolar to aromatic	ARD5	Not done	Metatropic dysplasia
18	-	F592L	Aromatic to nonpolar	TM4	Not done	Metatropic dysplasia
19	G1781A (exon 11)	R594H	Plus to plus	TM4	More conductivity	SMDK
20	A1805G (exon 11)	Y602C	Aromatic to polar	TM4-TM5	Not done	SEDM-PM2
21	C1812G (exon 11)	I604M	Nonpolar to nonpolar	TM4-TM5	Not done	Metatropic dysplasia
22	G1847A (exon 12)	R616Q	Plus to polar uncharged	TM5, pore region	More conductivity	Brachylomia
23	C 1851A (exon 12)	F617L	Aromatic to nonpolar	TM5, pore region	Not done	Metatropic dysplasia
24	T1853C (exon 12)	L618Q	Nonpolar to polar (uncharged)	TM5, pore region	Not done	Metatropic dysplasia
25	G858A (exon 12)	V620I	Nonpolar to nonpolar	TM5, pore region	More conductivity	Brachylomia
26	-	M625I	Nonpolar to nonpolar	TM5, pore region	Not done	SMDK
27	-	L709M	Nonpolar to nonpolar	TM5, pore region	Not done	SMDK
28	C2146T (exon 13)	A716S	Nonpolar to polar	Cytoplasmic side of TM6	Same as wild type	SMDK
29	-	R775K	Plus to plus	C-terminal region	Not done	Metatropic dysplasia
30	-	C777Y	Polar (uncharged) to aromatic	C-terminal region	Not done	SMDK
31	-	E797K	Negative to plus	C-terminal region	Not done	SEDM-PM2
32	-	P799R	Nonpolar to plus	C-terminal region	Not done	Metatropic dysplasia
33	-	P799S	Nonpolar to polar (uncharged)	C-terminal region	Not done	Metatropic dysplasia
34		P799A	Nonpolar to nonpolar	C-terminal region	Not done	Metatropic dysplasia
35	C2396T (exon 15)	P799L	Nonpolar to nonpolar	C-terminal	Not done	SMDK

As all these above mentioned mutants are naturally occurring, these mutants are not embryonically lethal (as most lethal mutants will be naturally excluded from the population). It is also important to note that none of these mutants show complete loss of their prime function, i.e., the ionic conductivity. Indeed, experimental results suggest that some of these mutants even have enhanced channel opening [179]. As most of the patients are heterozygous, it can be concluded that it is not only the ionic conductivity of the TRPV4 *per se*, but also the signalling events which is relevant with the development of pathophysiology. This is in agreement with the observation that TRPV4-KO animals do not reveal embryonic lethality but develop some pathophysiological disorders like hearing loss, impaired pressure sensation, reduced osmoregulation, defective bladder function and impaired release of antidiuretic hormone [63-66, 112].

1.6.2 Role of TRPV4 in the male and female reproductive tract

In the female oviducts cilia movements are necessary to ensure a correct transport of gametes [181]. As in the airways, TRPV4 is involved in the response to mechanical changes in the environment, which in turn control ciliary beat frequency (CBF). In hamster oviduct ciliated cells express functional TRPV4, which can be activated by its activator and it regulates the CBF through phospholipase A-dependent pathway [109]. Moreover TRPV4 expression is regulated by progesterone in mammary gland epithelial cells and also in airway epithelial cells, indicating that TRPV4 activity could be regulated by the female hormone cycle [182]. It has been also reported that TRPV4 is expressed at RNA level in rat testis but their functional role in spermatozoa maturation and other function was not characterized [183]. In addition, if TRPV4 is physically and functionally present in spermatozoa of other species has not been characterized.

1.6.3 TRPV4 in the airway epithelium

TRPV4 is present in airway epithelium to play a fundamental role in controlling the ciliary beat frequency (CBF). It has been suggested that activation of TRPV4 with agonist increases the calcium level in nasal epithelial cells and also regulates its CBF [184]. Cilia movement in airway epithelia is essential to maintain mucus clearance and provide a first line of defence against allergens or pathogens [185]. In this context, TRPV4-KO mice show significant reduction in CBF and display a reduction in Ca^{2+}-entry in ciliated cells [69]. In human, respiratory epithelia makes a protective barrier and clears diesel exhaust particles (DEP). It was reported that DEP in respiratory epithelia activates TRPV4 through proteinase-activated receptor-2 (PAR-2) and leads to massive influx of Ca^{2+} which leads to activation of human respiratory disease-enhancing matrix metalloproteinase-1 (MMP-1) [186]. Therefore pharmacological inhibition of TRPV4 opens possibilities for "targeted therapies" against human airway borne diseases.

1.6.4 TRPV4 in the vascular endothelium

Many TRPs channels are reported to be present in vascular endothelium but TRPV4 seem to be critically important for its key functions. Due to blood flow, vascular endothelium has to adapt to changes in shear-stress in order to maintain normal blood pressure and flow [187-189]. The "mechanical stress" generated during blood flow activates TRPV4 channel and also causes production of NO and results in vasodilation of blood vessels [163]. TRPV activation elevates the basal levels of Ca^{2+} which leads to hyperpolarization of endothelial cells [72, 190]. TRPV4-KO mice showed no shear-stress-induced vasodilatation, proving that Ca^{2+}- influx through TRPV4 contributes to endothelial mechanotransduction [188, 191]. In another case, it was reported that angiogenesis in cerebral hemisphere increased due shear-stress activation of TRPV4 [192]. This is mainly due to the fact that small capillaries are

anchored to the extracellular matrix and shear-stress increased the expression of TRPV4 in the membrane that induces collateral vessel growth [193]. Apart from controlling blood pressure and flow, other important endothelium functions such as transportation of liquids and solutes across the vascular endothelial barrier are also regulated by TRPV4. Damage or inflammation of the endothelium can lead to increased endothelial permeability or severe lung injury due to alveolar flooding [194].

1.6.5 Role of TRPV4 in stem cells

Ca^{2+} is a ubiquitous intracellular signal responsible for controlling numerous cellular processes such as cell differentiation, proliferation, and apoptosis. Recent evidence suggests that different Ca^{2+} signalling is related to cell proliferation and differentiation, critical functions that are important and relevant for stem cells [195, 196]. Human pluripotent stem cell-derived cardiomyocytes (hPSC-CMs) in culture are randomly organized and do not have typical directionality or axial alignment. It has been reported that activation of TRPV4 elicits changes in cytosolic Ca^{2+} and helps in natural directional alignment of cardiomyocytes cells. This effect (directional alignment) was abolished in presence of TRPV4 antagonist RN1734 and HC067047 [197]. It was proposed that TRPV4-mediated increase in Ca^{2+} results in phosphorylation of AKT which in turn helps in realignment of the cardiomyocytes cells [197].

Another report also suggests that TRPV4-mediated Ca^{2+}-signalling helps in differentiation of endothelial progenitor cells (EPCs) [198]. EPCs circulated into the blood to replace damaged endothelial cells and recapitulate the vascular network of injured tissues [198]. It was observed that circulating EPCs contain functional TRPV4 channel and TRPV4 activation helps in repair or replacement of new endothelial cells [198].

1.6.6 TRPV4 in the skin

In case of skin tissue, TRPV4 has been identified in Merkel cells and in the keratinocytes [165, 199]. Merkel cells (MCs) are associated with nerve terminals and forms MC-neurite complexes. However recent report suggests that TRPV3 is important for sensing warm temperature in keratinocytes cells [200]. TRPV4 is essential for the formation of cell-cell junctions and provides a hydrophobic barrier in the skin which is essential for protection. TRPV4-deficient mice reveal impaired intracellular junction dependent barrier function and TRPV4 is important for the homeostasis of the skin permeability barrier [165, 201].

1.6.7 TRPV4 and bone regulation

TRPV4 plays a crucial role in the skeletal system, where it is expressed in several tissues, such as cartilage and bone. Bones constantly undergo remodelling process to adapt to environmental stress. Shear or mechanical stress is an important stimulus for bone remodelling and is achieved by a balance between osteoclasts and osteoblasts where intracellular and extracellular Ca^{2+}-balance is crucial and tightly regulated. Interestingly, TRPV4 present in both osteoblast and osteoclast cells and precisely regulates the bone mass [61, 81]. The major role of osteoclasts is bone reabsorption, and their differentiations as well as maturations are dependent on the nuclear factor-activated T cells (NFAT) which translocate to nucleus. It was reported that TRPV4-mediated Ca^{2+}-influx causes translocation of NFAT in the nucleus where it activates osteoclast specific gene transcription [202]. Consequently TRPV4-KO mice show an impaired osteoclast function and an increased trabecular bone volume [60]. TRPV4-Wt mice induced with mechanical hind limb unloading present an increased rate of bone absorption and a higher number of osteoclasts. This bone remodelling was suppressed in TRPV4-KO mice that reveal bone thickening due to deficiencies in osteoclast differentiation [61].

1.6.8 TRPV4 in kidney and bladder

TRPV4 is widely expressed in different tissues but its expression is very high especially in kidney [56-58]. The kidney converts daily ~150 L of glomerular filtrate into ~1 L of urine by water reabsorption in the renal tubule. Water permeates and moves freely from the tubule lumen in the descending thin limb of the "Loop-of-Henle". This filtration is due to the hyperosmotic environment in the interstitium. The cells lining of the descending limb of kidney are freely permeable for water, and the filtrate becomes progressively more concentrated as water travelled to ascending limb of kidney. Interestingly, expression of TRPV4 is completely absent along the early parts of the kidney tubule (ascending limb) where passive water reabsorption takes place; however, it has been observed that in descending limb and distal nephron, the expression of TRPV4 is predominantly higher. In kidney, TRPV4 is able to sense changes in osmolarity in the medullary interstitium. Such functions are important for variety of physiological states and pathophysiological conditions, including even simple changes in urine flow rate. Few groups have described the functions of TRPV4 in presence of different drugs or antibiotics in *in vivo* conditions. For example, aminoglycoside antibiotics (Such as Kanamycin, an antibiotics widely prescribed in many medical cases) decreases renal expression of TRPV4 [203]. However, this effect is profoundly decreased in presence of antioxidant dihydroxybenzoate which can rescue the expression of TRPV4 [203].

1.7 AIMS OF THE PRESENT STUDY

In last few decades, TRP channels have been investigated extensively. Such studies have unravelled the localization of TRPV ion channels in the plasma membrane and also partly characterized their functions within certain subcellular organelles [204]. For example, TRPV1 and TRPV3 are physically and functionally present in ER and regulate its functions [205-206]. Similarly, surface expression and localization of TRPV4 depends on several key factors such as correct folding within ER, glycosylation, tetramer assembly, recycling and proteasomal degradation [132, 177]. Apart from membrane localization, subcellular localization of TRPV4 in nucleus and ER was also reported recently, though no functional significance was attributed in these cases [207, 208]. The surface expression of TRPV4 is largely reduced in case of its point mutations and different TRPV4-mutants localize in the cytoplasm as relatively big spots [146]. However, the exact identity and characterizations of these intracellular structures has not been done yet. Genetic analysis suggests that independent point mutations in either Mfn2 or TRPV4 results in development of same patho-physiological disorder, namely Charcot Marie Tooth (CMT) disease [209], though these two genes are located on two different chromosomes. TRPV4 is located on Chr 12 while Mfn2 is on Chr 1. Based on the literature describing genetic interaction with TRPV4 and regulation of biochemical pathway/s by TRPV4 the presence of TRPV4 in mitochondria can be speculated. However, so far no systematic studies have been conducted to explore whether TRPV4 is physically present in the mitochondria and regulates mitochondrial function/s. This thesis work explored TRPV4 in the context of mitochondrial localization and functional regulation. This work demonstrates that TRPV4 not only localizes into mitochondria but also regulates its critical functions in different manner. This work confirms that TRPV4 is endogenously present in the mitochondria of different cellular systems. *In vivo*, *in vitro* and *in silico* results

indicate that mitochondrial localization and its functional regulation by TRPV4 are common aspects in many cellular systems from vertebrate origin.

Major objectives:

1. Localization of TRPV4 in various intracellular organelles.

2. Exploring if TRPV4 interacts with mitochondria and with different mitochondrial proteins.

3. Regulation of mitochondrial morphology, Ca^{2+}-homeostasis, potentiality, metabolism and other functional parameters by TRPV4.

4. Characterization of the Mitochondrial Targeting Signal (MTS) present in TRPV4.

5. Characterization of TRPV4 in sperm cells and its functional association with mitochondria.

Chapter 2

Results

2.1. Characterization of TRPV4 in intracellular organelles

Most of the TRP ion channels are primarily located at the cell membrane in neuronal and non-neuronal tissue and regulate diverse cellular functions. However, recent findings suggest that many of these TRP channels are also localized at subcellular organelles or present in intracellular vesicular compartments [204, 210, 113]. For example, TRPV1 and TRPV3 are physically and functionally present in ER and regulate its functions [205, 206]. It has been reported that mutation in TRPML1 (mucolipin 1, also known as MCOLN1) present in late endosome or lysosomal compartment results in mucolipidosis type IV disease (ML4) [210]. These patients have motor impairment, mental retardation, retinal degeneration and iron-deficiency induced anaemia. TRPML1 mutants have unique ionic conductivity in which Fe^{2+} exchange occurs in endosome and lysosome [210]. Yeast TRP channel TRPY1 (also known as yeast vacuolar conductance 1; Yvc1) is known to be present in vacuolar membrane and causes influx of divalent cations in cell [10]. Nevertheless the molecular identity and characterization of TRP channel associated compartments are poorly identified. Membrane TRPV4 is regulated by several cues and signalling pathways but whether these signalling pathways are same for TRP channels localized in sub-cellular organelles is not well understood yet. Recent study in neonatal rat ventricular myocytes suggests that TRPV4 is predominantly located in nucleus but after exposure of hypotonic solution it translocates to the nucleus [207]. It seems that compartmentalization of TRPs is either an outcome of erroneous channel trafficking or systemic defect in the biosynthetic pathway which results in its localization at intermediate destinations like subcellular organelle and may regulate several signalling pathways. However among all the TRPV family members, sub-cellular localization of TRPV4 in any cellular system is not yet known. Here, in this work we have characterized if TRPV4 localizes in mitochondria irrespective of the cell type.

2.1.1. TRPV4 localizes in sub-cellular organelle in different cell lines

In order to characterise subcellular localization of TRPV4, TRPV4-GFP was expressed in different neuronal and non-neuronal cell lines like F11, COS-7, HaCaT and HeLa by transient over expression. In each case, apart from cell membrane, TRPV4 also localizes in the cytoplasm as big punctate aggregates (not diffused) and such localization in general suggest for an enriched amount of TRPV4 present in some specific organelles. In almost all cell types investigated, a large fraction of TRPV4 localized to the perinuclear region (**Fig 11**). Furthermore, to nullify the fact that such localization is not due to transient overexpression, immunostaining was performed in CHOK1 cells which are stably selected for TRPV4 (named as CHOK1-V4) and mock plasmid (named as CHOK1-Mock). Same perinuclear localization of TRPV4 was observed in CHOK1-V4 cells (**Fig 12**).

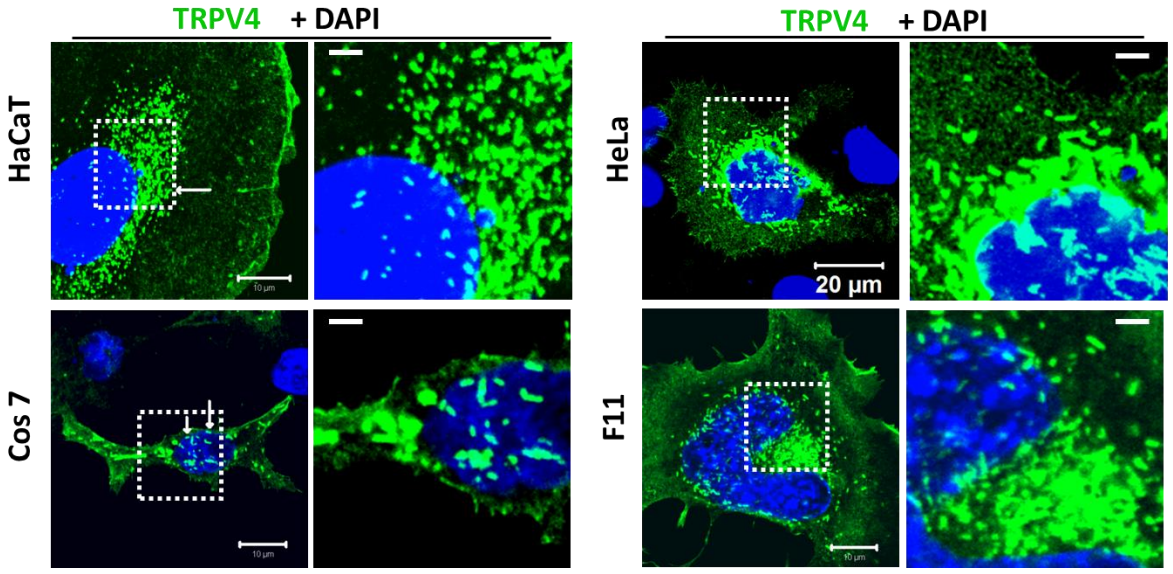

Fig 11: Perinuclear aggregation of TRPV4 in different cell lines. Confocal images of different cells expressing TRPV4 (green) and stained for DNA with DAPI dye (blue). TRPV4-GFP was transiently expressed in neuronal (F11) and non-neuronal (HaCaT, Cos7, HeLa) cell lines where TRPV4-specific clusters are present in the perinuclear regions. Enlarged confocal images of each are shown in the right side. Scale bar: 10 and 20 µm (for enlarge images) and 5 µm (for zoomed images).

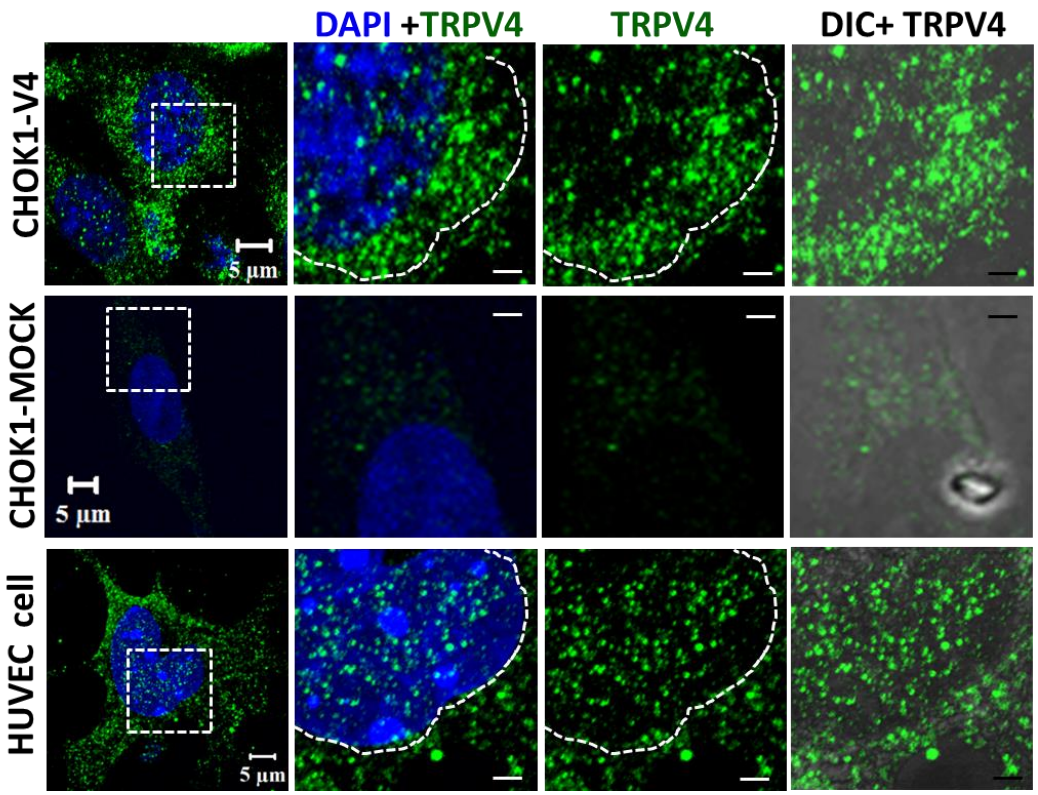

Fig 12: Perinuclear aggregation of TRPV4 is independent of transient over expression. Confocal images depicting localization of TRPV4 in cells stably expressing TRPV4 (named as CHOK1-V4) or an empty plasmid (named as CHOK1-Mock) are shown. Endogenous expression of TRPV4 in HUVEC cells are also shown in below. TRPV4 is detected by immunostaining with TRPV4-specific antibody (green) and nucleus was stained using DAPI (blue). The low level of TRPV4 immunoreacivity in CHOK1-Mock cell is due to the endogenous expression of TRPV4 at basal level. Scale bar: 5µm (for enlarge images) and 2 µm (for zoomed image).

2.1.2. TRPV4 localizes in mitochondria in different cell lines

For detailed characterization of these TRPV4-positive subcellular organelles, HaCaT cells were used as the preferred model system as these cells have a flat morphology (suitable for imaging) with more elongated mitochondria in control conditions. After transfecting the HaCaT cells with TRPV4, immunostaining was performed to determine whether the sub-organelles stained positive for TRPV4, represent mitochondria or not. For that purpose, two specific mitochondrial markers, namely Hsp60 and Cyt C were used to label mitochondria.

It was observed that TRPV4 colocalizes with mitochondrial markers, namely with Hsp60 and Cyt C in certain organelles (**Fig 13**). However, not all mitochondria reveal the presence of TRPV4 indicating that localization of TRPV4 to the mitochondria is

heterogeneous in nature. Furthermore to confirm if these TRPV4-positive organelles are indeed authentic mitochondria, another independent methodology was used. TRPV4-GFP was transiently expressed in HaCaT cells and these cells were labelled with MitoTracker Red. TRPV4-GFP expressing cells reveal colocalization with MitoTracker Red and therefore suggest that these organelles are indeed mitochondria (**Fig 13**). Another independent methodology was used to confirm if these organelles were indeed mitochondria. Therefore, colocalization experiments were performed in HaCaT cells expressing TRPV4-GFP and mitoDsRed. Both TRPV4-GFP and mitoDsRed co-localized in certain intra-cellular organelles. These results confirmed that TRPV4 indeed localizes in the mitochondria.

To rule out the possibility of co-localization as an outcome of fixation artefact, we performed live cell imaging of HaCaT cells transiently expressing TRPV4-GFP and mitoDsRed. We observed that even in live cells expressing very low level of TRPV4-GFP perfectly co-localized with mitoDsRed (**Fig 14**). Taken together, these results confirm that TRPV4 localizes into some mitochondria (but not all) and that is independent of cell types and its expression level.

2.1.3. Full-length hTRPV4 mutants also translocate inside the mitochondria

Previous result indicates that full-length TRPV4 colocalizes with different mitochondrial markers. In this regards, we explored if full-length mutants also localizes in the mitochondria. HaCaT cells were transiently transfected with full-length hTRPV4 "gain-of-function" mutants (R616Q, L618P and V620I) as GFP-tagged proteins and mitoDsRed for colocalization study (**Fig 15**). Results suggest that all these mutants colocalizes with mitochondrial marker mitoDsRed. This result indicates that not only TRPV4-Wt but also its gain-of-function mutants also localize in the mitochondria.

2.1.4. TRPV4 does not colocalize or co-localize moderately with other organelles

As TRPV4 colocalizes with mitochondrial marker/s, further experiments were performed to explore if TRPV4 localizes in other sub-cellular organelles other than mitochondria.

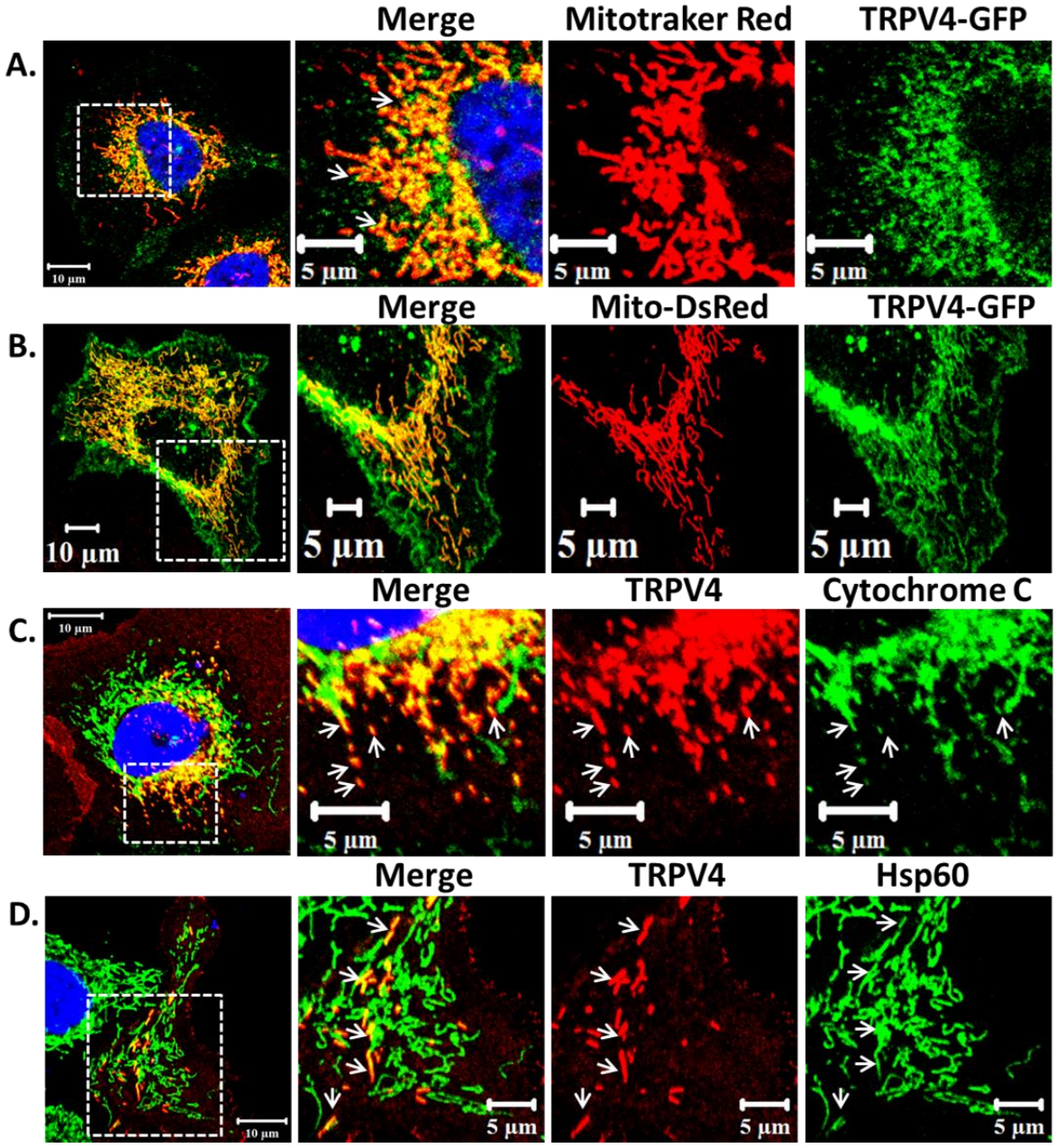

Fig 13: TRPV4 colocalizes with mitochondrial markers. In upper panel (A & B) describes the confocal images of HaCaT cells transiently expressing TRPV4-GFP and mitoDsRed both or only TRPV4-GFP. TRPV4-GFP shows colocalization with MitoTracker Red or mitoDsRed. TRPV4-GFP colocalizes with mitoDsRed (indicated by arrows). The lower panels (C and D) demonstrate the immunostaining of cells with antibodies specific for TRPV4 (red) with mitochondrial markers like Hsp60 and Cyt C (green). Colocalization results with Cyt C and Hsp60 indicates that TRPV4 colocalizes with mitochondrial marker proteins. However it was observed that all mitochondria are not positive for TRPV4, few of them do not colocalize at all with TRPV4.

For that HaCaT cells were doubly transfected with TRPV4-GFP and with either ER-CFP, or Golgi-CFP, or peroxisome-CFP. These colocalization experiments suggest that TRPV4 doesn't colocalize significantly with ER, Golgi and Peroxisome (**Fig 16**). However, in certain cases, some colocalization was observed with TRPV4 and peroxisome-CFP. Such minor degree of co-localization may appear due to the over expression of both proteins (TRPV4-GFP and peroxisome-CFP). Though it is unlikely, but such colocalization may appear due to spectral overlapping of the GFP and CFP also. To rule out such possibilities, only TRPV4-GFP was expressed and antibody staining for specific sub cellular organelles, namely for ER (with Anti-KDEL antibody), Golgi (with Anti-GM130 antibody) and lysosome (with Anti-Lamp1 antibody) respectively were performed (**Fig 17**). In all cases, TRPV4-GFP does not colocalize with these cell organelles.

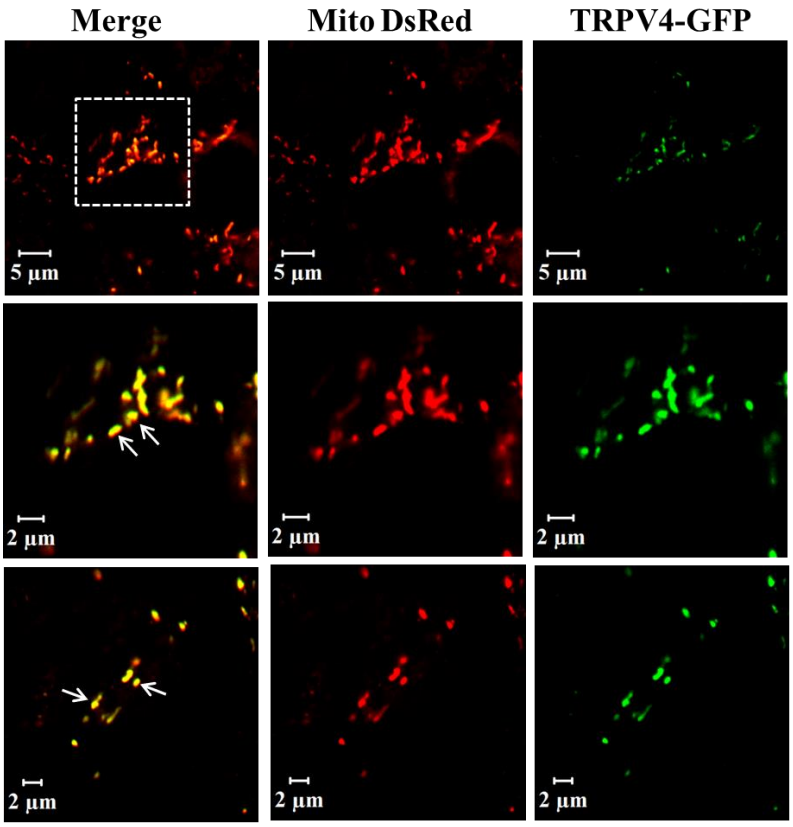

Fig 14: TRPV4 co-localizes with mitochondria in live cell. Confocal images from live HaCaT cells transiently expressing TRPV4-GFP and mitoDsRed. Enlarged confocal images depicting that in case of low expressing TRPV4-GFP positive cells, TRPV4 perfectly colocalizes with mitoDsRed within the mitochondria (indicated by arrows).

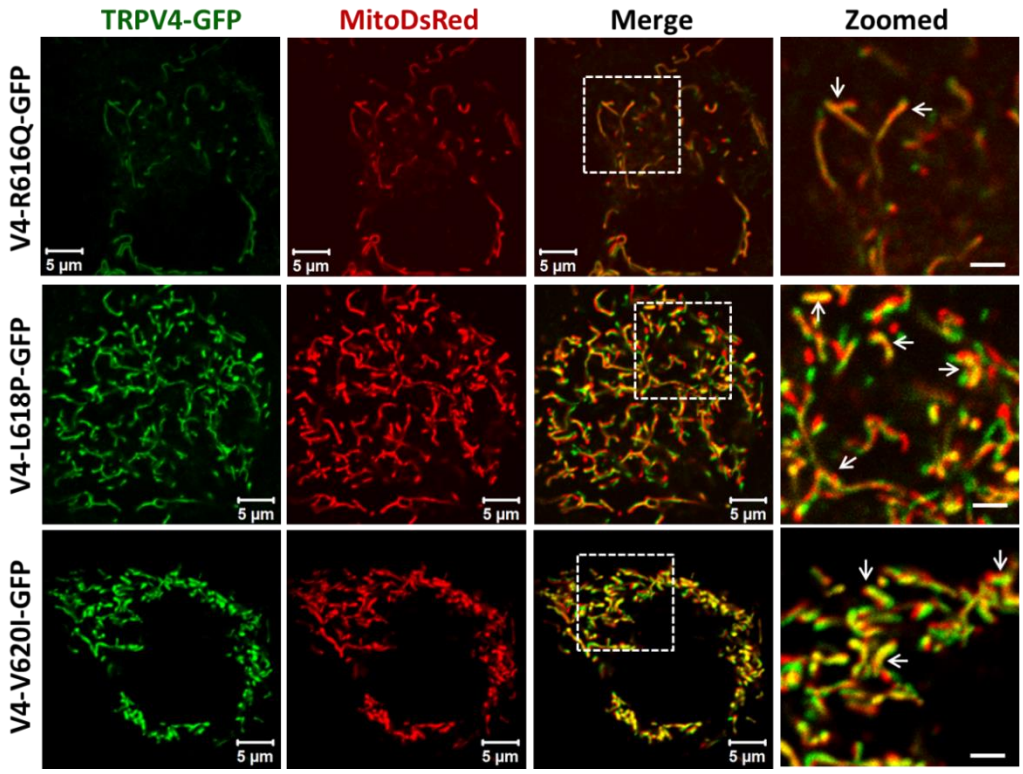

Fig 15: Full-length hTRPV4 mutants also colocalizes with mitochondria. Confocal colocalization images indicate that h-TRPV4 gain-of-function mutants (R616Q, L618P and V620I) colocalizes with mitoDsRed mitochondrial protein. Zoomed image shows distinct colocalization of hTRPV4 with tubular mitochondria (indicated by arrow). Scale bar: 2 µm.

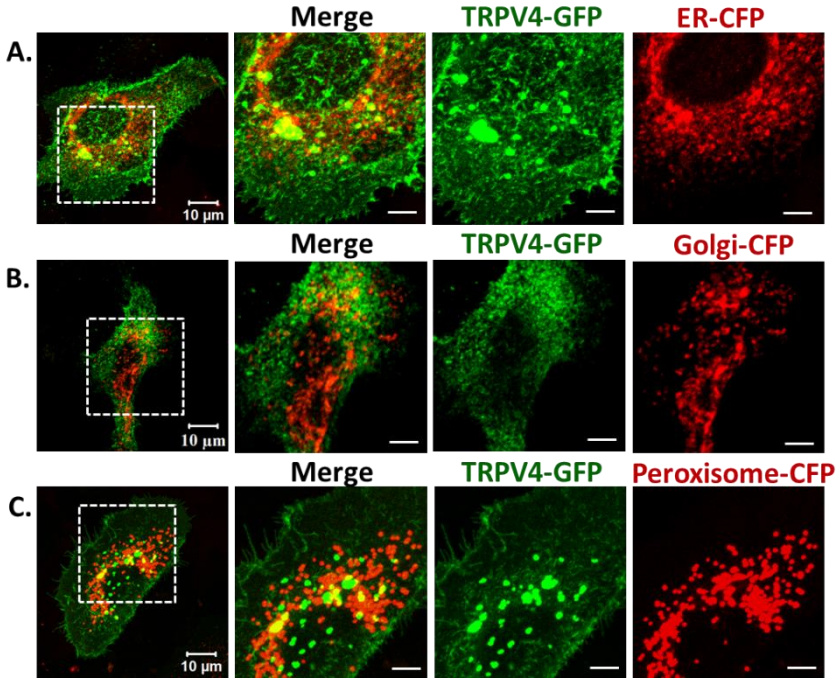

Fig 16: TRPV4 does not colocalizes with other subcellular organelles. Confocal images of HaCaT cells transiently expressing TRPV4-GFP and sub-cellular marker proteins such as ER-CFP, Golgi-CFP and Peroxisome-CFP are shown. Enlarged images (indicated by white dotted line) are shown in the right side. TRPV4 does not colocalize with ER or Golgi markers at all. TRPV4-GFP colocalizes with peroxisomal marker minimally. Scale bar: 5 µm (for enlarge images).

2.1.5. TRPV4 is endogenously present in isolated mitochondria

Next, we tried to explore if TRPV4 is endogenously present in mitochondria or not. For that purpose, mitochondrial fraction was purified from goat brain and western blot analysis was performed to detect endogenous TRPV4 in such fraction. Using an antibody specific for the C-terminal cytoplasmic domain of TRPV4, specific immunoreactivities (at ~ 72 kDa) was detected in this mitochondrial fraction (**Fig 18 A-D**). Band matching with the expected size of full-length TRPV4 (~ 98 kDa) was observed in that fraction (**Fig 18 B-C**). However, in many preparations, this ~ 98 kDa band becomes faint or totally invisible. This may suggest for a rapid proteolytic degradation or presence of a specific fragment which is tissue-specific (such as in brain).

To confirm that the isolated fraction is enriched in mitochondria and does not contain other cellular organelles, Western blot analysis for different sub-cellular markers were performed. All fractions were blotted with anti-Hsp60 and anti-Cyt C (for mitochondria), with anti-calnexin (for ER) and with anti-GM130 (for Golgi) (**Fig 18 A**). These confirmed the purity level of the mitochondrial fractions used in this study. The smaller yet strong specific band (~ 72 kDa) was enriched in the mitochondrial fraction in comparison to other fractions [S1 (supernatant after 1^{st} centrifugation), S2 and S3 (supernatant after 2^{nd} and wash fraction after 3^{rd} centrifugation)] (**Fig 18 A**). Taken together, these Western blots confirm that full-length TRPV4 (or a truncated part of TRPV4) is present in the mitochondrial fraction isolated from goat brain.

Mitochondria were isolated from CHOK1-V4 and CHOK1-Mock cell and Western blot was performed with the same C-terminus antibody. TRPV4 specific band was observed at ~100 kDa. This band is completely blocked by a specific peptide corresponding to the C-terminal sequence of TRPV4 (**Fig 18 B**). However, presence of the full-length TRPV4 is not prominent, though we observed the presence of the smaller band (at ~72 kDa) and it was

blocked by presence of this specific peptide suggesting that these bands are indeed specific for TRPV4 (**Fig 18 B**).

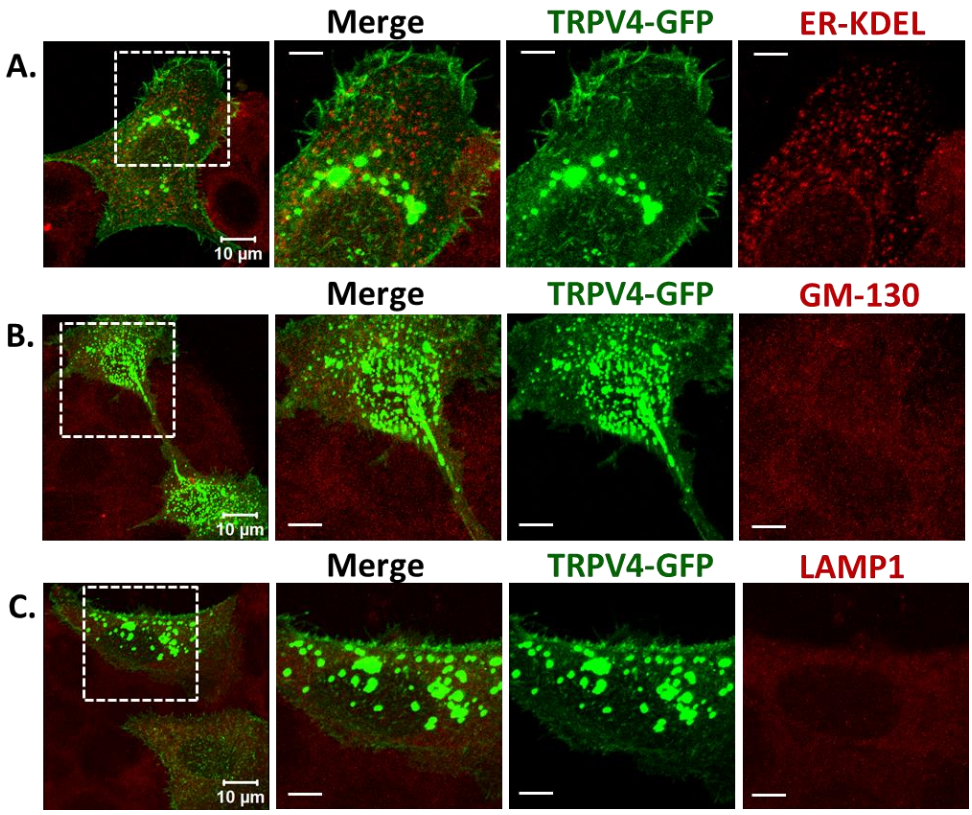

Fig 17: TRPV4 is not present in other intracellular organelles. Confocal images of HaCaT cells transiently expressing TRPV4-GFP and immunolabeled for sub-cellular organelles like ER (with Anti-KDEL ab), Golgi (with Anti-GM130 ab) and Lysosome (with Anti-Lamp1 ab) respectively. Enlarged images (indicated by white dotted line) represent the perinuclear region in details. TRPV4 does not colocalize with ER, Golgi and Lysosomal markers. Scale bar: 5 µm (for enlarged image)

Adipocytes are also known to respond to temperature changes. It has been reported that pharmacological inhibition of TRPV4 in white adipose tissue (abundantly present in adults) induces conversion of white adipose tissue in brown adipose tissue (very less in adults) by increasing the number of mitochondria [211]. Recent reports also suggest that TRPV4 present in white adipose tissue and regulates its thermogenic and oxidative metabolic properties [211]. In this context, we explored if TRPV4 is endogenously present in the mitochondria of white adipose tissue. We have isolated mitochondria from goat adipose tissue and Western blot was performed with this fraction using the same C-terminus antibody raised against TRPV4. The full length TRPV4-specific band was detected at ~ 100 kDa. The

size of the TRPV4 in adipose tissue mitochondria (lane one) exactly matches with positive control CHOK1-V4 mitochondria (lane two) (**Fig 18 C**). Our results strongly suggest that TRPV4 is indeed present in mitochondria but a smaller fragment is more prominent in mitochondria isolated from brain. This shorter fragment may arise due to specific photolytic cleavage of the full-length TRPV4 and such cleavage may be tissue specific in nature.

Synaptic junctions present in neuronal tissues are highly energy demanding area, therefore these regions are enriched with mitochondria to supply energy continuously. To explore the presence of endogenous TRPV4 in the synaptosomal structure, density gradient fractionation was performed with mouse fore brain homogenate. Different fractions were probed for TRPV4 with specific antibody. Result indicates that TRPV4-specific band is present in light membrane fraction (lane 2) and in synaptosomal fraction (lane 5) (**Fig 18 D**). TRPV4-specific faint band was observed at ~ 98kDa in light membrane fraction (lane 2) and in synaptosomal fraction (lane 5). However another strong band at ~ 72 kDa of TRPV4 was also observed in light membrane fraction (lane 2) and in synaptosomal fraction (lane 5). This band was not visible in any other fractions indicating that TRPV4 is specifically present in synaptosomal fraction and this band is completely abolished in presence of a blocking peptide, suggesting that this band indeed represents TRPV4.

2.2. TRPV4 interacts with intact mitochondria and mitochondrial proteins

Topological 3D structure of TRPV4 reveals that 70% of this channel is hanging towards the cytoplasmic area which makes it more accessible to interact with various regulatory molecules present in the cytosol [52].

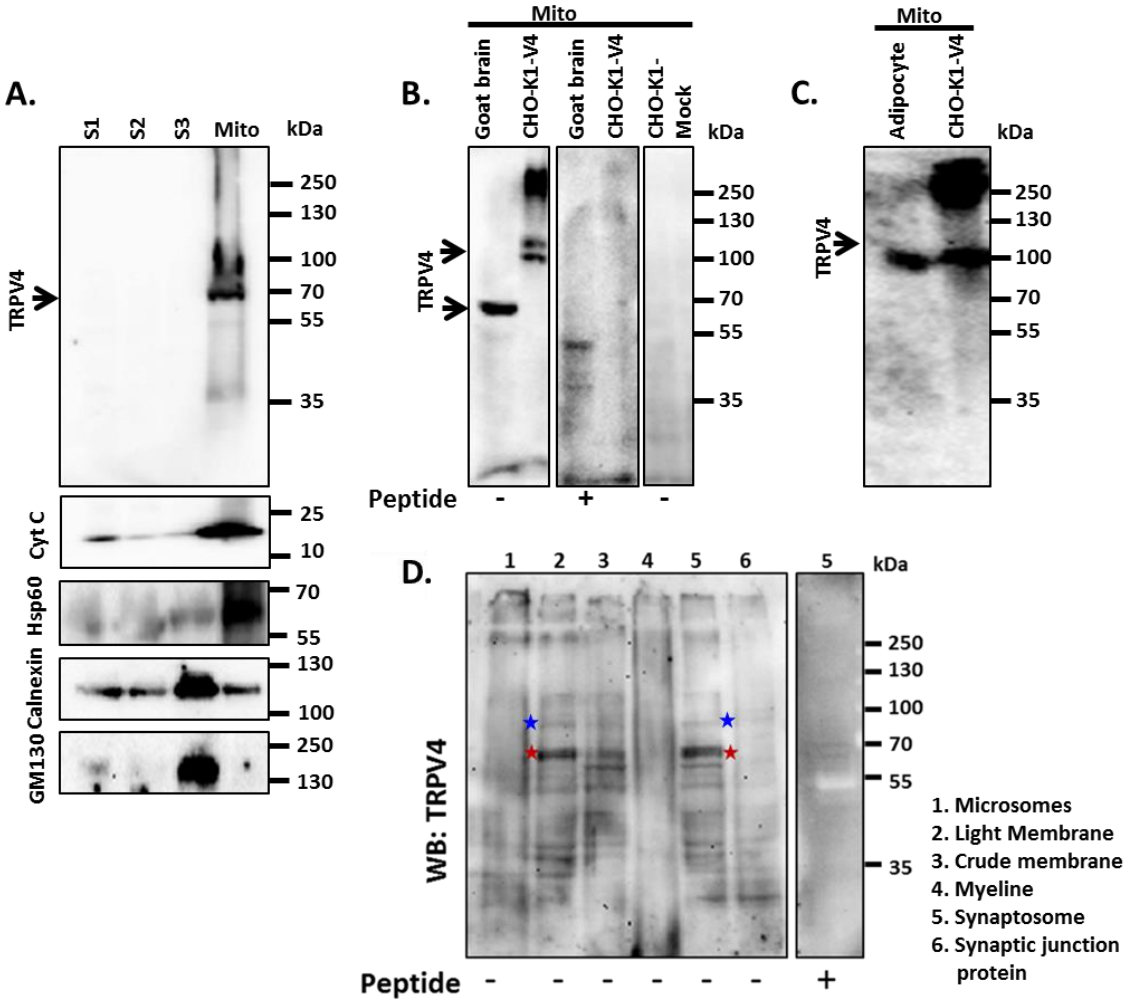

Fig 18: TRPV4 is endogenously present in mitochondria. Fresh mitochondria were isolated from Goat brain and different fractions were probed to explore if TRPV4 is endogenously present in mitochondria. **A.** The S1, S2, S3 and Mitochondrial fractions were probed with TRPV4-specific antibody (raised against the C-terminus of TRPV4) and the enrichment of TRPV4 was observed at ~ 72 kDa (expected band size of TRPV4 is ~ 98 kDa) in mitochondrial fraction. To check the purity of isolated mitochondria, Western blot was performed with specific marker antibodies like Cyt C and Hsp60 (for mitochondria), Calnexin (for ER) and GM130 (for Golgi). Results indicate that Cyt C and Hsp60 bands are intense in mitochondrial fractions as comparison to other lanes. Calnexin- or GM130-specifc immunoreactivities are very less or negligible in the same mitochondrial fraction. **B.** To check the specificity presence of TRPV4 in mitochondria, TRPV4-specific blots were developed from two different preparation of mitochondrial fractions, namely from goat brain and CHOK1-V4 stable cells. Results depicted that in mitochondria isolated from goat brain, TRPV4 band is lower in size (~ 72 kDa) as comparison to mitochondria isolated from CHOK1-V4 cells (~ 98 kDa). In presence of a specific peptide (corresponding to the C-terminus of TRPV4), the TRPV4-specific band is not detected suggesting that the immunoreactivity present in the mitochondrial fraction is very specific. **C.** Mitochondria was isolated from goat Adipocyte tissue and probed for TRPV4 by Western blot assay. In both lanes TRPV4 band (~ 100 kDa) was detected at the expected size. **D.** Tissue lysate was prepared from Rat forebrain and density gradient separation was done for different organelle fractions and subsequently Western blot was performed to detect the endogenous level of TRPV4. Result indicates that TRPV4-specific faint band (at ~ 98kDa, indicated by blue star) is present in light membrane fraction (lane 2) and in synaptosomal fraction (lane 5). In addition, another strong band for TRPV4 is also observed in these same fractions (indicated by red star). The presence of a specific peptide (corresponding to the C-terminus of TRPV4), the TRPV4-specifc band is abolished in the synaptosomal fraction (lane 5, right side). [S1 (supernatant after 1st centrifugation), S2 (supernatant after 2nd centrifugation, S3 (wash fraction, after 3rd centrifugation)].

Different domains of TRPV4 such as N-terminus, trans-membrane regions and the C-terminus are known to interact with different protein kinases, cytoskeletal proteins, different lipid derivatives and cholesterol [51, 110, 164, 212, 213, 214). The interaction of these proteins with TRPV4 modulates its structure, function and/or membrane localization. Recent reports suggest that point mutations (R269H, R315W) in the ankyrin repeat domain of TRPV4 result in loss-of-function due to reduced surface expression [146]. It was reported that these TRPV4 mutants largely aggregate in cytoplasm as puncta [146]. Yet the characterization of intra-cellular localization of TRPV4 remains largely uncharacterized. TRPV4 monomers are synthesized in ER and after tetramerization the functional channels are transported to the cell surface. The C-terminus of TRPV4 plays important role in tetramer assembly and sorting to its destination. It was reported that truncation of C-terminus leads to accumulation of TRPV4 in ER rather than membrane surface [208]. As TRPV4 is present in mitochondria, an attempt was given to explore if TRPV4 interacts with mitochondrial proteins.

2.2.1. Transmembrane (TM) regions and N-terminus of TRPV4 do not localize within mitochondria

In previous section it was shown that full-length TRPV4 is present in mitochondria. Next attempt was taken to decipher which segment of TRPV4 was imported inside mitochondria. Although mitochondrial import signal is generally present at the N-terminus of proteins in most cellular systems, recent reports suggest that C-terminus can also contain mitochondrial import signal [215, 216, 217]. To know that which segment of TRPV4 really goes inside the mitochondria, human TRPV4 N-terminus (1-465aa) and entire TM region (466-711aa) were cloned in RFP and GFP vector respectively. Subsequently transient transfection was performed in HaCaT cells and colocalization experiments were performed.

Images were acquired by confocal microscope. The N-terminal fragment of TRPV4 (TRPV4-Nt-RFP) appears to diffuse throughout the cytoplasm and the TM fragment of TRPV4 (TRPV4-TM-GFP appears as cytoplasmic puncta in HaCaT cell. Merged image of TRPV4-TM-GFP and TRPV4-Nt-RFP do not show any colocalization with immunostained Hsp60 or Mito-GFP respectively (**Fig 19**).

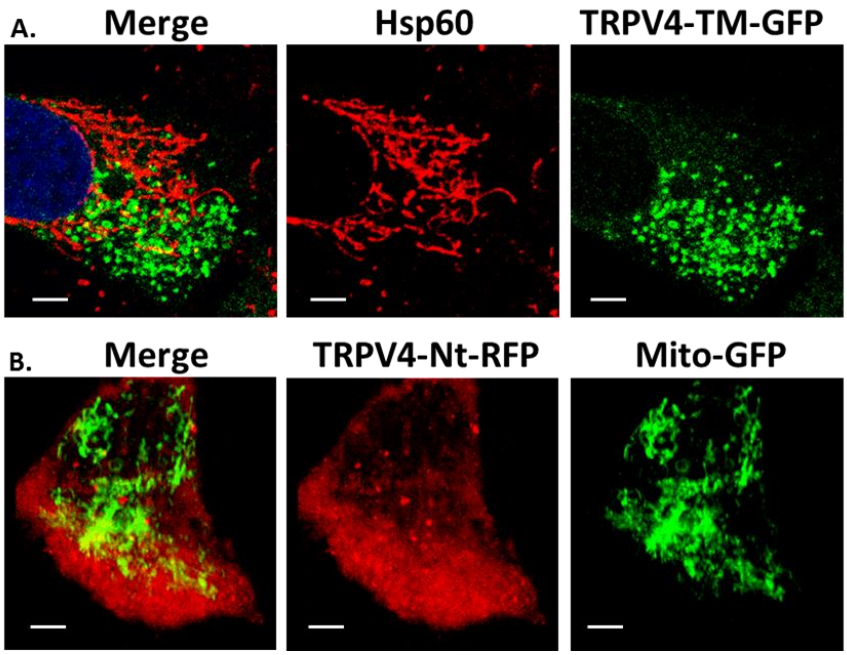

Fig 19: TRPV4 N-terminus and transmembrane region do not colocalize with mitochondrial markers. TRPV4-Nt-RFP, Mito-GFP and TM-GFP were transiently transfected in HaCaT cell. Upper panel (A) depicts that immunostained Hsp60 do not show any colocalization with TRPV4-TM-GFP. Lower panel (B) indicate that TRPV4-Nt-RFP do not show any colocalization with Mito-GFP. Scale bar: 5 μM

2.2.2. The C-terminus of TRPV4 localizes with mitochondria

Next attempt was taken to characterize the C-terminal region of TRPV4 (718-871aa) with respect to mitochondrial localization. In addition, previous studies indicate that the C-terminus of TRPV4 interacts with specific soluble cytosolic components such as PKCε, tubulin and even acetylated tubulin, which are also present in isolated mitochondria [51, 218, 219]. For that purpose, the C-terminus of TRPV4 was expressed in HaCaT cells as a RFP tagged protein and both TRPV4-Ct-RFP and Mito-GFP was co expressed in HaCaT cells by transient over expression. Cells which have higher expression of TRPV4-Ct-RFP appear as

larger aggregates and die soon suggesting that over expression of TRPV4-Ct-RFP is deleterious for cells. Nevertheless, TRPV4-Ct-RFP perfectly co-localizes with Mito-GFP in cells which over express TRPV4-Ct-RFP, suggesting that such larger aggregates can be actually aggregated mitochondria (**Fig 20**).

To confirm that TRPV4-Ct-RFP is indeed localizing in mitochondria, we tried to elucidate the colocalization between TRPV4-Ct-RFP and Mito-GFP in HaCaT cells which express both but at very low levels and at early time points. In such conditions, we observed that the C-terminus of TRPV4 appear as big-dots which are spherical in shape. In such cases, these dots are distributed throughout the cytoplasm and such dots perfectly colocalize with Mito-GFP (**Fig 20**). This suggests that these TRPV4-Ct-RFP positive dots are actually spherical-shaped mitochondria. It also indicates that localization of TRPV4-Ct inside mitochondria significantly alters mitochondrial morphology. To confirm that such localization of TRPV4-Ct-RFP in mitochondria is not due to over-expression, HaCaT cells expressing TRPV4-Ct-RFP were immunostained with Hsp60. Even in cells expressing very low levels of TRPV4-Ct-RFP, it perfectly colocalizes with Hsp60 (**Fig 20**).

2.2.3. C-terminus of TRPV4 is sufficient to bind with mitochondria

As TRPV4-CT-RFP is sufficient to localize within mitochondria, further attempt was taken to characterize if TRPV4-Ct interacts with intact mitochondria in *in vitro* experiments. For that purpose, *in vitro* binding experiments were performed with purified MBP-TRPV4-Ct, MBP-LacZ and intact mitochondria freshly isolated from Goat brain. MBP-TRPV4-Ct or MBP-LacZ was incubated in mitochondrial isolating buffer so that it maintains the osmolarity of mitochondria during incubation. This incubation was done for 30 minutes at 25°C and the buffers were supplemented with Ca^{2+} or combination of GTP and ATP (1 mM each) separately. Intact mitochondria and associated proteins were isolated by centrifugation.

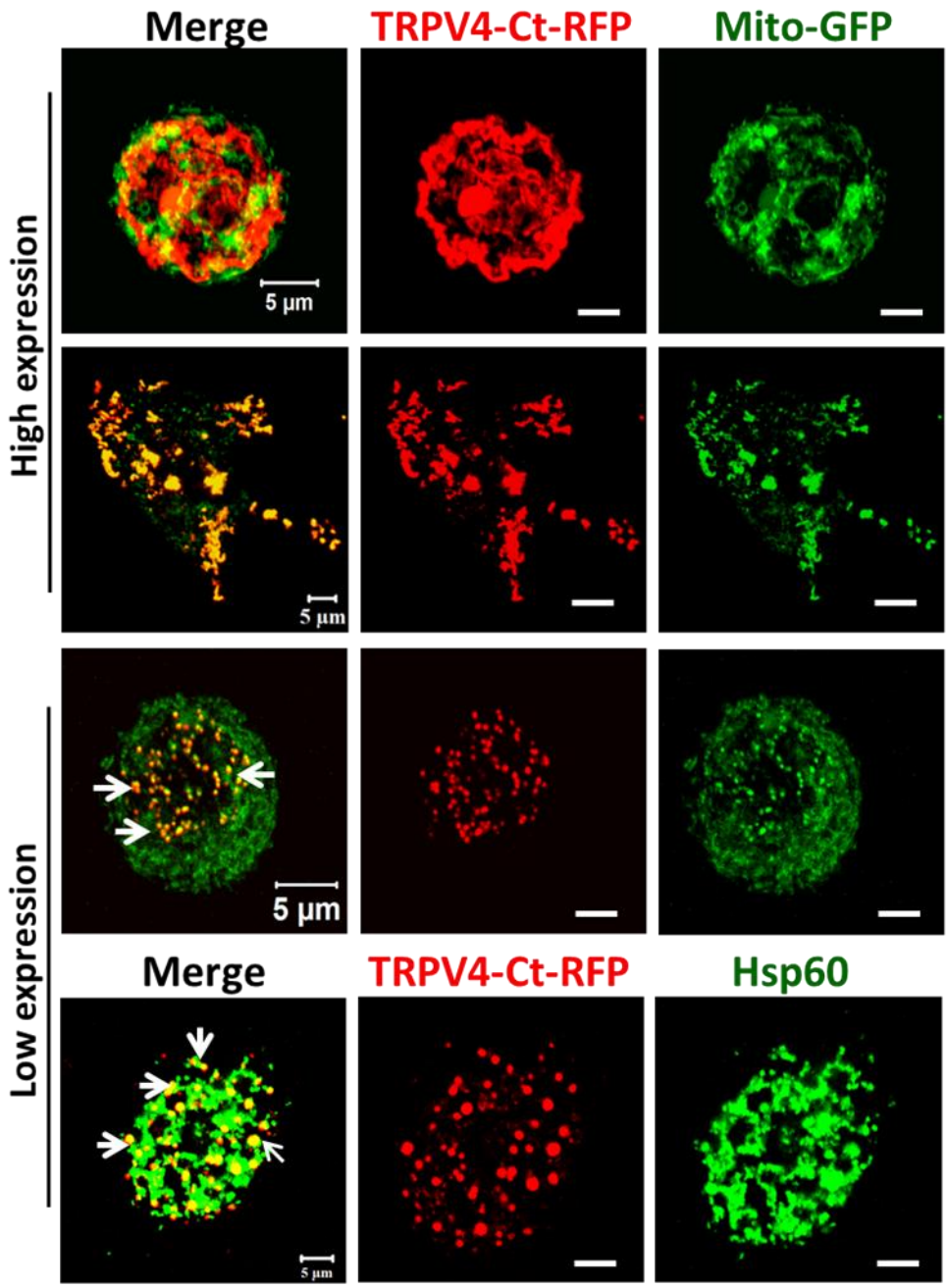

Fig 20: TRPV4 C-terminus colocalizes with mitochondria. TRPV4-Ct-RFP and mito-GFP was transiently expressed in HaCaT cell. It was observed that high expressing TRPV4-Ct-RFP alters mitochondrial morphology or it causes fragmentation of mitochondria but still merged images indicate that TRPV4 C-terminus colocalizes with mitochondria. In lower panel, low expressing TRPV4-Ct-RFP positive cell perfectly colocalizes with immunostained Hsp60 and Mito-GFP. Arrows indicate small round like mitochondria. Scale Bar: 5µm.

Subsequently (after two washing), gel samples were made for SDS-PAGE and/or Western Blot analysis. The mitochondrial pellet fraction was analysed for interaction of MBP-TRPV4-Ct or MBP-LacZ by Western blot analysis using anti-MBP antibody. Results suggest that MBP-TRPV4-Ct is enriched in mitochondrial fraction whereas MBP-LacZ does not appear in the

mitochondrial pellet fraction. Such interaction is independent of Ca^{2+} or combination of ATP and GTP as such. Notably, in wash fractions (W2), presence of MBP-TRPV4-Ct is minimum suggesting that the experiment was performed in below saturation conditions and the interaction of MBP-TRPV4-Ct in the mitochondrial pellet is specific in nature. To confirm that the pellet fraction truly contains mitochondria, the same samples were probed for Hsp60. The results suggest that the pellet fractions contain enriched amounts of Hsp60 suggesting that the pellet fraction indeed contains mitochondria (**Fig 21**).

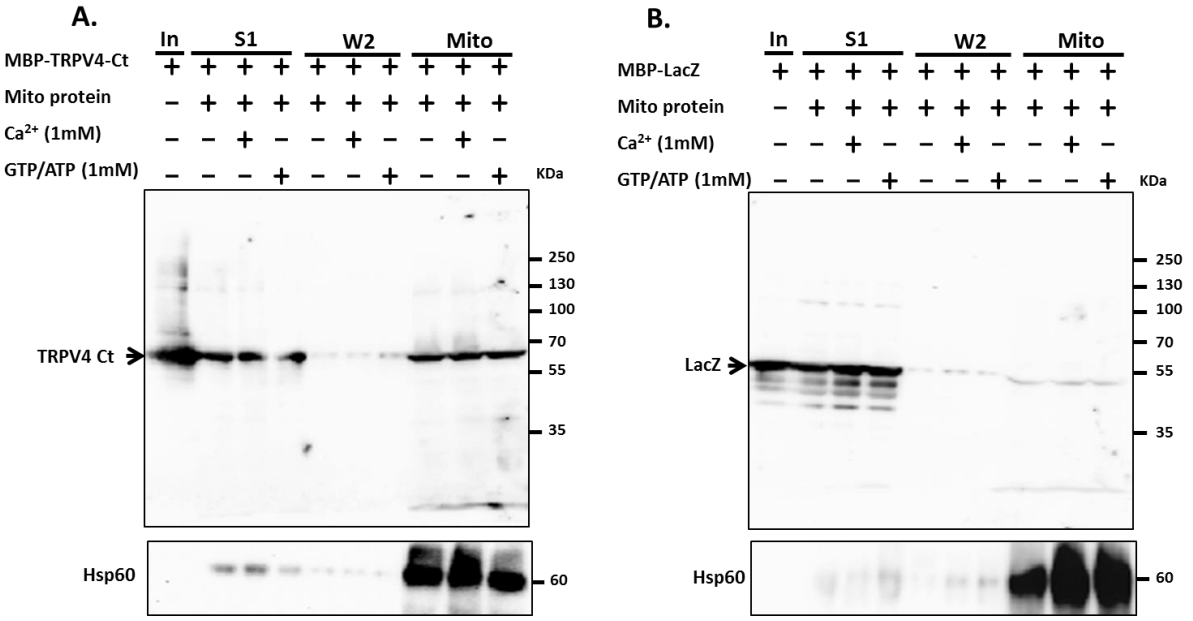

Fig 21: MBP-TRPV4-Ct but not MBP-LacZ binds to intact mitochondria independent of Ca^{2+} and/or ATP and GTP. MBP-TRPV4-Ct and MBP-LacZ were expressed in *E. coli* and purified by using amylose resin, quantified and same amount of fusion proteins were incubated for 30 minutes in mitochondrial isolation buffer with intact mitochondria freshly isolated from Goat brain. Subsequently they were washed twice, and protein samples were probed with anti-MBP antibody. In W2 fractions, neither MBP-TRPV4-Ct nor MBP-LacZ was observed indicating that unbound MBP-TRPV4-Ct or MBP-LacZ is washed away after second washing step. Presence of MBP-TRPV4-Ct but not MBP-LacZ in mitochondrial pellet fraction suggests that MBP-TRPV4-Ct specifically interacts with intact mitochondria and this interaction is independent of Ca^{2+} and/or GTP/ATP. (In: Input amount of MBP-TRPV4-Ct/MBP-LacZ, S1: Supernatant collected after incubation and 1st centrifugation, W2: 2nd wash fraction, Mito: Mitochondrial pellet fraction).

2.2.4. MBP-TRPV4-Ct interacts with different mitochondrial proteins

Previous result suggests that the C-terminus of TRPV4 interacts with mitochondria. Therefore next attempt was taken to identify mitochondrial proteins which can

potentially interact with MBP-TRPV4-Ct. An unrelated protein, namely MBP-LacZ was used as a negative control. Pull down experiment was performed with MBP-TRPV4-Ct and MBP-LacZ with goat brain mitochondrial lysate. MBP-TRPV4-Ct or MBP-LacZ were expressed in *E. coli* and these fusion proteins were immobilized on amylose beads and further incubated with mitochondrial lysates alone or supplemented with Ca^{2+}, GTP and ATP. All interacting proteins were eluted in 20 mM maltose and subjected for SDS-PAGE analysis. The pulled down proteins were further probed with specific antibodies for the presence of mitochondrial proteins. Western blot results indicate that Hsp60, Mfn1 and Mfn2 interact with MBP-TRPV4-Ct but not with the MBP-LacZ (**Fig 22 A-C**). These interactions remain same even in presence or absence of Ca^{2+} and ATP/GTP (1 mM each). However, Western blot with anti-Opa1, anti-Cyt C and anti-DRP1 failed to detect any interaction of these proteins with MBP-TRPV4-Ct (**Fig 22 D-F**). Coomassie staining results confirmed the presence of MBP-TRPV4-Ct or MBP-LacZ at equal amounts in the final eluted fractions (**Fig 22 G**). These results confirmed that the MBP-TRPV4-Ct interacts with Hsp60, Mfn1 and Mfn2.

2.2.5. The C-terminus of TRPV4 interacts directly with mitochondrial dynamics regulatory protein Mfn1 and Mfn2 independent of Ca^{2+} and GTP

Previous results were suggesting that MBP-TRPV4-Ct interacts with intact mitochondria and interacts with different mitochondrial proteins namely Hsp60, Mfn1 and Mfn2 present in mitochondrial lysates. Attempt was taken to confirm if the interaction of MBP-TRPV4-Ct with mitochondrial fusion protein Mfn1 and Mfn2 is direct and independent of any other proteins/factors present in the mitochondrial lysate.

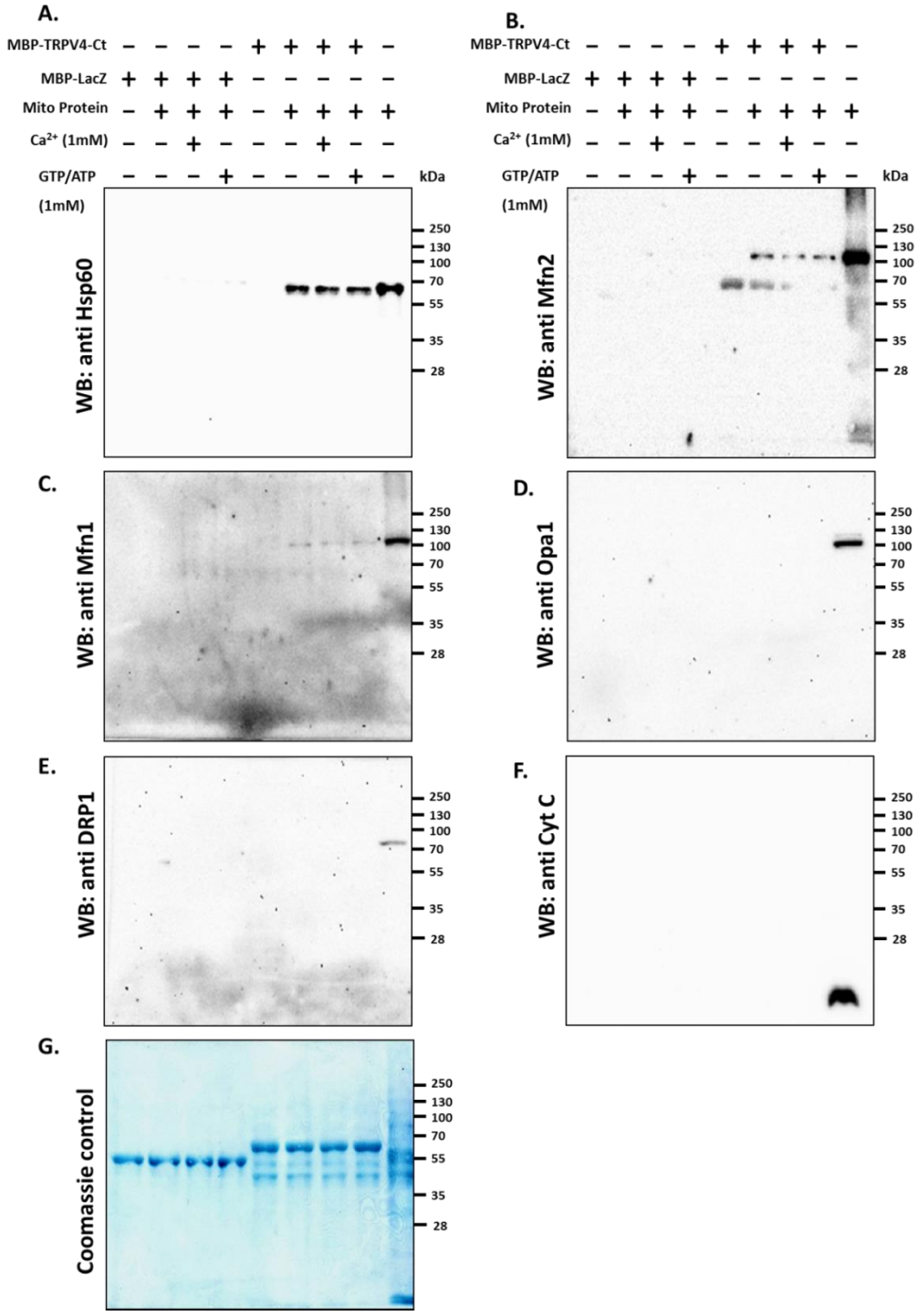

Fig 22: The C-terminus of TRPV4 interacts with different mitochondrial proteins. Pull down experiment was performed with mitochondrial lysate. MBP-TRPV4-Ct or MBP-LacZ was expressed and immobilized on amylose resin. Subsequently mitochondrial lysate was added for binding with MBP-TRPV4-Ct or with MBP-LacZ in presence of Ca^{2+} and GTP/ATP independently. Western blot was performed with different antibodies raised against different mitochondrial proteins. Results indicate that MBP-TRPV4-Ct but not MBP-LacZ interacts with mitochondrial protein Hsp60, Mfn2, Mfn1 (Panel **A, B, C**). This binding is independent of the presence or absence of Ca^{2+} and GTP/ATP. Presence of other mitochondrial proteins such as Opa1, DRP1 and Cyt C are not detectable in the eluates suggesting that these proteins probably do not interact with MBP-TRPV4-Ct (Panel **D, E. F**). MBP-LacZ was used as a negative control in each case. The right-most lane in all Western blot indicates the input of only mitochondrial lysate used as positive control for all Western blots. Presence of MBP-TRPV4-Ct or MBP-LacZ at equal amounts in the final eluted fractions is demonstrated by Coomassie staining (Panel **G**).

For that purpose, His-Mfn1 and His-Mfn2 were expressed in *E. coli*, purified and immobilized in Ni-NTA beads. Similarly, MBP-TRPV4-Ct and MBP-LacZ were expressed in *E. coli* and purified. Same amount of these purified MBP-tagged proteins were added on immobilized His-Mfn1 or His-Mfn2 column for direct interaction. In a similar manner, interaction with these purified proteins were analysed in the presence of catalytic amount of mitochondrial lysate and/or combination of Ca^{2+}/ATP/GTP. After interaction and substantial washing with 20 mM imidazole; all interacting proteins were eluted in 100 mM imidazole and subjected for SDS-PAGE. To see the interacting protein of MBP-TRPV4-Ct Western blot was performed with anti-MBP antibody. These results indicate that both His-Mfn1 and His-Mfn2 interacts directly with MBP-TRPV4-Ct but not with MBP-LacZ. This interaction is independent of the presence of catalytic amount of mitochondrial lysate, Ca^{2+}, ATP and GTP (**Fig 23 C-D**).

2.3. TRPV4 regulates mitochondrial morphology and other functional parameters

Several lines of evidence suggest that mitochondrial connectivity is dynamic in nature and it constantly changes its shape, size and subcellular distribution [220]. Mitochondrial number and its distribution is precisely regulated by fusion and fission mechanism and is mediated by several associated proteins namely by Mfn1, Mfn2, DRP1 and Opa1. Reports suggest that alteration of mitochondrial morphology largely occurs during early phases of apoptosis or in diseased conditions [221]. Mitochondria play an important role in Ca^{2+} buffering by sequestering excess intracellular Ca^{2+} and release extracellular fluid through uniporter pump [222].

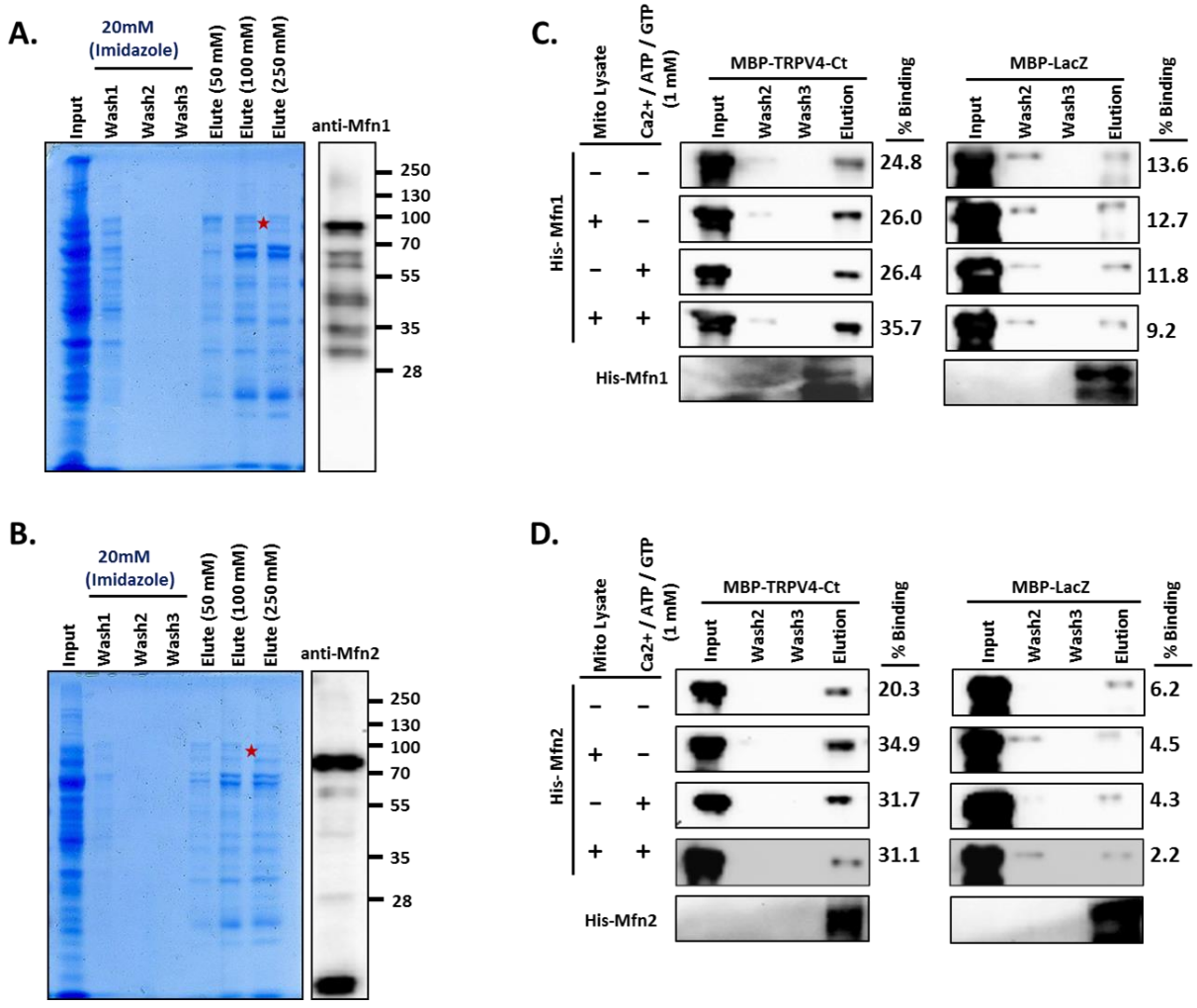

Fig 23: The C-terminus of TRPV4 interacts directly with mitochondrial dynamics regulatory protein Mfn1 and Mfn2 independent of Ca^{2+}, GTP and ATP. A-B. Purification profile of His-Mfn2 and His-Mfn1. The asterisk (*) symbol indicates the full-length size of His-Mfn1 or His-Mfn2. **C-D.** His-Mfn1, and His-Mfn2 interact directly to MBP-TRPV4-Ct but not with MBP-lacZ. His-Mfn1, His-Mfn2 were expressed in *E. coli*, purified and were immobilized in Ni-NTA beads. Purified MBP-TRPV4-Ct and MBP-LacZ were incubated separately on these immobilized beads alone or in presence of Ca^{2+}, GTP/ATP or catalytic amount of mitochondrial lysate respectively. Interaction of MBP-TRPV4-Ct is much higher compared to the interaction of MBP-LacZ. The values presented in the right side indicate the percentage [with respect to the input (MBP-TRPV4-Ct or MBP-LacZ)] of MBP-TRPV4-Ct or MBP-LacZ protein that binds to the immobilized beads. Western blot analysis with anti-His indicates the presence of purified His-tagged proteins in the eluted samples (In absence of mitochondrial lysate and Ca^{2+}, GTP/ATP).

It has been reported that excess Ca^{2+} load in mitochondria leads to mitochondrial dysfunction and altered mitochondrial morphology in several disease conditions [223, 224]. Since TRPV4 acts as a non-selective cationic channel, its activation causes Ca^{2+}-influx inside the cell. Results described in chapter two suggest that TRPV4 is physically present in the

mitochondria. Therefore the functional significance of TRPV4 in the context of mitochondrial structure-function relationship can be very important. In addition, it was observed that TRPV4-positive mitochondria become spherical or round-shaped as compared to normal tubular mitochondria, suggesting that TRPV4 may indeed regulate the mitochondrial structure and functions.

Results described in previous sections provide evidence that TRPV4 is present in mitochondria. Therefore the aim of the work described in this chapter is to explore the effect of TRPV4 activation or inhibition on mitochondrial structure and function.

2.3.1. TRPV4 regulates mitochondrial morphology

To visualize the effect of TRPV4 activator or inhibitor upon mitochondrial morphology, CHOK1-V4 and CHOK1-Mock cells were transiently transfected with mitochondrial marker mitoDsRed and subsequently treated with TRPV4 activator and inhibitor for 8 hrs and fixed subsequently. Confocal images were acquired after the immunostaing of TRPV4 in CHOK1-V4 and CHOK1-Mock cells. Results indicated that in CHOK1-V4 cell, mitochondrial morphology was mainly spherical or round ball shaped (**Fig 24 upper panel**). In CHOK1-Mock cells mitochondrial morphology was normally elongated and tubular in shape even when cells were treated with TRPV4 activator or inhibitor for the same duration. However in CHOK1-V4 cells, after the treatment of TRPV4 activator 4αPDD (5 µM), most of the spherical shape (small) mitochondria formed aggregates (Represented with arrow in right side, **Fig 24 upper second panel**). These aggregated mitochondria colocalizes with TRPV4. However in presence of TRPV4 inhibitor, RN1734 (10 µM) mitochondrial morphology did not change much as compared to its activator 4αPDD (5 µM). This indicates that activation of TRPV4 causes aggregation of mitochondria and increases its perimeter as well as area.

To confirm such changes in a more quantitative manner, several parameters (**Table 2**) were considered and more than 500 individual mitochondria were quantified against each parameter (**Fig 25 A-E**). It was observed that Aspect Ratio (AR; Major axis/Minor axis) of CHOK1-V4 mitochondria is not significantly different even in the presence of its activator or inhibitors. However AR change was significant with respect to mitochondria from CHOK1-Mock cell even in the control conditions suggesting that presence of TRPV4 is sufficient to bring certain changes in the mitochondrial morphology (**Fig 25**). "Aspect Ratio" is a reliable indicator of mitochondrial length; and therefore such results indicates that in CHOK1-V4 cell, the mitochondria is spherical in nature as compared to cylindrical or tubular mitochondria present in CHOK1-Mock cell. Similarly, mitochondrial "Form Factor" (FF, $Pm^2/4\pi A_m$) represent the branching or interconnectivity of mitochondria relevant for mitochondrial mass exchange. This FF is significantly high (1000 fold) in TRPV4 activator treated mitochondria as compared to control and RN1734 (10μM) treated mitochondria (p-value, **Table 3**). These results strongly indicate that in presence of 4αPDD (5μM), multiple spherical mitochondria fuse to each other to form big aggregated mitochondria. It seems that individual mitochondrial membrane entity is still intact during aggregation phase and only mitochondrial mass fuses with each other. Taken together, these results indicate that TRPV4 modulates mitochondrial morphology, at least in stable cell lines expressing TRPV4.

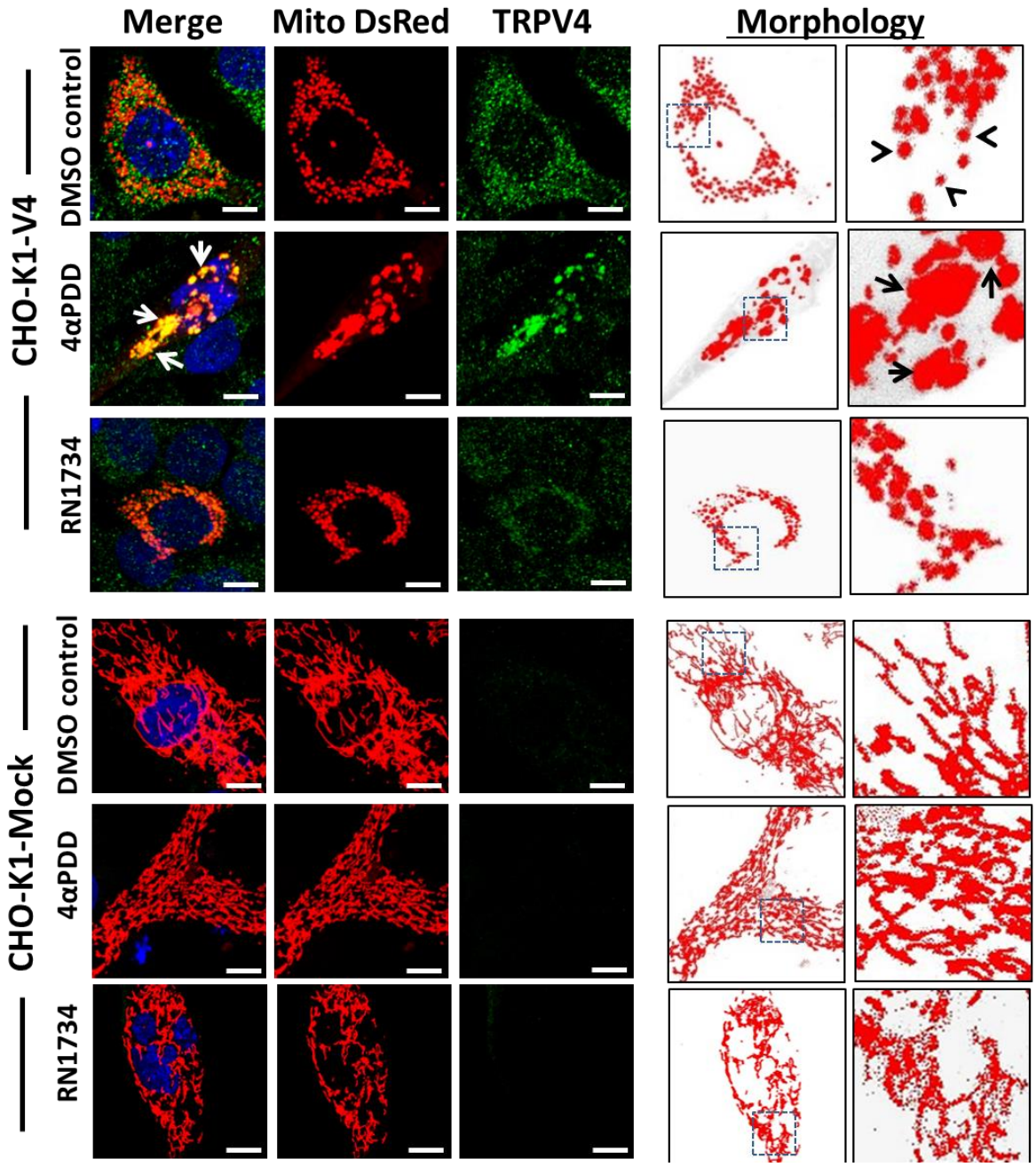

Fig 24: Activation or inhibition of TRPV4 alters mitochondrial morphology. mitoDsRed was transiently transfected in CHOK1-V4 and CHOK1-Mock cells. TRPV4 activator 4αPDD (5µM) and inhibitor RN1734 (10µM) was added to CHOK1-V4 and CHOK1-Mock cell for 8 hours, cells were fixed and stained for TRPV4 (green) and DAPI (blue). Subsequently images were acquired by confocal microscopy. Mitochondria in CHOK1-V4 cells become spherical or round ball-like in shape after activation with 4αPDD (shown as arrow head) as compared to cylindrical or rod-like normal mitochondria observed in CHOK1-Mock cell (lower panel). TRPV4 activator 4αPDD (5µM) treatment leads to mitochondrial aggregation in TRPV4-positive mitochondria as compared to DMSO control and RN1734 (10µM) treated mitochondria. The scale bar is 5 µm. The digitalized image of mitoDsRed intensity and an enlarged view filed of the same is represented on the right hand side.

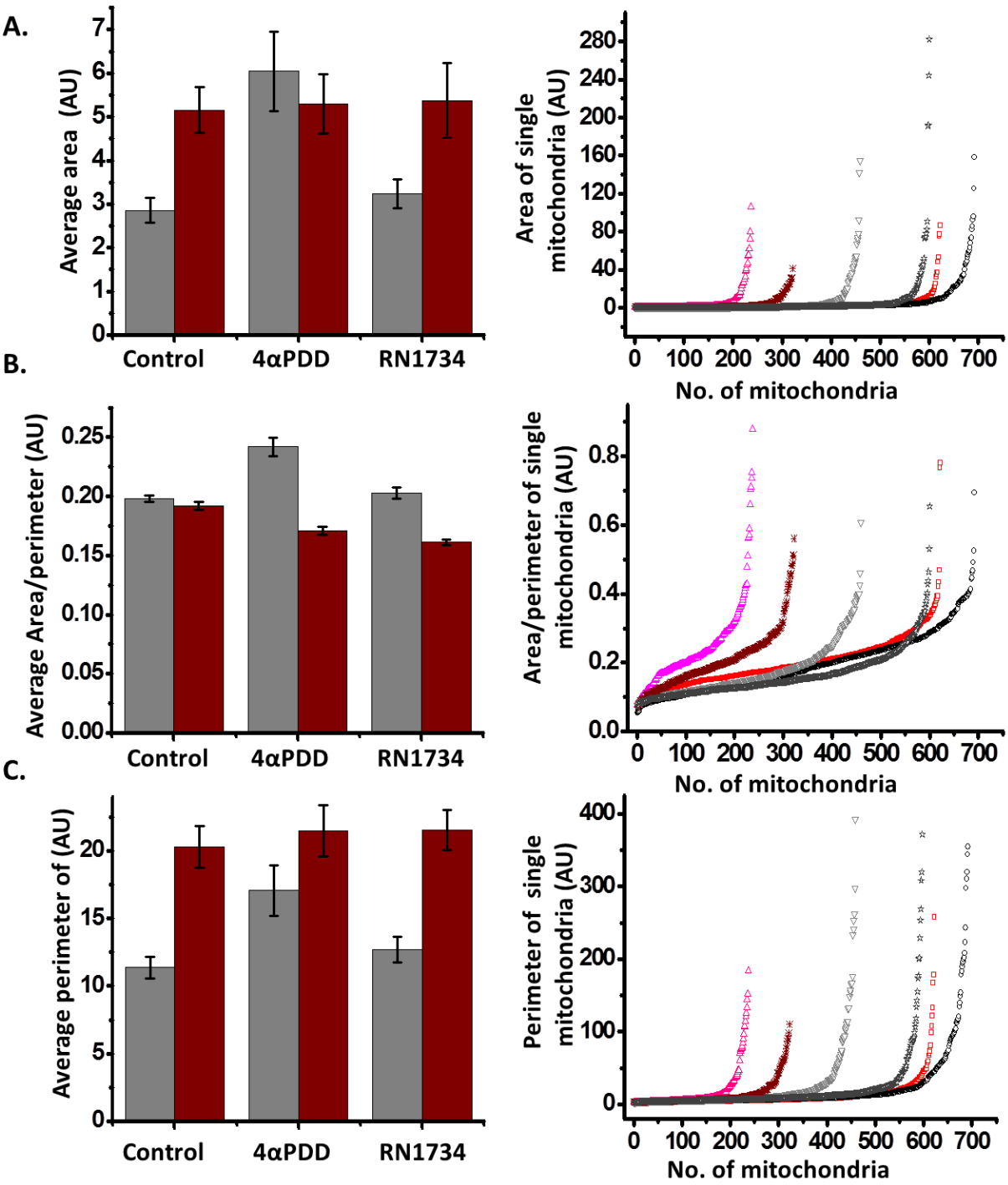
A.
Average area (AU)
Control
4αPDD
RN1734
Area of single mitochondria (AU)
No. of mitochondria
B.
Average Area/perimeter (AU)
Control
4αPDD
RN1734
Area/perimeter of single mitochondria (AU)
No. of mitochondria
C.
Average perimeter of (AU)
Control
4αPDD
RN1734
Perimeter of single mitochondria (AU)
No. of mitochondria

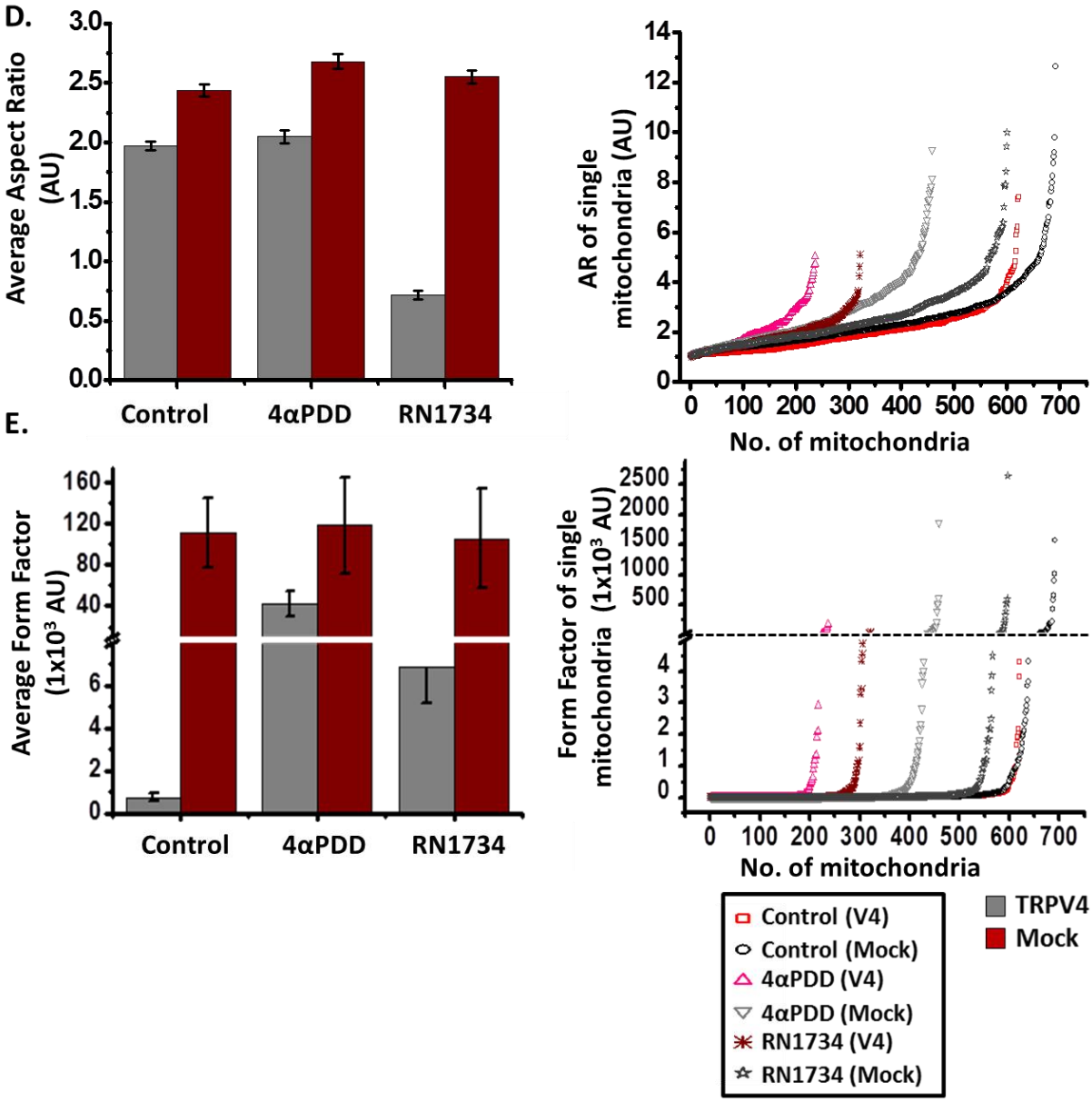

Fig 25: Quantitative analysis of mitochondrial morphology alteration in response to TRPV4 activation and inhibition. For quantitative analysis, images of mitoDsRed expressing CHOK1-V4 and CHOK1-Mock cells were processed by Image J software and all mitochondrial parameters were calculated by mitochondrial morphology plugin. Represented graph depicted that mitochondrial area, perimeter and area/perimeter increases significantly after treatment with TRPV4 agonist 4αPDD (5 µM) in CHOK1-V4. However these changes were not observed in CHOK1-Mock cells treated with same agonist 4αPDD **(A, B, C)**. Aspect Ratio (Major axis/ Minor axis) of mitochondria remain unchanged in presence of TRPV4 agonist or antagonist. However, in CHOK1-Mock cells mitochondrial AR is higher (elongated mitochondria) as compared to TRPV4-positive cell **(D)**. The Form Factor of TRPV4-postive mitochondria is 1000 fold higher in presence of 4αPDD as compared to control indicating that in 4αPDD treated condition mitochondria aggregates and gets interconnected to each other. Individual mitochondrial parameters for each mitochondrion are shown in scattered plot (right side).

Table 2: Parameter used for quantification of mitochondrial morphology

No.	Parameter	Designation	Remark
1.	Area	A_m	Area of mitochondrion
2.	Perimeter	P_m	Length of mitochondrial outline
3.	Area/Perimeter	A_m / P_m	Ratio between area and perimeter of mitochondria
4.	Major Axis	r_{max}	Maximum distance between mitochondrial centroid and outline
5.	Minor axis	r_{min}	Minimum distance between mitochondrial centroid and outline
6.	Aspect Ratio	AR	Ratio between r_{max} / r_{min} of elliptical mitochondria (Tubular mitochondria AR is higher)
7.	Form Factor	FF	$(Pm^2/4\pi A_m)$ Describe branching or interconnectivity of mitochondria

(Parameters adapted from Koopman et al.; 2005) [225]

Table 3: P-values of mitochondrial morphology

Average Area of Mitochondria					
	Control (Mock)	**4αPDD (V4)**	**4αPDD (Mock)**	**RN1734 (V4)**	**RN1734 (Mock)**
Control (V4)	0.0002	> 0.0001	0.0003	0.4212	0.0052
Control (Mock)		0.3932	0.8734	0.0161	0.8212
4αPDD (V4)			0.5146	0.0014	0.6556
4αPDD (Mock)				0.0171	0.9402
RN1734 (V4)					0.0759

Average Area/Perimeter of Mitochondria					
	Control (Mock)	**4αPDD (V4)**	**4αPDD (Mock)**	**RN1734 (V4)**	**RN1734 (Mock)**
Control (V4)	0.2142	> 0.0001	>0.0001	0.336	> 0.0001
Control (Mock)		> 0.0001	> 0.0001	0.0677	> 0.0001
4αPDD (V4)			> 0.0001	> 0.0001	> 0.0001
4αPDD (Mock)				> 0.0001	0.0194
RN1734 (V4)					> 0.0001

Average Perimeter of Mitochondria					
	Control (Mock)	**4αPDD (V4)**	**4αPDD (Mock)**	**RN1734 (V4)**	**RN1734 (Mock)**
Control (V4)	> 0.0001	0.0008	> 0.0001	0.3004	> 0.0001
Control (Mock)		0.2621	0.6268	0.0014	0.3083
4αPDD (V4)			0.1373	0.0251	0.7032
4αPDD (Mock)				0.0003	0.1529
RN1734 (V4)					0.0123

Average Aspect Ratio of Mitochondria					
	Control (Mock)	**4αPDD (V4)**	**4αPDD (Mock)**	**RN1734 (V4)**	**RN1734 (Mock)**
Control (V4)	> 0.0001	0.2394	> 0.0001	0.088	> 0.0001
Control (Mock)		> 0.0001	0.0035	> 0.0001	0.147
4αPDD (V4)			> 0.0001	0.006	> 0.0001
4αPDD (Mock)				> 0.0001	0.1087
RN1734 (V4)					> 0.0001

Average Form Factor (FF) of Mitochondria					
	Control (Mock)	**4αPDD (V4)**	**4αPDD (Mock)**	**RN1734 (V4)**	**RN1734 (Mock)**
Control (V4)	0.002	> 0.0001	0.0036	> 0.0001	0.0267
Control (Mock)		0.2387	0.895	0.0358	0.9244
4αPDD (V4)			0.2496	0.0019	0.4119
4αPDD (Mock)				0.0471	0.8509
RN1734 (V4)					0.1334

The next aim was to explore if endogenous TRPV4 regulates mitochondrial morphology in a similar manner. For that purpose we used HUVEC primary cell as TRPV4 is reported to be expressed endogenously in this cell [173]. Our Western blot analysis and immunofluorescence analysis also confirmed that these cells express TRPV4 endogenously (**Fig 26 B**). Therefore HUVEC cells were cultured and treated with TRPV4 activator or inhibitor for 8 hours. To explore the changes in mitochondrial morphology, treated cells were immunostained with Hsp60 and images were acquired by confocal microscope. Results indicate that in presence of TRPV4 activator 4αPPD (5 μM) mitochondria become aggregated in the perinuclear area (indicated by arrow). This effect was not observed in other cells that were treated with either RN1734 (20 μM) or 4αPPD (2 μM). In this condition mitochondrial morphology was tubular and branched similar to DMSO control (**Fig 26 A**). This result indicates that activation of endogenous TRPV4 is also able to induce changes in mitochondrial structure and morphology. This result also suggests that the regulation of mitochondria by TRPV4 may be a common phenomenon relevant in different types of cells and tissues, and is not restricted to specific cell types **(discussed later)**.

Furthermore to analyse if presence of TRPV4 can cause any ultra-structural changes, transmission electron microscopy was performed. For that purpose, either TRPV4-GFP or GFP, was transiently expressed in F11 cell and after fixation with glutaraldehyde cells were analysed by electron microscope. Electron micrograph images of mitochondria in F11 cells indicate that expression of TRPV4-GFP cause aggregation of mitochondrial cristae in corner and induce deformed structure (**Fig 27**). Some of the mitochondria become hollow or swollen (indicated by red arrow). F11 cells expressing only GFP do not develop such deformed mitochondria. Altogether, experimental evidences suggest that mitochondrial morphology is altered in TRPV4 positive cells.

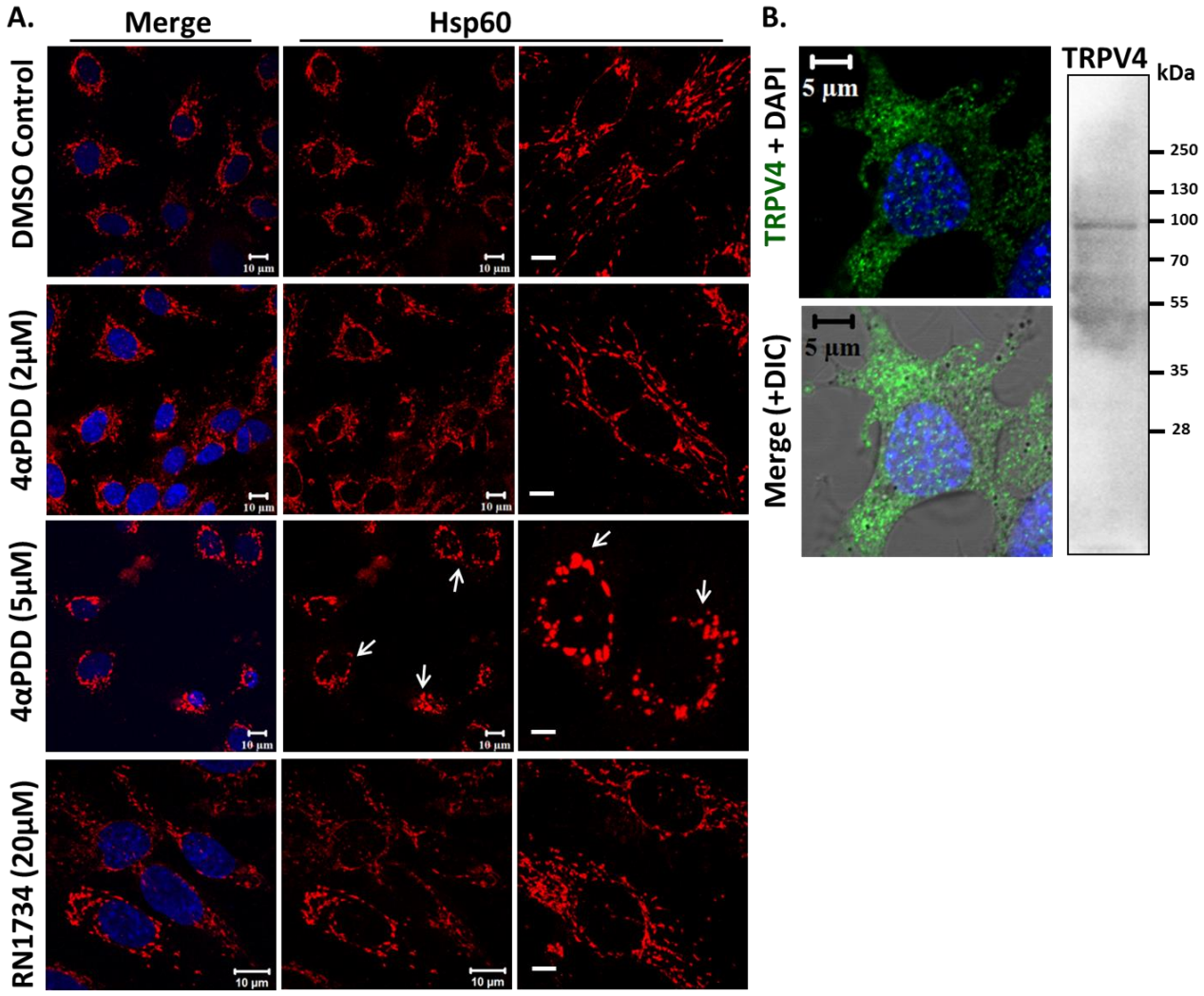

Fig 26: Endogenous TRPV4 regulates mitochondrial morphology in primary cell. **A.** HUVEC cells were grown on coverslips and treated with TRPV4 agonist 4αPDD and antagonist RN1734 for 8 hours and subsequently immunostained for Hsp60 and confocal images were acquired. Representative images depict that in presence of 4αPDD (5 μM) mitochondria becomes aggregated in perinuclear region (indicated by arrow). However mitochondrial morphology was filamentous or intact in presence of inhibitor RN1734 and control. Lower concentration of 4αPDD (2 μM) does not affect mitochondrial morphology significantly. **B.** Representative image showing the endogenous presence of TRPV4 in HUVEC cell. Western blot analysis of HUVEC cells for TRPV4 is also shown in right side. Scale bar: 5 μm.

2.3.2 TRPV4 regulates mitochondrial potentiality

Mitochondrial membrane potential ($\Delta\psi_m$) is the major component of proton motif force (Δp) [226]. Mitochondria maintain its membrane potential by utilizing oxidizable substrates and generates proton gradient across the inner membrane.

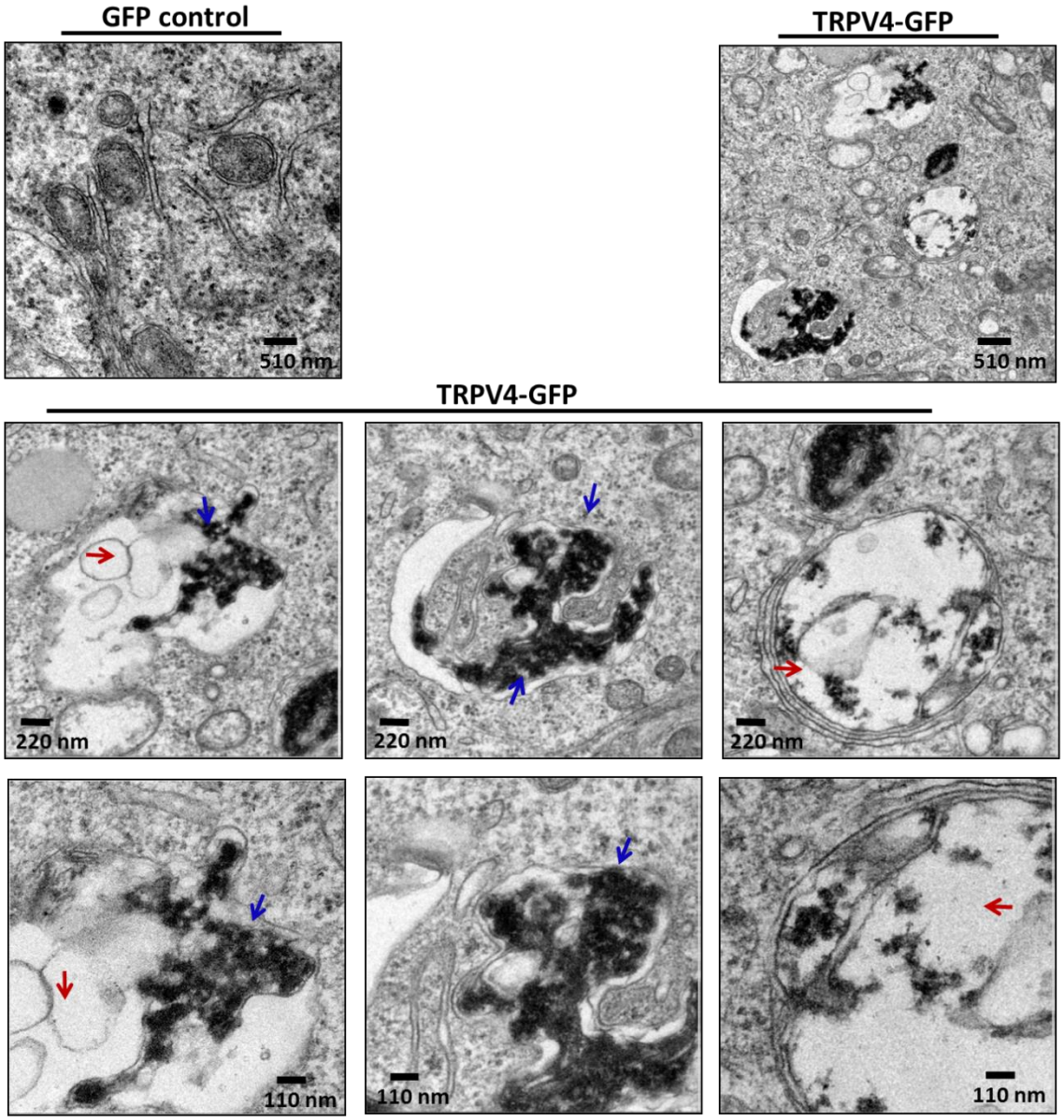

Fig 27: TRPV4 alters mitochondrial structure in neuronal cell. TRPV4-GFP was transiently expressed in F11 cells and subsequently fixed with glutaraldehyde. After sample preparation, images were acquired by electron microscope. Depicted EM images show that aggregation of mitochondrial cristae (indicated blue arrow). Some of the mitochondria completely lost the cristae structure and became hollow or swollen (indicated by red arrow). However in GFP expressing cells, mitochondrial structure remains normal.

Under normal conditions mitochondrial inner membrane is impermeable to any ions, therefore several Ca^{2+}-uniporter or exchanger cause influx of Ca^{2+} inside the mitochondria. It was reported that excess Ca^{2+}-influx inside the mitochondria results in collapse of mitochondrial membrane potential [227, 228]. In this context, it is important to explore if TRPV4 activation can cause changes in the mitochondrial potentiality. For this purpose

CHOK1-V4 and CHOK1-Mock cells were grown on coverslips and subsequently TRPV4 activator or inhibitor was added for 8 hours. After that JC-1 (5 μM) dye (Ratiomatric dye) was added in all for 40 minutes. Subsequently, confocal images were acquired from live cells. It was observed that in presence of TRPV4 activator 4αPDD (5μM), mitochondrial potential was significantly decreased in CHOK1-V4 cells as compared to DMSO control. TRPV4 inhibitor, RN1734 (10 μM) did not alter the mitochondrial potentiality in CHOK1-V4 and retains its potentiality similar to the control condition (**Fig 28 A**). This effect was not observed in CHOK1-Mock cell (**Fig 28 B**). Subsequently image intensity (Red and Green) was quantified by Image J. The Red intensity (Ex535/Em590) images representing higher membrane potential is shown at the right side. CCCP (5 μM), an uncoupler commonly used to reduce mitochondrial oxidative potential, was used as a positive control in this experiment separately. Represented JC-1 graph indicates that mitochondrial potential in control set of CHOK1-V4 cell is significantly less as compared to the CHOK1-Mock cells (**Fig 28 C**). Interestingly, effect of TRPV4 activator (4αPDD) on mitochondrial potential is significantly less in CHOK1-V4 cell and the values are comparable to that observed in case of CCCP, a mitochondrial oxidative potential uncoupler (P-value represented in **Table 4**).

2.3.3. TRPV4 regulates mitochondrial Ca^{2+}-dynamics

Ca^{2+}-influx inside the mitochondria occurs through outer mitochondrial membrane followed by inner membrane. Outer mitochondrial membrane allowed free transport of Ca^{2+} ions but the inner membrane is impermeable for Ca^{2+}. VDAC and many other unidentified ion channels are present on the outer membrane of mitochondria which allowed passing of cytoplasmic Ca^{2+} ions across the outer mitochondrial membrane. Likewise, different mitochondrial uniporters (MCU) and exchangers (Na^+/Ca^{2+}, Na^+/H^+ and Ca^{2+}/H^+) present on the inner membrane regulate the influx of mitochondrial Ca^{2+} [224, 229, 230, 231, 232]. As

TRPV4 is present in mitochondria, we explored if activation of TRPV4 can cause Ca^{2+} influx in mitochondria. To explore the mitochondrial Ca^{2+} dynamics in presence of TRPV4 activator or inhibitor, live cell imaging was performed in CHOK1-V4 and CHOK1-Mock cell. For this purpose, Mito-Perichem (Mitochondrial Ca^{2+}-sensing construct) was transiently transfected in CHOK1-V4 and CHOK1-Mock cell and live cell imaging was performed by confocal microscope. Cells exhibiting moderate levels of expression were considered for this Ca^{2+} imaging as such cells allow qualitative analysis of both increase as well as decrease in the intensities. Cells expressing very high level or very low level of Mito-Perichem were excluded from this study. This experiment suggests that Ca^{2+}-influx inside mitochondria increases after addition of TRPV4 activator 4αPDD in CHOK1-V4 cells (**Fig 29 A**). Addition of TRPV4 inhibitor RN1734 results in decrease in mitochondrial Ca^{2+} level (as indicted by fluorescence intensities of Mito-Perichem) with progress in time (**Fig 29 B**). However, Ca^{2+}-influx in CHOK1-Mock cell was not altered much in presence of TRPV4 activator or inhibitor (**Fig 29 A-B**). For quantitative analysis of Ca^{2+}-influx, similar experiments were repeated (n=4) in presence of TRPV4 activator or inhibitor and representative intensity graph indicating the same (**Fig 29 C**).

2.3.4. TRPV4 regulates Hsp60 levels in mitochondrial fractions

Hsp60 is a mitochondrial matrix protein that is essential for folding or assembly of newly synthesized proteins. It has been reported that HSPs (Hsp60, Hsp70 and Hsp90) plays a cytoprotective role during mitochondrial stress and maintain its oxidative potential and enzyme activities involved in TCA cycle [233]. The levels of HSPs are altered in case of inflammation or in cases where mitochondrial Ca^{2+} level is elevated [234].

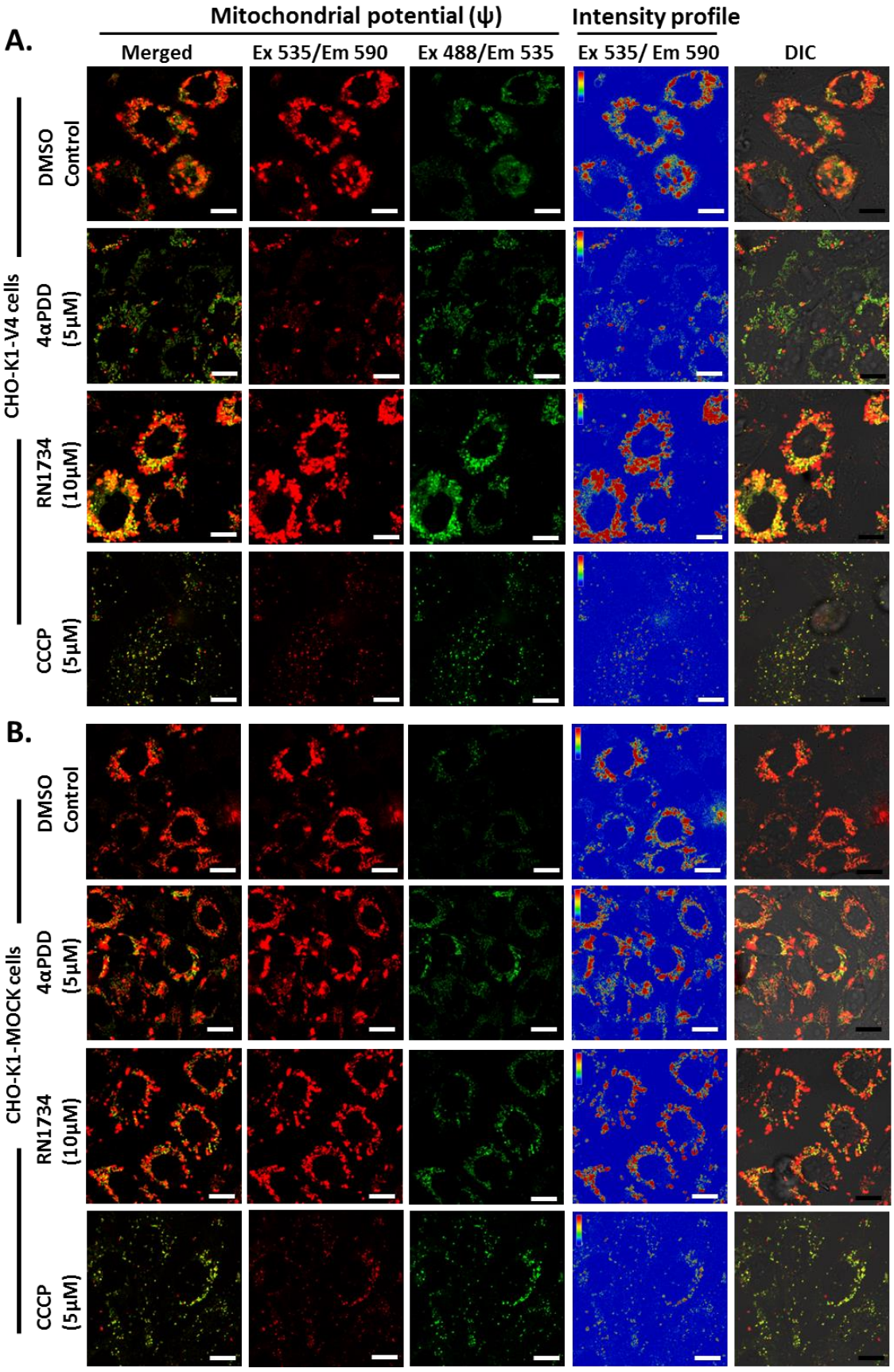
A.
Mitochondrial potential (ψ)
Intensity profile
Merged
Ex 535/Em 590
Ex 488/Em 535
Ex 535/ Em 590
DIC
CHO-K1-V4 cells
DMSO Control
4αPDD (5μM)
RN1734 (10μM)
CCCP (5μM)
B.
CHO-K1-MOCK cells
DMSO Control
4αPDD (5μM)
RN1734 (10μM)
CCCP (5μM)

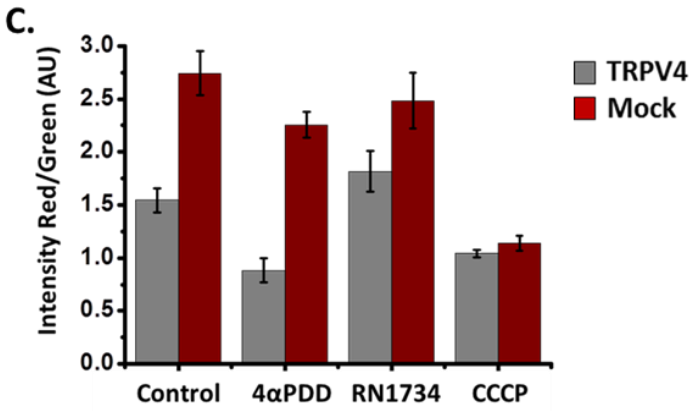

Table 4. P-value of mitochondrial potentiality

		CHOK1-V4			
		DMSO	**4αPDD**	**RN1734**	**CCCP**
CHOK1-Mock	**DMSO**	0.0001	0.0001	0.0003	0.0001
	4αPDD	0.0015	0.0001	0.1175	0.0001
	RN1734	0.0018	0.0001	0.0523	0.0001
	CCCP	0.0084	0.0751	0.0047	0.2765

Fig 28: TRPV4 regulates mitochondrial potentiality. CHOK1-V4 and CHOK1-Mock cells were grown on coverslip and subsequently TRPV4 activator 4αPDD (5 µM) and inhibitor RN1734 (10 µM) were added after 8 hours. After that JC-1 (5 µM) was added in the same culture media. Confocal images were acquired by dual excitation wavelength 488nm (Green, for mitochondria with formation of JC-1 monomers at low mitochondrial potential) and 535nm (Red, for mitochondria with formation of J-aggregates at high membrane potentials). Red/ Green intensity of more than 15 view fields for each condition was calculated by Image J. Represented graph shows that the basal level of mitochondrial potential is higher in CHOK1-Mock cell as compared to CHOK1-V4 cells. Statistical paired two test was performed and all P-values are represented in tabular form. Bar graph representing the ±SEM. Scale bar is 10 µm.

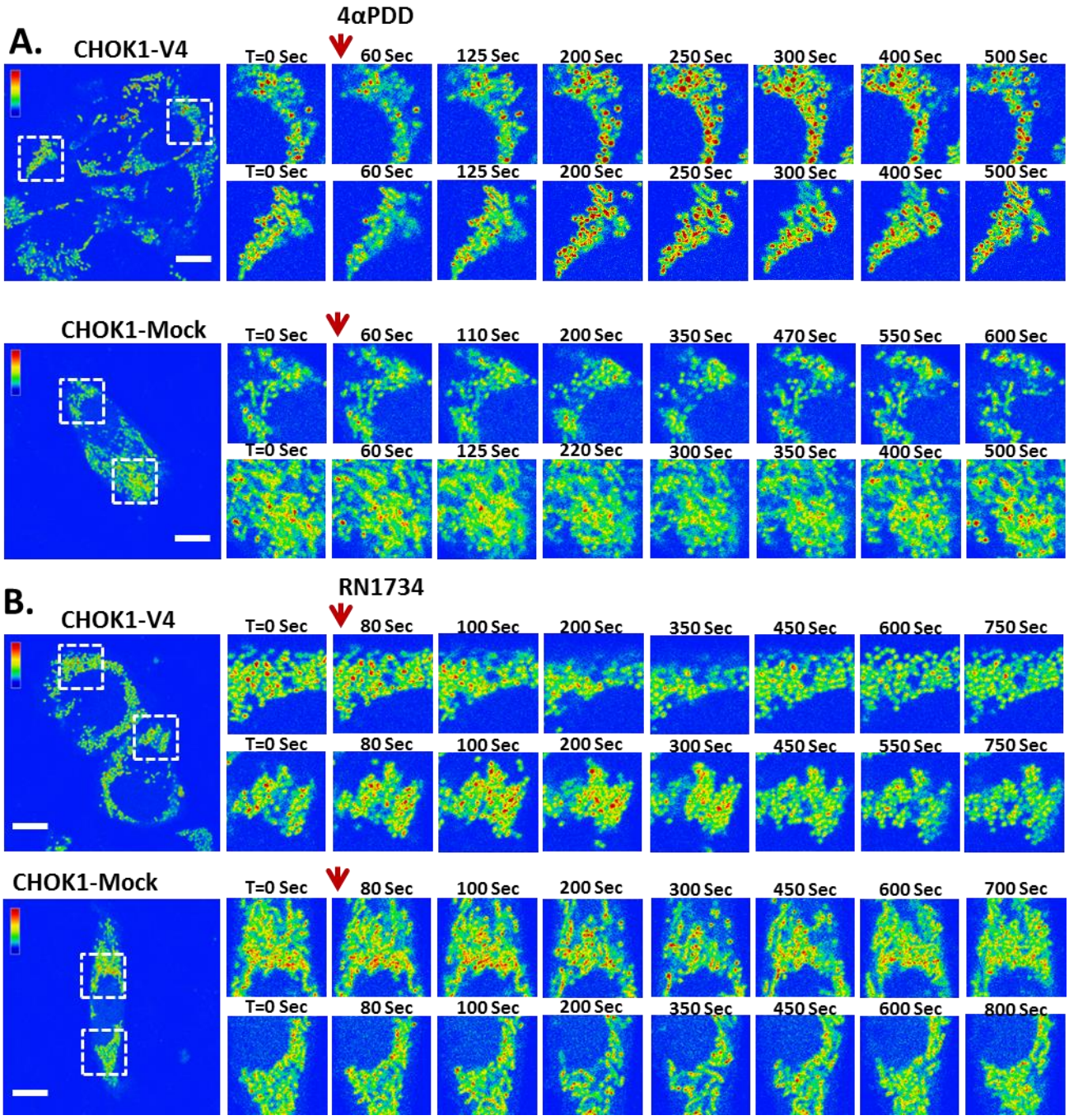
A.
CHOK1-V4
4αPDD
T=0 Sec
60 Sec
125 Sec
200 Sec
250 Sec
300 Sec
400 Sec
500 Sec
T=0 Sec
60 Sec
125 Sec
200 Sec
250 Sec
300 Sec
400 Sec
500 Sec
CHOK1-Mock
T=0 Sec
60 Sec
110 Sec
200 Sec
350 Sec
470 Sec
550 Sec
600 Sec
T=0 Sec
60 Sec
125 Sec
220 Sec
300 Sec
350 Sec
400 Sec
500 Sec
B.
CHOK1-V4
RN1734
T=0 Sec
80 Sec
100 Sec
200 Sec
350 Sec
450 Sec
600 Sec
750 Sec
T=0 Sec
80 Sec
100 Sec
200 Sec
300 Sec
450 Sec
550 Sec
750 Sec
CHOK1-Mock
T=0 Sec
80 Sec
100 Sec
200 Sec
300 Sec
450 Sec
600 Sec
700 Sec
T=0 Sec
80 Sec
100 Sec
200 Sec
350 Sec
450 Sec
600 Sec
800 Sec

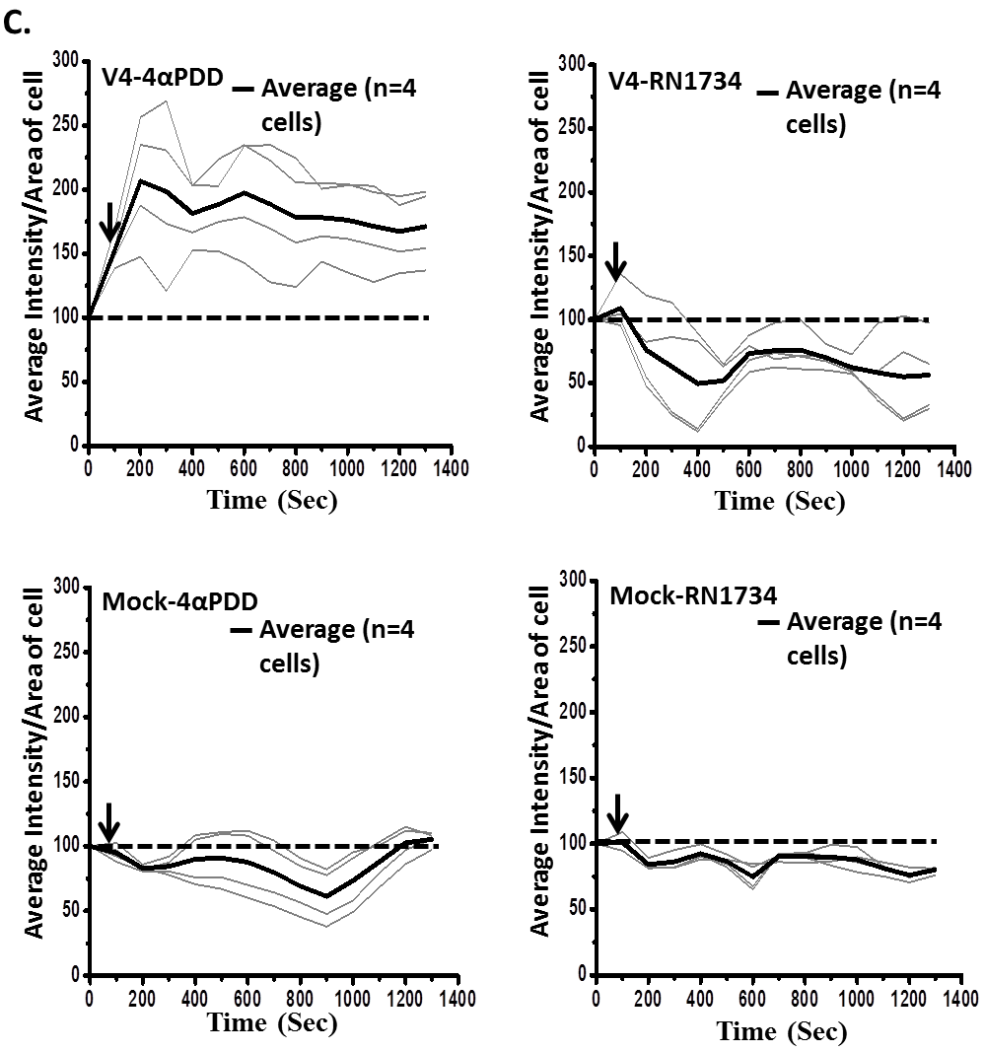

Fig 29: TRPV4 regulates mitochondrial Ca^{2+}-influx. Mito-Pericham (Mitochondrial targeting Ca^{2+}-sensing fluorescent protein) was transiently expressed in CHOK1-V4 and CHOK1-Mock cells and live cell imaging was performed by confocal microscope. TRPV4 activator 4αPDD (5 μM) and inhibitor RN1734 (10 μM) was added after 100 frames of imaging. Addition of 4αPDD causes massive influx of mitochondrial Ca^{2+} (panel **A**) in CHOK1-V4 positive cell. However in presence of RN1734, mitochondrial Ca^{2+}-influx decreases with time (panel **B**). In CHOK1-Mock cell, Ca^{2+}-level remained mostly unchanged in presence of TRPV4 activator or inhibitor. Represented Ca^{2+} intensity graph of four live cells in each condition was quantified by Image J (panel **C**). Average (thick dark black line) indicates that 4αPDD increases (~two fold) mitochondrial Ca^{2+}-level whereas RN1734 decrease the Ca^{2+}-level as comparison to CHOK1-Mock cell. Arrow indicates the time of addition of drug at 100^{th} frame. Scale bar: 20 μm.

Earlier studies suggest that TRPV1 activator (Capsaicin) upregulates the expression of Hsp70, Hsp90 and Hsp27 in non-neuronal epithelial cells [235]. In similar context, since our previous results suggest that TRPV4 is present inside mitochondria, we explored if TRPV4 regulates Hsp60 level. To explore that, TRPV4 was expressed transiently in HaCaT cells and immunostaining for Hsp60 was performed. Results indicate that TRPV4 expressing cells

almost lost the staining of Hsp60. It was observed that TRPV4 is present in tubular shaped mitochondria in HaCaT cell and the corresponding Hsp60 level was significantly low in such specific mitochondria (**Fig 30**).For better representation of Hsp60 level in TRPV4 positive mitochondria, intensity plots and intensity profile in pseudocolor are analysed. Results indicate that the green fluorescence intensity (corresponding to Hsp60 level) is very low whereas Red intensity (corresponding to the presence of TRPV4) is present.

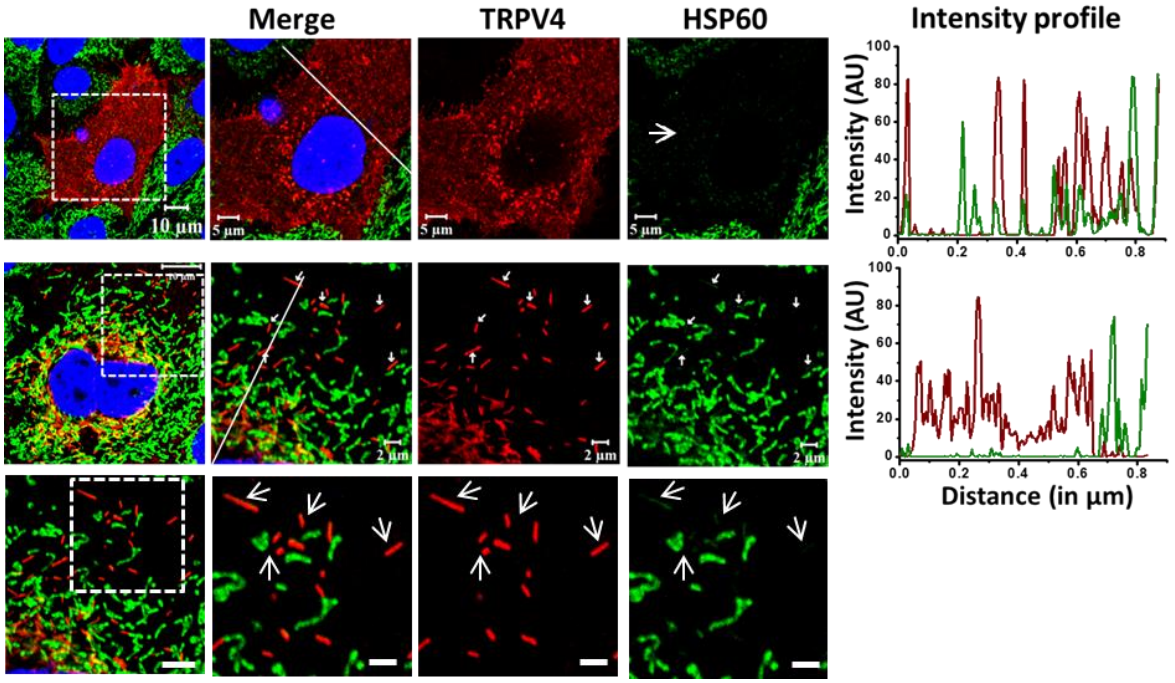

Fig 30: TRPV4 decreases Hsp60 expression in stable cell line. TRPV4-RFP was transiently transfected in HaCaT cells and after fixation cells were immunostained with Hsp60. Subsequently imaging was performed by confocal microscope. Represented image indicate that wherever TRPV4 (Red) was present, the expression of Hsp60 was reduced drastically (upper panel, A). For better visualization zoomed images were taken (lower panel) in which distinct tubular mitochondria were seen (white arrow). Corresponding Hsp60 image showed very faint expression. Which indicate that wherever TRPV4 level is high, Hsp60 expression goes down. On the right side, intensity graph represents TRPV4 (Red) and Hsp60 (Green) intensity which indicate that red peak area is higher as compared to green peak area. Scale bar: 1 µm (Zoomed image)

Furthermore, to explore the effect of TRPV4 agonist (4αPDD) on mitochondrial proteins, CHOK1-V4 and CHOK1-Mock cells were grown. Six hours after addition of TRPV4 agonist (4αPDD), total cellular fraction, cytoplasmic fraction and mitochondrial fraction were isolated for further characterization of Hsp60. All these fractions were analysed by Western blot analysis and Coomassie staining. Specific and prominent band corresponding

to full-length TRPV4 was observed in fractions obtained from CHOK1-V4 and enriched amount of TRPV4 was observed specifically in mitochondrial fraction. Such immunoreactivity was undetectable in fractions obtained from CHOK1-Mock cells. Same fractions were also probed with anti-Hsp60 antibodies and anti α-tubulin antibodies. Apart from the expected band of Hsp60 at 60 kDa, some smaller bands were observed by Western blot analysis, especially in the mitochondrial fraction purified from CHOK1-V4 cells but not from CHOK1-Mock cells. The intensity of such smaller bands are more when CHOK1-V4 cells are treated with 4αPDD (2 μM), suggesting that the full length Hsp60 is subject to degradation within mitochondria and such degradation is enhanced by activation of TRPV4 (**Fig 31**). The Western blot analysis of the same fractions with tubulin antibodies confirmed comparative protein loading and relative purity of these fractions.

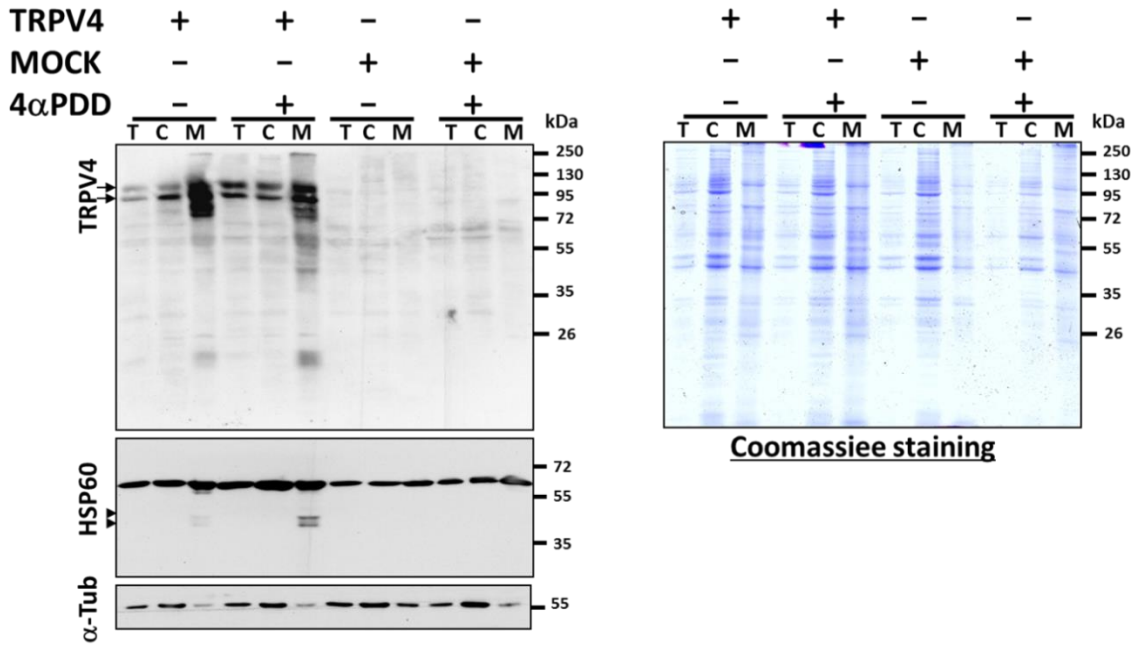

Fig 31: TRPV4 activation leads to degradation of Hsp60 in stable cell line. For more quantitative method, CHOK1-V4 and CHOK1-Mock cells were treated with TRPV4 activator 4αPDD (2 μM) for 6 hours. Subsequently mitochondria were isolated from both CHOK1-V4 or CHOK1-Mock cells and Western blot was performed with anti-TRPV4, anti-Hsp60 and anti-αTubulin antibodies. Represented blots indicate that enriched amount of TRPV4 is present in mitochondrial fraction apart from total and cytoplasmic fraction. Same fractions were probed with anti-Hsp60 and it was observed that apart from the expected size of Hsp60 (at 60 kDa), some small-sized yet specific bands are visible in the lane of mitochondrial fraction of CHOK1-V4. Such smaller bands are not observed in any fractions obtained from CHOK1-Mock cell. It seems that these bands are the specific proteolytic degradation products of Hsp60. Western blot against Tubulin and corresponding Coomassie gels are also shown. (T = Total protein extract, C = Cytoplasmic protein extract, M= Mitochondrial protein extract).

2.3.5. TRPV4 regulates mitochondrial metabolism and Electron Transport Chain (ETC)

Mitochondria are double membrane subcellular organelles that not only produces the cellular energy (ATP) but also important for several physiological functions such as apoptosis, redox potential, Ca^{2+}-homeostasis, synthesis or exchange of many small metabolite and different biosynthetic pathways. Mitochondrial ATP and heat are primarily generated through oxidative phosphorylation by using small metabolite precursor molecules such as carbohydrate (Tricarboxylic Acid Cycle) and lipids or fat (by β-oxidation). Mitochondrial electron transport chain or complexes (Complex I-V), act as carrier molecules by which electron flows across the complexes and finally reduces the oxygen to form water and energy (ATP) [236, 237]. Recent research suggests that Ca^{2+}-homeostasis inside the mitochondria is crucial for cellular physiology and mitochondrial function. Mitochondrial Ca^{2+} accumulation enhances the activity of OXPHOS and ATP production with the help of different Ca^{2+} ion channels. Mitochondrial Ca^{2+} binds with different key dehydrogenase enzymes such as glycerol phosphate dehydrogenase, pyruvate dehydrogenase, NAD^{+}-isocitrate dehydrogenase and α-ketoglutarate dehydrogenase and enhances the activity of these enzymes significantly [238, 239, 240]. Apart from dehydrogenase activity, mitochondrial small metabolite precursor molecules, such as aspartate and glutamate concentrations are also regulated by mitochondrial Ca^{2+}-influx. It has been reported that Aspartate/glutamate exchangers present into the inner mitochondrial membrane binds with Ca^{2+} and regulates its metabolite exchange [241, 242]. However overloading of Ca^{2+} inside the mitochondria is generally removed by "Mitochondrial Permeability Transition pores" (MPT). Indeed mitochondrial MPT leads to decrease in oxidative potential and also decrease in electron chain complex activity in isolated mitochondria and such universal properties have been reported in several pathophysiological conditions [243, 244].

Mitochondria are the important organelle for synthesis and transportation of different lipids, steroids/cholesterol or its derivatives, and metabolite precursors. It was reported that Ca^{2+}-influx inside the mitochondria largely regulates the biosynthesis of mitochondrial metabolite and steroid derivatives by several ways. Therefore abnormality in the mitochondrial energetics results in abnormalities in the synthesis of several small metabolites such as lipid derivatives, cholesterol and its derivatives, NAD^+/NADH, ADP/ATP and other small protein bio-metabolites. Since results described in previous sections indicate that TRPV4 is present in the mitochondria and plays functional role in Ca^{2+}-buffering and mitochondrial potentiality. In this context, understanding of the regulation related to mitochondrial metabolite synthesis and mitochondrial electron transport complex activity is very relevant.

2.3.6. Evolution of TRPV4 and analysis of linked genes involved in metabolite synthesis by Synteny analysis

To explore the molecular evolution of TRPV4, phylogenetic analysis was done by using Bayesian phylogenetic method. Results indicating that TRPV4-mediated functions in *C. elegans* can be rescued by hTRPV4, suggesting that certain functional features of TRPV4 are conserved throughout the evolution. However, hTRPV4 protein shares less identity (~ 20%) and homology (~36%) with Osm9 (TRPV4 homologue in *C. elegans*). Invertebrate homologues sequence of TRPV4 shows several insertions and deletions but TRPV4 sequences are well conserved in vertebrates (**Fig. 32 A**). Our analysis suggests that TRPV4 share high homology and identity during vertebrate evolution.

To understand the pattern of evolution, we calculated the changes in the number of amino acids per 100 amino acids in full-length TRPV4 sequences available for different species ranging from fish to human [245]. Histone (H4) and Cyt C was taken as a positive

control since these proteins are mostly conserved throughout the evolution. Results indicate that TRPV4 was originated at the point of emergence of vertebrates, ca. between 400 to 450 MYA, mostly during the transition of Silurian era from Devonian era (**Fig 32 B**). This analysis indicates that TRPV4 is evolutionary conserved though it is less conserved than histone H4 (highly conserved protein) and Cyt C (semi-conserved protein). Similar comparison indicates that TRPV1 and TRPV4 have been selected via different level of selection pressure during vertebrate evolution.

To investigate the evolution of TRPV4 gene (present in Chromosome 12) in context of biosynthesis pathway, we performed syntenic analysis of TRPV4 locus in different vertebrate genomes using Ensembl genome browser. Vertebrate-specific biosynthesis pathways such as "Cholesterol biosynthesis pathways" was investigated and genes involved in this pathway were analysed. Results suggest that TRPV4 and mevalonate kinase (MVK) genes are clustered into head to head orientation flanked by triad of potassium channel tetramerization domain containing 10 (KCTD10), Ubiquitin protein ligase E3B (UBE3B) and methylmalonic aciduria (cobalamin deficiency) cblB type (MMAB) on the one side and a tetrad of glycolipid transfer protein (GLTP), trichoplein, keratin filament binding (TCHP), G protein-coupled receptor kinase interacting ArfGAP 2 (GIT2) and ankyrin repeat domain 13A (ANKRD13A) in other side of human chromosome 12 within a 600 kb region (**Fig 33**). As mevalonate kinase (MVK) and glycolipid transfer protein (GLTP) are involved in cholesterol biosynthesis pathway [246, 247], this analysis suggests that TRPV4 may play an important role in this biosynthesis pathway.

2.3.7. TRPV4 altered mitochondrial Electron Transport Chain (ETC)

To explore the Role of TRPV4 activation or inhibition on the activities of enzymes involved in mitochondrial electron transport chain, mitochondria were freshly isolated from goat brain and mitochondrial complex activity assay were performed.

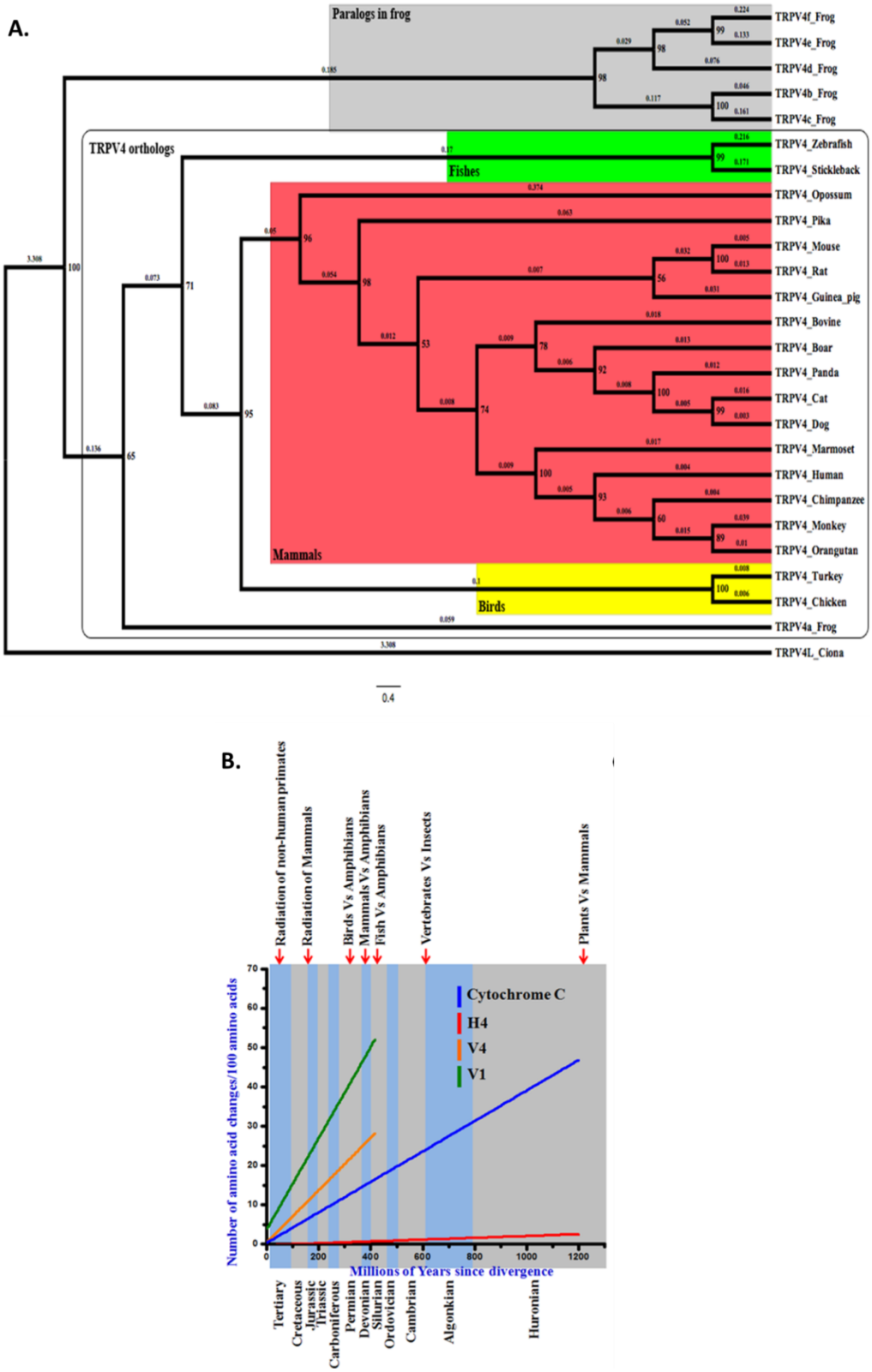

Fig 32: Molecular evolution of TRPV4. A. Bayesian phylogenetic tree illustrates six duplicates of TRPV4 in frogs (one ortholog: TRPV4a and five paralogs: TRPV4b–f, indicated in grey) while a single copy is maintained in other vertebrates (mammals: red; birds: yellow, fishes: green). This tree was generated using MrBayes 3.2 and the percentage posterior probabilities are marked at the node of the branches while mean branch length is marked in decimal on the respective branch. Putative TRPV4-like (TRPV4L) gene (gw1.02q.1264.1) from *Ciona intestinalis* served as ‘‘out-group-control’’. **B.** Conservation analysis of TRPV4. Histone-H4, Cytochrome-C and TRPV1 were used as controls (Kumari et al., 2015) [164].

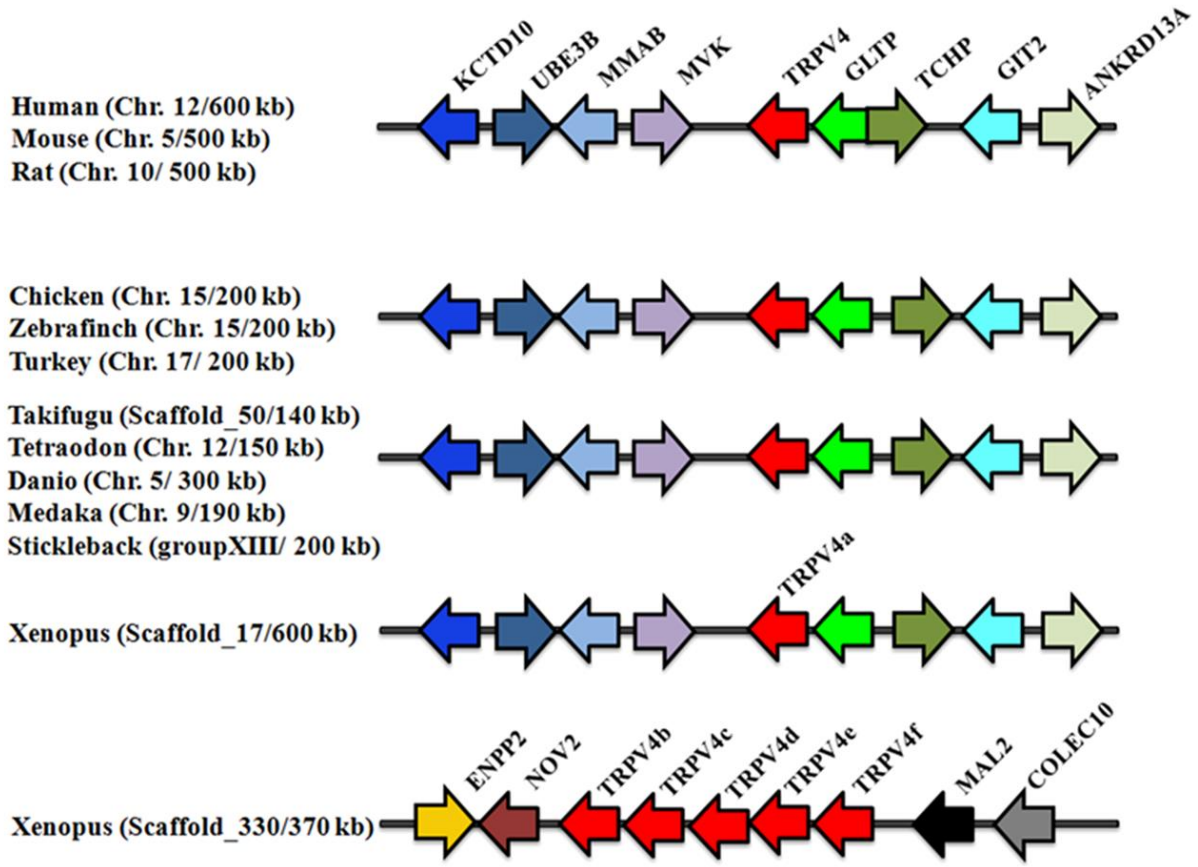

Fig 33: Genetic loci of TRPV4 and Synteny analysis. Two genes (MVK and GLTP) involved in cholesterol biosynthesis pathway have coevolved with TRPV4. This locus has maintained its organization since development of vertebrates (~450 MYA). Another locus in *Xenopus* contains five paralogous TRPV4 originated by tandem duplication.

TRPV4 activator and inhibitor were added in isolated mitochondria and activities were assayed against different mitochondrial Complexes (I-IV). This analysis indicates that neither activation nor inhibition altered the Complex I and Complex III activity (NADH: Ubiquinone oxidoreductase and CoQ Cyt C oxidoreductase) significantly. Addition of Complex I-specific inhibitor (Rotenone) and Complex II-specific inhibitor (Antimycine-A) shows significant decrease in the activities of these Complexes with respect to the control conditions (**Fig 34**). However, activity of Complex II decreased significantly in a dose-dependent manner in presence of TRPV4 activator 4αPDD (1 and 5 μM). At higher concentration of 4αPDD (10 μM) Complex II activity does not differ significantly as comparison to DMSO control.

However in presence of TRPV4 inhibitor RN1734 (20 μM), Complex II activity is significantly increased with comparison to control and 4αPDD (1, 5 and 10 μM). Calcium ionophore, namely Ionomycin and complex II inhibitor 3-NP (100 μM) also cause decreased activity of Complex II. The Complex IV activity was also measured in similar manner. In presence TRPV4 activator, 4αPDD (1 and 5 μM), the Complex IV activity was decreased significantly. In contrast, presence of TRPV4 inhibitor RN1734 (20 μM) increases the complex IV activity significantly as compared to 4αPDD treated sample. In presence of Ionomycin, Complex IV activity is significantly lower as compared to other conditions. Mitochondrial Complex activity assays suggest that TRPV4 activator or inhibitor largely regulate the function of Complex II and IV activity as comparison to the Complex I and III (**Fig 34**).

2.3.8 TRPV4 regulates Membrane Permeability Transition (MPT) pore in isolated mitochondria

Mitochondria formed large conducting pores in the inner mitochondrial membrane in case of over saturation of Ca^{2+} ions and this is known as Membrane Permeability Transition (MPT). To know the effect of TRPV4 activator or inhibitor upon the formation of mitochondrial membrane pore (Mitochondrial swelling), we performed MPT assay with mitochondria freshly isolated from goat brain. MPT results indicate that in presence of TRPV4 activator 4αPDD (10 μM) mitochondria got swollen up and formed MPT and its absorbance decreases with time (**Fig 35**). However in presence of TRPV4 inhibitor RN1734 (20 μM), the mitochondria did not form MPT as compared to others. Addition of $CaCl_2$ (1 mM, a known inducer of MPT) in mitochondria was taken as a positive control. The MPT graph of 4αPDD shows similar changes like $CaCl_2$ in later time point which suggest that TRPV4 activator regulates MPT in isolated mitochondria.

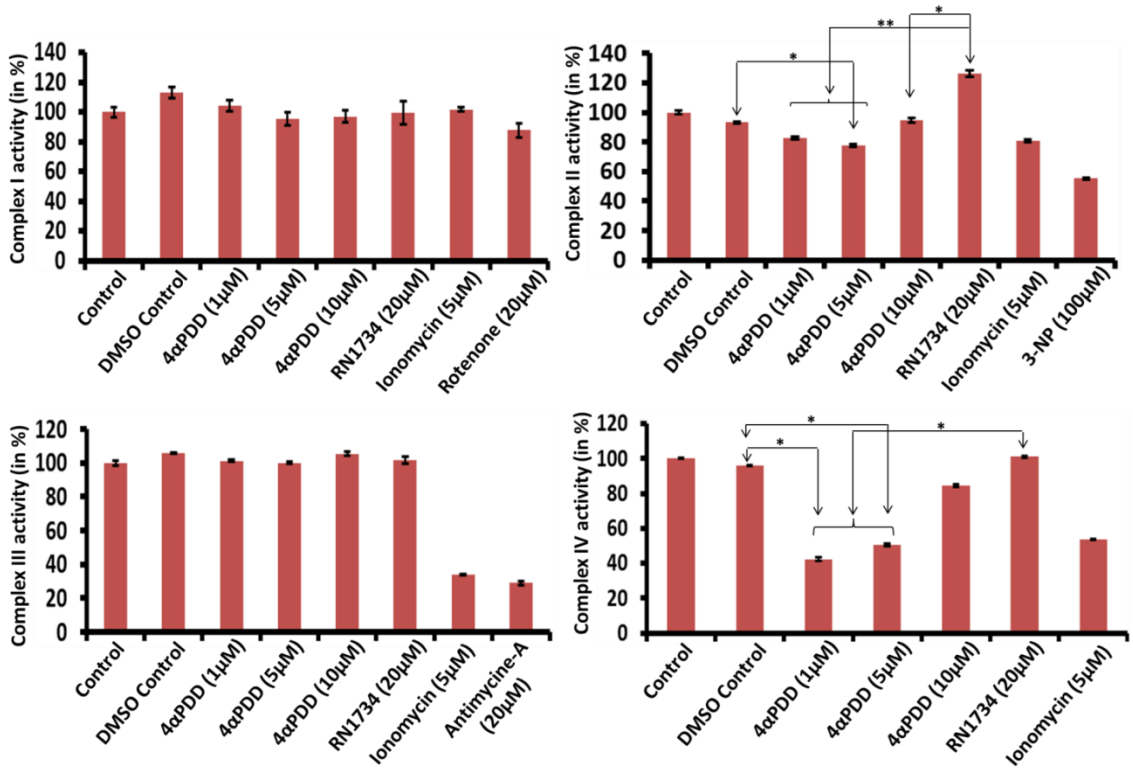

Fig 34: TRPV4 altered mitochondrial Electron Transport Chain (ETC). Enzymatic activity of mitochondrial complex I, II, III and IV was determined with mitochondria freshly isolated from goat brain. Mitochondria were pre incubated with TRPV4 activator/inhibitor in ice for 15 minutes and sample was taken for enzymatic activity. Results indicate that enzymatic activities of Complex I and III are not altered significantly in presence of TRPV4 activator or inhibitor. However enzymatic activities of complex II and IV is significantly altered in presence of TRPV4 activator and inhibitor. Complex II activity graph suggest that activation of TRPV4 by 4αPDD drastically decreases the enzymatic activity whereas inhibition of TRPV4 by RN1734 increases its activity significantly as compared to DMSO control. Enzymatic activity of complex IV was also decreased in presence of TRPV4 activator 4αPDD as compared to control and its increases in presence of TRPV4 inhibitor RN1734. In each represented enzymatic activity graph, Ionomycin (Ca^{2+} ionophore) and complex chain inhibitor shows significant decrease in complex activity.

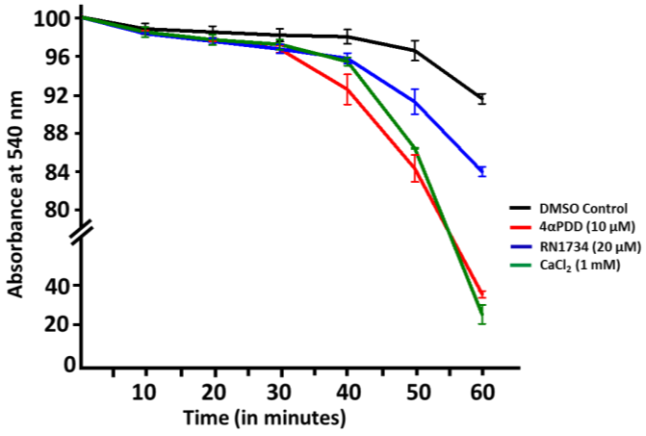

Fig 35: TRPV4 regulates Membrane Permeability Transition (MPT) in isolated mitochondria. Freshly isolated mitochondria from goat brain were pre-incubated with TRPV4 activator or inhibitor and absorbance was taken in different time points. Represented graph suggest that in presence of TRPV4 activator 4αPDD mitochondria formed MPT as comparison to control. However that TRPV4 inhibitor RN1734 reduces the formation of MPT inside the mitochondria. $CaCl_2$ was taken as a positive control for MPT in mitochondria.

2.3.9. TRPV4 regulates different metabolites present in isolated mitochondria

Our previous results indicate that TRPV4 activator or inhibitor alters the mitochondrial transport chain and also regulates the MPT pore, at least in case of isolated mitochondria. Therefore to evaluate the changes in the small metabolites or alteration in the metabolite synthesis pathway/s, freshly isolated mitochondria were treated with TRPV4 activator or inhibitor and all metabolite was extracted in perchloric acid. Subsequently, $_1H^2$ NMR was performed for identification and changes in the metabolite concentration after the TRPV4 drug treatment. The H_2O peak was taken as a reference peak and normalized for all conditions. Merged graph of NMR indicates the appearance of a new peak (3.45ppm) in case of Ionomycin-treated sample and this was not present at all in any drug-treated conditions tested (**Fig 36 A-B**). It was observed that the metabolite peak (5.51–5.53 ppm) reveals chemical shift towards the left side with respect to control. TRPV4 inhibitor RN1734 shows maximum shift as comparison to others (**Fig 36 C**). Peak shifts towards the left side indicating the addition of bulky groups, such as methyl or ethyl group or any electron donating group which can modify the chemical structure of these metabolites and ultimately cause peak shift. Other peaks indicate that in presence of RN1734, concentration of some metabolite increases significantly as compared to other drug-treated conditions (**Fig 36 D**). This peak (2.84 ppm) was completely abolished in presence of Ionomycin. Taken together, results indicate that the activation or inhibition of TRPV4 largely regulates the concentration of metabolites.

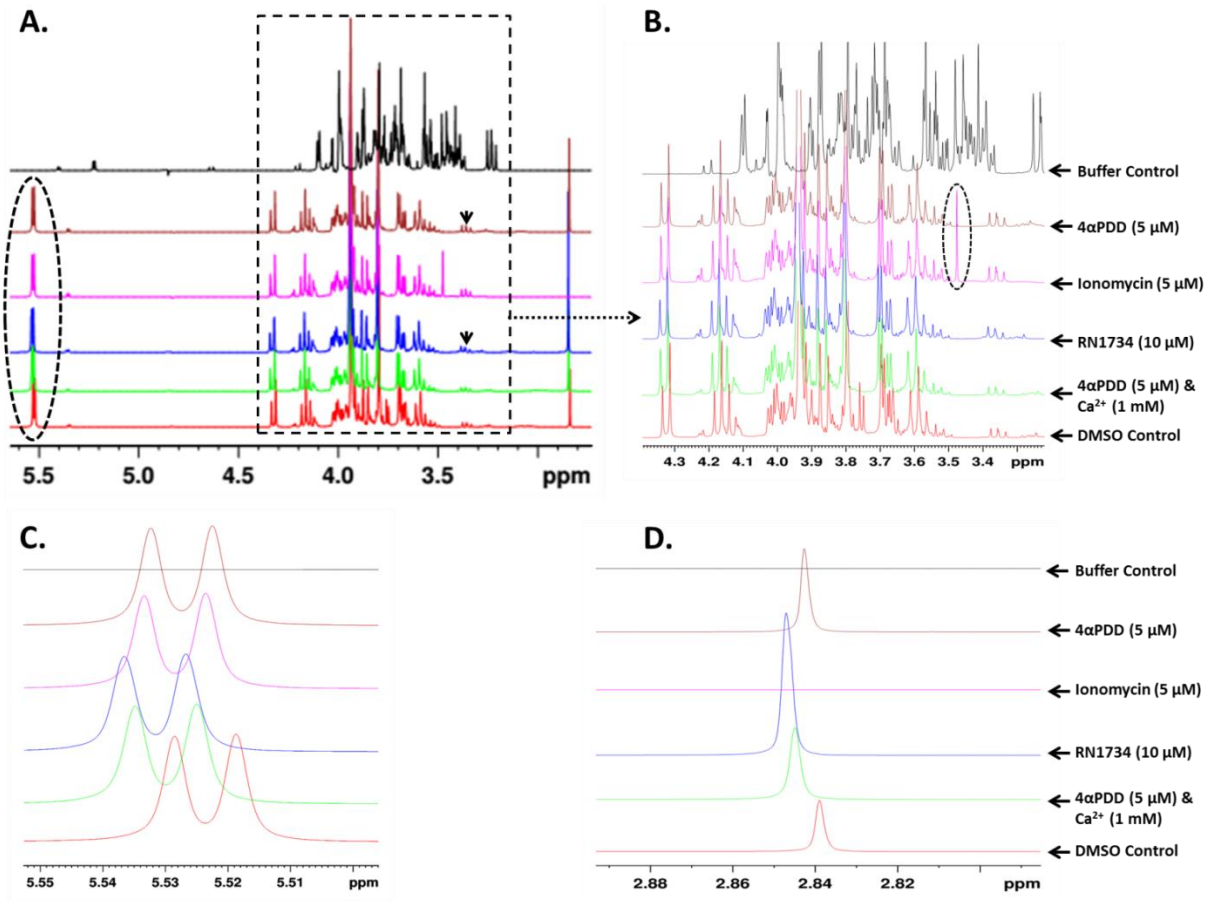

Fig 36: Activation or inhibition of TRPV alters mitochondrial metabolite synthesis. $_1H^2$ NMR (400 kHz) NMR was done with extracted mitochondrial metabolite of goat brain mitochondria. All samples were supplemented with 10% D_20 for peak detection. Merged NMR graph indicating that in presence of TRPV4 activator or inhibitor new peaks was appearing as compare to control or Ionomycin (**A** & **B**). Maximum chemical shift of peak was observed in presence of TRPV4 inhibitor RN1734 as compared to others (**c**). Area under the NMR peak was indicating the concentration of metabolite. Metabolite concentration was increased in presence of RN1734 at peak 2.84 ppm while others peak value, only showing chemical shift not in the area under the peak (**d**). This peak (2.28 ppm) was completely absent in presence of Ionomycin.

2.4. TRPV4 possess novel yet evolutionary conserved Mitochondrial Targeting Signal

Mitochondria are an important organelle for functions related to energy metabolism, different signalling pathway, synthesis of small metabolite precursors and lipid biosynthesis pathway [248]. Most of the mitochondrial proteins (about 99%) are coded by nuclear genes, are synthesized in the cytoplasm and transported or translocated to mitochondria for their functional and structural requirements [248]. Most of the mitochondrial proteins possesses conventional pre-sequences which is essential for its translocation into the mitochondria

called Mitochondrial Targeting Signal (MTS). Mitochondrial pre-sequence is typically a stretch sequence consisting of 15-40 amino acid residues present at the N-terminus of protein and it is generally enriched with positive charged residue [249, 216]. Previously it was believed that nearly all mitochondrial proteins have N-terminal MTS signal and this signal peptide is cleaved by TOM complexes for outer membrane resident proteins but for intermembrane space proteins or matrix proteins, the MTS sequence is not cleaved by TOM complexes [248]. Recent research suggests that MTS sequence can be present in the N-terminus or at the C-terminus [250]. Sometimes it can also be present at the middle position of a mitochondrial protein. For example, outer mitochondrial translocase proteins TOM6 and TOM22 contain a C-terminus anchor sequence which helps in mitochondrial import [217, 251, 252, 253]. Another protein which is present in intermembrane space is cytochrome C containing internal MTS sequence [254]. Some of the mitochondrial proteins contain nonconventional MTS sequence at their C-terminal regions too. Human apurinic/apyrimidinic endonuclease (APE1) plays important role in DNA repair mechanism, preferentially present in nucleus [250]. It was reported that this protein contains dually targeted signal sequence, NLS sequence at the N-terminus for nuclear localization and MTS sequence at the C-terminus for mitochondrial localization [250]. Notably, bioinformatics approach including MitoProt and TargetP failed to predict any mitochondrial signal in APE1 protein. However experimental approach indicates that APE1 protein translocates to the mitochondria in different conditions [250]. Therefore the exact sequence and the properties involved in the specific targeting of proteins to the mitochondria remain inconclusive and further characterization is certainly needed.

Recent experimental reports confirmed that TRPC3 is present in the mitochondria [255]. However, the exact sequence involved in the targeting of TRPC3 in to the mitochondria has not been characterized yet. Since our results suggest that full-length TRPV4

is imported to the mitochondria, we explored if TRPV4 possesses any mitochondrial target signal sequence. In this regard the main aim described in this chapter is to identify the mitochondrial target signal (MTS) sequence present in TRPV4 (592-630aa) and further characterization of that sequence.

2.4.1. *In silico* approach-based identification of novel MTS in TRPV4

The full-length as well as the C-terminus of TRPV4 alone are able to localize within the mitochondria. However, the TRPV4 sequence analysis using **TargetP1.1** does not show any relevant score which can be used as mitochondrial target sequence. Therefore, full-length of hTRPV4 and its systemic deleted sequences were analysed with WoLF PSORT (http://wolfpsort.org/) for predicting their sub-cellular localization. For potential localization in organelles, score was given for each set of sequences **(Represented in table 5)**. Total 19 different deletion sequences were analysed by this software for mitochondrial localization signal. Prediction results suggest that amino acid 592-630 of TRPV4 has the maximum mitochondrial localization score comparison to others and therefore likely to be localized to the mitochondria.

2.4.2. MTS sequence of TRPV4 is sufficient to localize within mitochondria

To confirm that the predicted sequence can indeed localize to the mitochondria, we cloned these 39 amino acid long sequence (AA number 592-630) into pEGFPN3 vector [named as TRPV4-(592-630)-GFP]. We expressed this segment in HaCaT cells along with the mitoDsRed (as mitochondrial markers) and performed colocalization experiments.

AMINO ACID NO	CYTOSOL	PM	ER	VACUOLAR	VESICLES OF SECRETORY SYSTEM	GOLGI	NUCLEAR	MITO	PEROXISOME
1-871	--	39.1	43.5	--	4.3	4.3	4.3	4.3	--
61-871	--	52.2	43.5	--	--	--	4.3	--	--
121-871	--	47.8	43.5	--	--	--	4.3	4.3	--
181-871	--	34.8	43.5	4.3	4.3	4.3	4.3	4.3	--
241-871	--	43.5	39.1	--	4.3	4.3	4.3	4.3	--
301-871	--	56.5	26.1	--	--	4.3	4.3	8.7	--
361-871	--	60.9	30.4	--	4.3	--	--	4.3	--
421-871	--	56.5	30.4	--	4.3	4.3	--	4.3	--
481-871	--	22.2	33.3	22.2	11.1	--	--	11.1	--
541-871	--	--	66.7	11.1	--	11.1	--	11.1	--
601-871	--	--	66.7	--	--	11.1	--	11.1	--
661-871	39.1	--	13	--	4.3	4.3	17.4	17.4	4.3
721-871	56.5	--	--	--	--	--	21.7	13	--
781-871							69.6		
601-840	--	--	66.7	--	--	11.1	--	11.1	--
601-660	11.1		22.2			44.4		22.2	
601-630	13	--	26.1	4.3	--	21.7	8.7	26.1	--
590-630	21.7		17.4	4.3		13		43.5	
592-630	17.4	--	21.7	4.3	--	8.7	--	47.8	--

Table 5: Prediction of subcellular organelle localization of TRPV4. Systemic deletion of hTRPV4 sequence was analysed with subcellular localization prediction software (WoLF PSORT site) and given score was represented in tabular form for all subcellular organelles. Blue colour indicating the amino acid stretch (592-630) which has highest mitochondrial localization score.

This experiments suggest that TRPV4-(592-630)-GFP localizes with mitoDsRed and it is present in mitochondria. In a similar manner, TRPV4-(592-630)-GFP was expressed and cells were immunostained with anti-Hsp60 antibody. This co-localization experiments indicate that TRPV4-(592-630)-GFP is indeed present in mitochondria and colocalizes with Hsp60. We therefore named this amino acid stretch (592-630) as TRPV4-MTS (**Fig 37**).

Previous reports suggest that the MTS sequence of TRPV4 harbour at least 11 different point mutations and each one is responsible for different channelopathies [176]. Out of these 11 mutations, few of these causes gain-of-function (R616Q and V620I) and other mutations lead to several pathophysiological disorders [177]. Since this mutation lies in this derived MTS sequence, therefore characterization of these mutants with respect to

mitochondrial targeting as well as functions were explored. In this regard, 4 different point mutations (R616Q, F617L, F618P and V620I) were cloned into the pEGFPN3 vector and subsequently analysed for its mitochondrial localization (**Fig 39**). Apart from MTS sequence of TRPV4, some other sequences of TRPV4 were also cloned into RFP or GFP vector and expressed in HaCaT cell, and analysed for their localization in to the mitochondria. Schematic diagram of all the constructs used in this study is represented (**Fig 38**).

Furthermore to explore the presence of mitochondrial targeting signal is present in this region (**Fig 38**) a bioinformatics approach was performed through **TargetP.1** website. This website prediction for mitochondrial pre-sequence (mTP) and Reliability Class (RC) score were represented in the tabular form (**Table 6**). Greater the RC value higher the prediction for its localization in mitochondria. In spite of the low TargetP.1 score, experimental results suggest that only full-length TRPV4 (1-871 aa), TRPV4-MTS (592-630 aa) and TRPV4-C terminus (718-871 aa) translocate to the mitochondria.

2.4.3. MTS sequence of TRPV4 is conserved throughout the vertebrate evolution

To explore if the Mitochondrial Targeting Signal of hTRPV4 is conserved in all species, hTRPV4-MTS sequence (592-630) was aligned in Mega 5 software package with full-length TRPV4 from more than 50 species. Alignment results indicate that TRPV4-MTS sequence is conserved throughout the vertebrate evolution. However in some species namely *Hyla japonica* (Japanese Tree frog) and *Oreochromis niloticus* (Nile tilapia) alignment was substituted with similar amino acids (**Fig 40**). Furthermore, to analyse the conservation of the MTS sequence (592-630) with respect to full-length TRPV4 (871 aa), a comparative conservation analysis was performed (box plot of divergence from more than 50 species) (**Fig 41**).

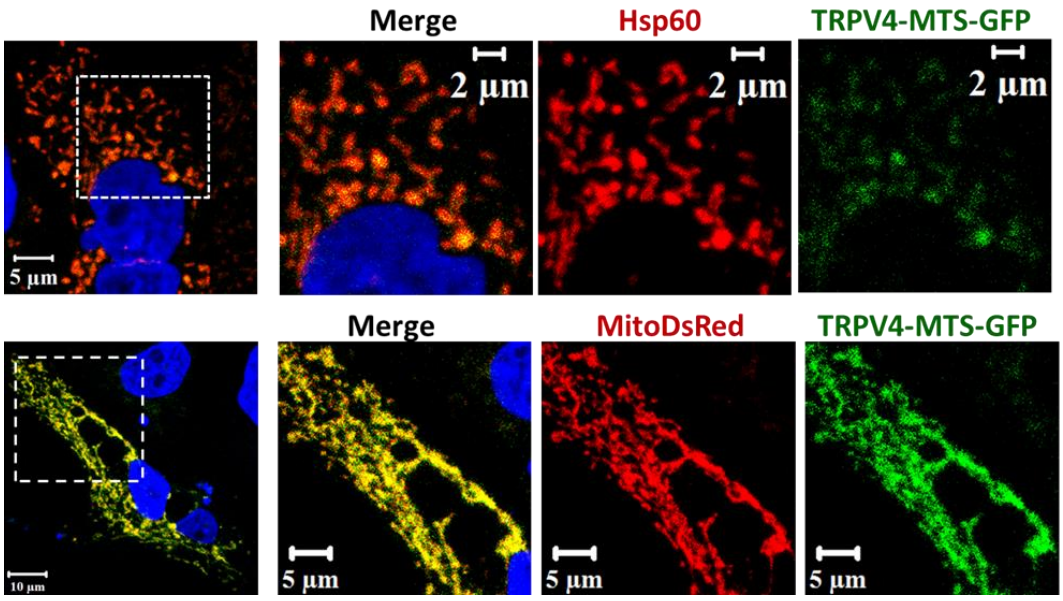

Fig 37: TRPV4-MTS localizes in mitochondria. Confocal images demonstrating that TRPV4-MTS-GFP colocalizes with different mitochondrial markers, namely with Hsp60 and mitoDsRed. TRPV4-MTS-GFP shows colocalization with mitochondrial protein.

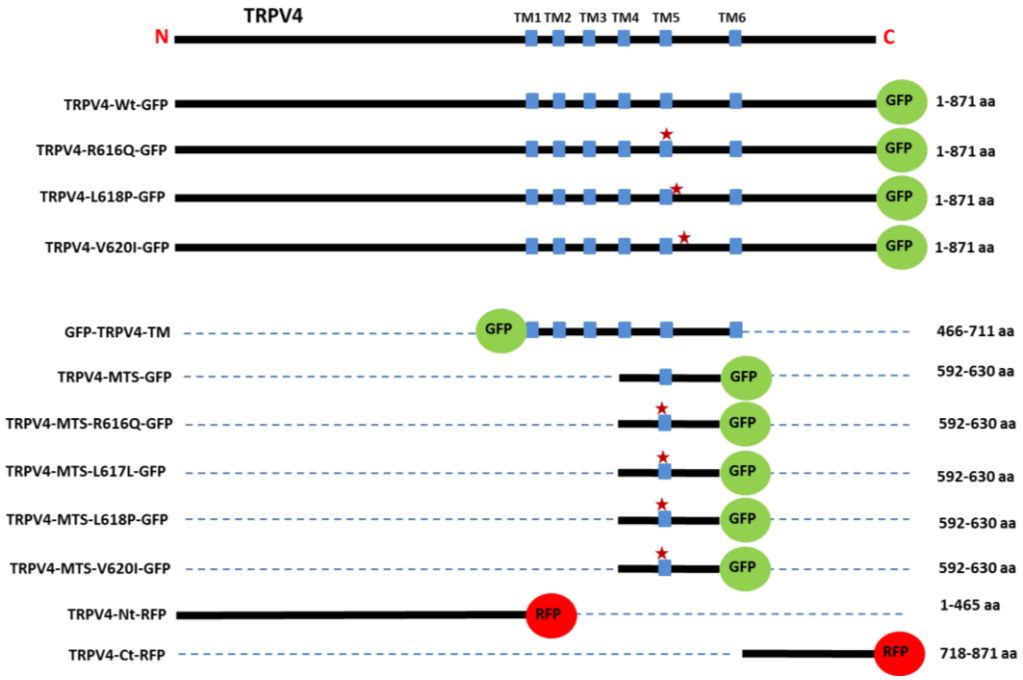

Fig 38: Schematic representation of TRPV4 deletion constructs used for mitochondrial localization. Schematic representation of constructs representing different deletion fragments of TRPV4 used in this study. Position of GFP or RFP attached eiher at the N-terminus or at the C-termnus is also indicated. The constructs with delatorious point mutations are indicated (red star). TRPV4-MTS and its mutants are described in this chapter and other constructs (TRPV4-Wt-GFP, TRPV4-R616Q-GFP, TRPV4-L618-GFP, TRPV4-V620I-GFP, GFP-TRPV4-TM, TRPV4-Nt-RFP and TRPV4-Ct-RFP) are mention in previous chapter (**chapter 2**).

Sequence of hTRPV4	Length	mTP Predicted score	RC	Colocalization with Mitochondria
TRPV4	1-871	0.066	1	Yes
Full TM	466-711	0.027	1	No
MTS	592-630	0.092	5	Yes
	R616Q*	0.040	4	No
	F617L*	0.071	5	No
	F618P*	0.218	5	No
	V620I*	0.100	5	No
TRPV4-Nt	1-465	0.066	1	No
TRPV4-Ct	718-871	0.104	3	Yes

Table 6: Prediction of TRPV4 Mitochondrial targeting signal: *In silico* approach was applied (Target P1.1 website) to predict the mitochondrial localization of different TRPV4 deletion constructs or point mutant constructs. Reliability Class (RC) score indicates the strong prediction. Lower the RC value more strong is the localization signal. Different point mutations (Indicated in red star) present within the MTS region are also included for this anaysis. Based on the colocalization with mitochondrial markers, "Yes" or "No" score was made for each constructs.

This result suggests that as TRPV4-MTS is more conserved in comparison to the full-length TRPV4 throughout the vertebrate evolution. Histone (an example of a conserved protein during the course of evolution) was taken as a positive control. Next we analysed if the MTS sequence of hTRPV4 is conserved in all other TRPVs (human TRPV1-6). The MTS of hTRPV4 was aligned by Mega 5 software and the results indicate that TRPV4-MTS is fairly conserved in all hTRPV family ion channels (**Fig 42**). Most conserved sequence of MTS was represented by red star. Among all aligned sequences only in two postions, the consensus score was less than 5 and rest other sequences are highly conserved.

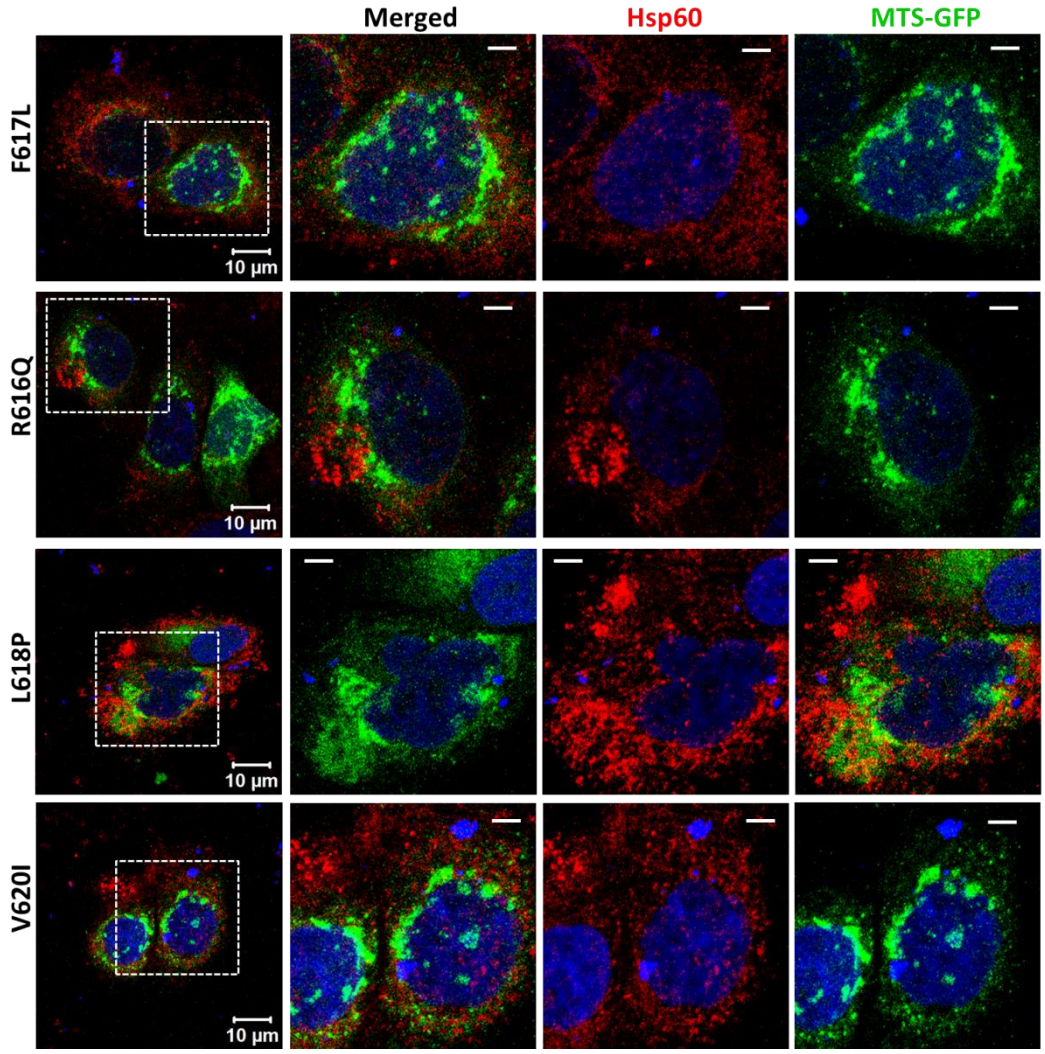

Fig 39: TRPV4-MTS mutants not localizes in mitochondria. Confocal images demonstrating that TRPV4-MTS-GFP mutants (R616Q, F617L, F618P and V620I) does not colocalizes with mitochondrial markers protein Hsp60.

As we discussed earlier, mitochondrial targeting signal are amphipathic in nature [249, 216]. In this regard we analysed the distribution of charges in this region. For that purpose, a homology modelling was performed (based on reported cryo-EM structure of TRPV1) [43]. TRPV4-MTS modelling was done with MODELLER 9.14 sowtware. Structure of TRPV4-MTS as visualized by ribbon-shapped model indicating its helical property and space-filled structure of TRPV4-MTS showing the positive charges are clustered at the N-terminus of this helix (**Fig 43**).

2.4.4. MTS of TRPV4 -interacts with mitochondrial proteins

To explore if TRPV4-MTS interacts with different mitochondrial proteins, pull-down experiments were performed using protein extract prepared from mitochondria isolated from goat brain. TRPV4-MTS was cloned into pGEX-6P1-GST vector and the fusion protein was expressed in *E. coli*. Only GST was used as a negative control. After expression, protein was immobilized on Glutathione Sepharose beads and mitochondrial protein extract was added in presence or in absence of Ca^{2+}, and combination of GTP/ATP. Subsequently eluted samples were probed for different mitochondrial protein antibodies namely with anti-Hsp60, anti-Mfn1, anti-Mfn2 and anti-Cyt C. Pull down results suggest that TRPV4-MTS interacts with Hsp60 in presence as well as in absence of Ca^{2+}, ATP and GTP (**Fig 44 A**). This suggests that TRPV4-MTS interaction with Hsp60 is independent of Ca^{2+}, ATP, and GTP. In the same experimental conditions, mitochondrial fusion regulatory proteins, namely Mfn1 and Mfn2 are not detectable suggesting these regulatory proteins are possibly not interacting with TRPV4-MTS. However pull down experiments indicate that Cyt C interacts with TRPV4-MTS specifically only in the presence of Ca^{2+} (**Fig 44 A**). Furthermore to explore if the interaction with Cyt C with TRPV4-MTS is direct, pull-down experiment was performed with purified Cyt C (oxidised form). GST-TRPV4-MTS was immobilized on Glutathione Sepharose beads and purified Cyt C protein was added for interaction in presence of EGTA (Ca^{2+} chelator) and different concentration of Ca^{2+}. Subsequently eluted samples were probed with anti-Cyt C antibody. Results indicate that Cyt C interacts with Ca^{2+} in dose-dependent manner and in presence of EGTA (5 mM), Cyt C interaction decreased as comparison to others (**Fig 44 B**). Such type of interaction was not observed with GST protein (Negative control). This result implies that Cyt C interaction with TRPV4-MTS is very specific and it is a Ca^{2+}-sensitive interaction.

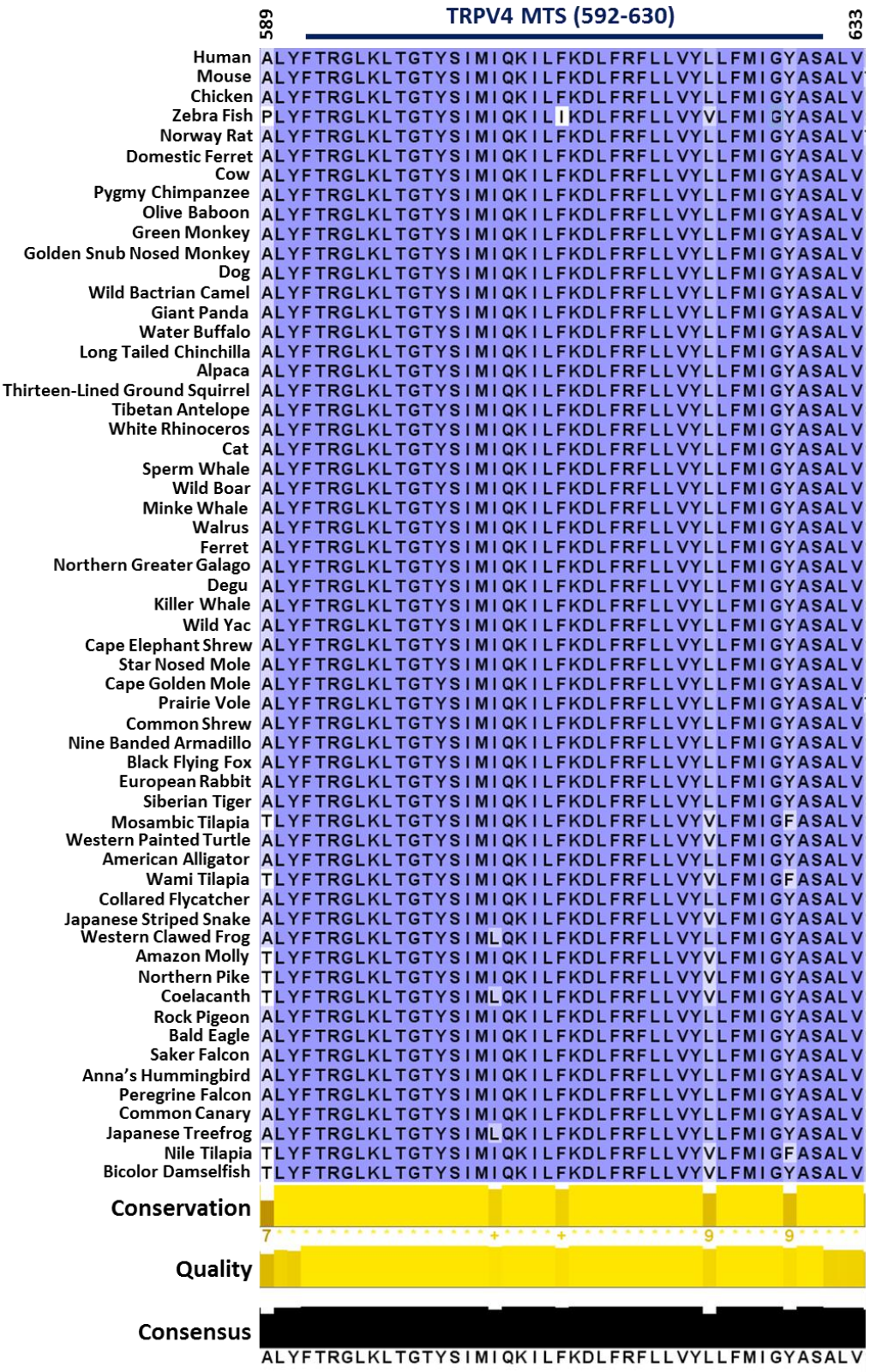

Fig 40. The MTS sequence of TRPV4 is conserved thoroghout the vertebrate evolution. The MTS of hTRPV4 was aligned with the full-length TRPV4 sequences from other species using the default parameters of MUSCLE in Mega 5 software. The alignment was further visualized using JalView. High homology of this squence suggest that this region is highly conserved in mammals. Substitution in few positions by similar amino acids was observed only in fish and in tree frog.

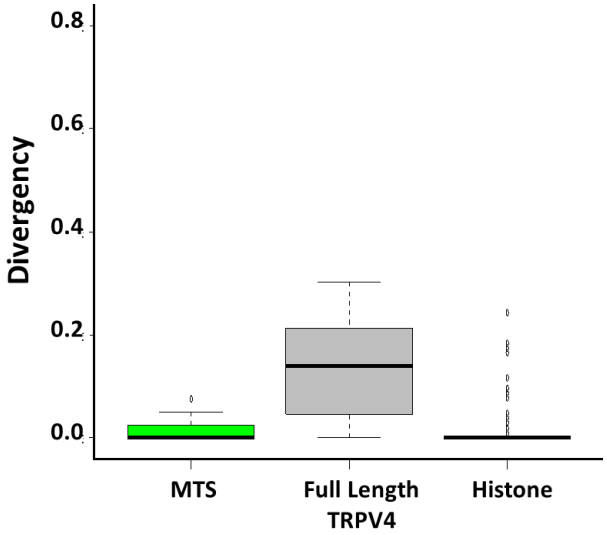

Fig 41. MTS of TRPV4 is more conserved as compared to the full-length TRPV4. Conservation is calculated from its divergence value (lower and higher values indicate more and less conservation respectively). Graph indicating that the TRPV4-MTS sequence is highly conserved almost in all species.

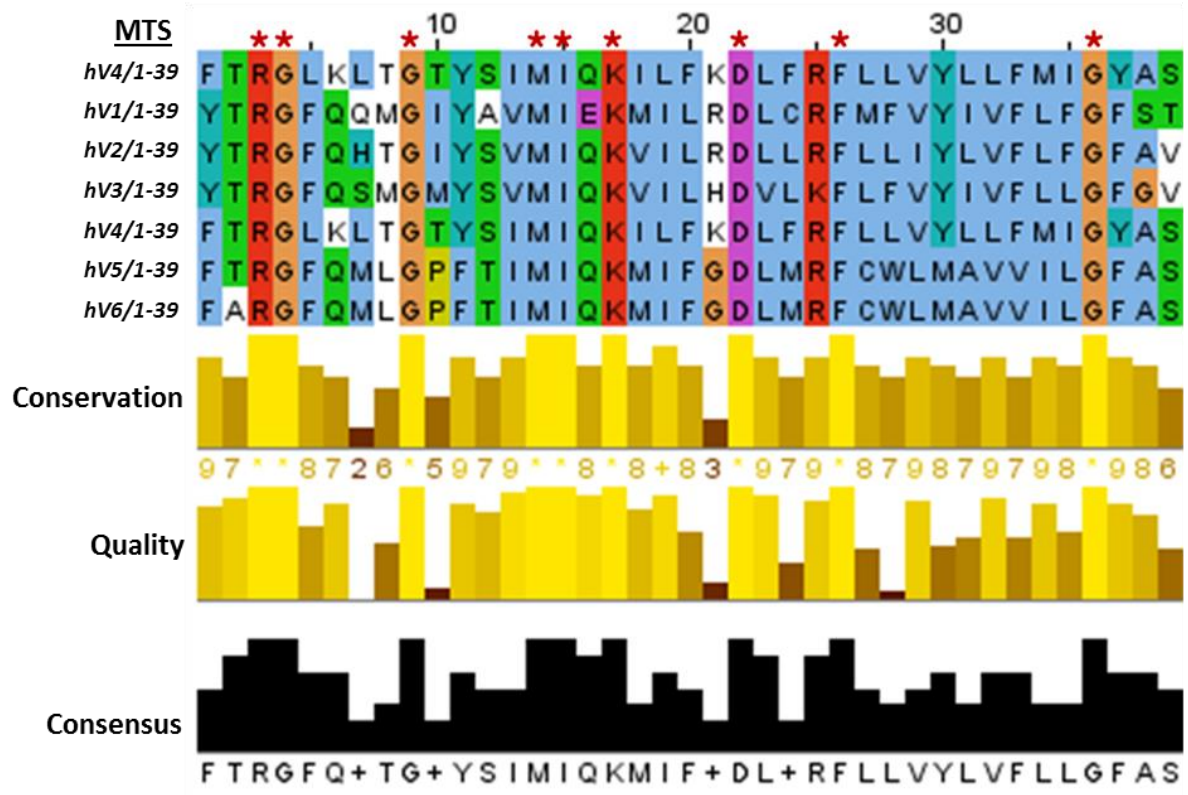

Fig 42. MTS sequence of TRPV4 is conserved in all other TRPV family members. The MTS of hTRPV4 was aligned (using the default parameters of MUSCLE in Mega 5 software package) with the full-length sequence of other TRPV members. The resulting alignment was further analysed using JalView. Results of conservation plot suggest that this region is highly conserved with homologous regions of other TRPV channels.

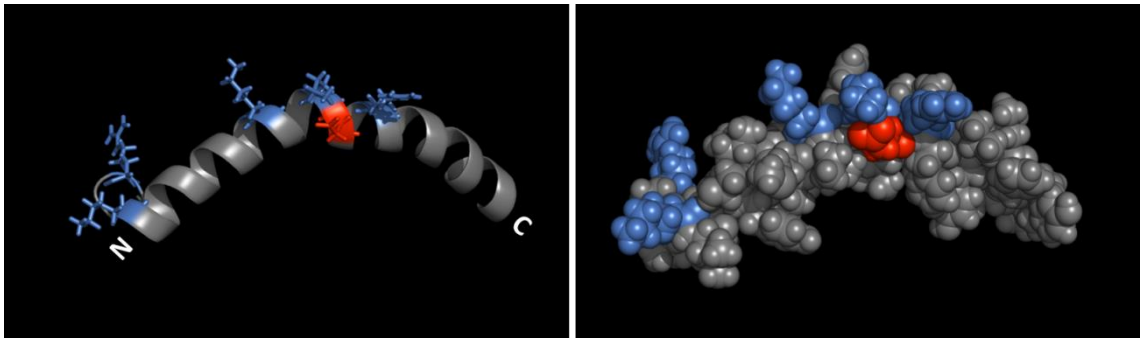

Fig 43. TRPV4-MTS structre prediction by homology modeling. A homology model of TRPV4 was made with MODELLER 9.14 using the B chain of TRPV1 (PDB Code: 3J5P) and energy minimized with YASARA Structure. The model quality was checked with MolProbity. The MTS region was extracted from the modelled TRPV4 structure. Left side image depicting the the ribbon-shaped model whilethe space-filled model is indicated in the right side. The positively charged and negatively charged residues are colored in marine blue and red respectively.

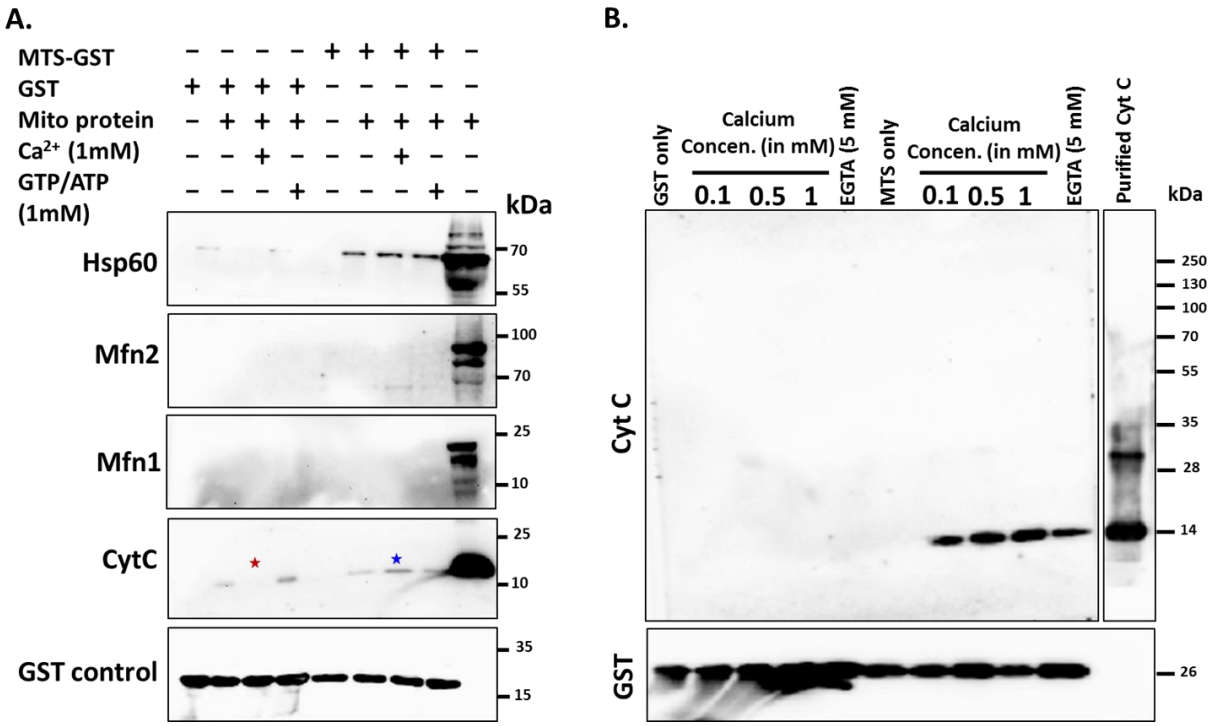

Fig 44: TRPV4-MTS interacts with mitochondrial protein. A. Pull down experiment was performed with GST-TRPV4-MTS and mitocondrial extract (isolated from goat brain) in presence of Ca^{2+} or GTP/ATP. Eluted pull down samples were probed with anti-Hsp60, anti-Mfn2, anti-Mfn1 and anti-Cyt C antibody. Results suggest that mitochondrial matix protein Hsp60 binds with TRPV4-MTS in a Ca^{2+} as well as ATP/GTP independent manner. Mitochondrial fusion regulatory proteins Mfn1 and Mfn2 do not show any interaction with TRPV4-MTS. Anotther mitochondrial protein Cyt C shows Ca^{2+}-sensitive interaction with TRPV4-MTS (indicated as blue star). **B.** Representing pull down experiments showing the direct interaction of purified Cyt C with TRPV4-MTS in presence of different concetration of Ca^{2+} and EGTA. Results indicating that Cyt C interaction with TRPV4-MTS increses in presence of higher concentration of Ca^{2+}. For each conditions, GST protein alone was taken as negative control.

2.5. Characterization of TRPV4 in sperm cells and associated mitochondrial dysfunction

Presence of TRPV4 in mitochondria and its importance in the regulation of mitochondrial structure as well as function in different cell line has been described in the previous chapters. In this chapter, effect of TRPV4 activation or inhibition upon the mitochondrial structure-function relationship was characterized using mature spermatozoa of different species as model systems. Sperm cells have high (and often almost fixed) number of mitochondria and are known to be transcriptionally as well as translationally silenced. Therefore, in order to study the effect of TRPV4 on the mitochondrial organization, mature sperm cells provide an excellent model system. In addition, specific sperm functions are mostly conserved throughout the evolution. In this context, it is relevant to study the regulation and characterization of TRPV4 in sperm with respect to mitochondrial organization and energetics. The work described in this chapter reveals the role of TRPV4 in the mitochondrial structure-function relationship in sperm cells in details.

2.5.1. TRPV4 is endogenously expressed in mature sperm cells ranging from lower to higher vertebrates

The sequence analysis of TRPV4 from different species indicates that TRPV4 is conserved in all vertebrates ranging from fish to human [164]. Therefore, comparative analysis of the localization pattern of TRPV4 in different regions of spermatozoa (head, neck and tail) was performed for different vertebrate classes. At least one species from five classes of subphylum vertebrata was selected for this study. Spermatozoa were collected and immunostained with TRPV4 antibody to visualize the localization of TRPV4 in spermatozoa. The specificity of antibody was confirmed by pre-incubating the antibody with a blocking peptide which completely abolished the immunostaining.

In the three classes of cold blooded vertebrates, a distinct difference in localization pattern was observed. While in fish/piscean group (osteichthyes class), TRPV4 was primarily seen at the tail and neck region of Rohu (*Labeo rohita*) sperm (**Fig 45 A**); for reptilian class TRPV4 was only detectable in the head region of house lizard (*Hemidactylus leschenaultii*) sperm (**Fig 45 C**). In contrast, for amphibian class, TRPV4 expression was present in head, neck and tail regions of Asian common toad (*Duttaphrynus melanostictus*) sperm (**Fig 45 B**).

Showing a similar trend of TRPV4 expression as in amphibian spermatozoa, warm blooded animals show TRPV4 distribution throughout the sperm. For the avian class, TRPV4 expression although present in all the regions, it was primarily concentrated in the sperm tail of duck (*Anas platrhyncos*) (**Fig 45 D**). As mammalian example, spermatozoa of bull (*Bos gaourus*) were taken which showed a faint yet distinct expression of TRPV4 in all the three regions (**Fig 45 E**). All these results suggest that TRPV4 is endogenously present in spermatozoa and such expression is evolutionarily conserved in all vertebrates.

2.5.2. TRPV4 localizes in sperm mitochondria: Analysis from different vertebrates

TRPV4 is endogenously expressed and distributed in different region of sperm, especially in the neck region. Therefore the next aim was to investigate if TRPV4 colocalizes with mitochondrial markers. Based on their localization pattern in neck region, fish, duck and human sperm were selected for co-localization experiment with mitochondrial markers such as mitochondrial specific dye (MitoTracker Red) or antibodies raised against specific mitochondrial markers (such as Hsp60, etc.). Subsequently immunostaining was performed with TRPV4 antibody and confocal microscopic images were acquired. Colocalization experiments indicate that not all but few mitochondria distinctly colocalizes with TRPV4 (**Fig 46**). Particularly in Fish and Human sperm, TRPV4 is enriched in mid piece region and there it colocalizes with few mitochondria that are labelled with MitoTracker Red (indicated

by arrow). Furthermore colocalization experiment was also performed with using antibody against Hsp60 in fish sperm. This result also suggested that TRPV4 colocalizes with mitochondria in neck region.

Similarly, in duck sperm, where atypical mitochondria are also present in the tip region, TRPV4 colocalization is observed in both, the tip region (of head) as well as in the mid piece of mitochondria. Duck sperm mitochondrial localization were analysed by confocal and Super Resolution Structured Illumination Microscopy (SR-SIM). Confocal microscopy reveals the presence of elongated and cylindrical nucleus within the head, but super-resolution microscopy distinctly revealed that the nucleus is actually bifurcated at the tip (**Fig 47 A-D**). In case of duck sperm, mid-piece labelled with MitoTracker Red suggesting that this region actually contains functional mitochondria (**Fig 47 A-B)**. However, both confocal and SR-SIM images reveal that the MitoTracker Red labelling can also be observed at the tip of the sperm head (**Fig 47 C-D)** [256]. Furthermore, sperm tip also showed the staining for other important mitochondrial markers such as Mitochondrial membrane ATP synthase (F_1F_0 ATP synthase or Complex V) and mitochondrial outer membrane protein Mitofusin2 (Mfn2) (**Fig 48 A-D**). Results indicate that in duck sperm, both tip and neck regions contain functional or atypical mitochondria and these regions seem to contain functional TRPV4 channel.

2.5.3 TRPV4 channel modulation affects Hsp60 level present in sperm

In previous chapter (Chapter 3) it has been described that TRPV4 regulates the level of Hsp60 in the mitochondria. As TRPV4 is endogenously present in the sperm cells, it was explored if TRPV4 can regulate the mitochondrial potentiality and mitochondrial matrix protein Hsp60 level.

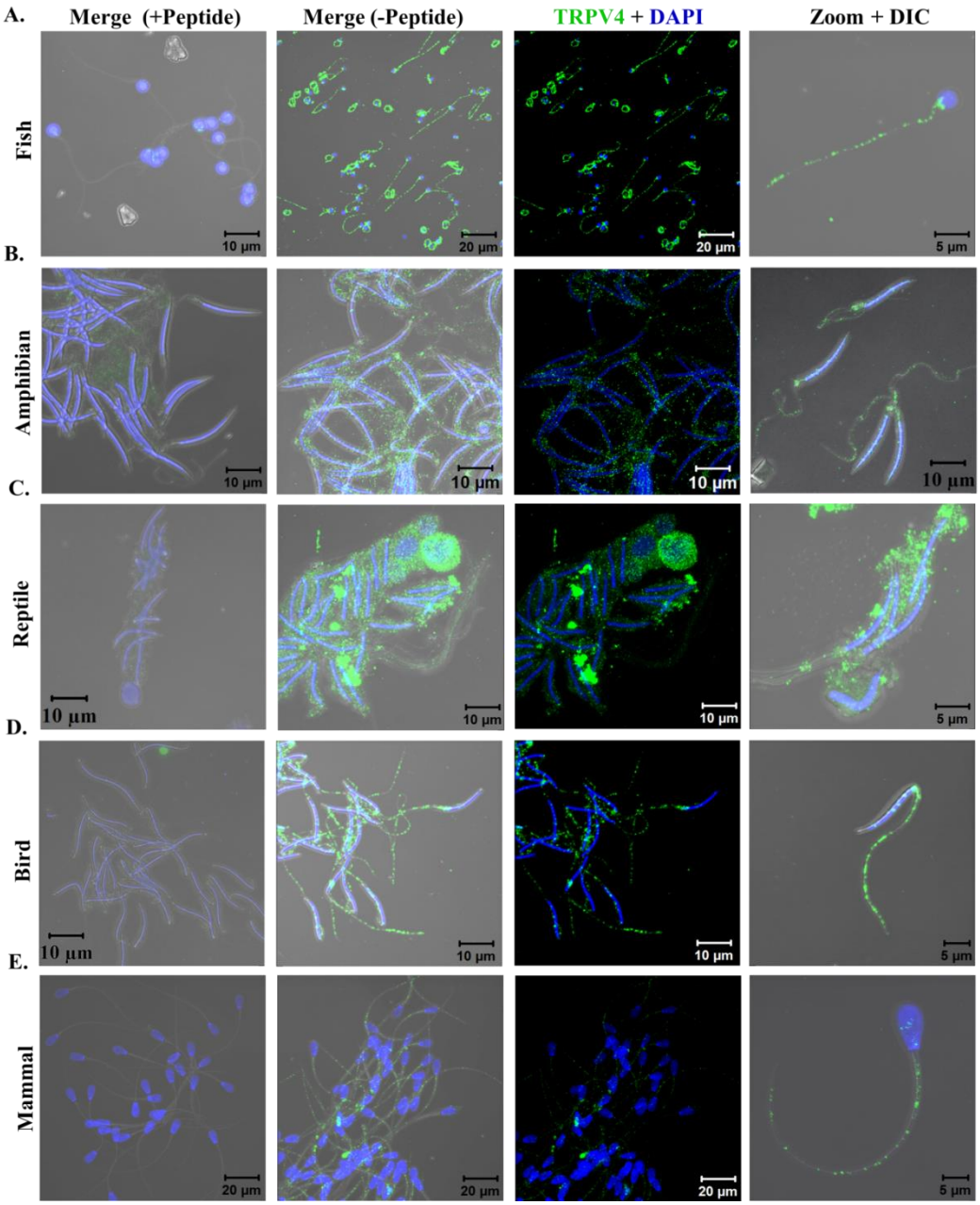

Fig 45. TRPV4 is endogenously expressed in vertebrate sperm cells. Confocal images demonstrating the presence of TRPV4 in Piscean (**A**, rohu fish), amphibian (**B**, common toad), reptilian (**C**, house lizard), avian (**D**, duck) and mammalian (**E**, bovine) sperm are shown. Cluster of sperm cells were immunostained for TRPV4-specific antibody in presence (left most column) or absence of a specific blocking peptide. Fluorescence images representing TRPV4 (green) and DNA (blue) were merged with DIC images. In the extreme right panel, confocal images of TRPV4 expression and localization in single sperm from different species are shown. In Piscean sperm, strong TRPV4 immunoreactivity is observed in the neck regions as well as the tail. In reptilian and amphibian sperm, faint yet specific TRPV4 expression is localized in the neck as well as in the tail regions. In avian sperm, it is localized throughout the sperm, but expression is highest in the tail region. In mammalian sperm TRPV4 is exclusively localized in the neck and tail regions whereas faint expression is present in the post-acrosomal region of the head.

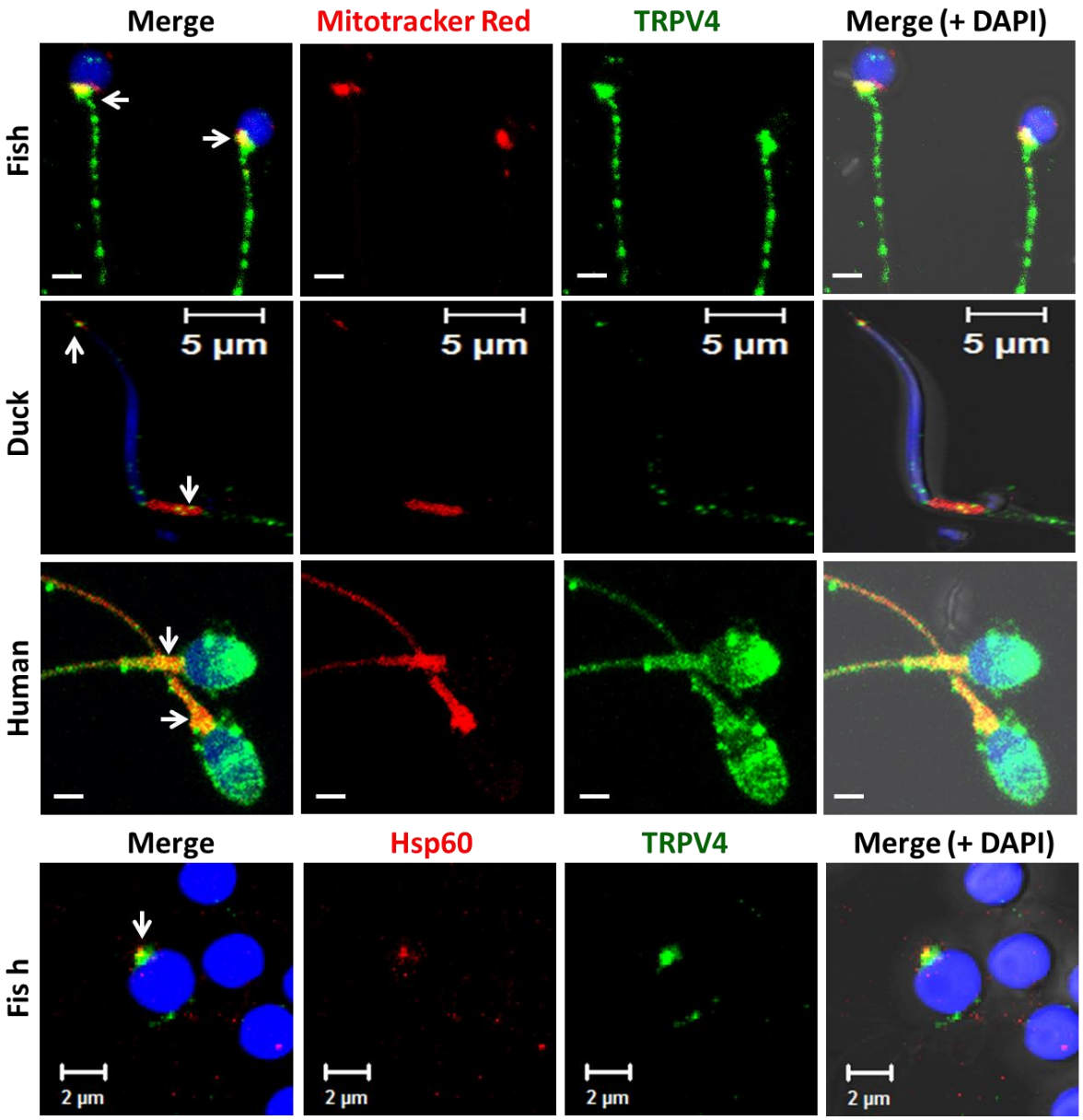

Fig 46: TRPV4 localizes in sperm mitochondria of different vertebrates system. These confocal images demonstrate the colocalization (indicated by arrows) of TRPV4 with mitochondrial markers in fish, duck and human sperm cell. Not all sperm mitochondria revels the presence of TRPV4 in the neck region. In case of duck sperm, apart from mid piece region, colocalization is also observed at the tip of the head (also see fig 47-48). In lower panel, immunostained image depicting that TRPV4 (green) colocalizes with Hsp60 (red) in the neck region in fish sperm.

To know the effect of TRPV4 modulation upon the duck sperm, we incubated the sperm at 39°C (specific body temperature suitable for duck sperm physiology) for 2 hours in presence of TRPV4 activator or inhibitor. Subsequently western blot was performed with anti-Hsp60 antibody. Western blot results indicate that presence of TRPV4 activator (4αPDD,

1 μM) induces degradation of Hsp60 which was observed as faint bands (**Fig 49**). These faint bands (degraded products) of Hsp60 were not observed in other cases such as in presence or absence of TRPV1 activators or inhibitors (high exposure blot). It suggests that activation of TRPV4 but not TRPV1 results in degradation of Hsp60 and therefore also suggests specific signalling events induced by TRPV4 activation only.

To explore if such changes in the Hsp60 level in response to TRPV4 activation is common in other species too, we explored bull sperm as a model system and performed immunofluorescence analysis. Bull sperm were treated with TRPV4 activator 4αPDD (1 μM) for 2 hours at 37°C. The mitochondria of the same samples were labelled with MitoTracker Red (Selectively bind to respiring mitochondria and become fluorescent after oxidation). Results indicate that in presence of TRPV4 activator 4αPDD decreases Hsp60 level as compared to the control conditions (**Fig 50**). Similarly MitoTracker Red labelling in sperm cell also decreases in presence of 4αPDD, which suggest that TRPV4 activator decreases the mitochondrial potentiality. Fluorescence intensity of both Hsp60 and MitoTracker Red was decreased drastically in presence of TRPV4 activator and overall very less colocalization was observed as comparison to control (indicated by arrow) (**Fig 50**).

2.5.4 Effect of TRPV4 channel activation on sperm mitochondrial organization and structure

Sperm mitochondria assembled in an organized fashion to form tight helix around the flagella of midpiece region [257]. Intact mitochondrial morphology and its coiling too are very much important for sperm motility and capacitation process [258, 259]. To know the changes in mitochondrial morphology and its coiling in bull sperm, TRPV4 activator 4αPDD (1μM) was added in sperm and incubated for 2 hours at 37°C. Subsequently, MitoTracker Red was added to label the mitochondria.

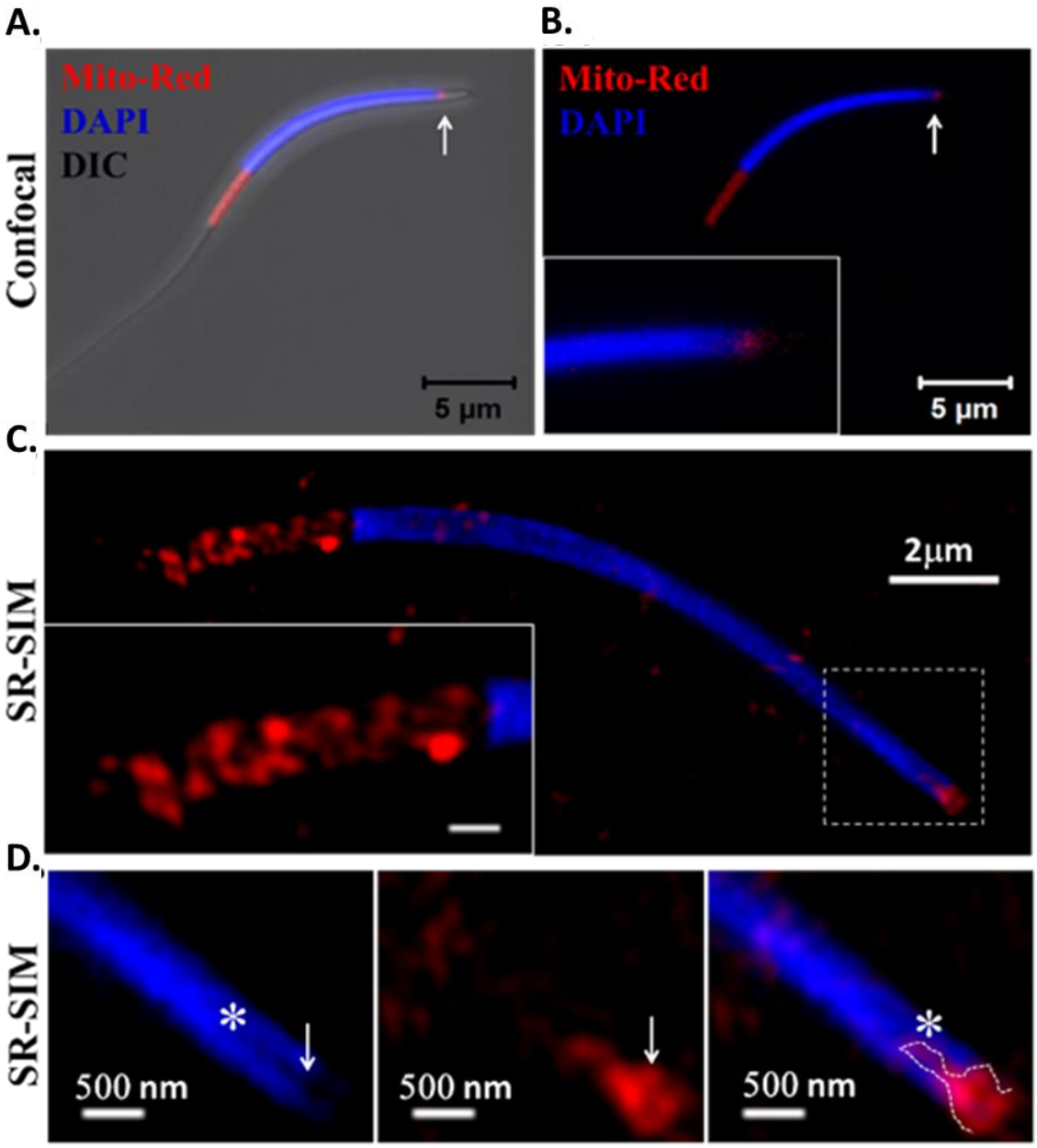

Fig 47: Duck (*White Pekin*) sperm tip contains bifurcated nucleus and atypical mitochondria-like organelle. A-B. Confocal image of duck sperm labelled with MitoTracker Red (red) and DAPI (blue) merged with DIC is shown, scale bar: 5µm. **C-D.** Super Resolution Structured Illumination Microscopy (SR-SIM) revealed the presence of a bifurcated nucleus in the head and the presence of MitoTracker Red labelled organelles which are embedded within the bifurcated tip. The asterisk indicates the start of bifurcation and arrow points out to the tip of bifurcated head. The enlarged image of the midpiece region is shown in set. Scale bar: 500 nm.

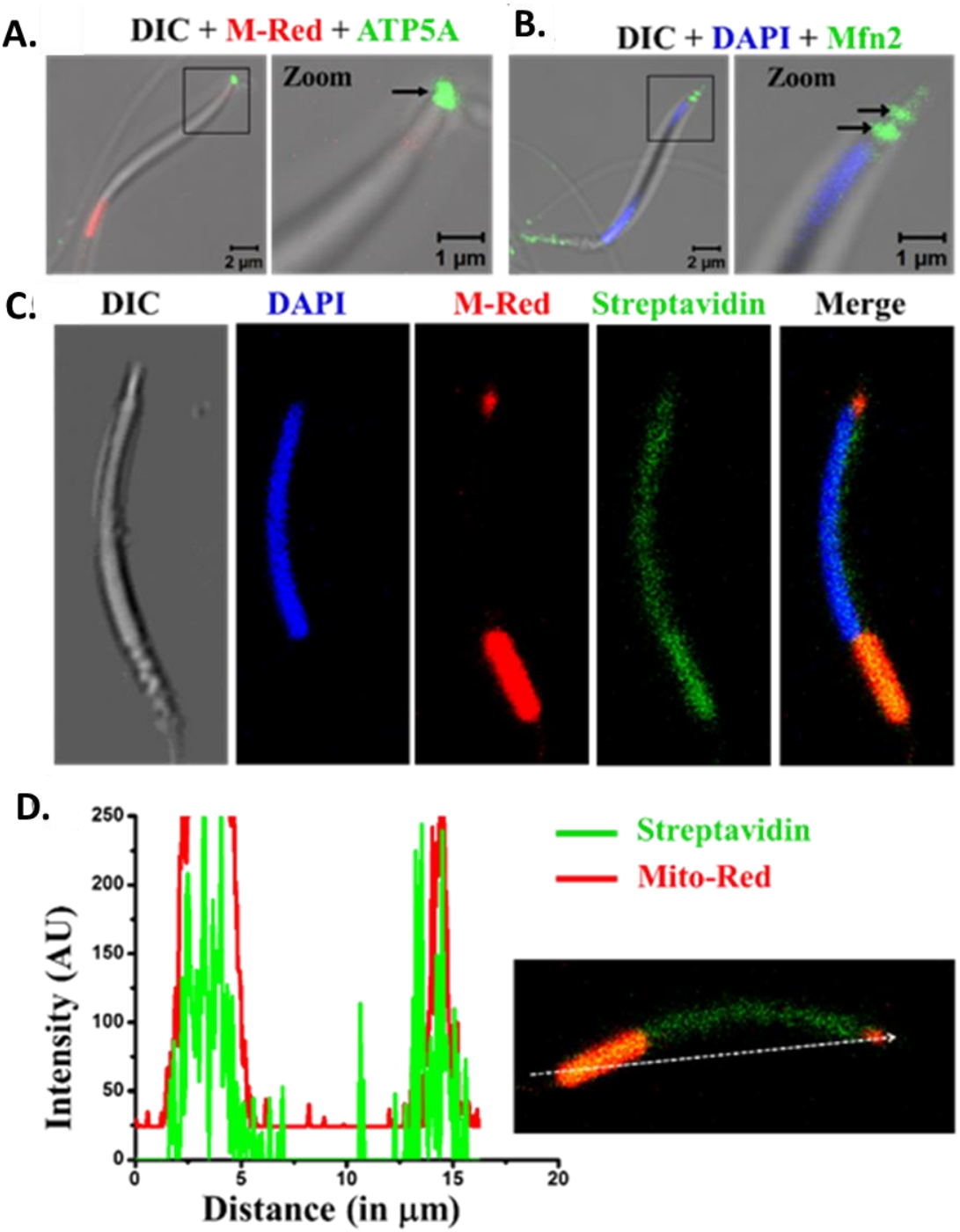

Fig 48: Duck (*White Pekin*) sperm tip contains atypical mitochondria-like structure. A. Confocal images of a duck sperm labelled with anti-ATP5A (green) and MitoTracker Red (Red). The enlarged portion of its head is shown in right side. The tip structure is indicated by an arrow. **B.** Confocal images of a duck sperm labelled with anti-Mfn2 (green) and DAPI. The enlarged portion of its head is shown in right side. The staining at tip region is indicated by arrows. **C.** Confocal images of the midpiece and head of White Pekin sperm stained with MitoTracker Red (Red) and Alexa flour 488 conjugated streptavidin (Green). DNA enriched region is counterstained with DAPI (blue). **D.** Intensity plot (of the same cell as shown in c) corresponding to white arrow region (shown in right side) is shown. Both MitoTracker Red and Alexa flour 488 conjugated streptavidin co-localize well at the mid-piece and also at the tip of the head.

Results indicate that in presence of TRPV4 activator, in many cases, sperm mitochondria developed blebs or split in the mitochondrial structure (**Fig 51**).Such abnormalities were not found in the control cases (n = ~500 cells). This in general suggests that TRPV4 activation induces extreme abnormalities in the mitochondrial organization. To observed minute changes in a better resolution, we performed super resolution microscopy of the same samples and analysed the mitochondrial coiling pattern in control and TRPV4 activated conditions. Results suggest that in control sperm, mitochondrial coiling was intact and form helix-like structure with regular thickness and pitch length in the midpiece region of sperm (**Fig 52**). It was observed that in presence of TRPV4 activator, mitochondrial coiling and its organization drastically changed. Helical organization of mitochondria was altered and they formed “kink” or “small cervices-like structure” in the mitochondrial ring structure (indicated by arrow).

2.5.5. TRPV4 is expressed in human spermatozoa

We tested the expression of TRPV4 in human (*Homo sapiens*) sperm. We noted that distribution of TRPV4 throughout the sperm; specifically it is enriched in the head and neck region while tail region shows faint expression. The TRPV4 signal is completely blocked by pre-incubating this antibody with specific antigenic peptide (**Fig 53 A**). To confirm the expression of TRPV4 in human sperm by western blot analysis, we used two different antibodies raised against TRPV4. One antibody (termed as Ab1) directed against the C-terminus of TRPV4 (Sigma-Aldrich) detected a band of 130 kDa (predicted size: 98 kDa) suggesting that in human sperm the TRPV4 is subject to post-translational modification.

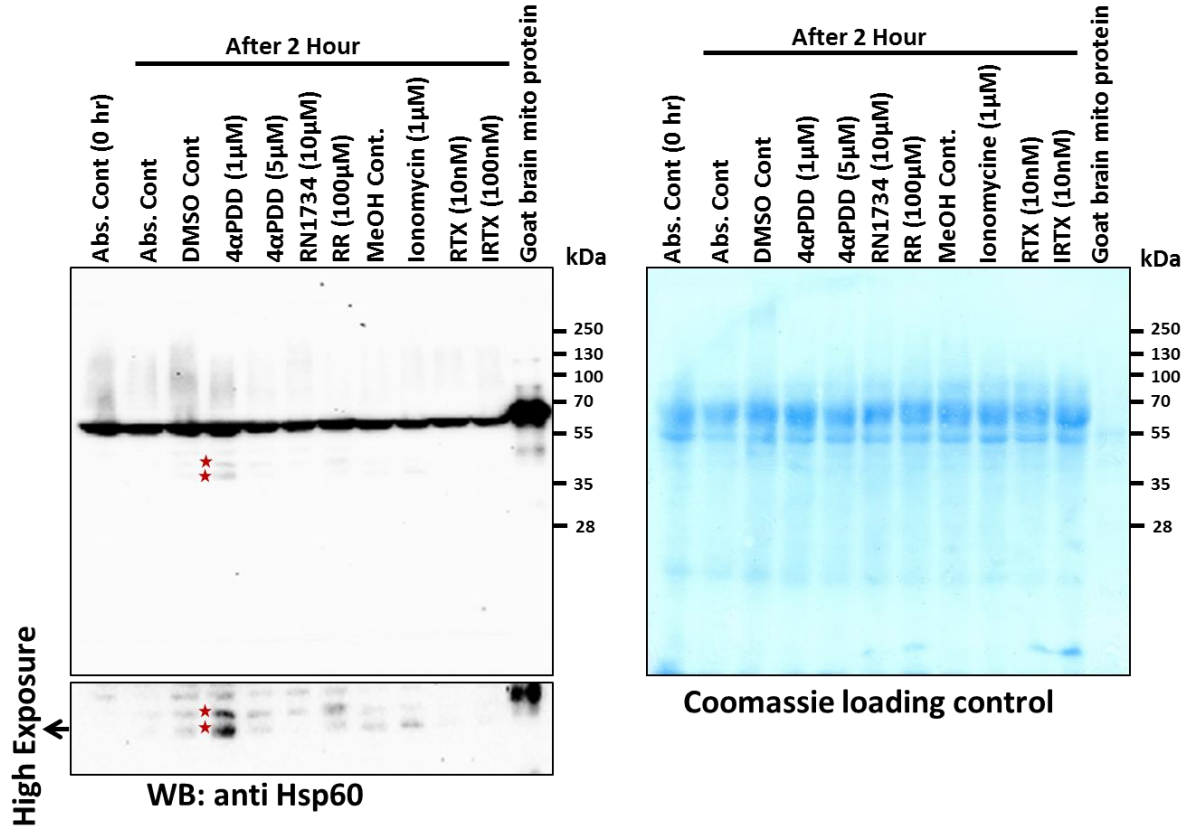

Fig 49: TRPV4 activation causes degradation of Hsp60. Represented western blot image indicating that in presence of TRPV4 activator 4αPDD (1 μM) Hsp60 protein degradation was higher as comparison to the trteatment of other drugs. At higher exposure time, smaller and degraded bands detected by Hsp60 antibody corresponding to the Hsp60 degradation is visiable only in 4αPDD treated sample (indicated by red asterisks). Such degradation is not detected in presence of TRPV1 activator (RTX) or inhibitor (IRTX). Right side coomasie image representing the loading conrol of these samples. Mitochndrial fraction purified from goat brain is used as a specific control.

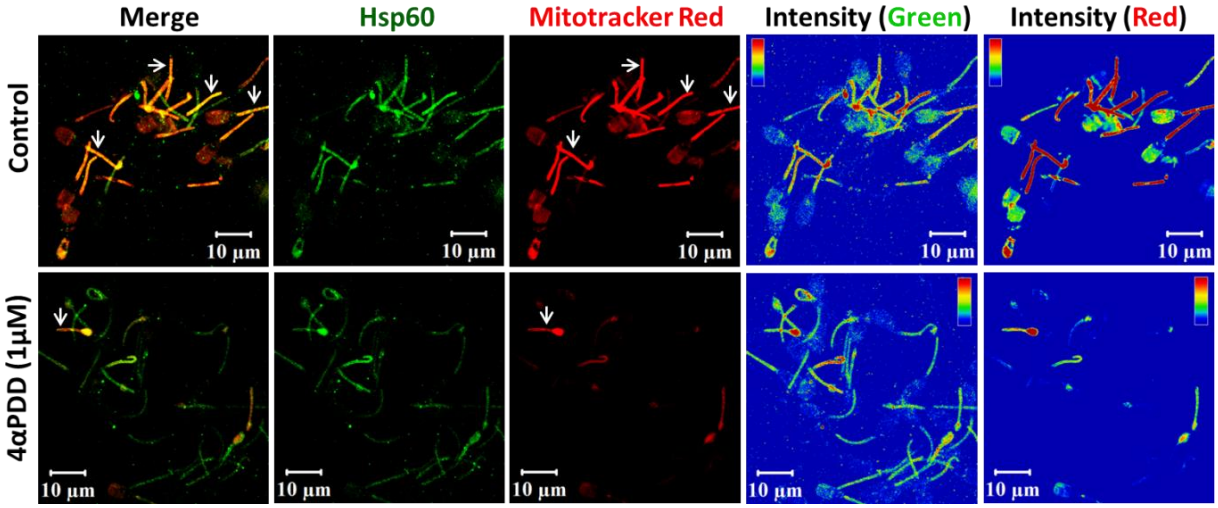

Fig 50: TRPV4 activation decrease both mitochondrial potentiality and Hsp60 level in bull sperm. Representing confocal image depicting that in presence of TRPV4 activator 4αPDD (1 μM), mitochondrial potentiality decreases drastically with comparison to control (indicated by arrow). In presence TRPV4 activator Hsp60 label goes down with comparison to control conditions. Since intensity of both MitoTracker Red and Hsp60 decreased in presence of TRPV4 activator, very less colocalization is observed in the midpiece of sperm. For better visualization, intensity profile of Hsp60 and MitoTracker Red are presented in right side of the panel.

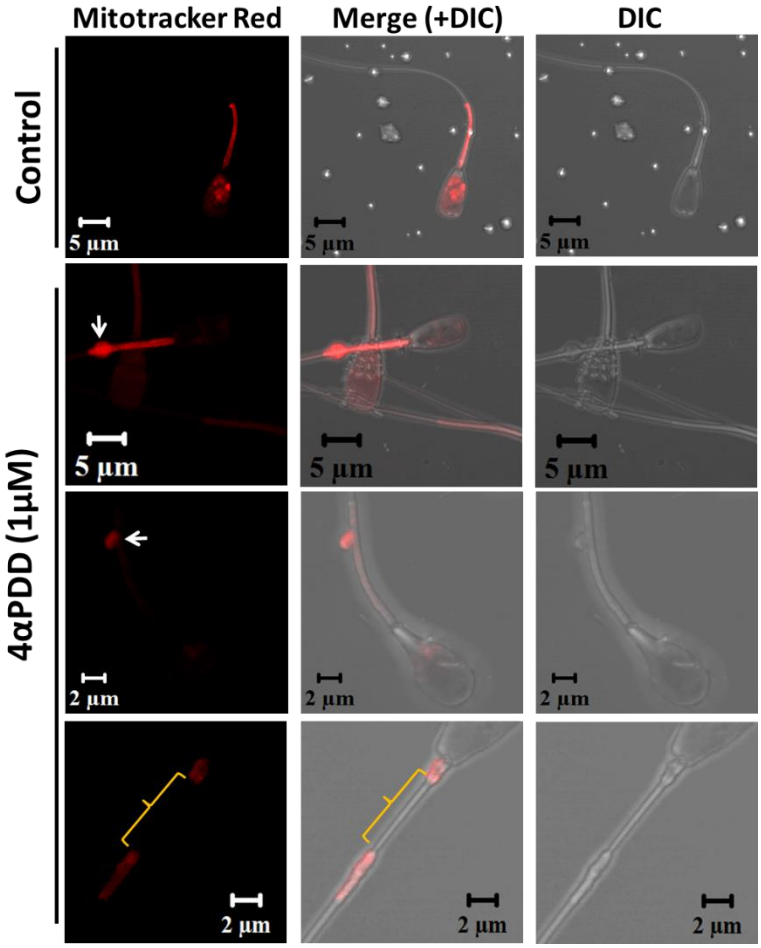

Fig 51: TRPV4 activation alters mitochondrial organization in bull sperm. Representing confocal images depicted the mitochondrial abnormality in bull sperm in presence of TRPV4 activator 4αPDD (1 μM). Activation of TRPV4 induces blabbing or node-like structure (indicated by arrow) in the midpiece regions. Some of the sperm mitochondrial structure becomes splitted into two halves. Such abnormalities can be correlated with the uncontrolled regulation of mitochondrial structure, fission and fusion.

A second antibody (termed as Ab2) that also binds to the C-terminus (Alomone Labs), showed two bands, one at 130 kDa and the other at 72 kDa and both these signals are blocked by using this specific peptide (**Fig 53 B**) suggesting that both these immunorectivities are specific in nature. Next we analysed the human spermatozoa by flow cytometry. Dot plot analysis further revealed that 98.98±0.34% spermatozoa were TRPV4 positive (n = 6). Upon pre-incubation with a specific blocking peptide, the same antibody detects less than 1% cells as TRPV4 positive, confirming the specificity of the TRPV4 antibody in FACS application also (**Fig 53 C-D**).

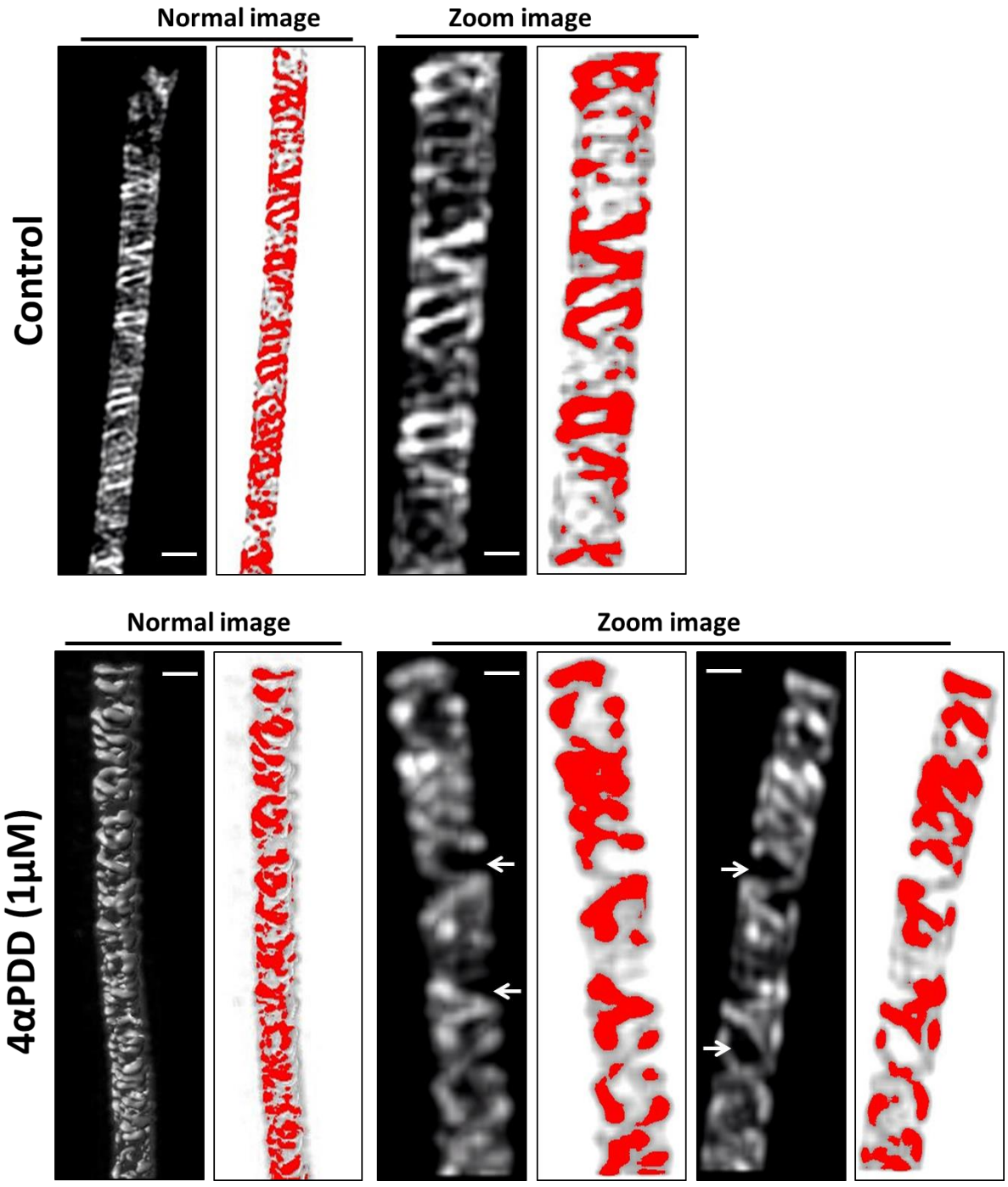

Fig 52: TRPV4 activation disrupts mitochondrial coiling and organization in bull sperm. Shown are the super resolution images demonstrating the mitochondrial coiling pattern in control and TRPV4 activated (by 4αPDD, 1 μM for 2 hours at 37°C) conditions. In control condition, mitochondrial coiling is intact and form regular helix-like structure. However in TRPV4 activated condition, the regular helical organization is disrupted (Kinks or cervices in the mitochondrial coiling region are indicated by arrows). For better visualization enlarged images are presented in each panel. Scale bar are 5 μm (for normal image) and 1 μm (for zoomed image).

In presence of this peptide, the mean fluorescence intensity (MFI) values reduced significantly (**Fig 53 E**). These experiments confirm the specific expression of TRPV4 in mature human spermatozoa.

2.5.6 TRPV4 is differentially expressed and localized in swim-up and swim-down human sperm

It is known that human spermatozoa are highly variable in nature and many have impaired motility. To explore if there is any difference in TRPV4 expression in case of immotile and highly motile sperm, we separated the total sperm population into these two fractions, namely swim-up (Su, cells with progressive motility) and swim-down (Sd, cells with mostly impaired motility) samples. We performed confocal microscopy and analysed expression and localization of TRPV4 in these two fractions. In case of swim-up cells, TRPV4 is primarily located in the head and faintly in the tail. However in case of swim-down cells, TRPV4 is mostly absent in the head region and is highly accumulated at the neck regions (**Fig 54 A-B**). In order to characterize these differences in TRPV4 expression, western blot analysis was performed using Su and Sd samples obtained from three individuals with proven fertility. The Ab1 detects a distinct band at 130 kDa in the Sd fraction of all three donors (**Fig 54 C**). However, the corresponding 130 kDa band is mostly absent or faintly present in Su fraction. In contrast, several smaller fragments of TRPV4 are observed in Su samples. Some of these smaller bands were also observed in the Sd samples, but with lesser intensities. Densitometry analysis of the 130 kDa region of all 3 donors revealed nearly 6 fold higher level of TRPV4 intensity in the Sd as compared to the Su fraction (**Fig 54 D**). This in general suggest for low level TRPV4 (corresponding to 130 kDa band) and more proteolytically-cleaved products in motile sample. Furthermore to analyse the

extent of proteolytic activity in Su and Sd samples, we probed the same samples for two other proteins which are abundant in the sperm cells, namely for β-tubulin and Hsp60. The western blot analysis suggests for higher proteolytic activity in Su samples as both Hsp60 and β-tubulin level in general is low in Su fraction compared to Sd fraction (**Fig 54 C**).

Next we analysed the expression of TRPV4 in Su and Sd samples in a more quantitative manner and performed FACS. Nearly 98.98 ± 0.34% and 96.15 ± 2.8% cells are TRPV4 positive in Su and Sd samples respectively. However, the mean fluorescence intensity (MFI) values for Su fraction is more (121.56 ± 37.79) compared to the Sd fraction (89.03 ± 23.76) (n = 6) (**Fig 54 E**). Though this difference may suggests for the more amount of TRPV4 in swim-up samples than compared to the swim-down sample, the difference turned out to be statistically non-significant ($p = 0.105$).

2.5.7 Effect of glycosidase treatment in human sperm TRPV4

In all other cellular system the expected molecular weight of TRPV4 is ~98 kDa but in sperm sample (Both in Su and Sd) it shows higher shift in molecular weight (130 kDa). To confirm that the upper band proteins of TRPV4 indeed results from complex glycosylation, we performed glycosidase treatment in sperm sample (Su and Sd) with two different glyosidic enzymes: Endoglycosidase H (Endo H) that cleaves N-linked high mannose-rich oligosaccharides and Peptide-N-Glycosidase F (PNGase F) that cleaves both N-linked high mannose-rich oligosaccharides and complex oligosaccharides. Results suggest that in presence of PNGase F enzyme but not in presence of Endo H, TRPV4 shows faster migration and resulting band is coming at expected molecular weight of TRPV4 (~ 98 kDa). It suggests that sperm TRPV4 contains complex glyosidic bonds with different types of oligosaccharides present there (**Fig 55**). As in western blot analysis, the TRPV4 band is not detectable in case of Su sample; it is not possible to comment on the glycosylation status of TRPV4 in Su cells.

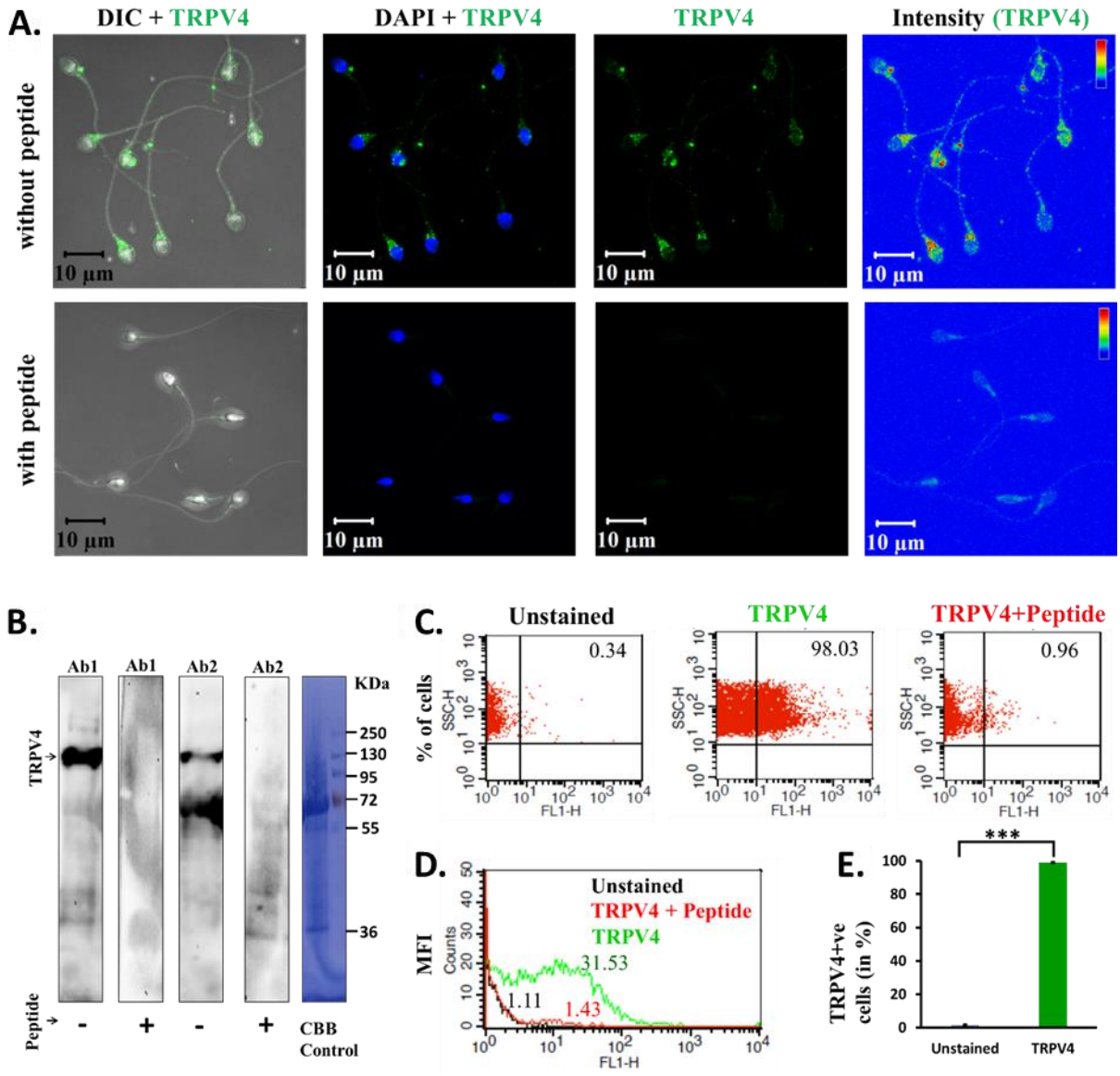

Fig 53: TRPV4 is endogenously expressed in human sperm. A. Confocal images showing the endogenous expression profile of TRPV4 (green) in human sperm. TRPV4 is localized in the post-acrosomal and neck regions, while faint expression is also present in the acrosomal and tail region (upper panel). TRPV4 signal is absent upon blocking the primary antibody with its antigenic peptide (lower panel). **B.** Western blot analysis using two different antibodies (Ab1 and Ab2) raised against the C-terminus of TRPV4 shows TRPV4-specific band at ~130 kDa (indicated by arrow). TRPV4 specific signal detected by Ab1 and Ab2 is absent when blocked with the antigenic peptide. Corresponding Coomassie-stained gel is shown in right side. **C.** Representative Dot Plot images showing the percentage of cells positive for TRPV4 (98.03%) obtained from Flow cytometric evaluation (n = 6). Application of blocking peptide reduced the number of positive cells to 0.96% only. **D.** Representative fluorescence intensity plot of TRPV4 expression is depicted as the Mean Fluorescence Intensity (MFI). **E.** Histogram representation of percentage of sperm cells positive for TRPV4 expression obtained from Flow cytometric evaluation (n = 6). About 98.98±0.34% cells were positive for TRPV4.

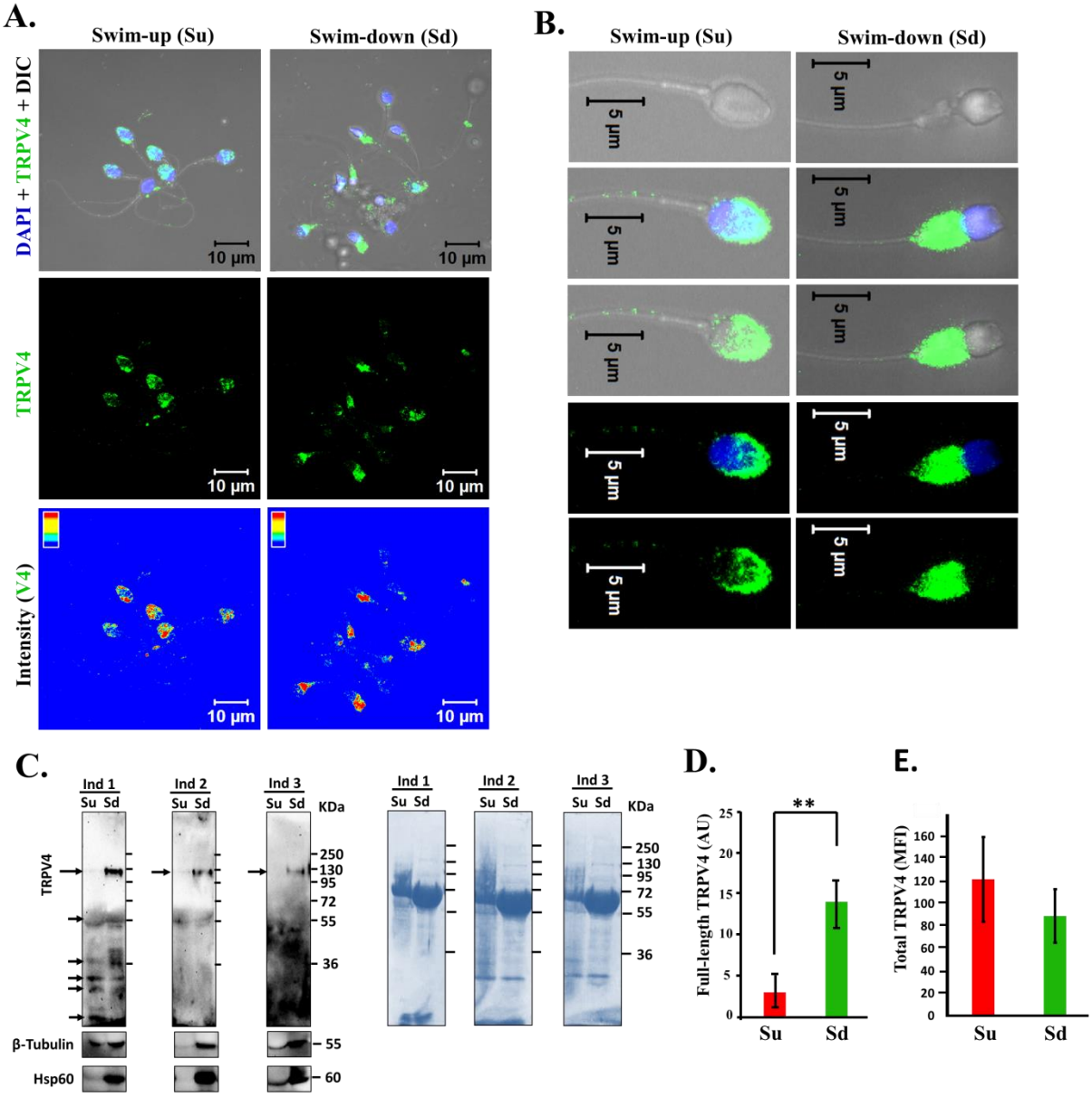

Fig 54: Swim-up and swim-down fractions of human sperm have different levels of TRPV4 expression. A-B. Cluster of sperm cells (A) and enlarged single cells (B) stained for TRPV4 (green) are shown. Strong signal for TRPV4 is observed throughout the head (primarily in acrosomal region) in the swim-up (Su) fraction while strong TRPV4 signal is present in the post-acrosomal and neck regions in the swim-down (Sd) fraction. Faint expression is present in the tail region. **C.** Western blot analysis of Su and Sd fractions of sperm from 3 individuals (Ind 1-3) were probed for TRPV4, β-tubulin and Hsp60. The 130 kDa band (longer arrow) and smaller bands (smaller arrows) represent the full-length (also the post-translationally modified form) and proteolytically degraded TRPV4 respectively. The corresponding Coomassie gels are provided at right. The prominent band/s around 70-50 kDa (in Su and Sd fraction) as observed by Coomassie staining represents protein/s present in sperm media. In each case, same number of cells in same volume was used for sample preparation. **D.** Densitometry analysis of western blot signal intensities for 130 kDa band of TRPV4 in Su and Sd fractions (n = 3, ANOVA test, ** p value< 0.005). **E.** Total TRPV4 fluorescence intensity from Su and Sd samples detected as Mean Fluorescence Intensity (MFI) values in flow cytometry measurements was found to be non-significant (n = 6, ANOVA test, p = 0.105). **F.** Histogram representation of percentage of sperm cells in Su and Sd fractions positive for TRPV4 expression obtained from Flow cytometric evaluation (n=6). More than 98% cells in each fraction express TRPV4.

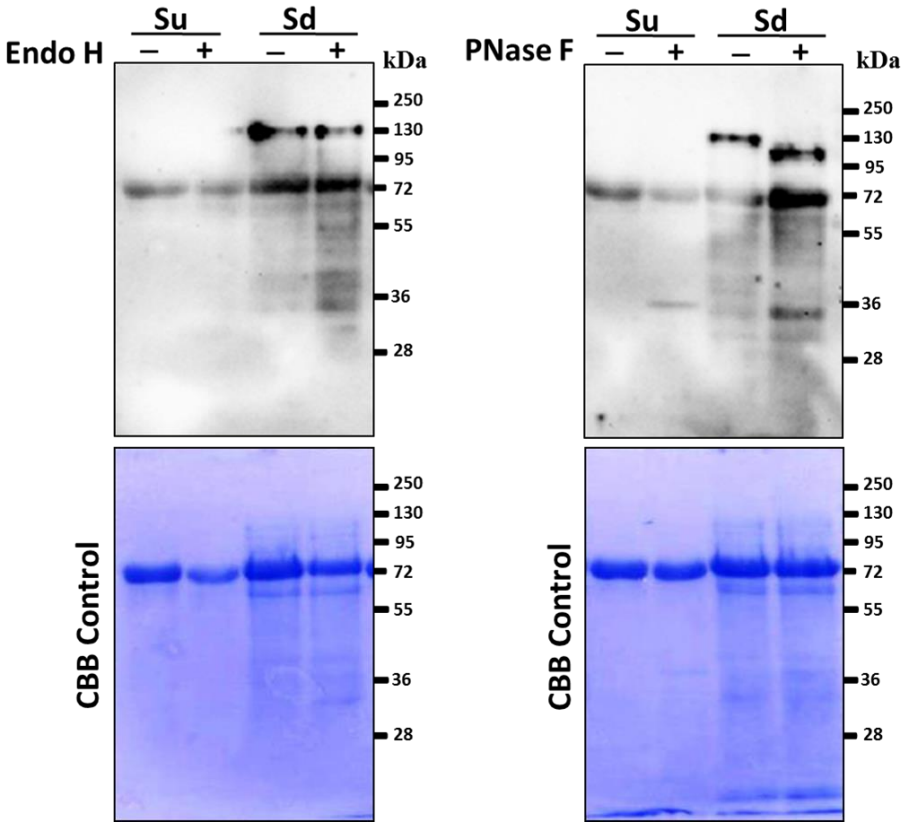

Fig 55: TRPV4 is present in glycosylated form in human sperm. Equal amount of sperm extract (obtained from same number of cells) representing swim-up (Su) and swim-down (Sd) fractions were treated with (+) or without (-) glycosidase enzymes Endo H or PNGase F for de-glycosylation reaction. Subsequent western blot with anti-TRPV4 antibody detects the shift in the molecular weight. Results suggest that TRPV4 has complex N-glycosidic linkage and branched complex glyosidic bond with glycosyl group, which shows shift in molecular weight (~30 kDa) only in presence of PNGase F (represented as red star). Enzymatic treatment with Endo H does not show any shift in molecular weight of TRPV4 (130 kDa) suggesting that the glycosylated TRPV4 is resistant against Endo H. In Su sample TRPV4 band is undetectable in western blot suggesting low abundance of full-length TRPV4. The corresponding Coomassie gels are shown below.

2.5.8 Activation of TRPV4 causes redistribution

We analyzed the localization pattern of TRPV4 in control and pharmacological modified conditions (**Fig 56**). DMSO-treated cells show TRPV4 localization primarily in the head region (both at the acrosomal region and post acrosomal regions) and faintly in the tail. Activation with 4αPDD (5 µM) induce re-distribution of TRPV4 mainly to the acrosomal, to the neck and tail regions as well. Activation by 4αPDD also increases the immunofluorescence signal for TRPV4 suggesting that such activation may also increases immunoreactivity against TRPV4 and possibly suggests for changes in epitope organization and/or removal of epitope masking. In contrast, RN1734 (10 µM) treated cells show reduced

TRPV4 levels. Progesterone (10 µM) treatment alone did not affect the localization profile of TRPV4 and majority of the TRPV4 is localized at the acrosomal regions only.

2.5.9 TRPV4 modulation altered premature capacitation in human sperm

In order to examine the role of TRPV4 in capacitation of human sperm, we treated the swim-up and swim-down fractions with TRPV4 activator (4αPDD at 1µM and 5µM) and inhibitor (RN1734, 10µM) for 1 hour and probed for total phosphotyrosination (using anti-phosphotyrosine antibody) and performed imaging analysis.

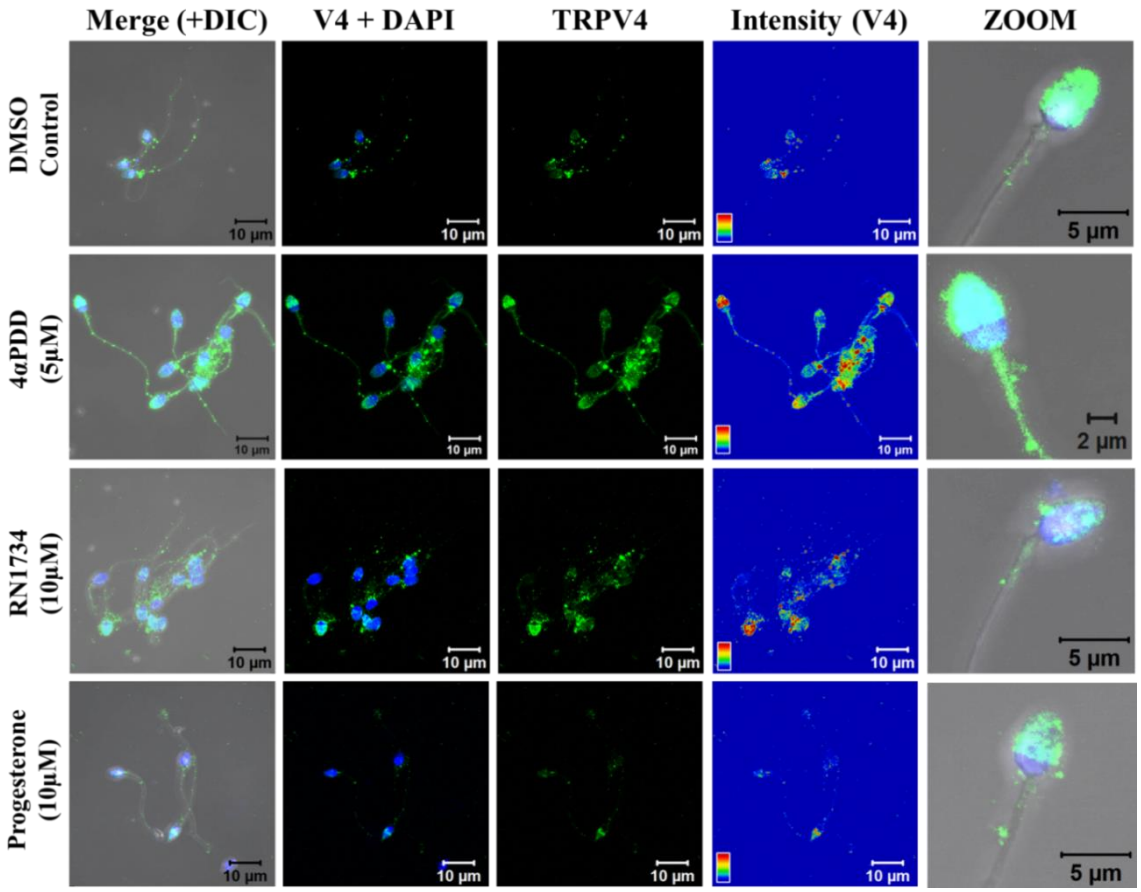

Fig 56. Translocation and relocalization of TRPV4 in human sperm upon activation or inhibition of TRPV4: Expression profiles of TRPV4 (green) in human sperm treated with either solvent control (DMSO) alone or by 4αPDD (activator, 5 µM), or RN1734 (inhibitor, 10 µM) or Progesterone is shown (in green). Depicted confocal images suggest that TRPV4 translocate upon pharmacological modulation and it is distributed into the midpiece and tail region. Overall immunoreactivity attributed for TRPV4 is also increased in presence of TRPV4 activator.

Depending on the level of phosphotyrosination, we classified the cells in three types (**Fig 57 A**). Extensive phosphotyrosinated cell is represented as "A-type", moderately phosphotyrosinated cell is represented as "B-type" while non-phosphotyrosinated cell is represented as "C-type". Quantification of phosphotyrosination pattern of >300 sperm cells per sample is represented (**Fig 57 B**).

In general, the swim-up samples have more phosphotyrosinated (A-type + B-type) cells than swim-down samples. Neither TRPV4 activation nor inhibition alters the phosphotyrosination pattern drastically in swim-up samples, especially in the percentage of B-type cells (~ 20% of the population in each of the treated conditions; indicated by double headed arrows). Strong activation as well as inhibition of TRPV4 however reduces certain percentage of A-type and increases C-type of cells.

In case of swim-down samples, ~35% and ~55% of the sperm population in DMSO-treated conditions show B-type and C-type cells respectively. This observation accords well with other reports suggesting that the level of phosphotyrosination is low in swim-down samples [260]. This percent distribution does not differ significantly when treated with RN1734 suggesting that in swim-down sample, the endogenous activity of TRPV4 is probably at the basal level. However, activation of TRPV4 with an optimum concentration of 4αPDD (1 μM) enhances the percentage of C-type cells, reduces B-type and A-type of cells when compared with DMSO control. This result suggests that TRPV4 activation in swim-down sample may reduce global phosphotyrosination. This may also suggest for the deactivation of tyrosine kinases activities and/or activation of phosphatases in a Ca^{2+}-dependent manner [261]. However, in the same swim-down sample, activation of TRPV4 with higher concentration 4αPDD (5 μM) enhances the percentage of A-type, reduces B-type and C-type remain unchanged (compared with DMSO control). This suggests that stronger activation of TRPV4 correlates well with the activation of tyrosine kinases and/or

deactivation of phosphatases in this condition. The difference between optimum activation (4αPDD at 1 μM) and stronger activation (4αPDD at 5 μM) is intriguing and may suggest that the difference in basal Ca^{2+}-level and/or Ca^{2+}-oscillation induced by TRPV4 can be relevant for phosphotyrosination and may have bio-medical application in case of treating infertility (by targeting this specific population having sperm with low motility).

For more quantitative analysis of phosphotyrosination in swim-up and swim-down sperm sample, we have performed flow cytometry-based analysis in different gated populations (**Fig 57 C**). As C-type cells represent no phosphotyrosination (probably also indicate a population which do not contribute in actual fertilization process), this analysis effectively reveals the changes in the phosphotyrosination status in B-type and A-type cells only. We separated swim-up and swim-down cells from 4 proven fertile donors and treated these cells with TRPV4 inhibitor (RN1734 at 10 μM) or activator (4αPDD at 1μM and 5μM) and subsequently compared the MFI-values in each samples.

In order to obtain more quantitative evaluation of effect of TRPV4 on phosphotyrosination, we performed flow cytometry-based experiments where at least 20,000 cells per sample (in each treatment group, from 4 independent individuals corresponding to a number of minimum 80,000 sperm cells in each category) were analyzed. Since the dot plot reflects the percent positive population as well as fluorescence intensities in log scale, we used dot plot analysis to categorize the sperm population in each sample into three classes based on the fluorescence intensities reflecting their phosphotyrosination levels. These different-gated populations in flow cytometry analysis are represented in (**Fig 57 D**). These 3 categories correlate well with Type-A, Type-B and Type-C represented in confocal image based classification as demonstrated in above (**Fig 57 B)**. We observed that activation or inhibition of TRPV4 does not alter the percentage of cells in these three sub types, both in swim-up or swim-down fractions (**Fig 57 D**). The MFI values of these sub-populations also

show no difference in phosphotyrosination levels upon TRPV4 modulation (**Fig 57 E**). We further analyzed the MFI values of the entire sperm population (Type-A + Type-B + Type-C) in each treated conditions and noted that TRPV4 modulation does not show significant differences in phosphotyrosination levels in either swim-up or in swim-down fractions (**Fig 57 F**). However, as expected, the overall MFI value is higher for swim-up population compared to the swim-down population. Based on these results, we can conclude that TRPV4 modulation does not induce premature capacitation in human sperm

2.5.10 TRPV4 regulates progesterone-induced motility

Progesterone-induced motility changes in motile sperm cells (Su fraction) were studied both in presence and in absence of TRPV4 modulators. Sperm cells were labelled with fluorescent dye (Fluo-4 AM) and time series acquisition was done by live cell imaging. The spatio-temporal information about the dynamics of motile cells was monitored by kymograph analysis. This is done by defining an unbiased line in the time series images which indicates about the cells passing through this line (**Fig 58 A)**. Intensities acquired along this line were stacked together to form a compiled image (as done in kymograph analysis) and such representative kymograph images are presented here (**Fig 58 B**). Total 500 frames (representing 1000s) were analysed for each condition.

In presence of DMSO only, the cells remain motile and application of progesterone results in hyper activation (cells become more motile). The cells remain motile in presence of only TRPV4 activators (4αPDD at 5μM) or inhibitor (RN1734 at 10μM or even at higher concentrations). In contrast to only RN1734-induced motility changes (**Fig 58 B**), a punctate type of cellular aggregation was seen after addition of RN1734 in progesterone-pre-treated cells. Most of the cells become immotile within ~10 minutes after adding RN1734 and forms clusters. It is likely that RN1734 alone does not induce detrimental effect on sperm motility,

but may impair the motility of hyperactivated sperm (progesterone-induced). It was evident with the finding of clumps of immotile cells in this treatment resulting in aggregated intensity observed from 235 frame (470s) onwards in kymograph (indicated by red arrow) (**Fig 58 B**). These results suggest that TRPV4 function is essential during progesterone-mediated hyper activation of sperm cells.

2.5.11 TRPV4 modulates Ca^{2+}-influx into human sperm

Ca^{2+}-homeostasis in sperm is precisely regulated by different Voltage Operated Channel (VOC) present in the membrane and female steroids like progesterone [262]. To evaluate the effect of TRPV4 activator and inhibitor upon the Ca^{+2}-influx in human sperm, cells (Su and Sd) were treated with 4αPDD (5µM) or RN1734 (10µM) for 1 hour and labelled with Fluo-4 AM to analyse the intracellular Ca^{2+}-levels. 4αPDD treatment in Su fraction resulted in increased intracellular Ca^{2+}-levels but inhibition by RN1734 (10 µM) did not decrease the intracellular Ca^{2+} levels below that of the control conditions (**Fig 59 A**). Notably, in Su fraction, the effect of TRPV4 activation by 4αPDD is comparable to the effect of Progesterone (10 µM), a standard inducer of Ca^{+2}-influx into sperm cells [263]. The above observation is supported by quantification of Fluo-4 AM signal intensity per unit area (n = 4 individuals), which revealed that in Su fraction the effect of 4αPDD and Progesterone is similar (**Fig 59 B**). In Sd fraction, there is no significant difference in basal Ca^{2+}-levels after modulation of TRPV4 by pharmacological agents (**Fig 59 B**).

In sperm cell cells, CatSper is well known ion channel exclusively present in spermatozoa and regulates calcium homeostasis. Furthermore, Ca^{2+}-levels was evaluated post activation of TRPV4 along with blocking of CatSper. As expected, reduction of Ca^{2+} levels was observed when motile fraction was treated with CatSper inhibitor (NNC-55-0396, 10 µM). The effect of CatSper inhibition on motility and intracellular Ca^{2+}-levels were restored

upon 4αPDD (5µM, 20min) treatment to NNC-55-0396 pre-treated cells (**Fig 59 C**). The bar-graph representing the average of three independent experiments and also confirms this finding. This data indicates that apart from CatSper channels, TRPV4 is also an important regulator of human sperm motility and intracellular Ca^{2+}-levels.

2.5.12 Pharmacological inhibition of TRPV4 blocks progesterone-induced hyper activation but not Ca^{2+}-influx in human sperm

Progesterone-induced hyper activation is essential to complete capacitation and subsequent acrosomal reaction as well as sperm-oocyte fusion [264-266]. We explored if TRPV4 can modulate the progesterone-mediated signalling events, intracellular Ca^{2+}-levels and functions in Su sample. For that purpose, cells were loaded with Fluo-4 AM and live cell images were performed. Addition of TRPV4 inhibitor RN1734 in progesterone (10 µM) pre-treated sample can block the hyper-activated motility and these cells form clusters soon after adding RN1734 (**Fig 60 A**). However, addition of RN1734 in progesterone pre-treated cells causes increased intracellular Ca^{2+}-levels (**Fig 60 A**). Quantification of Fluo-4 AM intensity values (of a total 100 frames) before and after addition of RN1734 in progesterone pre-treated samples also confirmed the same changes (**Fig 60, Right side**). This increment in basal Ca^{2+} level seems to correlate with the subsequent aggregation and death of sperm cells. In a reciprocal manner, addition of Progesterone to RN1734 pre-treated sperm, does not increase sperm motility further, but increases in intracellular Ca^{2+}-levels (**Fig 60 B**). However we could not find significant changes in basal Ca^{+2}-level and clustering effect in only progesterone or only RN1734 pre-treated cells (**Fig 60 C-D**). Taken together these results suggest that in presence of progesterone, endogenous TRPV4 activity is important for sperm cells.

2.5.13. TRPV4 regulates Ca^{2+}-buffering at the mid-piece and Ca^{2+}-wave propagation in sperm tail

To understand if and how TRPV4 regulates the intracellular Ca^{2+}-waves, we used Fluo-4 AM and performed live cell imaging followed by manual tracking of Ca^{2+}-wave propagation within single cells (**Fig 61 A**). In case of progesterone-treated cells, the level of Ca^{2+} is high in the head and neck regions. Progesterone-induced Ca^{2+}-wave originates in the mid-region of sperm head and spreads throughout the neck and then propagates to the tail and mostly covers a large portion of the tail. The Ca^{2+}-wave then subsides and a fresh wave originates in the head. This observation matches well with previous reports [263]. In case of 4αPDD-treated cells, the level of Ca^{2+} is also high in the head and neck regions. The patterns of 4αPDD-mediated waves are visible at the tail and mostly similar to progesterone-induced waves. Notably, application of RN1734 results in reduction in the intracellular Ca^{2+}-level in the head region. Nevertheless, the Ca^{2+}-wave propagation is observed in the tail region at times, though with less intensity and frequency.

However, application of RN1734 to the Progesterone pre-treated cells results in reduction in motility and majority of cells become immotile within 10 minutes of RN1734 addition. Majority of these immotile cells are unable to propagate any Ca^{2+}-wave to the mid-piece and tail resulting in a heavy increase in intracellular Ca^{2+} levels in the head regions (**Fig 61 A**). However, very few cells, which still remain motile in this condition, are able to transmit the Ca^{2+}-wave originated in the head to the mid piece and tail. This result suggests for a possible Ca^{2+}-buffering activity at the neck region of progesterone-induced hyper-motile cells and possible involvement of TRPV4 in such functions. Indeed, we observed wavy pattern of intracellular Ca^{2+}-level at the neck regions in case of progesterone- and 4αPDD-induced hyper motile cells (**Fig 61 B**). In contrast, such patterns were not observed when RN1734 was added in progesterone-treated cells (**Fig 61 B**).

2.5.14. Progesterone directly interacts with the conserved TM4-Loop4-TM5 region of TRPV4

Previously we demonstrated that TM4-Loop4-TM5 region of TRPV4 is highly conserved in all vertebrates and Loop4 region alone or in combination of TM4 and/or TM5 is sufficient for interaction with cholesterol and two derivatives namely stigmasterol and aldosterone [164]. In this work we explored if the same region can also interact with progesterone and thus performed blot overlay experiments. Our blot-overlay experiments confirmed that GST-TM4-Loop4-TM5 and GST-Loop4 alone can interact with progesterone while only GST does not interact (**Fig 62**). This confirms a direct interaction of progesterone to the TRPV4 and therefore suggests that TRPV4 can also act as an alternative progesterone receptor, at least in sperm cells.

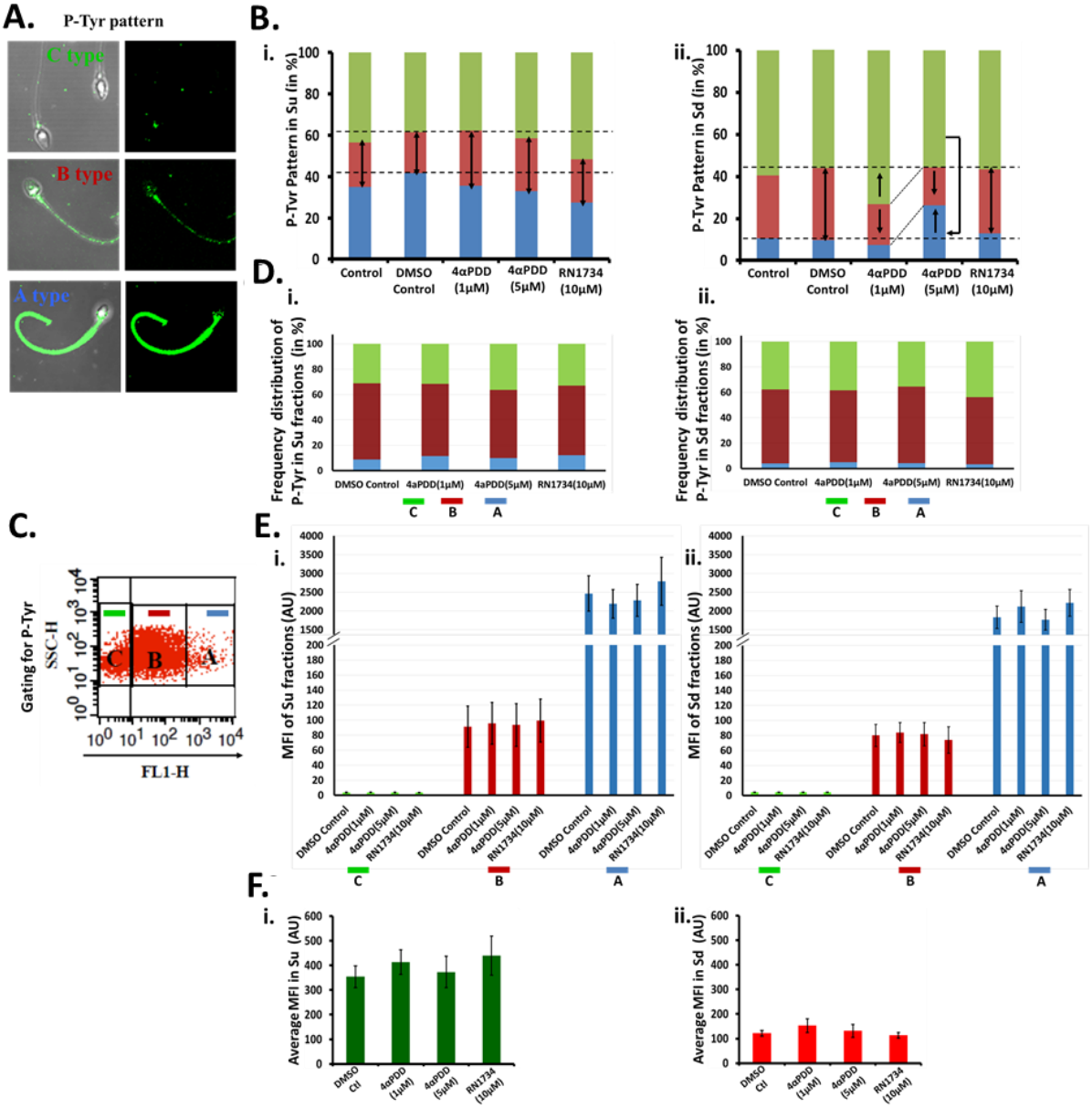

Fig 57: Effect of TRPV4 modulation on capacitation in human sperm. TRPV4 modulation does not induce premature capacitation. Human sperm cells were immunostained with phosphotyrosine (P-Tyr) antibody to determine the capacitation status. **A.** Representative confocal images showing distinct phosphotyrosination patterns: A-, B- and C-type representing strong (sky blue), weak (brick red) and absence of phosphotyrosination (light green) respectively. **B.** Quantification of phosphotyrosination pattern as visualized by confocal imaging in (b-i) swim-up (Su) and (b-ii) swim-down (Sd) sample. At least 300 cells obtained from 4 individuals in each conditions is depicted (as percent distribution). **C.** Representative dot-plot showing the gating of sperm cells classified into three populations (A, B, C-type) based on their fluorescence intensities representing phosphotyrosination levels. **D.** Frequency distribution of phosphotyrosination levels in Su (d-i) and Sd (d-ii) fractions as evaluated by flow cytometric analysis. **E.** Mean Fluorescence Intensity values (MFI) for Su (e-i) and Sd (e-ii) of the A-, B- and C-type under different treatments are represented (n < 80,000 cells from 4 independent samples). **F.** Average MFI values of phosphotyrosination levels in Su (f-i) and Sd (f-ii) fractions under different treatments (n = 5). TRPV4 modulation does not induce any change in phosphotyrosination levels neither in Su nor in Sd fractions.

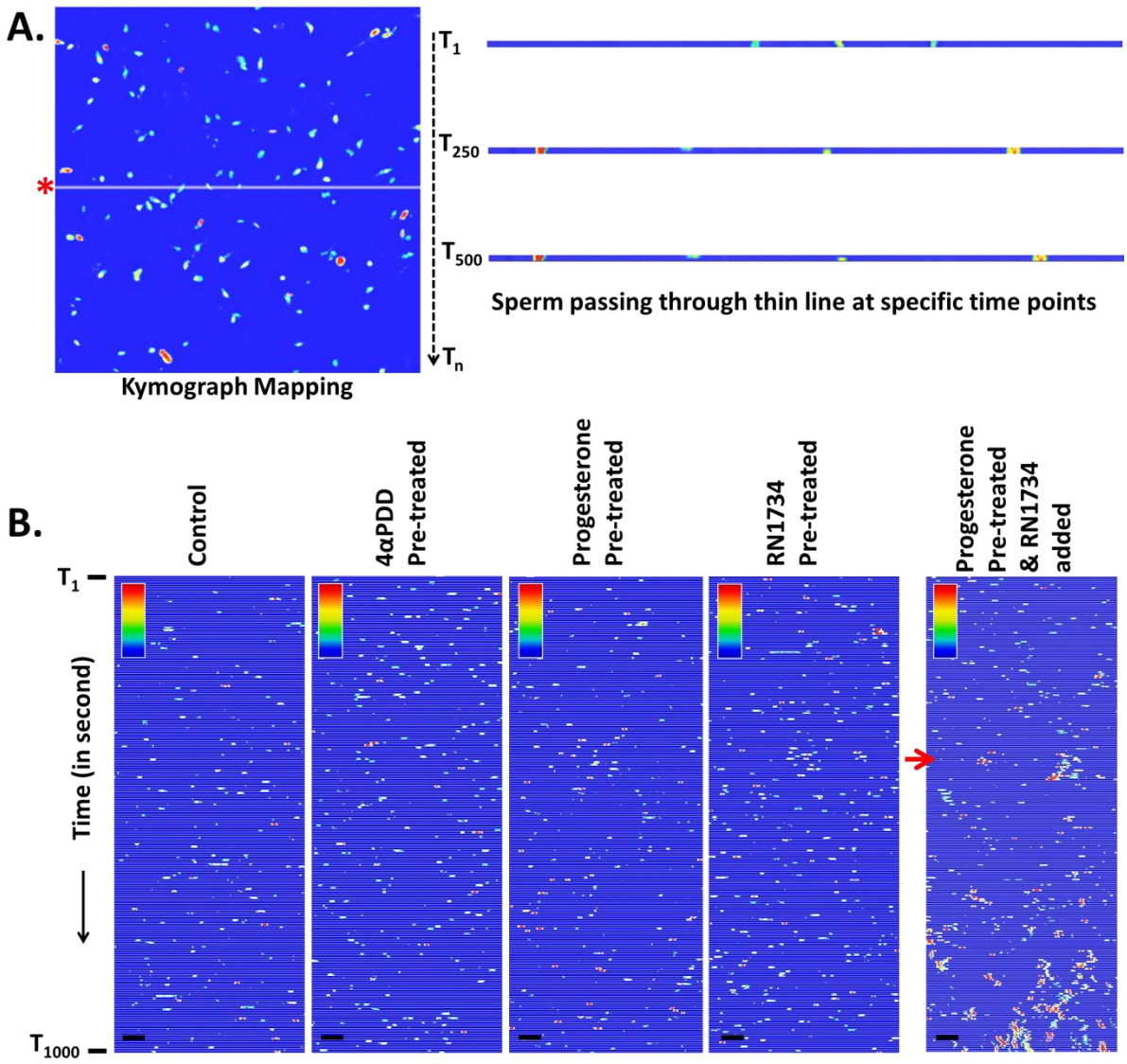

Fig 58: TRPV4 is involved in the progesterone-mediated hyper activation. Shown are the kymographs derived from human sperm (Su fraction) loaded with Fluo-4 AM and treated with different pharmacological agents. **A.** The time lapse imaging was acquired in presence or in absence of TRPV4 activator/inhibitor alone or applied on progesterone-pre-treated samples. An unbiased thin line (indicated by red asterisk) was drawn on the acquired images (equal dimension for all treatments) and respective kymographs were made for total time series. At each time points representing individual frames, the fluorescence intensity of cell/s crossing the thin line were represented as individual strips .This analysis represents the sperm movement through this line and relative level of intracellular Ca^{2+} observed as fluorescence intensity in all 500 frames (duration of 1000 sec). **B.** Kymographs of sperm movement under different treatment conditions is shown. Sperm motility drastically decreased as the cells get aggregated upon addition TRPV4 inhibitor RN1734 in the progesterone-pre-treated sample at 235 frame (470 sec, indicated by red arrow). Such aggregation pattern is not observed in cases when samples are treated with only 4αPDD (5 µM), RN1734 (10 µM) or progesterone (10 µM) each. Scale bar 5 µm. For more details, see supplementary movies.

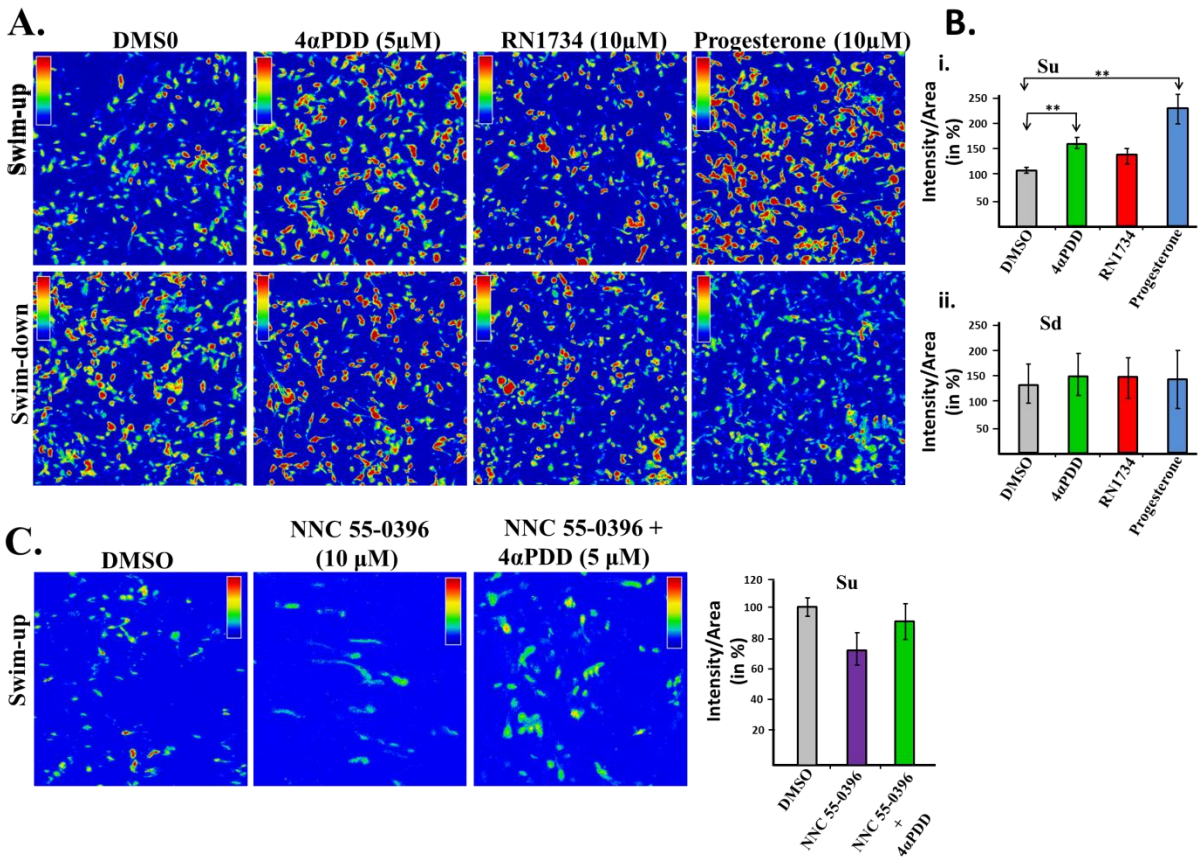

Fig 59: TRPV4 regulates intracellular Ca^{2+}-levels in human sperm. A. Sperm cells of swim up (Su) and swim down (Sd) fractions were pre-treated with TRPV4 activator (4αPDD, 5 μM) inhibitor (RN1734 (10 μM) or with Progesterone (10 μM) for 1 hour and Fluo-4 AM labelling followed by live cell imaging was performed. The intra cellular Ca^{2+}-levels are represented in pseudo color (rainbow scale, red and blue indicating highest and lowest intensity respectively). **B.** Quantification of average fluorescence intensity/area (in arbitrary unit) is shown. TRPV4 activator (4αPDD) and progesterone significantly increased the intracellular Ca^{2+} levels in sperm in comparison to control in Su sample ($p<0.05$). However in case of Sd sample, TRPV4 activator or inhibitor does not show any difference in intracellular Ca^{2+}-levels (n = 4 independent experiments). **C.** Live cell imaging revealed that CatSper inhibitor (NNC 55-0396) decreases the intracellular Ca^{2+} levels in comparison to control and this intracellular Ca^{2+}-level restored when the NNC-pre-treated cells were treated with TRPV4 activator for 20 minutes (4αPDD, 5 μM). These results suggest that apart from the CatSper channel, intracellular Ca^{2+} regulation, is also regulated by TRPV4. Quantification of average fluorescence intensity/area (in arbitrary unit) is represented in right side. (n = 4 independent experiments).

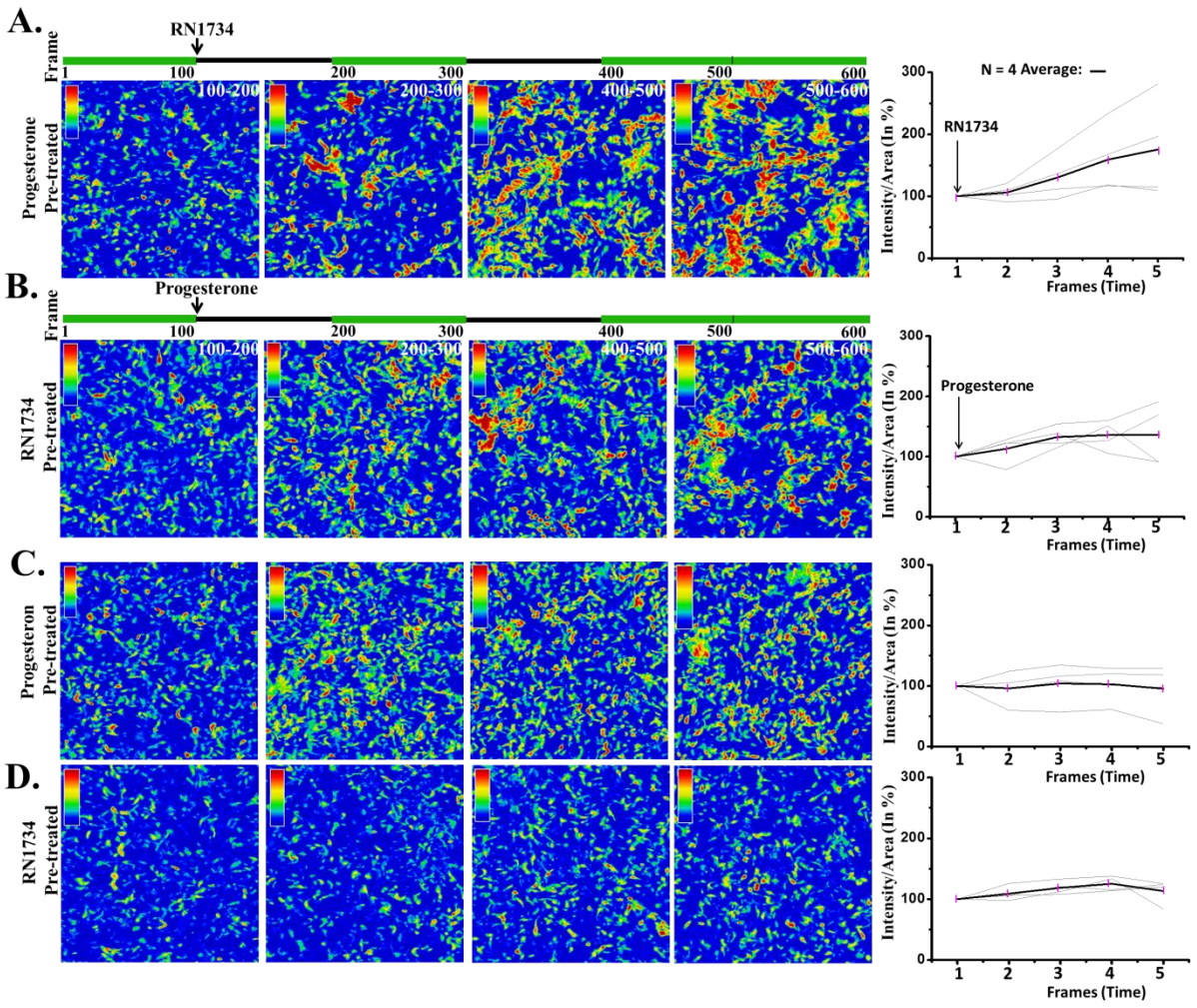

Fig 60: TRPV4 regulates progesterone-mediated Ca^{2+}-levels and motility. Time-series fluorescence images were acquired from Fluo-4 AM dye loaded highly motile swim-up sample. Cells were pre-incubated with different pharmacological agents for 1 hour and subsequently imaged for 600 time frames with or without further addition of a second agent at the 100th time frame. **A.** Intracellular Ca^{2+}-level of Progesterone (10 µM) pre-treated sperm upon addition of TRPV4 inhibitor RN1734 at 100th frame is shown TRPV4 inhibition in the presence of progesterone, induce high level of Ca^{2+} in the head, less cell motility and more cell aggregation. **B.** Intracellular Ca^{2+}-level in RN1734 (10 µM) pre-treated sperm upon addition of Progesterone at 100th frame are shown. **C-D.** Similarly, intracellular Ca^{2+}-level in Progesterone (10 µM) only pre-treated cells (**C**) or RN1734 (10 µM) pre-treated cells (**D**) are shown. For each condition, the fluorescence intensity is depicted in rainbow scale and total fluorescence intensity from 100 time frames (indicated by green thick line) are merged in to a single image. Quantification of Intensity/Area (initial value represented as 100%) at different time points are shown in the right side. A total of 4 independent experiments are shown (indicated by thin lines) and average values are indicated in dark black line (merged intensity values: 1 = 1-100th frame, 2 = 101 -200th frame, 3 = 201-300th frame, 4 = 301-400th frame, 5 = 401 -500th frame).

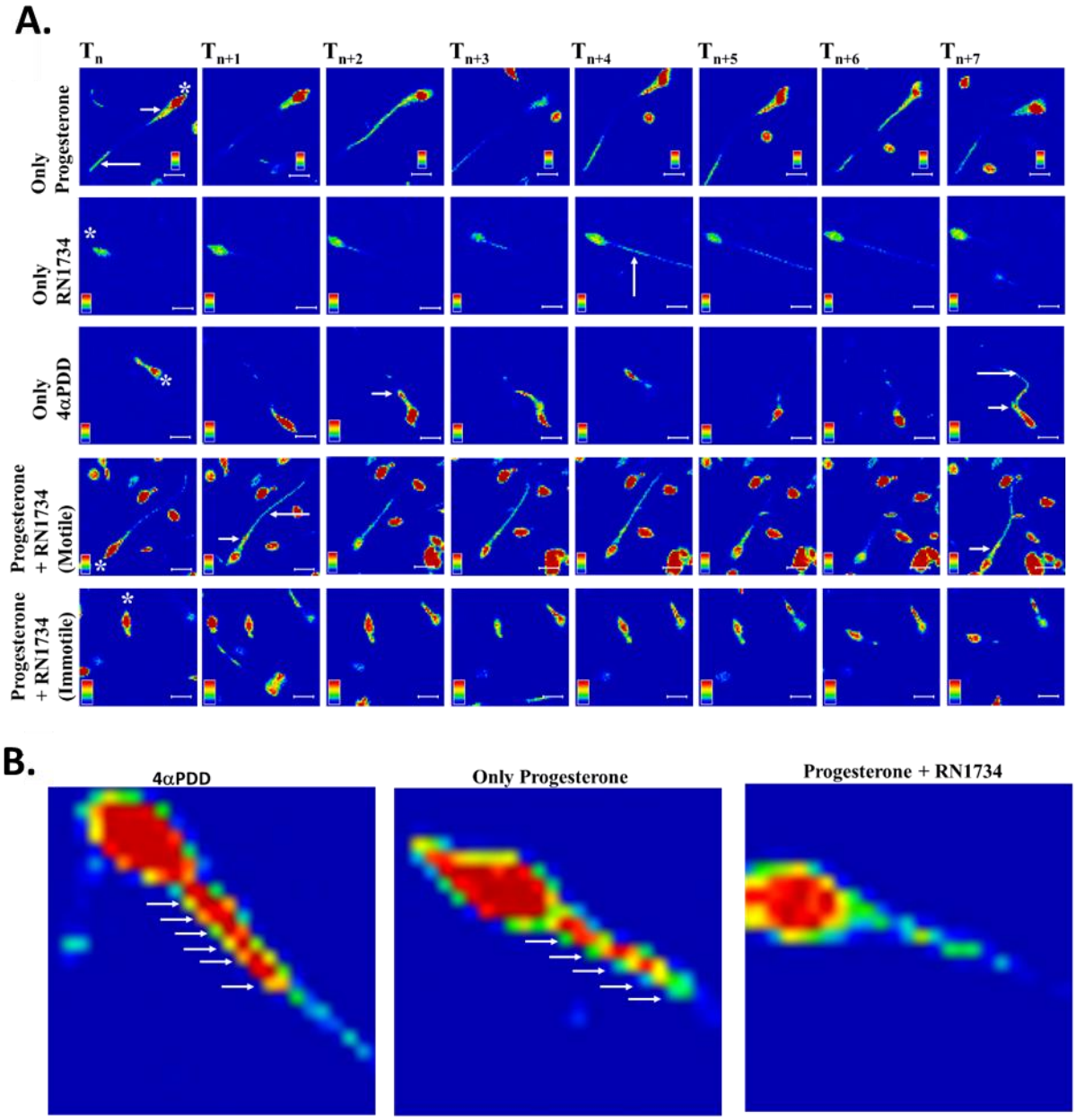

Fig 61. TRPV4 helps in Ca^{2+}-buffering in the neck region and acts as a progesterone receptor. A. Shown are the time-series images depicting the level of intracellular Ca^{2+} (indicated by pseudo color, red and blue indicating the highest and lowest level respectively) in human sperm cells loaded with Flou-4 AM and treated with different pharmacological agents alone or in sequential combinations. The cell which was tracked within a fixed time period (Tn to Tn + 7) is indicated by asterisk (*) symbol. The short- and long arrow indicate the high-level of Ca^{2+} in neck and tail respectively. Majority of the cells become immotile upon addition of RN1734 in progesterone pre-treated samples and have high-level of Ca^{2+} in the head regions and no/less Ca^{2+}-wave propagated to the tail. **B.** Shown are the magnified views of representative cells demonstrating the propagation of Ca^{2+}-waves from head to the tail through the neck region. In 4αPDD-treated and Progesterone-treated (representing motile, left side and middle) cells, Ca^{2+}-wave propagates through the mitochondrial coiling (green rings, indicated by arrows). High-level of Ca^{2+} (red) in the central stalk region is also visible in this case. Progesterone-treated cells when further treated with RN1734 (representing immotile cells, right side) do not propagate Ca^{2+}-waves through its mitochondrial coiling located at the neck regions. The central stalk region reveals mostly moderate- to low-level of Ca^{2+} there.

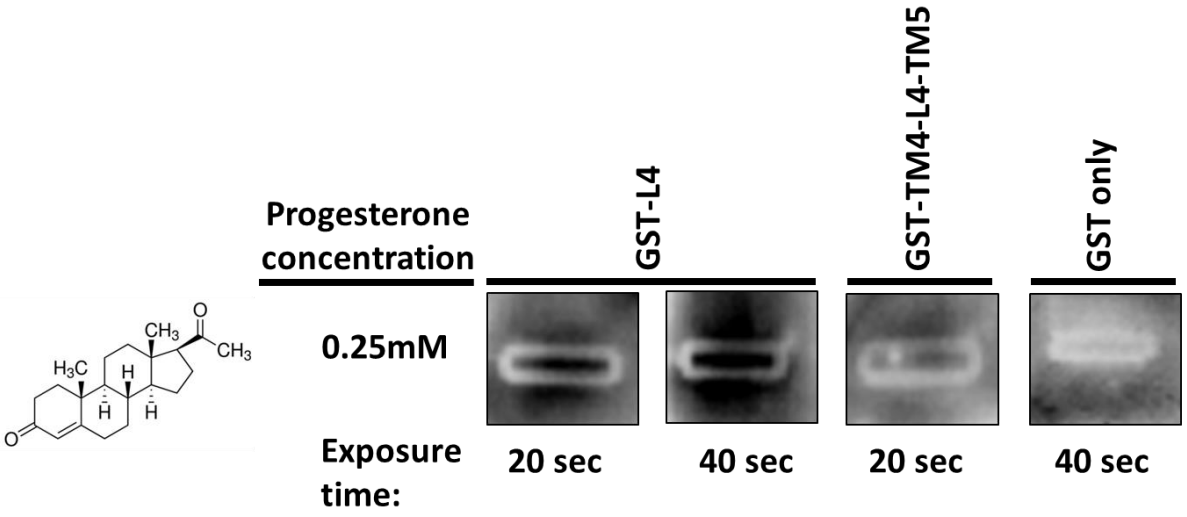

Fig 62: TRPV4 interacts with progesterone. Dot blot analysis depicting interaction between progesterone and TRPV4 fragments. Results suggest that Loop4 (L4) interacts strongly and TM4-Loop4-TM5 interacts weakly with progesterone (0.25 mM). Only GST protein was taken as a negative control which does not interact with progesterone at the same conditions.

Chapter 3

Discussion

3.1. TRPV4 is a mitochondrial protein

Transient receptor potential (TRP) is a cation channel superfamily which is divided into seven subfamilies involved in diverse physiological functions including thermosensation and mechanosensation [18, 21]. In last decades, intracellular localization of these ion channels was explored to some extent. Indeed, recent results demonstrate the intracellular localization of TRP ion channels in specific subcellular organelle and also characterized these TRP channels in the context of these organelles **(Fig 63)**. Among TRPV family ion channel, TRPV1 and TRPV3 are present in ER and regulates ER functions [205, 206]. However intracellular localization of TRPV4 in any cellular organelle not has been reported so far.

Accumulating evidence indicates that mitochondria have different channels and uniporters permeable for Ca^{2+}. Importance of these Ca^{2+}-channels have been linked with the several cellular functions such as cell signalling events, inter-organelle communications, cell aging, cell proliferation, pathophysiological disease and cell death. Voltage dependent anion channel (VDAC) present in the outer mitochondrial membrane is known to regulate mitochondrial Ca^{2+}-levels and thus mitochondrial metabolites and energetics; key functions of mitochondria [267]. Recent research demonstrated that VDAC channel is present in the mitochondria as well as the cell membrane and regulates its cellular function [268]. Recent report suggests that activation of TRPV4 in primary endothelial cells cause alteration in mitochondrial function and dilate the blood vessels because of ROS production, though it is an indirect effect of TRPV4 on mitochondria as it is primarily due to the TRPV4 present at the plasma membrane [102]. In another study it was reported that TRPV4 present in the endosymphatic sac of Rat and human ear where it acts as an osmosensor. Immunohistochemistry result of ear tissue section suggests that TRPV4 is present in the membranous region where mitochondrial number is very high and regulates the osmosensory functions of inner ear [269]. However these reports do not provide direct evidence that

TRPV4 is presents in the mitochondria and thus regulates the osmosensory function. So far, none of these reports suggest that TRPV4 is present into the mitochondria and can regulate mitochondrial function. In this thesis work we have investigated the presence of TRPV4 at the membrane as well as in the mitochondria and explored if TRPV4 can regulate critical functions of Mitochondria.

Previous studies on TRPV4 channel provided indirect evidences suggestive of its presence in mitochondria and its role in the regulation of mitochondrial activities. Earlier reports suggest that point mutations in TRPV4 (namely the R269C and R269H) lead to Charcot-Marie-Tooth disease type 2C (CMT2C), an autosomal dominant neuropathic disorder characterized by limb and laryngeal muscle weakness but normal motor nerve conduction [176]. Previous report also suggests that mutation in the mitochondrial fusion protein Mfn2 also leads to CMT2A disease, and pathophysiological symptoms similar to CMT2C which also characterized by peripheral nerve weakness [270]. However genetic loci of both these genes; i.e. Mfn2 (Chr 1) and TRPV4 (Chr 12) are different. However, as the resulting disease and pathophysiological symptoms are almost similar, and involve mitochondrial abnormalities, these results suggest that both candidate proteins are relevant with mitochondrial functions. In this regard, the results described in this thesis work strongly supports the previous reports and provides experimental evidence demonstrating that TRPV4 is present in cell membrane, and in the mitochondria. TRPV4 regulates mitochondrial structure and function in different manners.

3.1.1. Subcellular distribution of TRPV4: Unusual localization in the mitochondria

In last decade, few sporadic research have been conducted to characterize the intracellular characterization of TRPV4-Wt and its different mutants without any confirmatory results.

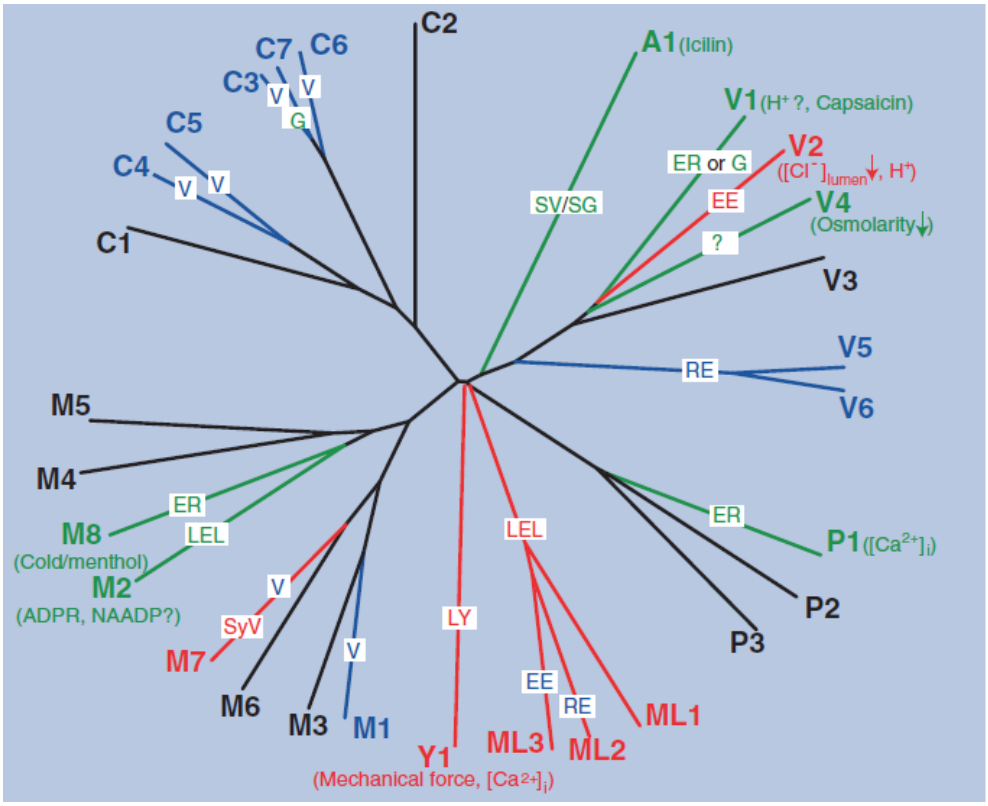

Fig 63: Subcellular localization of TRP channels. Represented image suggesting the localization of TRP channels present in different subcellular organelles. Apart from plasma membrane, ER and golgi; so far intracellular localization of TRPV4 has not been reported for any cellular systems. Image taken from Dong et al. 2010. [204]

However, immunofluorescence and Western blot analysis performed in this thesis work confirmed that TRPV4 is indeed present in the mitochondria. To establish the colocalization of TRPV4 with mitochondria, different mitochondrial marker proteins (Hsp60 and Cyt C) or specific dye (mitoTracker Red) were used in diverse cellular systems (HaCaT, CHOKI and HUVEC and in sperm cell). Furthermore to nullify the fixation artefact, live cell imaging was also performed to demonstrate the colocalization of TRPV4 in mitochondria in live cells **(Fig 13-15)**. The immunofluorescence results suggest that TRPV4 is primarily present in plasma membrane and in mitochondria but do not colocalize with other subcellular organelles such as ER, golgi and peroxisomes (**Fig 16-17**). Our results also suggest that not only TRPV4-Wt localizes in the mitochondria but other "gain-of-function" mutants (such as R616Q, V620I) and neonatal-lethal mutant (L618P) also localize in the mitochondria (**Fig**

15). Apart from the membrane localization, subcellular localization of TRPV4 in nucleus and ER was also reported, but functional significance of such localizations has not been characterized [208]. Among TRPV family ion channels, TRPV4 represents a molecular candidate which has been considered as a "hot spot" for several point mutations that play important role/s in the development of pathophysiologies [177, 178]. It was reported that the surface expression of TRPV4 is largely reduced in case of CMT2C mutants (R269H, R315W) and these mutants localize in the cytoplasm as a puncta [146]. In case of "gain-of-function" mutants (R616Q, V620I), the cell surface expression of these TRPV4 mutants are not altered much as compared to the TRPV4-Wt. It was suggested that gain in the total activity of the TRPV4 mutants may be because of the altered channel trafficking [208]. However comprehensive analysis for surface expression and subcellular localization of TRPV4 suggest that, TRPV4 surface expression not only depends on trafficking but other factors such as proper protein folding in ER, glycosylation, tetramer assembly, recycling and proteasomal degradation, etc. also regulate the localization of TRPV4 [132, 137, 177, 271, 272]. Nevertheless, a hypothetical model is proposed which partially described the surface expression or recycling of TRPV4-Wt and its mutants (**Fig 64**). Though all these studies have characterized the trafficking of TRPV4 to a large extent, the surface expression of TRPV4 and its involvement in the regulatory mechanisms are still uncharacterized. As both N- and C-terminal regions seem to be important, the reported self-interaction between N- and C-terminal of TRPV4 (which is also mediated by Calmodulin and Ca^{2+}) might play an important role here. Our results demonstrate that TRPV4 expression is not restricted to membrane as it could be localized in in the mitochondria as well. Our most of the colocalization results of TRPV4 with mitochondrial marker indicate that these mitochondria are located in perinuclear region, suggesting that during the trafficking of TRPV4 from ER to membrane, a fraction of it is recruited to the mitochondria.

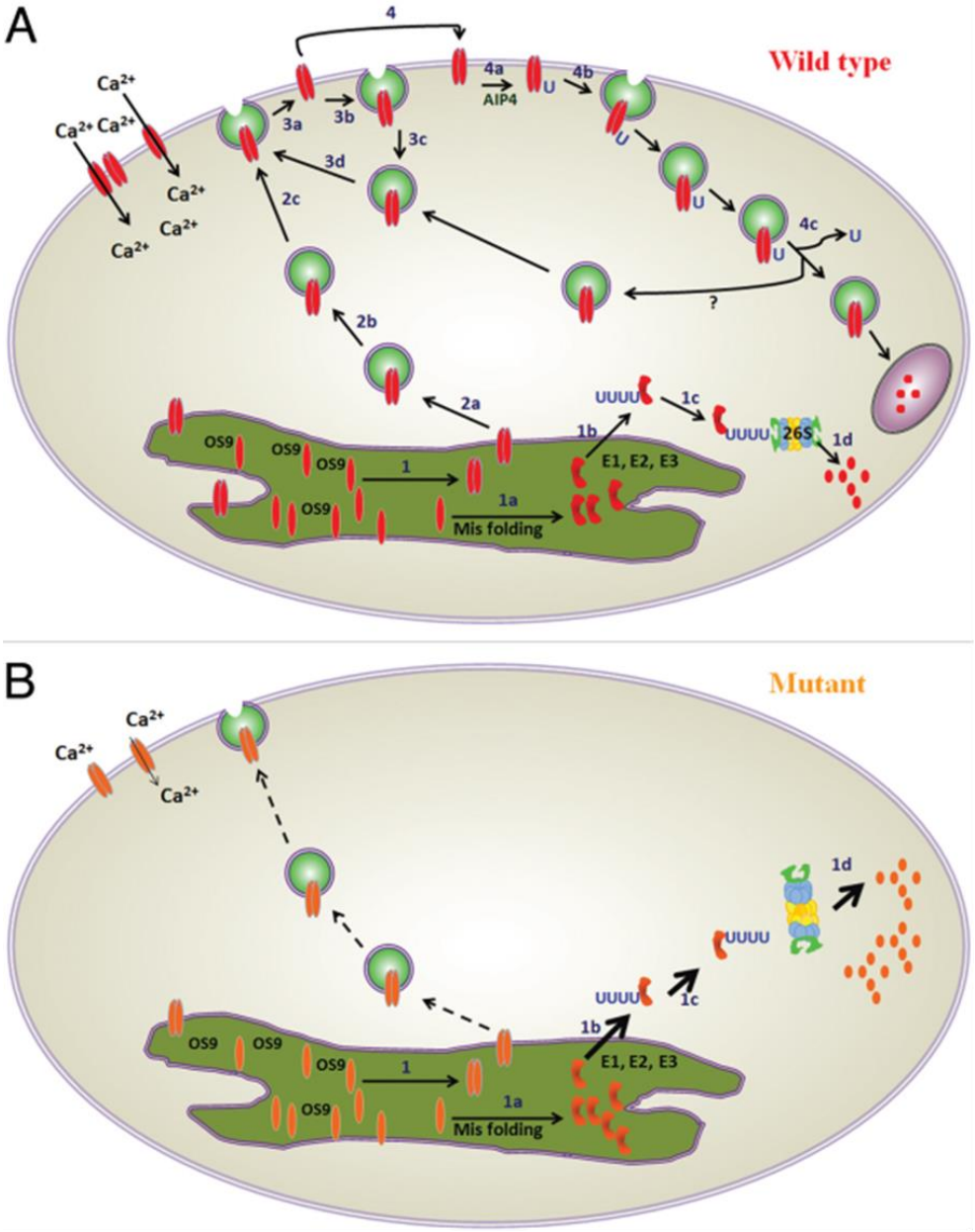

Fig 64: A hypothetical model depicting how surface expression of TRPV4 can be regulated. A. Surface expression of wild type TRPV4. OS9 protein with a chaperone-like activity assists TRPV4 monomer (indicated by red) to form tetramer. Misfolded TRPV4 is targeted for Ubiquitin-dependent 26S Proteasomal degradation pathway (ERAD, shown in steps 1a–d). Perfectly folded TRPV4 tetramer are inserted in vesicles and recruited to the plasma membrane (steps 2a and b). Most of the membrane inserted TRPV4 can be recycled (steps 3a–d). A fraction of the membrane inserted TRPV4 is regulated by AIP4, an E3 ligase and become monoubiquitinated (step 4a). This monoubiquitinated TRPV4 can be either degraded by lysosomes by multi-vesicular-body pathway (MVB pathway, indicated in steps 4a–d) or they get recycled back and become part of the recyclable vesicular pool located just beneath the plasma membrane. **B.** Reduced surface expression of TRPV4 mutant. In case of mutant (for example R269H, R316C and R315W in HeLa cell, indicated by yellow), a major fraction of total synthesized TRPV4 is misfolded and thus degraded by ERAD pathway as a quality control mechanism (steps 1a–d). Only a minor fraction of synthesized TRPV4, which is fully assembled and functional will be transported by vesicles and recruited to the plasma membrane (steps 2a and b). The other steps related to MVB pathway (steps 4a–d) and recycling of vesicles (steps 3a–d) are expected to be operational in case of mutants also. But for simplicity it is not shown in (**B**).

Furthermore to validate our immunofluorescence results we performed Western blot analysis of isolated mitochondria obtained from different cellular systems like goat brain, goat adipose tissue, synaptosomal fraction of fore brain and CHOK1-TRPV4 stable cell line using anti-TRPV4 antibodies. In each case, TRPV4-specific band was observed in mitochondrial fraction. Expected molecular weight (~ 98 kDa) was observed in mitochondrial fraction isolated from goat adipose tissue and from CHOK1-V4 cells. But in case of mitochondria isolated from goat brain, TRPV4-specifc band is observed at around 72 kDa. However in case of synaptosomal fraction isolated from fore brain, TRPV4-specific immunoreactivity was observed at a size of expected molecular weight (~ 98 kDa) and a lower band (~ 72 kDa) is also visible. In recent study, it was observed that TRPV4 unusually localizes in the nucleus and TRPV4-specific band of around ~ 70 kDa size has been detected by Western blot analysis of nuclear fraction [207]. The unusual band of TRPV4 (~ 70 kDa) can be a splice variant of TRPV4 or it may be a truncated product due to specific proteolytic action. It was reported that hTRPV4 consists of 871 amino acids (full-length), and has five splice variants including TRPV4-A (full-length form, expected molecular weight is 98, 100 and 110 kDa), TRPV4-B (lacking exon 7, expected molecular weight is 91 and 96 kDa), TRPV4-C (lacking exon 5, expected molecular weight is 92 and 97 kDa), TRPV4-D (short deletion inside exon 2, expected molecular weight is 98, 100 and 110 kDa) and TRPV4-E (lacking D237-284 and D384-444 amino acids, expected molecular weight is 86 and 90 kDa) [48]. The appearance of TRPV4-spepfic bands at different sizes can be due to the post-translational modification such as phosphorylation and glycosylation [137, 273]. Another possibility which can actually give rise to these smaller fragments is the specific proteolytic cleavage of TRPV4. Full-length TRPV4 can be subject to proteolytic cleavage inside the mitochondria or nucleus and this cleavage seem to be at the N-terminal region of TRPV4 as the lower molecular weight fragment can be detected by the C-terminal specific antibody. In this context, it is important

to mention that mitochondria contain more than 25 types of different proteases and only few of these proteases are characterized and most of these are not well established. These mitochondrial proteases play important role in mitochondrial proteostasis, i.e. maintenance of protein quality within mitochondria [274, 275]. The results suggest for a possibility where during the entry or translocation of TRPV4 from ER to mitochondria, active mitochondrial proteases act on TRPV4 and specifically cleave at the N-terminal side which results in the formation of lower molecular weight fragment of TRPV4.

3.1.2 Interaction of TRPV4 with mitochondrial proteins and its biological significance

Till now the interaction of any mitochondrial protein with TRPV4 not has been reported. However, some protein kinases (such as PKCε) and/or several other cytoplasmic proteins (such as tubulin) which are occasionally present in the mitochondria (or at the mitochondrial surface) known to interact with TRPV4 [51]. Here in this work we have characterized a few mitochondrial proteins (Hsp60, Mfn1 and Mfn2) which interact with the C-terminal of TRPV4 irrespective of the presence or absence of Ca^{2+}/GTP and ATP (**Fig 21-22**). Since full-length TRPV4 is difficult to express in bacterial system, and the N-terminus fragment or the entire transmembrane (TM) region of TRPV4 do not show any colocalization with mitochondrial markers, it is justified to prioritize the interaction study (with mitochondrial proteins) with the C-terminus of TRPV4 (718-871 aa) only. The *in vitro* experiments conducted with MBP-TRPV4-Ct is suitable for this kind of studies as the fusion protein is expressed as a "MBP fusion protein" which offers expression in higher amount and also increases the solubility of the fusion proteins.

Heat Shock Proteins (HSP) or stress proteins are the evolutionary conserved proteins present in almost all organism and are expressed in high quantity in response to physical and chemical stimuli. HSPs represent molecular chaperone proteins present in the mitochondrial

matrix which plays important role by facilitating the folding, intracellular transport, assembly, and disassembly of other proteins [276-278]. In this work we have demonstrated that Hsp60 interacts with MBP-TRPV4-Ct but how it helps in protein folding or assembly is not yet established. However previous studies suggested that TRPV1 agonist Capsaicin increased the level of different HSPs such as Hsp27, Hsp70 and Hsp90, though the same study has not characterized the level of Hsp60 [235]. It has been reported that Hsp60 is not present in mitochondria exclusively, as it is also present (about 20%) in ER luman and cell membrane [279-281]. It is possible that during tetramer assembly of TRPV4 in ER, Hsp60 binds to tetrameric TRPV4 and translocase to mitochondria as well as to the cell membrane. Our results suggest that TRPV4-Ct binds with Hsp60 which goes well with previous studies in which TRPV4-Ct plays an important role in tetrameric assembly [208].

The TRPV4-Ct interacts with two other mitochondrial fusion proteins, namely with Mfn1 and Mfn2, members of a GTPase family which are abundantly present in outer membrane of mitochondria and play a crucial role in mitochondrial fusion. Mfn2 is present in mitochondria and the mitochondria-associated membrane named as "MAM". The MAM consists of a region of close contact points between ER and mitochondria which communicate with associated mitochondria for lipids and/or lipid derivatives, metabolites and Ca^{2+}-exchange (**Fig 65**). It has been established that the contact site of ER and mitochondria regulates the mitochondrial dynamics through regulating the expression of Mfn1 and Mfn2 fusion protein [282, 283]. Although Mfn2 is an outer membrane mitochondrial protein, its amount is 14-fold higher in the region of MAM and helps in transiently tethering of ER towards mitochondria [284]. It seems that after tetrameric assembly of TRPV4 in ER, some of the tetrameric or monomeric TRPV4 undergoes leaky translocation and entered inside the mitochondria through MAM. Furthermore, we demonstrate the direct interaction of Mfn1 and

Mfn2 with TRPV4-Ct. This is demonstrated by using Mfn1 and Mfn2 as His-tagged fusion proteins which directly bind to the MBP-TRPV4-Ct **(Fig 23**).

3.1.3. Importance of TRPV4 in mitochondrial structure-function regulations

Mitochondrial dysfunction or mitochondrial abnormalities in the presence of TRPV4 activator or inhibitor are mostly because of mitochondrial ROS production, as demonstrated in case of endothelial cells [102]. However, in this study we demonstrate that TRPV4 activator 4αPDD regulates mitochondrial morphology and mitochondrial potentiality. Activation of TRPV4 induces mitochondrial aggregation or clustering in CHOK1-V4 stable cells as well as in HUVEC primary cell. However in presence of TRPV4 inhibitor mitochondrial morphology remains normal and reveals mostly tubular and/or elongated structure (**Fig 24-26**). Mitochondrial morphology is essential for continuous supply of ATP and mitochondrial metabolites to the cellular system. Mitochondria formed reticulate network radiating from nucleus to outer area and create a tubular network inside the cell [285]. This tubular network is precisely regulated by fusion and fission events in the cell mediated by several associated protein. Mitochondrial shape or morphology is not static in nature, because mitochondria divide and partition into daughter cells during cell division [286]. Altered mitochondrial morphology has also been linked with apoptosis and in this case fragmented mitochondria; altered cristae fusion and enlargement of cristae junctions are known [287, 288]. Mitochondrial fusion events carried out by group of GTPase family protein Mfn1, Mfn2 (present in outer membrane or MAM) and Opa1 (present in inner mitochondrial membrane) while mitochondrial fission carried out by Drp1 protein (present in outer membrane). Here in this work we have demonstrated that TRPV4 interacts with mitochondrial fusion protein Mfn1 and Mfn2 and also demonstrate that TRPV4 positive mitochondria have altered mitochondrial morphology, which gives strong evidence that

TRPV4 activator or inhibitor largely regulates mitochondrial structure. It seems that TRPV4 largely regulates the cristae curvature as in presence 4αPDD (activator of TRPV4), Ca^{2+}-influx inside the mitochondria is visible which may result in cristae aggregation and mitochondrial shape becomes spherical. Recent research indicates that mitochondrial morphology largely depended on the lipid composition or lipid signalling molecules present or associated with mitochondria [289]. Most of the mitochondrial lipids are synthesized in the MAM region and transported into the mitochondria for its metabolite requirements. Mitochondrial morphology is maintained by several lipids (which are present in lower eukaryotes to higher mammals such as in yeast and human) such as cardiolipin, phosphatidic acid, lysophosphatidic acid, diacylglycerol, and phosphatidylethanolamine and lipid related enzymes [289]. It seems that TRPV4 activator regulates or altered lipid composition or synthesis which is present in the mitochondria and because of that mitochondrial morphology change significantly.

3.1.4. Importance of TRPV4 in mitochondrial Ca^{2+} homeostasis

It is well established that intercellular Ca^{2+} homeostasis is maintained by Ca^{2+}-binding proteins present in cytoplasm, endoplasmic reticulum (ER) and mitochondria [290-292]. Mitochondria are important cellular organelles which can modulate both the amplitude and the spatio-temporal patterns of Ca^{2+}-signals [226, 293, 294]. Our results strongly suggest that TRPV4 is present in the mitochondria and regulates mitochondrial Ca^{2+}-influx. Although mitochondria plays an important role in Ca^{2+} homeostasis, but so far only very few calcium channels are known which are present in the mitochondria. Recently it has been reported that TRPC3 is present in the mitochondria and it regulates mitochondrial potentiality as well as Ca^{2+}-influx. Ca^{+2}-transport inside the mitochondria is mediated through outer mitochondrial membrane (OMM) and followed by inner mitochondrial membrane (IMM). The OMM is

able to transport small molecule (> 5 kDa) but the IMM are not freely permeable for Ca^{2+}. The permeability of divalent cations such as Ca^{2+} (but not anion) in OMM is known to be governed by Voltage Gated Anion Channels (VDAC) and its several isoforms [295, 296]. Once free Ca^{2+} ion crosses the OMM, it crosses further the IMM with the help of mitochondrial uniporters (MCU) abundantly present there [222]. However, the array of mitochondrial proteins involved in maintenance of mitochondrial Ca^{2+}-levels and subsequent signaling and the actual mechanisms remain as enigma. It has been demonstrated that the distribution of mitochondria is mainly high in the area where the cytoplasmic Ca^{2+} concentration is high (Heterogeneous in nature), because of different classes of Ca^{2+}-selective ion channels present in ER (such as IP3 receptor), sarcoplasmic reticulum (Rhynodine receptor) and plasma membrane (Voltage operated channels and Store operated channels) [297-300]. Therefore, mitochondria has evolved with a sensitivity for recognizing microdomains of high cytoplasmic Ca^{2+} which dissipates high influx and efflux of Ca^{2+} across the mitochondrial membrane. Because of this notion most of the mitochondria show close proximity with ER (in fact connected through MAM) and cause easy exchange of divalent cations such as Ca^{2+}. Experimental observation and chemiosmotic theory suggests that energized mitochondria sequestered positively charged cations such as Ca^{2+} inside the mitochondrial matrix [301]. In this study we have characterized TRPV4 as a unique ion channel present in mitochondria which regulates mitochondrial Ca^{2+} homeostasis and morphology. It has been reported that excesses of Ca^{2+} leads to reduction in mitochondrial potentiality and this extra Ca^{2+} efflux through new opening in the mitochondria called MPT. Therefore, our results fit well with this observation in which TRPV4 activator increases Ca^{2+}-influx and results in reduction in mitochondrial potentiality as compared to TRPV4 inhibitor, and it also shows the formation of MPT in mitochondria which helps in efflux of extra Ca^{2+}.

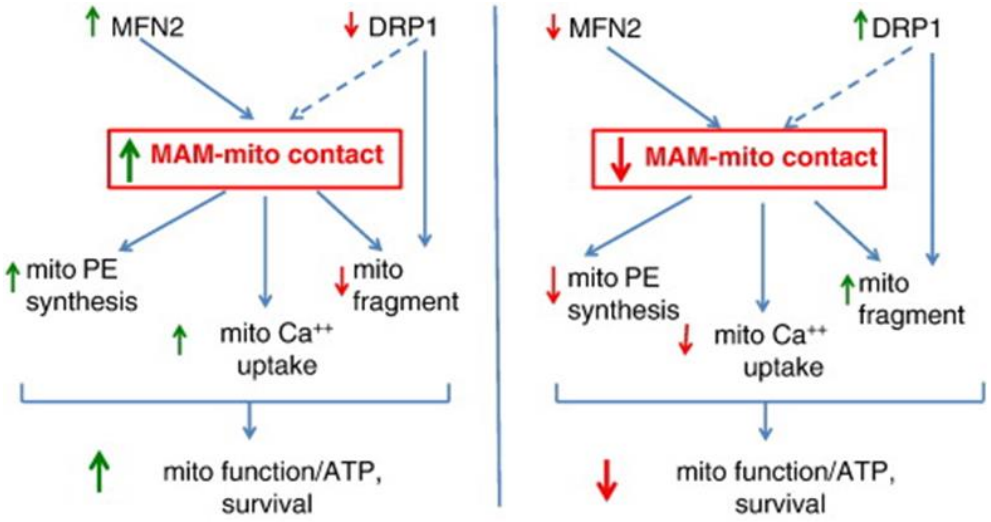

Fig 65: Role of MAM in mitochondrial dynamics and calcium regulation. Contact site between mitochondria-associated membranes (MAM) and mitochondria (mito) are increased when expression of the mitochondrial fusion protein, mitofusin-2 (Mfn2) is increased (left panel) and decreased by over-expression of the fission protein, Dynamin-related protein-1 (Drp1) (right panel). A reduction in MAM-mitochondria contacts (right panel) attenuates the import of phosphatidylserine (PS) into mitochondria via the MAM, thereby decreasing the mitochondrial production of phosphatidylethanolamine (PE) via PS decarboxylase (PSD). Reduction in the zones of contact between MAM and mitochondria reduces Ca^{2+} uptake into mitochondria from the ER and promotes mitochondrial fragmentation (Adapted from Jean E. Vance) [302].

3.1.5. TRPV4 interaction with mitochondrial protein or regulation of mitochondrial function is relevant for neuropathic pain other pathophysiology

TRPV4 is expressed in a broad range of tissues, including lung, spleen, kidney, testis, fat (Adipose tissue), brain, cochlea, skin, smooth muscle, liver, bone, cartilage and vascular endothelium where it regulates the physiology of the cellular system [53-58]. Not only does TRPV4 function as osmosensor, but also senses the mechano-transduction in A and C fibers of sensory neuron. It was demonstrated that in presence of nociceptive stimuli TRPV4 promote the release of the neuropeptides substance P and CGRP from the central projections of primary afferents nerve terminal in the spinal cord which indicate that TRPV4 plays a major role in nociceptive pain [90]. TRPV4 also plays an important role in mechanical hyperalgesia in presence of inflammatory molecule or compound. It was demonstrated that TRPV4 activates downstream Protein Kinase A (PKA) and Protein Kinase C (PKCε), Protein Lipase C (PLCβ) pathways and different inflammatory molecule which in turn activate

TRPV4 and results in TRPV4-mediated hyperalgesia [90, 91]. Recent study suggests that PKCε, a cytoplasmic kinases translocates to mitochondria and phosphorylates several other mitochondrial proteins or channel proteins such as Complex IV, glycogen synthatase kinase-3β, ATP-sensitive K^+ channel in case of mechanical hyperalgesia [92, 303-307]. Parallel study suggests that TRPV4 C-terminus binds to PKCε but how it regulates or effect mitochondrial function is not known [51]. Our results suggest that C-terminus of TRPV4 translocates inside the mitochondria and it may binds with the mitochondrial PKCε but how it regulates the mitochondrial function is still elusive. It is well known that mitochondrial dysfunction in neuronal cells or others also, produce ROS, NOS and excesses of calcium influx which in turns leads to generation of neuropathic and chronic pain [308-311]. It seems that TRPV4 containing mitochondria increases the calcium level of mitochondria which in turns increased the production of ROS and NOS and ultimately results in neuropathic or chronic pain perception in neuronal cell.

Mitochondrial number and its distribution is random in most of the cell but in case of differentiated cells like neuron and muscles cell its distribution as well as number are very specific. In neuronal cells mitochondrial number and its position are higher in high energy demanding area such as pre-synapse or post-synaptic junctions, active growth cones or axonal branches, nodes-of-Ranvier and dendritic spine which maintain the plasticity of neuron [312]. Recent report suggests that in mitochondrial position and its morphology altered as compared to other cellular type in neuropathic or inflammatory pain condition [313]. In this study, inflammation inducing compound was administered with adjuvant into the right hind paw of mice and after fixation mitochondrial distribution and morphology were studied in spinal nerve. It was observed that mitochondria shows perinuclear aggregation or clustering in presence of inflammatory molecule induced neuropathic pain [313]. However in control condition mitochondrial morphology was normal and granular in nature (**Fig 66**).

Though it was established that persistent inflammatory pain and neuropathic pain are different, mitochondrial aggregation or clustering (increased in area) nature was observed in both conditions. Our result fits well here, since we have demonstrated that mitochondrial morphology altered in presence of TRPV4 activator 4αPDD and that its number reduces significantly in CHOK1-V4 cells and HUVEC primary cells. These results indicate that TRPV4 mediated neuropathic pain is largely regulated by mitochondrial morphology and dynamics and its dysfunction results in several pathophysiology. Mitochondrial transportation or movement in neuronal cells largely depends on axonal microtubule and actin cytoskeleton and its associated protein. Microtubule is made up of polymer of α- and β- tubulin which arranged in polarized way plus and minus end. Microtubules accessory motor proteins KIF family proteins and dynein protein (ATPase protein) helps in mitochondrial anterograde and retrograde movement across the microtubules [314, 315].

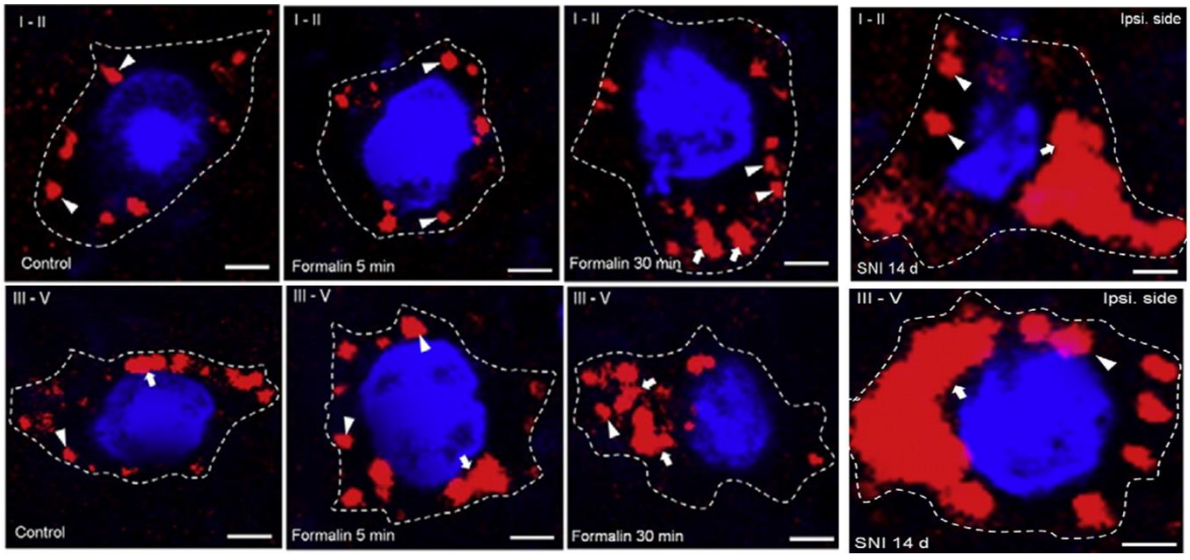

Fig 66: Mitochondrial morphology altered in case of neuropathic pain. Represented image shows the MitoTracker Red labelled mitochondrial morphology in spinal horn tissue after the induction of inflammatory molecule in the mice. Results indicate that mitochondrial distribution or morphology are strikingly different under normal and pain conditions: in normal control mice (left side), most of mitochondria exhibited granule; conversely, in mice of formalin -induced persistent inflammatory pain or Spared nerve injury (SNI) -induced neuropathic pain (right side), most of MitoTracker Red positive cells had a cluster and aggregated mitochondria. (Image adapted from Guo et al., 2013). [313]

The direct role of TRPV4 in mitochondrial transportation or movement is still elusive. However it has been reported that TRPV4 C-terminus binds with Microtubule Associated Protein (MAP7), soluble tubulin and polymerised tubulin and regulates the gating properties of channel (51, 149). It has been reported that Kif1b motor protein point mutation also leads to same CMT2A disease which was earlier shown with TRPV4 mutation. Same disease with two different genetic loci mutation indicates that TRPV4 involved in genetic-phenotypic interaction with same gene product. Several other proteins, namely Neurofilament L, Mfn2, Rab7a, Lamin A, Med25, GarS, Hsp 27, MPZ, GDAP1 and Hsp 22, which are also involved in CMT2 disease, are actually potential interacting partners of TRPV4 [209].

3.1.6. TRPV4 interaction and regulation of mitochondria is relevant for regulation of mitochondrial metabolite

In cellular system mitochondria and ER are the major organelle for metabolite synthesis and its exchange with cytoplasmic metabolite. Metabolic processes in mitochondria are compartmentalized into various functional units spanning over the outer membrane and the inner membrane because of their specialized structural and biochemical make up. Most of the lipid synthesis occur in ER and transported to mitochondria for further modification through MAM [302]. It was suggested that lipid molecule acts as a secondary signalling molecule or intracellular transmitter and may help in TRPs channel regulations [316-318]. Phosphatidylinositol 4,5-bisphosphate (PIP_2) is a lipid component found mostly in the plasma membrane (inner layer) and known to interacts various ion channel present in the membrane. PLC hydrolyses PIP_2 into DAG and inositol 1,4,5-trisphosphate (IP3). PIP_2 interacts with several TRPs family ion channels and regulates its gating property and sensitivity towards lipid signalling [319]. PIP_2 interacts with the positively charged residue present in the TRPs channel and it was reported that mutation in the positive charged amino acid residue altered

the binding affinity of PIP_2 and ultimately changed its gating property [320-322]. Recent report suggests that N-terminus of TRPV4 interacts with PIP_2 protein and regulates its gating property. PIP_2 binding site are closer to PASCIN binding site in N-terminus of TRPV4 [214]. In human, arachidonic acid oxidation carried out by three major enzymatic pathways: LOX, cyclooxygenase (COX) and cytochrome P450 epoxygenase. It was reported that 5,6-EET and 8,9-EET (Epoxyeicosatrienoic acids) are the products of cytochrome P450 epoxygenase pathway and that they help in opening and closing of TRPV4 channel.

Mitochondria are the major organelle for cholesterol biosynthesis pathway. Cholesterol biosynthesis starts from small carbon chain molecules through a series of chain reaction in the cytosol and the ER. The enzymes of cholesterol synthesis are located primarily on ER but the synthesis of steroids or its derivatives occurs in mitochondria [323, 324]. The main rate limiting step in the biosynthesis of steroid is the transport of cholesterol across the outer mitochondrial membrane (OMM) into the inner mitochondrial membrane (IMM) where cytchrome P450 enzyme converts all cholesterol into pregnenolone, the precursor of all steroids [323]. The direct role of cholesterol transportation into the mitochondria is not known but members of the StAR (steroidogenic acute regulatory) protein helps in cholesterol transportation into the inner membrane of mitochondria. Furthermore, it has been also proposed that transport of cholesterol across the IMM occurs through a complex of protein transporter called “transduceosome” which is primarily composed of OMM, VDAC and translocator protein [325]. Since mitochondria are the prime organelles whose role is reported in steroid biosynthesis, the alteration in mitochondrial dynamics or membrane potential might alter cholesterol biosynthesis. A recent study suggests that the levels of Mfn2, a mitochondrial fusion protein significantly increased during steroid synthesis [326]. It has been also reported that blocking mitochondrial fusion by knocking down Mfn2 expression has a negative impact on steroid synthesis [326]. It indicates that mitochondrial fusion is

central for the formation of multiprotein complex at OMM which helps in transport of cholesterol. Recently we have shown that TRPV4 interacts with cholesterol and it regulates the channel localization in membrane [164]. It seems that TRPV4 channels were present in the cholesterol enriched membrane microdomains and was also involved in regulating the biosynthesis of cholesterol. In this regards our bioinformatics results showed that TRPV4 was conserved throughout the evolution, as in the case of histone and Cyt C gene. Synteny analysis also suggested that TRPV4 and MVK (Mevalonate kinase) were located on the same chromosome 12, which indicate that cholesterol biosynthesis pathway coevolved with TRPV4. Mevalonate pathway is an important metabolic pathway which provides cholesterol, sterol isoprenoids, steroids and its derivatives to the cells [327]. We have also characterized some small molecular weight mitochondrial metabolite changes in presence of TRPV4 activator and inhibitor through NMR, and observed that TRPV4 activator significantly changes the metabolite molecular weight by adding or substituting the methyl or ethyl group in existing the mitochondrial metabolite. This indicates that TRPV4 directly or indirectly regulates the mitochondrial metabolite concentration or composition significantly. However the identity of the individual metabolite and its related or altered pathway are still not elucidated.

3.1.7. Regulation of mitochondrial function/s by other TRP ion channels

Recent studies suggested that mitochondrial dysfunction contributed to multiple diseases in cellular systems. Few other TRPs other than TRPV4 also regulate the mitochondrial morphology and function. For example, capsaicin, a TRPV1-specific agonist induced apoptosis in rat thymocytes cells [328]. The effect of capsaicin on cell death seems to be either specific (TRPV1-mediated) or non-specific (not mediated by TRPV1) in nature. Capsaicin can cause apoptosis or necrosis depending on the dose applied. In cultured rat

DRG cells, Capsaicin causes apoptosis by increasing the intracellular Ca^{2+} concentration, enhancing mitochondrial Ca^{2+} accumulation, dissipation of the inner trans-membrane potential ($\Delta\psi_m$), activation of Ca^{2+}-sensitive proteases and DNA fragmentation [329]. Capsaicin evokes similar signalling events in transformed and mitogen activated T- cells [330], and in human and rat glioblastoma cells [331, 332]. The intercellular Ca^{+2}-homeostasis is maintained by Ca^{+2}-binding proteins present in cytoplasm, endoplasmic reticulum (ER) and in mitochondria [290-292]. The elevated intracellular Ca^{+2} triggered by Capsaicin leads to activation of Ca^{2+}-dependent enzymes such as different phospholipases, proteases, endonucleases that can cause apoptosis in neuronal cells as well as non-neuronal cells [333, 334]. Though mitochondria are able to sequester intracellular Ca^{+2}, excess Ca^{+2}-influx into mitochondria leads to membrane permeability transition (MPT) pore in mitochondrial membrane [335]. This is considered as prototypical inducing factor. This MPT allows water and other small molecules to infiltrate inside the mitochondrial matrix which leads to osmotic swelling of mitochondria and may cause physical rupture of mitochondrial membrane [336-339].

However, several reports suggest that vanilloids may exert similar effects which are independent of Ca^{2+}-influx and involve different TRPV channels. This is due to the fact that Capsaicin has significant effects in biological systems that are much lower in the phylogenetic tree and in many cases do not contain TRPV1. For example, Capsaicin acts as inhibitor for organisms such as *Paracoccus denitrificans*, *Escherichia coli*, and *Thermus thermophilus* HB-8 where it affects ubiquinone reduction by NADH [340]. Vanilloids other than capsaicin such as dihydrocapsaicin and RTX, can also act as inhibitor of NADH oxidase [341]. Recently it has been shown that capsaicin can act as an inhibitor of tyrosyl-tRNA synthetase, therebyinducing cell death in hippocampal astrocytes [342, 343].

The TRPV1-independent functions of Capsaicin mostly indicate the deleterious effect of Capsaicin on mitochondria. Earlier research suggests that after the systemic application of Capsaicin leads to mitochondrial swelling resulting in the formation of atypical hollow mitochondria in the Aδ-type sensory neuron of adult rat as well as neonatal rat [344-349]. However, the real molecular mechanism behind the formation of hollow mitochondria is not clear. It seems that Capsaicin can also exert receptor-independent effects in addition to the TRPV1 receptor-mediated effects. Due to its structure, Capsaicin can act as analogue of Coenzyme Q, a lipophilic mobile electron carrier present in plasma membrane and involved in maintaining the redox potential of membrane. Indeed, it has been reported that pre-incubation of human lymphoblastoid cells with Coenzyme Q prevents Capsaicin-induced apoptosis [341, 350]. It suggests that Capsaicin competes for Coenzyme Q and alters the redox potential of plasma membrane. It has been also reported in transformed and activated T-cells, Capsaicin inhibits the plasma membrane NADH oxidoreductase (PMOR), an enzyme that transfers electrons from cytoplasmic NADH to external electron acceptors such as oxygen via Coenzyme Q (ubiquinone) [341, 350-352]. Capsaicin can also inhibit the NADH:Coenzyme Q oxidoreductase (Complex I) activity of the mitochondrial electron transport system [340, 353] which causes alteration on the mitochondrial membrane structure and its function [354, 355] (**Fig 67**). *In vitro* experiments in transformed cells as well as in activated T cells suggest that Capsaicin treatment enhances the generation of reactive oxygen species [330, 356, 357] causing depolarization of mitochondrial membrane and apoptosis [329]. Capsaicin suppresses the growth of cancer cells by NF-kB inactivation, reactive oxygen species (ROS) generation, cell-cycle arrest and modulating EGFR/HER-2 pathways [358-362].

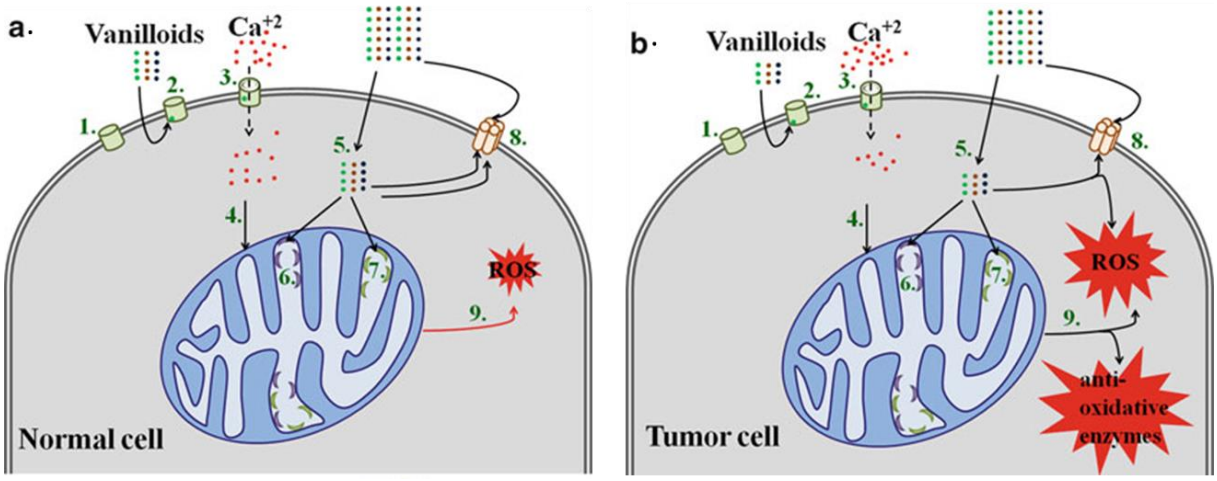

Fig 67: Model representing TRPV1-mediated mitochondrial dysfunction. TRPV1 present in the plasma membrane of normal cell (a) and tumor cell (b) can be activated by different vanilloids with different affinities and binding kinetics (Steps 1-2). Potent vanilloids such as Capsaicin or RTX activate TRPV1 at very low concentration and cause Ca^{2+} influx (Step 3). Vanilloids at much higher concentrations can cross plasma membrane and can also act on electron transport chain complex 1 (ETC1) and electron transport chain complex 3 (ETC3) (Steps 5–7). Vanilloids can also act on the Coenzyme Q and PMOR (Steps 8–9). All these factors result in production of ROS (indicated in red star).

Similarly, RTX was also reported to inhibit the NADH oxidase located in plasma membranes, to generate reactive oxygen species, and to induce apoptosis in transformed cells [142, 330, 341, 350]. The exact molecular mechanism by which Capsaicin causes oxidative stress and apoptosis remains unclear [363]. However, it is reported that activation of TRPV1 by Capsaicin increases mitochondrial fission, decreases mitochondrial membrane potential and reduces mitochondrial transport in the axons of murine DRG neurons [364]. Though it has been suggested that TRPV1 activity is involved in mitochondrial dysfunction, recent reports also suggest that other TRP channels also play significant role in mitochondrial function. For example, TRPA1 is stimulated by reactive oxygen species released during oxidative stress [365]. Diabetic Peripheral Neuropathy (DPN) and cancer are common comorbidities associated with Type I and Type II diabetes. DPN is characterized by increased sensitivity to cold pain as well as oxidative stress due to ROS overproduction. It has been already reported that TRPA1 mediates this enhanced sensitivity to cold and ROS in DPN patients.

Microtubule cytoskeleton is also involved in the development of atypical mitochondria. For example, Paclitaxel, an anti-cancer drug is associated with hypersensitity to cold, over expression of TRPA1, accumulation of atypical mitochondria and overproduction of reactive oxygen species in Diabetic subjects [309]. Cold hyperalgesia and production of ROS is significantly reduced in presence of TRPA1 inhibitors. Thus, TRPA1 channel seem to be a potential drug target for alleviating such ailments associated with Diabetes or other neurological disorders where atypical mitochondria is involved [309]. In this context, it is known that Vagal sensory nerves that line up respiratory airways and lungs are enriched with mitochondria. These nerves selectively express considerable amounts of TRPV1 and TRPA1. Reactive oxygen species generated by dysfunctional mitochondria in these regions (caused by noxious stimuli) activate these nerves via TRPA1 and thereby protects respiratory tracts and airways through various reflexes like coughing, bronchospasms, etc. [366]. Mitochondria are one of the major cell organelles that produce Reactive oxygen species (ROS). In addition to producing ROS, mitochondria harbour enzymes that catalyse the synthesis of hydrogen sulphide, which in turn scavenges these ROS. In brain, this creates a cytoprotective function. TRPA1 gets activated by polysulphides (H_2S derivatives) and thereby allows Ca^{2+}-influx through astrocytes. Once activated, astrocytes release D-serine at the synaptic junctions in order to enhance the activity of NMDA receptors which in turn stimulates hippocampal long term potentiation [367].

Activation of TRPC3 and TRPC6 is important for mitochondrial migration in hippocampal neurons [368]. Formation of superoxide and hydrogen peroxide in mitochondria is increased upon 4αPDD treatment in endothelial cells [102]. Expression of TRPM2 splice variant in tumour cells leads to decreased mitophagy, resulting in accumulation of dysfunctional/damaged mitochondria and increased ROS accumulation, thereby contributing to cell death and reduced tumor growth [369]. A fraction of TRPC3 has been shown to

localize in mitochondria and regulates mitochondrial Ca^{2+}-dynamics and mitochondrial membrane potential [255]. Mucolipidosis Type IV caused due to mutation in TRPML1 gene results in mitochondrial fragmentation and decreased mitochondrial Ca^{2+} buffering efficiency [370]. TRPM8 activation by menthol and icilin induces increase in mitochondrial membrane potential, glucose uptake and heat production in human white adipocytes [371]. Adult cardiac myocytes from TRPM2 KO mice show down-regulated levels of Complex I, III, and IV, and had lower mitochondrial membrane potential, mitochondrial Ca^{2+} uptake, ATP levels, and O_2 consumption but higher mitochondrial superoxide levels [372]. In mouse vagal neurons, Ca^{2+}-influx induced by the mitochondrial complex III inhibitor antimycin A was significantly reduced by pharmacological inhibition or genetic knockout of either TRPA1 or TRPV1. This Antimycin A effect is completely abolished by combined inhibition of both TRPA1 and TRPV1, thereby indicating that both these channels are critical for mitochondrial functions [366]. TRPC6 activation by hyperforin in isolated brain mitochondria collapses the mitochondrial membrane potential and induces the release of Ca^{2+} and Zn^{2+} from there [373].

3.2. TRPV4 has a novel Mitochondrial Target Signal (MTS)

Intracellular shorting of nucleus encoded mitochondrial protein depended on the N-terminal sequence of protein Mitochondrial Target Signal (MTS). The length of MTS cleavable sequence varies from 20-40 amino acids and carry spotted positively charged residue (mostly Arginine or Lysine) which is sufficient for import into the mitochondria [249, 216]. The positively charged residue of MTS formed α-helical structure which is amphipathic in nature, known to be important for recognition and translocation inside the mitochondria. However it was reported that some of the mitochondrial protein MTS, which do not form perfect amphipathic α-helical structure (low amphiphilicity index), also enter inside the mitochondria [249]. Though most of the MTS sequences localize at the N-terminus of

mitochondrial proteins, many mitochondrial proteins have been reported where MTS sequence lies either at the C-terminal or in the middle of the protein (Internal targeting signal). These mitochondrial proteins have unique targeting signal and the nature of this targeting signal is completely different from conventional MTS sequence (N-terminus) [46]. Among all TRPs family ion channel, only TRPC3 channel has been reported which is functionally present in the mitochondria. Nevertheless MTS sequence of TRPC3 has been not identified till date or its entry inside the mitochondria not clearly understood. Here in this thesis work we have identified a unique internal MTS sequence (39 aa) in TRPV4 which has potential to enter inside the mitochondria.

3.2.1 Importance of conserved MTS sequence in vertebrate evolution

We found that TRPV4 has originated at point of emergence of vertebrates between 400 to 450 MYA, mostly during the transition of Silurian era from Devonian era. This analysis indicates that TRPV4 is evolutionary conserved though it is less conserved than histone H4 (highly conserved protein) and Cytochrome-C (semi-conserved protein) [245, 374-376]. However box plot analysis of MTS (592-630aa) indicated that this region is conserved like the histone H4 throughout the vertebrate evolution. The hTRPV4 polypeptide is made of 871 amino acids, which contain 6 transmembrane regions, a pore domain and the N-terminal as well as C-terminal cytoplasmic domains [56]. Among all, Loop3, TM4, Loop4, TM5 and TRP-box reveal maximum degree of conservation [164]. In a similar manner, among all TM domains, the TM4 and TM5 regions are more conserved [164]. The TM4 reveals highest level of conservation indicating the importance of this region in the channel function. Our results suggest that TRPV-MTS lying in the Loop4-TM5 region shows its functional significance during the course of TRPV4 evolution. However in some species namely *Hyla japonica* (Japanese Tree frog) and *Oreochromis niloticus* (Nile tilapia), TRPV4-

MTS alignment was substituted with similar amino acids (**Fig 40**). Molecular evolution of TRPV4 suggests that it contains 1 ortholog and 5 paralogs gene isoform of TRPV4 in amphibian [164]. This indicates that amphibian passed through aquatic to terrestrial habitat transition and encountered with different osmotic environment during vertebrate evolution. It seems that TRPV4-MTS sequence also changed according to changing in the osmotic environment. MTS sequence is conserved in all other TRPV family ion channels also indicating that all TRPV family members have the potential MTS sequence and it may go inside the mitochondria under specific condition. However, characterization of MTS of all other TRPVs MTS has not been done so far. It has been reported that TM4-L4-TM5 of TRPV4 has potential to interact with cholesterol or cholesterol derivatives and lipid derivatives molecule (EETs and 17(S)-resolvin D1) and these interactions may regulates the channel activity [164, 377].

3.2.2 TRPV4-MTS interacting mitochondrial protein

TRPV4-MTS sequence (39 aa) enter inside the mitochondria; and our pull down results indicate that it interacts with mitochondrial protein Hsp60 and Cyt C but not interacts with outer membrane protein Mfn1 and Mfn2. Mitochondrial MTS enter inside the mitochondria with the help of "Mitochondria Import Stimulation Factor" (MSF) and "different translocase complex proteins". Mitochondrial Hsp60 is essential for the folding and assembly of newly imported proteins. Interaction of TRPV-MTS with Hsp60 shows that MTS sequence enter inside the mitochondria. TRPV4-MTS did not interact with outer membrane protein Mfn2 and Mfn1 indicating that MTS sequences may not localize in the outer mitochondria membrane. Furthermore, interactions of TRPV4-MTS with Cyt C (Cristae-associated protein) again confirm that this MTS sequence really enters inside the mitochondrial matrix. However results suggest that interaction of Cyt C (Oxidized form) with

TRPV4-MTS exclusively depends upon the presence of Ca^{2+}, which indicates that a critical concentration of Ca^{2+} is required for strong interaction of TRPV4-MTS and Cyt C. Nevertheless, the interaction of Cyt C (reduced form) with TRPV4-MTS has not been done in this study. Though many other mitochondrial proteins may interact with TRPV4-MTS, we have not characterized all the possible interacting proteins in this study.

3.2.3 Importance of TRPV4-MTS mutation in mitochondrial regulation and function

TRPV4-MTS sequence lies within the TM4-Loop4-TM5 segment of TRPV4 and this region has been reported to harbour more than 11 deleterious mutations which cause several pathophysiologies. Our results suggest that TRPV4-MTS-Wt colocalizes with mitochondrial marker protein but its mutants (R616Q, F617L, F618P and V620I) did not colocalizes with mitochondria. It is reported that MTS sequence contains positive charge and its hydrophobic residue which form α-helical structure which are important for the mitochondrial import [249]. Mitochondrial membrane potential (negative charge inside the outer membrane) also makes driving force for amphipathic MTS sequence and its import into the mitochondria. It seems that TRPV4-MTS point mutations may alter the amphipathicity index or α-helical structure of MTS sequence and ultimately prevent its import into the mitochondria. However detailed characterization of theses TRPV4-MTS mutants has been not done in this study.

3.3. TRPV4 and mitochondrial cross talk is conserved in other primary cells (mature sperm)

Sperm cells are truly remarkable as these cells have highly condensed DNA, no transcriptional activity, high number of mitochondria and very less to negligible translational activity. The sperm proteome possess a limited number of proteins which are extremely essential and are required for sperm development, maturation, motility and/or fertility. In addition, these cells are highly mobile and show extreme response against a large number of

variable factors such as slight changes in temperature, pH, osmolality, presence of salts, and other factors at very low concentrations indicating that these cells are equipped to detect and integrate these multiple physical and chemical stimuli precisely [378-381]. Notably, sperm cells perform all these tasks due to the presence of multiple ion channels and receptors regulating very complex yet efficient Ca^{2+}-signalling events [382]. In this work we report for the first time that TRPV4, a non-selective cation channel is endogenously present in the sperm cells of all vertebrate classes, ranging from fish to human and they play critical role in maintaining mitochondrial morphology and Ca^{2+}-influx. In general this also suggests that TRPV4 is "pleotropic" in nature and other channels present in the sperm cells can compensate the lack of TRPV4. Indeed, so far only TRPV1 channel is reported to be expressed in sperm cells from vertebrate origin [383-388].

3.3.1. TRPV4 expression is evolutionary conserved in almost all vertebrate sperms

The conserved expression of TRPV4 among all phyla of vertebrates strongly indicates that TRPV4 is probably involved in all vital functions of sperm. Presence of TRPV4 in the tail of the sperm of all vertebrates suggests that it could be a critical regulator of sperm motility. Immunostaining results suggest differential localization of TRPV4 in different species. Especially in human sperm, TRPV4 localizes in all the regions and it is significantly enriched in the head region. Different parts of the sperm cell, especially head, neck and tail region are the functionally important areas which regulates different specific functions. Sperms head is responsible for acrosomal reaction; neck region contains several mitochondria which continuously supply ATP and also act as the only available organelle for Ca^{2+}-buffering, and tail region is important for motility. In all conditions, Ca^{2+} plays an important role in all physiological conditions.

However our Western blot results from two different fractions indicate that the TRPV4 band at ~130 kDa is more abundant in swim-down (Sd) sample with respect to swim-up (Su) sample. On the other hand, the MFI values from FACS data suggest that the total TRPV4 immunoreactivity is more in swim-up fraction than that of the swim-down samples. These results in general may suggest that higher level of TRPV4 is present in the swim-up samples and the same is subject to more proteolytic degradation, probably due to higher level of Ca^{2+}-influx and Ca^{2+}-dependent proteolytic activity. Western blot analysis of β-tubulin (as an example of cytoplasmic protein) and Hsp60 (example of mitochondrial protein) from the same samples also suggest the same. Our Western blot results also suggest that in human sperm, TRPV4 migrates at 130 kDa, a size which is higher than the expected size and therefore suggest for the post-translational modification of TRPV4, such as glycosylation. In this context, it is worth mentioning that TRPV4 has also been reported previously at higher sizes (~110-120 kDa size) than expected 97 kDa [157, 389]. Interestingly, our results indicate that human sperm TRPV4 shows branched type of glycosylation, which is sensitive to PNGase F but resistant with Endo H glycosidase. It seems that TRPV4 does not contain any N-glyosidic linkage or due to the presence of branched oligosaccharides chain, the glyosidic bond is not freely accessible to the Endo H.

Precise localization of certain membrane and cytosolic proteins and their translocation in certain stages correlate well with the sperm function in general [390]. In this context, in swim-up fraction, TRPV4 localization is exclusively restricted in head region whereas it is mainly restricted to the neck region in swim-down cells. Similarly, 4αPDD-treated cells also show the presence of TRPV4 at the neck regions. This may also suggest for a possible and differential translocation or migration of TRPV4 upon capacitation. Similar translocation has also been observed in boar sperm where TRPV1 re-localizes from post-acrosomal region to apical region during capacitation process [384]. Re-localization of other membrane proteins

(such as TSC4 and OBF13 in mouse) has also been reported during capacitation [391, 392]. Another protein antigen from rat cauda epididymal spermatozoa has also been reported to relocalize from head to tail [393].

3.3.2. TRPV4 precisely regulates the organization and structure of sperm mitochondria

Sperm morphometry and molecular details of any organism is an indicator of several relevant factors such as reproductive uniqueness, energetics, adaptation, evolution, speciation, population structure, male-female ratio and other complex behaviours [394-399]. In sperm cell, mitochondrial mass and its number increases during its maturation stage from spermatogonia to spermatozoa. Fully differentiated sperm cells from vertebrates have ~ 22-75 numbers of mitochondria, coiled around the axonemal microtubule [400, 401]. Mature spermatozoa have condensed, compact and metabolically active mitochondria which regulate critical functions of sperm such as fertilization and capacitation and act as the only organelle for Ca^{2+}-homeostasis [401]. However our results suggest that TRPV4 activation (4αPDD, 1 μM) for long time altered the mitochondrial morphology and its helical organization in bull sperm (**Fig 51, 52**). It was also observed that activation of TRPV4 causes reduction in the mitochondrial potential and degradation of Hsp60 in sperm cell (**Fig 49, 50**). The alteration in the mitochondrial morphology, potential and level of Hsp60 in sperm cell, showed similar trends which were observed in other neuronal or non-neuronal cell line.

Long term activation of TRPV4 caused massive influx of Ca^{2+} and subsequently results in excess production of ROS and free radicals which may alter the mitochondrial morphology. In other cellular system (Endothelial cell) it was reported that TRPV4 activation increases Ca^{2+} level and leads to production of ROS and NOS [102]. Our results also suggest that TRPV4 is present in the mitochondria of sperm cell (**Fig 46**). Therefore it seems that massive intracellular Ca^{2+}-influx, after TRPV4 activation, is the cumulative effect of both

sperm membrane and mitochondrial TRPV4, which may alter the mitochondrial morphology significantly.

3.3.3. TRPV4 acts as a progesterone receptor and regulates Ca^{2+}-homeostasis in sperm

We show the importance of TRPV4 in progesterone-mediated Ca^{2+}-signalling. Progesterone induces Ca^{2+}-influx into spermatozoa and stimulates several Ca^{2+}-dependent physiological events including Ca^{2+}-waves which are essential for successful fertilization, such as sperm hyperactivation, acrosome reaction and chemotaxis towards the egg [402-409]. However the true identity of the progesterone receptor present in the sperm cell remains elusive. In case of sperm, the involvements of nuclear progesterone receptors (involved in genomic action of progesterone) can easily be ruled out by the fact that progesterone induced responses are rapid and sperm is transcriptionally inactive [403, 410, 411]. Besides, progesterone induced effects on sperm are not responsive to the antagonists of the classic progesterone receptor [411]. In addition, membrane impermeable BSA-conjugated Progesterone can also induce increased intracellular Ca^{2+} concentrations and acrosome reaction suggesting that an alternative progesterone receptor is most likely present on the on the sperm surface [411, 412]. In this context, involvement of voltage-sensitive or second messenger-operated channel-mediated Ca^{2+} entry in response to progesterone was ruled out by inhibitor based studies [413]. Recent papers have suggested that progesterone-induced effects could be (at least partly) due to direct activation of CatSper channels, mainly due to the fact that in human sperm, progesterone at nanomolar concentrations can potentiate currents which are similar to CatSper-activated currents [414, 415]. However, for several reasons, our results indicate that TRPV4 (in addition to CatSper as proposed) may also act as "the progesterone receptor" in higher mammalian sperms (**Fig 59-60**). Firstly, involvement of CatSper in progesterone signalling is not observed in all species, even in all mammals

whereas TRPV4 is present in all vertebrate sperms. In addition, progesterone does not induce CatSper-currents in mice although CatSper is essential for hyper-activation and fertility of mice sperm [411, 416-419]. Thirdly, it has been shown that nearly 27% of unselected and 53% of swim up fraction of human sperm are positive for CatSper [420]. The fact that >90% of all spermatozoa bind to progesterone indicates that apart from CatSper, some other channel is also involved in the rapid signalling in response to progesterone [421]. Notably, so far the direct interaction of progesterone with CatSper has not been demonstrated. In the absence of direct physical interaction, it has been suggested that some other CatSper-associated progesterone receptor may be mediating the effect of progesterone in sperm [415, 422]. In this context, our results confirm that TRPV4 is also involved in progesterone-mediated signalling events and importantly, TRPV4 interacts directly with progesterone through its TM4-Loop4-TM5 region. Previously we have reported that this intracellular Loop4 of TRPV4 alone or in combination with TM 4 and/or with transmembrane 5 binds to cholesterol and cholesterol derived steroids [164]. For such interactions, Loop4 is sufficient and this region is highly conserved in all vertebrates. In this work we demonstrate that the same Loop4 region of human TRPV4 directly binds to progesterone (**Fig 62**). In addition, our observation confirmed that >95% of both the swim-up and swim-down cells are positive for TRPV4. These numbers also fit well with the overall responsiveness of cells towards progesterone reported before [421]. Therefore, our results strongly indicate that TRPV4 may also act as "the progesterone receptor" in human sperm. Indeed the localization of TRPV4 in human sperm also correlates well with the Ca^{2+}-waves observed in cell. Progesterone induced Ca^{2+}-waves move immediately, mostly within few seconds and such high level of intracellular Ca^{2+} is followed by a plateau phase lasting for several minutes. Progesterone treatment of spermatozoa induces wave-like increase in intracellular Ca^{2+} level in the sperm head, which initiates near the equatorial segment and then spreads throughout the rest of the

head [263]. Positioning of TRPV4 in the equatorial region and sperm tip correlates well with the unique position to mediate immediate progesterone induced Ca^{2+} signals. TRPV4 activation-induced Ca^{2+}-wave pattern is similar with the progesterone evoked Ca^{2+}-waves also. In contrast, CatSper is reported to be located in the sperm tail [420].

We demonstrate that TRPV4 activation (by 4αPDD at 5 μM) increases the sperm motility suggesting that TRPV4 is an important regulator of sperm functions. Notably, addition of Progesterone (10 μM) or TRPV4 activator 4αPDD (5 μM) induced similar hyper activation of motility. Besides, progesterone (10 μM) induced hyper activated motility is completely arrested within ~5-10 minutes of RN1734 treatment and the cells float in single plane as aggregates suggesting that during progesterone-mediated hyper-activation stage, TRPV4 function is essential (**Fig 60**). We correlate TRPV4 with a possible Ca^{2+}-buffering activity at the neck region, especially in case of progesterone-treated hyper active cells.

In this work we demonstrate that there is a massive increase in Ca^{2+} levels upon addition of TRPV4 inhibitor RN1734 in progesterone pre-treated sperm cells. This could be attributed to sudden release of Ca^{2+}-from the nucleus and the outer acrosomal membrane which act as the calcium storage sites [423, 424]. However, treatment with RN1734 alone (even at higher concentrations) did not increase intracellular calcium levels as such over a period of time and in fact reduce the intracellular Ca^{2+} at the head region (**Fig 61**). These probably suggest that TRPV4 is involved in the Ca^{2+}-syphoning and thus maintenance of Ca^{2+}-homeostasis in progesterone treated cells. As RN1734 treatment to progesterone-pretreated cells blocks Ca^{2+}-wave propagation to the tail (in most of the cells), involvement of TRPV4 in such Ca^{2+}-buffering functions at the neck region is highly important. It seems that progesterone as well as many other steroids derivatives may interact (direct or indirect) with membrane bound TRP channel and regulates their gating mechanism significantly (**Fig 68**).

Steroids can potentially induce complex conformational changes in the TRP channel leading to bidirectional changes such as channel opening or channel closing. However further characterization of steroid-TRP interactions are required by systematic exploration of different steroids and TRP family members.

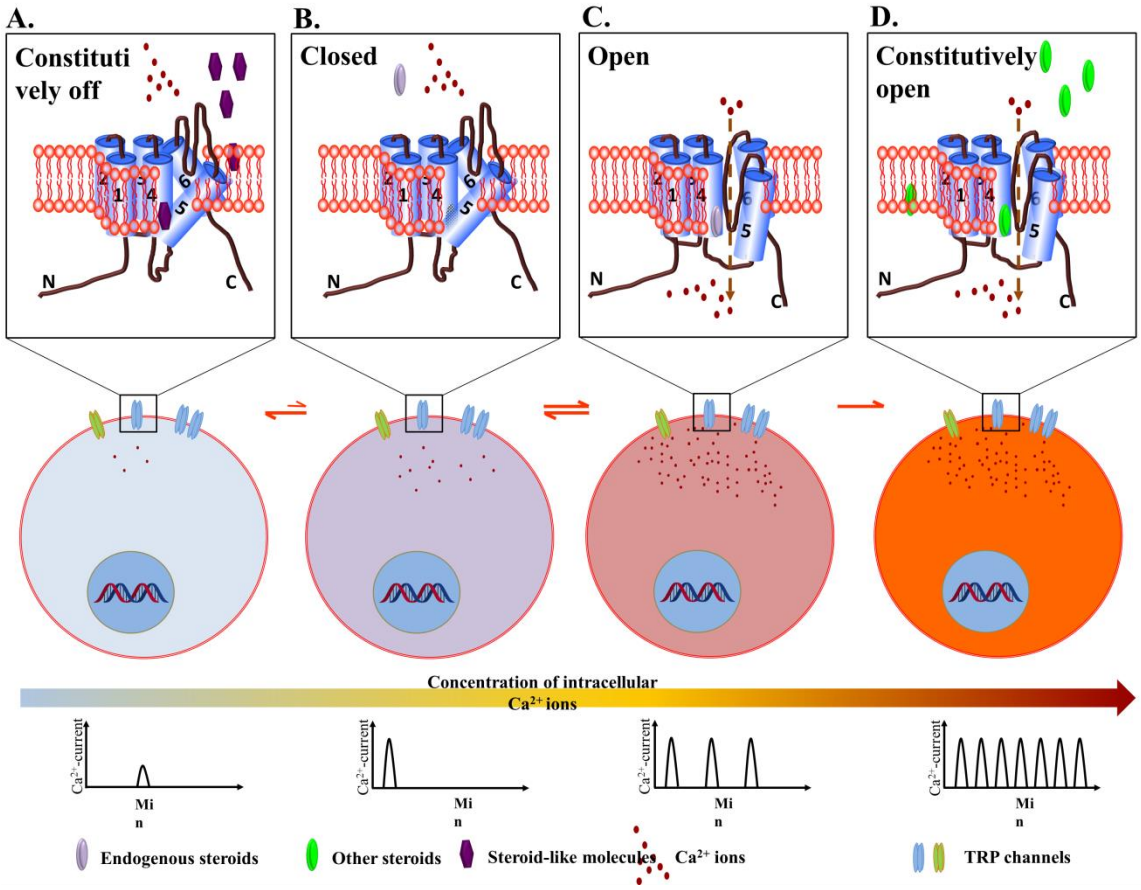

Fig 68: Non-genomic action of different steroids and steroid-like molecules on TRP channels. The schematic diagram suggests that endogenous steroids readily diffuse to the plasmamembrane and binds to certain steroid-binding pockets (mainly located at the transmembrane and/or loop region) of the TRP channels. Such binding alters the channel conformation resulting in reversible regulation of ‘‘on-and-off’’ mode of TRP channels and thus regulate intracellular concentration of Ca^{2+} ions as well as cellular response leading to physiological functions (described in B–C). However excess steroids as well as different steroid-like molecules bind with different TRP channels with different kinetics leading to irreversible changes such as either constitutive on (described in D) or constitutive off (described in a) mode leading to abnormal intracellular Ca^{2+} and defective cellular functions. Under this scenario, expected Ca^{2+}-currents due to TRP channels are plotted at the bottom.

Chapter 4

Conclusion and Future prospect

Conclusion and future prospect:

Transient Receptor Potential Vanilloid sub-type 4 (TRPV4) is a non-selective cationic channel expressed broad range of cellular/tissue system where it regulates diverse cellular physiology. In last few decades, intracellular localization of TRP channels was investigated. Such studies have unravelled the intracellular localization of TRP ion channels and have also partly characterized their functions within these subcellular organelles. However sub-cellular localization and characterization of TRPV4 in context of cellular functions are largely rudimentary. Therefore, in this study we have delineated the presence of TRPV4 in the mitochondria of different cellular system (neuronal and non-neuronal) which potentially regulates different mitochondrial functions such as morphology, potentiality, dynamics (Fusion/Fission) and Ca^{2+}- homeostasis.

The salient findings from this thesis work:

- Localization and characterization of TRPV4 in different subcellular organelles (in neuronal and non-neuronal cells).
- TRPV4 is endogenously present in mitochondria (in neuronal and non-neuronal cells).
- TRPV4 agonist or antagonist largely regulates mitochondrial function and morphology.
- C-terminus of TRPV4 interacts with mitochondrial proteins (Mfn1, Mfn2 and Hsp60).
- Natural occurring TRPV4 mutants (L618P, R616Q and V620I) also translocated in the mitochondria.
- TRPV4 has a novel and conserved Mitochondrial Target Signal (MTS) which is conserved throughout the vertebrate evolution.
- TRPV4 agonist or antagonist regulates mitochondrial metabolite and electron transport chain activity.

- TRPV4 physically interacts with progesterone/cholesterol and it shows parallel evolution with cholesterol biosynthesis pathway/ steroids synthesis pathway.
- TRPV4 endogenously present in mitochondria of vertebrate sperm and it regulates mitochondrial organization or coiling.
- TRPV4 agonist or antagonist regulates progesterone-mediated hyperactivation in human spermatozoa.
- TRPV4 agonist or antagonist also regulates Ca^{2+}- dynamics and its propagation from head to tail in human spermatozoa.

This work established the functional and physical presence of TRPV4 in the mitochondria of diverse cellular system; and this not only regulates mitochondrial morphology but also regulates the mitochondrial calcium homeostasis, oxidative potentiality and metabolism. These findings will open a new avenue to understand several pathophysiological disorders where TRPV4 and/or mitochondrial abnormalities are involved. However future work will be aimed to understand the other interacting mitochondrial proteins with TRPV4 and how it regulates mitochondrial function as well as signalling events. Functional characterization of other TRPV4 mutants (more then 30) with mitochondria and with other subcellular organelles will reveal the mitochondrial associated pathophysiology at molecular level. Other TRPV family ion channels also need to be endogenously characterized with respect to other subcellular organelle which will signify the contribution of TRPV4 with mitochondrial functions.

Chapter 5

Material and Method

5.1. Materials used

5.1.1. Chemicals	Source
Acetic Acid	Merck Millipore
Acrylamide	Sigma - Aldrich
Agar	Himedia
Agarose	Lonza
Ampicillin	Sigma - Aldrich
Amylose resin	NEB
APS (Ammonium persulphate)	Sigma - Aldrich
ATP	Sigma - Aldrich
β-mercaptoethanol	Sigma - Aldrich
Bis-acryalamide	Sigma - Aldrich
Bromophenol Blue	Sigma - Aldrich
BSA	Sigma - Aldrich
Capsaicin	Sigma - Aldrich
Cover Slip	Fisher
Complete protease inhibitor	Sigma - Aldrich
Coomassie Brilliant Blue G250	MP biomedical
Cytochrome C (Purified)	Sigma - Aldrich
Decylubiquinone	Sigma - Aldrich
DCPIP	Sigma - Aldrich
DAPI	Invitrogen
Dipotassium phosphate	Sigma - Aldrich
DMSO	Sigma - Aldrich
dNTPs	NEB
DTT	Sigma - Aldrich
EDTA	Sigma - Aldrich
EGTA	Sigma - Aldrich
Endo H	NEB
Ethanol	Merck
Ethidium Bromide	Sigma - Aldrich
Fluoromount G	Southern Biotechnology
Glutamate	MP biomedical
Glutathione sepharose	GE healthcare
Paraformaldehyde	Sigma - Aldrich
Glycerol	Sigma - Aldrich
Glycine	Sigma - Aldrich
GTP	MP biomedical
Hydrogen Chloride	Merck

HEPES	Sigma - Aldrich
Ionomycin	Sigma - Aldrich
IPTG	MP biomedical
JC-1	Sigma - Aldrich
Kanamycin	MP biomedical
LB powder	Himedia
Maltose	Sigma - Aldrich
Malate	MP biomedical
Methanol	Merck
MitoTracker Red	Invitrogen
$MgCl_2$	Sigma - Aldrich
NADH	Sigma - Aldrich
$NaBH_4$	MP biomedical
Ni-NTA Agarose	Qiagen
4αPDD	Sigma - Aldrich
PMSF	Sigma - Aldrich
PNGase F	NEB
Perchloric acid	ACS
PIPES	Sigma - Aldrich
Potassium phosphate monobasic	Sigma - Aldrich
Progesterone	Sigma - Aldrich
PVDF membrane	Millipore
Ponceau S	Sigma - Aldrich
Potassium Hydroxide	Sigma - Aldrich
RTX	Sigma - Aldrich
RN1734	Sigma - Aldrich
Skimmed milk powder	Himedia
Sodium Chloride	Sigma - Aldrich
Sodium Dodecyl Sulphate	Sigma - Aldrich
Sodium Hydroxide	Sigma - Aldrich
Sperm wash media	Sar clinic
Succinic acid	MP biomedical
Sucrose	Sigma - Aldrich
TEMED	Sigma - Aldrich
Tris base	Sigma - Aldrich
Triton X100	Sigma - Aldrich
Tryptone	Himedia
Tween 20	Sigma - Aldrich
Whatman paper	Whattman
Xylene cyanol	Sigma - Aldrich

Yeast extracts	Himedia

5.1.2.

Kits and markers	Source
Plasmid DNA isolation (maxi prep) kit	Qiagen
Plasmid DNA isolation (mini prep) kit	Qiagen
Gel extraction kit	Qiagen
Lipofectamine Cell transfection kit	Invitrogen
ECL	Thermoscientific
Bradford protein estimation kit	Sigma
Cytochrome C oxidase assay Kit	Sigma
SDS-PAGE protein marker High range	Thermoscientific
1 kb DNA ladder	Fermentas
100 bp DNA ladder	Fermentas
Restriction Enzyme	NEB, Fermentas
T4 DNA ligase	NEB

5.1.3. Primary antibodies

Primary antibodies used

Antibodies	Host	Source	Application/s	Dilution♠
ATP5A	Mo	Abcam	WB	250
Cyt C	Mo	Abcam	WB	500
Drp1	Mo	Abcam	WB	250
His	Mo	Sigma	WB	500
Hsp60	Mo	Abcam	IHC, WB	500
Mfn1	Mo	Abcam	WB	250
Mfn2	Mo	Abcam	WB	250
MBP	Mo	NEB	WB	10000
Opa1	Mo	Abcam	WB	250
TRPV4	Rb	Almone lab	IHC, WB	500
TRPV4	Rb	Sigma	IHC, WB	500
β-Tubulin	Mo	Sigma	WB	500

Mo: mouse monoclonal; **Rb:** rabbit polyclonal; **IHC:** Immuno Histochemistry; **WB:** Western Blot; ♠ With respect to Western Blot analysis.

5.1.4. Secondary antibodies and related reagents

Secondary antibodies and reagents for immunofluorescence:

Description	Host	Source	Dilution
Alexa-594-labelled anti-mouse	Chicken	Molecular Probe	500
Alexa-594-labelled anti-rabbit	Chicken	Molecular Probe	500
Alexa-488-labelled anti-rabbit	Chicken	Molecular Probe	1000
Alexa-488-labelled anti-mouse	Chicken	Molecular Probe	1000
Alexa-488-labelled anti-rabbit	Chicken	Molecular Probe	1000
Alexa-488-conjugated streptavidin	Rabbit	Molecular Probe	500

Secondary antibodies and reagents for western blot analysis:

Description	Host	Source	Dilution
HRP labelled anti mouse	Donkey	GE Healthcare	5000
HRP labelled anti rabbit	Donkey	GE Healthcare	5000

Peptide:

Sequence	Blocking activity against	Source
CDGHQQGYAP KWRAEDAPL	**Rabbit polyclonal anti-TRPV4antibody**	**Alomone**

5.1.5. Vectors

Vectors	Source
pCDNA3.1	Prof. Jon D Levine (UCSF, San Francisco)
pDSRed-Monomer	Invitrogen
pEGFPN3	Prof. J. Berreiter-Hahn (Frankfurt, Germany)
pGEX6P1	Dr. P V Alone (NISER)
pMALc2x	NEB
mitoDsRed	Clontech
pmTurquoise2-Golgi (Golgi-CFP)	Addgene
pmTurquoise2-ER (ER-CFP)	Addgene
pmTurquoise2-Peroxi (Peroxisome-CFP)	Addgene
pSEGFP-C1	Addgene
mito-GFP (AtNOS-GFP)	Prof. Stefan Mundlos (Berlin, Germany)

5.1.6. Cell lines and Primary cells

Cell lines and Primary cells	Source
F11	Prof. F. Hucho (FU, Berlin)
HaCaT	Prof. F. Hucho (FU, Berlin)
HeLa	Prof. F. Hucho (FU, Berlin)
HEK	Prof. F. Hucho (FU, Berlin)
Cos7	Prof. F. Hucho (FU, Berlin)
CHOK1-V4	Prof. Jon D Levine (UCSF, USA)
CHOK1-Mock	Prof. Jon D Levine (UCSF, USA)
HUVEC	Lonza
Fish sperm (*Labeo rohita*)*****	CIFA, Bhubaneswar, India
House Lizard sperm (*Hemidactylus leschenaultii*)*****	NISER, Bhubaneswar, India
Amphibian sperm (*Duttaphrynus melanostictus*)*****	NISER, Bhubaneswar, India
Duck sperm (*Anas platrhyncos*)*****	CARI, Bhubaneswar, India
Bovine sperm (*Bos gaourus*)*****	FSB, Cuttack, India
Human sperm (*Homo sapiens*)******	Kar clinic Pvt Ltd, Bhubaneswar, India

***IAEC number:** NISER-IAEC/SBS-AH/07/13/10, ****IEC numbers:** KHPL-04/2013, NISER/IEC/2015-11

5.1.7. Bacterial cell lines

Bacterial cell lines	Source
BL21DE3pLys, DH5α	CG Lab

5.1.8. Constructs

Constructs used	Vector	Expression system	Source
GFP-TRPV4-TM	pSGFP2-C1	Mammalian	CG lab*
GST-TRPV4-MTS	pGEX6P-1	*E. coli*	CG lab*
GST-TRPV4-TM4-Loop4-TM5	pGEX6P-1	*E. coli*	CG lab*
GST-TRPV4-Loop4	pGEX6P-1	*E. coli*	CG lab*
His-Mfn1	PET28a	*E. coli*	Ishihara et al.; 2004
His-Mfn2	PET28a	*E. coli*	Ishihara et al.; 2004
MBP-TRPV4-Ct	pMALc2x	*E. coli*	Goswami et al.; 2010
Mito Pericam	pEYFP	Mammalian	Nagai et al., 2001
TRPV4-GFP	pEGFPN3	Mammalian	Becker et al.; 2005
TRPV4-R616Q-GFP	pEGFPN3	Mammalian	CG lab*
TRPV4-L618P-GFP	pEGFPN3	Mammalian	CG lab*
TRPV4-V620I-GFP	pEGFPN3	Mammalian	CG lab*
TRPV4-Nt-RFP	pDSRed-Monomer	Mammalian	CG lab*
TRPV4-Ct-RFP	pDSRed-Monomer	Mammalian	CG lab*
TRPV4-MTS-GFP	pEGFPN3	Mammalian	CG lab*
TRPV4-MTS-L596P-GFP	pEGFPN3	Mammalian	CG lab*
TRPV4-MTS-R616Q-GFP	pEGFPN3	Mammalian	CG lab*
TRPV4-MTS-F617L-GFP	pEGFPN3	Mammalian	CG lab*
TRPV4-MTS-L618P-GFP	pEGFPN3	Mammalian	CG lab*
TRPV4-MTS-V620I-GFP	pEGFPN3	Mammalian	CG lab*

***** = Generated in this study

5.1.9. Primers

No.	Sequence	Use	Construct
1f.	CCG***CTCGAG***CTATGGGTGAGACCGTGGGCCA	F/L	V4-Ct-RFP
1r.	CGC***GGATTC***CTACAGTGGTGCGTCCTCCG	R/L	V4-Ct-RFP
2f.	CCG***CTCGAG***CTATGGCAGATCCTGGTGATGT	F/L	V4-Nt-RFP
2r.	CGC***GGATTC***CTA ACGCCACTTGTCCCTCA	R/L	V4-Nt-RFP
3f.	GTT***GAATTC***TTCGGGGCCGTCTCCTTCTAC	F/L	V4-TM-GFP
3r.	GCC***GTCGAC***TTAGAGGAGCAGCACAAAGGTGAG	R/L	V4-TM-GFP
4f.	GCA***GCTAGC***ATGTTCACCCGTGGGCTGAAG	F/L	V4-MTS-GFP
4r.	GCA***GGATCC***TGAAGCGTAGCCGATCATGAA	R/L	V4-MTS-GFP
5f.	GTA***GGATCC***ATGTTCACCCGTGGGCTGAAG	F/L	V4-MTS-GST
5r.	GTT***GTCGAC***TGAAGCGTAGCCGATCATGAA	R/L	V4-MTS-GST
6f.	GAT***GGATCC***TTCACCCGTGGGCTGAAGCT	F/L	V4-L4-TM5-GST
6r.	GAT***GTCGAC***TTAGTTGGCACACGGGTTCAGGA	R/L	V4-L4-TM5-GST
7f.	GAT***GGATCC***TTCACCCGTGGGCTGAAGCT	F/L	V4-L4-GST
7r.	GAT***GTCGAC***TTACCCGAGCAGGAATCGGAAAAGGT	R/L	V4-L4-GST
8f.	CCTTTACTTCACCCGTGGGC**C**GAAGCTGACGGGGACC	F/L	V4 (L596P)
8r.	GGTCCCCGTCAGCTTC**G**GCCCACGGGTGAAGTAAAGG	R/L	V4 (L596P)
9f.	CTCTTCAAGGACCTTTTCCGATT**A**CTGCTCGTCTACTTG CTCTTCATG	F/L	V4 (F617L)
9r.	CATGAAGAGCAAGTAGACGAGCAG**T**AATCGGAAAAGG TCCTTGAAGAG	R/L	V4 (F617L)
10f.	CTTCAAGGACCTTTTCCGATTCC**C**GCTCGTCTACTTGCT CTTCATG	F/L	V4 (L618P)
10r.	CATGAAGAGCAAGTAGACGAGC**G**GGAATCGGAAAAGGT CCTTGAAG	R/L	V4 (L618P)

Bold & Italics: Restriction enzyme in primer; **Only Bold:** Point mutation in Primer

5.2. Methods related to molecular biology

5.2.1. Construct preparation

DNA constructs were synthesized in the following manner: DNA fragments corresponding to the desired coding regions were secured by either performing PCR amplification with a specific pair of primer or by digesting them with suitable restriction enzymes. The specific vector and PCR amplified insert were subsequently digested by restriction enzyme/s to generate cohesive overhanging ends. Restriction-digested vector and insert were extracted from agarose gel, ligated and the ligated product was transformed into *E. coli*. Transformed *E. coli* cells were allowed to grow by antibiotic selection on LB plates. Plasmid DNA was isolated from those colonies by using commercially available DNA miniprep kits. Presence of desired insert in the vector was testified by subjecting the miniprep plasmid DNA to restriction digestion, PCR amplification using insert specific primers and eventually sequencing.

5.2.2. Polymerase Chain Reaction (PCR)

For preparation of different constructs in specific expression vectors, PCR reactions were executed to amplify the different coding regions with specific restriction sites at the ends. For the purpose of sub-cloning, specific inserts in different expression vectors were synthesized by digesting the PCR-amplified-DNA with restriction enzymes. Using miniprep-DNA isolated from *E. coli*, PCR reaction was repeated to screen and confirm the existence of desired insert in particular colonies grown on transformed plates after ligation. All PCR reactions were carried out using the below-mentioned conditions and Taq DNA-polymerase (NEB) as the enzyme. All PCR-amplified DNA were further confirmed by agarose gel electrophoresis.

PCR components:

Constituents	Quantity
DNA template	0.5 µl
10 X buffer	2.5 µl
dNTPs (10 mM)	2 µl
Forward Primer (100 nM)	1 µl
Reverse Primer (100 nM)	1 µl
H_2O	17 µl
DNA polymerase	1 µl
Total volume	**25 µl**

PCR conditions:

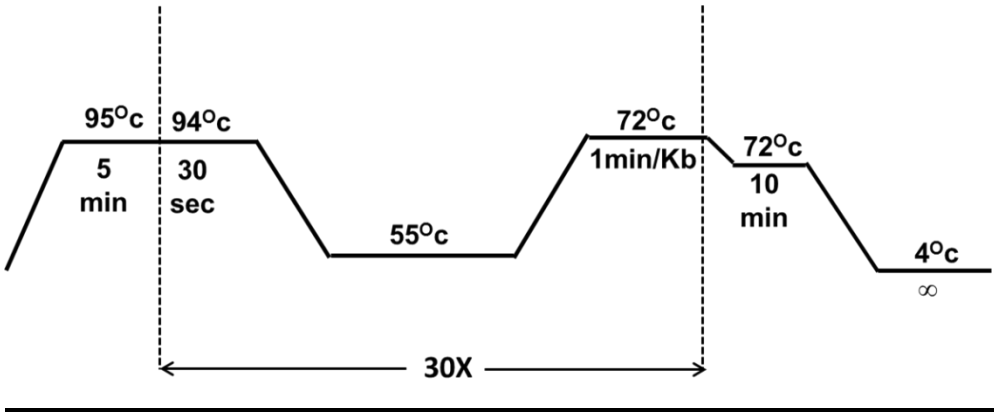

5.2.3. Restriction digestion of dsDNA

For conducting restriction digestion, 20 µl of restriction digestion mixture containing approximately 1 µg of dsDNA was used. This mixture comprises of restriction enzyme-compatible buffer of 1 X concentration, enzymes and doubly distilled autoclaved water. Based on the activity of restriction enzymes, the amount of enzyme added was in the ratio of 1 unit/µg of DNA and the incubation time of the reaction mixture was either set to 37°C for 3

hours or for overnight. For restriction digestion using two different enzymes, a compatible buffer was selected according to the manufacturer's (NEB) instruction.

5.2.4. Ligation of dsDNA

In order to ligate the restriction-digested insert and vector, the DNA was first run on an agarose gel and bands at desired sizes were excised from the gel. The dsDNA were subsequently purified from the gel by using Qiagen Gel Extraction kit according to the manufacturer's instruction. The purified insert and vector dsDNA were mixed with doubled distilled autoclaved water and ligation buffer so that the final concentration of ligation buffer in the reaction mixture becomes 1 X. Finally T4-DNA ligase was added to the reaction mixture. The mixture was incubated over night at 16°C. For a better efficiency of ligation, insert and vector in the ligation mixture was maintained as molar ratio (3:1 for insert to vector). This enhances the probability of ligation reaction.

5.2.5. Agarose gel electrophoresis

A horizontal agarose-gel electrophoresis apparatus and 1 X TAE buffer was used for the purpose of electrophoretic separation of dsDNA. The procedure can be summarized as follows:

Depending on the length of the dsDNA that needs to be separated, the desired percentage of agarose gel (0.8 - 1.2%) is casted by dissolving agarose powder in electrophoresis buffer (1 X TAE) by heating in a microwave oven. Ethidium bromide (EtBr, at a final concentration of 0.1 to 0.5 μg/ml) was added to the liquefied gel solution at this point (when its temperature is approximately 60°C) to enable visualization of DNA after electrophoresis. The molten gel was then poured into a casting tray containing a sample comb and allowed to solidify at room temperature. Once solidified, the comb was removed from the gel without tampering the well

bases. The gel along with the casting tray was immersed into the electrophoresis chamber containing electrophoretic buffer. DNA samples mixed with loading dye were then loaded into the wells and the apparatus was connected to a constant electricity supply source. DNA migration was assessed by visualization of tracking dye. After adequate migration, DNA fragment/s are visualized on an ultraviolet trans-illuminator (during electrophoresis, due to intercalation of ethidium bromide in between DNA base pairs, DNA becomes fluorescent) and photographed by a camera attached with a gel-documentation system.

Solutions and buffer required:

(1 X) TAE buffer: 40 mM Tris/Acetic acid, pH7.8; 1 mM EDTA, pH 8.0

(5 X) DNA loading buffer: 40% (w/v) Sucrose, 240 mM Tris/Acetic acid, pH7.8, 5 mM EDTA, pH 0.8, 0.25% (w/v) Bromophenol blue, 0.25% (w/v) Xylene cyanol FF

5.2.6. Competent *E. coli* cell preparation

a. $CaCl_2$ method:

Competent *E. coli* cells were prepared in the following manner. A single colony of *E. coli* bacteria (DH5α) was added to 3 ml of Luria-Bertani (LB) broth and allowed to grow over night. From this fully grown bacterial culture, 1 ml was added to 100 ml of fresh LB liquid medium and incubated at 37°C. The cells were grown until an OD of 0.4-0.5 was reached at 600 nm. The entire bacterial culture was then incubated in ice for 10 minutes and centrifuged at 3000 RPM for 5 minutes at 4°C. The pellet was re-suspended in 30 ml of ice-cold $CaCl_2$ (100 mM) solution and incubated for 30 minutes on ice. The suspension was further centrifuged for 5 minutes at 4°C. Finally the pellet was resuspended in ice-cold $CaCl_2$ (100 mM) solution supplemented with 10% glycerol, distributed in tubes and stored at -80°C.

b. RbCl method:

Competent *E. coli* cells were prepared in the following manner. A single colony of *E. coli* bacteria (DH5α) was added to 3 ml of Luria-Bertani (LB) broth and allowed to grow over night. From this fully grown bacterial culture, 1ml was added to 100 ml of fresh LB liquid medium and incubated at 37°C. The cells were grown until an OD of 0.4-0.5 was reached at 600 nm. The entire bacterial culture was then incubated in ice for 10 minutes and centrifuged at 4500 RPM for 10 minutes at 4°C. The supernatant was discarded and the entire 100 ml culture was pelleted by repeated centrifugation. The pellet was first resuspended in 30 ml of TfbI buffer and incubated in ice for 15 minutes. This was followed by centrifugation at 4000 RPM for 5 minutes at 4°C. The pellet obtained was again resuspended in 6 ml of TfbII buffer. Bacterial cells suspended in TfbII buffer were eventually aliquoted in microcentrifuge tubes. These competent cells containing tubes were snap-chilled in liquid nitrogen and stored in -80°C for further use.

Solutions and buffer required:

TfbI buffer: Rubidium Chloride (100 mM), Manganese Chloride (50 mM), Potassium Acetate (30 mM), Calcium Chloride (10 mM), Glycerol (15%). Adjust to pH 5.8 with dilute acetic acid (0.2%; 1.0 M). Filter sterilize (Do not autoclave) and store at 4^{o}C.

TfbII buffer: MOPS (10 mM), Rubidium Chloride (10 mM), Calcium Chloride (75 mM), Glycerol (15%). Adjust pH to 6.5 with KOH. Filter sterilize (Do not autoclave) and store at 4^{o}C.

5.2.7. Transformation of *E.coli*

E. coli competent cells (DH5α or DE3 strain) were taken out from -80°C and thawed on ice for 10 minutes. Cells (100 μL) were taken in a 1.5mL tube and approximately 100 ng of plasmid DNA was added to the competent cells. The mix was incubated for 10 minutes on ice. After incubation, the mix was given a heat shock for 45 seconds by dipping the tube in water bath set at 42°C. Immediately after heat shock, the tube was kept on ice for 2 minutes

after which 800 µL LB media was added to the mix. The cells were allowed to grow for 1 hour at 37°C in incubator-shaker with constant shaking. After 1 hour, the transformed cells were centrifuged at 13,500 RPM for 30 seconds, resuspended in 100 µL supernatant and plated on the LB plates containing the desired antibiotic and the plate was kept at 37°C for 14 hours. Single colonies were obtained after 14 hour incubation.

5.3. Methods related to protein and Biochemistry

5.3.1. Separation of denatured proteins by SDS-PAGE

For electrophoretic separation of proteins, SDS-PAGE was performed with 10-12% acrylamide gel using Biorad mini-apparatus. The nomenclature of this technique is based on the fact that sodium dodecyl sulphate (SDS), a strong anionic detergent is used to denature the proteins and a discontinuous polyacrylamide gel is used as a support medium to separate the denatured proteins according to their molecular size. The most commonly used system is also called the Laemmli method after U.K. Laemmli, who was the first to demonstrate SDS-PAGE as a technique for separation of proteins [425].

Sample preparation for SDS-PAGE was done in the following manner. Protein samples were completely denatured by adding Laemmli protein loading buffer in 1:4 v/v (from a 5 X stock of Laemmli protein loading buffer) and then the mixture was heated at 95°C for 5 minutes. SDS-PAGE cassettes were set by using a pair of clean glass plate (10 cm wide and 7 cm high) separated by spacer (1 mm thickness for thin gel or 1.5 mm thickness for thick gel). Approximately, 5 cm of the Cassettes were filled up with liquid resolving gel mixture and allowed to polymerize. Top-most surface of the resolving gel was smoothened by gradual addition of water on it to form a thin film coating the resolving gel. On completion of polymerization of resolving gel, stacking gel mixture was layered on top of the resolving

gel and a 15 or 10- well comb was inserted within. After polymerization of the stacking gel, the comb was removed carefully without disrupting the wells. Cassettes were inserted into the electrophoresis chamber vertically, filled with electrophoresis running buffer and denatured protein samples were loaded into the wells using a Hamilton syringe. The apparatus was connected to a constant power supply (10 mAmp for thin gel and 20 mAmp for thick gel) for electrophoresis. Protein migration within gel was assessed by visually tracking the movement of bromophenol blue added in the protein-loading buffer. As the dye front approached the end of the gel, electrophoresis was stopped and the gel was fixed with fixer. Separated proteins in the gel were visualized by Coomassie blue staining. In case of Western blot analysis, an unfixed gel was used to transfer the proteins on a PVDF membrane.

Bis-Acrylamide stock solution (30%), APS stock solution (10%), TEMED solution (100%), SDS solution (20%) and Tris HCl solution (1.5 M, pH 8.8 for resolving gel; or 0.5M M, pH 6.8 for stacking gel) were used to prepare separating and stacking solutions. APS and TEMED were added just prior to pouring the gels.

Buffers required:

SDS-PAGE running buffer (1 X): 196 mM glycine, 0.1% SDS, 50 mM Tris-HCl (pH 8.3)

Laemmli protein loading buffer (5 X): 62.5 mM Tris HCl (pH 6.8), 5% β-mercaptoethanol (v/v), 50% Glycerol (v/v), 2% SDS (w/v), 0.1% (w/v) Bromo phenol Blue. Volume was adjusted by adding water.

Resolving gel mixture: 10% Bis-Acrylamide (v/v), 375 mM Tris HCl (pH 8.8), 0.1% SDS (w/v), 0.1% ammonium persulfate, 0.005% TEMED in water.

Stacking gel mixture: 4% Bis-Acrylamide (v/v), 125 mM Tris HCl (pH 6.8), 0.1% SDS (w/v), 0.1% ammonium persulfate, 0.005% TEMED in water.

5.3.2. Coomassie staining of the protein bands in gel.

Commonly 0.1% Coomassie blue dye, which is dissolved in 10% glacial acetic acid and 50% methanol, was used to stain the proteins in a gel separated by SDS-PAGE. Staining

was usually done over-night by agitating the gel in the above mentioned solution. Continuous agitation causes circulation of the dye, facilitates its penetration into the gel, and helps ensure uniformity of staining. Though the dye permeates into the entire gel, it only sticks to the proteins permanently. Excess dye was washed out by agitating the gel in a destaining solution containing acetic acid/methanol. The two steps that most efficiently destain the gel is done by initially washing the gel with 50% methanol and 10% acetic acid for 1-2 hours, followed by washing with 7% methanol, 10% acetic acid. The first solution causes the gel to shrink and extracts much of the liquid component whereas the second solution causes swelling and eventual cleaning of the gel. Properly stained - destained gels exhibited a pattern of blue protein bands against a clear background. The gels were scanned in a scanner attached to a computer. Coomassie blue dye may fail to stain proteins present in scanty amounts as well as those proteins having high carbohydrate content.

5.3.3. Western blot analysis

For Western blot analysis, proteins were first separated by SDS-PAGE and subsequently electro-transferred on a PVDF membrane by semi-dry method. Briefly, unfixed gels were shortly incubated in a transfer buffer. PVDF membranes and Whatman paper were also soaked in the same transfer buffer. At first, the gel was placed on the membrane. Then, in order to make the transfer set; two layers of Whatman paper were placed on either sides of the gel-membrane combination. Air bubbles were removed from the whole transfer-set by rolling a glass rod over it. Finally this set was placed on a transfer unit in such a way that the gel is connected to the cathode while the membrane is connected to the anode. The apparatus was connected to a power supply and the electro-transfer was done at a constant voltage 17V (for a single gel) for 1 hour. Transfer of proteins from the gel to the membrane was confirmed by staining the membranes with Ponceau Red dye solution. Next, the membranes were

blocked with 5% non-fat milk dissolved in TBS-T buffer. Blocked membranes were incubated with primary antibody in TBS-T buffer for 1 hour, washed 3 times with TBS-T buffer and then incubated with secondary antibody in TBS-T buffer for 1 hour. Finally, the membranes were washed with TBS-T again and Bound proteins were probed by enhanced chemiluminescence method (Super Signal™ West Femto Maximum Sensitivity Substrate, Thermo Scientific) and detected by chemidoc apparatus (Bio-Rad). In some experiments, blots were stripped-off by incubating the blots in a stripping buffer at 37°C for 30 minutes and re-probed again with a different primary antibody.

Buffers and solutions required:

Transfer buffer: 0.1% SDS, 20% (v/v) MeOH, 48 mM TRIS/HCl, 39 mM Glycine

Ponceau Red solution: 5% (w/v) Ponceau S dye, 5% (v/v) Acetic acid

TBS-T: 20 mM Tris, 150 mM NaCl. 0.1% (w/v) Tween-20

Stripping buffer: 1% SDS, 20 mM TRIS/HCl (pH 6.8), 1% (v/v) β-Mercaptoethanol

5.3.4. Isolation of mitochondria from Goat brain and CHOK1 cell lines.

Adult goat brains were obtained from a local slaughterhouse. The meninges were separated from the brain and the tissues were taken to the laboratory in isotonic mitochondrial isolating buffer (10 mM HEPES, 1 mM EDTA, 320 mM sucrose, pH 7.4). Isolation of mitochondria was based on the method established previously with some minor modifications [426, 427]. Briefly, goat brain was homogenized in mitochondrial isolating buffer containing a complete protease inhibitor cocktail (Sigma Aldrich). After homogenization, the homogenate was equally distributed in centrifuge tubes and centrifuged at 1000g for 10 minutes. The supernatant (S1, which contain mitochondria and other cell organelles) was collected in a separate tube and the pellet was homogenized again in mitochondrial isolating buffer with 5-7 strokes of pestle. The homogenized sample was centrifuged again at 1000g for 10 minutes. The supernatant fractions (S1′) was pooled and centrifuged at 10,000g for 20

minutes to get crude mitochondrial pellet fraction (P1, brown in colour) and supernatant fraction (S2). The pellet fraction (mitochondria) was washed twice with same buffer and centrifuged again at 10,000g for 20 minutes. The mitochondrial fraction was isolated as pellet (P2) and separated from wash fractions (W). Subsequently, the brown mitochondrial pellet was resuspended in isolating buffer, aliquoted and kept at -80°C for long-term storage. All isolation procedure and centrifugation steps were carried out at 4°C. For isolation of mitochondria from CHOK1 cells, 90% confluent cells were splitted and seeded in 100 mm dishes and grown for 24 hours. After that, seeded cells were treated with TRPV4 activator, inhibitor or only DMSO for 8 hours and then the cells were scrapped with media and centrifuged. Mitochondrial fraction and cytoplasmic fraction were isolated by using Mitochondrial isolation kit according to the manufacturer's protocol (Sigma Aldrich, Bangalore).

3.3.5. Enzymatic assay for mitochondrial electron transport chain

All enzymatic activity analysis was done with freshly isolated goat brain mitochondria and performed at 30°C. Before starting the enzymatic assay, isolated mitochondria were pre-incubated with TRPV4-specific activator namely 4αPDD (5 μM) or specific inhibitor, namely RN1734 (10 μM). In each conditions changes in absorbance was recorded for 3 minutes. For electron transport chain complex I activity assays, NADH-based spectroscopic analysis was performed with some minor modification [428, 429]. Mitochondrial complex I oxidizes cellular NADH ($NADH \rightarrow NAD^+ + H^+$), and the electron released due to oxidation of NADH (Extinction coefficient 5.4 $mM^{-1}cm^{-1}$) is captured by artificial electron acceptor decylubiquinone (DU). The electron subsequently transferred to 2,6-dichloroindophenol (DCPIP). The absorbance of reduced DCPIP was measured spectrophotometrically at 600 nm. This method is advantageous, as electrons produced by

other cellular NADH-dehydrogenases are not accepted by decylubiquinone, therefore reduction of DCPIP is almost completely caused by complex I activity, resulting in very high rotenone-sensitive activity. The reaction mixture (1 ml) consists of 20 mM potassium phosphate buffer (pH 7.2), 0.1 mM EDTA, 10 mM $MgCl_2$, mitochondrial fraction (sonicated mitochondria) (30 µg protein), NADH (50 µM) and decylubiquinone (150 µM). In all cases NADH was added in the end to minimize variation due to handling.

The electron transport chain Complex II activity was measured at 600 nm using 2,6-Dichlorophenolindophenol {(DCPIP), extinction coefficient 21 $mM^{-1}cm^{-1}$} as acceptor [430, 431]. After adding artificial substrate decylubiquinone (DU), it accepts electron from complex II and transfers to DCPIP. The reaction mixture (1 ml) consists of 20 mM potassium phosphate buffer (pH 7.2), 0.1 mM EDTA, 10 mM $MgCl_2$, 20 mM succinate, 50 µM DCPIP, mitochondrial (sonicated mitochondria) protein (30 µg) and the reaction was started after addition of 50 µM DU.

Mitochondrial Complex III activity was measured by monitoring the reduction of cytochrome C at 550-540 nm (extinction coefficient 19 $mM^{-1}cm^{-1}$) [432]. The reaction mixture (1 ml) consist of 20 mM potassium phosphate buffer (pH 7.2), 0.1 mM EDTA, 10 mM $MgCl_2$, 100 µM cytochrome C, mitochondrial lysate (30 µg) and the reaction was started after addition of 100 µM reduced decylubiquinone (DUH_2).

Mitochondrial Complex IV activity was measured by the oxidation of reduced cytochrome C at 550 nm (Extinction coefficient 19 $mM^{-1}cm^{-1}$) [433]. Complex IV activity was measured by cytochrome C oxidase assay kit (Sigma Aldrich, Bangalore). Cytochrome C oxidase is located in the inner mitochondrial membrane that divides the mitochondrial matrix from the intermembrane space and it has been used as a specific marker for this membrane. The reaction mixture (1 ml) consists of Mitochondrial isolating buffer, 50 µM cytochrome C

and the reaction was started after adding 20 µg mitochondrial lysate and the decrease in absorbance at 550 nm were recorded for 3 minutes.

5.3.6. Assay for mitochondrial permeability transition pore

Mitochondrial swelling or membrane permeability transition pore induced by influx of excesses of calcium inside the mitochondria which can be detected as a decrease in light scattering property in isolated mitochondria at 540 nm [434]. Briefly, Mitochondria (100 µg) were treated with TRPV4 activator and inhibitor drug for 15 minutes in the same mitochondrial isolating buffer in ice. Subsequently, treated mitochondria were transferred to mitochondrial swelling buffer (final volume 1 ml) and decay in absorbance was taken at 540 nm wavelength by spectrophotometer in time kinetics mode (5 minutes interval) for 1 hour.

Mitochondrial swelling buffer: HEPES (20 mM), KH_2PO_4 (2 mM), KCl (125 mM), EGTA (1 µM), $MgCl_2$ (1 mM), Malate (5 mM), Glutamate (5 mM), pH: 7.4

5.3.7. Metabolite extraction from isolated mitochondria

The protocol for metabolite extraction from isolated mitochondria and sample preparation was done following previously published research methodology [435]. Briefly, freshly isolated mitochondria were incubated with TRPV4 specific drugs such as 4αPDD (5 µM), RN1734 (10 µM), 4αPDD (5 µM) and Ca^{2+} (1 mM), Ionomycin (5 µM) for 30 minutes in the same mitochondria isolating buffer at room temperature. After drug incubation, mitochondria were centrifuged at 8000 RPM for 10 minutes and the supernatant was taken out as S1. In the remaining mitochondrial pellet, 12% perchloric acid was added to extract the acid soluble metabolite and centrifuged at 10000 RPM for 10 minutes. After centrifugation supernatant S2 was taken out and mixed with previously extracted fraction S1, now the resultant metabolite solution is S3. To neutralize perchloric acid in fraction S3, 5 M NaOH

was added which gave a white precipitate of sodium perchlorate. The titrated fraction S3 was again centrifuged at 10000 RPM for 10 minutes and supernatant S4 was taken out. Furthermore, the pH of metabolite fraction S4 was adjusted to 7.2 by adding 1-2 µL NaOH (5 M). Finally pH of metabolite fraction S4 was measured by using litmus paper.

5.3.8. Glycosidase enzymatic treatment in sperm lysate

Equal amount of protein lysate of Swim-down (Sd) and Swim-up (Su) sperm sample was taken for Endo H and PNGase F glycosidase treatment according to manufacture instruction (New England Biolabs) with minor modifications. Briefly, sperm protein lysate were mixed with glycoprotein denaturing buffer (1 X) and subsequently denaturation reaction was carried out at 100°C for 5 minutes. After that sample (denatured glycoprotein) were chill in ice for 5 minutes. Subsequently Glyco buffer (1 X) and NP-40 was added for proper enzymatic activity. The sample mixture was incubated in the presence or absence of Endo H and PNGase F at 37°C for 6 hours. Subsequently sample was separated on one-dimensional SDS-PAGE and Western blot with anti-TRPV4 antibody.

5.3.9. Protein estimation by Bradford method

Quantification of the purified protein or isolated mitochondrial protein was done using Bradford protein estimation method [436]. For standard curve preparation, different concentrations of BSA protein (20, 40, 60, 80 and 100 µg) were made in 100 µL of PBS solution. Subsequently 900 µL of Bradford reagent (Sigma Aldrich) was added to the tubes containing different BSA concentrations and incubated for 5 minutes after which the OD was measured at 595 nm. Blank solution was made by adding 100 µL of PBS and 900 µL of Bradford reagent.

5.4. Method related protein expression, purification and protein interaction

5.4.1. MBP-Pull-down assay for identifying TRPV4 interacting proteins

Expression and purification of the C-terminal cytoplasmic domain of TRPV4 fused with MBP (MBP-TRPV4-Ct) as well as LacZ fused with MBP (MBP-LacZ) are based on the protocol described previously [437]. In brief, the expression constructs were introduced into *Escherichia coli* strain BL21DE3 by heat shock method of transformation. Expression of fusion proteins were induced by addition of isopropyl thiogalactoside (IPTG) for 2 hours. Cells were lysed by either rapid-freezing and thawing (by using Liquid N_2 and 37°C water bath) or by sonication (60 Hz, 10 cycle with 5 sec pulse interval) cycles or freezing and thawing method in lysis buffer (PBS pH 7.4, lysozyme and protease inhibitor cocktail). The lysed extracts were cleared by centrifugation (35000 RPM for 2 hours) and applied to amylose resin for binding. The resins with bound proteins were washed thoroughly and finally the proteins were eluted with 20 mM maltose in elution buffer (50 mM PIPES, pH 6.8, 150 mM NaCl, 1 mM EGTA and 0.2 mM $MgCl_2$).

For TRPV4-Ct interaction study, approximately 50 µL of amylose resin per tube with the bound fusion protein was used for further pull-down experiments. Depending on the respective experiments, the resin with coupled fusion protein (MBP-TRPV4-Ct and MBP-LacZ) were incubated with 50 µL of mitochondrial protein (0.7 mg/ml protein) for 2 hours at 4°C in the presence or absence of Ca^{2+} (1 mM) or a mixture of GTP and ATP (1 mM). The amylose resin present in each tube was washed three times (each time with 500 µL) with PEM-S buffer. The proteins were eluted by using 100 µL elution buffer (PEM-S supplemented with 20 mM maltose). Eluted samples were analysed by 10% sodium dodecyl

sulphate polyacrylamide gel electrophoresis (SDS–PAGE) and Western blot analysis with candidate specific antibodies.

5.4.2. GST-Pull-down assay for identifying TRPV4-MTS interacting protein

GST-TRPV4-MTS and only GST were expressed in *E. coli* strain BL21DE3 and the cleared cell lysates were applied to amylose resin (NEB) and incubated for 2 hours at RT. *E. coli* cells were induced to express the proteins by isopropyl thiogalactoside (IPTG) (0.25 mM) for 2 hours at 37°C. Thereafter, the pelleted cells were lysed by incubating in lysis buffer (1 X PBS pH 7.4, lysozyme, protease inhibitor, PMSF) followed by sonication. The lysed extracts were cleared by spinning at 35000 RPM at 4°C for 2 hours. For purification, the cleared lysate containing the desired expressed proteins were incubated with Glutathione sepharose beads for 12 hours at 4°C with constant rotation after which the beads were washed thrice with GST wash buffer (50 mM Tris pH 7.4, 0.25 M NaCl, 1 mM EDTA) followed by elution of bound proteins from the beads using elution buffer (20 mM Glutathione reduced, 50 mM Tris-Cl pH 8.0). Protein estimation was done using Bradford estimation method immediately after protein purification.

For interaction study with GST-TRPV4-MTS with mitochondrial protein, expressed protein were coupled with sepharose beads for 2 hours at 4°C. Subsequently washed with GST wash buffer and mitochondrial protein 50 µL of mitochondrial protein (0.4 mg/ml protein) were added into the sepharose beads bound with GST-TRPV4-MTS protein in the presence or absence of Ca^{2+} (1 mM) or a mixture of GTP and ATP (1 mM), and incubated for 2 hours at 4°C. Thereafter washed 3 times with GST wash buffer and all bound protein eluted in 100 µL of elution buffer (20 mM Glutathione reduced 50 mM Tris-Cl pH 8.0). Further eluted samples were analysed by 12% sodium dodecyl sulphate polyacrylamide gel electrophoresis (SDS–PAGE) and Western blot analysis with candidate specific antibodies.

5.4.3. His-Tagged Pull down assay for Mfn1 and Mfn2 with MBP-TRPV4-Ct

His-tagged Mfn1 and His-tagged Mfn2 constructs were received as a gift from Prof. Naotada Ishihara (Dept. of Protein Biochemistry, Institute of Life Science, Kurume University) [438]. His-Mfn1 and Mfn2 were freshly transformed into BL21-DE3 and a single colony of each type was inoculated in 3 ml of 2 X YT media. The culture was grown in presence of 25 μg/ml kanamycin (in each steps same concentration of antibiotic was used) overnight. The next day, 1 ml of this overnight grown culture media was transferred to 100 ml of 2 X YT media and was allowed to grow overnight under same conditions. From this 100 ml, 50 ml of overnight grown culture was transferred to 200 ml of 2 X YT media in a 1 L conical flask and incubated for 3 hours in shaker at 37°C and 220 RPM till the OD reached to 1.2. Subsequently 0.3 mM IPTG was added and kept for 2 more hours until the OD reached 2.4. Thereafter, the culture was kept in cold room for 30 minutes. The culture was then pelleted at 8000 RPM for 5 minutes and kept at -80°C for further use. Next day, the pellet was suspended in lysis buffer (20 mM HEPES, pH 7.4, 250 mM NaCl, 1 mM PMSF and 1 X EDTA free protease inhibitor) for 2 hr in ice. The cells in this solution were disrupted by sonication (60 Hz, 10 cycle with 5 sec pulse interval) in ice cold condition. The sonicated lysate was then centrifuged at 15000 RPM for 2 hours and the supernatant was discarded as Mfn2 and Mfn1 appears inside the inclusion body. The pellet was again resuspended in lysis buffer and made up to 30 ml by sonication. This was followed by the addition of 1 ml 20% Triton X 100 and was then rotated in cold room for 30 minutes. Thereafter, it was centrifuged at 15000 RPM for 40 minutes and the collected supernatant was incubated with Ni-NTA beads (pre-washed with pre-equilibration buffer: 20 mM HEPES, pH 7.4, 250 mM NaCl, 10 mM imidazole) for 2 hours in cold room. It was then washed thrice with washing buffer (20 mM HEPES, pH 7.4, 250 mM NaCl, 20 mM imidazole) and then centrifuged at 2000 RPM

for 3 minutes. Thereafter all His-tagged Mfn2 and Mfn1 were eluted in 50, 100 and 250 mM imidazole solution.

2 X YT Media (1L): Tryptone- 16 g, Yeast Extract- 10 g, NaCl- 5 g. Adjust pH to 7 by adding 5N NaOH.

5.4.4. MBP-TRPV4-Ct binding assay with isolated mitochondria

Freshly isolated mitochondria (30 µg) from goat brain were incubated with equal concentration of purified MBP-TRPV4-Ct and MBP-LacZ at 25°C in the same mitochondrial isolating buffer. The isolated mitochondria were kept for binding with MBP-TRPV4-Ct and MBP-LacZ in presence or absence of Ca^{2+} or a mixture of GTP and ATP (1 mM each). After 30 minutes of incubation, mitochondria were washed two times (centrifuged at 8000 RPM for 5 minutes) with mitochondrial isolating buffer which separated most of the unbound protein of MBP-TRPV4-Ct and MBP-LacZ. The mitochondrial pellet was suspended in PEMS buffer which breaks the intact mitochondrial membrane by osmotic shock. The complete protease inhibitor cocktail was added in each fraction and the sample was boiled with (1 X) Laemmli buffer for preparation of SDS-PAGE gel samples.

5.4.5. Blot overlay

PVDF membrane was cut and charged in 100% methanol followed by rehydrating and washing with 1 X PBS. Membrane was arranged in a dot blot apparatus and fixed volumes of progesterone solutions of different concentrations was applied into the wells and suctioned through a vacuum pump. The membrane was blocked with 3% BSA solution for 1 hour. After blocking, the membranes were incubated with GST, GST-TRPV4-TM4-L4-TM5 and GST-TRPV4-L4 purified protein solutions made in 3% BSA and 1 X PBS for 12 hours at 4°C without shaking. Membranes were then washed thrice for 5 minutes with 1 X PBS and incubated with primary anti-GST antibody (1:750 in blocking buffer and 1 X PBS) for 6

hours at 4°C and then washed with 1 X PBS thrice for 5 minutes each. Secondary antibody conjugated to horseradish peroxidase (1:10,000, GE healthcare) was applied to the membranes for 1 hour at room temperature and washed thrice with 1 X PBS. Bound protein was visualized by adding equal amount of substrate and luminol solution to the membranes and detecting on the chemidoc apparatus (Bio-Rad).

5.5. Method related to cell biology

5.5.1. Cell culture and transfection

Chinese hamster ovary (CHO-K1) cells stably selected for TRPV4 (cloned in pCDNA5.1 vector) and CHOK1-Mock cells (which contains pCDNA5.1 empty vector only) [51] were grown in F-12 HAMES medium containing 10% (v/v) of FBS, 2mM L-glutamine, 100 µg/ml streptomycin, 100 U/ml penicillin, in a humidity controlled incubator maintained with 5% CO_2 and at 37°C. HaCaT, HEK, Cos7 and F11 cells were cultured in DMEM media supplemented with 10% (v/v) FBS, 2mM L-glutamine, 100 µg/ml streptomycin, 100 U/ml penicillin, in a humidity controlled incubator with 5% CO_2 and at 37°C. The growing cells were splitted and grown further for 24 hours in suitable flasks and dishes. Similarly, Human Umbilical Vein Endothelial cells (HUVEC) (purchased from Lonza) were cultured in endothelial cell growth media (EGM, Lonza) containing heat-inactivated 2% fetal bovine serum (FBS), human VEGF, epidermal growth factor (EGF), insulin-like growth factor-1 (IGF-1), basic fibroblast growth factor (FGFB) and amphotericin-B. All cells were maintained at 37°C incubator with 5% CO_2 in a humid atmosphere. For transient over expression of the cells with desired constructs, purified DNA plasmids were used. Transient over expression was performed by using Lipofectamine 2000 and Plus reagent according to the manufacturers protocol (Invitrogen). Generally 24-36 hours after transfection, the cells were used for live cell imaging and for immunocytochemistry cells were fixed by 4%PFA.

5.5.2. TRPV4 activation/inhibition in stable cell line and primary HUVEC cells

CHOK1-V4 / CHOK1-Mock / HUVEC cells were seeded on coverslip in 24 well plates for 12 hours. Subsequently TRPV4 activator 4αPDD (1 μM or 5 μM) and inhibitor RN1734 (10 μM) were added for 8 hours. To explore the changes in the mitochondrial morphology and potentiality, cells were labelled with MitoTracker Red FM (1 μM) or J-C1 dye (5 μM) for 30 minutes in incubator. Thereafter, MitoTracker Red FM labelled cells were fixed with 4% paraformaldehyde for further imaging. JC-1-labelled cell were washed with PBS (1 X) and taken out gently from incubator for life cell imaging.

5.5.3. Calcium imaging of adherent cells and floating cells

Adherent cells such as CHOK1-V4 and CHOK1-Mock were seeded on 24 mm coverslip in 60 mm dishes and kept in incubator. After 24 hours, Ca^{2+}-sensing dye Fluo-4 AM (5 μM) was added in culture dishes for 40 minutes. Subsequently two wash was given with PBS (1 X) and the cells were used for live cell imaging.

Floating cells such as sperm cells and others were incubated with Fluo-4 AM (1 μM) at 37°C in water bath (For sperm cells) or in incubator (for other Primary cells) for 30 minutes. Subsequently two times washing was performed with 1 X PBS through centrifugation at 2000 RPM for 4 minutes and cells were pelleted in 1.5 ml Eppendorf tube. Thereafter cells were resuspended in respective media for live cell imaging. All steps of washing and resuspension were carried out at 37°C. Approximately 20 μL of suspended cells were dropped onto the live cell chamber which contain optimum number of floating cells and live cell imaging was performed with confocal microscope with 488 nm argon laser.

5.5.4. Mitochondrial Calcium imaging

Mitochondrial Ca^{2+} imaging was performed with ratiometric mitochondrial pericam construct (A gift from Dr. Atsushi Miyawaki, RIKEN Brain Science Institute, Wako City, Saitama, Japan) [439]. Ratiometric pericam is a Ca^{2+}-indicator fusion of two permuted protein yellow fluorescent protein (YFP) and Calmodulin which goes inside the mitochondria. Binding of single molecule of calcium with Mito-pericam changes their excitation wavelengths from 415 nm to 494 nm while its emission spectra at 515 nm. CHOK1-V4 and CHOK1-Mock cells were transfected with Mito-pericam construct in live cell dishes and after 24 hours cells were imaged with confocal microscope.

5.5.5. JC-1 (Ratiometric dye) staining in floating and adherent cells

Mitochondrial potential staining in floating cell such as sperm cells were performed with 5,5,6,6-tetrachloro-1,1,3,3-tetraethylbenzimidazolylcarbocyanine iodide (JC-1) cationic dye. JC-1 dye exhibits potential-dependent accumulation inside the mitochondria and also has fluorescence emission properties that shift from green (525 nm) to red (590 nm) region [440]. After TRPV4-specific drug treatment, floating cells were incubated with JC-1 (1 µM) for 20 minutes at 37°C. Subsequently cells was pelleted down at 2000 RPM for 4 minutes and resuspended in media. Resuspendend cells at high density were placed onto the live cell chamber and images were acquired by confocal microscope (Zeiss LSM780) in the respective excitation and emission regions.

In adherent cells line such as CHOK1-V4 and CHOK1-Mock, cells were seeded in 25 mm coverslip for overnight. TRPV4 specific activator 4αPDD (5 µM) and inhibitor RN1734 (10 µM) was added for 6 hours and after that JC-1 (5 µM) was added for 40 minutes and kept at incubator. Subsequently cells were washed by 1 X PBS and coverslip were taken for live cell imaging by confocal microscope (Zeiss LSM780).

5.5.6. MitoTracker Red staining in adherent and floating cells

Adherent cells were grown and transfected on 12 mm glass cover slips. Two days after seeding or transfection, cells were incubated with MitoTracker Red (1 μM) for 20 minutes in cell culture incubator. Subsequently cells were washed with 1 X PBS and fixed by 4% PFA at RT. Similarly for sperm cells (floating cell) after drug treatment, MitoTracker Red (2 μM) was added in sperm incubating media and kept at 37°C in water bath for 20 minutes. Subsequently incubated cells were diluted in 3 ml of 1 X PBS to avoid any clumping or aggregation during PFA fixation and immediately equal volume of 3 ml PFA (4% PFA) were added in diluted sperm for fixation.

5.6. Method related Immunocytochemistry and microscopy

5.6.1. Immunocytochemistry

Cells were grown and transfected on 12 mm glass cover slips. Two days after seeding or transfection, the cells were fixed either with 4% paraformaldehyde at room temperature (RT). Cells were permeabilized with 0.1% Triton X 100 in PBS for 5 minutes, followed by two times washing with 0.1% PBS-T (0.1% Tween 20 in 1 X PBS). The cells were blocked with 5% bovine serum albumin (BSA) prepared in PBS-T. Subsequently cells were incubated with primary antibody for overnight (Dilution varies depending upon primary antibody type) at cold room. Thereafter cells were washed three times with PBS-T (PBS supplemented with 0.1% Tween 20). The cells were further incubated for 1 hour with Alexa dye labelled secondary antibody (anti-mouse or anti-rabbit) diluted (1: 1000) in PBS-T and 5% bovine serum albumin (BSA) in 1:1 ratio. After incubation with secondary antibody/ies, the cells were washed three times with PBS-T buffer. Further for nucleus staining cells were incubated with DAPI (5 μM) in PBS-T for 30 minutes at RT. Subsequently cells were washed with PBS

two times and cover slips were finally mounted onto glass slides with Fluoromount G (Southern Biotech).

5.6.2. Live cell imaging

Live cell imaging were performed to see the changes in mitochondrial potentiality, mitochondrial calcium, total Ca^{2+}-influx and mitochondrial morphology in different adherent (CHOK1-V4, CHOK1-Mock, HaCaT cells) and floating cell (sperm cell). Depending upon the requirements, cells were transfected with respective construct or labelled with relevant mitochondrial dye (MitoTracker Red FM, JC-1) and coverslip were imaged with Zeiss confocal microscope (1.4 NA, 63X objectives). TRPV4-specific pharmacological agents were gently added to the live cell imaging chamber during the imaging and care was taken to avoid any focal drift due to pipetting or vibration of microscope stage. Since sperm cells are motile, therefore to visualize the changes in calcium level across the head to tail region, live cell imaging was done with minimum time gap between image acquisitions.

5.6.3. Image processing, analysis and quantification by different software

All confocal images were processed with LSM 510 and Zen 2010 software. Live cell time series images, movies depicting sperm motility and spatio-temporal changes in the Ca^{2+}-levels calculation and image processing were performed with Image J and Fiji software. To see the changes in mitochondrial area, Aspect ratio, perimeter, Form Factor and all parameter related to mitochondrial morphology were quantified by *mitochondrial morphology plugin* by using Image J software [225]. Image resolution and labelling was done by Adobe Photoshop software.

Chapter 6

Bibliography

References:

1. Minke, B. (1977) Drosophila mutant with a transducer defect, *Biophysics of structure and mechanism.* **3**, 59-64.

2. Cosens, D. J. & Manning, A. (1969) Abnormal electroretinogram from a Drosophila mutant, *Nature.* **224**, 285-7.

3. Minke, B., Wu, C. & Pak, W. L. (1975) Induction of photoreceptor voltage noise in the dark in Drosophila mutant, *Nature.* **258**, 84-7.

4. Montell, C., Jones, K., Hafen, E. & Rubin, G. (1985) Rescue of the Drosophila phototransduction mutation trp by germline transformation, *Science.* **230**, 1040-3.

5. Montell, C. & Rubin, G. M. (1989) Molecular characterization of the Drosophila trp locus: a putative integral membrane protein required for phototransduction, *Neuron.* **2**, 1313-23.

6. Montell, C. (2011) The history of TRP channels, a commentary and reflection, *Pflugers Archiv : European journal of physiology.* **461**, 499-506.

7. Grynkiewicz, G., Poenie, M. & Tsien, R. Y. (1985) A new generation of Ca2+ indicators with greatly improved fluorescence properties, *The Journal of biological chemistry.* **260**, 3440-50.

8. Caterina, M. J., Schumacher, M. A., Tominaga, M., Rosen, T. A., Levine, J. D. & Julius, D. (1997) The capsaicin receptor: a heat-activated ion channel in the pain pathway, *Nature.* **389**, 816-24.

9. Denis, V. & Cyert, M. S. (2002) Internal Ca(2+) release in yeast is triggered by hypertonic shock and mediated by a TRP channel homologue, *The Journal of cell biology.* **156**, 29-34.

10. Palmer, C. P., Zhou, X. L., Lin, J., Loukin, S. H., Kung, C. & Saimi, Y. (2001) A TRP homolog in Saccharomyces cerevisiae forms an intracellular Ca(2+)-permeable channel in the yeast vacuolar membrane, *Proceedings of the National Academy of Sciences of the United States of America.* **98**, 7801-5.

11. Finka, A., Cuendet, A. F., Maathuis, F. J., Saidi, Y. & Goloubinoff, P. (2012) Plasma membrane cyclic nucleotide gated calcium channels control land plant thermal sensing and acquired thermotolerance, *The Plant cell.* **24**, 3333-48.

12. Finka, A. & Goloubinoff, P. (2014) The CNGCb and CNGCd genes from Physcomitrella patens moss encode for thermosensory calcium channels responding to fluidity changes in the plasma membrane, *Cell stress & chaperones.* **19**, 83-90.

13. Venkatachalam, K., Hofmann, T. & Montell, C. (2006) Lysosomal localization of TRPML3 depends on TRPML2 and the mucolipidosis-associated protein TRPML1, *The Journal of biological chemistry.* **281**, 17517-27.

14. Cai, X. & Clapham, D. E. (2012) Ancestral Ca2+ signaling machinery in early animal and fungal evolution, *Molecular biology and evolution.* **29**, 91-100.

15. Boenigk, J. & Arndt, H. (2002) Bacterivory by heterotrophic flagellates: community structure and feeding strategies, *Antonie van Leeuwenhoek.* **81**, 465-80.

16. Leys, S. P. & Degnan, B. M. (2001) Cytological basis of photoresponsive behavior in a sponge larva, *The Biological bulletin.* **201**, 323-38.

17. Peng, G., Shi, X. & Kadowaki, T. (2015) Evolution of TRP channels inferred by their classification in diverse animal species, *Molecular phylogenetics and evolution.* **84**, 145-57.

18. Clapham, D. E. (2003) TRP channels as cellular sensors, *Nature.* **426**, 517-24.

19. Clapham, D. E., Runnels, L. W. & Strubing, C. (2001) The TRP ion channel family, *Nature reviews Neuroscience.* **2**, 387-96.

20. Ramsey, I. S., Delling, M. & Clapham, D. E. (2006) An introduction to TRP channels, *Annual review of physiology.* **68**, 619-47.

21. Montell, C. (2005) The TRP superfamily of cation channels, *Science's STKE : signal transduction knowledge environment.* **2005**, re3.

22. Duncan, L. M., Deeds, J., Hunter, J., Shao, J., Holmgren, L. M., Woolf, E. A., Tepper, R. I. & Shyjan, A. W. (1998) Down-regulation of the novel gene melastatin correlates with potential for melanoma metastasis, *Cancer research.* **58**, 1515-20.

23. Kiselyov, K., Chen, J., Rbaibi, Y., Oberdick, D., Tjon-Kon-Sang, S., Shcheynikov, N., Muallem, S. & Soyombo, A. (2005) TRP-ML1 is a lysosomal monovalent cation channel that undergoes proteolytic cleavage, *The Journal of biological chemistry.* **280**, 43218-23.

24. Mochizuki, T., Wu, G., Hayashi, T., Xenophontos, S. L., Veldhuisen, B., Saris, J. J., Reynolds, D. M., Cai, Y., Gabow, P. A., Pierides, A., Kimberling, W. J., Breuning, M. H., Deltas, C. C., Peters, D. J. & Somlo, S. (1996) PKD2, a gene for polycystic kidney disease that encodes an integral membrane protein, *Science.* **272**, 1339-42.

25. Zheng, J. (2013) Molecular mechanism of TRP channels, *Comprehensive Physiology.* **3**, 221-42.

26. Berridge, M. J., Lipp, P. & Bootman, M. D. (2000) The versatility and universality of calcium signalling, *Nature reviews Molecular cell biology.* **1**, 11-21.

27. Bootman, M. D., Collins, T. J., Peppiatt, C. M., Prothero, L. S., MacKenzie, L., De Smet, P., Travers, M., Tovey, S. C., Seo, J. T., Berridge, M. J., Ciccolini, F. & Lipp, P. (2001) Calcium signalling--an overview, *Seminars in cell & developmental biology.* **12**, 3-10.

28. Vennekens, R., Hoenderop, J. G., Prenen, J., Stuiver, M., Willems, P. H., Droogmans, G., Nilius, B. & Bindels, R. J. (2000) Permeation and gating properties of the novel epithelial Ca(2+) channel, *The Journal of biological chemistry.* **275**, 3963-9.

29. Voets, T., Droogmans, G., Wissenbach, U., Janssens, A., Flockerzi, V. & Nilius, B. (2004) The principle of temperature-dependent gating in cold- and heat-sensitive TRP channels, *Nature.* **430**, 748-54.

30. Chung, M. K., Guler, A. D. & Caterina, M. J. (2008) TRPV1 shows dynamic ionic selectivity during agonist stimulation, *Nature neuroscience.* **11**, 555-64.

31. Karashima, Y., Prenen, J., Talavera, K., Janssens, A., Voets, T. & Nilius, B. (2010) Agonist-induced changes in Ca(2+) permeation through the nociceptor cation channel TRPA1, *Biophysical journal.* **98**, 773-83.

32. Ellinor, P. T., Yang, J., Sather, W. A., Zhang, J. F. & Tsien, R. W. (1995) Ca2+ channel selectivity at a single locus for high-affinity Ca2+ interactions, *Neuron.* **15**, 1121-32.

33. Hoenderop, J. G., Voets, T., Hoefs, S., Weidema, F., Prenen, J., Nilius, B. & Bindels, R. J. (2003) Homo- and heterotetrameric architecture of the epithelial Ca2+ channels TRPV5 and TRPV6, *The EMBO journal.* **22**, 776-85.

34. Nilius, B. & Droogmans, G. (2001) Ion channels and their functional role in vascular endothelium, *Physiological reviews.* **81**, 1415-59.

35. Gees, M., Colsoul, B. & Nilius, B. (2010) The role of transient receptor potential cation channels in Ca2+ signaling, *Cold Spring Harbor perspectives in biology.* **2**, a003962.

36. Gaudet, R. (2008) TRP channels entering the structural era, *The Journal of physiology.* **586**, 3565-75.

37. Owsianik, G., D'Hoedt, D., Voets, T. & Nilius, B. (2006) Structure-function relationship of the TRP channel superfamily, *Reviews of physiology, biochemistry and pharmacology.* **156**, 61-90.

38. Lis, A., Wissenbach, U. & Philipp, S. E. (2005) Transcriptional regulation and processing increase the functional variability of TRPM channels, *Naunyn-Schmiedeberg's archives of pharmacology.* **371**, 315-24.

39. Rohacs, T. (2007) Regulation of TRP channels by PIP(2), *Pflugers Archiv : European journal of physiology.* **453**, 753-62.

40. Moiseenkova-Bell, V. Y., Stanciu, L. A., Serysheva, II, Tobe, B. J. & Wensel, T. G. (2008) Structure of TRPV1 channel revealed by electron cryomicroscopy, *Proceedings of the National Academy of Sciences of the United States of America.* **105**, 7451-5.

41. Sokolova, O., Kolmakova-Partensky, L. & Grigorieff, N. (2001) Three-dimensional structure of a voltage-gated potassium channel at 2.5 nm resolution, *Structure.* **9**, 215-20.

42. Higgins, M. K., Weitz, D., Warne, T., Schertler, G. F. & Kaupp, U. B. (2002) Molecular architecture of a retinal cGMP-gated channel: the arrangement of the cytoplasmic domains, *The EMBO journal.* **21**, 2087-94.

43. Cao, E., Liao, M., Cheng, Y. & Julius, D. (2013) TRPV1 structures in distinct conformations reveal activation mechanisms, *Nature.* **504**, 113-8.

44. Liao, M., Cao, E., Julius, D. & Cheng, Y. (2013) Structure of the TRPV1 ion channel determined by electron cryo-microscopy, *Nature.* **504**, 107-12.

45. Zubcevic, L., Herzik, M. A., Jr., Chung, B. C., Liu, Z., Lander, G. C. & Lee, S. Y. (2016) Cryo-electron microscopy structure of the TRPV2 ion channel, *Nature structural & molecular biology*.

46. Benham, C. D., Davis, J. B. & Randall, A. D. (2002) Vanilloid and TRP channels: a family of lipid-gated cation channels, *Neuropharmacology.* **42**, 873-88.

47. Gunthorpe, M. J., Benham, C. D., Randall, A. & Davis, J. B. (2002) The diversity in the vanilloid (TRPV) receptor family of ion channels, *Trends in pharmacological sciences.* **23**, 183-91.

48. Zhang, Z., Ferraris, J. D., Brooks, H. L., Brisc, I. & Burg, M. B. (2003) Expression of osmotic stress-related genes in tissues of normal and hyposmotic rats, *American journal of physiology Renal physiology.* **285**, F688-93.

49. Denker, S. P. & Barber, D. L. (2002) Cell migration requires both ion translocation and cytoskeletal anchoring by the Na-H exchanger NHE1, *The Journal of cell biology.* **159**, 1087-96.

50. Sedgwick, S. G. & Smerdon, S. J. (1999) The ankyrin repeat: a diversity of interactions on a common structural framework, *Trends in biochemical sciences.* **24**, 311-6.

51. Goswami, C., Kuhn, J., Heppenstall, P. A. & Hucho, T. (2010) Importance of non-selective cation channel TRPV4 interaction with cytoskeleton and their reciprocal regulations in cultured cells, *PloS one.* **5**, e11654.

52. Shigematsu, H., Sokabe, T., Danev, R., Tominaga, M. & Nagayama, K. (2010) A 3.5-nm structure of rat TRPV4 cation channel revealed by Zernike phase-contrast cryoelectron microscopy, *The Journal of biological chemistry.* **285**, 11210-8.

53. Chung, M. K., Lee, H. & Caterina, M. J. (2003) Warm temperatures activate TRPV4 in mouse 308 keratinocytes, *The Journal of biological chemistry.* **278**, 32037-46.

54. Fernandez-Fernandez, J. M., Nobles, M., Currid, A., Vazquez, E. & Valverde, M. A. (2002) Maxi K+ channel mediates regulatory volume decrease response in a human bronchial epithelial cell line, *American journal of physiology Cell physiology.* **283**, C1705-14.

55. Jia, Y., McLeod, R. L., Wang, X., Parra, L. E., Egan, R. W. & Hey, J. A. (2002) Anandamide induces cough in conscious guinea-pigs through VR1 receptors, *British journal of pharmacology.* **137**, 831-6.

56. Liedtke, W., Choe, Y., Marti-Renom, M. A., Bell, A. M., Denis, C. S., Sali, A., Hudspeth, A. J., Friedman, J. M. & Heller, S. (2000) Vanilloid receptor-related osmotically activated channel (VR-OAC), a candidate vertebrate osmoreceptor, *Cell.* **103**, 525-35.

57. Strotmann, R., Harteneck, C., Nunnenmacher, K., Schultz, G. & Plant, T. D. (2000) OTRPC4, a nonselective cation channel that confers sensitivity to extracellular osmolarity, *Nature cell biology.* **2**, 695-702.

58. Wissenbach, U., Bodding, M., Freichel, M. & Flockerzi, V. (2000) Trp12, a novel Trp related protein from kidney, *FEBS letters.* **485**, 127-34.

59. Chung, M. K., Lee, H., Mizuno, A., Suzuki, M. & Caterina, M. J. (2004) 2-aminoethoxydiphenyl borate activates and sensitizes the heat-gated ion channel TRPV3, *The Journal of neuroscience : the official journal of the Society for Neuroscience.* **24**, 5177-82.

60. Masuyama, R., Vriens, J., Voets, T., Karashima, Y., Owsianik, G., Vennekens, R., Lieben, L., Torrekens, S., Moermans, K., Vanden Bosch, A., Bouillon, R., Nilius, B. & Carmeliet, G. (2008) TRPV4-mediated calcium influx regulates terminal differentiation of osteoclasts, *Cell metabolism.* **8**, 257-65.

61. Mizoguchi, F., Mizuno, A., Hayata, T., Nakashima, K., Heller, S., Ushida, T., Sokabe, M., Miyasaka, N., Suzuki, M., Ezura, Y. & Noda, M. (2008) Transient receptor potential vanilloid 4 deficiency suppresses unloading-induced bone loss, *Journal of cellular physiology.* **216**, 47-53.

62. Muramatsu, S., Wakabayashi, M., Ohno, T., Amano, K., Ooishi, R., Sugahara, T., Shiojiri, S., Tashiro, K., Suzuki, Y., Nishimura, R., Kuhara, S., Sugano, S., Yoneda, T. & Matsuda, A. (2007) Functional gene screening system identified TRPV4 as a regulator of chondrogenic differentiation, *The Journal of biological chemistry.* **282**, 32158-67.

63. Gevaert, T., Vriens, J., Segal, A., Everaerts, W., Roskams, T., Talavera, K., Owsianik, G., Liedtke, W., Daelemans, D., Dewachter, I., Van Leuven, F., Voets, T., De Ridder, D. & Nilius, B. (2007) Deletion of the transient receptor potential cation channel TRPV4 impairs murine bladder voiding, *The Journal of clinical investigation.* **117**, 3453-62.

64. Suzuki, M., Mizuno, A., Kodaira, K. & Imai, M. (2003) Impaired pressure sensation in mice lacking TRPV4, *The Journal of biological chemistry.* **278**, 22664-8.

65. Tabuchi, K., Suzuki, M., Mizuno, A. & Hara, A. (2005) Hearing impairment in TRPV4 knockout mice, *Neuroscience letters.* **382**, 304-8.

66. Liedtke, W. & Friedman, J. M. (2003) Abnormal osmotic regulation in trpv4-/- mice, *Proceedings of the National Academy of Sciences of the United States of America.* **100**, 13698-703.

67. Lee, H., Iida, T., Mizuno, A., Suzuki, M. & Caterina, M. J. (2005) Altered thermal selection behavior in mice lacking transient receptor potential vanilloid 4, *The Journal of neuroscience : the official journal of the Society for Neuroscience.* **25**, 1304-10.

68. Birder, L., Kullmann, F. A., Lee, H., Barrick, S., de Groat, W., Kanai, A. & Caterina, M. (2007) Activation of urothelial transient receptor potential vanilloid 4 by 4alpha-phorbol 12,13-didecanoate contributes to altered bladder reflexes in the rat, *The Journal of pharmacology and experimental therapeutics.* **323**, 227-35.

69. Lorenzo, I. M., Liedtke, W., Sanderson, M. J. & Valverde, M. A. (2008) TRPV4 channel participates in receptor-operated calcium entry and ciliary beat frequency regulation in mouse airway epithelial cells, *Proceedings of the National Academy of Sciences of the United States of America.* **105**, 12611-6.

70. Gradilone, S. A., Masyuk, A. I., Splinter, P. L., Banales, J. M., Huang, B. Q., Tietz, P. S., Masyuk, T. V. & Larusso, N. F. (2007) Cholangiocyte cilia express TRPV4 and detect changes in luminal tonicity inducing bicarbonate secretion, *Proceedings of the National Academy of Sciences of the United States of America.* **104**, 19138-43.

71. Teilmann, S. C., Byskov, A. G., Pedersen, P. A., Wheatley, D. N., Pazour, G. J. & Christensen, S. T. (2005) Localization of transient receptor potential ion channels in primary and motile cilia of the female murine reproductive organs, *Molecular reproduction and development.* **71**, 444-52.

72. Earley, S., Heppner, T. J., Nelson, M. T. & Brayden, J. E. (2005) TRPV4 forms a novel Ca2+ signaling complex with ryanodine receptors and BKCa channels, *Circulation research.* **97**, 1270-9.

73. Yang, X. R., Lin, M. J., McIntosh, L. S. & Sham, J. S. (2006) Functional expression of transient receptor potential melastatin- and vanilloid-related channels in pulmonary arterial and aortic smooth muscle, *American journal of physiology Lung cellular and molecular physiology.* **290**, L1267-76.

74. Fian, R., Grasser, E., Treiber, F., Schmidt, R., Niederl, P. & Rosker, C. (2007) The contribution of TRPV4-mediated calcium signaling to calcium homeostasis in endothelial cells, *Journal of receptor and signal transduction research.* **27**, 113-24.

75. Benfenati, V., Amiry-Moghaddam, M., Caprini, M., Mylonakou, M. N., Rapisarda, C., Ottersen, O. P. & Ferroni, S. (2007) Expression and functional characterization of transient receptor potential vanilloid-related channel 4 (TRPV4) in rat cortical astrocytes, *Neuroscience.* **148**, 876-92.

76. Delany, N. S., Hurle, M., Facer, P., Alnadaf, T., Plumpton, C., Kinghorn, I., See, C. G., Costigan, M., Anand, P., Woolf, C. J., Crowther, D., Sanseau, P. & Tate, S. N. (2001) Identification and characterization of a novel human vanilloid receptor-like protein, VRL-2, *Physiological genomics.* **4**, 165-74.

77. Shen, J., Harada, N., Kubo, N., Liu, B., Mizuno, A., Suzuki, M. & Yamashita, T. (2006) Functional expression of transient receptor potential vanilloid 4 in the mouse cochlea, *Neuroreport.* **17**, 135-9.

78. Kumagami, H., Terakado, M., Sainoo, Y., Baba, A., Fujiyama, D., Fukuda, T., Takasaki, K. & Takahashi, H. (2009) Expression of the osmotically responsive cationic channel TRPV4 in the endolymphatic sac, *Audiology & neuro-otology.* **14**, 190-7.

79. Majhi, R. K., Sahoo, S. S., Yadav, M., Pratheek, B. M., Chattopadhyay, S. & Goswami, C. (2015) Functional expression of TRPV channels in T cells and their implications in immune regulation, *The FEBS journal.* **282**, 2661-81.

80. Watanabe, H., Vriens, J., Prenen, J., Droogmans, G., Voets, T. & Nilius, B. (2003) Anandamide and arachidonic acid use epoxyeicosatrienoic acids to activate TRPV4 channels, *Nature.* **424**, 434-8.

81. Masuyama, R., Mizuno, A., Komori, H., Kajiya, H., Uekawa, A., Kitaura, H., Okabe, K., Ohyama, K. & Komori, T. (2012) Calcium/calmodulin-signaling supports TRPV4 activation in osteoclasts and regulates bone mass, *Journal of bone and mineral research : the official journal of the American Society for Bone and Mineral Research.* **27**, 1708-21.

82. Cesare, P., Dekker, L. V., Sardini, A., Parker, P. J. & McNaughton, P. A. (1999) Specific involvement of PKC-epsilon in sensitization of the neuronal response to painful heat, *Neuron.* **23**, 617-24.

83. Cesare, P. & McNaughton, P. (1996) A novel heat-activated current in nociceptive neurons and its sensitization by bradykinin, *Proceedings of the National Academy of Sciences of the United States of America.* **93**, 15435-9.

84. Bhave, G., Zhu, W., Wang, H., Brasier, D. J., Oxford, G. S. & Gereau, R. W. t. (2002) cAMP-dependent protein kinase regulates desensitization of the capsaicin receptor (VR1) by direct phosphorylation, *Neuron.* **35**, 721-31.

85. Fan, H. C., Zhang, X. & McNaughton, P. A. (2009) Activation of the TRPV4 ion channel is enhanced by phosphorylation, *The Journal of biological chemistry.* **284**, 27884-91.

86. Goswami, C. (2012) TRPV1-tubulin complex: involvement of membrane tubulin in the regulation of chemotherapy-induced peripheral neuropathy, *Journal of neurochemistry.* **123**, 1-13.

87. Mercado, J., Baylie, R., Navedo, M. F., Yuan, C., Scott, J. D., Nelson, M. T., Brayden, J. E. & Santana, L. F. (2014) Local control of TRPV4 channels by AKAP150-targeted PKC in arterial smooth muscle, *The Journal of general physiology.* **143**, 559-75.

88. Wegierski, T., Lewandrowski, U., Muller, B., Sickmann, A. & Walz, G. (2009) Tyrosine phosphorylation modulates the activity of TRPV4 in response to defined stimuli, *The Journal of biological chemistry.* **284**, 2923-33.

89. Xu, H., Zhao, H., Tian, W., Yoshida, K., Roullet, J. B. & Cohen, D. M. (2003) Regulation of a transient receptor potential (TRP) channel by tyrosine phosphorylation. SRC family kinase-dependent tyrosine phosphorylation of TRPV4 on TYR-253 mediates its response to hypotonic stress, *The Journal of biological chemistry.* **278**, 11520-7.

90. Grant, A. D., Cottrell, G. S., Amadesi, S., Trevisani, M., Nicoletti, P., Materazzi, S., Altier, C., Cenac, N., Zamponi, G. W., Bautista-Cruz, F., Lopez, C. B., Joseph, E. K., Levine, J. D., Liedtke, W., Vanner, S., Vergnolle, N., Geppetti, P. & Bunnett, N. W. (2007) Protease-activated receptor 2 sensitizes the transient receptor potential vanilloid 4 ion channel to cause mechanical hyperalgesia in mice, *The Journal of physiology.* **578**, 715-33.

91. Alessandri-Haber, N., Dina, O. A., Joseph, E. K., Reichling, D. & Levine, J. D. (2006) A transient receptor potential vanilloid 4-dependent mechanism of hyperalgesia is engaged by concerted action of inflammatory mediators, *The Journal of neuroscience : the official journal of the Society for Neuroscience.* **26**, 3864-74.

92. Joseph, E. K. & Levine, J. D. (2006) Mitochondrial electron transport in models of neuropathic and inflammatory pain, *Pain.* **121**, 105-14.

93. Winkler, A., Arkind, C., Mattison, C. P., Burkholder, A., Knoche, K. & Ota, I. (2002) Heat stress activates the yeast high-osmolarity glycerol mitogen-activated protein kinase pathway, and protein tyrosine phosphatases are essential under heat stress, *Eukaryotic cell.* **1**, 163-73.

94. Hdud, I. M., Mobasheri, A. & Loughna, P. T. (2014) Effect of osmotic stress on the expression of TRPV4 and BKCa channels and possible interaction with ERK1/2 and p38 in cultured equine chondrocytes, *American journal of physiology Cell physiology.* **306**, C1050-7.

95. Thoppil, R. J., Adapala, R. K., Cappelli, H. C., Kondeti, V., Dudley, A. C., Gary Meszaros, J., Paruchuri, S. & Thodeti, C. K. (2015) TRPV4 channel activation selectively inhibits tumor endothelial cell proliferation, *Scientific reports.* **5**, 14257.

96. Chen, Y., Kanju, P., Fang, Q., Lee, S. H., Parekh, P. K., Lee, W., Moore, C., Brenner, D., Gereau, R. W. t., Wang, F. & Liedtke, W. (2014) TRPV4 is necessary for trigeminal irritant pain and functions as a cellular formalin receptor, *Pain.* **155**, 2662-72.

97. Levine, J. D. & Alessandri-Haber, N. (2007) TRP channels: targets for the relief of pain, *Biochimica et biophysica acta.* **1772**, 989-1003.

98. Liedtke, W. (2008) Molecular mechanisms of TRPV4-mediated neural signaling, *Annals of the New York Academy of Sciences.* **1144**, 42-52.

99. Segond von Banchet, G., Boettger, M. K., Konig, C., Iwakura, Y., Brauer, R. & Schaible, H. G. (2013) Neuronal IL-17 receptor upregulates TRPV4 but not TRPV1 receptors in DRG neurons and mediates mechanical but not thermal hyperalgesia, *Molecular and cellular neurosciences.* **52**, 152-60.

100. Phan, M. N., Leddy, H. A., Votta, B. J., Kumar, S., Levy, D. S., Lipshutz, D. B., Lee, S. H., Liedtke, W. & Guilak, F. (2009) Functional characterization of TRPV4 as an osmotically sensitive ion channel in porcine articular chondrocytes, *Arthritis and rheumatism.* **60**, 3028-37.

101. Adam-Vizi, V. & Starkov, A. A. (2010) Calcium and mitochondrial reactive oxygen species generation: how to read the facts, *Journal of Alzheimer's disease : JAD.* **20 Suppl 2**, S413-26.

102. Bubolz, A. H., Mendoza, S. A., Zheng, X., Zinkevich, N. S., Li, R., Gutterman, D. D. & Zhang, D. X. (2012) Activation of endothelial TRPV4 channels mediates flow-induced dilation in human coronary arterioles: role of Ca2+ entry and mitochondrial ROS signaling, *American journal of physiology Heart and circulatory physiology.* **302**, H634-42.

103. Cabral, P. D. & Garvin, J. L. (2014) TRPV4 activation mediates flow-induced nitric oxide production in the rat thick ascending limb, *American journal of physiology Renal physiology.* **307**, F666-72.

104. Mendoza, S. A., Fang, J., Gutterman, D. D., Wilcox, D. A., Bubolz, A. H., Li, R., Suzuki, M. & Zhang, D. X. (2010) TRPV4-mediated endothelial Ca2+ influx and vasodilation in response to shear stress, *American journal of physiology Heart and circulatory physiology.* **298**, H466-76.

105. Wang, J., Wang, X. W., Zhang, Y., Yin, C. P. & Yue, S. W. (2015) Ca(2+) influx mediates the TRPV4-NO pathway in neuropathic hyperalgesia following chronic compression of the dorsal root ganglion, *Neuroscience letters.* **588**, 159-65.

106. Wang, C., Ning, L. P., Wang, Y. H., Zhang, Y., Ding, X. L., Ge, H. Y., Arendt-Nielsen, L. & Yue, S. W. (2011) Nuclear factor-kappa B mediates TRPV4-NO pathway involved in thermal hyperalgesia following chronic compression of the dorsal root ganglion in rats, *Behavioural brain research.* **221**, 19-24.

107. De Giusti, V. C., Caldiz, C. I., Ennis, I. L., Perez, N. G., Cingolani, H. E. & Aiello, E. A. (2013) Mitochondrial reactive oxygen species (ROS) as signaling molecules of intracellular pathways triggered by the cardiac renin-angiotensin II-aldosterone system (RAAS), *Frontiers in physiology.* **4**, 126.

108. Liedtke, W., Tobin, D. M., Bargmann, C. I. & Friedman, J. M. (2003) Mammalian TRPV4 (VR-OAC) directs behavioral responses to osmotic and mechanical stimuli in Caenorhabditis elegans, *Proceedings of the National Academy of Sciences of the United States of America.* **100 Suppl 2**, 14531-6.

109. Andrade, Y. N., Fernandes, J., Vazquez, E., Fernandez-Fernandez, J. M., Arniges, M., Sanchez, T. M., Villalon, M. & Valverde, M. A. (2005) TRPV4 channel is involved in the coupling of fluid viscosity changes to epithelial ciliary activity, *The Journal of cell biology.* **168**, 869-74.

110. Gao, X., Wu, L. & O'Neil, R. G. (2003) Temperature-modulated diversity of TRPV4 channel gating: activation by physical stresses and phorbol ester derivatives through protein kinase C-dependent and -independent pathways, *The Journal of biological chemistry.* **278**, 27129-37.

111. O'Neil, R. G. & Heller, S. (2005) The mechanosensitive nature of TRPV channels, *Pflugers Archiv : European journal of physiology.* **451**, 193-203.

112. Mizuno, A., Matsumoto, N., Imai, M. & Suzuki, M. (2003) Impaired osmotic sensation in mice lacking TRPV4, *American journal of physiology Cell physiology.* **285**, C96-101.

113. Vriens, J., Owsianik, G., Fisslthaler, B., Suzuki, M., Janssens, A., Voets, T., Morisseau, C., Hammock, B. D., Fleming, I., Busse, R. & Nilius, B. (2005) Modulation of the Ca2 permeable cation channel TRPV4 by cytochrome P450 epoxygenases in vascular endothelium, *Circulation research.* **97**, 908-15.

114. Todaka, H., Taniguchi, J., Satoh, J., Mizuno, A. & Suzuki, M. (2004) Warm temperature-sensitive transient receptor potential vanilloid 4 (TRPV4) plays an essential role in thermal hyperalgesia, *The Journal of biological chemistry.* **279**, 35133-8.

115. Jordt, S. E. & Julius, D. (2002) Molecular basis for species-specific sensitivity to "hot" chili peppers, *Cell.* **108**, 421-30.

116. Caterina, M. J., Rosen, T. A., Tominaga, M., Brake, A. J. & Julius, D. (1999) A capsaicin-receptor homologue with a high threshold for noxious heat, *Nature.* **398**, 436-41.

117. Peier, A. M., Reeve, A. J., Andersson, D. A., Moqrich, A., Earley, T. J., Hergarden, A. C., Story, G. M., Colley, S., Hogenesch, J. B., McIntyre, P., Bevan, S. & Patapoutian, A. (2002) A heat-sensitive TRP channel expressed in keratinocytes, *Science.* **296**, 2046-9.

118. Smith, G. D., Gunthorpe, M. J., Kelsell, R. E., Hayes, P. D., Reilly, P., Facer, P., Wright, J. E., Jerman, J. C., Walhin, J. P., Ooi, L., Egerton, J., Charles, K. J., Smart, D., Randall, A. D., Anand, P. & Davis, J. B. (2002) TRPV3 is a temperature-sensitive vanilloid receptor-like protein, *Nature.* **418**, 186-90.

119. Xu, H., Ramsey, I. S., Kotecha, S. A., Moran, M. M., Chong, J. A., Lawson, D., Ge, P., Lilly, J., Silos-Santiago, I., Xie, Y., DiStefano, P. S., Curtis, R. & Clapham, D. E. (2002) TRPV3 is a calcium-permeable temperature-sensitive cation channel, *Nature.* **418**, 181-6.

120. Guler, A. D., Lee, H., Iida, T., Shimizu, I., Tominaga, M. & Caterina, M. (2002) Heat-evoked activation of the ion channel, TRPV4, *The Journal of neuroscience : the official journal of the Society for Neuroscience.* **22**, 6408-14.

121. Watanabe, H., Davis, J. B., Smart, D., Jerman, J. C., Smith, G. D., Hayes, P., Vriens, J., Cairns, W., Wissenbach, U., Prenen, J., Flockerzi, V., Droogmans, G., Benham, C. D. & Nilius, B. (2002) Activation of TRPV4 channels (hVRL-2/mTRP12) by phorbol derivatives, *The Journal of biological chemistry.* **277**, 13569-77.

122. Tominaga, M. & Caterina, M. J. (2004) Thermosensation and pain, *Journal of neurobiology.* **61**, 3-12.

123. Vriens, J., Owsianik, G., Janssens, A., Voets, T. & Nilius, B. (2007) Determinants of 4 alpha-phorbol sensitivity in transmembrane domains 3 and 4 of the cation channel TRPV4, *The Journal of biological chemistry.* **282**, 12796-803.

124. Kim, K. S., Shin, D. H., Nam, J. H., Park, K. S., Zhang, Y. H., Kim, W. K. & Kim, S. J. (2010) Functional Expression of TRPV4 Cation Channels in Human Mast Cell Line (HMC-1), *The Korean journal of physiology & pharmacology: official journal of the Korean Physiological Society and the Korean Society of Pharmacology.* **14**, 419-25.

125. Nilius, B., Vriens, J., Prenen, J., Droogmans, G. & Voets, T. (2004) TRPV4 calcium entry channel: a paradigm for gating diversity, *American journal of physiology Cell physiology.* **286**, C195-205.

126. Vriens, J., Watanabe, H., Janssens, A., Droogmans, G., Voets, T. & Nilius, B. (2004) Cell swelling, heat, and chemical agonists use distinct pathways for the activation of the cation channel TRPV4, *Proceedings of the National Academy of Sciences of the United States of America.* **101**, 396-401.

127. Moore, C., Cevikbas, F., Pasolli, H. A., Chen, Y., Kong, W., Kempkes, C., Parekh, P., Lee, S. H., Kontchou, N. A., Yeh, I., Jokerst, N. M., Fuchs, E., Steinhoff, M. & Liedtke, W. B. (2013) UVB radiation generates sunburn pain and affects skin by activating epidermal TRPV4 ion channels and triggering endothelin-1 signaling, *Proceedings of the National Academy of Sciences of the United States of America.* **110**, E3225-34.

128. Stotz, S. C., Vriens, J., Martyn, D., Clardy, J. & Clapham, D. E. (2008) Citral sensing by Transient [corrected] receptor potential channels in dorsal root ganglion neurons, *PloS one.* **3**, e2082.

129. Everaerts, W., Zhen, X., Ghosh, D., Vriens, J., Gevaert, T., Gilbert, J. P., Hayward, N. J., McNamara, C. R., Xue, F., Moran, M. M., Strassmaier, T., Uykal, E., Owsianik, G., Vennekens, R., De Ridder, D., Nilius, B., Fanger, C. M. & Voets, T. (2010) Inhibition of the cation channel TRPV4 improves bladder function in mice and rats with cyclophosphamide-induced cystitis, *Proceedings of the National Academy of Sciences of the United States of America.* **107**, 19084-9.

130. Vincent, F., Acevedo, A., Nguyen, M. T., Dourado, M., DeFalco, J., Gustafson, A., Spiro, P., Emerling, D. E., Kelly, M. G. & Duncton, M. A. (2009) Identification and characterization of novel TRPV4 modulators, *Biochemical and biophysical research communications.* **389**, 490-4.

131. Bezzerides, V. J., Ramsey, I. S., Kotecha, S., Greka, A. & Clapham, D. E. (2004) Rapid vesicular translocation and insertion of TRP channels, *Nature cell biology.* **6**, 709-20.

132. Xu, H., Fu, Y., Tian, W. & Cohen, D. M. (2006) Glycosylation of the osmoresponsive transient receptor potential channel TRPV4 on Asn-651 influences membrane trafficking, *American journal of physiology Renal physiology.* **290**, F1103-9.

133. D'Hoedt, D., Owsianik, G., Prenen, J., Cuajungco, M. P., Grimm, C., Heller, S., Voets, T. & Nilius, B. (2008) Stimulus-specific modulation of the cation channel TRPV4 by PACSIN 3, *The Journal of biological chemistry.* **283**, 6272-80.

134. Miranda, M. & Sorkin, A. (2007) Regulation of receptors and transporters by ubiquitination: new insights into surprisingly similar mechanisms, *Molecular interventions.* **7**, 157-67.

135. Garcia-Elias, A., Lorenzo, I. M., Vicente, R. & Valverde, M. A. (2008) IP3 receptor binds to and sensitizes TRPV4 channel to osmotic stimuli via a calmodulin-binding site, *The Journal of biological chemistry.* **283**, 31284-8.

136. Strotmann, R., Semtner, M., Kepura, F., Plant, T. D. & Schoneberg, T. (2010) Interdomain interactions control Ca^{2+}-dependent potentiation in the cation channel TRPV4, *PloS one.* **5**, e10580.

137. Arniges, M., Fernandez-Fernandez, J. M., Albrecht, N., Schaefer, M. & Valverde, M. A. (2006) Human TRPV4 channel splice variants revealed a key role of ankyrin domains in multimerization and trafficking, *The Journal of biological chemistry.* **281**, 1580-6.

138. Alessandri-Haber, N., Yeh, J. J., Boyd, A. E., Parada, C. A., Chen, X., Reichling, D. B. & Levine, J. D. (2003) Hypotonicity induces TRPV4-mediated nociception in rat, *Neuron.* **39**, 497-511.

139. Wegierski, T., Hill, K., Schaefer, M. & Walz, G. (2006) The HECT ubiquitin ligase AIP4 regulates the cell surface expression of select TRP channels, *The EMBO journal.* **25**, 5659-69.

140. Morenilla-Palao, C., Planells-Cases, R., Garcia-Sanz, N. & Ferrer-Montiel, A. (2004) Regulated exocytosis contributes to protein kinase C potentiation of vanilloid receptor activity, *The Journal of biological chemistry.* **279**, 25665-72.

141. Pizzirusso, M. & Chang, A. (2004) Ubiquitin-mediated targeting of a mutant plasma membrane ATPase, Pma1-7, to the endosomal/vacuolar system in yeast, *Molecular biology of the cell.* **15**, 2401-9.

142. Pickart, C. M. (1997) Targeting of substrates to the 26S proteasome, *FASEB journal : official publication of the Federation of American Societies for Experimental Biology.* **11**, 1055-66.

143. Katzmann, D. J., Babst, M. & Emr, S. D. (2001) Ubiquitin-dependent sorting into the multivesicular body pathway requires the function of a conserved endosomal protein sorting complex, ESCRT-I, *Cell.* **106**, 145-55.

144. Katzmann, D. J., Sarkar, S., Chu, T., Audhya, A. & Emr, S. D. (2004) Multivesicular body sorting: ubiquitin ligase Rsp5 is required for the modification and sorting of carboxypeptidase S, *Molecular biology of the cell.* **15**, 468-80.

145. Woodman, P. (2009) ESCRT proteins, endosome organization and mitogenic receptor down-regulation, *Biochemical Society transactions.* **37**, 146-50.

146. Auer-Grumbach, M., Olschewski, A., Papic, L., Kremer, H., McEntagart, M. E., Uhrig, S., Fischer, C., Frohlich, E., Balint, Z., Tang, B., Strohmaier, H., Lochmuller, H., Schlotter-Weigel, B., Senderek, J., Krebs, A., Dick, K. J., Petty, R., Longman, C., Anderson, N. E., Padberg, G. W., Schelhaas, H. J., van Ravenswaaij-Arts, C. M., Pieber, T. R., Crosby, A. H. & Guelly, C. (2010) Alterations in the ankyrin domain of TRPV4 cause congenital distal SMA, scapuloperoneal SMA and HMSN2C, *Nature genetics.* **42**, 160-4.

147. Deng, H. X., Klein, C. J., Yan, J., Shi, Y., Wu, Y., Fecto, F., Yau, H. J., Yang, Y., Zhai, H., Siddique, N., Hedley-Whyte, E. T., Delong, R., Martina, M., Dyck, P. J. & Siddique, T. (2010) Scapuloperoneal spinal muscular atrophy and CMT2C are allelic disorders caused by alterations in TRPV4, *Nature genetics.* **42**, 165-9.

148. Shikano, S. & Li, M. (2003) Membrane receptor trafficking: evidence of proximal and distal zones conferred by two independent endoplasmic reticulum localization signals, *Proceedings of the National Academy of Sciences of the United States of America.* **100**, 5783-8.

149. Suzuki, M., Hirao, A. & Mizuno, A. (2003) Microtubule-associated [corrected] protein 7 increases the membrane expression of transient receptor potential vanilloid 4 (TRPV4), *The Journal of biological chemistry.* **278**, 51448-53.

150. Sumoy, L., Pluvinet, R., Andreu, N., Estivill, X. & Escarceller, M. (2001) PACSIN 3 is a novel SH3 domain cytoplasmic adapter protein of the pacsin-syndapin-FAP52 gene family, *Gene.* **262**, 199-205.

151. Roberts-Galbraith, R. H. & Gould, K. L. (2010) Setting the F-BAR: functions and regulation of the F-BAR protein family, *Cell cycle.* **9**, 4091-7.

152. Cuajungco, M. P., Grimm, C., Oshima, K., D'Hoedt, D., Nilius, B., Mensenkamp, A. R., Bindels, R. J., Plomann, M. & Heller, S. (2006) PACSINs bind to the TRPV4 cation channel. PACSIN 3 modulates the subcellular localization of TRPV4, *The Journal of biological chemistry.* **281**, 18753-62.

153. Roach, W. & Plomann, M. (2007) PACSIN3 overexpression increases adipocyte glucose transport through GLUT1, *Biochemical and biophysical research communications.* **355**, 745-50.

154. Wang, Y., Fu, X., Gaiser, S., Kottgen, M., Kramer-Zucker, A., Walz, G. & Wegierski, T. (2007) OS-9 regulates the transit and polyubiquitination of TRPV4 in the endoplasmic reticulum, *The Journal of biological chemistry.* **282**, 36561-70.

155. Sidhaye, V. K., Guler, A. D., Schweitzer, K. S., D'Alessio, F., Caterina, M. J. & King, L. S. (2006) Transient receptor potential vanilloid 4 regulates aquaporin-5 abundance under hypotonic conditions, *Proceedings of the National Academy of Sciences of the United States of America.* **103**, 4747-52.

156. Liu, X., Bandyopadhyay, B. C., Nakamoto, T., Singh, B., Liedtke, W., Melvin, J. E. & Ambudkar, I. (2006) A role for AQP5 in activation of TRPV4 by hypotonicity: concerted involvement of AQP5 and TRPV4 in regulation of cell volume recovery, *The Journal of biological chemistry.* **281**, 15485-95.

157. Benfenati, V., Caprini, M., Dovizio, M., Mylonakou, M. N., Ferroni, S., Ottersen, O. P. & Amiry-Moghaddam, M. (2011) An aquaporin-4/transient receptor potential vanilloid 4 (AQP4/TRPV4) complex is essential for cell-volume control in astrocytes, *Proceedings of the National Academy of Sciences of the United States of America.* **108**, 2563-8.

158. Fabre-Jonca, N., Allaman, J. M., Radlgruber, G., Meda, P., Kiss, J. Z., French, L. E. & Masson, D. (1998) The distribution of murine 115-kDa epithelial microtubule-associated protein (E-MAP-115) during embryogenesis and in adult organs suggests a role in epithelial polarization and differentiation, *Differentiation; research in biological diversity.* **63**, 169-80.

159. Becker, D., Bereiter-Hahn, J. & Jendrach, M. (2009) Functional interaction of the cation channel transient receptor potential vanilloid 4 (TRPV4) and actin in volume regulation, *European journal of cell biology.* **88**, 141-52.

160. Ramadass, R., Becker, D., Jendrach, M. & Bereiter-Hahn, J. (2007) Spectrally and spatially resolved fluorescence lifetime imaging in living cells: TRPV4-microfilament interactions, *Archives of biochemistry and biophysics.* **463**, 27-36.

161. Goswami, C. & Hucho, T. (2007) TRPV1 expression-dependent initiation and regulation of filopodia, *Journal of neurochemistry.* **103**, 1319-33.

162. Cohen, D. M. (2003) Of rafts and moving water, *Science's STKE : signal transduction knowledge environment.* **2003**, pe36.

163. Saliez, J., Bouzin, C., Rath, G., Ghisdal, P., Desjardins, F., Rezzani, R., Rodella, L. F., Vriens, J., Nilius, B., Feron, O., Balligand, J. L. & Dessy, C. (2008) Role of caveolar compartmentation in endothelium-derived hyperpolarizing factor-mediated relaxation: Ca2+ signals and gap junction function are regulated by caveolin in endothelial cells, *Circulation.* **117**, 1065-74.

164. Kumari, S., Kumar, A., Sardar, P., Yadav, M., Majhi, R. K., Kumar, A. & Goswami, C. (2015) Influence of membrane cholesterol in the molecular evolution and functional regulation of TRPV4, *Biochemical and biophysical research communications.* **456**, 312-9.

165. Sokabe, T., Fukumi-Tominaga, T., Yonemura, S., Mizuno, A. & Tominaga, M. (2010) The TRPV4 channel contributes to intercellular junction formation in keratinocytes, *The Journal of biological chemistry.* **285**, 18749-58.

166. Shin, S. H., Lee, E. J., Hyun, S., Chun, J., Kim, Y. & Kang, S. S. (2012) Phosphorylation on the Ser 824 residue of TRPV4 prefers to bind with F-actin than with microtubules to expand the cell surface area, *Cellular signalling.* **24**, 641-51.

167. Shukla, A. K., Kim, J., Ahn, S., Xiao, K., Shenoy, S. K., Liedtke, W. & Lefkowitz, R. J. (2010) Arresting a transient receptor potential (TRP) channel: beta-arrestin 1 mediates ubiquitination and functional down-regulation of TRPV4, *The Journal of biological chemistry.* **285**, 30115-25.

168. Pitcher, J. A., Freedman, N. J. & Lefkowitz, R. J. (1998) G protein-coupled receptor kinases, *Annual review of biochemistry.* **67**, 653-92.

169. Matsusaka, T. & Ichikawa, I. (1997) Biological functions of angiotensin and its receptors, *Annual review of physiology.* **59**, 395-412.

170. Kohler, R., Heyken, W. T., Heinau, P., Schubert, R., Si, H., Kacik, M., Busch, C., Grgic, I., Maier, T. & Hoyer, J. (2006) Evidence for a functional role of endothelial transient receptor potential V4 in shear stress-induced vasodilatation, *Arteriosclerosis, thrombosis, and vascular biology.* **26**, 1495-502.

171. Hellwig, N., Albrecht, N., Harteneck, C., Schultz, G. & Schaefer, M. (2005) Homo- and heteromeric assembly of TRPV channel subunits, *Journal of cell science.* **118**, 917-28.

172. Kottgen, M., Buchholz, B., Garcia-Gonzalez, M. A., Kotsis, F., Fu, X., Doerken, M., Boehlke, C., Steffl, D., Tauber, R., Wegierski, T., Nitschke, R., Suzuki, M., Kramer-Zucker, A., Germino, G. G., Watnick, T., Prenen, J., Nilius, B., Kuehn, E. W. & Walz, G. (2008) TRPP2 and TRPV4 form a polymodal sensory channel complex, *The Journal of cell biology.* **182**, 437-47.

173. Ma, X., Qiu, S., Luo, J., Ma, Y., Ngai, C. Y., Shen, B., Wong, C. O., Huang, Y. & Yao, X. (2010) Functional role of vanilloid transient receptor potential 4-canonical transient receptor potential 1 complex in flow-induced Ca2+ influx, *Arteriosclerosis, thrombosis, and vascular biology.* **30**, 851-8.

174. Du, J., Ma, X., Shen, B., Huang, Y., Birnbaumer, L. & Yao, X. (2014) TRPV4, TRPC1, and TRPP2 assemble to form a flow-sensitive heteromeric channel, *FASEB journal : official publication of the Federation of American Societies for Experimental Biology.* **28**, 4677-85.

175. Baratchi, S., Almazi, J. G., Darby, W., Tovar-Lopez, F. J., Mitchell, A. & McIntyre, P. (2016) Shear stress mediates exocytosis of functional TRPV4 channels in endothelial cells, *Cellular and molecular life sciences : CMLS.* **73**, 649-66.

176. Lamande, S. R., Yuan, Y., Gresshoff, I. L., Rowley, L., Belluoccio, D., Kaluarachchi, K., Little, C. B., Botzenhart, E., Zerres, K., Amor, D. J., Cole, W. G., Savarirayan, R., McIntyre, P. & Bateman, J. F. (2011) Mutations in TRPV4 cause an inherited arthropathy of hands and feet, *Nature genetics.* **43**, 1142-6.

177. Verma, P., Kumar, A. & Goswami, C. (2010) TRPV4-mediated channelopathies, *Channels.* **4**, 319-28.

178. Nilius, B. & Voets, T. (2013) The puzzle of TRPV4 channelopathies, *EMBO reports.* **14**, 152-63.

179. Rock, M. J., Prenen, J., Funari, V. A., Funari, T. L., Merriman, B., Nelson, S. F., Lachman, R. S., Wilcox, W. R., Reyno, S., Quadrelli, R., Vaglio, A., Owsianik, G., Janssens, A., Voets, T., Ikegawa, S., Nagai, T., Rimoin, D. L., Nilius, B. & Cohn, D. H. (2008) Gain-of-function mutations in TRPV4 cause autosomal dominant brachyolmia, *Nature genetics.* **40**, 999-1003.

180. Krakow, D., Vriens, J., Camacho, N., Luong, P., Deixler, H., Funari, T. L., Bacino, C. A., Irons, M. B., Holm, I. A., Sadler, L., Okenfuss, E. B., Janssens, A., Voets, T., Rimoin, D. L., Lachman, R. S., Nilius, B. & Cohn, D. H. (2009) Mutations in the gene encoding the calcium-permeable ion channel TRPV4 produce spondylometaphyseal dysplasia, Kozlowski type and metatropic dysplasia, *American journal of human genetics.* **84**, 307-15.

181. Halbert, S. A., Tam, P. Y. & Blandau, R. J. (1976) Egg transport in the rabbit oviduct: the roles of cilia and muscle, *Science.* **191**, 1052-3.

182. Jung, C., Fandos, C., Lorenzo, I. M., Plata, C., Fernandes, J., Gene, G. G., Vazquez, E. & Valverde, M. A. (2009) The progesterone receptor regulates the expression of TRPV4 channel, *Pflugers Archiv : European journal of physiology.* **459**, 105-13.

183. Xu, Z. P., Gao, W. C., Wang, H. P. & Wang, X. H. (2009) [Expression of transient receptor potential subfamily mRNAs in rat testes], *Nan fang yi ke da xue xue bao = Journal of Southern Medical University.* **29**, 519-20.

184. Alenmyr, L., Uller, L., Greiff, L., Hogestatt, E. D. & Zygmunt, P. M. (2014) TRPV4-mediated calcium influx and ciliary activity in human native airway epithelial cells, *Basic & clinical pharmacology & toxicology.* **114**, 210-6.

185. Knowles, M. R. & Boucher, R. C. (2002) Mucus clearance as a primary innate defense mechanism for mammalian airways, *The Journal of clinical investigation.* **109**, 571-7.

186. Li, J., Kanju, P., Patterson, M., Chew, W. L., Cho, S. H., Gilmour, I., Oliver, T., Yasuda, R., Ghio, A., Simon, S. A. & Liedtke, W. (2011) TRPV4-mediated calcium influx into human bronchial epithelia upon exposure to diesel exhaust particles, *Environmental health perspectives.* **119**, 784-93.

187. Watanabe, H., Murakami, M., Ohba, T., Takahashi, Y. & Ito, H. (2008) TRP channel and cardiovascular disease, *Pharmacology & therapeutics.* **118**, 337-51.

188. Zhang, D. X., Mendoza, S. A., Bubolz, A. H., Mizuno, A., Ge, Z. D., Li, R., Warltier, D. C., Suzuki, M. & Gutterman, D. D. (2009) Transient receptor potential vanilloid type 4-deficient mice exhibit impaired endothelium-dependent relaxation induced by acetylcholine in vitro and in vivo, *Hypertension.* **53**, 532-8.

189. Kohler, R. & Hoyer, J. (2007) Role of TRPV4 in the Mechanotransduction of Shear Stress in Endothelial Cells in *TRP Ion Channel Function in Sensory Transduction and Cellular Signaling Cascades* (Liedtke, W. B. & Heller, S., eds), Boca Raton (FL).

190. Loot, A. E., Popp, R., Fisslthaler, B., Vriens, J., Nilius, B. & Fleming, I. (2008) Role of cytochrome P450-dependent transient receptor potential V4 activation in flow-induced vasodilatation, *Cardiovascular research.* **80**, 445-52.

191. Hartmannsgruber, V., Heyken, W. T., Kacik, M., Kaistha, A., Grgic, I., Harteneck, C., Liedtke, W., Hoyer, J. & Kohler, R. (2007) Arterial response to shear stress critically depends on endothelial TRPV4 expression, *PloS one.* **2**, e827.

192. Schierling, W., Troidl, K., Apfelbeck, H., Troidl, C., Kasprzak, P. M., Schaper, W. & Schmitz-Rixen, T. (2011) Cerebral arteriogenesis is enhanced by pharmacological as well as fluid-shear-stress activation of the Trpv4 calcium channel, *European journal of vascular and endovascular surgery : the official journal of the European Society for Vascular Surgery.* **41**, 589-96.

193. Troidl, C., Troidl, K., Schierling, W., Cai, W. J., Nef, H., Mollmann, H., Kostin, S., Schimanski, S., Hammer, L., Elsasser, A., Schmitz-Rixen, T. & Schaper, W. (2009) Trpv4 induces collateral vessel growth during regeneration of the arterial circulation, *Journal of cellular and molecular medicine.* **13**, 2613-21.

194. Alvarez, D. F., King, J. A., Weber, D., Addison, E., Liedtke, W. & Townsley, M. I. (2006) Transient receptor potential vanilloid 4-mediated disruption of the alveolar septal barrier: a novel mechanism of acute lung injury, *Circulation research.* **99**, 988-95.

195. Kawano, S., Shoji, S., Ichinose, S., Yamagata, K., Tagami, M. & Hiraoka, M. (2002) Characterization of Ca(2+) signaling pathways in human mesenchymal stem cells, *Cell calcium.* **32**, 165-74.

196. Heubach, J. F., Graf, E. M., Leutheuser, J., Bock, M., Balana, B., Zahanich, I., Christ, T., Boxberger, S., Wettwer, E. & Ravens, U. (2004) Electrophysiological properties of human mesenchymal stem cells, *The Journal of physiology.* **554**, 659-72.

197. Qi, Y., Li, Z., Kong, C. W., Tang, N. L., Huang, Y., Li, R. A. & Yao, X. (2015) Uniaxial cyclic stretch stimulates TRPV4 to induce realignment of human embryonic stem cell-derived cardiomyocytes, *Journal of molecular and cellular cardiology.* **87**, 65-73.

198. Dragoni, S., Guerra, G., Fiorio Pla, A., Bertoni, G., Rappa, A., Poletto, V., Bottino, C., Aronica, A., Lodola, F., Cinelli, M. P., Laforenza, U., Rosti, V., Tanzi, F., Munaron, L. & Moccia, F. (2015) A functional transient receptor potential vanilloid 4 (TRPV4) channel is expressed in human endothelial progenitor cells, *Journal of cellular physiology.* **230**, 95-104.

199. Boulais, N., Pennec, J. P., Lebonvallet, N., Pereira, U., Rougier, N., Dorange, G., Chesne, C. & Misery, L. (2009) Rat Merkel cells are mechanoreceptors and osmoreceptors, *PloS one.* **4**, e7759.

200. Mandadi, S., Sokabe, T., Shibasaki, K., Katanosaka, K., Mizuno, A., Moqrich, A., Patapoutian, A., Fukumi-Tominaga, T., Mizumura, K. & Tominaga, M. (2009) TRPV3 in keratinocytes transmits temperature information to sensory neurons via ATP, *Pflugers Archiv : European journal of physiology.* **458**, 1093-102.

201. Denda, M., Sokabe, T., Fukumi-Tominaga, T. & Tominaga, M. (2007) Effects of skin surface temperature on epidermal permeability barrier homeostasis, *The Journal of investigative dermatology.* **127**, 654-9.

202. Takayanagi, H., Kim, S., Koga, T., Nishina, H., Isshiki, M., Yoshida, H., Saiura, A., Isobe, M., Yokochi, T., Inoue, J., Wagner, E. F., Mak, T. W., Kodama, T. & Taniguchi, T. (2002) Induction and activation of the transcription factor NFATc1 (NFAT2) integrate RANKL signaling in terminal differentiation of osteoclasts, *Developmental cell.* **3**, 889-901.

203. Kitahara, T., Li, H. S. & Balaban, C. D. (2005) Changes in transient receptor potential cation channel superfamily V (TRPV) mRNA expression in the mouse inner ear ganglia after kanamycin challenge, *Hearing research.* **201**, 132-44.

204. Dong, X. P., Wang, X. & Xu, H. (2010) TRP channels of intracellular membranes, *Journal of neurochemistry.* **113**, 313-28.

205. Gallego-Sandin, S., Rodriguez-Garcia, A., Alonso, M. T. & Garcia-Sancho, J. (2009) The endoplasmic reticulum of dorsal root ganglion neurons contains functional TRPV1 channels, *The Journal of biological chemistry.* **284**, 32591-601.

206. Lo, I. C., Chan, H. C., Qi, Z., Ng, K. L., So, C. & Tsang, S. Y. (2016) TRPV3 Channel Negatively Regulates Cell Cycle Progression and Safeguards the Pluripotency of Embryonic Stem Cells, *Journal of cellular physiology.* **231**, 403-13.

207. Zhao, Y., Huang, H., Jiang, Y., Wei, H., Liu, P., Wang, W. & Niu, W. (2012) Unusual localization and translocation of TRPV4 protein in cultured ventricular myocytes of the neonatal rat, *European journal of histochemistry : EJH.* **56**, e32.

208. Becker, D., Muller, M., Leuner, K. & Jendrach, M. (2008) The C-terminal domain of TRPV4 is essential for plasma membrane localization, *Molecular membrane biology.* **25**, 139-51.

209. Bird TD. Charcot-Marie-Tooth Neuropathy Type 2 1993, University of Washingtion, Seattle, USA

210. Dong, X. P., Cheng, X., Mills, E., Delling, M., Wang, F., Kurz, T. & Xu, H. (2008) The type IV mucolipidosis-associated protein TRPML1 is an endolysosomal iron release channel, *Nature.* **455**, 992-6.

211. Ye, L., Kleiner, S., Wu, J., Sah, R., Gupta, R. K., Banks, A. S., Cohen, P., Khandekar, M. J., Bostrom, P., Mepani, R. J., Laznik, D., Kamenecka, T. M., Song, X., Liedtke, W., Mootha, V. K., Puigserver, P., Griffin, P.

R., Clapham, D. E. & Spiegelman, B. M. (2012) TRPV4 is a regulator of adipose oxidative metabolism, inflammation, and energy homeostasis, *Cell.* **151**, 96-110.

212. Mamenko, M., Zaika, O. L., Boukelmoune, N., Berrout, J., O'Neil, R. G. & Pochynyuk, O. (2013) Discrete control of TRPV4 channel function in the distal nephron by protein kinases A and C, *The Journal of biological chemistry.* **288**, 20306-14.

213. Gamba, G. (2006) TRPV4: a new target for the hypertension-related kinases WNK1 and WNK4, *American journal of physiology Renal physiology.* **290**, F1303-4.

214. Garcia-Elias, A., Mrkonjic, S., Pardo-Pastor, C., Inada, H., Hellmich, U. A., Rubio-Moscardo, F., Plata, C., Gaudet, R., Vicente, R. & Valverde, M. A. (2013) Phosphatidylinositol-4,5-biphosphate-dependent rearrangement of TRPV4 cytosolic tails enables channel activation by physiological stimuli, *Proceedings of the National Academy of Sciences of the United States of America.* **110**, 9553-8.

215. Omura, T. (1998) Mitochondria-targeting sequence, a multi-role sorting sequence recognized at all steps of protein import into mitochondria, *Journal of biochemistry.* **123**, 1010-6.

216. Stan, T., Brix, J., Schneider-Mergener, J., Pfanner, N., Neupert, W. & Rapaport, D. (2003) Mitochondrial protein import: recognition of internal import signals of BCS1 by the TOM complex, *Molecular and cellular biology.* **23**, 2239-50.

217. Cao, W. & Douglas, M. G. (1996) Specific targeting of ISP6 to mitochondria is mediated by sequences other than its amino terminus, *Biochemical and biophysical research communications.* **224**, 457-61.

218. Joseph, E. K. & Levine, J. D. (2010) Multiple PKCepsilon-dependent mechanisms mediating mechanical hyperalgesia, *Pain.* **150**, 17-21.

219. Carre, M., Andre, N., Carles, G., Borghi, H., Brichese, L., Briand, C. & Braguer, D. (2002) Tubulin is an inherent component of mitochondrial membranes that interacts with the voltage-dependent anion channel, *The Journal of biological chemistry.* **277**, 33664-9.

220. Detmer, S. A. & Chan, D. C. (2007) Functions and dysfunctions of mitochondrial dynamics, *Nature reviews Molecular cell biology.* **8**, 870-9.

221. Karbowski, M. & Youle, R. J. (2003) Dynamics of mitochondrial morphology in healthy cells and during apoptosis, *Cell death and differentiation.* **10**, 870-80.

222. Kirichok, Y., Krapivinsky, G. & Clapham, D. E. (2004) The mitochondrial calcium uniporter is a highly selective ion channel, *Nature.* **427**, 360-4.

223. Szabadkai, G., Bianchi, K., Varnai, P., De Stefani, D., Wieckowski, M. R., Cavagna, D., Nagy, A. I., Balla, T. & Rizzuto, R. (2006) Chaperone-mediated coupling of endoplasmic reticulum and mitochondrial Ca2+ channels, *The Journal of cell biology.* **175**, 901-11.

224. De Stefani, D., Raffaello, A., Teardo, E., Szabo, I. & Rizzuto, R. (2011) A forty-kilodalton protein of the inner membrane is the mitochondrial calcium uniporter, *Nature.* **476**, 336-40.

225. Koopman, W. J., Verkaart, S., Visch, H. J., van der Westhuizen, F. H., Murphy, M. P., van den Heuvel, L. W., Smeitink, J. A. & Willems, P. H. (2005) Inhibition of complex I of the electron transport chain causes O2-. -mediated mitochondrial outgrowth, *American journal of physiology Cell physiology.* **288**, C1440-50.

226. Nicholls, D. G. & Ward, M. W. (2000) Mitochondrial membrane potential and neuronal glutamate excitotoxicity: mortality and millivolts, *Trends in neurosciences.* **23**, 166-74.

227. Chalmers, S. & McCarron, J. G. (2008) The mitochondrial membrane potential and Ca2+ oscillations in smooth muscle, *Journal of cell science.* **121**, 75-85.

228. Talbot, J., Barrett, J. N., Barrett, E. F. & David, G. (2007) Stimulation-induced changes in NADH fluorescence and mitochondrial membrane potential in lizard motor nerve terminals, *The Journal of physiology.* **579**, 783-98.

229. Perocchi, F., Gohil, V. M., Girgis, H. S., Bao, X. R., McCombs, J. E., Palmer, A. E. & Mootha, V. K. (2010) MICU1 encodes a mitochondrial EF hand protein required for Ca(2+) uptake, *Nature.* **467**, 291-6.

230. Jiang, D., Zhao, L. & Clapham, D. E. (2009) Genome-wide RNAi screen identifies Letm1 as a mitochondrial Ca2+/H+ antiporter, *Science.* **326**, 144-7.

231. Nowikovsky, K., Froschauer, E. M., Zsurka, G., Samaj, J., Reipert, S., Kolisek, M., Wiesenberger, G. & Schweyen, R. J. (2004) The LETM1/YOL027 gene family encodes a factor of the mitochondrial K+ homeostasis with a potential role in the Wolf-Hirschhorn syndrome, *The Journal of biological chemistry.* **279**, 30307-15.

232. Palty, R., Silverman, W. F., Hershfinkel, M., Caporale, T., Sensi, S. L., Parnis, J., Nolte, C., Fishman, D., Shoshan-Barmatz, V., Herrmann, S., Khananshvili, D. & Sekler, I. (2010) NCLX is an essential component of mitochondrial Na+/Ca2+ exchange, *Proceedings of the National Academy of Sciences of the United States of America.* **107**, 436-41.

233. Veereshwarayya, V., Kumar, P., Rosen, K. M., Mestril, R. & Querfurth, H. W. (2006) Differential effects of mitochondrial heat shock protein 60 and related molecular chaperones to prevent intracellular beta-amyloid-induced inhibition of complex IV and limit apoptosis, *The Journal of biological chemistry.* **281**, 29468-78.

234. Grundtman, C., Kreutmayer, S. B., Almanzar, G., Wick, M. C. & Wick, G. (2011) Heat shock protein 60 and immune inflammatory responses in atherosclerosis, *Arteriosclerosis, thrombosis, and vascular biology.* **31**, 960-8.

235. Bromberg, Z., Goloubinoff, P., Saidi, Y. & Weiss, Y. G. (2013) The membrane-associated transient receptor potential vanilloid channel is the central heat shock receptor controlling the cellular heat shock response in epithelial cells, *PloS one.* **8**, e57149.

236. Hatefi, Y. (1985) The mitochondrial electron transport and oxidative phosphorylation system, *Annual review of biochemistry.* **54**, 1015-69.

237. Saraste, M. (1999) Oxidative phosphorylation at the fin de siecle, *Science.* **283**, 1488-93.

238. McCormack, J. G. & Denton, R. M. (1979) The effects of calcium ions and adenine nucleotides on the activity of pig heart 2-oxoglutarate dehydrogenase complex, *The Biochemical journal.* **180**, 533-44.

239. McCormack, J. G., Halestrap, A. P. & Denton, R. M. (1990) Role of calcium ions in regulation of mammalian intramitochondrial metabolism, *Physiological reviews.* **70**, 391-425.

240. Hansford, R. G. (1994) Physiological role of mitochondrial Ca2+ transport, *Journal of bioenergetics and biomembranes.* **26**, 495-508.

241. Lasorsa, F. M., Pinton, P., Palmieri, L., Fiermonte, G., Rizzuto, R. & Palmieri, F. (2003) Recombinant expression of the Ca(2+)-sensitive aspartate/glutamate carrier increases mitochondrial ATP production in agonist-stimulated Chinese hamster ovary cells, *The Journal of biological chemistry.* **278**, 38686-92.

242. Contreras, L., Gomez-Puertas, P., Iijima, M., Kobayashi, K., Saheki, T. & Satrustegui, J. (2007) Ca2+ Activation kinetics of the two aspartate-glutamate mitochondrial carriers, aralar and citrin: role in the heart malate-aspartate NADH shuttle, *The Journal of biological chemistry.* **282**, 7098-106.

243. Hajnoczky, G., Csordas, G., Das, S., Garcia-Perez, C., Saotome, M., Sinha Roy, S. & Yi, M. (2006) Mitochondrial calcium signalling and cell death: approaches for assessing the role of mitochondrial Ca2+ uptake in apoptosis, *Cell calcium.* **40**, 553-60.

244. Rizzuto, R. & Pozzan, T. (2006) Microdomains of intracellular Ca2+: molecular determinants and functional consequences, *Physiological reviews.* **86**, 369-408.

245. Dickerson, R. E. (1971) The structures of cytochrome c and the rates of molecular evolution, *Journal of molecular evolution.* **1**, 26-45.

246. Hinson, D. D., Chambliss, K. L., Toth, M. J., Tanaka, R. D. & Gibson, K. M. (1997) Post-translational regulation of mevalonate kinase by intermediates of the cholesterol and nonsterol isoprene biosynthetic pathways, *Journal of lipid research.* **38**, 2216-23.

247. Kjellberg, M. A., Backman, A. P., Ohvo-Rekila, H. & Mattjus, P. (2014) Alternation in the glycolipid transfer protein expression causes changes in the cellular lipidome, *PloS one.* **9**, e97263.

248. Chacinska, A., Koehler, C. M., Milenkovic, D., Lithgow, T. & Pfanner, N. (2009) Importing mitochondrial proteins: machineries and mechanisms, *Cell.* **138**, 628-44.

249. Roise, D. & Schatz, G. (1988) Mitochondrial presequences, *The Journal of biological chemistry.* **263**, 4509-11.

250. Li, M., Zhong, Z., Zhu, J., Xiang, D., Dai, N., Cao, X., Qing, Y., Yang, Z., Xie, J., Li, Z., Baugh, L., Wang, G. & Wang, D. (2010) Identification and characterization of mitochondrial targeting sequence of human apurinic/apyrimidinic endonuclease 1, *The Journal of biological chemistry.* **285**, 14871-81.

251. Dembowski, M., Kunkele, K. P., Nargang, F. E., Neupert, W. & Rapaport, D. (2001) Assembly of Tom6 and Tom7 into the TOM core complex of Neurospora crassa, *The Journal of biological chemistry.* **276**, 17679-85.

252. Egan, B., Beilharz, T., George, R., Isenmann, S., Gratzer, S., Wattenberg, B. & Lithgow, T. (1999) Targeting of tail-anchored proteins to yeast mitochondria in vivo, *FEBS letters.* **451**, 243-8.

253. Rodriguez-Cousino, N., Nargang, F. E., Baardman, R., Neupert, W., Lill, R. & Court, D. A. (1998) An import signal in the cytosolic domain of the Neurospora mitochondrial outer membrane protein TOM22, *The Journal of biological chemistry.* **273**, 11527-32.

254. Diekert, K., Kispal, G., Guiard, B. & Lill, R. (1999) An internal targeting signal directing proteins into the mitochondrial intermembrane space, *Proceedings of the National Academy of Sciences of the United States of America.* **96**, 11752-7.

255. Feng, S., Li, H., Tai, Y., Huang, J., Su, Y., Abramowitz, J., Zhu, M. X., Birnbaumer, L. & Wang, Y. (2013) Canonical transient receptor potential 3 channels regulate mitochondrial calcium uptake, *Proceedings of the National Academy of Sciences of the United States of America.* **110**, 11011-6.

256. Majhi, R. K., Kumar, A., Yadav, M., Kumar, P., Maity, A., Giri, S. C. & Goswami, C. (2016) Light and electron microscopic study of mature spermatozoa from White Pekin duck (Anas platyrhynchos): an ultrastructural and molecular analysis, *Andrology*. doi: 10.1111/andr.12130.

257. Ankel-Simons, F. & Cummins, J. M. (1996) Misconceptions about mitochondria and mammalian fertilization: implications for theories on human evolution, *Proceedings of the National Academy of Sciences of the United States of America*. **93**, 13859-63.

258. Piomboni, P., Focarelli, R., Stendardi, A., Ferramosca, A. & Zara, V. (2012) The role of mitochondria in energy production for human sperm motility, *International journal of andrology.* **35**, 109-24.

259. Shivaji, S., Kota, V. & Siva, A. B. (2009) The role of mitochondrial proteins in sperm capacitation, *Journal of reproductive immunology.* **83**, 14-8.

260. Chan CC, Shui HA, Wu CH, Wang CY, Sun GH, Chen HM & Wu GJ (2009) Motility and protein phosphorylation in healthy and asthenozoospermic sperm. *J. Proteome Res.* **8**, 5382–5386.

261. Dorval V, Dufour M & Leclerc, P. (2002) Regulation of the phosphotyrosine content of human sperm proteins by intracellular Ca^{2+}: role of Ca2+-adenosine triphosphatases. *Biol. Reprod.* **67**, 1538–1545

262. Florman HM, Arnoult C, Kazam IG, Li C & O'Toole CM (1998) A perspective on the control of mammalian fertilization by egg-activated ion channels in sperm: a tale of two channels. *Biol. Reprod.* **59**, 12–16.

263. Meizel S, Turner KO, Nuccitelli R (1997) Progesterone triggers a wave of increased free calcium during the human sperm acrosome reaction. *Dev. Biol.* **182**, 67-75.

264. Tesarik J, Carreras A, Mendoza C (1993) Differential sensitivity of progesterone- and zona pellucida-induced acrosome reactions to pertussis toxin. *Mol Reprod Dev*. **34**, 183-9.

265. Bielfeld P, Anderson RA, Mack SR, De Jonge CJ, Zaneveld LJ (1994) Are capacitation or calcium ion influx required for the human sperm acrosome reaction? *Fertil Steril*. **62**, 1255-61.

266. Liu DY, Baker HW (1996) Relationship between the zona pellucida (ZP) and ionophore A23187-induced acrosome reaction and the ability of sperm to penetrate the ZP in men with normal sperm-ZP binding. *Fertil Steril*. **66**, 312-5.

267. Shoshan-Barmatz, V., De Pinto, V., Zweckstetter, M., Raviv, Z., Keinan, N. & Arbel, N. (2010) VDAC, a multi-functional mitochondrial protein regulating cell life and death, *Molecular aspects of medicine.* **31**, 227-85.

268. Lisanti, M. P., Scherer, P. E., Vidugiriene, J., Tang, Z., Hermanowski-Vosatka, A., Tu, Y. H., Cook, R. F. & Sargiacomo, M. (1994) Characterization of caveolin-rich membrane domains isolated from an endothelial-rich source: implications for human disease, *The Journal of cell biology.* **126**, 111-26.

269. Kumagami, H., Terakado, M., Sainoo, Y., Baba, A., Fujiyama, D., Fukuda, T., Takasaki, K. & Takahashi, H. (2009) Expression of the osmotically responsive cationic channel TRPV4 in the endolymphatic sac, *Audiology & neuro-otology.* **14**, 190-7.

270. Kijima, K., Numakura, C., Goto, T., Takahashi, T., Otagiri, T., Umetsu, K. & Hayasaka, K. (2005) Small heat shock protein 27 mutation in a Japanese patient with distal hereditary motor neuropathy, *Journal of human genetics.* **50**, 473-6.

271. Cayouette, S. & Boulay, G. (2007) Intracellular trafficking of TRP channels, *Cell calcium.* **42**, 225-32.

272. Lei, L., Cao, X., Yang, F., Shi, D. J., Tang, Y. Q., Zheng, J. & Wang, K. (2013) A TRPV4 channel C-terminal folding recognition domain critical for trafficking and function, *The Journal of biological chemistry.* **288**, 10427-39.

273. Alessandri-Haber, N., Dina, O. A., Chen, X. & Levine, J. D. (2009) TRPC1 and TRPC6 channels cooperate with TRPV4 to mediate mechanical hyperalgesia and nociceptor sensitization, *The Journal of neuroscience : the official journal of the Society for Neuroscience.* **29**, 6217-28.

274. Quiros, P. M., Langer, T. & Lopez-Otin, C. (2015) New roles for mitochondrial proteases in health, ageing and disease, *Nature reviews Molecular cell biology.* **16**, 345-59.

275. Gerdes, F., Tatsuta, T. & Langer, T. (2012) Mitochondrial AAA proteases--towards a molecular understanding of membrane-bound proteolytic machines, *Biochimica et biophysica acta.* **1823**, 49-55.

276. Cheng, M. Y., Hartl, F. U. & Horwich, A. L. (1990) The mitochondrial chaperonin hsp60 is required for its own assembly, *Nature.* **348**, 455-8.

277. Cheng, M. Y., Hartl, F. U., Martin, J., Pollock, R. A., Kalousek, F., Neupert, W., Hallberg, E. M., Hallberg, R. L. & Horwich, A. L. (1989) Mitochondrial heat-shock protein hsp60 is essential for assembly of proteins imported into yeast mitochondria, *Nature.* **337**, 620-5.

278. Ellis, R. J. & van der Vies, S. M. (1991) Molecular chaperones, *Annual review of biochemistry.* **60**, 321-47.

279. Soltys, B. J. & Gupta, R. S. (1996) Immunoelectron microscopic localization of the 60-kDa heat shock chaperonin protein (Hsp60) in mammalian cells, *Experimental cell research.* **222**, 16-27.

280. Soltys, B. J. & Gupta, R. S. (1997) Cell surface localization of the 60 kDa heat shock chaperonin protein (hsp60) in mammalian cells, *Cell biology international.* **21**, 315-20.

281. Soltys, B. J. & Gupta, R. S. (1999) Mitochondrial-matrix proteins at unexpected locations: are they exported?, *Trends in biochemical sciences.* **24**, 174-7.

282. Nunnari, J. & Suomalainen, A. (2012) Mitochondria: in sickness and in health, *Cell.* **148**, 1145-59.

283. Chen, H., Detmer, S. A., Ewald, A. J., Griffin, E. E., Fraser, S. E. & Chan, D. C. (2003) Mitofusins Mfn1 and Mfn2 coordinately regulate mitochondrial fusion and are essential for embryonic development, *The Journal of cell biology.* **160**, 189-200.

284. de Brito, O. M. & Scorrano, L. (2008) Mitofusin 2 tethers endoplasmic reticulum to mitochondria, *Nature.* **456**, 605-10.

285. Frazier, A. E., Kiu, C., Stojanovski, D., Hoogenraad, N. J. & Ryan, M. T. (2006) Mitochondrial morphology and distribution in mammalian cells, *Biological chemistry.* **387**, 1551-8.

286. Catlett, N. L. & Weisman, L. S. (2000) Divide and multiply: organelle partitioning in yeast, *Current opinion in cell biology.* **12**, 509-16.

287. Frank, S., Gaume, B., Bergmann-Leitner, E. S., Leitner, W. W., Robert, E. G., Catez, F., Smith, C. L. & Youle, R. J. (2001) The role of dynamin-related protein 1, a mediator of mitochondrial fission, in apoptosis, *Developmental cell.* **1**, 515-25.

288. Scorrano, L., Ashiya, M., Buttle, K., Weiler, S., Oakes, S. A., Mannella, C. A. & Korsmeyer, S. J. (2002) A distinct pathway remodels mitochondrial cristae and mobilizes cytochrome c during apoptosis, *Developmental cell.* **2**, 55-67.

289. Ha, E. E. & Frohman, M. A. (2014) Regulation of mitochondrial morphology by lipids, *BioFactors.* **40**, 419-24.

290. Kostyuk, P. & Verkhratsky, A. (1994) Calcium stores in neurons and glia, *Neuroscience.* **63**, 381-404.

291. Svichar, N., Kostyuk, P. & Verkhratsky, A. (1997) Mitochondria buffer Ca2+ entry but not intracellular Ca^{2+} release in mouse DRG neurones, *Neuroreport.* **8**, 3929-32.

292. Verkhratsky, A. J. & Petersen, O. H. (1998) Neuronal calcium stores, *Cell calcium.* **24**, 333-43.

293. Duchen, M. R. (1999) Contributions of mitochondria to animal physiology: from homeostatic sensor to calcium signalling and cell death, *The Journal of physiology.* **516 (Pt 1)**, 1-17.

294. Jouaville, L. S., Ichas, F., Holmuhamedov, E. L., Camacho, P. & Lechleiter, J. D. (1995) Synchronization of calcium waves by mitochondrial substrates in Xenopus laevis oocytes, *Nature.* **377**, 438-41.

295. Blachly-Dyson, E. & Forte, M. (2001) VDAC channels, *IUBMB life.* **52**, 113-8.

296. Blachly-Dyson, E., Zambronicz, E. B., Yu, W. H., Adams, V., McCabe, E. R., Adelman, J., Colombini, M. & Forte, M. (1993) Cloning and functional expression in yeast of two human isoforms of the outer mitochondrial membrane channel, the voltage-dependent anion channel, *The Journal of biological chemistry.* **268**, 1835-41.

297. Rizzuto, R., Pinton, P., Carrington, W., Fay, F. S., Fogarty, K. E., Lifshitz, L. M., Tuft, R. A. & Pozzan, T. (1998) Close contacts with the endoplasmic reticulum as determinants of mitochondrial Ca2+ responses, *Science.* **280**, 1763-6.

298. Csordas, G., Thomas, A. P. & Hajnoczky, G. (1999) Quasi-synaptic calcium signal transmission between endoplasmic reticulum and mitochondria, *The EMBO journal.* **18**, 96-108.

299. Szalai, G., Csordas, G., Hantash, B. M., Thomas, A. P. & Hajnoczky, G. (2000) Calcium signal transmission between ryanodine receptors and mitochondria, *The Journal of biological chemistry.* **275**, 15305-13.

300. Mannella, C. A., Buttle, K., Rath, B. K. & Marko, M. (1998) Electron microscopic tomography of rat-liver mitochondria and their interaction with the endoplasmic reticulum, *BioFactors.* **8**, 225-8.

301. Mitchell, P. & Moyle, J. (1967) Chemiosmotic hypothesis of oxidative phosphorylation, *Nature.* **213**, 137-9.

302. Vance, J. E. (2014) MAM (mitochondria-associated membranes) in mammalian cells: lipids and beyond, *Biochimica et biophysica acta.* **1841**, 595-609.

303. Barnett, M., Lin, D., Akoyev, V., Willard, L. & Takemoto, D. (2008) Protein kinase C epsilon activates lens mitochondrial cytochrome c oxidase subunit IV during hypoxia, *Experimental eye research.* **86**, 226-34.

304. Dave, K. R., DeFazio, R. A., Raval, A. P., Torraco, A., Saul, I., Barrientos, A. & Perez-Pinzon, M. A. (2008) Ischemic preconditioning targets the respiration of synaptic mitochondria via protein kinase C epsilon, *The Journal of neuroscience : the official journal of the Society for Neuroscience.* **28**, 4172-82.

305. Costa, A. D. & Garlid, K. D. (2008) Intramitochondrial signaling: interactions among mitoKATP, PKCepsilon, ROS, and MPT, *American journal of physiology Heart and circulatory physiology.* **295**, H874-82.

306. McCarthy, J., McLeod, C. J., Minners, J., Essop, M. F., Ping, P. & Sack, M. N. (2005) PKCepsilon activation augments cardiac mitochondrial respiratory post-anoxic reserve--a putative mechanism in PKCepsilon cardioprotection, *Journal of molecular and cellular cardiology.* **38**, 697-700.

307. Korzick, D. H., Kostyak, J. C., Hunter, J. C. & Saupe, K. W. (2007) Local delivery of PKCepsilon-activating peptide mimics ischemic preconditioning in aged hearts through GSK-3beta but not F1-ATPase inactivation, *American journal of physiology Heart and circulatory physiology.* **293**, H2056-63.

308. Kim, H. Y., Wang, J., Lu, Y., Chung, J. M. & Chung, K. (2009) Superoxide signaling in pain is independent of nitric oxide signaling, *Neuroreport.* **20**, 1424-8.

309. Barriere, D. A., Rieusset, J., Chanteranne, D., Busserolles, J., Chauvin, M. A., Chapuis, L., Salles, J., Dubray, C. & Morio, B. (2012) Paclitaxel therapy potentiates cold hyperalgesia in streptozotocin-induced diabetic rats through enhanced mitochondrial reactive oxygen species production and TRPA1 sensitization, *Pain.* **153**, 553-61.

310. Li, J., Kanju, P., Patterson, M., Chew, W. L., Cho, S. H., Gilmour, I., Oliver, T., Yasuda, R., Ghio, A., Simon, S. A. & Liedtke, W. (2011) TRPV4-mediated calcium influx into human bronchial epithelia upon exposure to diesel exhaust particles, *Environmental health perspectives.* **119**, 784-93.

311. Xiao, W. H. & Bennett, G. J. (2012) Effects of mitochondrial poisons on the neuropathic pain produced by the chemotherapeutic agents, paclitaxel and oxaliplatin, *Pain.* **153**, 704-9.

312. Hollenbeck, P. J. & Saxton, W. M. (2005) The axonal transport of mitochondria, *Journal of cell science.* **118**, 5411-9.

313. Guo, B. L., Sui, B. D., Wang, X. Y., Wei, Y. Y., Huang, J., Chen, J., Wu, S. X., Li, Y. Q., Wang, Y. Y. & Yang, Y. L. (2013) Significant changes in mitochondrial distribution in different pain models of mice, *Mitochondrion.* **13**, 292-7.

314. Martin, M., Iyadurai, S. J., Gassman, A., Gindhart, J. G., Jr., Hays, T. S. & Saxton, W. M. (1999) Cytoplasmic dynein, the dynactin complex, and kinesin are interdependent and essential for fast axonal transport, *Molecular biology of the cell.* **10**, 3717-28.

315. Hirokawa, N. & Takemura, R. (2005) Molecular motors and mechanisms of directional transport in neurons, *Nature reviews Neuroscience.* **6**, 201-14.

316. Piomelli, D., Volterra, A., Dale, N., Siegelbaum, S. A., Kandel, E. R., Schwartz, J. H. & Belardetti, F. (1987) Lipoxygenase metabolites of arachidonic acid as second messengers for presynaptic inhibition of Aplysia sensory cells, *Nature.* **328**, 38-43.

317. Buttner, N., Siegelbaum, S. A. & Volterra, A. (1989) Direct modulation of Aplysia S-K+ channels by a 12-lipoxygenase metabolite of arachidonic acid, *Nature.* **342**, 553-5.

318. Kim, D., Lewis, D. L., Graziadei, L., Neer, E. J., Bar-Sagi, D. & Clapham, D. E. (1989) G-protein beta gamma-subunits activate the cardiac muscarinic K+-channel via phospholipase A2, *Nature.* **337**, 557-60.

319. Rohacs, T. (2007) Regulation of TRP channels by PIP(2), *Pflugers Archiv : European journal of physiology.* **453**, 753-62.

320. Prescott, E. D. & Julius, D. (2003) A modular PIP2 binding site as a determinant of capsaicin receptor sensitivity, *Science.* **300**, 1284-8.

321. Brauchi, S., Orta, G., Salazar, M., Rosenmann, E. & Latorre, R. (2006) A hot-sensing cold receptor: C-terminal domain determines thermosensation in transient receptor potential channels, *The Journal of neuroscience : the official journal of the Society for Neuroscience.* **26**, 4835-40.

322. Lukacs, V., Thyagarajan, B., Varnai, P., Balla, A., Balla, T. & Rohacs, T. (2007) Dual regulation of TRPV1 by phosphoinositides, *The Journal of neuroscience : the official journal of the Society for Neuroscience.* **27**, 7070-80.

323. Rone, M. B., Fan, J. & Papadopoulos, V. (2009) Cholesterol transport in steroid biosynthesis: role of protein-protein interactions and implications in disease states, *Biochimica et biophysica acta.* **1791**, 646-58.

324. Miller, W. L. & Bose, H. S. (2011) Early steps in steroidogenesis: intracellular cholesterol trafficking, *Journal of lipid research.* **52**, 2111-35.

325. Hauet, T., Yao, Z. X., Bose, H. S., Wall, C. T., Han, Z., Li, W., Hales, D. B., Miller, W. L., Culty, M. & Papadopoulos, V. (2005) Peripheral-type benzodiazepine receptor-mediated action of steroidogenic acute regulatory protein on cholesterol entry into leydig cell mitochondria, *Molecular endocrinology.* **19**, 540-54.

326. Duarte, A., Poderoso, C., Cooke, M., Soria, G., Cornejo Maciel, F., Gottifredi, V. & Podesta, E. J. (2012) Mitochondrial fusion is essential for steroid biosynthesis, *PloS one.* **7**, e45829.

327. Brown, M. S. & Goldstein, J. L. (1986) A receptor-mediated pathway for cholesterol homeostasis, *Science.* **232**, 34-47.

328. Amantini, C., Mosca, M., Lucciarini, R., Perfumi, M., Morrone, S., Piccoli, M. & Santoni, G. (2004) Distinct thymocyte subsets express the vanilloid receptor VR1 that mediates capsaicin-induced apoptotic cell death, *Cell death and differentiation.* **11**, 1342-56.

329. Dedov, V. N., Mandadi, S., Armati, P. J. & Verkhratsky, A. (2001) Capsaicin-induced depolarisation of mitochondria in dorsal root ganglion neurons is enhanced by vanilloid receptors, *Neuroscience.* **103**, 219-26.

330. Macho, A., Calzado, M. A., Munoz-Blanco, J., Gomez-Diaz, C., Gajate, C., Mollinedo, F., Navas, P. & Munoz, E. (1999) Selective induction of apoptosis by capsaicin in transformed cells: the role of reactive oxygen species and calcium, *Cell death and differentiation.* **6**, 155-65.

331. Biro, T., Brodie, C., Modarres, S., Lewin, N. E., Acs, P. & Blumberg, P. M. (1998) Specific vanilloid responses in C6 rat glioma cells, *Brain research Molecular brain research.* **56**, 89-98.

332. Lee, Y. S., Nam, D. H. & Kim, J. A. (2000) Induction of apoptosis by capsaicin in A172 human glioblastoma cells, *Cancer letters.* **161**, 121-30.

333. McConkey, D. J. & Orrenius, S. (1996) The role of calcium in the regulation of apoptosis, *Journal of leukocyte biology.* **59**, 775-83.

334. Wood, J. N., Winter, J., James, I. F., Rang, H. P., Yeats, J. & Bevan, S. (1988) Capsaicin-induced ion fluxes in dorsal root ganglion cells in culture, *The Journal of neuroscience : the official journal of the Society for Neuroscience.* **8**, 3208-20.

335. Wong, R., Steenbergen, C. & Murphy, E. (2012) Mitochondrial permeability transition pore and calcium handling, *Methods in molecular biology.* **810**, 235-42.

336. Green, D. R. & Reed, J. C. (1998) Mitochondria and apoptosis, *Science.* **281**, 1309-12.

337. Bernardi, P. (1992) Modulation of the mitochondrial cyclosporin A-sensitive permeability transition pore by the proton electrochemical gradient. Evidence that the pore can be opened by membrane depolarization, *The Journal of biological chemistry.* **267**, 8834-9.

338. Crompton, M. (1999) The mitochondrial permeability transition pore and its role in cell death, *The Biochemical journal.* **341 (Pt 2)**, 233-49.

339. Kroemer, G. & Reed, J. C. (2000) Mitochondrial control of cell death, *Nature medicine.* **6**, 513-9.

340. Yagi, T. (1990) Inhibition by capsaicin of NADH-quinone oxidoreductases is correlated with the presence of energy-coupling site 1 in various organisms, *Archives of biochemistry and biophysics.* **281**, 305-11.

341. Wolvetang, E. J., Larm, J. A., Moutsoulas, P. & Lawen, A. (1996) Apoptosis induced by inhibitors of the plasma membrane NADH-oxidase involves Bcl-2 and calcineurin, *Cell growth & differentiation : the molecular biology journal of the American Association for Cancer Research.* **7**, 1315-25.

342. Cochereau, C., Sanchez, D., Bourhaoui, A. & Creppy, E. E. (1996) Capsaicin, a structural analog of tyrosine, inhibits the aminoacylation of tRNA(Tyr), *Toxicology and applied pharmacology.* **141**, 133-7.

343. Cochereau, C., Sanchez, D. & Creppy, E. E. (1997) Tyrosine prevents capsaicin-induced protein synthesis inhibition in cultured cells, *Toxicology.* **117**, 133-9.

344. Joo, F., Szolcsanyi, J. & Jancso-Gabor, A. (1969) Mitochondrial alterations in the spinal ganglion cells of the rat accompanying the long-lasting sensory disturbance induced by capsaicin, *Life sciences.* **8**, 621-6.

345. Szolcsanyi, J., Jancso-Gabor, A. & Joo, F. (1975) Functional and fine structural characteristics of the sensory neuron blocking effect of capsaicin, *Naunyn-Schmiedeberg's archives of pharmacology.* **287**, 157-69.

346. Jancso, G., Kiraly, E. & Jancso-Gabor, A. (1977) Pharmacologically induced selective degeneration of chemosensitive primary sensory neurones, *Nature.* **270**, 741-3.

347. Jancso, G. & Kiraly, E. (1981) Sensory neurotoxins: chemically induced selective destruction of primary sensory neurons, *Brain research.* **210**, 83-9.

348. Szoke, E., Seress, L. & Szolcsanyi, J. (1998) Reevaluation of the effect of neonatal capsaicin treatment on the basis of morphometrical studies, *Neurobiology.* **6**, 477-8.

349. Szoke, E., Seress, L. & Szolcsanyi, J. (2002) Neonatal capsaicin treatment results in prolonged mitochondrial damage and delayed cell death of B cells in the rat trigeminal ganglia, *Neuroscience.* **113**, 925-37.

350. Macho, A., Lucena, C., Calzado, M. A., Blanco, M., Donnay, I., Appendino, G. & Munoz, E. (2000) Phorboid 20-homovanillates induce apoptosis through a VR1-independent mechanism, *Chemistry & biology.* **7**, 483-92.

351. Morre, D. J., Chueh, P. J. & Morre, D. M. (1995) Capsaicin inhibits preferentially the NADH oxidase and growth of transformed cells in culture, *Proceedings of the National Academy of Sciences of the United States of America.* **92**, 1831-5.

352. Morre, D. J., Sun, E., Geilen, C., Wu, L. Y., de Cabo, R., Krasagakis, K., Orfanos, C. E. & Morre, D. M. (1996) Capsaicin inhibits plasma membrane NADH oxidase and growth of human and mouse melanoma lines, *European journal of cancer.* **32A**, 1995-2003.

353. Shimomura, Y., Kawada, T. & Suzuki, M. (1989) Capsaicin and its analogs inhibit the activity of NADH-coenzyme Q oxidoreductase of the mitochondrial respiratory chain, *Archives of biochemistry and biophysics.* **270**, 573-7.

354. Aranda, F. J., Villalain, J. & Gomez-Fernandez, J. C. (1995) Capsaicin affects the structure and phase organization of phospholipid membranes, *Biochimica et biophysica acta.* **1234**, 225-34.

355. Tsuchiya, H. (2001) Biphasic membrane effects of capsaicin, an active component in Capsicum species, *Journal of ethnopharmacology.* **75**, 295-9.

356. Macho, A., Blazquez, M. V., Navas, P. & Munoz, E. (1998) Induction of apoptosis by vanilloid compounds does not require de novo gene transcription and activator protein 1 activity, *Cell growth & differentiation : the molecular biology journal of the American Association for Cancer Research.* **9**, 277-86.

357. Garle, M. J., Knight, A., Downing, A. T., Jassi, K. L., Clothier, R. H. & Fry, J. R. (2000) Stimulation of dichlorofluorescin oxidation by capsaicin and analogues in RAW 264 monocyte/macrophages: lack of involvement of the vanilloid receptor, *Biochemical pharmacology.* **59**, 563-72.

358. Hail, N., Jr. (2003) Mechanisms of vanilloid-induced apoptosis, *Apoptosis : an international journal on programmed cell death.* **8**, 251-62.

359. Kang, H. J., Soh, Y., Kim, M. S., Lee, E. J., Surh, Y. J., Kim, H. R., Kim, S. H. & Moon, A. (2003) Roles of JNK-1 and p38 in selective induction of apoptosis by capsaicin in ras-transformed human breast epithelial cells, *International journal of cancer Journal international du cancer.* **103**, 475-82.

360. Lee, Y. S., Kang, Y. S., Lee, J. S., Nicolova, S. & Kim, J. A. (2004) Involvement of NADPH oxidase-mediated generation of reactive oxygen species in the apototic cell death by capsaicin in HepG2 human hepatoma cells, *Free radical research.* **38**, 405-12.

361. Min, J. K., Han, K. Y., Kim, E. C., Kim, Y. M., Lee, S. W., Kim, O. H., Kim, K. W., Gho, Y. S. & Kwon, Y. G. (2004) Capsaicin inhibits in vitro and in vivo angiogenesis, *Cancer research.* **64**, 644-51.

362. Thoennissen, N. H., O'Kelly, J., Lu, D., Iwanski, G. B., La, D. T., Abbassi, S., Leiter, A., Karlan, B., Mehta, R. & Koeffler, H. P. (2010) Capsaicin causes cell-cycle arrest and apoptosis in ER-positive and -negative breast cancer cells by modulating the EGFR/HER-2 pathway, *Oncogene.* **29**, 285-96.

363. Pramanik, K. C., Boreddy, S. R. & Srivastava, S. K. (2011) Role of mitochondrial electron transport chain complexes in capsaicin mediated oxidative stress leading to apoptosis in pancreatic cancer cells, *PloS one.* **6**, e20151.

364. Chiang, H., Ohno, N., Hsieh, Y. L., Mahad, D. J., Kikuchi, S., Komuro, H., Hsieh, S. T. & Trapp, B. D. (2015) Mitochondrial fission augments capsaicin-induced axonal degeneration, *Acta neuropathologica.* **129**, 81-96.

365. Wei, H., Koivisto, A., Saarnilehto, M., Chapman, H., Kuokkanen, K., Hao, B., Huang, J. L., Wang, Y. X. & Pertovaara, A. (2011) Spinal transient receptor potential ankyrin 1 channel contributes to central pain hypersensitivity in various pathophysiological conditions in the rat, *Pain.* **152**, 582-91.

366. Nesuashvili, L., Hadley, S. H., Bahia, P. K. & Taylor-Clark, T. E. (2013) Sensory nerve terminal mitochondrial dysfunction activates airway sensory nerves via transient receptor potential (TRP) channels, *Molecular pharmacology.* **83**, 1007-19.

367. Kimura, H. (2013) Physiological role of hydrogen sulfide and polysulfide in the central nervous system, *Neurochemistry international.* **63**, 492-7.

368. Su, B., Ji, Y. S., Sun, X. L., Liu, X. H. & Chen, Z. Y. (2014) Brain-derived neurotrophic factor (BDNF)-induced mitochondrial motility arrest and presynaptic docking contribute to BDNF-enhanced synaptic transmission, *The Journal of biological chemistry.* **289**, 1213-26.

369. Chen, S. J., Hoffman, N. E., Shanmughapriya, S., Bao, L., Keefer, K., Conrad, K., Merali, S., Takahashi, Y., Abraham, T., Hirschler-Laszkiewicz, I., Wang, J., Zhang, X. Q., Song, J., Barrero, C., Shi, Y., Kawasawa, Y. I., Bayerl, M., Sun, T., Barbour, M., Wang, H. G., Madesh, M., Cheung, J. Y. & Miller, B. A. (2014) A splice variant of the human ion channel TRPM2 modulates neuroblastoma tumor growth through hypoxia-inducible factor (HIF)-1/2alpha, *The Journal of biological chemistry.* **289**, 36284-302.

370. Jennings, J. J., Jr., Zhu, J. H., Rbaibi, Y., Luo, X., Chu, C. T. & Kiselyov, K. (2006) Mitochondrial aberrations in mucolipidosis Type IV, *The Journal of biological chemistry.* **281**, 39041-50.

371. Rossato, M., Granzotto, M., Macchi, V., Porzionato, A., Petrelli, L., Calcagno, A., Vencato, J., De Stefani, D., Silvestrin, V., Rizzuto, R., Bassetto, F., De Caro, R. & Vettor, R. (2014) Human white adipocytes express the cold receptor TRPM8 which activation induces UCP1 expression, mitochondrial activation and heat production, *Molecular and cellular endocrinology.* **383**, 137-46.

372. Miller, B. A., Hoffman, N. E., Merali, S., Zhang, X. Q., Wang, J., Rajan, S., Shanmughapriya, S., Gao, E., Barrero, C. A., Mallilankaraman, K., Song, J., Gu, T., Hirschler-Laszkiewicz, I., Koch, W. J., Feldman, A. M., Madesh, M. & Cheung, J. Y. (2014) TRPM2 channels protect against cardiac ischemia-reperfusion injury: role of mitochondria, *The Journal of biological chemistry.* **289**, 7615-29.

373. Tu, P., Gibon, J. & Bouron, A. (2010) The TRPC6 channel activator hyperforin induces the release of zinc and calcium from mitochondria, *Journal of neurochemistry.* **112**, 204-13.

374. Flicek, P., Aken, B. L., Ballester, B., Beal, K., Bragin, E., Brent, S., Chen, Y., Clapham, P., Coates, G., Fairley, S., Fitzgerald, S., Fernandez-Banet, J., Gordon, L., Graf, S., Haider, S., Hammond, M., Howe, K., Jenkinson, A., Johnson, N., Kahari, A., Keefe, D., Keenan, S., Kinsella, R., Kokocinski, F., Koscielny, G., Kulesha, E., Lawson, D., Longden, I., Massingham, T., McLaren, W., Megy, K., Overduin, B., Pritchard, B., Rios, D., Ruffier, M., Schuster, M., Slater, G., Smedley, D., Spudich, G., Tang, Y. A., Trevanion, S., Vilella, A., Vogel, J., White, S., Wilder, S. P., Zadissa, A., Birney, E., Cunningham, F., Dunham, I., Durbin, R., Fernandez-Suarez, X. M., Herrero, J., Hubbard, T. J., Parker, A., Proctor, G., Smith, J. & Searle, S. M. (2010) Ensembl's 10th year, *Nucleic acids research.* **38**, D557-62.

375. Hubbard, T. J., Aken, B. L., Ayling, S., Ballester, B., Beal, K., Bragin, E., Brent, S., Chen, Y., Clapham, P., Clarke, L., Coates, G., Fairley, S., Fitzgerald, S., Fernandez-Banet, J., Gordon, L., Graf, S., Haider, S., Hammond, M., Holland, R., Howe, K., Jenkinson, A., Johnson, N., Kahari, A., Keefe, D., Keenan, S., Kinsella, R., Kokocinski, F., Kulesha, E., Lawson, D., Longden, I., Megy, K., Meidl, P., Overduin, B., Parker, A., Pritchard, B., Rios, D., Schuster, M., Slater, G., Smedley, D., Spooner, W., Spudich, G., Trevanion, S., Vilella, A., Vogel, J., White, S., Wilder, S., Zadissa, A., Birney, E., Cunningham, F., Curwen, V., Durbin, R., Fernandez-Suarez, X. M., Herrero, J., Kasprzyk, A., Proctor, G., Smith, J., Searle, S. & Flicek, P. (2009) Ensembl 2009, *Nucleic acids research.* **37**, D690-7.

376. Baxevanis, A. D. & Landsman, D. (1996) Histone Sequence Database: a compilation of highly-conserved nucleoprotein sequences, *Nucleic acids research.* **24**, 245-7.

377. Bang, S., Yoo, S., Yang, T. J., Cho, H. & Hwang, S. W. (2010) Farnesyl pyrophosphate is a novel pain-producing molecule via specific activation of TRPV3, *The Journal of biological chemistry.* **285**, 19362-71.

378. Bahat A, Tur-Kaspa I, Gakamsky A, Giojalas LC, Breitbart H & Eisenbach M (2003) Thermotaxis of mammalian sperm cells: a potential navigation mechanism in the female genital tract. *Nat. Med.* **9**, 149–150.

379. Hamamah S & Gatti JL (1998) Role of the ionic environment and internal pH on sperm activity. *Hum. Reprod.* **13 Suppl 4**, 20–30.

380. Yeung CH, Anapolski M, Depenbusch M, Zitzmann M & Cooper TG (2003) Human sperm volume regulation. Response to physiological changes in osmolality, channel blockers and potential sperm osmolytes. *Hum. Reprod.* **18**, 1029–1036.

381. Rossato M, Balercia G, Lucarelli G, Foresta C & Mantero F (2002) Role of seminal osmolarity in the reduction of human sperm motility. *Int. J. Androl.* **25**, 230–235.

382. Alasmari W, Barratt CLR, Publicover SJ, Whalley KM, Foster E, Kay V, Martins Da Silva S & Oxenham SK (2013) The clinical significance of calcium-signalling pathways mediating human sperm hyperactivation. *Hum. Reprod.* **28**, 866–876.

383. Auzanneau C, Norez C, Antigny F, Thoreau V, Jougla C, Cantereau A, Becq F & Vandebrouck C (2008) Transient receptor potential vanilloid 1 (TRPV1) channels in cultured rat Sertoli cells regulate an acid sensing chloride channel. *Biochem. Pharmacol.* **75**, 476–483.

384. Bernabò N, Pistilli MG, Mattioli M & Barboni B (2010) Role of TRPV1 channels in boar spermatozoa acquisition of fertilizing ability. *Mol. Cell. Endocrinol.* **323**, 224–231.

385. Botto L, Bernabò N, Palestini P & Barboni B (2010) Bicarbonate induces membrane reorganization and CBR1 and TRPV1 endocannabinoid receptor migration in lipid microdomains in capacitating boar spermatozoa. *J. Membr. Biol.* **238**, 33–41.

386. De Blas GA, Darszon A, Ocampo AY, Serrano CJ, Castellano LE, Hernández-Gonzá EO, Chirinos M, Larrea F, Beltrán C & Treviño CL (2009) TRPM8, a versatile channel in human sperm. *PLoS One* **4**. e6095

387. Gervasi MG, Osycka-Salut C, Caballero J, Vazquez-Levin M, Pereyra E, Billi S, Franchi A & Perez-Martinez S (2011) Anandamide capacitates bull spermatozoa through CB1 and TRPV1 activation. *PLoS One* **6** e16993.

388. Majhi RK, Kumar A, Yadav M, Swain N, Kumari S, Saha A, Pradhan A, Goswami L, Saha S, Samanta L, Maity A, Nayak TK, Chattopadhyay S, Rajakuberan C, Kumar A & Goswami C (2013) Thermosensitive ion channel TRPV1 is endogenously expressed in the sperm of a fresh water teleost fish (Labeo rohita) and regulates sperm motility. *Channels* **7**, 483–492.

389. Hills CE, Bland R & Squires PE (2012) Functional expression of trpv4 channels in human collecting duct cells: Implications for secondary hypertension in diabetic nephropathy. *Exp. Diabetes Res.* **2012,** 936518.

390. Spinaci M, Volpe S, Bernardini C, De Ambrogi M, Tamanini C, Seren E & Galeati G (2005) Immunolocalization of heat shock protein 70 (Hsp 70) in boar spermatozoa and its role during fertilization. *Mol. Reprod. Dev.* **72**, 534–541.

391. Okabe M, Takada K, Adachi T, Kohama Y, Mimura T & Aonuma S (1986) Studies on sperm capacitation using monoclonal anti-body--disappearance of an antigen from the anterior part of mouse sperm head. *J. Pharmacobiodyn.* **9**, 55–60.

392. Okabe M, Yagasaki M, Oda H, Matzno S, Kohama Y & Mimura T (1988) Effect of a monoclonal anti-mouse sperm antibody (OBF13) on the interaction of mouse sperm with zona-free mouse and hamster eggs. *J. Reprod. Immunol.* **13**, 211–219.

393. Shalgi R, Matityahu A, Gaunt SJ & Jones R (1990) Antigens on rat spermatozoa with a potential role in fertilization. *Mol. Reprod. Dev.* **25**, 286–296.

394. Lattao, R., Bonaccorsi, S. & Gatti, M. (2012) Giant meiotic spindles in males from Drosophila species with giant sperm tails, *Journal of cell science.* **125**, 584-8.

395. Bjork, A., Dallai, R. & Pitnick, S. (2007) Adaptive modulation of sperm production rate in Drosophila bifurca, a species with giant sperm, *Biology letters.* **3**, 517-9.

396. Bjork, A. & Pitnick, S. (2006) Intensity of sexual selection along the anisogamy-isogamy continuum, *Nature.* **441**, 742-5.

397. Korn, N., Thurston, R. J., Pooser, B. P. & Scott, T. R. (2000) Ultrastructure of spermatozoa from Japanese quail, *Poultry science.* **79**, 407-14.

398. Rowe, M., Laskemoen, T., Johnsen, A. & Lifjeld, J. T. (2013) Evolution of sperm structure and energetics in passerine birds, *Proceedings Biological sciences / The Royal Society.* **280**, 20122616.

399. Immler, S. & Birkhead, T. R. (2007) Sperm competition and sperm midpiece size: no consistent pattern in passerine birds, *Proceedings Biological sciences / The Royal Society.* **274**, 561-8.

400. Otani, H., Tanaka, O., Kasai, K. & Yoshioka, T. (1988) Development of mitochondrial helical sheath in the middle piece of the mouse spermatid tail: regular dispositions and synchronized changes, *The Anatomical record.* **222**, 26-33.

401. Ramalho-Santos, J. & Amaral, S. (2013) Mitochondria and mammalian reproduction, *Molecular and cellular endocrinology.* **379**, 74-84.

402. Publicover S, Harper C V & Barratt C (2007) [Ca2+]i signalling in sperm--making the most of what you've got. *Nat. Cell Biol.* **9**, 235–242.

403. Blackmore PF, Beebe SJ, Danforth DR & Alexander N (1990) Progesterone and 17 alpha-hydroxyprogesterone. Novel stimulators of calcium influx in human sperm. *J. Biol. Chem.* **265**, 1376–1380.

404. Harper CV, Barratt CL, Publicover SJ. (2004) Stimulation of human spermatozoa with progesterone gradients to simulate approach to the oocyte. Induction of [Ca(2+)](i) oscillations and cyclical transitions in flagellar beating. *J Biol Chem*. **279**, 46315-25.

405. Eisenbach M & Giojalas LC (2006) Sperm guidance in mammals - an unpaved road to the egg. *Nat. Rev. Mol. Cell Biol.* **7**, 276–285.

406. Revelli A, Massobrio M, Tesarik J (1998) Nongenomic actions of steroid hormones in reproductive tissues. *Endocr Rev*. **19**, 3-17.

407. Roldan ER, Murase T, Shi QX (1994) Exocytosis in spermatozoa in response to progesterone and zona pellucida. *Science*. **266**, 1578-81.

408. Teves ME, Barbano F, Guidobaldi HA, Sanchez R, Miska W, Giojalas LC (2006) Progesterone at the picomolar range is a chemoattractant for mammalian spermatozoa. *Fertil Steril*. **86**, 745-9.

409. Uhler ML, Leung A, Chan SY, Wang C (1992) Direct effects of progesterone and antiprogesterone on human sperm hyperactivated motility and acrosome reaction. *Fertil Steril*. **58**, 1191-8.

410. Thomas P & Meizel S (1989) Phosphatidylinositol 4,5-bisphosphate hydrolysis in human sperm stimulated with follicular fluid or progesterone is dependent upon Ca2+ influx. *Biochem. J.* **264**, 539–546.

411. Blackmore PF, Neulen J, Lattanzio F & Beebe SJ (1991) Cell surface-binding sites for progesterone mediate calcium uptake in human sperm. *J. Biol. Chem.* **266**, 18655–18659.

412. Meizel S & Turner KO (1991) Progesterone acts at the plasma membrane of human sperm. *Mol. Cell. Endocrinol.* **77**, R1–5.

413. Aitken RJ, Buckingham DW & Irvine DS (1996) The extragenomic action of progesterone on human spermatozoa: Evidence for a ubiquitous response that is rapidly down-regulated. *Endocrinology* **137**, 3999–4009.

414. Lishko P V, Botchkina IL & Kirichok Y (2011) Progesterone activates the principal Ca2+ channel of human sperm. *Nature* **471**, 387–391.

415. Strünker T, Goodwin N, Brenker C, Kashikar ND, Weyand I, Seifert R & Kaupp UB (2011) The CatSper channel mediates progesterone-induced Ca2+ influx in human sperm. *Nature* **471**, 382–386.

416. Carlson AE, Westenbroek RE, Quill T, Ren D, Clapham DE, Hille B, Garbers DL & Babcock DF (2003) CatSper1 required for evoked Ca2+ entry and control of flagellar function in sperm. *Proc. Natl. Acad. Sci. U. S. A.* **100**, 14864–14868.

417. Ren D, Navarro B, Perez G, Jackson AC, Hsu S, Shi Q, Tilly JL & Clapham DE (2001) A sperm ion channel required for sperm motility and male fertility. *Nature* **413**, 603–609.

418. Quill TA, Sugden SA, Rossi KL, Doolittle LK, Hammer RE & Garbers DL (2003) Hyperactivated sperm motility driven by CatSper2 is required for fertilization. *Proc. Natl. Acad. Sci. U. S. A.* **100**, 14869–14874.

419. Qi H, Moran MM, Navarro B, Chong JA, Krapivinsky G, Krapivinsky L, Kirichok Y, Ramsey IS, Quill TA & Clapham DE (2007) All four CatSper ion channel proteins are required for male fertility and sperm cell hyperactivated motility. *Proc. Natl. Acad. Sci. U. S. A.* **104**, 1219–1223.

420. Tamburrino L, Marchiani S, Minetti F, Forti G, Muratori M & Baldi E (2014) The CatSper calcium channel in human sperm: Relation with motility and involvement in progesterone-induced acrosome reaction. *Hum. Reprod.* **29**, 418–428.

421. Plant A, McLaughlin EA & Ford WC (1995) Intracellular calcium measurements in individual human sperm demonstrate that the majority can respond to progesterone. *Fertil. Steril.* **64**, 1213–1215.

422. Kumar A, Kumari S, Majhi RK, Swain N, Yadav M & Goswami C (2015) Regulation of TRP channels by steroids: Implications in physiology and diseases. *Gen. Comp. Endocrinol.* **220**, 23–32.

423. Blackmore PF (1993) Rapid non-genomic actions of progesterone stimulate Ca2+ influx and the acrosome reaction in human sperm. *Cell. Signal.* **5**, 531–538.

424. Meizel S & Turner K O (1993) Initiation of the human sperm acrosome reaction by thapsigargin. *J. Exp. Zool.* **267**, 350–355.

425. Laemmli, U. K. (1970) Cleavage of structural proteins during the assembly of the head of bacteriophage T4, *Nature.* **227**, 680-5.

426. Whittaker, V. P. (1968) The morphology of fractions of rat forebrain synaptosomes separated on continuous sucrose density gradients, *The Biochemical journal.* **106**, 412-7.

427. Frezza, C., Cipolat, S. & Scorrano, L. (2007) Organelle isolation: functional mitochondria from mouse liver, muscle and cultured fibroblasts, *Nature protocols.* **2**, 287-95.

428. Kramer, K. A., Oglesbee, D., Hartman, S. J., Huey, J., Anderson, B., Magera, M. J., Matern, D., Rinaldo, P., Robinson, B. H., Cameron, J. M. & Hahn, S. H. (2005) Automated spectrophotometric analysis of mitochondrial respiratory chain complex enzyme activities in cultured skin fibroblasts, *Clinical chemistry.* **51**, 2110-6.

429. Humphries, K. M. & Szweda, L. I. (1998) Selective inactivation of alpha-ketoglutarate dehydrogenase and pyruvate dehydrogenase: reaction of lipoic acid with 4-hydroxy-2-nonenal, *Biochemistry.* **37**, 15835-41.

430. Singer, T. P. (1974) Determination of the activity of succinate, NADH, choline, and alpha-glycerophosphate dehydrogenases, *Methods of biochemical analysis.* **22**, 123-75.

431. Dayal, D., Martin, S. M., Owens, K. M., Aykin-Burns, N., Zhu, Y., Boominathan, A., Pain, D., Limoli, C. L., Goswami, P. C., Domann, F. E. & Spitz, D. R. (2009) Mitochondrial complex II dysfunction can contribute significantly to genomic instability after exposure to ionizing radiation, *Radiation research.* **172**, 737-45.

432. Minchenko, J., Williams, A. J. & Christodoulou, J. (2003) Adaptation of a mitochondrial complex III assay for automation: examination of reproducibility and precision, *Clinical chemistry.* **49**, 330-2.

433. Spinazzi, M., Casarin, A., Pertegato, V., Salviati, L. & Angelini, C. (2012) Assessment of mitochondrial respiratory chain enzymatic activities on tissues and cultured cells, *Nature protocols.* **7**, 1235-46.

434. Kobayashi, T., Kuroda, S., Tada, M., Houkin, K., Iwasaki, Y. & Abe, H. (2003) Calcium-induced mitochondrial swelling and cytochrome c release in the brain: its biochemical characteristics and implication in ischemic neuronal injury, *Brain research.* **960**, 62-70.

435. Baykal, A. T., Jain, M. R. & Li, H. (2008) Aberrant regulation of choline metabolism by mitochondrial electron transport system inhibition in neuroblastoma cells, *Metabolomics : Official journal of the Metabolomic Society*. **4**, 347-356.

436. Bradford, M. M. (1976) A rapid and sensitive method for the quantitation of microgram quantities of protein utilizing the principle of protein-dye binding, *Analytical biochemistry*. **72**, 248-54.

437. Goswami, C., Dreger, M., Jahnel, R., Bogen, O., Gillen, C. & Hucho, F. (2004) Identification and characterization of a Ca2+ -sensitive interaction of the vanilloid receptor TRPV1 with tubulin, *Journal of neurochemistry*. **91**, 1092-103.

438. Ishihara, N., Eura, Y. & Mihara, K. (2004) Mitofusin 1 and 2 play distinct roles in mitochondrial fusion reactions via GTPase activity, *Journal of cell science*. **117**, 6535-46.

439. Nagai, T., Sawano, A., Park, E. S. & Miyawaki, A. (2001) Circularly permuted green fluorescent proteins engineered to sense Ca2+, *Proceedings of the National Academy of Sciences of the United States of America*. **98**, 3197-202.

440. Reers, M., Smiley, S. T., Mottola-Hartshorn, C., Chen, A., Lin, M. & Chen, L. B. (1995) Mitochondrial membrane potential monitored by JC-1 dye, *Methods in enzymology*. **260**, 406-17.

Chapter 7

Publications

REVIEW

Channels 4:4, 1-10; July/August 2010; © 2010 Landes Bioscience

TRPV4-mediated channelopathies

Pratibha Verma, Ashutosh Kumar and Chandan Goswami*

National Institute of Science Education and Research; Institute of Physics Campus; Sachivalaya Marg; Bhubaneswar, India

Key words: TRPV4, surface expression, ubiquitin, vesicle, mutation

Abbreviations: 2-APB, 2-aminoethoxydiphenyl borate; 4αPDD, 4α Phorbol 12; 13-didecanoate; AD, association domain; AIP4, atrophin-1-interacting protein 4; ARD, ankyrin repeat domain; ATP, adenosine-5-triphosphate; CAM, calmodulin; CMT2C, charcot marie tooth disease type 2C; EM, electron microscope; ERAD, endoplasmic reticulum associated degradation; FRET, fluorescence resonance energy transfer; HECT, homologous to E6-AP carboxyl terminus; HEK cell, human embryonic kidney cell**;** HMSN2C, hereditary motor and sensory neuropathy type 2; MVB, multi vesicular body; NMR, nuclear magnetic resonance; OSM9, OSMotic avoidance abnormal family member 9; OS9, osteosarcoma amplified 9; PASCIN, protein kinase C and casein kinase substrate in neurons protein 1; PRD, proline-rich domain; RGA, recombinase gene activator; SEDM-PM2, spondylo-epiphyseal dysplasia, maroteaux type (pseudo-morquio syndrome type 2); STAM, signal transducing adaptor molecule; SMA, spinal muscular atrophy; SMDK, spondylometaphyseal dysplasia kozlowski; SPSMA, scapuloperoneal spinal muscular atrophy; TM, transmembrane; TRP, transient receptor potential; TRPP2, transient receptor potential polycystin; TRPV, transient receptor potential vanilloid; TRPV1, transient receptor potential vanilloid sub type 1; TRPV4, transient receptor potential vanilloid sub type 4

Transient Receptor Potential Vanilloid sub type 4 (TRPV4) is a member of non-selective cation channel that is important for sensation of several physical and chemical stimuli and also involved in multiple physiological functions. Recently it gained immense medical and clinical interest as several independent studies have demonstrated that mutations in the TRPV4 gene can results in genetic disorders like Brachyolmia, Charcot-Marie-Tooth disease type 2C, Spinal Muscular Atrophy and Hereditary Motor and Sensory Neuropathy type 2. Close analysis of the data obtained from these naturally occurring as well as other TRPV4 mutants suggest that it is not the altered channel activity of these mutants per se, but the involvement and interaction of other factors that seem to modulate oligomerization, trafficking and degradation of TRPV4 channels. Also, these factors can either enhance or reduce the activity of TRPV4. In addition, there are some potential signaling events that can also be involved in these genetic disorders. In this review, we analyzed how and what extent certain cellular and molecular functions like oligomerization, surface expression, ubiquitination and functional interactions might be affected by these mutations.

Introduction

In spite of sharing high degree of homology and identity, members of TRPV channels retain their uniqueness in terms of structure, function and ability to recognize different physical and chemical stimuli. Among all TRPV channels, TRPV4 is unique as it can be activated by temperature, pressure and also by specific chemical ligands.[1] TRPV4 is functionally conserved throughout the evolution as mammalian TRPV4 can rescue the mechanosensitive defects observed in OSM9 mutants in *C. elegans*,[2] suggesting that the functional and interacting network related to TRPV4 may be conserved to a large extent and TRPV4 functionality is important for some organism. Recent studies demonstrated that missense mutations result in either constitutively-active or constitutively-inactive TRPV4 channels,[3-7] which leads to inheritable genetic disorders. To make it more complicated, point mutations at the same position generates different mutant TRPV4 channels that not only exhibit different electrophysiological properties in vitro but also reveals different level of surface expression. Based on the available data, we summarize the latest understanding of the structure—function relationship of TRPV4 and critically analyze how different mutations can affect the structure, function as well as the regulation of TRPV4 at the cellular level. Our analysis also indicates some other factors that may act as a missing link and probably also contributing in these genetic disorders and involved in TRPV4 functions.

*Correspondence to: Chandan Goswami; Email: chandan@niser.ac.in
Submitted: 06/07/10; Revised: 06/25/10; Accepted: 07/06/10
Previously published online:
www.landesbioscience.com/journals/channels/article/12905

Structure of TRPV4 and Different Interacting Proteins

At the functional level, four subunit of TRPV4 assemble in proper order to form a functional channel which can conduct ionic influx.[8] At present, no crystallographic or nuclear magnetic resonance (NMR) data is available that can shed light on the fine atomic structure of functional TRPV4. However, recently, structure of Rat TRPV4 was analyzed at a resolution of 3.5 nm by cryo-electron microscopy.[9] This electron microscopic (EM) study was conducted on His-tagged TRPV4 expressed in Baculovirus infected Sf9 cells, solubilized with detergents and further purified by several chromatography columns. This study reveals that functional TRPV4 forms a "hanging basket"-like structure, which

is approximately 130 Å in length (from top to bottom) and 85 Å in width respectively. Approximately 30% volume of the functional channel lies in the plasma membrane and 70% of the total volume remains hanging from the plasma membrane. This 3D structure indicates that trans-membrane and/or membrane-integral proteins as well as several cytoplasmic proteins can interact with the TRPV4 and these interactions can modulate the structure—function relationship of TRPV4. As TRPV1 and TRPV4 share a high-degree (~41%) of sequence identity and functional TRPV1 also forms a similar "hanging basket"-like structure,[10] it is justified to assume that TRPV4 and TRPV1 share similarity in structure—function relationship to some extent.

In addition to this EM structure, certain structural information can also be extracted on the basis of characterizations performed on smaller fragments of TRPV4. The mammalian [based on Rat (gi62901120), Mice (gi62901468) and Human (gi62901470) sequence] TRPV4 polypeptide is 871 amino acid long with both the N- and C-terminal domains located at the cytoplasmic side. The N-terminal cytoplasmic domain contains six Ankyrin Repeat Domains (ARD) that are specifically located between amino acid residues 132–383.[5] These ARDs are predicted to be involved in the interaction with several proteins (Discussed later). These ARDs are also the key molecular determinants assumed to be important for subunit assembly and interaction with different molecules.[11,12] Apparently, the C-terminal cytoplasmic region of TRPV4 does not have any specific domain or motifs that can impart some especial structure-function prediction related to TRPV4. However, the C-terminal cytoplasmic domain of TRPV4 contains a conserved TRP motif, which is a specific characteristic signature present in many other TRP channels.[13]

At present, only few proteins have been identified which are known to interact with TRPV4. The C-terminus of TRPV4 is known to interact with IP3 receptor and Calmodulin.[14,15] The Calmodulin interaction seems to regulate the self interaction of N- and C-terminal of TRPV4 in a Ca^{2+}-dependent manner.[16] In addition, C-terminus of TRPV4 shares a high homology with the tubulin-binding motif sequence of TRPV1 which suggests that TRPV4 can also be a part of microtubule cytoskeleton.[17] Indeed, MAP7, a microtubule binding protein and soluble tubulin as well as polymerized microtubule interact with TRPV4, especially at the C-terminal region of TRPV4.[18,19] In a similar manner, close proximity of TRPV4 and actin filaments has been demonstrated by using fluorescence resonance energy transfer (FRET).[20]

As TRPV4 is involved in the Charcot-Marie-Tooth disease type 2 (CMT2), it suggests that TRPV4 is genetically linked with other genes which are also involved in the same disease and thus TRPV4 share a special genotype-phenotype correlation with this gene products.[21] Thus, several proteins, namely Kif1b, Neurofilament L, Mfn2, Rab7a, Lamin A, Med25, GarS, Heat shock protein 27, MPZ, GDAP1 and Heat Shock Protein 22, which are also involved in CMT2 disease, are actually potential TRPV4 interacting partners.[21] Indeed, our recent study confirmed that Neurofilament protein physically interacts with TRPV4.[19] In the same context, Kif1B, which is also involved in the CMT2 disease and/or peripheral neuropathic pain development, may be responsible for cellular transport and surface expression of TRPV4.[22]

Naturally Occurring TRPV4 Mutants and Genetic Disorder

Recently, few naturally occurring TRPV4 mutants have been identified. Interestingly, most of these missense and nonsense point mutations are linked with the development of genetic disorders in human and a detailed list of naturally occurring TRPV4 mutations and related disease is documented (**Table 1**). Here we briefly discuss some of these mutations gained importance in terms of genetic disease.

Brachyolmia. Using a linkage analysis and candidate gene sequencing, Rock et al. have identified that some patients affected with brachylomia have missense mutation in TRPV4, specifically at position R616Q or V620I respectively.[7] These mutations are located at the 5th-transmembrane region which is a part of the functional pore. Each of these two mutations increases basal level activity when compared to the wild type TRPV4. Also the response to 4αPDD (a TRPV4 specific agonist) is more in the mutants when compared with the wild type. This result also indicates that these two mutations preferably stabilize TRPV4 in its "open stage" resulting in constitutive activity of the channel.

Spinal muscular atrophy (SMA). SMA is a heterogeneous disorder of peripheral nervous system. Patients with SMA have been reported to have several missense mutations in the TRPV4, namely at R316C, R269H and R315W.[4] These mutations are located at the ARD of TRPV4. These (mutants R316C, R269H and R315W) reveal loss of function when challenged by hyposmotic solution and 4αPDD.[4]

Hereditary motor and sensory neuropathy type 2 (HMSN2C). Charcot Maries Tooth disease type 2C (CMT2C) and Scapuloperoneal Spinal Muscular Atrophy (SPSMA) are also known as HMSN2C. SPSMA patients are characterized by weakness of scapular muscle and bone abnormalities. CMT2C leads to weakness of distal limbs, vocal cords and often impairs hearing and vision. Genetic analyses of these patients have shown the presence of missense mutations at the TRPV4, especially at the R269H, R315W and R316C positions.[4]

Spondylometaphyseal dysplasias (SMDK) and metatropic dyplasia. SMDK is an autosomal dominant dysplasia. Genetic mapping of the patients affected with this disease have shown missense mutation in TRPV4, either at R594H, D333G or A716S.[27] Any of these mutations seems to alter the basal level activity. In addition, I331F and P799L mutations are known to induce metatropic dysplasia.[27]

As all these above mentioned mutants are naturally occurring, these mutants are not embryonically lethal (as most lethal mutants will be naturally excluded from the population). It is also important to note that none of these mutants show complete loss of their prime function, i.e., the ionic conductivity. Indeed, experimental results suggest that some of these mutants even have enhanced channel opening.[7] As most of the patients are heterozygous, it can be concluded that it is not only the ionic conductivity of the TRPV4 per se, but also the signaling events which

Table 1. Naturally occurring TRPV4 mutations

	Mutation	Residue	Change in charge	Domain/motif effected	Effects on ion conductivity	Genetic disorder	Ref
1	-	P19S	Nonpolar to polar	N-terminal	Less conductivity	hyponatermia	23
2	C366T (exon 2)	T89I	Polar (uncharged) to nonpolar	N-terminal	Not done	Metatropic dysplasia	24
3	G547A (exon 3)	E183K	Negative to plus	ARD1	Not done	SEDM-PM2	25
4	A590G (exon 4)	K197R	Plus to plus	ARD2	Not done	Metatropic dysplasia	24
5	-	L199F	Nonpolar to aromatic	ARD2	Not done	Metatropic dysplaisa	26
6	G806A (exon 5)	R269H	Plus to plus	ARD3	Less conductivity	SMA	4
7	G806A (exon 5)	R269H	Plus to plus	ARD3	More conductivity	CMT2C, SPSMA	6
8	G806A (exon 5)	R269H	Plus to plus	ARD3	More conductivity	CMT2C	5
9	G806A (exon 5)	R269C	Plus to polar un charged	ARD3	More conductivity	CMT2C	5
10	-	E278K	Negative to plus	ARD3	Not done	SMDK	26
11	-	T295A	Polar (uncharged) to nonpolar	ARD4	Not done	Metatropic dysplaisa	26
12	C943T (exon 6)	R315W	Plus to aromatic	ARD4	Less conductivity	HMSN2C	4
13	C946T (exon 6)	R316C	Plus to polar (uncharged)	ARD4	Less conductivity	HMSN2C	4
14	A1080T (exon 6)	I331F	Nonpolar to aromatic	ARD5	Not done	Metatropic dysplasia	27
15	-	I331T	Nonpolar to polar (uncharged)	ARD5	Not done	Metatropic dysplasia	26
16	A992G (exon 6)	D333G	Negative to nonploar	ARD4	More conductivity	SMDK	27
17	-	V342F	Nonpolar to aromatic	ARD5	Not done	Metatropic dysplasia	26
18	-	F592L	Aromatic to nonpolar	TM4	Not done	Metatropic dysplasia	26
19	G1781A (exon 11)	R594H	Plus to plus	TM4	More conductivity	SMDK	27
20	A1805G (exon 11)	Y602C	Aromatic to polar	TM4-TM5	Not done	SEDM-PM2	25
21	C1812G (exon 11)	I604M	Nonpolar to nonpolar	TM4-TM5	Not done	Metatropic dyslpasia	24
22	G1847A (exon 12)	R616Q	Plus to polar uncharged	TM5, pore region	More conductivity	Brachylomia	7
23	C1851A (exon 12)	F617L	Aromatic to nonpolar	TM5, pore region	Not done	Metatropic dysplasia	24
24	T1853C (exon 12)	L618Q	Nonpolar to polar (uncharged)	TM5, pore region	Not done	Metatropic dysplasia	24
25	G858A (exon 12)	V620I	Nonpolar to nonpolar	TM5, pore region	More conductivity	Brachylomia	7
26	-	M625I	Nonpolar to nonpolar	TM5, pore region	Not done	SMDK	26
27	-	L709M	Nonpolar to nonpolar	TM5, pore region	Not done	SMDK	26
28	C2146T (exon 13)	A716S	Nonpolar to polar	Cytoplasmic side of TM6	Same as wild type	SMDK	27
29	-	R775K	Plus to plus	C-terminal region	Not done	Metatropic dysplasia	26
30	-	C777Y	Polar (uncharged) to aromatic	C-terminal region	Not done	SMDK	26
31	-	E797K	Negative to plus	C-terminal region	Not done	SEDM-PM2	26
32	-	P799R	Nonpolar to plus	C-terminal region	Not done	Metatropic dysplasia	26
33	-	P799S	Nonpolar to polar (uncharged)	C-terminal region	Not done	Metatropic dysplasia	26
34	-	P799A	Nonpolar to non polar	C-terminal region	Not done	Metatropic dysplasia	26
35	C2396T (exon 15)	P799L	Nonpolar to nonpolar	C-terminal	Not done	SMDK	27

is relevant with the development of pathophysiology. This is in agreement with the observation that TRPV4 knock out animals do not reveal embryonic lethality but develop some pathophysiological disorders like hearing loss, impaired pressure sensation, reduced osmoregulation, defective bladder function and impaired release of antidiuretic hormone.[2,28-31]

A better and further understanding of TRPV4 structure, interaction and function can also be derived from studies that have generated and characterized several artificial TRPV4 mutations (**Table 2**). All these mutations mostly alter single amino acids or cause deletion of specific regions. The change (or loss) of these residues (or regions) correlates well with the change in

Table 2. Other artificially generated TRPV4 mutations

No	Mutation	Domain	Change	Effects	Species	Refs
1	P142A	Proline-rich domain	Nonpolar to nonpolar	PASCIN binding abolished	Murine	32
2	P143L	Proline-rich domain	Nonpolar to nonpolar	PASCIN binding abolished	Murine	32
3	R151D	Proline-rich domain	Plus to negative	No change in response to 4αPDD	Murine	33
4	R151A	Proline-rich domain	Plus to nonpolar	No change in response to 4αPDD	Murine	33
5	R151Q	Proline-rich domain	Plus to polar (uncharged)	No change in response to 4αPDD	Murine	33
6	R151K	Proline-rich domain	Plus to plus	No change in response to 4αPDD	Murine	33
7	P152A	Proline-rich domain	Nonpolar to nonpolar	No effect	Murine	32
8	K178A	ARD 2	Plus to nonpolar	Reduced binding to CAM and ATP	Chicken	34
9	K183A	ARD2	Plus to nonpolar	Reduced binding to CAM and ATP	Chicken	34
10	K185A	ARD2	Plus to nonpolar	Reduced binding to CAM and ATP	Chicken	34
11	Y253F	TM3	Aromatic to aromatic	No response in Ca^{2+}-permeability to hyopotonic swelling	Mouse	35
12	N456H	TRP box	Polar (uncharged) to plus	Marginal response to APB	Mouse	36
13	Y555A	TM3	Aromatic to nonpolar	Strongly impaired permeability, lower basal level	Mouse	35
14	Y555F	TM3	Aromatic to nonpolar	Same as wild type	Mouse	35
15	S556A	TM3	Polar to nonpolar	Lower basal level activity	Mouse	35
16	Y566A	TM4	Aromatic to nonpolar	Increased basal level Activity	Murine	37
17	L584M	TM4	Nonpolar to nonpolar	Increased basal level Activity	Murine	37
18	W586A	TM4	Aromatic to nonpolar	Increased basal level Activity	Murine	37
19	M587A	TM4	Nonpolar to nonpolar	Marginal response	Murine	37
20	N588A	TM4	Polar (uncharged) to polar	Marginal response	Murine	37
21	Y591A	TM4	Aromatic to nonpolar	Marginal response	Murine	37
22	R594Q	TM4	Plus to polar (uncharged)	No response	Murine	37
23	R594A	TM4	Plus to nonpolar	No response	Murine	37
24	R594K	TM4	Plus to plus	Increased response to 4αPDD	Murine	37
25	L619P	TM5	Nonpolar to nopolar	Iincrease in response to 4αPDD (Gain of function)	Rat	38
26	L623P	TM5	Nonpolar to nonpolar	Not done	Rat	38
27	N651Q	TM5-TM6, pore region	Polar (uncharged) to polar (uncharged)	Increase at surface expression and increase in response (Gain of function)	Murine	39
28	D672A	Pore region	Negative to nonpolar	Reduced Ca^{2+}-permeability	Mouse	40
29	D672K	Pore region	Negative to plus	Decreased osmotic response	Rat	2
30	K675A	Cytoplasmic pore region	Plus to nonpolar (uncharged)	No change	Mouse	40
31	M680A	Pore region	Nonpolar to nonpolar	Decreased Ca^{2+}-selectivity	Mouse	40
32	M680K	Pore region	Nonpolar to plus	Lack of channel activity	Rat	2
33	M680D	Pore region	Nonpolar to negative	Complete loss of Ca^{2+}-selectivity	Mouse	40
34	D682A	Pore region	Negative to nonpolar	Decreased Ca^{2+}selectivity	Mouse	40
35	D682K	Pore region	Negative to plus	Decreased osmotic response	Rat	2
36	F707A	TM6	Aromatic to nonpolar	Increased response to 4αPDD	Murine	33
37	F707K	TM6	Aromatic to plus	Resulted in non-functional channel	Murine	33
38	F707D	TM6	Aromatic to negative	Resulted in non-functional channel	Murine	33
39	M713V	TM6	Nonpolar to nonpolar	Not done	Rat	38
40	M713I	TM6	Nonpolar to nonpolar	Gain of function	Rat	38
41	W733R	C-terminal region	Aromatic to plus	Not done	Rat	38
42	W737R	TRP-BOX	Aromatic to plus	Increased sensitivity to APB (Gain of function)	Mouse	36

Table 2. Other artificially generated TRPV4 mutations

43	E797K	C-terminal	Negative to plus	Gain of function	Murine	33
44	E797A	C-terminal	Negative to nonpolar	Gain of function	Murine	33
45	S824A	C-terminal	Polar (uncharged) to nonpolar	No significant difference in channel activity	Mouse	41
46	S824D	C-terminal	Polar (uncharged) to negative	Increased channel activity than wild type	Mouse	41
47	TRPV4 Δ1–410	N-terminal	Deletion	Decreased channel activity	Rat	2
48	TRPV4-Δ40–112	N-terminal region	Deletion	Not retained in ER and detected at cell periphery	Mouse	42
49	TRPV4-Δ40–235	ARD	Deletion	Retained in ER	Mouse	42
50	TRPV4-Δ132–144	Loss of Proline-rich domain (PRD)	Deletion	Less channel activity	Human	14
51	TRPV4-Δ226–437	Ankyrin repeats	Deletion	Retained in ER	Mouse	42
52	TRPV4-Δ235–398	Ankyrin repeats	Deletion	Less channel activity	Murine	43
53	TRPV4-Δ411–437	PY-motif	Deletion	No effect on ubiquitination in presence of AIP4	Mouse	44
54	TRPV4-Δ741–871	C-termianl region	Deletion	Decreased channel activity	Rat	2
55	TRPV4-Δ812–831	Deletion of CAM-binding region	Deletion	Prevent IP3 binding, Loss of function	Human	14
56	TRPV4-Δ868–871	Deletion of C- terminal PDZ domain	Deletion	Same as wild type	Human	14

certain interaction and function attributed for TRPV4. All these mutational analysis indicate that the structure—function relationship is determined by whole TRPV4 sequence. However, two "hot spots" in TRPV4 sequences are prominent, one at the pore region and the second one in the ARDs.

Can these Mutations Affect TRPV4 Oligomerization?

Recently a number of studies have characterized the assembly and oligomerization of TRP channels.[45,46] Members of TRP family can also form homo- or hetero-tetramer.[47-50] It has been also postulated that the assembly and oligomerization can occurs in phases to get functional conformation of the channel. For example, in TRPC, tetramerization occurs through interaction of association domain 1 (AD1) (N-terminal region) followed by interaction with AD2 (putative pore region S4-S5 and C-terminal region).[13,51] However, in spite of several studies, the molecular mechanism underlying the assembly of TRPV monomers into functional tetramer is still at infancy. In addition, the regions of TRPV channels and the sequence specificity, which regulates the homo- or hetero-tetramer formation, are not well understood.[52,53]

In spite of some sequence similarity, all TRPV members prefer to form homo-tetramer and different regions like ARD, colied coil domain and transmembrane regions are important for oligomerization.[53,54] For example, a small region located at the C-terminus of TRPV1 is important for homotetramer formation[55] while TRPV5 and TRPV6 can form a hetero tetramer due to interaction at the N- and C-terminus.[47] The N-terminal region, especially the ARD3 and ARD5 have been shown to play an important role for oligomerization of TRPV6.[56] It has been proposed that ARD3 and ARD5 form a molecular zipper that stabilizes the channel assembly.[56] In case of TRPV4, both N- and C-terminal domains as well as transmembrane regions contribute to overall assembly and functionality of TRPV4 channel.[53]

Within the N-terminus, the ARD regions (amino acid residues 132–383) seem to be important for assembly and maturation of TRPV4.[57,58] This conclusion is drawn on the basis of the fact that TRPV4 splice variants namely B, C and E isotypes cannot assemble into functional channel.[57] These isotypes lack regions located at the N-terminal region, are sequestered in endoplasmic reticulum and thus cannot reach to the plasma membrane. In contrast, A and D isotypes are transported to the membrane and can form functional channels. Thus cells expressing A and D isotypes can response against TRPV4-specific stimuli.[57] This result is in line with another study which demonstrated that the N-terminal region of TRPV4 is responsible for homotetramer formation.[53] In the agreement with the role of ARDs in the oligomerization and surface expression, mutations namely R269H, R315W and R316C result in loss of function due to reduced surface expression, at least when expressed in HeLa cells.[4] This conclusion is drawn from the reduced Ca^{2+}-peaks observed after activation with 4α-PDD in cells expressing TRPV4 mutants. Cells expressing these mutants also contain aggregated patches distributed all over the cytoplasm.[4] As all these mutations are located at the ARDs, these results strongly suggest that ARDs located at the N-terminal region play important role in subunit assembly and act as prime site for binding auxiliary proteins.

How the N-terminal region contributes and regulates all these properties is currently unknown. The ARDs can possibly act as scaffold or adaptor and helps the interaction of TRPV4 with other proteins. In a bigger context, these results suggest

that oligomerization of TRPV4 is important not only for its trafficking and surface expression but also for functional properties like selectivity and gating mechanisms. Like all other membrane proteins, assembly of TRPV4 also occurs in endoplasmic reticulum and it undergoes diverse modifications like disulfide bond formation and glycosylation.[59] Coiled-coil domain (protein oligomerization unit), ARDs and transmembrane domains of TRPV4 seem to be important for tetrameric assembly.[52] Thus, any mutation in these regions can potentially result in abnormal channel assembly and/or activity. Within endoplasmic reticulum, proper folding of TRPV4 and further tetramer formation seems to be facilitated by interaction with OS-9 which has chaperone-like activity.[42] Though the exact position where OS-9 interacts with monomeric TRPV4 is not known, it is known to interact at the N-terminus of TRPV4 and especially within amino acid 40–235.[42] This interaction can prevent misfolding of TRPV4 and further polyubiquitination of misfolded monomeric TRPV4. Therefore this interaction can potentially reduce the degradation of TRPV4 by endoplasmic reticulum-associated degradation (ERAD) pathway and/or by 26S proteasome.[42,60]

How These Mutations can Affect Function and Surface Expression of TRPV4?

Previously it has been shown that deletion of extreme C-terminal 16 amino acid residues does not alter the surface expression as truncated TRPV4 having 1–855 amino acids can exported to the membrane and this surface expression is equivalent to the wild type TRPV4 (amino acid 1–871).[61] However, the same study revealed that the deletion of 16 amino acids at the region of 828–844 results in accumulation of TRPV4-Δ828-844 in the ER. Another report demonstrate that deletion of amino acid residue 132–144 (located at the N-terminal cytoplasmic domain), i.e., deletion of Proline-rich domain (PRD) results in loss of channel function despite having proper trafficking at the membrane.[14] It has also been demonstrated that interaction of PACSIN 3, a cytoskeletal protein to the N-terminal region of TRPV4 enhances the membrane localization.[32] Though all these studies characterized the trafficking of TRPV4 to a large extent, the understanding of surface expression of TRPV4 and actual regulation/s underlying this is still fragmented. As both N- and C-terminal regions seems to be important, the reported self interaction between N- and C-terminal of TRPV4 mediated by Calmodulin and Ca^{2+} might play an important role here.[16]

TRPV4-R269H mutant mostly accumulated in the cytoplasm, indicating that amino acid R269 located at the 3rd ARD is important for the surface expression, at least in case of HeLa cells.[4] However, using a different cellular system, namely HEK cell, another group has reported that the same TRPV4-R269H mutant has proper cell surface expression.[6] A similar study revealed that a different mutation at the same position, i.e., TRPV4-R269C does not have an altered surface expression in HeLa cells.[4] In contrast, R316C reveals a loss of function (compared to the wild type) when expressed in HeLa cells[4] while the same mutation reveals a gain of function in HEK cells.[6] Though, these results appear as contradicting to each other, these data reveal important clues about the surface expression of TRPV4 and also raise an important and interesting question: how the surface expression of TRPV4 is regulated? As the R residues at the position of 269 and 315–316 cannot act as potential phosphorylation sites, altered functions of the relevant mutations cannot be explained by direct phosphorylation-mediated regulation on TRPV4. Preliminary bioinformatic analysis (AGADIR prediction algorithm, available at http://agadir.crg.es/) with human TRPV4 sequence (NCBI number gi62901470) indicate that substitution of R to H (R269H) or R to C (R269C) at the position of 269 and substitution of R to W (R315W) or R to C (R316C) at the position of 315–316 can potentially change the structure of these regions, especially the alpha-helical propensity and/or helical percentage of that region to some extent. These changes might be important if compared in case of permissive temperature (T = >37°C to 45°C, a temperature range in which TRPV4 can be activated) with in non-permissive temperature (T = <37°C to 15°C, a temperature range in which TRPV4 should not be activated). R to K substitutions (R269K and R315K) in these positions is known to rescue the functions of the mutants (R269H and R315C) respectively.[4] Interestingly, the bioinformatic analysis reveals that these rescue mutants may have helical properties in these regions that are similar to the wild type. However, at present, the true helicity of these two important regions are not known and further experimental proof is required to confirm if these mutations can indeed alter the helicity/secondary structure of these regions.

Interestingly, R269 is located within the ARD-helix and brings a positive charge at the surface of the ARD3 and thus may be crucial for interaction with other protein. Though R269K mutation rescue the effect of R269H mutation,[4] critical analysis of relevant mutations reveal few important clues: first, a specific positive charge at the position of 269 is neither very important nor plays the prime determining factor. This is due to the fact that substitution of polar R (10.75) with another polar residue H (7.59, though having a different side chain and size) results in abnormal trafficking and accumulation of mutant TRPV4 at the cytoplasm.[4] Secondly, substitution of polar R (10.75) with a non-polar residue C (5.07) does not alter the surface expression.[5] Also substitution of R with K (9.74) can rescue the effect. Thus, a change in the size and/or at the side chain of the residues at 269 and mutation-induced local yet minute change in the structure seems to be more important than the positive charge. The contradictory results from Auer-Grumbach et al. and Deng et al. may also suggest a differential interaction and/or regulation of surface expression of TRPV4 even in different cell lines of Human origin (HeLa and HEK).[44] As most of the point mutations are observed in the N-terminal region, specifically at the position of ARDs (R269H, R315W, R316C), a loss or at least a different route of trafficking seems to be relevant. Considering that constitutive activation of any ion channel is harmful and in general, most of the ion channels stay in their closed state, it seems logical to assume that proteins interacting with TRPV4 may act as inhibitory complex and thus stabilize TRPV4 in its closed state, thermodynamically most stable state. Thus, it is tempting to speculate that substitution of R with other amino acids (like H, C and W)

at the position of 269 and 315–316 might result in either weak or strong interaction of at least one molecular component that works as a inhibitory complex for TRPV4 (**Fig. 1**).

Significant information can be imparted from these results: How is the surface expression of TRPV4 regulated? Generally, surface expression of TRP channels is an important aspect regulated in several manners. Depending on the signaling events, new functional channels are recruited to the plasmamembrane when required.[44,62,63] The pre-existing channels will be either recycled by endocytosis and exocytosis or internalized and degraded by 26S proteasomal pathway if not required.[64] These regulations are essential and form the basis of channel homeostasis at the plasma membrane. In that context, multi vesicular body (MVB) pathway is important as it regulates the level of surface expression by degrading the internalized transmembrane protein at lysosome.[65] Surface expression of transmembrane proteins can also be regulated by Ubiquitin, a 76 amino acid long chain that serves as a degradation signal in Ubiquitin-mediated Proteasomal degradation pathway.[66] Ubiquitin attachment is carried out by three enzymes E1 (Ubiquitin activating enzyme), E2 (Ubiquitin conjugating enzyme) and E3 (Ubiquitin ligase) and internalized ubiquitinated proteins are known to be degraded at lysosome.[67] However, recent studies demonstrated that Ubiquitin can also be used as a sorting signal for MVB pathway.[68-70]

In case of TRPV4, surface expression seems to be regulated by Ubiquitination, at least in parts. Atrophin-1-interacting protein 4 (AIP4) is a member of HECT ligases which acts as an E3 ligase.[71] AIP4 is known to add Ubiquitin on TRPV4, especially within amino acid residues 411–437 located at the N-terminal cytoplasmic domain.[44] It has been demonstrated that AIP4 actually promotes endocytosis and thus increases the intracellular pool of TRPV4.[44] These internalized TRPV4 containing vesicles efficiently recycles to the plasma membrane.[44] However, it has been observed that in spite of tagged with Ubiquitin, some of the TRPV4 does not get degraded, but become accumulated beneath plasma membrane.[44] Thus, AIP4 seems to plays a role which is not only relevant in the context of Ubiquitination of the TRPV4 but also can direct the TRPV4 under regulation by MVB pathway. As AIP4 binds to the N-terminal region of the TRPV4,[44] mutations in this region can leads to altered Ubiquitination. This altered Ubiquitination might affect the surface expression and Ca^{2+}-influx via TRPV4 that is relevant in the context of cellular function (**Fig. 2**).

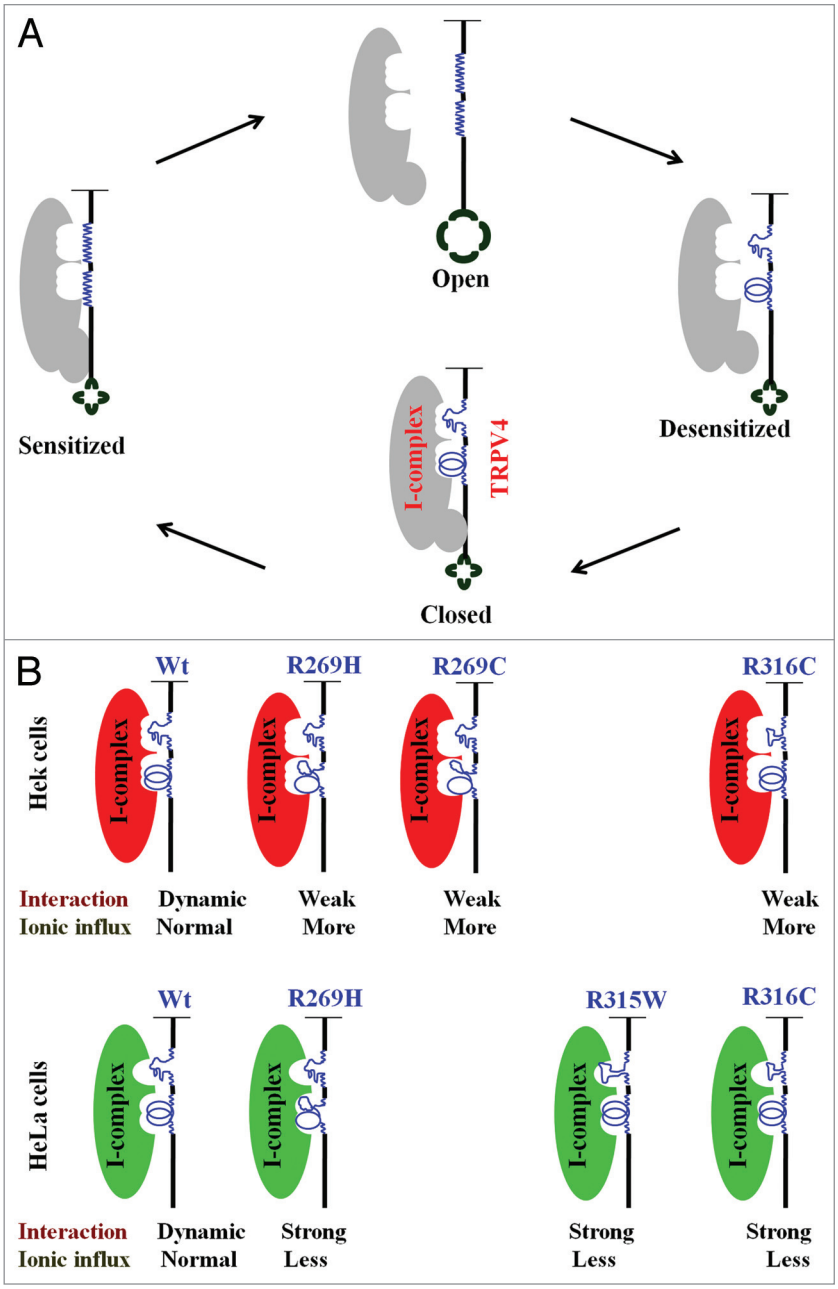

Figure 1. A hypothetical model demonstrating how mutations in the ARD region can alter the TRPV4 function. (A) Interaction of the inhibitory complex (indicated by gray object) can stabilize the TRPV4 in its closed conformation and dissociation of this complex can be a pre-requisite for TRPV4 channel opening. Differential interaction of TRPV4 mutants with this inhibitory complex can stabilize the TRPV4 channel either in closed state or in open state. (B) Altered characteristics of wild type and mutant TRPV4 can be explained if the interaction of this inhibitory complex with TRPV4 can be stabilized and/or regulated by two key positions, namely by R269 and RR315-6. A change in these positions can alter the association-dissociation of this inhibitory complex with TRPV4 as indicated in the figure. The biophysical properties of this inhibitory complex, like structure, association-dissociation kinetics seems to be different in HEK (indicated by Red) and HeLa cells (indicated by Green). The cartoons represent the interaction of the TRPV4 with the inhibitory complex in the closed-state mainly.

Sequence analysis also shed light on the differential distribution of the wild type and mutant TRPV4. Both carboxyl-terminal dilysine KKXX motif which interacts with coat protein I (CopI

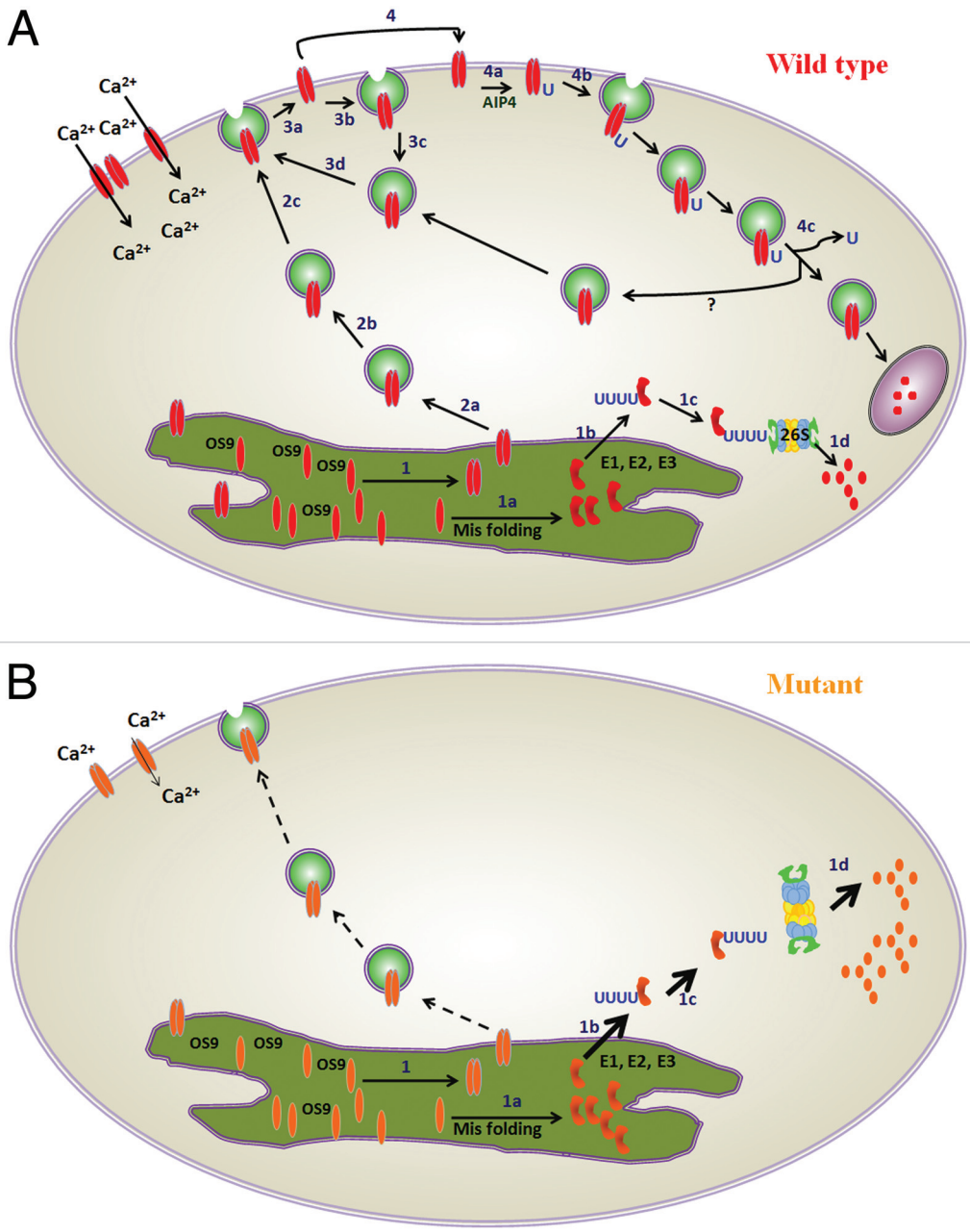

Figure 2. A hypothetical model depicting how surface expression of TRPV4 can be regulated. (A) Surface expression of wild type TRPV4. OS9 protein with a chaperone-like activity assists TRPV4 monomer (indicated by red) to form tetramer. Misfolded TRPV4 is targeted for Ubiquitin-dependent 26S Proteasomal degradation pathway (ERAD, shown in steps 1a–d). Perfectly folded TRPV4 tetramer are inserted in vesicles and recruited to the plasma membrane (steps 2a and b). Most of the membrane inserted TRPV4 can be recycled (steps 3a–d). A fraction of the membrane inserted TRPV4 is regulated by AIP4, an E3 ligase and become monoubiquitinated (step 4a). This monoubiquitinated TRPV4 can be either degraded by lysosomes by multi-vesicular-body pathway (MVB pathway, indicated in steps 4a–d) or they get recycled back and become part of the recyclable vesicular pool located just beneath the plasma membrane. (B) Reduced surface expression of TRPV4 mutant. In case of mutant (for example R269H, R316C and R315W in HeLa cell, indicated by yellow), a major fraction of total synthesized TRPV4 is misfolded and thus degraded by ERAD pathway as a quality control mechanism (steps 1a–d). Only a minor fraction of synthesized TRPV4, which is fully assembled and functional will be transported by vesicles and recruited to the plasma membrane (steps 2a and b). The other steps related to MVB pathway (steps 4a–d) and recycling of vesicles (steps 3a–d) are expected to be operational in case of mutants also. But for simplicity it is not shown in (B).

complex) and the internally positioned RXR motif regulate the retention of any protein within endoplasmic reticulum.[72] Apparently, TRPV4 polypeptide contains four RXR motifs, two on the N-terminal region (122RWR and 269RGR) and two at the C-terminal (816RLR and 819RDR) cytoplasmic domain. Interestingly, mutation at R269 (R269C and R269H) can destroy

the function of one RXR motif located at the N-terminal domain and thus regulate the surface expression significantly. However, this possibility needs to be verified experimentally in future.

Future Direction and Conclusion

The relation between assembly, trafficking, surface expression and functionality of TRP channels is poorly understood and seems to be specific for each TRP channels. In many cases the TRPV channel can assemble and expressed at the plasma membrane but remain non functional. For example, substitution of TRP domain (684–721, which is highly conserved in all TRP family and known as TRP box) from TRPV1 to TRPV2-TRPV6 results assembly of TRP channels and proper surface expression also. However, these TRPV chimeras remain non functional.[73] In case of TRPV4, OS-9 seems to be important for its surface expression. In this regard it is important to mention that ectopic expression of TRPV4 causes deformities in body and bone in zebra fish embryos.[42] Interestingly, expression of OS-9 can rescue these TRPV4-mediated defects in zebra fish.[42] Therefore, similar lethal phenotype observed in patients suffering from Brachyolmia and in the zebra fish embryos largely suggest that the fine regulation of the basal level activity of TRPV4 is extremely important for normal bone function.[7-42] This similarities in human as well as zebra fish may also hint that the OS-9-mediated regulation of TRPV4 is conserved throughout the evolution.[7-42] However, further experimental proof is needed to validate this.

The proteins which are actually involved in insertion of TRPV4-containing vesicles to the plasma membrane and for recognizing Ubiquitin-tagged TRPV4 as sorting signal has not been identified yet. In this regard, recent studies on other TRP channels indicate that membrane trafficking of TRPs are complex and different Rab-GTPase, dynamin, 80KH, annexins and kinesins might be involved.[74-77] Based on the structural information available and existing sequence homology among other TRPs, especially with TRPV members and the manner by which the surface expression of TRP channels are regulated, it can be speculated that proteins like Signal Transducing Adaptor Molecule (STAM), Hrs (which downregulate TRPP2 in *C. elegans*) and Recombinase Gene Activator (RGA, which regulates cell surface expression of TRPV2) may also be involved in the surface expression of TRPV4.[78-80] However, further detailed studies are needed to confirm if these proteins really interact and are involved in the surface expression of TRPV4.

Acknowledgements and Notes

Funding from National Institute of Science Education and Research is acknowledged. We regret for not including all the scientific works due to space limitation. This critical review reflects the views of the authors based on the data available. The authors undertake no formal responsibility for the scientific authenticity/reproducibility of the data.

References

1. Plant TD, Strotmann R. TRPV4. Handb Exp Pharmacol 2007; 179:189-205.
2. Liedtke W, Tobin DM, Bargmann CI, Friedman JM. Mammalian TRPV4 (VR-OAC) directs behavioral responses to osmotic and mechanical stimuli in *Caenorhabditis elegans*. Proc Natl Acad Sci USA 2003; 100:14531-6.
3. Nilius B, Owsianik G. Transient receptor potential chanellopathies. Pflugers Arch 2010; 460:437-50.
4. Auer-Grumbach M, Olschewski A, Papic L, Kremer H, McEntagart ME, Uhrig S, et al. Alterations in the ankyrin domain of TRPV4 cause congenital distal SMA, scapuloperoneal SMA and HMSN2C. Nat Genet 2010; 42:160-4.
5. Landouré G, Zdebik AA, Martinez TL, Burnett BG, Stanescu HC, Inada H, et al. Mutations in TRPV4 cause Charcot-Marie-Tooth disease type 2C. Nat Genet 2010; 42:170-4.
6. Deng HX, Klein CJ, Yan J, Shi Y, Wu Y, Fecto F, et al. Scapuloperoneal spinal muscular atrophy and CMT2C are allelic disorders caused by alterations in TRPV4. Nat Genet 2010; 42:165-9.
7. Rock MJ, Prenen J, Funari VA, Funari TL, Merriman B, Nelson SF, et al. Gain-of-function mutations in TRPV4 cause autosomal dominant brachyolmia. Nat Genet 2008; 40:999-1003.
8. Everaerts W, Nilius B, Owsianik G. The vanilloid transient receptor potential channel TRPV4: From structure to disease. Prog Biophys Mol Biol 2009; (Epub ahead of print).
9. Shigematsu H, Sokabe T, Danev R, Tominaga M, Nagayama K. A 3.5 nm structure of rat TRPV4 cation channel revealed by zernike phase-contrast cryo-EM. J Biol Chem 2010; 285:11210-8.
10. Moiseenkova-Bell VY, Stanciu LA, Serysheva II, Tobe BJ, Wensel TG. Structure of TRPV1 channel revealed by electron cryomicroscopy. Proc Natl Acad Sci USA 2008; 105:7451-5.
11. Gaudet R. TRP channels entering the structural era. J Physiol 2008; 586:3565-75.
12. Denker SP, Barber DL. Ion transport proteins anchor and regulate the cytoskeleton. Curr Opin Cell Biol 2002; 14:214-20.
13. Lepage PK, Boulay G. Molecular determinant of assembly. J Biochem Soc Trans 2007; 35:81-3.
14. Garcia-Elias A, Lorenzo IM, Vicente R, Valverde MA. IP3 receptor binds to and sensitizes TRPV4 channel to osmotic stimuli via a calmodulin-binding site. J Biol Chem 2008; 283:31284-8.
15. Strotmann R, Schultz G, Plant TD. Ca^{2+}-dependent potentiation of the nonselective cation channel TRPV4 is mediated by a C-terminal Calmodulin binding site. J Biol Chem 2003; 278:26541-9.
16. Strotmann R, Semtner M, Kepura F, Plant TD, Schöneberg T. Interdomain interactions control Ca^{2+}-dependent potentiation in the cation channel TRPV4. PLoSOne 2010; 5:10580.
17. Goswami C, Hucho T, Hucho F. Identification and characterisation of novel tubulin-binding motifs located within the C-terminus of TRPV1. J Neurochem 2007; 101:250-62.
18. Suzuki M, Hirao A, Mizuno A. Microfilament-associated Protein 7 increases the membrane expression of Transient Receptor Potential Vanilloid 4. J Biol Chem 2003; 278:51448-53.
19. Goswami C, Khun J, Heppenstall P, Hucho T. Importance of non-selective cation channel TRPV4 interaction with cytoskeleton and their reciprocal regulations in cultured cells. Plos One (Accepted) 2010.
20. Ramadass R, Becker D, Jendrach M, Bereiter-Hahn J. Spectrally and spatially resolved fluorescence lifetime imaging in living cells: TRPV4-microfilament interactions. Arch Biochem Biophys 2007; 463:27-36.
21. Bird TD. Charcot-Marie-Tooth Neuropathy Type 2. GeneReviews 2010.
22. Zhao C, Takita J, Tanaka Y, Setou M, Nakagawa T, Takeda S, et al. Charcot-Marie-Tooth disease type 2A caused by mutation in a microtubule motor KIF1Bbeta. Cell 2001; 105:587-97.
23. Tian W, Fu Y, Garcia-Elias A, Fernández-Fernández JM, Vicente R, Kramer PL, et al. A loss-of-function nonsynonymous polymorphism in the osmoregulatory TRPV4 gene is associated with human hyponatremia. Proc Natl Acad Sci 2009; 106:14034-9.
24. Camacho N, Krakow D, Johnykutty S, Katzman PJ, Pepkowitz S, Vriens J, et al. Dominant TRPV4 mutations in nonlethal and lethal metatropic dysplasia. Am J Med Genet A 2010; 152:1169-77.
25. Nishimura G, Dai J, Lausch E, Unger S, Megarbané A, Kitoh H, et al. Spondylo-epiphyseal dysplasia, Maroteaux type (pseudo-Morquio syndrome type 2) and parastremmatic dysplasia are caused by TRPV4 mutations. Am J Med Genet A 2010; 152:1443-9.
26. Dai J, Cho TJ, Unger S, Lausch E, Nishimura G, Kim OH, et al. TRPV4-pathy, a novel channelopathy affecting diverse systems. J Hum Genet 2010; (Epub ahead of print).
27. Krakow D, Vriens J, Camacho N, Luong P, Deixler H, Funari TL, et al. Mutations in the gene encoding the calcium-permeable ion channel TRPV4 produce spondylometaphyseal dysplasia, Kozlowski type and metatropic dysplasia. Am J Hum Genet 2009; 84:307-15.
28. Tabuchi K, Suzuki M, Mizuno A, Hara A. Hearing impairment in TRPV4 knockout mice. Neurosci Lett 2005; 382:304-8.

29. Gevaert T, Vriens J, Segal A, Everaerts W, Roskams T, Talavera K, et al. Deletion of the transient receptor potential cation channel TRPV4 impairs murine bladder voiding. J Clin Invest 2007; 117:3453-62.
30. Mizuno A, Matsumoto N, Imai M, Suzuki M. Impaired osmotic sensation in mice lacking TRPV4. Am J Physiology 2003; 285:96-101.
31. Suzuki M, Mizuno A, Kodaira K, Imai M. Impaired pressure sensation in mice lacking TRPV4. Biol Chem 2003; 278:22664-8.
32. D'hoedt D, Owsianik G, Prenen J, Cuajungco MP, Grimm C, Heller S, et al. Stimulus-specific modulation of the cation channel TRPV4 by PACSIN 3. J Biol Chem 2008; 283:6272-80.
33. Watanabe H, Vriens J, Janssens A, Wondergem R, Droogmans G, Nilius B. Modulation of TRPV4 gating by intra- and extracellular Ca^{2+}. Cell Calcium 2003; 33:489-95.
34. Phelps CB, Wang RR, Choo SS, Gaudet R. Differential regulation of TRPV1, TRPV3 and TRPV4 sensitivity through a conserved binding site on ankyrin repeat domain. J Biol Chem 2009; 285:731-40.
35. Vriens J, Watanabe H, Janssens A, Droogmans G, Voets T, Nilius B. Cell swelling, heat and chemical agonists use distinct pathways for the activation of the cation channel TRPV4. Proc Natl Acad Sci USA 2004; 101:396-401.
36. Hu H, Grandl J, Bandell M, Petrus M, Patapoutian A. Two amino acid residues determine 2-APB sensitivity of the ion channels TRPV3 and TRPV4. Proc Natl Acad Sci USA 2009; 106:1626-31.
37. Vriens J, Owsianik G, Janssens A, Voets T, Nilius B. Determinants of 4-Phorbol sensitivity in transmembrane domains 3 and 4 of the cation channel TRPV4. J Biol Chem 2007; 282:12796-803.
38. Loukin S, Su Z, Zhou X, Kung C. Forward genetic analysis reveals multiple gating mechanisms of TRPV4. J Biol Chem 2010; 285:19884-90.
39. Xu H, Fu Y, Tian W, Cohen DM. Glycosylation of the osmoresponsive transient receptor potential channel TRPV4 on Asn-651 influences membrane trafficking. Am J Physiol Renal Physiol 2006; 290:1103-9.
40. Voets T, Prenen J, Vriens J, Watanabe H, Janssens A, Wissenbach U, et al. Molecular Determinants of Permeation through the Cation Channel TRPV4. J Biol Chem 2002; 277:33704-10.
41. Peng H, Lewandrowski U, Müller B, Sickmann A, Walz G, Wegierski T. Identification of a Protein Kinase C-dependent phosphorylation site involved in sensitization of TPV4 channel. Biochem Biophys Res Commun 2010; 391:1721-5.
42. Wang Y, Fu X, Gaiser S, Köttgen M, Kramer-Zucker A, Walz Gand, et al. OS-9 regulates the transit and polyubiquitination of TRPV4 in the endoplasmic reticulum. J Biol Chem 2007; 282:36561-70.
43. Watanabe H, Vriens J, Suh SH, Benham CD, Droogmans G, Nilius B. Heat-evoked activation of TRPV4 channels in a HEK293 cell expression system and in native mouse aorta endothelial cells. J Biol Chem 2002; 277:47044-51.
44. Wegierski T, Hill K, Schaefer M, Walz G. The HECT ubiquitin ligase AIP4 regulates the cell surface expression of select TRP channels. EMBO J 2006; 25:5659-69.
45. Yu Y, Ulbrich MH, Li MH, Buraei Z, Chen XZ, Ong AC, et al. Structural and molecular basis of the assembly of the TRPP2/PKD1 complex. Proc Natl Acad Sci 2009; 106:11558-63.
46. Goswami C, Islam MS. TRP channels: What's happening? Reflections in the wake of the 2009 TRP Meeting, Karolinska Institutet, Stockholm. Channels 2010; 4:1-12.
47. Hoenderop JG, Voets T, Hoefs S, Weidema F, Prenen J, Nilius B, et al. Homo- and heterotetrameric architecture of the epithelial Ca^{2+} channels TRPV5 and TRPV6. EMBO J 2003; 22:776-85.
48. Poteser M, Graziani A, Rosker C, Eder P, Derler I, Kahr H, et al. TRPC3 and TRPC4 associate to form a redox-sensitive cation channel. Evidence for expression of native TRPC3-TRPC4 heteromeric channels in endothelial cells. J Biol Chem 2006; 281:13588-95.
49. Rutter AR, Ma QP, Leveridge M, Bonnert TP. Heteromerization and colocalization of TrpV1 and TrpV2 in mammalian cell lines and rat dorsal root ganglia. Neuroreport 2005; 16:1735-9.
50. Cheng W, Yang F, Takanishi LC, Zheng J. Thermosensitive TRPV channel subunits co-assemble into heteromeric channels with intermediate conductance and gating. J Gen Physiol 2007; 129:191-207.
51. Lepage PK, Lussier MP, Barajas-Martinez H, Bousquet SM, Blanchard AP, Francoeur N, et al. Identification of two domains involved in the assembly of Transient Receptor Potential Canonical channels. J Biol Chem 2006; 281:30356-64.
52. Schaefer M. Homo- and heteromeric assembly of TRP channel subunits. Pflugers Arch 2005; 451:35-42.
53. Hellwig N, Albrecht N, Harteneck C, Schultz G, Schaefer M. Homo and hetero assembly of TRPV channel subunits. J Cell Sci 2005; 118:917-28.
54. Schindl R, Romanin C. Assembly domains in TRP channels. Biochem Soc Trans 2007; 35:84-5.
55. Garcia-Sanz N, Fernandez-Carvajal A, Morenilla-Palao C, Planells-Cases R, Fajardo-Sanchez E, Fernandez-Ballester G, et al. Identification of a tetramerization domain in the C-terminus of the Vanilloid Receptor. J Neurosci 2004; 24:5307-14.
56. Erler I, Hirnet D, Wissenbach U, Flockerzi V, Niemeyer BA. Ca^{2+}-selective Transient Receptor Potential V channel architecture and function require a specific Ankyrin Repeat. J Biol Chem 2004; 279:34456-63.
57. Arniges M, Fernandez-Fernandez JM, Albrecht N, Schaefer M, Valverde MA. Human TRPV4 channel splice variants revealed a key role of Ankyrin domains in multimerization and trafficking. J Biol Chem 2005; 281:1580-6.
58. Alessandri-Haber N, Yeh JJ, Boyd AE, Parada CA, Chen X, Reichling DB, et al. Hypotonicity induces TRPV4-mediated nociception in rat. Neuron 2003; 39:497-511.
59. Ellgaard L, Helenius A. Quality control in the endoplasmic reticulum. Nat Rev Mol Cell Biol 2003; 4:181-91.
60. Alcock F, Swanton E. Mammalian OS-9 is upregulated in response to E.R stress and facilitates ubiquitination of misfolded glycoprotein. J Mol Biol 2009; 385:1032-42.
61. Becker D, Müller M, Leuner K, Jendrach M. The C-terminal domain of TRPV4 is essential for plasma membrane localization. Mol Membr Biol 2008; 25:139-51.
62. Miranda M, Sorkin A. Regulation of receptors and transporters by ubiquitination: new insights into surprisingly similar mechanisms. Mol Interv 2007; 7:157-67.
63. Morenilla-Palao C, Planells-Cases R, Garcia-Sanz N, Ferrer-Montiel A. Regulated exocytosis contributes to protein kinase C potentiation of vanilloid receptor activity. J Biol Chem 2004; 279:25665-72.
64. Glickman MH, Ciechanover A. The ubiquitin-proteasome proteolytic pathway: destruction for the sake of construction. Physiol Rev 2002; 82:373-428.
65. Pizzirusso M, Chang A. Ubiquitin-mediated targeting of mutant plasma membrane ATPase, Pma1-7 to the endosomal vacuolar system in yeast. Mol Biol Cell 2004; 15:2401-9.
66. Pickaart CM. Targetting substrate to the 26S Proteasome. FASEB J 1997; 11:1055-66.
67. Raiborg C, Rusten TE, Stenmark H. Protein sorting into multi-vesicular endosomes. Curr Opin Cell Biol 2003; 15:446-55.
68. Katzmann DJ, Babst M, Emr DS. Ubiquitin dependent sorting into multivesicular body pathway requires the function of conserved endosomal protein sorting complex ESCRT-1. Cell 2001; 106:145-55.
69. Katzmann DJ, Sarkar S, Chu T, Audhya A, Emr SD. Multivesicular body sorting: Ubiquitin ligase Rsp5 is required for the modification and sorting of carboxypeptidase S. Mol Biol Cell 2004; 15:13943-53.
70. Woodman P. ESCRT proteins, endosome organization and mitogenic receptor downregulation. Biochem Soc Trans 2009; 37:146-50.
71. d'Azzo A, Bongiovanni A, Nastasi T. E3 ubiquitin ligases as regulators of membrane protein trafficking and degradation. Traffic 2005; 6:429-41.
72. Shikano S, Li M. Membrane receptor trafficking: evidence of proximal and distal zones conferred by two independent endoplasmic reticulum localization signals. Proc Natl Acad Sci 2003; 100:5783-8.
73. Garcia-Sanz N, Valente P, Gomis A, Fernandez-Carvajal A, Fernandez-Ballester G, Viana F, et al. A role of the transient receptor potential domain of vanilloid receptor I in channel gating. J Neurosci 2007; 27:11641-50.
74. Goel M, Sinkins WG, Schilling WP. Selective association of TRPC channel subunits in rat brain synaptosomes. J Biol Chem 2002; 277:48303-10.
75. Graaf SFJ, Chang Q, Mensenkamp AR, Hoenderop JG, Bindels RJ. Direct interaction with Rab11a targets the epithelial Ca^{2+} channels TRPV5 and TRPV6 to the plasma membrane. Mol Cell Biol 2006; 26:303-12.
76. Gkika D, Mahieu F, Nilius B, Hoenderop JG, Bindels RJ. 80K-H as a new Ca^{2+}-sensor regulating the activity of the epithelial Ca^{2+} channel transient receptor potential cation channel V5 (TRPV5). J Biol Chem 2004; 279:26351-7.
77. Goswami C, Rademacher N, Smalla KH, Kalscheuer V, Ropers HH, Gundelfinger ED, et al. TRPV1 acts as a synaptic protein and regulates vesicle recycling. J Cell Sci 2010; 123:2045-57.
78. Hu J, Wittekind GS, Barr MM. STAM and Hrs downregulate ciliary TRP receptors. Mol Biol Cell 2007; 18:3277-89.
79. Stokes AJ, Wakano C, Del Carmen KA, Koblan-Huberson M, Turner H. Formation of a physiological complex between TRPV2 and RGA protein promotes cell surface expression of TRPV2. J Cell Biochem 2005; 94:669-83.
80. Phelps CB, Huang RJ, Lishko PV, Wang RR, Gaudet R. Structural analyses of the ankyrin repeat domain of TRPV6 and related TRPV ion channels. Biochemistry 2008; 47:2476-84.

[Frontiers in Bioscience, Scholar, 5, 19-38, January 1, 2013]

Importance of TRP channels in pain: implications for stress

Ashutosh Kumar[1], Luna Goswami[2], Chandan Goswami[1]

[1]National Institute of Science Education and Research, Institute of Physics Campus, Sachivalaya Marg, Bhubaneswar, Orissa, 751005, India, [2]School of Biotechnology, KIIT University, Patia, Bhubaneswar, 751024, India

TABLE OF CONTENTS

1. ABSTRACT

Though stress is an integrated part of the modern life, defining stress in biological systems is difficult. Anxiety, medication, metabolic disorder, neuro-endocrinological abnormalities, immunological responses, neuro-immune interaction and several other internal and external factors are important which induce stress and pain in higher organisms. Stress and pain are often synonymous and overlapping to a large extent, but these two responses are different at the behavioral, cellular and molecular levels. Importance of Transient Receptor Potential (TRP) group of non-selective cation channels in the development and regulation of different forms of pain is well established. However, recent studies confirmed that TRPs can regulate neuroplastic changes through neuro-endocrine signaling, neuro-immune interactions and psychological state variables suggesting that abnormalities in TRP-signaling can indeed affect the hypothalamic-pituitary-adrenal (HPA) axis and several other metabolic pathways and thus may generate stress at various levels. Therefore, TRPs are important factors that can link stress with pain. This review summarizes the role of TRPs, their effects and clinical implications in the context of different types of pain which can be relevant for stress too.

2. STRESS AND PAIN: OVERLAPPING YET DIFFERENT GAME?

Due to changes in the modern life style and other associated factors, increased level of stress and pain has become a prominent clinical, social and economic problem (1). An increasing number of individuals worldwide suffer from chronic stress and pain. Both life quality and duration are adversely affected in these conditions. It has been predicted that chronic stress and pain-related problems are going to be the next biggest epidemic outbreak which makes the need to understand stress and pain at the molecular and cellular level. Understanding the relation between pain and stress at the behavioral context is a high priority and developing effective methods to nullify these responses are clinically important.

Apparently stress and pain seems to be synonymous and often overlap in many situations, mostly at the gross behavioral level. Stress can be defined as the nonspecific response of the body to any demand made upon it (2). Commonly, stress is referred to as any adverse condition observed at the cellular, organelle and/or individual behavioral level and is often associated with negative situations and settings (Box 1). Every individual

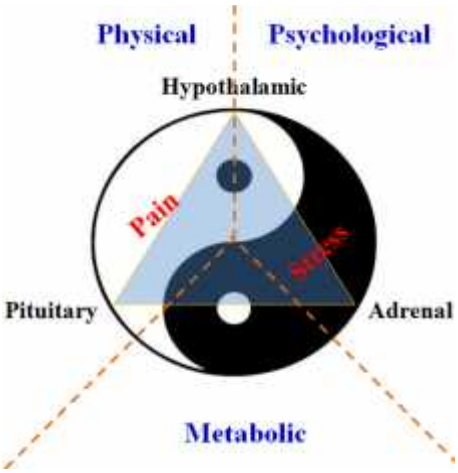

Figure 1. "Mind-body"- and HPA-axis are involved in feedback amplification of stress and pain. In altered conditions, physical, psychological and metabolic stimuli initiates individual perception of chronic stress and pain. If prolonged, stress and pain influence each other and forms a noxious cycle of negative events. This cycle is linked to the HPA-axis and affects the individual adversely. In addition, the HPA-axis also affects the physical, psychological and metabolic status of the individual and thus modulates the vicious cycle of stress and pain.

can handle stress to an optimal level which has been referred to as "eustress". In contrast, the stress which becomes harmful is referred to as "distress". The International Association of Study of Pain (IASP) has defined "pain" as an unpleasant sensory and emotional experience associated with actual or potential tissue damage, or described in terms of such damage (Box 1). Pain is a sensation in a part or parts of the body, but it is also always unpleasant and therefore triggers an emotional experience. Pain is partly contextual. For example, it has been shown that pain sensitivity may or may not differ within the context of a conditioned fear response (3).

There are several common factors that correlate well with the development of stress and pain. In most cases, the causes, the outcomes and the symptoms of these two conditions are similar. Indeed, an increasing number of studies indicate that stress and pain often share a common "cause-effect" vicious cycle of events (Figure 1). This is because prolonged stress can be considered as an upstream event for the development of a chronic painful condition. In reverse, chronic pain can also induce severe stress at the physical and psychological level (4). Interestingly, both stress and pain seem to have a shared evolutionary origin. Certainly, pain is advantageous as it warns the body of potential damages. Similarly, a stress-free life may also be detrimental as an individual may lose his/her ability to react to the different challenges in a stress-free life. At present our understanding of stress, pain and their crosstalk is rudimentary, but these two seems to be different at the molecular, cellular and behavioral level. Thus, it might be possible to mark the boundary between stress and pain. Indeed, studies indicate that mis-regulation of ion channels is a key factor behind the development of chronic pain and other pathophysiological conditions. Therefore pain has been recently considered as a channelopathy (5-11).

So far stress and pain has been analyzed in terms of several factors/stimuli with different properties. Most of these factors can be categorized as physical or chemical stimuli (either endogenous or exogenous component). In addition, psychological stimuli are also involved in modulation of stress and/or pain (discussed later). As several studies have already identified the different physical and chemical stimuli contributing to pain development, this review will not repeat such information in further details. In contrast, this review will highlight the different psychological, neurobiological and biochemical factors and involvement of TRP channels that are relevant in the context of stress and pain.

3. FACTORS THAT GENERATE STRESS AND PAIN

It is known that certain physical stimuli like noxious temperature (hot as well as cold) and mechanical pressure can cause pain. However, the molecular basis of how different physical stimuli induce pain remains poorly understood. Molecular characterization of temperature-induced pain effectively started with the cloning of Vanilloid Receptor sub-type 1 (VR1) (12). This is commonly known as capsaicin receptor and now named as Transient Receptor Potential Vanilloid sub-type 1, (TRPV1) which can conducts a Ca^{2+}-influx in response to noxious temperature like 42°C (12). Subsequently, several other Transient Receptor Potential (TRP) channels were cloned and many of these are activated by noxious stimuli (like high or low temperatures, mechanical pressure) (13). TRPs were previously considered to be molecular detectors for physical noxious stimuli and associated with the transmission of pain signals. Therefore, TRPs are involved in the execution of noxious temperature- and pressure-induced deleterious effects. All these results in general indicate that TRPs are involved in thermosensation and mechanosensation (14). However, later studies confirmed that animals lacking these channels (knockout studies) have normal sensation suggesting the existence of functional redundancy among these closely related ion channels (15-17). For example, TRPV1 knockout mice have no thermal selection when tested against temperature gradients. However, the same animals reveal enhanced mechanical responses. Similarly, TRPV3 and TRPV4 knockout animals reveal a similar thermal preference comparable to wild type animals (18). These contradictory results indicate that TRPs may have overlapping yet different functions and signaling events relevant in the context of physiological sensation and pain.

In contrast to physical stimuli, chemical stimuli-induced acute and chronic pain development is relatively well-studied. So far a large number of studies have been conducted to identify and characterize several compounds (as exogenous or endogenous stimuli) that can induce and modulate acute or chronic pain (19-21). The endogenous components include different steroids and their derivatives, lipid metabolites, inflammatory and immune secretary

compounds (like histamine, interleukins, prostaglandins, bradykinin and others), growth factors (like NGF, BDNF, EGF), neuropeptides/ neurotransmitters (like GABA, SP, NPY), different hormones, other metabolic products, low pH and many other biomolecules (Table 1). These arrays of nociceptive molecules are recognized by a set of molecular detectors present in the nociceptive neurons and thereby induce pain (20). In most cases, different transmembrane-receptors, ion channels (including TRP channels) and pro-nociceptive kinases are the first set of target molecules that are stimulated by these nociceptive stimuli. Availability of these stimuli, expression and activity of these molecular detectors, and changes in the neuronal contacts are the prime factors that regulate the pain transmission and the degree of pain perception (21-23). In last few years significant progress has also been made to unearth the signaling pathways and cellular changes leading to the development of hyperalgesia and allodynia (Box 1). However, the detailed molecular mechanisms and pathways remain unclear and these pathways seem to vary depending on species and the stimuli used (21, 24).

In spite of extensive studies conducted to characterize different factors, still only few have been currently identified that can be considered as key effectors/modulators of pain (21, 25). TRPs not only act as key molecules that integrate several pain producing signaling events but also play a much bigger role as molecular regulators (26). Apart from their role in ionic conductance, these channels interact with several proteins and form dynamic signaling complexes at the membrane alternatively known as the signalplex (27). Further studies are needed to understand how different factors and stimuli can alter the organization, regulation and function of these complexes. A detailed biochemical and cellular understanding of these signalplexes has clinical and pharmacological interest too.

So far a magnitude of work has also been done to characterize stress-inducing physical and chemical factors (termed as stressors) and their effects. In contrast to different forms of pain, understanding the physical and biochemical basis of stress at the molecular level is just at its beginning and remains largely undefined. Though, the number of stressors is large, our understandings about the stressors, their mode of action and effects remain largely fragmented. Often the effects of different stressors differ largely in quality, quantity and from subject to subject. For example, changes in the day-light cycle perceived by individual can also be stressful for some while others may remain unaffected (27). So far very few endogenous bio-molecules have been identified in higher animals that can be considered as stress markers. The correlation of these markers with the actual development of stress also remains disputed. Thus, the outcome of all these studies can largely be categorized in parts: the effect of stressors at the level of metabolism and development of stressor-mediated abnormalities at the level of cell, tissue and/or behavior.

Interestingly, altered levels of a few bio-molecules (such as higher level of steroid hormones) correlate well with the development of stressed conditions. However, the reasons behind this altered level of steroids are not clear (28). It has been demonstrated that school boys who are occasionally bullied have higher levels of cortisol (Box 1) than their peers who are not bullied (29). In contrast, bullied girls seem to have cortisol at low levels (29). Similarly, elevated corticosterone in the amygdala increases anxiety-like behavior and pain sensitivity (30). Similarly, higher level of blood cholesterol positively correlates with the conditions characterized by hypertension, stress and depression (31-32). It has been demonstrated that depressed female primates have higher total plasma cholesterol (TPC) and lower level of high density lipoprotein cholesterol (HDLC) than non-depressed female primates (31). A contribution by the immune system in stress-response has also been demonstrated (33-34). However, it is difficult to make general conclusions based on these studies for several reasons. First, the molecular mechanisms behind the individual to individual differences are not clear. Second, the variability observed in these studies is generally large and often differs from species to species and population to population.

4. PHYSICAL, BIOCHEMICAL AND CELLULAR BASIS OF PSYCHOLOGICAL STRESS AND PAIN

Recent studies have confirmed that psychological state contributes robustly to the manifestation of pain and thus is referred to as psychogenic pain (35). Psychogenic pain has some common symptoms like headache, back pain, or stomach pain. Previously, this type of pain was considered an emotional phenomenon which is exclusively independent of stimulation or damage of the peripheral nervous system. However, later studies indicate that psychogenic pain is more complex in nature. Functional magnetic resonance imaging (fMRI) confirmed that sadness enhances the experience of pain via neural activation in the anterior cingulate cortex and amygdala (36). In a similar context, “Phantom pain” and “emotional pain” have a large degree of psychological association and these forms of pain can affect physiology too. “Phantom limb pain”, is a kind of neuropathic pain which is common in almost 85% of the amputees who report this type of pain in their amputated limb after surgery (37). Emotional pain is also another form of pain where psychological contribution is significant (38). High blood pressure, pain in the chest and heart, an abnormally elevated mood, inflated self esteem, acute insomnia, obsessive-compulsive disorder, anorexia, depression, loss of concentration, and tearfulness, are some of the commonly considered symptoms of stressful situations which are often brought by a romantic break up or by a "crush".

In contrast to pain, understanding the psychological contribution in stress is even more difficult as it affects the “mind-body” correlation by several complex mechanisms. Although a correlation (either positive or negative) exists between “mind-body interaction” and the development of stress and/or pain, how psychological states actually contribute to these conditions remains poorly understood. Why and how different individuals perceive stress with a different threshold level and gradually build or avoid stressed conditions also

Table1. Cross-talk between several stress-related factors and TRP channels

	Compound	TRP channel	Effect(s)
Neuropeptides	Neuropeptide-Y	TRPV1	Suppresses Ca^{+2}-influx via TRPV1
		TRPV1	Inhibits activity of capsaicin-sensitive nociceptors and decrease capsaicin-induced CGRP release
	Substance-P	TRPV1 & TRPV4	Contributes in vasodilation regulated by Substance-P during osmotic stress
		TRPV1	TRPV1 activation results in release of Substance-P from capsaicin -sensitive spinal cord afferent terminals
	CGRP	TRPV1 & TRPV4	Contributes in vasodilation regulated by CGRP during osmotic stress
Neurotransmitters	Dopamine	TRPV1	Activation of TRPV1 excites dopaminergic neurons and increases dopamine release
	NADA (Dopamine-derivative)	TRPV1	Activates TRPV1 and causes retraction of TRPV1 positive neuronal growth cones
	N-acyldopamines	TRPV1	Activate TRPV1 and causes Ca^{2+}-influx
	OLDA	TRPV1	Activate TRPV1, causes Ca^{2+}-influx and pain
	Oleic acid, NAE	TRPV1	Activate TRPV1, causes Ca^{2+}-influx
	Linoleic acid	TRPV1, TRPV3 & TRPM8	Increases open channel block (OCB) activity in which metal ion binds to receptor and decreases its ionic conductivity
	GABA	TRPC4	TRPC4 controls the GABA release from dendrites
	Glutamate	TRPV1	TRPV1 activation induces glutamate release from spinal cord synaptosomes
	Noradrenaline	TRPV1	TRPV1 activation stimulates release of noradrenaline
	Serotonin	TRPV4	Activates TRPV4 and results in Ca^{2+}-influx
Steroids and derivatives	Estrogen	TRPV1	Enhances the expression of TRPV1 channel in c-fibres
	Androgen	TRPV4	Reduces the expression of TRP4 in bovine aortic endothelial cells
		TRPV5	Activates TRPV5 and induces Ca^{2+}-influx
		TRPV1	TRPV1 activation induces expression of androgen receptor in prostate LNCaP cells
	Testosterone	TRPM8	Androgen regulates the expression of TRPM8
		TRPC3	Increases Ca^{2+}-influx in muscles cells
	Progesterone	TRPV4	Decreases the cationic current and Ca^{2+}-influx in human airways, mammary gland epithelial cells and vascular smooth muscle cells
	Insulin	TRPC5	Decreases activity of channels and Ca^{2+}-influx
		TRPV1	Present in islet beta cells and promotes insulin secretion and Ca^{2+}-influx
Protein hormones	Klotho	TRPC3	Interacts with GLUT4 and promotes glucose uptake
		TRPV5	Klotho, a β-glucuronidase hydrolyzes extracellular sugar residues on TRPV5 and increases Ca^{2+}-influx, prevents internalization and inactivation of the channels in Kidney cells
	Leptin	TRPC1 & TRPC4-7 TRPV1	Activates POMC neuron by generating action potential and causes Ca^{2+}-influx Activation of TRPV1 blocks Leptin-CCK regulation
	NGF	TRPV1	Increases expression of TRPV1, CB2, Leptin receptor and attenuate the ischemetic injury in brain
		TRPV4	Activates TRPV4 and sensitizes bladder for urine filling
Growth factors	BDNF	TRPV1	Sensitizes TRPV1 and causes Ca^{2+}-influx
	EGF	TRPC5	Effects rapid translocation, insertion of channels in the plasma membrane and causes Ca^{2+}-influx
	Transforming growth factor α (TGF-α)	TRPV3	Activates channels (in keretinocytes) and regulates proliferation, differentiation and also controls hair morphogenesis
	Transforming growth factor -β1 (TGF-β1)	TRPM7	Induces differentiation of fibroblasts cells and increases the expression of TRPM7
Immuno-secretory compounds	IL2	TRPM4	Prevents in T-lymphocytes and induces Ca^{+2}-influx and IL-2 production during T-cells activation
	IL4	TRPA1	Increases the production of inflammatory molecule during allergic condition in airway lungs
	IL5	TRPA1	Increases the production of inflammatory molecule during allergic condition in airway lungs
	IL6	TRPV1	Sensitizes TRPV1 via PKCδ pathway and produces pain
	IL13	TRPA1	Increases the production of inflammatory molecule during allergic condition in airway lungs
	Histamine	TRPV1/ TRPV4	Activates and excites sensory neurons by producing 12-HPETE, a downstream metabolite of PLA2 and LO (lipoxygenase)
	Bradykinin	TRPA1/ TRPV1	Activates TRPA1 which acts via GPCR and phospholipase-C pathways Causes excitation of vagal sensory airway pathways via nitration of TRPV1
	Prostaglandin	TRPV1, TRPV3 TRPA1	Sensitizes and activates TRPV1 Influences acute nociception and hyperalgesia by activating TRPV3 Directly activates TRPA1
	Macrophage Inflammatory Protein-2 (MIP-2)	TRPC6	Present in neutrophil granulocytes and promotes fast cell migration via rearrangement of actin filament
	IFN-γ	TRPV1	Increases intracellular Ca^{+2} due to production of inflammatory molecule in microglial cells
	NO	TRPV1 & TRPA1	Increases intracellular Ca^{+2} and expression of ion channels in DRG-neurons that helps in nociception
Other metabolites and byproducts	Reactive Oxygen	TRPA1	Increases intracellular Ca^{+2} and membrane current in lung sensory neuron
	Arachodonic acid	TRPV3 & TRPV4	Directly potentiates responses via TRPV3 expressing cells Activates TRPV4 and regulates cell swelling and metabolism of epoxyeicosatrienoic Acid,
	Acetaminophen	TRPV1	Induces analgesic effect by activating TRPV1 at the brain
	Epoxyeicosatrienoic acid (AA-derivative)	TRPC5 & TRPC6	Increases intracellular Ca^{+2} and also helps in translocation of channels to membrane in endothelial cells
	20-HETE (AA-derivative)	TRPC6	Activates TRPC6 channels
	12-(S)-HPETE (lipoxygenase product)	TRPV1	Activates TRPV1 and causes nociception
	15-(S)-HPETE (lipoxygenase product)	TRPV1	Activate TRPV1 and cause nociception
	5-(S)-HETE (lipoxygenase product)	TRPV1	Activates TRPV1 and causes nociception
	Leukotriene B4 (lipoxygenase product)	TRPV1	Activates TRPV1 and causes nociception
	LPS	TRPV2	Increases mobilization of intracellular Ca^{+2} via TRPV2 and IP3 receptor in macrophage cells

remains unclear. However, the psychological contribution in manifestation of stress and pain can further be explained on the basis of biochemical pathways. For example certain forms of pain can be reduced by using placebo and/or certain psychotropic drugs (23, 39-42). Interestingly, the placebo-induced analgesic effect is often gender specific suggesting that sex hormones might also be involved in this process (43). These placebo-induced analgesic effects can

be reversed by using Naloxone (a competitive antagonist of opioid receptors) suggesting that placebo, which is equivalent to a positive expectation, stimulates opioid pathways (44-48). In a similar fashion, Duloxetine (a balanced serotonin and noradrenaline reuptake inhibitor) is used for the treatment of major depressive disorders, urinary stress, incontinence and the management of neuropathic pain associated with diabetic peripheral neuropathy (42). Post-operative Phantom-pain can also be blocked by tricyclic antidepressants, namely by Milnacipran and Venlafaxine (a class of novel serotonin and noradrenaline reuptake inhibitors) (37, 41, 49-51). These indicate that psychology and neuro-chemical signaling events involving serotonin receptors play a role in case of phantom pain. Notably, memantine, milnacipran and ketamine (inhibitors of NMDA-receptor) effectively block phantom pain indicating that the involvement of NMDA-receptor in this process (41, 50, 52-53). Neuropathic and chronic pain inducing stimuli are known to increase the neuronal secretion of β-endorphin and down regulate transmission through the central μ-opioid and dopaminergic neurons (54). Often more than one pathways may interact functionally. For example, corticotropin-releasing factor and serotonin together contribute to the anxiety-related disorders (55).

A few studies have indicated that genetic factors contribute in the perception and amplification of stress and pain. Due to genetic variation, individual responses to local and changing environments varies and often initiates psychological and/or physical stress (56). For example, it is well-characterized that people exhibit changes in mood and behavior with changing seasons which are often characterized by anxiety, depression and stress. These changes are known as “seasonality problem” and termed as “seasonal affective disorder” (SAD) which is mostly hereditary. Indeed, gene variants of GABA (A) receptor, the μ-opioid receptor, the serotonin transporter, catechol O-methyltransferase (COMT), monoamine oxidase (MAOA), alpha (2)-adrenergic receptor, brain-derived neurotrophic factor and the anginotensin-converting enzymes are known to affect the HPA-axis in a different manner (57). The involvement of genetic factors in psychological stress and in schizophrenia (and several other psychological disorders) is best illustrated by the serotonin metabolism and signaling pathways (58). A few studies have indicated that promoter repeat length polymorphism of serotonin transporter (5-HTT, which is encoded by a single gene SLC6A4) correlates well with the onset of the mood and/or seasonal affective disorders (59-61). The promoter is characterized by insertion/deletion of 44-bp which generates either long or short allele of 5-HTT respectively. This shorter allele is a well-established risk factor for stress, anxiety, disorder in mood changes, food uptake and obesity in adolescents (54-64). In agreement with the involvement of serotonin in several disorders, enzymes involved in serotonin biosynthesize and factors involved in recognition and/or uptake of serotonin are also important genetic factors that contribute in psychological, physiological disorder (65). For example, mutations in the gene encoding for the tryptophan hydroxylase (TPH, the rate-limiting enzyme involved in serotonin biosynthesis) reveal psychological and physiological abnormalities including stress (65-66).

5. HPA-AXIS IN STRESS AND PAIN: IMPORTANCE OF TRP CHANNELS

Involvement of HPA-axis in stress was first demonstrated experimentally by H.F. Harlow. His experiments confirmed that physical separation of infant from mother induce strong stress to the infant as well as to the mother (67). Interestingly, prolong stress perceived in the early phase of development seems to have a long-lasting effect on learning and memory formation and seem to affect neural circuit like HPA-axis and limbic system (hippocampus, amygdala, prefrontal cortex etc.). At the behavioral level, attachment of infants with mother helps them to develop their learning circuit which is induced by maternal odor and nursing. Thus separation of infants from mother during early life shows several abnormalities in the later part (68-70). Often, the stress perceived by mother can be transmitted to the next generation too. For example, stress applied to rodents in the form of a physical exercise during pregnancy results in transient increases in postnatal hippocampal neurogenesis in the offspring after birth (71). Nevertheless, several studies indicate that psychology plays an important role in development or reduction of stress and pain. The exact nature, extent and pathways by which psychology modulates the mind-body interaction are different. Notably, the underlying mechanisms are not clear yet though the involvement of HPA-axis in stress and pain seems to be prominent (33, 72).

The altered behavior and function during stressful and painful conditions can partly be explained by changes in synaptic adaptations, neuronal structure, function, networking and alteration in the brain structures. Different forms of stress and pain can induce changes in the neuronal density (brain volume), number, subtype, connectivity, function, synaptic plasticity, neuro-immune interactions, neuro-endocrine secretion and regulation too. In that regard, changes in neuronal plasticity have been identified as a major link between stress and mood disorders (73). Stress seems to have a direct effect on the structure – function – regulation of the brain. For example, the amygdala plays a role in processing of anxiety and threat-related stimuli which are crucial in stress responses (74). A change in gray matter density within the bilateral amygdala has been associated with a stress response. In this context, reductions in stress correlate positively with decreases in right basolateral amygdala gray matter density (75). In a similar manner, acute psychosocial stress reduces cell survival during adult hippocampal neurogenesis (76). Similarly, stress-induced prefrontal cortical impairment has been linked with the development of mental illness. In addition, chronic stress induces contrasting patterns of dendritic remodeling in hippocampal and amygdaloid neurons and results in changes in the neuronal contacts as well as synaptic connectivity (77). In contrast, stress reduction correlates with structural changes in the amygdala (75). Reductions in stress also correlate positively with decreases in right basolateral amygdala gray matter density (75).

Similar to several stress-related disorders, changes in the brain structure and hypocortisolism seem to also occur during several painful conditions and thus have been considered as common characteristics of some functional pain syndromes (78-80). For example, patients with chronic pain perform impaired emotional decision-making tasks (79). By using Magnetic Resonance Imaging (MRI) technology, it was observed that patients with chronic back pain (CBP) had a reduction in the outer layer of the brain and have 5–11% less neocortical gray matter volume than control subjects (80). The magnitude of loss after normalization with the skull volume is equivalent to the loss observed following 10-20 years of normal aging. These studies strongly indicate that CBP is accompanied by brain atrophy and involves thalamocortical processes. It is noteworthy to mention that hippocampus plays a role in learning and spatial memory formation which is vulnerable in stressed conditions. Similarly, impairment in the prefrontal cortical has been linked with the development of mental illness induced by stress. A complementary effect on gray matter volume has also been observed by studying subjects who perform meditation regularly (81). It is well accepted that meditation has several positive effects and it improves psychological and physiological states (82). By using MRI it has been shown that long-term meditation correlates well with anatomical changes of the brain, especially in the right orbito-frontal cortex (as well as in the right thalamus and left inferior temporal gyrus. In addition, people performing regular meditation show significantly larger volumes of the right hippocampus. It is important to mention here that these regions are involved in emotional regulation and response control.

Noteworthy, TRPs can play a significant role in all these above-mentioned processes. Recent studies confirmed the physical and functional presence of different TRP channels (especially TRPVs and TRPCs) in specific regions of brain, namely in the thalamic and hypothalamic nuclei, locus coeruleus, periaqueductal gray, cerebellum, cortical and limbic structures which regulate the neuronal functions and networking in presence of stressor (83-86). In the same notion, involvement of TRP channels in schizophrenia and other neuropsychiatric problems have been suggested (87). Several endogenous and small molecules (such as endovanilloids, anandamide, estrogen, other steroids) have also been identified in the brain and other regions of central nervous system suggesting that these compounds can activate several TRPs either in a specific or non-specific manner (Table 1). For example, NADA, an endovanilloid can regulate neuronal structure, function and synaptic transmissions by activating TRPV1 (88). It has been reported that under stressed conditions, endocannabinoids within the paraventricular nucleus of the hypothalamus decreased excitatory inputs to HPA and cause release of corticotropin hormone into the portal blood at high levels as well as ACTH from anterior pituitary and corticosterone from adrenal gland. Similar results in general suggest that endogenous ligands of TRPs can regulate the behavioral responses and synaptic effects.

It is well established that TRPs regulate neuronal differentiation, networking and synaptic functions. Differential expression of TRP channels in DRG neurons helps in development of Isolectin-B4 (IB4) positive neuron (89). This in turn contributes to the maintenance of functional heterogeneity in sensory neurons involved in perception of touch (mechanoreceptors), temperature (thermoreceptors) and pain (nociceptor) (89). TRP channels are also involved in the regulation of neuronal functions which are related to cognition, pain perception and in neuropsychiatric disorders (90-91). For example, TRPV and TRPC channels are involved in neuronal survival, regulation of growth cone migration and neuronal networking (92-96). TRPC channels are involved in the migration of the growth cone and neuronal connection formation (93). Activation of TRPV1 also results in shortening of the IB4-positive nociceptive neurons and in the protection of hippocampal neurons against oxidative stress (97). In the same notion, TRPV1, TRPV4 and several other TRPC channels are localized in the synaptic sites (88, 98-99). At the synaptic sites, TRPs can modulate the synaptic organizations, regulations and transmissions and are involved with the release as well as uptake of several neurotransmitters and neuropeptides (Table 1). For example, recently we demonstrated that TRPV1 activation increases spine lengths (88). TRPV1 regulates metabotropic glutamate receptor and thereby regulate the function of dopaminergic neurons in rat (100). Activation of TRPV1 also induces release of substance-P and glutamate from synaptic sites. In the same notion, TRPC4 contributes to the control of GABA release from dendrites and can modulate the synaptic output. TRPV1 present in hippocampus neuron is known to increases long-term potentiation (LTP) and decrease long-term depression (LTD) (101). Genetic and behavioral experiments also confirmed that TRPV1 knockout animals (*trpv1* -/-) have reduced anxiety, conditioned fear, and hippocampal LTP (102). The increased LTP prevents the synaptic plasticity in hippocampus area and helps in learning in acute stress. However, the exact involvement of TRPV1 in LTP and LTD in CNS is still unclear. This is due to the fact that endogenous presence of TRPV1 in the microglia cells may add complexity under stressed conditions.

6. PHYSIOLOGICAL EFFECT OF CHRONIC STRESS AND PAIN

Stress is known to alter behavioral responses to certain stimuli which correlate with changes at the cellular and/or molecular level. As a result, neuronal connections, morphology as well as function are altered. These neuronal changes seem to be more prominent at the level of dendritic spines. While detailed characterizations of the biochemical and metabolic pathways that underlie these changes are still fragmentary, these changes have largely been analyzed at the level of gene expression and proteome. However, it is difficult to conclude if these changes in gene expression and the proteome are cause or effect of stress and/or painful conditions. Here we describe some of these changes in details.

6.1. Changes in the proteome and local protein synthesis

Few studies confirmed that the total proteome of tissues and cells, especially neurons are altered drastically

when subjects are exposed to chronic (both physical as well as psychological) stress and/or pain. Such studies have identified key proteins that show differential expression in normal and stressed/painful conditions (103-105). For example, 17 proteins were identified which are involved in anti-nociception (105). These proteins mostly represent factors involved in signal transduction, vesicular trafficking and neurotransmitter release, energy metabolism, and ion transport. Another study addressed the proteome changes of the synaptosome (isolated from spinal cord dorsal horn), especially after peripheral nerve injury (104). This study identified 27 proteins that are involved in transmission and modulation of noxious information, cellular metabolism, membrane receptor trafficking, oxidative stress, apoptosis, and degeneration. Another study indicated that nearly 200 proteins (representing cytoskeletal proteins, enzymes and proteins associated with oxidative stress) are up-regulated in hyper-excitable nerves (105). Notably, this work indicated that the differential expression was due to local protein synthesis which was altered in hyper-excitable nerves, a condition which correlates well with peripheral nerve injury-induced neuropathic pain.

Apart from direct regulation at the transcript level, post-transcriptional regulation seem to be another major mechanism by which chronic stress and pain can alter the proteome. Indeed, a proteomic study has revealed changes in the protein but not in the mRNA level of some proteins (unc-18 protein homolog 67K, CRMP-2 and CRMP-4) which are involved in the neurotransmitter release and/or axon elongation (105). The abundance of these proteins is regulated by post-translational regulation like proteolysis and/or phosphorylation. Similarly, another report confirmed the involvement of stress-granules, P-bodies and other transcript-related regulatory factors in stress and pain (106). For example, formation of stress-granules and P-bodies in DRG-neurons is regulated by many stress-related signaling events (106-107). In summary, these recent studies indicate that total protein synthesis at the cellular level and specific protein synthesis in sub-cellular regions like in dendritic spine have a profound role in stress and pain. Recently this hypothesis has gained credibility as it can explain many of the observed changes in the proteome in response to stress and pain.

Recent studies have demonstrated the involvement of microRNAs in the different forms of pain and stress (106-113). DRG-neurons of adult rats express three micro RNAs, namely miR-96, miR-182, and miR-183 which are involved in the regulation of mechanical hypersensitivity (106). Interestingly, miR-96, miR-182, and miR-183 are down-regulated in case of spinal nerve ligation, an experimental condition which correlates strongly with the development of neuropathic pain (106). MicroRNA-mediated regulation of dopaminergic neuron differentiation, expression of nociceptor-associated mRNA transcripts like Nav1.8, P2xr3, and Runx-1 and μ-opioid receptor has been linked with the regulation of pain (107-110). Regulation of TRPs by micro-RNA has also been reported recently. It has been shown that in kidney, the expression of PC2 is regulated by mir17 and RNA-binding protein Bicaudal C (114). However very little has been investigated in this aspect and certainly more studies are needed to demonstrate the involvement of microRNAs in the regulation of stress and pain. The small RNA and microRNA-mediated regulation of stress and pain might be of pharmacological interest also.

6.2. Changes in the novel PKCs-mediated signaling events

Stress and different forms of pain have strong effects on the peripheral and central nervous system through several neuro-chemical pathways. However, among all distinct pathways, activation of different PKCs, mostly atypical and/or novel PKCs (this group of PKCs are activated in a Ca^{2+}-independent manner) are the common pathways reported in several stress and pain conditions (21, 115-117). Interestingly, the activation of these novel PKCs in response to different stressors and types of pain correlates well at the behavioral level as well as the cellular level. For example, the level of PKCε increases in stress and pain (mechanical as well as thermal), and modulates NGF and mitogen activated protein kinases (MAP kinase)-mediated signaling events (117). Mechanical stress can also activate PKCδ and thus activate the Smad pathway in osteoblasts present in bone. This in turn enhances interleukin-11 (IL-11) expression and this may affect several other systems (116). Mechanical stress also induces sarcomere assembly which alters the morphology of cardiac muscles, a process where PKCs are involved (117). In the same notion, up-regulation and redistribution of PKCδ is observed in chronically hypoxic heart (115). PKC-mediated pathways are also involved in other stress signaling, such as oxidative stress.

6.3. Changes in the neuronal organization

Chronic stress induces transient plastic changes and may even induce long-term changes in the dendritic spine and neuronal patterns in the amygdala. For example, chronic unpredictable stress had little effect on CA3 pyramidal neurons and induced atrophy only in BLA-bipolar neurons (75-76). Thus chronic stress can induce contrasting patterns of dendritic remodeling in neurons of the amygdala and hippocampus. In addition the structures of neuronal ends and dendritic spines are altered. Even the distribution of neuronal ends in the peripheral tissue and spinal cord can be altered in response to stress/pain (22). Stress is known to induce synaptic changes. For example, stress-induced changes in synaptic connectivity have been shown in the neurons of the basolateral amygdala.

Stress and pain may have a role in “unsilencing of dendritic spines”, a mechanism by which activation of “silent synapse” can occur and result in activity- and sensory-dependent refinement of neuronal circuits. Silent spines are morphologically similar to other dendritic spines though these entities do not contribute to the total neuronal communications. Thus activation of silent spines can be one of the key phenomena involved in chronic manifestation of the stress and/or pain. This notion is supported by observations that β-estradiol, heat and mechanical pressure increase the neuronal output via

sensory neurons per unit area of the skin (118-119). However, further work is needed to confirm this.

7. TRPS AS DETECTORS AND MEDIATORS OF STRESS AND PAIN

As TRPs can be activated by different physical and endogenous chemical stimuli (Table 1), these channels have role in the regulation of several physiological and metabolic functions. The expression of TRPs is often tissues-specific which correlate well with the development and functions of specialized organs. Indeed, TRPs are critical elements that define the regulation, structure, development and function of certain organs, tissues and cells. For example, endogenous activity of TRPs are important for proper Ca^{2+}-signaling and functioning of brain, spinal cord, liver, immune cells, pancreatic cells, skin cells, keratinocytes, retinal cells, cardiac mayocytes, gut and many other specific organs and cells. So far several studies have confirmed (or indicated a strong correlation) that altered expression, function and/or regulation of TRPs are key changes which induce patho-physiological conditions like stress, neuropathic pain and cancer. For example, TRPV1 and TRPA1 participate in visceral hyperalgesia in chronic water avoidance stress (120). TRPM2 and TRPV4 are involved in oxidative stress-induced cell death of hippocampal neurons (121). TRPs are also involved in programmed death of different type of cells in response to stress-signaling. Rats exposed to chronic stress reveal reciprocal change in TRPV1 expression induced by corticosterone (122).

In a defined cellular system, TRPs mainly act as molecular detectors of stress- and pain-inducing stimuli (physical and chemical). TRPs also recognize several endogenous noxious compounds and their different metabolites that are often associated with the development of stress and pain (123). For example, a number of lipid derivatives can activate a battery of TRPs (Table 1). So far the effects of only limited lipid derivatives on few TRPs have been explored and the effect of the entire array of these lipid derivatives on all the TRPs remains untested. A better understanding of the effect of different lipid derivatives on all TRPs has medical and pharmacological importance. Apart from the lipid derivatives, several TRPs can also be activated by estrogen, endrogen, testosterone, cortisol and many other steroids (Table 1). In addition, the expressions of TRPs are often under the regulation of these steroids, neurotransmitters and neuropeptides (Table 1). These studies may explain why most of the steroids that are often used as pharmacological drugs exert side effects like pain and stress. Cholesterol, which may be up-regulated during stress, seems to have a regulatory effect on the function of TRPs too. This is due to the fact that most of the TRPs are located in the lipid raft regions (defined as cholesterol-rich lipid micro-domains) and function/behave differently when they are present in the lipid raft. In the same notion, recent studies confirmed that TRPs may have specific cholesterol-binding motif sequences and the cholesterol binding has regulatory roles on the ion channel properties (124-125). All this studies suggests that effects of neurotransmitters, neuropeptides, steroids and other noxious compounds on TRPs are relevant in the context of stress and pain and these effects are conserved to some extent throughout the evolution.

Activation of TRPs induces influx of Ca^{2+} and other cations. Thus TRPs act as mediators of different cellular signaling events and can have direct and opposite effects related to stress and pain. While the basal expression and endogenous activation of TRPs are involved in maintaining homeostasis for several ions, over-activation and constitutive inactivation seems to have major setbacks on the cellular system and are linked with the development of stress and pain. For example, over-stimulation of TRPs leads to an influx of excess Ca^{2+} which is generally associated with the cell death (126). Therefore deletion of certain cell types may have an adverse effect on tissue homeostasis. TRPs are also important for cellular uptake of Co, Fe, Ni and other important metal ions that are essential for several physiological and metabolic functions like bone formation, vitamin synthesis and maintenance of urine composition.

8. HOW TRPS REGULATE METABOLIC PATHOGENESIS IN STRESS AND PAIN?

TRPs are ubiquitously expressed in many tissues and cell types and have considerable functional and/or regulatory diversities. The distribution of TRPs in several tissues, like kidney, pancreas, and lungs is important for tissue specific metabolism and physiological functions. Recently, involvement of TRPs in different types of cancer and cancer pain has been demonstrated (127). As there are few reviews which already have addressed the involvement of TRPs in cancer, this review will not repeat the same. While cancer cells can certainly a factor for stress at the gross level, if secretion of noxious components from cancer cells are specifically regulated by and/or act on TRPs that remain to be explored. In addition to cancer, TRPs are regulated by a number of exogenous and endogenous components including several metabolic byproducts (Table 1). Therefore, misregulation of TRP's function leads to various pathophysiological disorders. Indeed, TRPs are involved in disorders like diabetes, obesity, dyslipidaemia, metabolic syndrome, atherosclerosis, metabolic bone diseases, male sterility and electrolyte disturbances which are linked with stress and pain (Figure 3) (128). TRPs are also involved in addiction and thus in behavioral responses. Therefore, the link between metabolic pathogenesis and the deregulation of TRPs are of pharmacological, clinical, social and economic importance as this will help to identify and develop potential means for better treatment (128). Here we discuss in detail the involvement of TRPs in metabolic disorders.

8.1. Involvement of TRPs in obesity

Whole genome scanning analysis for obesity genes implicated few TRPs, namely TRPC3, TRPC4, TRPM8, TRPP2, TRPML and TRPV6 which may play important roles in obesity (129). The best example of the involvement of TRPs in obesity was provided by TRPV1 and involvement of other TRPs in obesity needs further characterization. It has been reported that the consumption

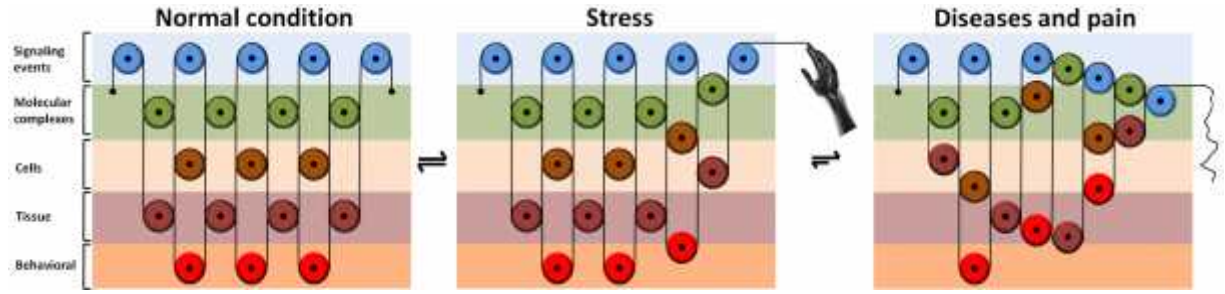

Figure 2. Stress is an altered state of mind and body which threatens biochemical and cellular balance, equilibrium and/or behavioral harmony which eventually disturbs the physiological, psychological and metabolic homeostasis of individual. Individual's function and behavior in stressed and painful conditions can be explained in terms of an organized set of signaling events controlled by cellular and molecular complexes. These can be best portrayed as multiple pulleys and levers connected to each other where each pulley denotes a key event essential at biochemical, cellular or tissue context. In stressed condition, the organized setup is challenged fully or partially but still remains functional. This setup may come back to its initial condition in absence of the prolonged and/or strong challenge. However, further challenges and stretching of the system results in an altered state where further adjustment is not possible. As a result of this prolonged stress and/or pain, the mind-body balance becomes minimum.

of chili in food increases the oxidation of fat present in adipose tissue of both mice and humans suggesting a potential role for TRPV1 in that process (130). Indeed, capsaicin decreases obesity in a dose-dependent manner by increasing oxidation of fat molecules (131). TRPV1 regulates food absorption, emesis, colitis and also regulates the gut - brain axis mainly by responding to endovanilloids and endocannabinoids (132-133). Pancreatic sensory nerves as well as pancreatic cells express TRPV1 and activation of TRPV1 induces preadipocyte differentiation, obesity-induced chronic inflammation and fat distribution (134-136). TRPV1-null mice are smaller and exhibit significantly greater thermogenic capacity compared to wild-type mice when supplemented with 11% fat diet (136). Interestingly, genetic deletion of TRPV1 is protective against obesity only in young animals. Aged TRPV1 knockout mice are more obese than their wild-type littermates (137). The reasons for this specific effect in the young stage are not clear. This probably indicates that factors, which are different in juvenile and adult stages, may control obesity through TRPV1. However, further studies are needed in this context.

The TRPV1-positive sensory nerves present in the intestine are activated by capsaicin and other spices and cause increased blood flow in intestinal region. This in turn reduces visceral adiposity but exerts very little effect on body weight (138). However the role of oral capsaicin on visceral adipogenesis is debatable as the oral capsaicin get metabolized before absorption from the gut lumen and thus very little remains available for circulation in adipose tissue (138). Capsaicin can also modulate energy balance and obesity by modulating signaling pathways. Recently, Kang *et al*. showed that capsaicin can suppress obesity-induced inflammation through nuclear factor (NF)-κB inactivation and/or PPAR-γ activation in the adipose tissues of obese mice (139). Taken together it suggests that TRPV1 and other TRPs are involved in food absorption and obesity regulation. These results are in agreement with the fact that in case of chronic stress, eating behavior is altered and appetite is reduced due to persistent high level of cortisol in circulating blood which activate the *ob* gene that causes obesity (140). Involvement of TRPV1 in obesity can also be explained by the crosstalk between TRPV1 with Cholecystokinin (CCK, released postprandially and elicits satiety signals) and the leptin (a circulating protein involved in the long-term regulation of food intake and body weight by inhibiting the food uptake) (141-144). Capsaicin-sensitive vagal primary afferents control the release of CCK. In reverse, leptin also affects capsaicin sensitive nerves. This feedback mechanism is supported by the fact that capsaicin stimulates electrical vagal nerve which in turn control the food intake and body mass (141). TRPV1 activation also blocks Leptin-CCK action, abolished the inhibitory effects of leptin and metabolic response to abdominal sepsis (142-144).

8.2. Involvement of TRP channels in diabetes mellitus

Diabetes mellitus is a life-style related metabolic disorder in which level of blood glucose, insulin secretion and insulin sensitivity are defective. Several TRP channels act as mediators of oxidative stress and have been associated with these disorders (126, 145). For example, TRPC, TRPV and TRPM channels are expressed in the pancreas and are involved in the regulation of insulin secretion and maintenance of Ca^{+2}-homeostasis (146). However, among all TRPs, TRPV1 seems to play an important role in diabetes. The TRPV1 containing sensory nerve fibres present in the pancreas regulate insulin secretion (147-148). Apart from the sensory nerve ending, TRPV1 is also present in islet β-cells, in the RIN and INS1 β-cell lines where activation of TRPV1 promotes insulin secretion by increasing Ca^{2+} concentration. Interestingly, either a TRPV1 inhibitor or EDTA (a Ca^{2+}-chelator) prevents this secretion (148). Secreted insulin binds to insulin receptors in the brain and TRPV1-positive sensory neuronal junctions and lowers the activation threshold of TRPV1. Subsequently, Ca^{2+}-influx mediated by TRPV1 induces local release of neuropeptides (e.g. substance-P, CGRP). In that context, recent studies have also shown that insulin not only sensitizes TRPV1 on sensory nerve endings but also increases the release of calcitonin gene-

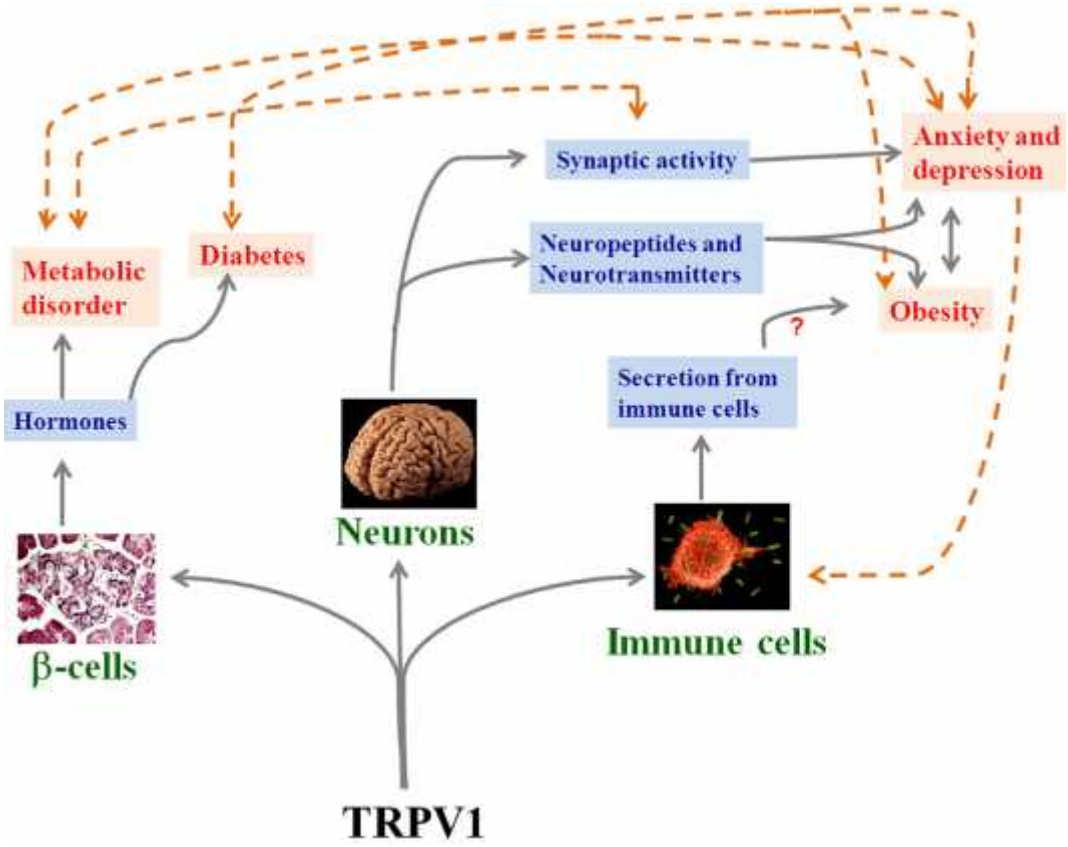

Figure 3. Involvement of TRP channels in stress. TRPV1, a member of TRP channel is present in different cells, like in neurons, pancreatic-β cells and immune cells. TRPV1 can regulate the secretion of neurotransmitters, neuropeptides, hormones, immnuochemicals and many other substances respectively. These substances in turn can induce altered synaptic activity, metabolic disorders, diabetes, obesity, anxiety, depression and many other physiological and psychological abnormalities relevant in stress and pain.

related peptide (CGRP) from pancreatic islets (149-150). The released CGRP provides a negative feedback regulation by reducing insulin release from islet β-cells. Razavi *et al.* demonstrated a pivotal role for TRPV1 in type-1 diabetes (151). In this case, T cell-mediated death of pancreatic β-cells results in insulin deficiency (152). TRPV1-positive sensory neurons in the pancreas also control islet inflammation and insulin resistance. It has been reported that elimination of these neurons in non-obese diabetic mice (NOD-mice) prevents insulitis and diabetes, despite systemic persistence of pathogenic T-cells (152). It seems that TRPV1 regulates insulin level in stressed condition and this regulation also involves cortisol and epinepherin, which are present in high-level in stressed conditions.

Apart from TRPV1, TRPV5 and TRPV6 are also involved in diabetes by regulating insulin secretion under the control of vitamin-D level (153). Earlier studies suggest that Vitamin-D is essential for normal insulin secretion and dietary intake of Ca^{+2} in pancreatic tissue. This is evident as insulin secretion is impaired in vitamin D-deficient rats but can be restored by 1,25 (OH)2D3 supplementation because the expression of TRPV5 and TRPV6 is low in case of vitamin-D deficient rat (153). In a similar manner, TRPM2 is activated by hydrogen peroxide causing Ca^{2+}-influx and thereby regulating insulin secretion in rodent and human β-cells (154- 155). TRPM3 also regulates β-cell activity in response to steroids (156). However, detailed research is required to elucidate how these TRPs regulate insulin secretion and determine their roles in the pathogenesis of diabetes.

8.3. Involvement of TRPs in addiction and neuropathy

TRPs are extensively involved in alcoholism, smoking and other addictions which are life-style and stress-related phenomena that lead to several metabolic changes subsequently. Consumption of alcohol is a chronic and clinical problem that gives rise to several physiological manifestations like liver disease, pancreatitis, gastrointestinal and neurological disorder e.g. polyneuropathies which are common in alcohol addicted patients (157). Ethanol-induced peripheral neuropathy develops in as many as 48% of chronic alcoholics and often involves the development of painful hyperalgesia via mechanisms that are largely unclear (158-160). Interestingly, TRPs seem to be involved in these addictions and alter the state of physiology by several mechanisms.

Endogenous TRPs are also present in various parts of the brain, namely in substantia nigra, hippocampal pyramidal neurons, hypothalamus, brainstem and cortex (83-86). These endogenous TRPs can affect the HPA-axis and thus may account for these addictions. TRPs share a functional cross talk with other receptors including opioid receptors that are involved in addiction. For example, blockade of opioid receptor affects the processing of thermal stimuli by neurons (161).

Interestingly, some of addictive agents directly activate TRPs at pharmacological concentrations. For example, ethanol can directly activate as well as potentiates TRPV1 (162). In the presence of ethanol the threshold for heat activation of TRPV1 decreases from 42°C to 34°C, at which spontaneous activation of TRPV1 can occur in the tongue and skin (163). Other TRPs are also involved in the development of addictive behavior. For example, TRPM8 is also involved in ethanol-induced behavioral response (164). TRPs are also involved in nicotine addiction (165). Interestingly, the effect of nicotine on TRPs seems to be conserved throughout the animal kingdom. Xu *et al.* showed that the TRP1 and TRP2 in *C. elegans* are involved in nicotine sensitivity (166). Similarly, Nilius *et al.* also showed that nicotine directly activates TRPA1 (167). These studies may explain why nicotine patches produce some burning sensation, itching and skin irritation.

Alcoholism apparently changes lipid metabolism and signaling events via opioid receptors, μ-opioid receptors and other TRPs which in turn modulates the synaptic structure and functions leading to ethanol-induced metabolic disorders (168). Indeed, regular ethanol uptake increases the levels of endocannabinoids in brain, decreases AEA (169-170) and the expression of CB1 receptors during chronic ethanol-induced dependence and withdrawal (171). Thus it is possible that addictive ethanol intake modulates the endocannabinoid levels which in turn alter the behavior through actions on both CB1 and TRPV1. It was also reported that the μ-opioid receptor (MOP) agonist morphine can inhibit ethanol-activated TRPV1 responses by decreasing cAMP-dependent PKA pathway (172). However, recent studies indicate that potentiation of TRPV1 by ethanol can modulate the PIP_2 interaction with TRPV1 and this potentiation is not sensitive to opioids (173). Consistent with these observations, TRPM8 reveals less ionic conductance in response to ethanol by regulating the PIP_2 interaction with TRPM8 (164). How ethanol, nicotine and other addictives modulate different TRPs requires more studies and these studies may help to further understand addiction and other related physiological problems.

Progress has also been made to understand the role of TRPs in chemotherapy-induced neuropathy. This is particularly important for cancer treatment where Taxol, a microtubule stabilizer-based drug is routinely used as a life-saving chemotherapeutic agent. Why administration of Taxol produces strong neuropathy including other psychological and physical stress is not clear (174). However, TRPs, especially TRPV1 and TRPV4 seem to be involved in this Taxol-induced neuropathy. For example, administration of TRPV4-specific antisense oligodeoxynucleotides to the spinal cord reduces the expression of TRPV4 in sensory nerves and also abolishes Taxol-induced mechanical hyperalgesia and attenuates hypotonic hyperalgesia by 42% (175). This indicates that TRPV4 is involved if not essential in Taxol-induced neuropathic pain. This is in full agreement with the fact that TRPV4 and TRPV1 interacts with polymerized microtubules and with soluble tubulin dimer by their C-terminal cytoplasmic region (176). Though the exact mechanism is not clear, TRPV-tubulin complexes seem to be involved in multiple signaling events including neuropathy. Further detailed studies are required to clarify this aspect.

8.4. Involvement of TRPs in ageing

Aging is influenced by complex factors such as circumstances, living habits and genetic backgrounds. Though the exact molecular mechanism of aging has not been elucidated yet, premature aging has been considered as a stress-related problem. Recent studies have pointed that TRPs are involved in the aging process by several means. In case of chronic stress, endogenous corticosteroid level is high and the expression of respective receptor is low. This results in imbalance in Ca^{+2}-homeostasis and causes ageing of hippocampous neuron, a process where involvement of TRPs is plausible. Similarly, the ageing of human skin is induced by both intrinsic ageing and photo-ageing processes (176-177). It has been reported that TRPV1 channels play an important role in heat shock-induced MMP-1 expression in human keratinocytes in which the expression of some matrix metalloproteinases (MMPs) is up-regulated (178-179). Enhanced MMPs cause degradation of dermal collagen during UV-induced photo-ageing.

TRPs are also involved in aging process by regulating the anti-aging hormone, namely Klotho, a type I membrane glycoprotein. The extracellular domain of Klotho has two tandem copies of a β-glucuronidase-like sequence, which can be released as soluble factor after cleaved by metalloproteinases such as ADAM10 and ADAM17 (180). It has been demonstrated that Klotho regulates TRPV5 (181). The α-Klotho co-localizes with TRPV5 in the distal convoluted tubule in the kidney. Moreover, Ca^{2+}-uptake is increased in cells that are positive for both TRPV5 and Klotho as compared to cells that express only TRPV5. Interestingly, sugar residues seem to be important for TRPV5 activation. This is evident by the fact that salicydase, endo-F or Klotho treatment results in the activation of TRPV5 (181). Extracellular soluble Klotho induces deglycosylation of TRPV5. This retains TRPV5 at the plasma membrane for a longer time and also prevents its recycling. Therefore Klotho not only stimulates TRPV5 but also accumulates more TRPV5 in the plasma membrane. In agreement with the regulation of TRPV5 by Klotho, age-related disorders are observed in many TRPV5 expressing tissues like kidney, lung, bone, gastric wall and in the skin of Klotho knockout mice. It remains to be explored whether other TRPs are also involved in the aging process.

8.4. Involvement of TRPs in male sterility

It is well known that emotional and psychological stress has deleterious effect on reproductive abilities and results in decreased conception (182-183). But how stress actually modulates these aspects are not clear. Recent studies indicate that TRPs are involved in this process. So far several TRPs have been detected in the spermatozoa and in mature sperm cells. Notably, the localization of TRPs in the sperm cells is conserved throughout the evolution and thus somewhat functionally important. The involvement of TRPs in the sperm motility and fertility seem to be important as these channels allow Ca^{2+}-influx. In *Drosophila*, TRPC homolog (TRP-3) is present in intracellular vesicles of spermatids and after activation these vesicles translocate to the cell membrane (184). In human sperm cells, TRPV1 is located in the post-acrosomal area and in the mid-piece (185). In addition, several endogenous stimulators have been identified in the seminal plasma and other reproductive fluids. For example, N-acylethanolamides (NAEs) and lipid derivatives able to activate TRPs are present in seminal plasma as well as in other reproductive fluids (186). There are several other endogenous lipid ligands like arachidonylethanolamide (AEA; also known as anandamide), palmitoylethanolamide (PEA), and oleoylethanolamide (OEA) that are present in seminal plasma and oviductal fluid and can therefore regulate the localization of the TRPV1 in sperm cells (187). Activities of TRPs seem to be important for the sperm acrosomal reaction as inhibition of TRPV1 inhibits sperm fusion with oocytes (185). Excess production of reactive oxygen species (ROS) (a condition relevant in oxidative stress situations when superoxide anion, hydroxyl radical, nitric oxide, peroxides, and peroxynitrile are produced more and/or antioxidant enzymes are insufficient) can also exert deleterious effect on sperm cells via TRPs (188-189). In normal conditions, ROS have an important physiological role and are required for sperm capacitation and acrosomal reaction. Excess ROS generation may results in immature and abnormal spermatozoa leading to male sterility.

9. CONCLUSION AND FUTURE OUTLOOK

In the last few years' significant progress has been made in understanding pain and stress at the molecular, cellular, psychological and behavioral level. Interestingly, both stress and pain seem to have a shared evolutionary origin as these processes help individuals to avoid unpleasant environments and cope better with different adverse situations. Ultimately, this leads to better adaptation. As stress and pain are complex disorders having environmental, genetic, physical and/or psychological backgrounds, a more "tailor-made" approach to cure stress and pain is required. It is relevant to mention here that so far there is no effective and tailor-made treatment available for stress and/or chronic pain (1). In this context, meditation and mental capacity to cultivate positive emotion seems to activate certain neuronal circuitries which may prove helpful. For example, it has also been demonstrated that zen practitioners display a reduced duration of neural responses linked to certain functions (190). In a similar manner, central and autonomic nervous system interactions are also altered by short-term meditation (191).

Tough the present understanding of how TRPs are involved in different forms of stress and pain are just at their beginning stage, involvement of TRPs in stress and pain has gained tremendous medical attention. This is mainly due to the fact that TRPs represent key yet diverse pharmacological targets which can be useful to treat different forms of stress and pain in a systematic manner. At presently very little is known about the identity of different endogenous small molecules that can either act as modulators of these TRPs or are secreted due to activation of TRPs. Also how these components and their derivatives act on and modulate arrays of TRPs remains to be characterized. The fact that certain TRPs can be modulated by physical stimuli like temperature, mechanical pressure, osmolarity and different odors gives hope that certain form of stress and pain can be cured by physical stimuli without the use of chemical agents (**192**). This is particularly fascinating as TRPs can modulate the HPA-axis at the upstream as well as the downstream direction. Indeed, commonly practiced analgesic, anxiety- and stress-removal methods like meditation, body massage, acupuncture, water and music therapy, etc most likely to affect the HPA-axis via modulating relevant TRPs in the peripheral tissues (**193**). For example, it has been shown that activation of TRPV1 in the brain contributes to the analgesic effect of acetaminophen. However, more studies are needed to and future research should address to explore these possibilities.

10. ACKNOWLEDGEMENT

This review reflects the views of the authors based on their interpretation of data available in the literature. The authors also regret not being able to include all relevant scientific works due to space limitations. The authors acknowledge support and intellectual inputs from all the lab members and colleagues. Input from Dr. P. S. Singru during the manuscript preparation is appreciated. Financial support from NISER and KIIT University is appreciated.

11. REFERENCES

1. C. L. Stucky, M. S. Gold and X. Zhang: Mechanisms of pain. *Proc Natl Acad Sci U S A*, 98 (21), 11845-6 (2001)

2. Jones, T. L: Definition of stress. In J. J. Robert-McComb (Ed.), *Eating disorders in women and children: Prevention, stress management, and treatment, (*pp. 89-100). Boca Raton, FL: CRC Press (2001)

3. M. Lehner, A. Wislowska-Stanek, P. Maciejak, J. Szyndler, A. Sobolewska, P. Krzascik and A. Plaznik: The relationship between pain sensitivity and conditioned fear response in rats. *Acta Neurobiol Exp (Wars)*, 70 (1), 56-66 (2010)

4. M. Hummel, T. Cummons, P. Lu, L. Mark, J. E. Harrison, J. D. Kennedy and G. T. Whiteside: Pain is a salient "stressor" that is mediated by corticotropin-releasing factor-1 receptors. *Neuropharmacology*, 59 (3), 160-6 (2010)

5. R. Raouf, K. Quick and J. N. Wood: Pain as a channelopathy. *J Clin Invest*, 120 (11), 3745-52 (2010)

6. D. P. Ryan and L. J. Ptacek: Episodic neurological channelopathies. *Neuron*, 68 (2), 282-92 (2010)

7. Verma P, Kumar A, Goswami C: TRPV4-mediated channelopathies. Channels (Austin), Jul-Aug;4 (4):319-28 (2010)

8. Nilius B, Owsianik G: Transient receptor potential chanellopathies. Pflugers Arch, 460:437-50 (2010)

9. Auer-Grumbach M, Olschewski A, Papic L, Kremer H, McEntagart ME, Uhrig S, et al. Alterations in the ankyrin domain of TRPV4 cause congenital distal SMA, scapuloperoneal SMA and HMSN2C. Nat Genet, 42:160-4 (2010)

10. Landouré G, Zdebik AA, Martinez TL, Burnett BG, Stanescu HC, Inada H, et al. Mutations in TRPV4 cause Charcot-Marie-Tooth disease type 2C. Nat Genet, 42:170-4 (2010)

11. Deng HX, Klein CJ, Yan J, Shi Y, Wu Y, Fecto F, et al. Scapuloperoneal spinal muscular atrophy and CMT2C are allelic disorders caused by alterations in TRPV4. Nat Genet, 42:165-9 (2010)

12. M. J. Caterina, M. A. Schumacher, M. Tominaga, T. A. Rosen, J. D. Levine and D. Julius: The capsaicin receptor: a heat-activated ion channel in the pain pathway. Nature, 389 (6653), 816-24 (1997)

13. M. Tominaga and M. J. Caterina: Thermosensation and pain. J Neurobiol, 61 (1), 3-12 (2004)

14. J. Fernandes, I. M. Lorenzo, Y. N. Andrade, A. Garcia-Elias, S. A. Serra, J. M. Fernandez-Fernandez and M. A. Valverde: IP3 sensitizes TRPV4 channel to the mechano- and osmotransducing messenger 5'-6'-epoxyeicosatrienoic acid. J Gen Physiol, 131 (5), i2 (2008)

15. C. J. Woodbury, M. Zwick, S. Wang, J. J. Lawson, M. J. Caterina, M. Koltzenburg, K. M. Albers, H. R. Koerber and B. M. Davis: Nociceptors lacking TRPV1 and TRPV2 have normal heat responses. J Neurosci, 24 (28), 6410-5 (2004)

16. M. J. Caterina, A. Leffler, A. B. Malmberg, W. J. Martin, J. Trafton, K. R. Petersen-Zeitz, M. Koltzenburg, A. I. Basbaum and D. Julius: Impaired nociception and pain sensation in mice lacking the capsaicin receptor. Science, 288 (5464), 306-13 (2000)

17. K. Talavera, B. Nilius and T. Voets: Neuronal TRP channels: thermometers, pathfinders and life-savers. Trends Neurosci, 31 (6), 287-95 (2008)

18. Caterina, M. J: Transient receptor potential ion channels as participants in thermosensation and thermoregulation. *Am J Physiol Regul Integr Comp Physiol*, 292, R64-76 (2007)

19. K. Venkatachalam and C. Montell: TRP channels. *Annu Rev Biochem*, 76, 387-417 (2007)

20. D. Julius and A. I. Basbaum: Molecular mechanisms of nociception. *Nature*, 413 (6852), 203-10 (2001)

21. T. Hucho and J. D. Levine: Signaling pathways in sensitization: toward a nociceptor cell biology. *Neuron*, 55 (3), 365-76 (2007)

22. R. Kuner: Central mechanisms of pathological pain. *Nat Med*, 16 (11), 1258-66 (2010)

23. M. H. Ossipov, G. O. Dussor and F. Porreca: Central modulation of pain. *J Clin Invest*, 120 (11), 3779-87 (2010)

24. E. S. Smith, G. R. Blass, G. R. Lewin and T. J. Park: Absence of histamine-induced itch in the African naked mole-rat and "rescue" by Substance P. *Mol Pain*, 6, 29 (2010)

25. A. E. Dubin and A. Patapoutian: Nociceptors: the sensors of the pain pathway. *J Clin Invest*, 120 (11), 3760-72 (2010)

26. C. Goswami and M. S. Islam: Transient Receptor Potential channels: What's happening? Reflections in the wake of the 2009 TRP Meeting, Karolinska Institutet, Stockholm. *Channels (Austin)*, 4 (2), 124-35 (2010)

27. A. Fujioka, T. Fujioka, R. Tsuruta, T. Izumi, S. Kasaoka and T. Maekawa: Effects of a constant light environment on hippocampal neurogenesis and memory in mice. *Neurosci Lett*, 488 (1), 41-4 (2010)

28. B. S. McEwen and M. Kalia: The role of corticosteroids and stress in chronic pain conditions. *Metabolism*, 59 Suppl 1, S9-15 (2010)

29. T. Vaillancourt, E. Duku, D. Decatanzaro, H. Macmillan, C. Muir and L. A. Schmidt: Variation in hypothalamic-pituitary-adrenal axis activity among bullied and non-bullied children. *Aggress Behav*, 34 (3), 294-305 (2008)

30. B. Myers and B. Greenwood-Van Meerveld: Elevated corticosterone in the amygdala leads to persistent increases in anxiety-like behavior and pain sensitivity. *Behav Brain Res*, 214 (2), 465-9 (2010)

31. C. A. Shively, T. C. Register, D. P. Friedman, T. M. Morgan, J. Thompson and T. Lanier: Social stress-associated depression in adult female cynomolgus monkeys (Macaca fascicularis). *Biol Psychol*, 69 (1), 67-84 (2005)

32. C. A. Shively, D. L. Musselman and S. L. Willard: Stress, depression, and coronary artery disease: modeling comorbidity in female primates. *Neurosci Biobehav Rev*, 33 (2), 133-44 (2009)

33. G. P. Chrousos: The stress response and immune function: clinical implications. The 1999 Novera H. Spector Lecture. *Ann N Y Acad Sci*, 917, 38-67 (2000)

34. G. P. Chrousos: The HPA axis and the stress response. *Endocr Res*, 26 (4), 513-4 (2000)

35. S. Tyrer: Psychosomatic pain. *Br J Psychiatry*, 188, 91-3 (2006)

36. A. Yoshino, Y. Okamoto, K. Onoda, S. Yoshimura, Y. Kunisato, Y. Demoto, G. Okada and S. Yamawaki: Sadness enhances the experience of pain via neural activation in the anterior cingulate cortex and amygdala: an fMRI study. *Neuroimage*, 50 (3), 1194-201 (2009)

37. R. P. Iacono, J. Linford and R. Sandyk: Pain management after lower extremity amputation. *Neurosurgery*, 20 (3), 496-500 (1987)

38. J. E. LeDoux: Emotion circuits in the brain. *Annu Rev Neurosci*, 23, 155-84 (2000)

39. J. D. Levine and N. C. Gordon: Influence of the method of drug administration on analgesic response. *Nature*, 312 (5996), 755-6 (1984)

40. A. K. Malhotra, G. M. Murphy, Jr. and J. L. Kennedy: Pharmacogenetics of psychotropic drug response. *Am J Psychiatry*, 161 (5), 780-96 (2004)

41. R. J. Hackworth, K. A. Tokarz, I. M. Fowler, S. C. Wallace and E. T. Stedje-Larsen: Profound pain reduction after induction of memantine treatment in two patients with severe phantom limb pain. *Anesth Analg*, 107 (4), 1377-9 (2008)

42. M. P. Lunn, R. A. Hughes and P. J. Wiffen: Duloxetine for treating painful neuropathy or chronic pain. *Cochrane Database Syst Rev* (4), CD007115 (2009)

43. P. M. Aslaksen, M. Bystad, S. M. Vambheim and M. A. Flaten: Gender differences in placebo analgesia: event-related potentials and emotional modulation. *Psychosom Med*, 73 (2), 193-9 (2011)

44. J. K. Zubieta, J. A. Bueller, L. R. Jackson, D. J. Scott, Y. Xu, R. A. Koeppe, T. E. Nichols and C. S. Stohler: Placebo effects mediated by endogenous opioid activity on μopioid receptors. *J Neurosci*, 25 (34), 7754-62 (2005)

45. R. H. Gracely, R. Dubner, P. J. Wolskee and W. R. Deeter: Placebo and naloxone can alter post-surgical pain by separate mechanisms. *Nature*, 306 (5940), 264-5 (1983)

46. P. Grevert, L. H. Albert and A. Goldstein: Partial antagonism of placebo analgesia by naloxone. *Pain*, 16 (2), 129-43 (1983)

47. F. Benedetti: The opposite effects of the opiate antagonist naloxone and the cholecystokinin antagonist proglumide on placebo analgesia. *Pain*, 64 (3), 535-43 (1996)

48. P. Mason: Central mechanisms of pain modulation. *Curr Opin Neurobiol*, 9 (4), 436-41 (1999)

49. C. Mattia, F. Paoletti, F. Coluzzi and A. Boanelli: New antidepressants in the treatment of neuropathic pain. A review. *Minerva Anestesiol*, 68 (3), 105-14 (2002)

50. K. Sato, H. Higuchi and Y. Hishikawa: Management of phantom limb pain and sensation with milnacipran. *J Neuropsychiatry Clin Neurosci*, 20 (3), 368 (2008)

51. D. Mochizuki, R. Tsujita, S. Yamada, K. Kawasaki, Y. Otsuka, S. Hashimoto, T. Hattori, Y. Kitamura and N. Miki: Neurochemical and behavioural characterization of milnacipran, a serotonin and noradrenaline reuptake inhibitor in rats. *Psychopharmacology (Berl)*, 162 (3), 323-32 (2002)

52. A. Buvanendran and J. S. Kroin: Early use of memantine for neuropathic pain. *Anesth Analg*, 107 (4), 1093-4 (2008)

53. H. Shanthanna, M. Huilgol and V. K. Manivackam: Early and effective use of ketamine for treatment of phantom limb pain. *Indian J Anaesth*, 54 (2), 157-9 (2010)

54. K. Niikura, M. Narita, E. R. Butelman, M. J. Kreek and T. Suzuki: Neuropathic and chronic pain stimuli downregulate central μopioid and dopaminergic transmission. *Trends Pharmacol Sci*, 31 (7), 299-305 (2010)

55. J. R. Homberg and C. Contet: Deciphering the interaction of the corticotropin-releasing factor and serotonin brain systems in anxiety-related disorders. *J Neurosci*, 29 (44), 13743-5 (2009)

56. W. El Hage, J. F. Powell and S. A. Surguladze: Vulnerability to depression: what is the role of stress genes in gene x environment interaction? *Psychol Med*, 39 (9), 1407-11 (2009)

57. R. H. Derijk: Single nucleotide polymorphisms related to HPA axis reactivity. *Neuroimmunomodulation*, 16 (5), 340-52 (2009)

58. D. L. Murphy, A. Lerner, G. Rudnick and K. P. Lesch: Serotonin transporter: gene, genetic disorders, and pharmacogenetics. *Mol Interv*, 4 (2), 109-23 (2004)

59. K. P. Lesch, D. Bengel, A. Heils, S. Z. Sabol, B. D. Greenberg, S. Petri, J. Benjamin, C. R. Muller, D. H. Hamer and D. L. Murphy: Association of anxiety-related traits with a polymorphism in the serotonin transporter gene regulatory region. *Science*, 274 (5292), 1527-31 (1996)

60. L. Sher, T. A. Hardin, B. D. Greenberg, D. L. Murphy, Q. Li and N. E. Rosenthal: Seasonality associated with the serotonin transporter promoter repeat length polymorphism. *Am J Psychiatry*, 156 (11), 1837 (1999)

61. A. Caspi, A. R. Hariri, A. Holmes, R. Uher and T. E. Moffitt: Genetic sensitivity to the environment: the case of the serotonin transporter gene and its implications for studying complex diseases and traits. *Am J Psychiatry*, 167 (5), 509-27 (2010)

62. N. E. Rosenthal, C. M. Mazzanti, R. L. Barnett, T. A. Hardin, E. H. Turner, G. K. Lam, N. Ozaki and D. Goldman: Role of serotonin transporter promoter repeat length polymorphism (5-HTTLPR) in seasonality and seasonal affective disorder. *Mol Psychiatry*, 3 (2), 175-7 (1998)

63. S. Sookoian, C. Gemma, S. I. Garcia, T. F. Gianotti, G. Dieuzeide, A. Roussos, M. Tonietti, L. Trifone, D. Kanevsky, C. D. Gonzalez and C. J. Pirola: Short allele of serotonin transporter gene promoter is a risk factor for obesity in adolescents. *Obesity (Silver Spring)*, 15 (2), 271-6 (2007)

64. Goldman, D: High anxiety. Science, 274 (5292): p. 1483. (1996)

65. B. Bondy, A. Buettner and P. Zill: Genetics of suicide. *Mol Psychiatry*, 11 (4), 336-51 (2006)

66. N. K. Popova: From genes to aggressive behavior: the role of serotonergic system. *Bioessays*, 28 (5), 495-503 (2006)

67. H. F. Harlow and R. R. Zimmermann: Affectional responses in the infant monkey; orphaned baby monkeys develop a strong and persistent attachment to inanimate surrogate mothers. *Science*, 130 (3373), 421-32 (1959)

68. S. Moriceau, K. Shionoya, K. Jakubs and R. M. Sullivan: Early-life stress disrupts attachment learning: the role of amygdala corticosterone, locus ceruleus corticotropin releasing hormone, and olfactory bulb norepinephrine. *J Neurosci*, 29 (50), 15745-55 (2009)

69. J. Lukkes, S. Vuong, J. Scholl, H. Oliver and G. Forster: Corticotropin-releasing factor receptor antagonism within the dorsal raphe nucleus reduces social anxiety-like behavior after early-life social isolation. *J Neurosci*, 29 (32), 9955-60 (2009)

70. J. L. Lukkes, C. H. Summers, J. L. Scholl, K. J. Renner and G. L. Forster: Early life social isolation alters corticotropin-releasing factor responses in adult rats. *Neuroscience*, 158 (2), 845-55 (2009)

71. A. Bick-Sander, B. Steiner, S. A. Wolf, H. Babu and G. Kempermann: Running in pregnancy transiently increases postnatal hippocampal neurogenesis in the offspring. *Proc Natl Acad Sci U S A*, 103 (10), 3852-7 (2006)

72. S. F. Bomholt, M. S. Harbuz, G. Blackburn-Munro and R. E. Blackburn-Munro: Involvement and role of the hypothalamo-pituitary-adrenal (HPA) stress axis in animal models of chronic pain and inflammation. *Stress*, 7 (1), 1-14 (2004)

73. F. Calabrese, R. Molteni, G. Racagni and M. A. Riva: Neuronal plasticity: a link between stress and mood disorders. *Psychoneuroendocrinology*, 34 Suppl 1, S208-16 (2009)

74. S. J. Bishop, J. Duncan and A. D. Lawrence: State anxiety modulation of the amygdala response to unattended threat-related stimuli. *J Neurosci*, 24 (46), 10364-8 (2004)

75. B. K. Holzel, J. Carmody, K. C. Evans, E. A. Hoge, J. A. Dusek, L. Morgan, R. K. Pitman and S. W. Lazar: Stress reduction correlates with structural changes in the amygdala. *Soc Cogn Affect Neurosci*, 5 (1), 11-7 (2010)

76. Thomas, R.M., G. Hotsenpiller, and D.A. Peterson, Acute psychosocial stress reduces cell survival in adult hippocampal neurogenesis without altering proliferation. J Neurosci. 27 (11): p. 2734-43 (2007)

77. A. Vyas, R. Mitra, B. S. Shankaranarayana Rao and S. Chattarji: Chronic stress induces contrasting patterns of dendritic remodeling in hippocampal and amygdaloid neurons. *J Neurosci*, 22 (15), 6810-8 (2002)

78. A. May: Chronic pain may change the structure of the brain. *Pain*, 137 (1), 7-15 (2008)

79. A. V. Apkarian, Y. Sosa, B. R. Krauss, P. S. Thomas, B. E. Fredrickson, R. E. Levy, R. N. Harden and D. R. Chialvo: Chronic pain patients are impaired on an emotional decision-making task. *Pain*, 108 (1-2), 129-36 (2004)

80. A. V. Apkarian, Y. Sosa, S. Sonty, R. M. Levy, R. N. Harden, T. B. Parrish and D. R. Gitelman: Chronic back pain is associated with decreased prefrontal and thalamic gray matter density. *J Neurosci*, 24 (46), 10410-5 (2004)

81. E. Luders, A. W. Toga, N. Lepore and C. Gaser: The underlying anatomical correlates of long-term meditation: larger hippocampal and frontal volumes of gray matter. *Neuroimage*, 45 (3), 672-8 (2009)

82. K. W. Brown and R. M. Ryan: The benefits of being present: mindfulness and its role in psychological well-being. *J Pers Soc Psychol*, 84 (4), 822-48 (2003)

83. Sasamura, T., M. Sasaki, C. Tohda & Y. Kuraishi: Existence of capsaicin-sensitive glutamatergic terminals in rat hypothalamus. *Neuroreport*, 9, 2045-8 (1998)

84. Mezey, E., Z. E. Toth, D. N. Cortright, M. K. Arzubi, J. E. Krause, R. Elde, A. Guo, P. M. Blumberg & A. Szallasi: Distribution of mRNA for vanilloid receptor subtype 1 (VR1), and VR1-like immunoreactivity, in the central nervous system of the rat and human. *Proc Natl Acad Sci U S A*, 97, 3655-60 (2000)

85. Sanchez, J. F., J. E. Krause & D. N. Cortright: The distribution and regulation of vanilloid receptor VR1 and VR1 5' splice variant RNA expression in rat. *Neuroscience*, 107, 373-81 (2001)

86. Toth, A., J. Boczan, N. Kedei, E. Lizanecz, Z. Bagi, Z. Papp, I. Edes, L. Csiba & P. M. Blumberg: Expression and distribution of vanilloid receptor 1 (TRPV1) in the adult rat brain. *Brain Res Mol Brain Res*, 135, 162-8 (2005)

87. L. A. Chahl: TRP's: links to schizophrenia? *Biochim Biophys Acta*, 1772 (8), 968-77 (2007)

88. C. Goswami, N. Rademacher, K. H. Smalla, V. Kalscheuer, H. H. Ropers, E. D. Gundelfinger and T. Hucho: TRPV1 acts as a synaptic protein and regulates vesicle recycling. *J Cell Sci*, 123 (Pt 12), 2045-57 (2010)

89. Hjerling-Leffler, J., M. Alqatari, P. Ernfors & M. Koltzenburg: Emergence of functional sensory subtypes as defined by transient receptor potential channel expression. *J Neurosci*, 27, 2435-43 (2007)

90. V. Di Marzo, G. Gobbi and A. Szallasi: Brain TRPV1: a depressing TR (i)P down memory lane? *Trends Pharmacol Sci*, 29 (12), 594-600 (2008)

91. A. Toth, J. Boczan, N. Kedei, E. Lizanecz, Z. Bagi, Z. Papp, I. Edes, L. Csiba and P. M. Blumberg: Expression and distribution of vanilloid receptor 1 (TRPV1) in the adult rat brain. *Brain Res Mol Brain Res*, 135 (1-2), 162-8 (2005)

92. Goswami, C., H. Schmidt & F. Hucho: TRPV1 at nerve endings regulates growth cone morphology and movement through cytoskeleton reorganization. *Febs J*, 274, 760-72 (2007)

93. Montell, C: Exciting trips for TRPs. *Nat Cell Biol*, 6, 690-2 (2004)

94. Li, Y., Y. C. Jia, K. Cui, N. Li, Z. Y. Zheng, Y. Z. Wang & X. B. Yuan: Essential role of TRPC channels in the guidance of nerve growth cones by brain-derived neurotrophic factor. *Nature*, 434, 894-8 (2005)

95. Wang, G. X. & M. M. Poo: Requirement of TRPC channels in netrin-1-induced chemotropic turning of nerve growth cones. *Nature*, 434, 898-904 (2005)

96. Shim, S., E. L. Goh, S. Ge, K. Sailor, J. P. Yuan, H. L. Roderick, M. D. Bootman, P. F. Worley, H. Song & G. L. Ming: XTRPC1-dependent chemotropic guidance of neuronal growth cones. *Nat Neurosci*, 8, 730-5 (2005)

97. N. Crouzin, M. C. Ferreira, C. Cohen-Solal, G. Barbanel, J. Guiramand and M. Vignes: Neuroprotection induced by vitamin E against oxidative stress in hippocampal neurons: involvement of TRPV1 channels. *Mol Nutr Food Res*, 54 (4), 496-505 (2010)

98. C. Goswami and T. Hucho: TRPV1 expression-dependent initiation and regulation of filopodia. *J Neurochem*, 103 (4), 1319-33 (2007)

99. K. Shibasaki, M. Suzuki, A. Mizuno and M. Tominaga: Effects of body temperature on neural activity in the hippocampus: regulation of resting membrane potentials by transient receptor potential vanilloid 4. *J Neurosci*, 27 (7), 1566-75 (2007)

100. C. P. Bengtson, A. Tozzi, G. Bernardi and N. B. Mercuri: Transient receptor potential-like channels mediate metabotropic glutamate receptor EPSCs in rat dopamine neurones. *J Physiol*, 555 (Pt 2), 323-30 (2004)

101. Li, H. B., R. R. Mao, J. C. Zhang, Y. Yang, J. Cao & L. Xu: Antistress effect of TRPV1 channel on synaptic plasticity and spatial memory. *Biol Psychiatry*, 64, 286-92 (2008)

102. Marsch, R., E. Foeller, G. Rammes, M. Bunck, M. Kossl, F. Holsboer, W. Zieglgansberger, R. Landgraf, B. Lutz & C. T. Wotjak: Reduced anxiety, conditioned fear, and hippocampal long-term potentiation in transient receptor potential vanilloid type 1 receptor-deficient mice. *J Neurosci*, 27, 832-9 (2007)

103. O. V. Singh, M. Yaster, J. T. Xu, Y. Guan, X. Guan, A. M. Dharmarajan, S. N. Raja, P. L. Zeitlin and Y. X. Tao: Proteome of synaptosome-associated proteins in spinal cord dorsal horn after peripheral nerve injury. *Proteomics*, 9 (5), 1241-53 (2009)

104. H. L. Huang, C. M. Cendan, C. Roza, K. Okuse, R. Cramer, J. F. Timms and J. N. Wood: Proteomic profiling of neuromas reveals alterations in protein composition and local protein synthesis in hyper-excitable nerves. *Mol Pain*, 4, 33 (2008)

105. H. Fujisawa, R. Ohtani-Kaneko, M. Naiki, T. Okada, K. Masuko, K. Yudoh, N. Suematsu, K. Okamoto, K. Nishioka and T. Kato: Involvement of post-translational modification of neuronal plasticity-related proteins in hyperalgesia revealed by a proteomic analysis. *Proteomics*, 8 (8), 1706-19 (2008)

106. B. T. Aldrich, E. P. Frakes, J. Kasuya, D. L. Hammond and T. Kitamoto: Changes in expression of sensory organ-specific microRNAs in rat dorsal root ganglia in association with mechanical hypersensitivity induced by spinal nerve ligation. *Neuroscience*, 164 (2), 711-23 (2009)

107. Y. He, C. Yang, C. M. Kirkmire and Z. J. Wang: Regulation of opioid tolerance by let-7 family microRNA targeting the mu opioid receptor. *J Neurosci*, 30 (30), 10251-8 (2010)

108. F. M. Sanchez-Simon, X. X. Zhang, H. H. Loh, P. Y. Law and R. E. Rodriguez: Morphine regulates dopaminergic neuron differentiation via miR-133b. *Mol Pharmacol*, 78 (5), 935-42 (2010)

109. V. Sanchez Freire, F. C. Burkhard, T. M. Kessler, A. Kuhn, A. Draeger and K. Monastyrskaya: MicroRNAs may mediate the down-regulation of neurokinin-1 receptor in chronic bladder pain syndrome. *Am J Pathol*, 176 (1), 288-303 (2010)

110. J. Zhao, M. C. Lee, A. Momin, C. M. Cendan, S. T. Shepherd, M. D. Baker, C. Asante, L. Bee, A. Bethry, J. R. Perkins, M. A. Nassar, B. Abrahamsen, A. Dickenson, B. S. Cobb, M. Merkenschlager and J. N. Wood: Small RNAs control sodium channel expression,

nociceptor excitability, and pain thresholds. *J Neurosci*, 30 (32), 10860-71 (2010)

111. Dwivedi, Y: Evidence demonstrating role of microRNAs in the etiopathology of major depression. *J Chem Neuroanat*, (2011)

112. Hulsmans, M., D. De Keyzer & P. Holvoet: MicroRNAs regulating oxidative stress and inflammation in relation to obesity and atherosclerosis. *Faseb J*, 25, 2515-27 (2011)

113. Ferguson, L. R: RNA silencing: Mechanism, biology and responses to environmental stress. *Mutat Res* (2011)

114. Tran, U., L. Zakin, A. Schweickert, R. Agrawal, R. Doger, M. Blum, E. M. De Robertis & O. Wessely: The RNA-binding protein bicaudal C regulates polycystin 2 in the kidney by antagonizing miR-17 activity. *Development*, 137, 1107-16 (2010)

115. M. Hlavackova, K. Kozichova, J. Neckar, F. Kolar, R. J. Musters, F. Novak and O. Novakova: Up-regulation and redistribution of protein kinase C-delta in chronically hypoxic heart. *Mol Cell Biochem*, 345 (1-2), 271-82 (2010)

116. S. Kido, R. Kuriwaka-Kido, Y. Umino-Miyatani, I. Endo, D. Inoue, H. Taniguchi, Y. Inoue, T. Imamura and T. Matsumoto: Mechanical stress activates Smad pathway through PKCdelta to enhance interleukin-11 gene transcription in osteoblasts. *PLoS One*, 5 (9) (2010)

117. S. G. Khasar, Y. H. Lin, A. Martin, J. Dadgar, T. McMahon, D. Wang, B. Hundle, K. O. Aley, W. Isenberg, G. McCarter, P. G. Green, C. W. Hodge, J. D. Levine and R. O. Messing: A novel nociceptor signaling pathway revealed in protein kinase C epsilon mutant mice. *Neuron*, 24 (1), 253-60 (1999)

118. S. B. McMahon and M. Koltzenburg: Novel classes of nociceptors: beyond Sherrington. *Trends Neurosci*, 13 (6), 199-201 (1990)

119. H. O. Handwerker, S. Kilo and P. W. Reeh: Unresponsive afferent nerve fibres in the sural nerve of the rat. *J Physiol*, 435, 229-42 (1991)

120. Y. B. Yu, J. Yang, X. L. Zuo, L. J. Gao, P. Wang and Y. Q. Li: Transient receptor potential vanilloid-1 (TRPV1) and ankyrin-1 (TRPA1) participate in visceral hyperalgesia in chronic water avoidance stress rat model. *Neurochem Res*, 35 (5), 797-803 (2010)

121. J. Z. Bai and J. Lipski: Differential expression of TRPM2 and TRPV4 channels and their potential role in oxidative stress-induced cell death in organotypic hippocampal culture. *Neurotoxicology*, 31 (2), 204-14 (2010)

122. S. Hong, G. Zheng, X. Wu, N. T. Snider, C. Owyang and J. W. Wiley: Corticosterone Mediates Reciprocal Changes in CB 1 and TRPV1 Receptors in Primary Sensory Neurons in the Chronically Stressed Rat. *Gastroenterology*, 140 (2), 627-637 e4 (2010)

123. N. Rimmerman, H. B. Bradshaw, A. Basnet, B. Tan, T. S. Widlanski and J. M. Walker: Microsomal omega-hydroxylated metabolites of N-arachidonoyl dopamine are active at recombinant human TRPV1 receptors. *Prostaglandins Other Lipid Mediat*, 88 (1-2), 10-7 (2009)

124. Picazo-Juarez, G., S. Romero-Suarez, A. Nieto-Posadas, I. Llorente, A. Jara-Oseguera, M. Briggs, T. J. McIntosh, S. A. Simon, E. Ladron-de-Guevara, L. D. Islas & T. Rosenbaum: Identification of a Binding Motif in the S5 Helix That Confers Cholesterol Sensitivity to the TRPV1 Ion Channel. *J Biol Chem*, 286, 24966-76 (2011)

125. Liu, M., W. Huang, D. Wu & J. V. Priestley: TRPV1, but not P2X, requires cholesterol for its function and membrane expression in rat nociceptors. *Eur J Neurosci*, 24, 1-6 (2006)

.

126. B. A. Miller and W. Zhang: TRP Channels as Mediators of Oxidative Stress. *Adv Exp Med Biol*, 704, 531-44 (2011)

127. N. Prevarskaya, L. Zhang and G. Barritt: TRP channels in cancer. *Biochim Biophys Acta*, 1772 (8), 937-46 (2007)

128. Z. Zhu, Z. Luo, S. Ma and D. Liu: TRP channels and their implications in metabolic diseases. *Pflugers Arch*, 461 (2), 211-23 (2010)

129. D. A. Jacobson and L. H. Philipson: TRP channels of the pancreatic beta cell. *Handb Exp Pharmacol* (179), 409-24 (2007)

130. K. M. Kim, T. Kawada, K. Ishihara, K. Inoue and T. Fushiki: Increase in swimming endurance capacity of mice by capsaicin-induced adrenal catecholamine secretion. *Biosci Biotechnol Biochem*, 61 (10), 1718-23 (1997) 1997. 61 (10): p. 1718-23.

131. N. Inoue, Y. Matsunaga, H. Satoh and M. Takahashi: Enhanced energy expenditure and fat oxidation in humans with high BMI scores by the ingestion of novel and non-pungent capsaicin analogues (capsinoids). *Biosci Biotechnol Biochem*, 71 (2), 380-9 (2007)

132. F. Massa, A. Sibaev, G. Marsicano, H. Blaudzun, M. Storr and B. Lutz: Vanilloid receptor (TRPV1)-deficient mice show increased susceptibility to dinitrobenzene sulfonic acid induced colitis. *J Mol Med*, 84 (2), 142-6 (2006)

133. M. A. Storr and K. A. Sharkey: The endocannabinoid system and gut-brain signalling. *Curr Opin Pharmacol*, 7 (6), 575-82 (2007)

134. A. Suri and A. Szallasi: The emerging role of TRPV1 in diabetes and obesity. *Trends Pharmacol Sci*, 29 (1), 29-36 (2008)

135. C. Wang, J. Zhou, S. Wang, M. Ye, C. Jiang, G. Fan and H. Zou: Combined comparative and chemical proteomics on the mechanisms of levo-tetrahydropalmatine-induced antinociception in the formalin test. *J Proteome Res*, 9 (6), 3225-34 (2010)

136. A. L. Motter and G. P. Ahern: TRPV1-null mice are protected from diet-induced obesity. *FEBS Lett*, 582 (15), 2257-62 (2008)

137. Zhang, L. L., D. Yan Liu, L. Q. Ma, Z. D. Luo, T. B. Cao, J. Zhong, Z. C. Yan, L. J. Wang, Z. G. Zhao, S. J. Zhu, M. Schrader, F. Thilo, Z. M. Zhu & M. Tepel: Activation of transient receptor potential vanilloid type-1 channel prevents adipogenesis and obesity. *Circ Res*, 100, 1063-70 (2007)

138. F. W. Leung: Capsaicin-sensitive intestinal mucosal afferent mechanism and body fat distribution. *Life Sci*, 83 (1-2), 1-5 (2008)

139. J. H. Kang, C. S. Kim, I. S. Han, T. Kawada and R. Yu: Capsaicin, a spicy component of hot peppers, modulates adipokine gene expression and protein release from obese-mouse adipose tissues and isolated adipocytes, and suppresses the inflammatory responses of adipose tissue macrophages. *FEBS Lett*, 581 (23), 4389-96 (2007)

140. S. W. Janssen, J. G. Hoenderop, A. R. Hermus, F. C. Sweep, G. J. Martens and R. J. Bindels: Expression of the novel epithelial Ca^{2+} channel ECaC1 in rat pancreatic islets. *J Histochem Cytochem*, 50 (6), 789-98 (2002)

141. J. Laskiewicz, G. Królczyk, D. Zurowski, P. Enck and P. J. Thor: Capasaicin induced deafferentation enhances the effect of electrical vagal nerve stimulation on food intake and body mass. *J Physiol Pharmacol*. 55 (1 Pt 2):155-63 (2004)

142. M. D. Barrachina, V. Martínez, L Wang, J. Y. Wei, Y Taché: Synergistic interaction between leptin and cholecystokinin to reduce short-term food intake in lean mice. *Proc Natl Acad Sci U S A*. 94 (19):10455-60. (1997)

143. J. D. Patel, I.S. Ebenezer IS: The effect of intraperitoneal administration of leptin on short-term food intake in rats. Eur J Pharmacol. 580 (1-2):143-52. (2008)

144. P. Bryant, M. Shumate, G. Yumet, C. H. Lang, T. C. Vary, R. N. Cooney: Capsaicin-sensitive nerves regulate the metabolic response to abdominal sepsis. *J Surg Res*. 112 (2):152-61 (2003).

145. E. Epel, R. Lapidus, B. McEwen and K. Brownell: Stress may add bite to appetite in women: a laboratory study of stress-induced cortisol and eating behavior. *Psychoneuroendocrinology*, 26 (1), 37-49 (2001)

146. Uchida, K. & M. Tominaga: The role of thermosensitive TRP (transient receptor potential) channels in insulin secretion. *Endocr J*, (2011)

147. D. X. Gram, B. Ahren, I. Nagy, U. B. Olsen, C. L. Brand, F. Sundler, R. Tabanera, O. Svendsen, R. D. Carr, P. Santha, N. Wierup and A. J. Hansen: Capsaicin-sensitive sensory fibers in the islets of Langerhans contribute to defective insulin secretion in Zucker diabetic rat, an animal model for some aspects of human type 2 diabetes. *Eur J Neurosci*, 25 (1), 213-23 (2007)

148. Y. Akiba, S. Kato, K. Katsube, M. Nakamura, K. Takeuchi, H. Ishii and T. Hibi: Transient receptor potential vanilloid subfamily 1 expressed in pancreatic islet beta cells modulates insulin secretion in rats. *Biochem Biophys Res Commun*, 321 (1), 219-25 (2004)

149. Zhang, Z., C. S. Winborn, B. Marquez de Prado & A. F. Russo: Sensitization of calcitonin gene-related peptide receptors by receptor activity-modifying protein-1 in the trigeminal ganglion. *J Neurosci*, 27, 2693-703 (2007)

150. M. Pettersson, B. Ahren, G. Bottcher and F. Sundler: Calcitonin gene-related peptide: occurrence in pancreatic islets in the mouse and the rat and inhibition of insulin secretion in the mouse. *Endocrinology*, 119 (2), 865-9 (1986)

151. R. Razavi, Y. Chan, F. N. Afifiyan, X. J. Liu, X. Wan, J. Yantha, H. Tsui, L. Tang, S. Tsai, P. Santamaria, J. P. Driver, D. Serreze, M. W. Salter and H. M. Dosch: TRPV1+ sensory neurons control beta cell stress and islet inflammation in autoimmune diabetes. *Cell*, 127 (6), 1123-35 (2006)

152. J. J. Van Buren, S. Bhat, R. Rotello, M. E. Pauza and L. S. Premkumar: Sensitization and translocation of TRPV1 by insulin and IGF-I. *Mol Pain*, 1, 17 (2005)

153. A. W. Norman, J. B. Frankel, A. M. Heldt and G. M. Grodsky: Vitamin D deficiency inhibits pancreatic secretion of insulin. *Science*, 209 (4458), 823-5 (1980)

154. K. Inamura, Y. Sano, S. Mochizuki, H. Yokoi, A. Miyake, K. Nozawa, C. Kitada, H. Matsushime and K. Furuichi: Response to ADP-ribose by activation of TRPM2 in the CRI-G1 insulinoma cell line. *J Membr Biol*, 191 (3), 201-7 (2003)

155. P. S. Herson, K. A. Dulock and M. L. Ashford: Characterization of a nicotinamide-adenine dinucleotide-dependent cation channel in the CRI-G1 rat insulinoma cell line. *J Physiol*, 505 (Pt 1), 65-76 (1997)

156. T. F. Wagner, S. Loch, S. Lambert, I. Straub, S. Mannebach, I. Mathar, M. Dufer, A. Lis, V. Flockerzi, S. E. Philipp and J. Oberwinkler: Transient receptor potential M3 channels are ionotropic steroid receptors in pancreatic beta cells. *Nat Cell Biol*, 10 (12), 1421-30 (2008)

157. C. S. Lieber: Hepatic and other medical disorders of alcoholism: from pathogenesis to treatment. *J Stud Alcohol*, 59 (1), 9-25 (1998)

158. G. Vittadini, M. Buonocore, G. Colli, M. Terzi, R. Fonte and G. Biscaldi: Alcoholic polyneuropathy: a clinical

and epidemiological study. *Alcohol Alcohol*, 36 (5), 393-400 (2001)

159. H. Koike and G. Sobue: Alcoholic neuropathy. *Curr Opin Neurol*, 19 (5), 481-6 (2006)

160. O. A. Dina, R. W. Gear, R. O. Messing and J. D. Levine: Severity of alcohol-induced painful peripheral neuropathy in female rats: role of estrogen and protein kinase (A and Cepsilon). *Neuroscience*, 145 (1), 350-6 (2007)

161. E. D. Schoell, U. Bingel, F. Eippert, J. Yacubian, K. Christiansen, H. Andresen, A. May and C. Buechel: The effect of opioid receptor blockade on the neural processing of thermal stimuli. *PLoS One*, 5 (8), e12344 (2010)

162. M. Trevisani, D. Gazzieri, F. Benvenuti, B. Campi, Q. T. Dinh, D. A. Groneberg, M. Rigoni, X. Emonds-Alt, C. Creminon, A. Fischer, P. Geppetti and S. Harrison: Ethanol causes inflammation in the airways by a neurogenic and TRPV1-dependent mechanism. *J Pharmacol Exp Ther*, 309 (3), 1167-73 (2004)

163. K. Hirota, D. Smart and D. G. Lambert: The effects of local and intravenous anesthetics on recombinant rat VR1 vanilloid receptors. *Anesth Analg*, 96 (6), 1656-60, table of contents (2003)

164. J. Benedikt, J. Teisinger, L. Vyklicky and V. Vlachova: Ethanol inhibits cold-menthol receptor TRPM8 by modulating its interaction with membrane phosphatidylinositol 4,5-bisphosphate. *J Neurochem*, 100 (1), 211-24 (2007)

165. E. Andre, B. Campi, S. Materazzi, M. Trevisani, S. Amadesi, D. Massi, C. Creminon, N. Vaksman, R. Nassini, M. Civelli, P. G. Baraldi, D. P. Poole, N. W. Bunnett, P. Geppetti and R. Patacchini: Cigarette smoke-induced neurogenic inflammation is mediated by alpha,beta-unsaturated aldehydes and the TRPA1 receptor in rodents. *J Clin Invest*, 118 (7), 2574-82 (2008)

166. R. Xiao and X. Z. Xu: Function and regulation of TRP family channels in C. elegans. *Pflugers Arch*, 458 (5), 851-60 (2009)

167. K. Talavera, M. Gees, Y. Karashima, V. M. Meseguer, J. A. Vanoirbeek, N. Damann, W. Everaerts, M. Benoit, A. Janssens, R. Vennekens, F. Viana, B. Nemery, B. Nilius and T. Voets: Nicotine activates the chemosensory cation channel TRPA1. *Nat Neurosci*, 12 (10), 1293-9 (2009)

168. B. L. Hungund and B. S. Basavarajappa: Role of endocannabinoids and cannabinoid CB1 receptors in alcohol-related behaviors. *Ann N Y Acad Sci*, 1025, 515-27 (2004)

169. M. Rubio, D. McHugh, J. Fernandez-Ruiz, H. Bradshaw and J. M. Walker: Short-term exposure to alcohol in rats affects brain levels of anandamide, other N-acylethanolamines and 2-arachidonoyl-glycerol. *Neurosci Lett*, 421 (3), 270-4 (2007)

170. B. Ferrer, F. J. Bermudez-Silva, A. Bilbao, L. Alvarez-Jaimes, I. Sanchez-Vera, A. Giuffrida, A. Serrano, E. Baixeras, S. Khaturia, M. Navarro, L. H. Parsons, D. Piomelli and F. Rodriguez de Fonseca: Regulation of brain anandamide by acute administration of ethanol. *Biochem J*, 404 (1), 97-104 (2007)

171. B. S. Basavarajappa, T. B. Cooper and B. L. Hungund: Chronic ethanol administration down-regulates cannabinoid receptors in mouse brain synaptic plasma membrane. *Brain Res*, 793 (1-2), 212-8 (1998)

172. I. Vetter, B. D. Wyse, G. R. Monteith, S. J. Roberts-Thomson and P. J. Cabot: The mu opioid agonist morphine modulates potentiation of capsaicin-evoked TRPV1 responses through a cyclic AMP-dependent protein kinase A pathway. *Mol Pain*, 2, 22 (2006)

173. I. Vetter, B. D. Wyse, S. J. Roberts-Thomson, G. R. Monteith and P. J. Cabot: Mechanisms involved in potentiation of transient receptor potential vanilloid 1 responses by ethanol. *Eur J Pain*, 12 (4), 441-54 (2008)

174. C. Goswami and L. Goswami: Filamentous microtubules in the neuronal spinous process and the role of microtubule regulatory drugs in neuropathic pain. *Neurochem Int*, 57 (5), 497-503

175. N. Alessandri-Haber, O. A. Dina, J. J. Yeh, C. A. Parada, D. B. Reichling and J. D. Levine: Transient receptor potential vanilloid 4 is essential in chemotherapy-induced neuropathic pain in the rat. *J Neurosci*, 24 (18), 4444-52 (2004)

176. C. Goswami, M. Dreger, R. Jahnel, O. Bogen, C. Gillen and F. Hucho: Identification and characterization of a Ca2+ -sensitive interaction of the vanilloid receptor TRPV1 with tubulin. *J Neurochem*, 91 (5), 1092-103 (2004)

177. B. A. Gilchrest, J. S. Stoff and N. A. Soter: Chronologic aging alters the response to ultraviolet-induced inflammation in human skin. *J Invest Dermatol*, 79 (1), 11-5 (1982)

178. B. A. Gilchrest: Age-associated changes in the skin. *J Am Geriatr Soc*, 30 (2), 139-43 (1982)

179. W. H. Li, Y. M. Lee, J. Y. Kim, S. Kang, S. Kim, K. H. Kim, C. H. Park and J. H. Chung: Transient receptor potential vanilloid-1 mediates heat-shock-induced matrix metalloproteinase-1 expression in human epidermal keratinocytes. *J Invest Dermatol*, 127 (10), 2328-35 (2007)

180. R. T. Alexander, T. E. Woudenberg-Vrenken, J. Buurman, H. Dijkman, B. C. van der Eerden, J. P. van Leeuwen, R. J. Bindels and J. G. Hoenderop: Klotho prevents renal calcium loss. *J Am Soc Nephrol*, 20 (11), 2371-9 (2009)

181. Q. Chang, S. Hoefs, A. W. van der Kemp, C. N. Topala, R. J. Bindels and J. G. Hoenderop: The beta-

glucuronidase klotho hydrolyzes and activates the TRPV5 channel. *Science*, 310 (5747), 490-3 (2005)

182. G. Collodel, E. Moretti, V. Fontani, S. Rinaldi, L. Aravagli, G. Sarago, S. Capitani and C. Anichini: Effect of emotional stress on sperm quality. *Indian J Med Res*, 128 (3), 254-61 (2008)

183. G. M. Buck Louis, K. J. Lum, R. Sundaram, Z. Chen, S. Kim, C. D. Lynch, E. F. Schisterman and C. Pyper: Stress reduces conception probabilities across the fertile window: evidence in support of relaxation. *Fertil Steril* (2010)

184. X. Z. Xu and P. W. Sternberg: A C. elegans sperm TRP protein required for sperm-egg interactions during fertilization. *Cell*, 114 (3), 285-97 (2003)

185. F. Francavilla, N. Battista, A. Barbonetti, M. R. Vassallo, C. Rapino, C. Antonangelo, N. Pasquariello, G. Catanzaro, B. Barboni and M. Maccarrone: Characterization of the endocannabinoid system in human spermatozoa and involvement of transient receptor potential vanilloid 1 receptor in their fertilizing ability. *Endocrinology*, 150 (10), 4692-700 (2009)

186. H. Schuel, L. J. Burkman, J. Lippes, K. Crickard, E. Forester, D. Piomelli and A. Giuffrida: N-Acylethanolamines in human reproductive fluids. *Chem Phys Lipids*, 121 (1-2), 211-27 (2002)

187. S. Minowa, S. Ishihara, S. Tsuchiya, S. Horie and T. Murayama: Capsaicin- and anandamide-induced gastric acid secretion via vanilloid receptor type 1 (TRPV1) in rat brain. *Brain Res*, 1039 (1-2), 75-83 (2005)

188. Y. Koca, O. L. Ozdal, M. Celik, S. Unal and N. Balaban: Antioxidant activity of seminal plasma in fertile and infertile men. *Arch Androl*, 49 (5), 355-9 (2003)

189. G. Balercia, T. Armeni, F. Mantero, G. Principato and F. Regoli: Total oxyradical scavenging capacity toward different reactive oxygen species in seminal plasma and sperm cells. *Clin Chem Lab Med*, 41 (1), 13-9 (2003)

190. G. Pagnoni, M. Cekic and Y. Guo: "Thinking about not-thinking": neural correlates of conceptual processing during Zen meditation. *PLoS One*, 3 (9), e3083 (2008)

191. Y. Y. Tang, Y. Ma, Y. Fan, H. Feng, J. Wang, S. Feng, Q. Lu, B. Hu, Y. Lin, J. Li, Y. Zhang, Y. Wang, L. Zhou and M. Fan: Central and autonomic nervous system interaction is altered by short-term meditation. *Proc Natl Acad Sci U S A*, 106 (22), 8865-70 (2009)

192. J. D. Levine and N. Alessandri-Haber: TRP channels: targets for the relief of pain. *Biochim Biophys Acta*, 1772 (8), 989-1003 (2007)

193. D. Austin: The psychophysiological effects of music therapy in intensive care units. *Paediatr Nurs*, 22 (3), 14-20, (2010)

Abbreviations: ACTH: Adrenocorticotrophic Hormone, BDNF: Brain-derived neurotrophic factor, CBP: Chronic back pain,CCK: Cholecystokinin, CGRP: Calcitonin gene-related peptide, CRH: Corticotrophin-Releasing Hormone, EGF: Epidermal Growth Factor, GABA: γ-Aminobutyric acid, GC: Glucocorticoid, HDLC: High Density Lipoprotein Cholesterol, HPA axis: Hypothalamic-Pituitary-Adrenal axis, LTD: Long Term Depression, LTP: Long Term Potentiation, MRI: Magnetic Resonance Imaging, NGF: Nerve Growth Factor, NOD-mice: Non-Obese Diabetic mice, NPY: Neuropeptide Y, PAR2: Protease Activated Receptor, PKC: Protein Kinase C, SP: Substance-P, TPC: Total Plasma Cholesterol, TRPs: Transient Receptor Potential channels, TRPV: Transient Receptor Potential Vanilloid

Key Words: TRP channels, HPA-axis, Neuropeptides, Neurotransmitters, Review

Send correspondence to: Chandan Goswami, National Institute of Science Education and Research, Institute of Physics Campus, Sachivalaya Marg, Bhubaneswar, Orissa, 751005, India, Tel: 91-674-2304044, Fax: 91-674-230243, E-mail: chandan@niser.ac.in

Metadata of the chapter that will be visualized online

Chapter Title	TRPV1 Activators (“Vanilloids”) as Neurotoxins	
Copyright Year	2013	
Copyright Holder	Springer Science+Business Media New York	
Author	Family Name	**Kumar**
	Particle	
	Given Name	**Ashutosh**
	Suffix	
	Division/Department	National Institute of Science Education and Research
	Organization/University	Institute of Physics Campus
	Street	Sachivalaya Marg
	City	Bhubaneswar
	State	Orissa
	Country	India
Author	Family Name	**Majhi**
	Particle	
	Given Name	**Rakesh Kumar**
	Suffix	
	Division/Department	National Institute of Science Education and Research
	Organization/University	Institute of Physics Campus
	Street	Sachivalaya Marg
	City	Bhubaneswar
	State	Orissa
	Country	India
Author	Family Name	**Yadav**
	Particle	
	Given Name	**Manoj**
	Suffix	
	Division/Department	National Institute of Science Education and Research
	Organization/University	Institute of Physics Campus
	Street	Sachivalaya Marg
	City	Bhubaneswar
	State	Orissa
	Country	India
Corresponding Author	Family Name	**Szallasi**

	Particle	
	Given Name	**Arpad**
	Suffix	
	Organization/University	Monmouth Medical Center
	City	Long Branch
	State	NJ
	Country	USA
	Email	ASzallasi@barnabashealth.org
	Email	ASzallasi@sbhcs.com
Corresponding Author	Family Name	**Goswami**
	Particle	
	Given Name	**Chandan**
	Suffix	
	Division/Department	National Institute of Science Education and Research
	Organization/University	Institute of Physics Campus
	Street	Sachivalaya Marg
	City	Bhubaneswar
	State	Orissa
	Country	India
	Email	chandan@niser.ac.in

Abstract

A distinct subset of primary sensory neurons is distinguished by their unique sensitivity to capsaicin, the pungent ingredient in hot chili peppers. The initial excitation by capsaicin of these neurons is followed by a long-lasting, but fully reversible, refractory state (traditionally termed as desensitization) or under certain conditions, like neonatal treatment, frank neurotoxicity. This neurotoxic action was extensively used to identify capsaicin-sensitive neuronal pathways and to explore their physiological function. In 1997, a specific receptor for capsaicin and related compounds (collectively referred to as vanilloids) was identified as transient receptor potential cation channel subfamily V member 1 (TRPV1), a multifunctional channel involved in thermosensation (heat) and taste perception (e.g., peppers and vinegar). Importantly, TRPV1 also functions as a molecular integrator for a broad range of seemingly unrelated noxious stimuli including venoms from spiders and jellyfish. Indeed, TRPV1 is thought to be a major transducer of the thermal hyperalgesia that follows inflammation and/or tissue injury. Ablation of sensory neurons by vanilloids is, however, not only a research tool but also has a clear therapeutic potential. Currently, site-specific resiniferatoxin (an ultrapotent capsaicin analog) injections are being evaluated as "molecular scalpels" to achieve permanent analgesia in cancer patients with chronic, intractable pain. In this chapter, we review our knowledge of the molecular mechanisms underlying

	vanilloid-induced neurotoxicity, which includes both TRPV1-mediated and independent signalling pathways.
Keywords (separated by “-”)	Capsaicin - Resiniferatoxin - The capsaicin (vanilloid) receptor TRPV1 - Vanilloids

TRPV1 Activators ("Vanilloids") as Neurotoxins

Ashutosh Kumar, Rakesh Kumar Majhi, Manoj Yadav, Arpad Szallasi, and Chandan Goswami

Contents

Abstract

A distinct subset of primary sensory neurons is distinguished by their unique sensitivity to capsaicin, the pungent ingredient in hot chili peppers. The initial excitation by capsaicin of these neurons is followed by a long-lasting, but fully reversible, refractory state (traditionally termed as desensitization) or under certain conditions, like neonatal treatment, frank neurotoxicity. This neurotoxic action was extensively used to identify capsaicin-sensitive neuronal pathways and to explore their physiological function. In 1997, a specific receptor for capsaicin and related compounds (collectively referred to as vanilloids) was identified as transient receptor potential cation

Authors Ashutosh Kumar and Rakesh Kumar Majhi have equally contributed.

A. Kumar • R.K. Majhi • M. Yadav • C. Goswami (✉)
National Institute of Science Education and Research, Institute of Physics Campus, Bhubaneswar, Orissa, India
e-mail: chandan@niser.ac.in

A. Szallasi (✉)
Monmouth Medical Center, Long Branch, NJ, USA
e-mail: ASzallasi@barnabashealth.org; ASzallasi@sbhcs.com

R.M. Kostrzewa (ed.), *Handbook of Neurotoxicity*,
DOI 10.1007/978-1-4614-5836-4_94,

channel subfamily V member 1 (TRPV1), a multifunctional channel involved in thermosensation (heat) and taste perception (e.g., peppers and vinegar). Importantly, TRPV1 also functions as a molecular integrator for a broad range of seemingly unrelated noxious stimuli including venoms from spiders and jellyfish. Indeed, TRPV1 is thought to be a major transducer of the thermal hyperalgesia that follows inflammation and/or tissue injury. Ablation of sensory neurons by vanilloids is, however, not only a research tool but also has a clear therapeutic potential. Currently, site-specific resiniferatoxin (an ultrapotent capsaicin analog) injections are being evaluated as "molecular scalpels" to achieve permanent analgesia in cancer patients with chronic, intractable pain. In this chapter, we review our knowledge of the molecular mechanisms underlying vanilloid-induced neurotoxicity, which includes both TRPV1-mediated and independent signalling pathways.

Keywords

Capsaicin • Resiniferatoxin • The capsaicin (vanilloid) receptor TRPV1 • Vanilloids

List of Abbreviations

CCK-B	Cholecystokinin receptor-B
CGRP	Calcitonin gene-related peptide
CNS	Central nervous system
CTB	Cholera toxin subunit B
DRG neuron	Dorsal root ganglion neuron
ETC1	Electron transport chain complex 1
ETC3	Electron transport chain complex 3
ICK-peptides	Inhibitory cystine knot peptides
ISH	In situ hybridization
MPT	Membrane permeability transition
NADA	*N*-arachidonoyl-dopamine
NNOS	Neuronal nitric oxide synthase
OLDA	*N*-oleoyldopamine
PALDA	*N*-palmitoyldopamine
PCR	Polymerase chain reaction
PKC	Protein kinase C
PMOR	Plasma membrane NADH oxidoreductase
ROPA	Resiniferonol 9,13,14-orthophenylacetate
ROS	Reactive oxygen species
RTX	Resiniferatoxin
SP	Substance P
STEARDA	*N*-stearoyldopamine
TG-neurons	Trigeminal ganglion neurons

TiTX	Tinyatoxin
TRPV1	Transient receptor potential cation channel subfamily V member 1

1 Introduction: Historical Perspectives

Natural products provide a window of opportunity to identify new targets for pharmacological intervention. Capsaicin, the active principle in hot chili peppers (*Capsicum annum*), is a prime example. Connoisseurs of hot spicy food are intimately familiar with the predominant pharmacological actions of capsaicin from personal experience: it induces profuse perspiration (known as gustatory sweating) as well as a hot, burning sensation that dissipates upon repeated challenge (desensitization). Evolutionary selective pressure seems to have maximized the pungency of capsaicin. It was speculated that the compound's pungency is able to deter ambulatory animals from eating chili pepper fruits, favoring those plants whose seeds were dispersed widely by birds. Indeed, the avian TRPV1 receptor is not activated by capsaicin, and hence birds are undeterred from ingesting chili pepper fruits and can excrete the pepper seeds large distances away. This forms the basis of the development of hot pepper-flavored "squirrel-free" bird feed. It is still a mystery, however, why the same pungency that repels squirrels is perceived as pleasurable by many human beings.

Although topical capsaicin has been used in folk medicine to relieve pain for centuries, it took the genius of the late Miklós (Nicholas) Jancsó to ask the obvious question: how can an irritant molecule paradoxically cause analgesia? Jancsó noticed that the initial transient irritation by capsaicin was followed by a long-lasting refractory state in which the neurons not only did not respond to a repeated capsaicin challenge but were also insensitive to various unrelated stimuli, and he termed this state as "desensitization" (Jancsó and Jancsó 1949; Jancsó-Gábor et al. 1970). Per definition, capsaicin-mediated desensitization is reversible. However, following neonatal treatment or when sufficiently high doses are used in adult animals, capsaicin induces neuronal death and causes permanent analgesia (Jancsó et al. 1984). This forms the experimental foundation for the use of site-specific resiniferatoxin (an ultrapotent capsaicin analog) injections to achieve permanent relief of otherwise intractable pain in cancer patients. Furthermore, chemical ablation of sensitive neurons by capsaicin turned out to be an invaluable tool to dissect capsaicin-sensitive pathways and to explore their physiological function. Generally speaking, these neurons comprise a functional subset of peptidergic primary sensory neurons with unmyelinated (C-type) fibers that respond to noxious stimuli and initiate the cascade of neurogenic inflammation.

The molecular mechanisms underlying capsaicin-mediated desensitization are poorly understood, and the line between desensitization and neurotoxicity is most likely ill defined and arbitrary. The sensitization of TRPV1 by different kinases and involvement of different pathways also remain unclear (Vellani et al. 2006;

Otten et al. 1983; Negri et al. 2006). The cloned capsaicin (vanilloid) receptor TRPV1 is an inwardly rectifying cation channel with limited selectivity for Ca^{2+}, and Ca^{2+}-overload is a well-established cause of neurotoxicity (Chard et al. 1995; Caterina et al. 1997; Sugimoto et al. 1998; Czaja et al. 2008). Indeed, neurochemical calcium and other ions such as cobalt stains were historically used to visualize sensitive neurons in capsaicin-treated animals (Winter 1987). At the ultrastructural level, neuronal calcium staining is coupled to swollen mitochondria, but it is still hotly debated if this reflects a buffering of cytoplasmic Ca^{2+} by the mitochondria (a direct TRPV1-mediated effect) or an indirect, TRPV1-independent interference of capsaicin with the mitochondrial electron transport chains (ETCs) (Szolcsányi et al. 1971).

The first vanilloids to be identified were pungent phytochemical compounds that typically contain a vanillyl (4-hydroxy-3-methoxybenzyl) moiety essential for bioactivity (hence the name "vanilloid") and are present in nature, mainly as plant resources (Table 1). Prime examples include capsaicin (the pungent ingredient in chili peppers), piperine (responsible for the piquancy of black pepper), resiniferatoxin (isolated from the latex of the cactus-like plant *Euphorbia resinifera*), curcumin (from *Curcuma longa*), eugenol (in clove), and zingerone (from ginger). Subsequently, vanilloids (so-called endovanilloids) were isolated from animal tissues (e.g., *N*-arachidonoyl-dopamine, NADA, isolated from rat brain) or were obtained via chemical synthesis to explore structure-activity relations (Huang et al. 2002). Few more examples are *N*-oleoyldopamine (OLDA), *N*-palmitoyldopamine (PALDA), and *N*-stearoyldopamine (STEARDA) (Chu et al. 2003). Indeed, the existence of a specific capsaicin receptor was first postulated based on the fairly strict structural requirements for capsaicin-like bioactivity.

2 Capsaicin-Sensitive Neurons

In culture, capsaicin kills ~35 % of dorsal root ganglion (DRG) neurons. It was postulated that capsaicin destroys these neurons due to influx of excess Ca^{2+} (Chard et al. 1995). Indeed, capsaicin causes a drastic increase in basal intracellular Ca^{2+} concentration when applied to the cultured DRG neuron. This in vitro toxicity correlates with the observation that application of capsaicin in vivo for prolonged periods can cause irreversible toxic effect leading to loss of pain-sensing neurons (Holzer 1991; Maggi 1991). The DRG neurons abolished by capsaicin are small in size, possess either unmyelinated C- or thinly myelinated Aδ–fibers, and show large inward intracellular Ca^{2+} currents in response to capsaicin. Both Ca^{2+} current and the neurotoxic effect of capsaicin were prevented by pre-treating the cells with ruthenium red, currently recognized as a general, nonspecific blocker of TRP channels. The neurotoxic action of capsaicin can also be prevented by chelating extracellular Ca^{2+} and/or by blocking Ca^{2+}-activated proteases like calcineurin (Docherty et al. 1996). Taken together, these results imply that capsaicin exerts its neurotoxic effects predominantly due to

t1.1 **Table 1** Example of some vanilloids

t1.2 Vanilloids	Chemical structure	Molecular formula	Origin	Properties and action	Reference
Capsaicin	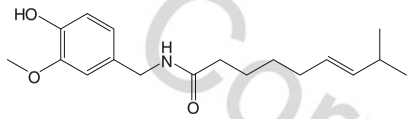	$C_{18}H_{27}NO_3$	*Capsicum* genus	Analgesic, anticancer, antiobesity, anti-inflammatory, antioxidant activates TRPV1 at 10–8 to 10–6 M	Caterina et al. 1997; Luo et al. 2011; Knotkova et al. 2008.
Resiniferatoxin	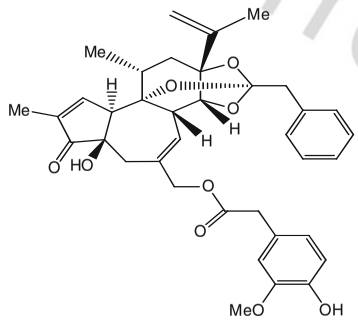	$C_{37}H_{40}O_9$	*Euphorbia resinifera*	Inhibits inflammatory hyperalgesia, activates TRPV1 at 10–10 to 10–8 M	Neubert et al. 2008; Caterina et al. 1997.
Paradol	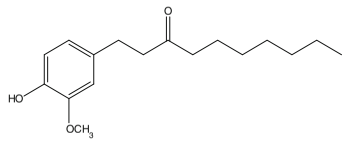	$C_{17}H_{26}O_3$	*Aframomum melegueta*	Antioxidative, antitumor, activates TRPA1 and TRPV1	Chung et al. 2001; Riera et al. 2009.

(*continued*)

t1.3 **Table 1** (continued)

t1.4 Vanilloids	Chemical structure	Molecular formula	Origin	Properties and action	Reference
Curcumin	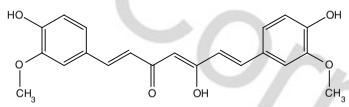	$C_{21}H_{20}O_6$	*Zingiberaceae* family	Used for pain relief, anticarcinogenic and food additive	Kuptniratsaikul et al. 2009; Aggarwal and Shishodia 2004.
Rotenone	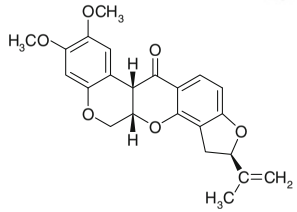	$C_{23}H_{22}O_6$	*Lonchocarpus nicou*	Used as pesticide, insecticide, piscicide, and neurotoxin	Swarnkar et al. 2012; Cabeza-Arvelaiz and Schiestl 2012
Coenzyme Q	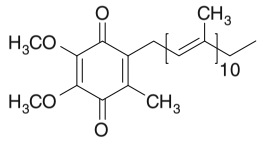	$C_{59}H_{90}O_4$	Most eukaryotic cells	Antioxidant	Littarru and Tiano 2007; Hoppe et al. 1999

consequences of both increased Ca^{2+} concentration inside the cell and cascades of cellular signalling events (Chard et al. 1995).

Capsaicin-sensitive sensory neurons are bipolar neurons with somata in dorsal root and trigeminal ganglia. The peripheral fibers innervate the skin as well as the viscera, whereas the central axons enter the central nervous system (CNS) where they form synapse at second-order neurons in the dorsal horn of the spinal cord and the spinal nucleus of the trigeminal tract, respectively. The vagal nerve also supplies capsaicin-sensitive innervations to some visceral organs: the cell bodies of these neurons are in the nodose ganglia, and they centrally project to the area postrema. The presence of TRPV1 in these neuronal pathways is firmly established by a combination of [^{3}H]-labeled resiniferatoxin (RTX) autoradiography, TRPV1 immunostaining, and other molecular methods (Szallasi and Blumberg 1999). The existence of TRPV1-expressing brain nuclei is, however, controversial.

In 1988, using a silver impregnation method, Ritter and Dinh described unexpected neuronal degeneration in several discrete forebrain and hindbrain areas of adult rats following i.p. capsaicin administration (50 or 90 mg/kg) (Ritter and Dinh. 1988). Subsequently, the presence of TRPV1 receptors was reported in corresponding (and also in additional) rat brain nuclei (and also in other parts) and the cortex in [^{3}H]RTX-binding experiments as well as by polymerase chain reaction (PCR), in situ hybridization (ISH), Western blot analysis, and immunostaining studies targeting to detect TRPV1 at RNA and protein level (Acs et al. 1996; Tóth et al. 2005; Doyle et al. 2002; Valtschanoff et al. 2001; Caterina et al. 1997; Goswami et al. 2010; Sasamura et al. 1998). Recordings obtained from rat brain slices implied that these TRPV1 receptors were functional and might be involved in learning and memory formation. Indeed, TRPV1 has been linked to the pathogenesis of Alzheimer disease (Micale et al. 2010; Pákáski et al. 2009). An additional important role for brain TRPV1 in anxiety and fear was postulated based on studies in TRPV1 knockout animals (Marsch et al. 2007). Most recently, however, only weak and minimal TRPV1 expression was found in rodent brain using a sensitive and selective reporter-mouse model (Tóth et al. 2005). This discrepancy is puzzling. Furthermore, relevant to the topic of this review, it clearly questions the value of capsaicin-induced toxicity to dissect "capsaicin sensitive" (i.e., TRPV1-expressing) pathways.

3 Plant-Derived Vanilloid Toxins

Though there are handful examples of vanilloids from plant origin, in this chapter, only vanilloids, namely, capsinoid and resiniferanoids, will be discussed in details.

Capsinoids: Capsaicin, the archetypal vanilloid, is responsible for the piquancy of hot chili peppers (Buck and Burks 1986). Capsaicin and related compounds are collectively called capsinoids. Naturally occurring capsinoids include capsiate, dihydrocapsiate, and nordihydrocapsiate. Like capsaicin, capsinoids activate TRPV1 (Iida et al. 2003), yet, they were reported to be sweet-tasting. Of synthetic capsinoids,

in the past olvanil and nuvanil had attracted attention as "improved" (candidate molecules that can be given per os to achieve desensitization) in preclinical models of chronic pain. The synthetic capsaicin, civamide (*cis*-capsaicin), is under clinical development by Winston Pharmaceuticals for indications like cluster headache.

Resiniferanoids: Resiniferatoxin (RTX) is a naturally occurring ultrapotent capsaicin analog isolated from the dried latex of the cactus-like perennial *Euphorbia resinifera*, a native of the Anti-Atlas Mountains in Morocco (Appendino and Szallasi 1997). The closely related tinyatoxin (TiTX) is present in the soap of *Euphorbia poissonii*, a succulent plant in Nigeria, which is traditionally used as a pesticide. TiTX is somewhat (approximately threefold) less potent than RTX. Although a method for the full synthesis of RTX is available, the molecule is still isolated from its natural host or obtained semi-synthetically from its parent diterpene, resiniferonol 9,13,14-orthophenylacetate (ROPA). Attempts to recapitulate the ultra potency of RTX by synthesizing phorbol-based vanilloids (phorbol is inexpensive and its chemistry is well known) met limited success. Of note, ROPA is a potent activator of protein kinase C (PKC) and acts as a tumor promoter (Frey et al. 2004). At nanomolar concentrations RTX activates TRPV1, but does not activate PKC, and does not promote the formation of tumor either in the mouse skin model of two-stage carcinogenesis (Driedger and Blumberg 1980). RTX, however, did show unexpected activity against various cancer cell lines in a most likely TRPV1-independent manner (discussed later in details).

4 Venoms as Toxins for Vanilloid Receptors

Venomous creatures such as spiders, scorpions, snakes, and snails contain a wealth of peptide toxins which can activate or block different ion channels including vanilloid receptors and produce shock, paralysis, or death (Escoubas and Rash 2004; Miller 1995; Terlau and Olivera 2004). Often such venoms and toxins and their activity on ion channels define the pray-predator relationship and exert selection pressure of certain species in specific environmental niches (Fry et al. 2006). Some venoms contain toxins which act on somatosensory neurons and provoke a noxious sensation, primarily in mammals (Siemens et al. 2006; Bohlen and Julius 2012). Somewhat unexpectedly, bites or stings by such venomous creatures were shown to activate the TRPV1 receptor and produce inflammatory pain (Siemens et al. 2006; Cuypers et al. 2006).

Venom from a *Tarantula* sp., *Psalmopoeus cambridgei*, commonly found in the West Indies, has three inhibitory cystine knot (ICK) peptides present in one peptide (Siemens et al. 2006). Previously, it was shown that venoms and toxins from spiders, snakes, and scorpions mainly target three members of the TRP channel family, namely, TRPV1, TRPA1, and TRPM8 (Siemens et al. 2006). By reverse phase chromatographic technique, the *Tarantula* venom was purified and fractionated further. When testing the bioactive fractions on HEK-293 cells heterogeneously expressing different TRP channels, it was demonstrated that the toxin was selective to TRPV1 (Siemens et al. 2006). Edman sequencing revealed the

presence of three closely related peptides named vanillotoxin 1, vanillotoxin 2, and vanillotoxin 3, all of which can act as agonists for TRPV1. Similar to the ICK peptide, these vanillotoxins have six cysteine residues in each toxin sequence (Zhu et al. 2003). Recently, another tarantula, namely, *Ornithoctonus huwena*, from China has been reported to produce a toxin that functions as a TRPV1 agonist (Bohlen et al. 2010). Interestingly, this toxin is similar to the vanillotoxin 1–3. This toxin is named double knot toxin because it has two ISK motifs repeated in tandem (Bohlen et al. 2010).

For the sake of completeness, it should be mentioned that there are venoms which contain inhibitory components against TRPV1. For example, extract from a nematocyte (sea anemone *Heteractis crispa*) contains a peptide, named APHC1, which blocks TRPV1 (Andreev et al. 2008). Furthermore, venom from a funnel web spider (*Agelenopsis aperta*) has two toxin components (AG489 and AG505) which inhibit TRPV1 (Kitaguchi and Swartz 2005).

5 The Diversity of Vanilloid Actions

The spectrum of vanilloid actions depends not only on the pharmacophore but also on the species and the route of administration. One has to carefully consider all these factors before selecting the appropriate compound for the studies.

Pharmacophore: RTX functions as an ultrapotent capsaicin analog with a peculiar spectrum of pharmacological activities. For example, in the rat, RTX is several thousandfold more potent than capsaicin in inhibiting the xylene-induced neurogenic inflammatory response or in causing twitch inhibition in the vas deferens (Wardle et al. 1996). By contrast, RTX is only similar in potency to capsaicin in evoking the eye-wiping response upon intraocular instillation. RTX also has unique actions: unlike capsaicin which repeatedly evokes the pulmonary chemo-reflex with no evidence of desensitization, RTX desensitizes this reflex without causing any detectable prior activation. Interestingly, RTX and capsaicin congeners showed distinct structure-activity relations for receptor binding and Ca^{2+} uptake, respectively. Resiniferanoids displayed high affinity in the binding assay and low activity in the Ca^{2+} uptake assay, whereas capsinoids showed the opposite pattern. Based on these observations, the existence of two types of vanilloid receptor was postulated, an R-type (presumably metabotropic) vanilloid receptor responsible for desensitization and a C-type (most likely) ionotropic receptor mediating irritation. This hypothesis, however, turned out to be not true: following the cloning of TRPV1, it was recognized that the same receptor mediates both R-type binding and C-type calcium responses (Caterina et al. 1997). Pharmacokinetics appears to play an important role in determining RTX-like and capsaicin-like activities. In most cases, capsaicin-evoked Ca^{2+} current is rapid in onset, large in magnitude, and short in duration. By contrast, RTX induces sustained, slowly developing and long-lasting currents. This observation might explain why RTX treatment shows a better desensitization-to-excitation ratio than capsaicin for most end-points examined.

Species Differences: Evolutionary, heat, and capsaicin sensitivity seems to have developed over a time in different species. However, different species reveal differences in responsiveness against heat and capsaicin (Nagy and Rang 2000; Phillips et al. 2004; Jordt and Julius 2002; Sardar et al. 2012). Even mammalian species show striking differences in the way they react to capsaicin challenge (Gavva et al. 2004). Reptiles, such as snakes, seem to be insensitive to capsaicin as trigeminal ganglion (TG) neurons from snakes do not respond to capsaicin (Gracheva et al. 2010). Birds do not respond to capsaicin. In keeping with this, chicken DRG neurons lack specific [^{3}H]RTX-binding sites, and the treatment of DRG neurons from chicken with capsaicin does not results in Ca^{2+} influx (Jordt and Julius 2002; Goswami et al. 2007). Chicken, however, do possess TRPV1 but it is resistant to capsaicin due to a point mutation at the position of S512 which confers capsaicin sensitivity in mammals (Jordt and Julius 2002). Within mammals, rats and rabbits are a good example for species-related differences in capsaicin sensitivity (Gavva et al. 2004). In rats, application of 1 % capsaicin to the saphenous nerve resulted in a 35 % decrease in the C:Aδ fiber ratio (Pini et al. 1990), while the same concentration of capsaicin administration to saphenous nerve of rabbits did not change the C: Aδ fiber ratio (Lynn and Shakhanbeh 1988). This implies the existence of low density and/or low capsaicin-affinity TRPV1 receptors in the rabbit. Indeed, no high-affinity RTX binding was detected in rabbit DRG neuron membranes (Gavva et al. 2004). An intriguing species-related difference in RTX actions was reported in the cat. Unlike in rats where, as described above, RTX desensitizes the pulmonary chemoreflex without prior activation, in the cat, RTX evokes the full reflex triad (Pórszász and Szolcsányi 1991–1992; Sculptoreanu et al. 2005). Bat has two isoforms of TRPV1 of which one is responsive to infrared (Gracheva et al. 2011). However, both isoforms are responsive to capsaicin and high temperature.

Routes of Administration: The site of administration of vanilloids can be an important factor in determining neurotoxicity. This is due to the fact that intrathecal, perineural, intraganglionic, subcutaneous, intraperitoneal, and topical application of vanilloids exposes different parts of sensory neurons to differential vanilloid concentrations. For example, intraganglionic injections expose the cell bodies of sensitive neurons to high vanilloid concentrations, leaving the peripheral terminals intact. By contrast, topical vanilloid administration mainly targets the peripheral nerve terminals with no detectable effect on perikarya. As an added complication, different parts of the primary afferent neurons (central terminals, cell bodies, axons, and peripheral terminals) have their own range of sensitivity to vanilloid agonists. For example, peripheral sensory axons have different sensitivity to capsaicin, with the most vulnerable part being the subepidermal part of the axon (Chung et al. 1990). Intrathecal or intraganglionic administration of RTX selectively deletes TRPV1-expressing neurons and confers irreversible thermal, inflammatory, and cancer pain relief (Brown et al. 2005; Karai et al. 2004; Tender et al. 2005). By contrast, peripheral administration of a single dose of RTX produces a long-lasting but reversible analgesia by ablating nociceptive nerve terminals (Karai et al. 2004; Kissin 2008; Neubert et al. 2003; Goswami et al. 2007). This effect could last from

few days to few weeks and is preceded by a rapid loss of specific [^{3}H]RTX-binding sites which is already apparent 1 h after RTX treatment. Similarly, a long-lasting (up to 1 month) but fully reversible loss of TRPV1-like immunoreactivity was observed in skin biopsies taken from volunteers following exposure to a high-concentration capsaicin patch (Qutenza) (Inoue et al. 2002). Taken together, these results imply that it is impossible to extrapolate vanilloid actions from one species to another, especially if the route of administration is also changed.

6 Vanilloid Interaction with Receptors

Among all TRPV channels, TRPV1 represents the best characterized channel in terms of the vanilloid-mediated activation. It has been demonstrated that the temperature gating of TRPV1 is actually a voltage-dependent process (Voets et al. 2005). In a similar manner, vanilloids also modulate the voltage dependency of the TRP channel in ambient temperature and thus eliminates the requirement for high temperatures. In a simplified manner, it can be said that at molecular level, interaction of vanilloids with TRPV1 results in a conformational change which reduces the requirements for high temperature and thus is suitable for channel opening. However, information regarding the species-specific interaction of vanilloids to TRPV1 remains insufficient and discrepancies in the vanilloid-binding sites remain ambiguous.

Initially, it was demonstrated that capsaicin and capsazepine are competitive inhibitors of RTX binding on membrane fraction suggesting that these compounds probably bind at the same region (Szallasi et al. 1993). Capsaicin was originally believed to activate TRPV1 by binding to its extracellular loops. However, use of a membrane impermeable analog of capsaicin, i.e., DA-5018.HCl, reveals opposite effect on the TRPV1 present in the inside-out patched membrane. This compound activates TRPV1 when applied outside of the pipet, but failed to activate TRPV1 when applied from inside of the patch. This result confirms that capsaicin, being lipophilic in nature, can cross the plasma membrane and thus can bind to an intracellular/intramembranous region of TRPV1 (Jung et al. 1999). Indeed, it was demonstrated that capsaicin binds to the TM regions of TRPV1. The capsaicin-binding region was mapped down to a critical residue (Y511) located at the region between the 1st intracellular loop joining TM2 and TM3 regions of rat TRPV1 (Jordt and Julius 2002). The same position is responsible for capsaicin sensitivity too. In agreement with the involvement of that residues in capsaicin sensitivity, two mutants, namely, TRPV1-Y511A and TRPV1-S512Y (rat TRPV1), abolished capsaicin-mediated activation, while TRPV1-Y511A mutant failed to respond to anandamide also (an endogenous vanilloid that activates TRPV1) (Jordt and Julius 2002). Functional studies with the capsaicin-insensitive orthologs of TRPV1 (avian and rabbit) have demonstrated that capsaicin-mediated gating requires a small region of the TRPV1 which includes residues at positions 511 and 512 (Jordt and Julius 2002; Gavva et al. 2004). Interestingly, the mutant, namely, TRPV1-S512Y, converted the activity of the antagonist 5'I-RTX into an intrinsic agonist, albeit

with a lower potency than its parent compound, RTX (Sutton et al. 2005). Notably, these two residues are present between transmembrane domain 3 (TM3) and the first intracellular loop region. Based on these observations, it was proposed that gating of this channel may involve a sequential movement of a paddle structure. According to this concept, the TM3 and TM4 region of the channel is predicted to form a gating paddle (Chou et al. 2004), with residues such as M547 (Rat) and L547 (human) forming a part of the key agonist-binding site which is accessible from the intracellular interface (Johnson et al. 2006). However, this suggests that the critical agonist-binding region is not buried deep within the transmembrane region as suggested by the traditional homology models (Jordt and Julius 2002; Gavva et al. 2004; Phillips et al. 2004). This concept is also supported by the recent observation made in voltage-dependent potassium channel KvAP where X-ray crystal structure confirmed that amino acids at position 512 and 547 are located in close proximity (Jiang et al. 2003). In agreement with the joint action of TM3 and TM4 in agonist recognition, residue M/L547 located at the TM4 mediates significant species differences in resiniferatoxin (RTX) sensitivity, and the S512 is critical for discriminating between pH and capsaicin gating of TRPV1 (Jordt and Julius 2002).

However, a number of studies indicated the involvement of additional residues located within TM4, the putative S5–S6 pore region, and also at the N- and C-termini of TRPV1 on vanilloid-mediated activities and capsaicin responsiveness (Welch et al. 2000; Vlachova et al. 2003; Gavva et al. 2004; Phillips et al. 2004; Jung et al. 2002). For example, involvement of residues (R114 and E761) located in the N- and C-cytosolic tails of rat TRPV1 respectively has influence on the RTX-binding and RTX-mediated response to TRPV1 (Jung et al. 2002). Similarly, a number of critical residues located within the TM3 and TM4 (also considered as voltage sensor) regions have been shown to be responsible for major species-specific differences in vanilloid activity (Chou et al. 2004; Gavva et al. 2004; Phillips et al. 2004). In agreement with the involvement of TM3 and TM4 in the capsaicin activity in different species, M547 and T550 located in TM3 and TM4 region of TRPV1 (rat as well as human) confer vanilloid sensitivity, [^{3}H]RTX-binding and capsazepine-binding, parameters which are different in rabbit TRPV1 (Gavva et al. 2004). Changing the single residue at 550 in rabbit TRPV1 to the corresponding residue found in rat and human TRPV1 (I550T) was sufficient to confer gain of function for activation by capsaicin (Gavva et al. 2004). Furthermore, TRPV1 (rat as well as in human) mutants, namely, TRPV1-T550I and TRPV1-Y511A, demonstrate a loss of sensitivity to capsaicin (Gavva et al. 2004). A single mutation embedded in the TM4 region of TRPV1 (human), namely, TRPV1-L547M, produced a 30-fold increase in sensitivity to [^{3}H]RTX, whereas the reverse mutation in the rat isoform caused a decrease in sensitivity of equal amplitude (Chou et al. 2004). These critical residues affect ligand recognition to some extent and also affect channel function in response to ligand binding (Gavva et al. 2004).

Three amino acid residues located near the pore region of the rat TRPV1 are also involved in the capsaicin responsiveness. This is confirmed by the TRPV1 mutants,

namely, TRPV1-E636Q, TRPV1-D646N, and TRPV1-E648Q mutants, which affects capsaicin-mediated gating but not the heat or proton-mediated activation of TRPV1 (Welch et al. 2000). In addition, mutation of three residues located in TM6 (NML676FAP) also abolished capsaicin-mediated activation with little effect on ligand binding to rat TRPV1 (Kuzhikandathil et al. 2001). Similarly, another mutant, namely, TRPV1-L547M (Human) located at the 4th TM region, causes a decrease in capsaicin potency (Johnson et al. 2006).

7 Vanilloid-Induced Messenger Plasticity

It was postulated that vanilloids do not affect non-nociceptive neurons and/or mechanosensitive nociceptive neurons (Karai et al. 2004). This is important because, unlike local anaesthetics which target ubiquitous sodium channels in all axons, vanilloids selectively block heat-sensitive TRPV1-positive nociceptors and thus leave other sensory modalities intact, rendering these molecules a better choice for pain relief. In the rat spinal cord, RTX treatment ameliorated the so-called "wind-up" phenomenon after repeated peripheral C-fiber stimulation that is believed to correspond to central sensitization (Xu et al. 1997). This effect on the "wind-up" response correlated to the time course of the thermal hypoalgesia in the hot plate test (Xu et al. 1997). Unexpectedly, RTX treatment also resulted in reduced sensitivity to mechanical stimulation (Pan et al. 2003). The mechanical hypoalgesia was, however, transient (a few days) compared to the thermal hypoalgesia (several weeks). Since TRPV1-expressing C-fiber neurons do not respond to mechanical stimuli (and mechanosensitive A neurons do not express TRPV1), it is unclear how RTX treatment elevates the threshold for mechanical stimulation. One might wonder, however, if this is somehow part of the "messenger plasticity" that follows vanilloid administration.

Paradoxically, RTX treatment can cause mechanical allodynia. Pan et al. injected 200 μg/kg RTX i.p. to rats and observed rapid increase in the paw withdrawal latency to a heat stimulus, while profound tactile allodynia developed in 3 weeks (Pan et al. 2003). This unexpected increase in mechanical sensitivity lasted for at least 6 weeks (Pan et al. 2003). In the RTX-treated rats, IB4-labeled unmyelinated C-fiber terminals in the dorsal horn were significantly reduced, and cholera toxin subunit B (CTB)-labeled myelinated fiber terminals appeared to sprout into lamina II of the spinal dorsal horn (Pan et al. 2003). Electron microscopic examination of the sciatic nerve also revealed significant loss of unmyelinated fibers and extensive ultrastructural damage of myelinated fibers in RTX-treated rats (Pan et al. 2003). Immunofluorescence labeling showed diminished TRPV1-like immunoreactivity in DRG neurons and the spinal dorsal horn following RTX administration. This study suggests that systemic (i.p.) RTX administration diminishes the thermal pain sensitivity by depletion of unmyelinated afferent fibers. At the same time, RTX damages the myelinated afferent fibers and causes their abnormal sprouting in lamina II of the spinal dorsal horn. The latter anatomical change might be the reason behind delayed tactile allodynia (Pan et al. 2003).

As discussed above, desensitization to vanilloids is reversible and thus contrasts to irreversible neurotoxicity. For example, it has been reported that a single topical application of RTX to the rat cornea reduces the capsaicin-evoked eye-wiping response in a dose-dependent manner for 3–5 days, while the normal nociceptive responses return by 5–7 days (Bates et al. 2010). Importantly, RTX administration did not impair epithelial wound healing and blink reflex or cause detectable histological damage to the cornea (Bates et al. 2010). Immunohistochemistry experiments revealed that RTX treatment caused a temporary loss of calcitonin gene-related peptide (CGRP) expressing nociceptive fibers: the majority of fibers reappeared within 12 days and full recovery was attained within 4 months (Bates et al. 2010). Systemic (s.c.) RTX treatment also inhibits the capsaicin-induced eye-wiping response and depletes CGRP-like immuoreactivity in the dorsal horn of the spinal cord: these effects last much longer (months) than those observed after topical administration (less than 2 weeks) but are fully reversible. Subcutaneous RTX, however, causes skin ulcerations (that can be severe in some animals) in the head (mostly in the facial skin and around the ears), the cause of which is unclear. It was suggested that RTX may cause paradoxical itch and the ulcers are secondary to the scratching behavior of the animals. This effect of RTX is somewhat different than other vanilloids such as capsaicin and curcumin which reveal anticarcinogenic and antitumor activity (Surh et al. 1995; Park and Surh 1997; Limtrakul et al. 1997; Jang et al. 1989; Huang et al. 1997; Tanaka et al. 2002). Also, high-concentration RTX (leaking from the injection site) may damage the epithelium, either directly (there are reports that keratinocytes may express functional TRPV1 receptors) or indirectly (Li et al. 2007). Finally, intraganglionic RTX injection (into the trigeminal ganglion) was reported to abolish eye wiping in response to capsaicin in an irreversible fashion; this was associated with a loss of TRPV1/CGRP-positive neurons (Karai et al. 2004).

The effect of RTX-induced denervation on TRPV1 expression in surrounding tissues has been recently examined. Surgical removal of both the sciatic and saphenous nerves from rat right hind legs and a parallel setup administration of RTX to the rat leg subcutaneously were performed (Kun et al. 2012). Two weeks after administration, the dorsal and plantar paw skin samples of hind legs, as well as the oral mucosa, were excised. Neither chemical nor surgical denervation influenced the level of TRPV1 receptor mRNA and protein expression in non-neural cells of either skin regions or mucosa (Kun et al. 2012). This indicates that RTX pretreatment is cytotoxic only to TRPV1-positive neurons and does not affect surrounding non-neural tissues.

As discussed above, vanilloid treatment depletes the proinflammatory neuropeptides substance-P (SP) and CGRP from capsaicin-sensitive sensory neurons. It was proposed that capsaicin blocks centripetal intra-axonal transport and thereby starves the cell bodies of nerve growth factor (NGF) which is produced in the periphery and is important for neuropeptide synthesis. Indeed, RTX treatment causes a marked decrease in pre-protachykinin mRNA levels encoding SP (Szallasi et al. 1999). Subsequently, it was discovered that vanilloid-induced changes in neuropeptide levels are, in fact, bidirectional: while SP and CGRP are

downregulated after capsaicin or RTX treatment, the expression of an endogenous analgesic peptide galanin is increased. Moreover, increased neuronal nitric oxide synthase (nNOS) and cholecystokinin receptor-B (CCK-B) levels were observed in the RTX-treated animals (Burliński et al. 2011). Collectively, these changes were termed "vanilloid-induced messenger plasticity" (Szallasi and Blumberg 1999). It was postulated that vanilloid treatment alters the phenotype of sensory neurons from proinflammatory to analgesic/anti-inflammatory. Thus, vanilloid-induced messenger plasticity may represent a major mechanism of desensitization.

8 Vanilloids and Mitochondrial Dysfunction

In cultured DRG neurons, there is a clear separation between concentrations at which capsaicin activates TRPV1 ($ED_{50}<100$ nM) and at which it becomes neurotoxic (30–100 μM) (Chard et al. 1995; Wood et al. 1988). Moreover, capsaicin was reported to kill a variety of non-neuronal cells such as in human B-cells, mouse myeloid cell lines, and Jurkat T-cells as well as squamous cell carcinoma cell lines (Wolvetang et al. 1996; Macho et al. 1999; Lee and Surh. 1998; Hail and Lotan. 2002). Capsaicin-induced apoptosis was also described in rat thymocytes (Amantini et al. 2004). It is still hotly debated if these non-neuronal cells express functional TRPV1. For example, in dendritic cells, both the presence and absence of TRPV1 were reported (O'Connell et al. 2005; Tóth et al. 2009).

The effect of capsaicin on cell death seems to be either specific (TRPV1 mediated) or nonspecific (not mediated by TPV1) in nature. Capsaicin can cause apoptosis or necrosis depending on the dose applied. In cultured rat DRG cells, capsaicin causes apoptosis by increasing the intracellular Ca^{2+} concentration, enhancing mitochondrial Ca^{2+} accumulation, dissipation of the inner transmembrane potential ($\Delta\psi_m$), activation of Ca^{2+}-sensitive proteases, and DNA fragmentation (Dedov et al. 2001). Capsaicin evokes similar signalling events in transformed and mitogen-activated T-cells (Macho et al. 1999) and in human and rat glioblastoma cells (Bíró et al. 1998; Lee et al. 2000).

The intercellular Ca^{2+} homeostasis is maintained by Ca^{2+}-binding proteins present in cytoplasm, endoplasmic reticulum (ER), and mitochondria (Kostyuk and Verkhratsky 1994; Svichar et al 1997; Verkhratsky and Petersen 1998). The elevated intracellular Ca^{2+} triggered by capsaicin leads to activation of Ca^{2+}-dependent enzymes such as different phospholipases, proteases, and endonucleases that can cause apoptosis in neuronal cells as well as non-neuronal cells (McConkey and Orrenius 1996; Wood et al. 1988). Though in general mitochondria are able to sequester intracellular Ca^{2+}, excess Ca^{2+}-influx into mitochondria causes membrane permeability transition (MPT) pore in mitochondrial membrane (Wong et al. 2012). This is considered as prototypical inducing factor. This MPT allows water and other small molecules to infiltrate inside the mitochondrial matrix which leads to osmotic swelling of mitochondria and may cause physical rupture of mitochondrial membrane (Green and Reed 1998; Bernardi 1992; Crompton 1999; Kroemer and Reed 2000).

However, several reports suggest that vanilloids may exert effects which are independent of Ca^{2+}-influx and TRPV1 receptors. This is due to the fact that capsaicin has significant effects in biological systems that are much lower in the phylogenetic tree and do not contain TRPV1. For example, capsaicin acts as inhibitor for organisms such as *Paracoccus denitrificans*, *Escherichia coli*, and *Thermus thermophilus* HB-8 where it affects ubiquinone reduction by NADH (Yagi 1990). Not only pure capsaicin, other vanilloids such as dihydrocapsaicin and RTX can also act as inhibitor of NADH oxidase (Wolvetang et al. 1996). Indeed, these inhibitors are able to induce apoptosis in human B-cell and mouse myeloid cell line (Wolvetang et al. 1996). In contrast, it was shown that in organisms which do not have the energy transducing site, such as in *Saccharomyces cerevisiae* mitochondria and *Bacillus subtilis* membranes, capsaicin does not inhibit NADH-ubiquinone reductase, suggesting that mitochondria can be a potential target of capsaicin action (Yagi 1990). In addition to mitochondria, recently it has been shown that in hippocampal astrocytes capsaicin can act as an inhibitor of tyrosyl tRNA synthetase and by inhibiting this enzyme, it induces cell death (Cochereau et al. 1996, 1997).

The TRPV1-independent functions of capsaicin mostly indicate the deleterious effect of capsaicin on mitochondria. Earlier research suggests that after the systemic application of capsaicin in the Aβ-type sensory neuron of adult rat as well as neonatal rat leads to mitochondrial swelling and results in the formation of atypical hollow mitochondria (Joó et al. 1969; Szolcsányi et al. 1975; Jancsó et al. 1977; Jancsó and Király 1981; Szöke et al. 1998, 2002). However, the real molecular mechanism behind the formation of hollow mitochondria is not clear. In addition to the TRPV1 receptor-mediated effects, it seems that capsaicin can also exert receptor-independent effects on the mitochondria. Due to its structure, capsaicin can act as analog of coenzyme Q, a lipophilic mobile electron carrier present in plasma membrane and involved in maintaining the redox potential of membrane. Indeed, it has been reported that preincubation of human lymphoblastoid cells with coenzyme Q prevents capsaicin-induced apoptosis (Wolvetang et al. 1996; Macho et al. 2000). It suggests that capsaicin competes for coenzyme Q and alters the redox potential of plasma membrane. Apart from that it has been also reported in transformed and activated T-cells; capsaicin inhibits the plasma membrane NADH oxidoreductase (PMOR), an enzyme that transfers electrons from cytoplasmic NADH to external electron acceptors such as oxygen via coenzyme Q (ubiquinone) (Morré et al. 1995, 1996; Wolvetang et al. 1996; Macho et al. 2000). Capsaicin can also inhibit the NADH:coenzyme Q oxidoreductase (complex I) activity of the mitochondrial electron transport system (Shimomura et al. 1989; Yagi 1990) which causes alteration on the mitochondrial membrane structure and its function (Aranda et al. 1995; Tsuchiya 2001). In vitro experiments in transformed cells as well as in activated T-cells suggest that capsaicin treatment enhances the generation of reactive oxygen species (Macho et al. 1998, 1999; Garle et al. 2000) and depolarization of mitochondrial membrane (Dedov et al. 2001) and apoptosis. Capsaicin suppresses the growth of cancer cells by NF-kB inactivation, reactive oxygen species (ROS) generations, cell-cycle arrest, and modulating EGFR/HER-2

pathways (Hail 2003; Kang et al. 2003; Lee et al. 2004; Min et al. 2004; Surh 2002; Thoennissen et al. 2010). Similarly, RTX was also reported to inhibit the NADH oxidase located in plasma membranes, to generate reactive oxygen species, and to induce apoptosis in transformed cells (Wolvetang et al. 1996; Macho et al. 1999, 2000; Garle et al. 2000). The exact molecular mechanism by which capsaicin causes oxidative stress and apoptosis remains rudimentary (Pramanik et al. 2011).

9 Conclusions and Future Research Directions

Historically, capsaicin and RTX proved to be invaluable tools in defining a fundamental subdivision of the peripheral nervous system (Appendino and Szallasi 1997; Buck and Burks 1986). Capsaicin-sensitive neurons are peptidergic nociceptive (primary sensory) neurons that express the vanilloid (capsaicin) receptor TRPV1. The activation of these neurons not only transmits painful stimuli to the CNS but also initiates the neurogenic inflammatory response. In turn, neurogenic inflammation was postulated to play a pivotal role in the pathogenesis of diverse diseases states, ranging from migraine through asthma to irritable bowel disease.

What makes capsaicin unique among naturally occurring irritant agents is that the initial stimulation of these neurons is followed by a lasting but fully reversible refractory state (traditionally termed desensitization) or irreversible neurotoxicity. Desensitization to capsaicin has a clear therapeutic potential. Indeed, capsaicin-containing creams and patches have clinical application for decades for indications like diabetic polyneuropathy. Irreversible neurotoxicity can also be exploited for therapeutic purposes. Indeed, at present site-specific RTX injections are undergoing clinical trials to achieve permanent analgesia in cancer patients with chronic, intractable pain secondary to metastatic disease.

Despite the tremendous progress that has been made after the identification and molecular cloning of TRPV1 in understanding capsaicin mechanisms, several outstanding questions remain unsolved. Most important, the exact molecular mechanisms underlying reversible desensitization versus irreversible toxicity are yet to be established. At high concentrations, the specificity of vanilloids for TRPV1 is lost, and the distinction between specific (TRPV1-mediated) and nonspecific (non-TRPV1-mediated) vanilloid actions becomes problematic. As an added complication, the existence of functional TRPV1 receptors in cells other than capsaicin-sensitive primary sensory neurons remains controversial. For example, TRPV1 knockout mice show altered behavior (e.g., reduced fear response) and capsaicin causes extensive neurodegenerative changes in the rat brain; yet, reporter mice show essentially no TRPV1 expression in the brain (Cavanaugh et al. 2011; Marsch et al. 2007; Tóth et al. 2005; Roberts et al. 2004; Starowicz et al. 2008; Goswami et al. 2010). In this context it is worth to mention that involvement of TRPV1 in the regulation of spine morphology and synaptic transmission has been demonstrated (Goswami et al. 2010). Another puzzling example is the keratinocytes present in skin. Keratinocytes were reported to express TRPV1 (both mRNA and protein) and

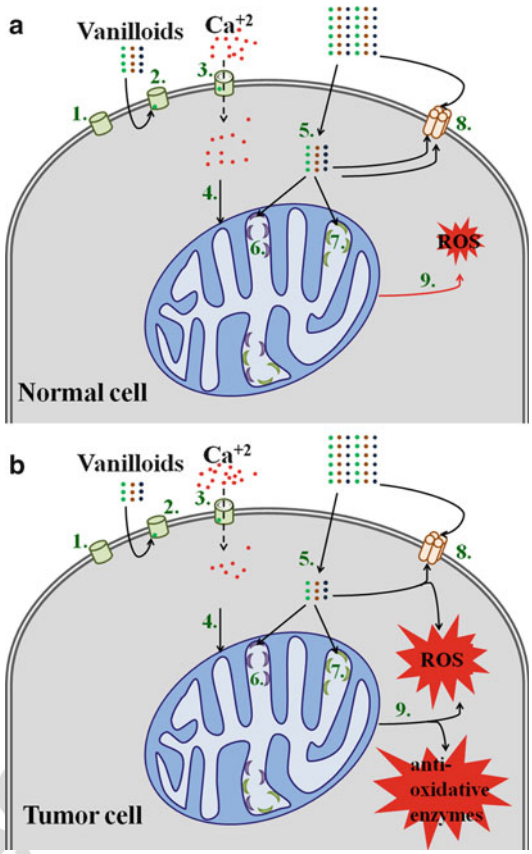

Fig. 1 TRPV1-dependent and TRPV1-independent vanilloid actions in normal cell (**a**) and tumor cell (**b**). TRPV1 present in the plasma membrane can be activated by different vanilloids with different affinities and binding kinetics (*Steps 1–2*). Potent vanilloids such as capsaicin or RTX activate TRPV1 at very low concentration and cause Ca^{2+} influx (*Step 3*). Vanilloids at much higher concentrations can cross plasma membrane and can also act on electron transport chain complex 1 (*ETC1*) and electron transport chain complex 3 (*ETC3*) (*Steps 5–7*). Vanilloids can also act on the coenzyme Q and PMOR (*Steps 8–9*). All these factors result in production of ROS (*Step 10*) relevant for neurotoxicity

respond to capsaicin with Ca^{2+}-uptake (Southall et al. 2003; Lee et al. 2008; Pecze et al. 2008). Yet, capsaicin evokes no responses in the rat skin after skin denervation (Fig. 1).

The mechanisms responsible for the marked species-related differences in vanilloid actions are only partially understood. It is now clear that birds do not respond to capsaicin because the avian TRPV1 receptor lacks the functional vanilloid-binding motif of mammalian TRPV1 receptors. However, it remains a mystery why the pulmonary chemoreflex is differentially regulated by RTX in rats (desensitization without prior excitation) and cats (repeatable excitation with no desensitization). However, much more and detailed studies are needed to characterize vanilloids for therapeutic applications in near future.

Acknowledgements Funding from National Institute of Science Education and Research and Department of Biotechnology (Govt. India, grant number BT-BRB-TF-2-2011) is acknowledged. The funders had no role in study design, data collection and analysis, decision to publish, or preparation of the manuscript. The authors declare existence of no competing interests.

References

Acs, G., Palkovits, M., & Blumberg, P. M. (1996). Specific binding of [3H]resiniferatoxin by human and rat preoptic area, locus ceruleus, medial hypothalamus, reticular formation and ventral thalamus membrane preparations. *Life Sciences, 59*, 1899–1908.

Aggarwal, B. B., & Shishodia, S. (2004). Suppression of the nuclear factor-kappaB activation pathway by spice-derived phytochemicals: Reasoning for seasoning. *Annals of the New York Academy of Sciences, 1030*, 434–441.

Amantini, C., Mosca, M., Lucciarini, R., Perfumi, M., Morrone, S., Piccoli, M., & Santoni, G. (2004). Distinct thymocyte subsets express the vanilloid receptor VR1 that mediates capsaicin-induced apoptotic cell death. *Cell Death and Differentiation, 11*, 1342–1356.

Andreev, Y. A., Kozlov, S. A., Koshelev, S. G., Ivanova, E. A., Monastyrnaya, M. M., Kozlovskaya, E. P., & Grishin, E. V. (2008). Analgesic compound from sea anemone Heteractis crispa is the first polypeptide inhibitor of vanilloid receptor 1 (TRPV1). *The Journal of Biological Chemistry, 283*, 23914–23921.

Appendino, G., & Szallasi, A. (1997). Euphorbium: Modern research on its active principle, resiniferatoxin, revives an ancient medicine. *Life Sciences, 60*, 681–696.

Aranda, F. J., Villalaín, J., & Gómez-Fernández, J. C. (1995). Capsaicin affects the structure and phase organization of phospholipid membranes. *Biochimica et Biophysica Acta, 1234*, 225–234.

Bates, B. D., Mitchell, K., Keller, J. M., Chan, C. C., Swaim, W. D., Yaskovich, R., Mannes, A. J., & Iadarola, M. J. (2010). Prolonged analgesic response of cornea to topical resiniferatoxin, a potent TRPV1 agonist. *Pain, 149*, 522–528.

Bernardi, P. (1992). Modulation of the mitochondrial cyclosporin A-sensitive permeability transition pore by the proton electrochemical gradient. Evidence that the pore can be opened by membrane depolarization. *The Journal of Biological Chemistry, 267*, 8834–8839.

Bíró, T., Brodie, C., Modarres, S., Lewin, N. E., Acs, P., & Blumberg, P. M. (1998). Specific vanilloid responses in C6 rat glioma cells. *Brain Research. Molecular Brain Research, 56*, 89–98.

Bohlen, C. J., & Julius, D. (2012). Receptor-targeting mechanisms of pain-causing toxins: How ow? *Toxicon, 60*, 254–264.

Bohlen, C. J., Priel, A., Zhou, S., King, D., Siemens, J., & Julius, D. (2010). A bivalent tarantula toxin activates the capsaicin receptor, TRPV1, by targeting the outer pore domain. *Cell, 141*, 834–845.

Brown, D. C., Iadarola, M. J., Perkowski, S. Z., Erin, H., Shofer, F., Laszlo, K. J., Olah, Z., & Mannes, A. J. (2005). Physiologic and antinociceptive effects of intrathecal resiniferatoxin in a canine bone cancer model. *Anesthesiology, 103*, 1052–1059.

Buck, S. H., & Burks, T. F. (1986). The neuropharmacology of capsaicin: Review of some recent observations. *Pharmacological Reviews, 38*, 179–226.

Burliński, P. J., Gonkowski, S., & Całka, J. (2011). Tetrodotoxin- and resiniferatoxin-induced changes in paracervical ganglion ChAT- and nNOS-IR neurons supplying the urinary bladder in female pigs. *Acta Veterinaria Hungarica, 59*, 455–463.

Cabeza-Arvelaiz, Y., & Schiestl, R. H. (2012). Transcriptome analysis of a rotenone model of parkinsonism reveals complex I-tied and -untied toxicity mechanisms common to neurodegenerative diseases. *PloS One, 7*, e44700.

Caterina, M. J., Schumacher, M. A., Tominaga, M., Rosen, T. A., Levine, J. D., & Julius, D. (1997). The capsaicin receptor: A heat-activated ion channel in the pain pathway. *Nature, 389*, 816–824.

Cavanaugh, D. J., Chesler, A. T., Jackson, A. C., Sigal, Y. M., Yamanaka, H., Grant, R., O'Donnell, D., Nicoll, R. A., Shah, N. M., Julius, D., & Basbaum, A. I. (2011). Trpv1 reporter mice reveal highly restricted brain distribution and functional expression in arteriolar smooth muscle cells. *The Journal of Neuroscience, 31*, 5067–5077.

675 Chard, P. S., Bleakman, D., Savidge, J. R., & Miller, R. J. (1995). Capsaicin-induced neurotoxicity
676 in cultured dorsal root ganglion neurons: Involvement of calcium-activated proteases. *Neuro-*
677 *science, 65*, 1099–1108.
678 Chou, M. Z., Mtui, T., Gao, Y. D., Kohler, M., & Middleton, R. E. (2004). Resiniferatoxin binds to
679 the capsaicin receptor (TRPV1) near the extracellular side of the S4 transmembrane domain.
680 *Biochemistry, 43*, 2501–2511.
681 Chu, C. J., Huang, S. M., De Petrocellis, L., Bisogno, T., Ewing, S. A., Miller, J. D., Zipkin, R. E.,
682 Daddario, N., Appendino, G., Di Marzo, V., & Walker, J. M. (2003). N-oleoyldopamine,
683 a novel endogenous capsaicin-like lipid that produces hyperalgesia. *The Journal of Biological*
684 *Chemistry, 278*, 13633–13639.
685 Chung, K., Klein, C. M., & Coggeshall, R. E. (1990). The receptive part of the primary afferent
686 axon is most vulnerable to systemic capsaicin in adult rats. *Brain Research, 511*, 222–226.
687 Chung, W. Y., Jung, Y. J., Surh, Y. J., Lee, S. S., & Park, K. K. (2001). Antioxidative and antitumor
688 promoting effects of [6]-paradol and its homologs. *Mutation Research, 496*, 199–206.
689 Cochereau, C., Sanchez, D., Bourhaoui, A., & Creppy, E. E. (1996). Capsaicin, a structural analog
690 of tyrosine, inhibits the aminoacylation of tRNA(Tyr). *Toxicology and Applied Pharmacology,*
691 *141*, 133–137.
692 Cochereau, C., Sanchez, D., & Creppy, E. E. (1997). Tyrosine prevents capsaicin-induced protein
693 synthesis inhibition in cultured cells. *Toxicology, 117*, 133–139.
694 Crompton, M. (1999). The mitochondrial permeability transition pore and its role in cell death. *The*
695 *Biochemical Journal, 341*, 233–249.
696 Cuypers, E., Yanagihara, A., Karlsson, E., & Tytgat, J. (2006). Jellyfish and other cnidarian
697 envenomations cause pain by affecting TRPV1 channels. *FEBS Letters, 580*, 5728–5732.
698 Czaja, K., Burns, G. A., & Ritter, R. C. (2008). Capsaicin-induced neuronal death and proliferation
699 of the primary sensory neurons located in the nodose ganglia of adult rats. *Neuroscience, 154*,
700 621–630.
701 Dedov, V. N., Mandadi, S., Armati, P. J., & Verkhratsky, A. (2001). Capsaicin-induced
702 depolarisation of mitochondria in dorsal root ganglion neurons is enhanced by vanilloid
703 receptors. *Neuroscience, 103*, 219–226.
704 Docherty, R. J., Yeats, J. C., Bevan, S., & Boddeke, H. W. (1996). Inhibition of calcineurin inhibits
705 the desensitization of capsaicin-evoked currents in cultured dorsal root ganglion neurones from
706 adult rats. *Pflügers Archiv, 431*, 828–837.
707 Doyle, M. W., Bailey, T. W., Jin, Y. H., & Andresen, M. C. (2002). Vanilloid receptors
708 presynaptically modulate cranial visceral afferent synaptic transmission in nucleus tractus
709 solitarius. *The Journal of Neuroscience, 22*, 8222–8229.
710 Driedger, P. E., & Blumberg, P. M. (1980). Different biological targets for resiniferatoxin and
711 phorbol 12 myristate 13-acetate. *Cancer Research, 40*, 1400–1404.
712 Escoubas, P., & Rash, L. (2004). Tarantulas: eight-legged pharmacists and combinatorial chem-
713 ists. *Toxicon, 43*, 555–574.
714 Frey, M. R., Clark, J. A., Bateman, N. W., Kazanietz, M. G., Black, A. R., & Black, J. D. (2004).
715 Cell cycle- and protein kinase C-specific effects of resiniferatoxin and resiniferonol 9,13,14-
716 ortho-phenylacetate in intestinal epithelial cells. *Biochemical Pharmacology, 67*, 1873–1886.
717 Fry, B. G., Vidal, N., Norman, J. A., Vonk, F. J., Scheib, H., Ramjan, S. F., Kuruppu, S., Fung, K.,
718 Hedges, S. B., Richardson, M. K., Hodgson, W. C., Ignjatovic, V., Summerhayes, R., & Kochva, E.
719 (2006). Early evolution of the venom system in lizards and snakes. *Nature, 439*, 584–588.
720 Garle, M. J., Knight, A., Downing, A. T., Jassi, K. L., Clothier, R. H., & Fry, J. R. (2000).
721 Stimulation of dichlorofluorescin oxidation by capsaicin and analogues in RAW 264 mono-
722 cyte/macrophages: Lack of involvement of the vanilloid receptor. *Biochemical Pharmacology,*
723 *59*, 563–572.
724 Gavva, N. R., Klionsky, L., Qu, Y., Shi, L., Tamir, R., Edenson, S., Zhang, T. J., Viswanadhan, V. N.,
725 Toth, A., Pearce, L. V., Vanderah, T. W., Porreca, F., Blumberg, P. M., Lile, J., Sun, Y., Wild, K.,
726 Louis, J. C., & Treanor, J. J. (2004). Molecular determinants of vanilloid sensitivity in TRPV1. *The*
727 *Journal of Biological Chemistry, 279*, 20283–20295.

728 Goswami, C., Schmidt, H., & Hucho, F. (2007). TRPV1 at nerve endings regulates growth cone
729 morphology and movement through cytoskeleton reorganization. *The FEBS Journal, 274*,
730 760–772.
731 Goswami, C., Rademacher, N., Smalla, K. H., Kalscheuer, V., Ropers, H. H., Gundelfinger, E. D.,
732 & Hucho, T. (2010). TRPV1 acts as a synaptic protein and regulates vesicle recycling. *Journal*
733 *of Cell Science, 123*, 2045–2057.
734 Gracheva, E. O., Ingolia, N. T., Kelly, Y. M., Cordero-Morales, J. F., Hollopeter, G., Chesler, A. T.,
735 Sánchez, E. E., Perez, J. C., Weissman, J. S., & Julius, D. (2010). Molecular basis of infrared
736 detection by snakes. *Nature, 464*, 1006–1011.
737 Gracheva, E. O., Cordero-Morales, J. F., González-Carcacía, J. A., Ingolia, N. T., Manno, C.,
738 Aranguren, C. I., Weissman, J. S., & Julius, D. (2011). Ganglion-specific splicing of TRPV1
739 underlies infrared sensation in vampire bats. *Nature, 476*, 88–91.
740 Green, D. R., & Reed, J. C. (1998). Mitochondria and apoptosis. *Science, 281*, 1309–1312.
741 Hail, N., Jr., & Lotan, R. (2002). Examining the role of mitochondrial respiration in vanilloid-
742 induced apoptosis. *Journal of the National Cancer Institute, 94*, 1281–1292.
743 Hail, N., Jr. (2003). Mechanisms of vanilloid-induced apoptosis. *Apoptosis, 8*, 251–262.
744 Holzer, P. (1991). Capsaicin: cellular targets, mechanisms of action, and selectivity for thin
745 sensory neurons. *Pharmacological Reviews, 43*, 143–201.
746 Hoppe, U., Bergemann, J., Diembeck, W., Ennen, J., Gohla, S., Harris, I., Jacob, J., Kielholz, J.,
747 Mei, W., Pollet, D., Schachtschabel, D., Sauermann, G., Schreiner, V., Stäb, F., & Steckel, F.
748 (1999). Coenzyme Q10, a cutaneous antioxidant and energizer. *BioFactors, 9*, 371–378.
749 Huang, M. T., Ma, W., Yen, P., Xie, J. G., Han, J., Frenkel, K., Grunberger, D., & Conney, A. H.
750 (1997). Inhibitory effects of topical application of low doses of curcumin on 12-O-tetradeca-
751 noylphorbol-13-acetate-induced tumor promotion and oxidized DNA bases in mouse epider-
752 mis. *Carcinogenesis, 18*, 83–88.
753 Huang, S. M., Bisogno, T., Trevisani, M., Al-Hayani, A., De Petrocellis, L., Fezza, F., Tognetto, M.,
754 Petros, T. J., Krey, J. F., Chu, C. J., Miller, J. D., Davies, S. N., Geppetti, P., Walker, J. M., &
755 Di Marzo, V. (2002). An endogenous capsaicin-like substance with high potency at recombinant
756 and native vanilloid VR1 receptors. *Proceedings of the National Academy of Sciences USA, 99*,
757 8400–8405.
758 Iida, T., Moriyama, T., Kobata, K., Morita, A., Murayama, N., Hashizume, S., Fushiki, T.,
759 Yazawa, S., Watanabe, T., & Tominaga, M. (2003). TRPV1 activation and induction of
760 nociceptive response by a non-pungent capsaicin-like compound, capsiate. *Neuropharmacol-*
761 *ogy, 44*, 958–967.
762 Inoue, K., Koizumi, S., Fuziwara, S., Denda, S., Inoue, K., & Denda, M. (2002). Functional
763 vanilloid receptors in cultured normal human epidermal keratinocytes. *Biochemical and*
764 *Biophysical Research Communications, 291*, 124–129.
765 Jancsó, N., & Jancsó, A. (1949). Desensitization of sensory nerve endings (in Hungarian). *Kísé*
766 *rletes Orvostudomány, 2*(Suppl), 15.
767 Jancsó, G., & Király, E. (1981). Sensory neurotoxins: Chemically induced selective destruction of
768 primary sensory neurons. *Brain Research, 210*, 83–89.
769 Jancsó, G., Kiraly, E., & Jancsó-Gábor, A. (1977). Pharmacologically induced selective degener-
770 ation of chemosensitive primary sensory neurones. *Nature, 270*, 741–743.
771 Jancsó, G., Karcsú, S., Király, E., Szebeni, A., Tóth, L., Bácsy, E., Joó, F., & Párducz, A. (1984).
772 Neurotoxin induced nerve cell degeneration: Possible involvement of calcium. *Brain*
773 *Research, 295*, 211–216.
774 Jancsó-Gábor, A., Szolcsányi, J., & Jancsó, N. (1970). Stimulation and desensitization of the
775 hypothalamic heat-sensitive structures by capsaicin in rats. *The Journal of Physiology, 208*,
776 449–459.
777 Jang, J. J., Kim, S. H., & Yun, T. K. (1989). Inhibitory effect of capsaicin on mouse lung tumor
778 development. *In Vivo, 3*, 49–53.
779 Jiang, Y., Ruta, V., Chen, J., Lee, A., & MacKinnon, R. (2003). The principle of gating charge
780 movement in a voltage-dependent K^+ channel. *Nature (London), 423*, 42–48.

781 Johnson, D. M., Garrett, E. M., Rutter, R., Bonnert, T. P., Gao, Y. D., Middleton, R. E., & Sutton, K. G.
782 (2006). Functional mapping of the transient receptor potential vanilloid 1 intracellular binding site.
783 *Molecular Pharmacology, 70*, 1005–1012.
784 Joó, F., Szolcsányi, J., & Jancsó-Gábor, A. (1969). Mitochondrial alterations in the spinal ganglion
785 cells of the rat accompanying the long-lasting sensory disturbance induced by capsaicin. *Life*
786 *Sciences, 8*, 621–626.
787 Jordt, S. E., & Julius, D. (2002). Molecular basis for species-specific sensitivity to "hot" chili
788 peppers. *Cell, 108*, 421–430.
789 Jung, J., Hwang, S. W., Kwak, J., Lee, S. Y., Kang, C. J., Kim, W. B., Kim, D., & Oh, U. (1999).
790 Capsaicin binds to the intracellular domain of the capsaicin-activated ion channel. *The Journal*
791 *of Neuroscience, 19*, 529–538.
792 Jung, J., Lee, S. Y., Hwang, S. W., Cho, H., Shin, J., Kang, Y. S., Kim, S., & Oh, U. (2002).
793 Agonist recognition sites in the cytosolic tails of vanilloid receptor 1. *The Journal of Biological*
794 *Chemistry, 277*, 44448–44454.
795 Kang, H. J., Soh, Y., Kim, M. S., Lee, E. J., Surh, Y. J., Kim, H. R., Kim, S. H., & Moon, A. (2003).
796 Roles of JNK-1 and p38 in selective induction of apoptosis by capsaicin in ras-transformed
797 human breast epithelial cells. *International Journal of Cancer, 103*, 475–482.
798 Karai, L., Brown, D. C., Mannes, A. J., Connelly, S. T., Brown, J., Gandal, M., Wellisch, O. M.,
799 Neubert, J. K., Olah, Z., & Iadarola, M. J. (2004). Deletion of vanilloid receptor 1-expressing
800 primary afferent neurons for pain control. *The Journal of Clinical Investigation, 113*,
801 1344–1352.
802 Kissin, I. (2008). Vanilloid-induced conduction analgesia: Selective, dose-dependent, long-
803 lasting, with a low level of potential neurotoxicity. *Anesthesia and Analgesia, 107*, 271–281.
804 Kitaguchi, T., & Swartz, K. J. (2005). An inhibitor of TRPV1 channels isolated from funnel Web
805 spider venom. *Biochemistry, 44*, 15544–15549.
806 Knotkova, H., Pappagallo, M., & Szallasi, A. (2008). Capsaicin (TRPV1 Agonist) therapy for pain
807 relief: Farewell or revival? *The Clinical Journal of Pain, 24*, 142–154.
808 Kostyuk, P., & Verkhratsky, A. (1994). Calcium stores in neurons and glia. *Neuroscience, 63*,
809 381–404.
810 Kroemer, G., & Reed, J. C. (2000). Mitochondrial control of cell death. *Nature Medicine, 6*,
811 513–519.
812 Kun, J., Helyes, Z., Perkecz, A., Bán, A., Polgár, B., Szolcsányi, J., & Pintér, E. (2012). Effect of
813 surgical and chemical sensory denervation on non-neural expression of the Transient Receptor
814 Potential Vanilloid 1 (TRPV1) receptors in the rat. *Journal of Molecular Neuroscience, 48*,
815 795–803.
816 Kuptniratsaikul, V., Thanakhumtorn, S., Chinswangwatanakul, P., Wattanamongkonsil, L., &
817 Thamlikitkul, V. (2009). Efficacy and safety of Curcuma domestica extracts in patients with
818 knee osteoarthritis. *Journal of Alternative and Complementary Medicine, 15*, 891–897.
819 Kuzhikandathil, E. V., Wang, H., Szabo, T., Morozova, N., Blumberg, P. M., & Oxford, G. S.
820 (2001). Functional analysis of capsaicin receptor (vanilloid receptor subtype 1)
821 multimerization and agonist responsiveness using a dominant negative mutation. *The Journal*
822 *of Neuroscience, 21*, 8697–8706.
823 Lee, E., & Surh, Y. J. (1998). Induction of apoptosis in HL-60 cells by pungent vanilloids, [6]-
824 gingerol and [6]-paradol. *Cancer Letters, 134*, 163–168.
825 Lee, Y. S., Nam, D. H., & Kim, J. A. (2000). Induction of apoptosis by capsaicin in A172 human
826 glioblastoma cells. *Cancer Letters, 161*, 121–130.
827 Lee, Y. S., Kang, Y. S., Lee, J. S., Nicolova, S., & Kim, J. A. (2004). Involvement of NADPH
828 oxidase-mediated generation of reactive oxygen species in the apototic cell death by capsaicin
829 in HepG2 human hepatoma cells. *Free Radical Research, 38*, 405–412.
830 Lee, Y. M., Li, W. H., Kim, Y. K., Kim, K. H., & Chung, J. H. (2008). Heat-induced MMP-1
831 expression is mediated by TRPV1 through PKCalpha signaling in HaCaT cells. *Experimental*
832 *Dermatology, 17*, 864–870.

Li, W. H., Lee, Y. M., Kim, J. Y., Kang, S., Kim, S., Kim, K. H., Park, C. H., & Chung, J. H. (2007). Transient receptor potential vanilloid-1 mediates heat-shock-induced matrix metalloproteinase-1 expression in human epidermal keratinocytes. *The Journal of Investigative Dermatology, 127*, 2328–2335.

Limtrakul, P., Lipigorngoson, S., Namwong, O., Apisariyakul, A., & Dunn, F. W. (1997). Inhibitory effect of dietary curcumin on skin carcinogenesis in mice. *Cancer Letters, 116*, 197–203.

Littarru, G. P., & Tiano, L. (2007). Bioenergetic and antioxidant properties of coenzyme Q10: Recent developments. *Molecular Biotechnology, 37*, 31–37.

Luo, X. J., Peng, J., & Li, Y. J. (2011). Recent advances in the study on capsaicinoids and capsinoids. *European Journal of Pharmacology, 650*, 1–7.

Lynn, B., & Shakhanbeh, J. (1988). Substance P content of the skin, neurogenic inflammation and numbers of C-fibres following capsaicin application to a cutaneous nerve in the rabbit. *Neuroscience, 24*, 769–775.

Macho, A., Blázquez, M. V., Navas, P., & Muñoz, E. (1998). Induction of apoptosis by vanilloid compounds does not require de novo gene transcription and activator protein 1 activity. *Cell Growth & Differentiation, 9*, 277–286.

Macho, A., Calzado, M. A., Muñoz-Blanco, J., Gómez-Díaz, C., Gajate, C., Mollinedo, F., Navas, P., & Muñoz, E. (1999). Selective induction of apoptosis by capsaicin in transformed cells: The role of reactive oxygen species and calcium. *Cell Death and Differentiation, 6*, 155–165.

Macho, A., Lucena, C., Calzado, M. A., Blanco, M., Donnay, I., Appendino, G., & Muñoz, E. (2000). Phorboid 20-homovanillates induce apoptosis through a VR1-independent mechanism. *Chemistry & Biology, 7*, 483–492.

Maggi, C. A. (1991). Capsaicin and primary afferent neurons: From basic science to human therapy? *Journal of the Autonomic Nervous System, 33*, 1–14.

Marsch, R., Foeller, E., Rammes, G., Bunck, M., Kössl, M., Holsboer, F., Zieglgänsberger, W., Landgraf, R., Lutz, B., & Wotjak, C. T. (2007). Reduced anxiety, conditioned fear, and hippocampal long-term potentiation in transient receptor potential vanilloid type 1 receptor-deficient mice. *The Journal of Neuroscience, 27*, 832–839.

McConkey, D. J., & Orrenius, S. (1996). The role of calcium in the regulation of apoptosis. *Journal of Leukocyte Biology, 59*, 775–783.

Micale, V., Cristino, L., Tamburella, A., Petrosino, S., Leggio, G. M., Di Marzo, V., & Drago, F. (2010). Enhanced cognitive performance of dopamine D3 receptor "knock-out" mice in the step-through passive-avoidance test: assessing the role of the endocannabinoid/endovanilloid systems. *Pharmacological Research, 61*, 531–536.

Miller, C. (1995). The charybdotoxin family of K+ channel-blocking peptides. *Neuron, 15*, 5–10.

Min, J. K., Han, K. Y., Kim, E. C., Kim, Y. M., Lee, S. W., Kim, O. H., Kim, K. W., Gho, Y. S., & Kwon, Y. G. (2004). Capsaicin inhibits in vitro and in vivo angiogenesis. *Cancer Research, 64*, 644–651.

Morré, D. J., Chueh, P. J., & Morré, D. M. (1995). Capsaicin inhibits preferentially the NADH oxidase and growth of transformed cells in culture. *Proceedings of the National Academy of Sciences USA, 92*, 1831–1835.

Morré, D. J., Sun, E., Geilen, C., Wu, L. Y., de Cabo, R., Krasagakis, K., Orfanos, C. E., & Morré, D. M. (1996). Capsaicin inhibits plasma membrane NADH oxidase and growth of human and mouse melanoma lines. *European Journal of Cancer, 32A*, 1995–2003.

Nagy, I., & Rang, H. (2000). Comparison of currents activated by noxious heat in rat and chicken primary sensory neurons. *Regulatory Peptides, 96*, 3–6.

Negri, L., Lattanzi, R., Giannini, E., Colucci, M., Margheriti, F., Melchiorri, P., Vellani, V., Tian, H., De Felice, M., & Porreca, F. (2006). Impaired nociception and inflammatory pain sensation in mice lacking the prokineticin receptor PKR1: Focus on interaction between PKR1 and the capsaicin receptor TRPV1 in pain behavior. *The Journal of Neuroscience, 26*, 6716–6727.

Neubert, J. K., Karai, L., Jun, J. H., Kim, H. S., Olah, Z., & Iadarola, M. J. (2003). Peripherally induced resiniferatoxin analgesia. *Pain, 104*, 219–228.

885 Neubert, J. K., Mannes, A. J., Karai, L. J., Jenkins, A. C., Zawatski, L., Abu-Asab, M., & Iadarola,
886 M. J. (2008). Perineural resiniferatoxin selectively inhibits inflammatory hyperalgesia. *Molec-*
887 *ular Pain, 4*, 03–13.
888 O'Connell, P. J., Pingle, S. C., & Ahern, G. P. (2005). Dendritic cells do not transduce inflamma-
889 tory stimuli via the capsaicin receptor TRPV1. *FEBS Letters, 579*, 5135–5139.
890 Otten, U., Lorez, H. P., & Businger, F. (1983). Nerve growth factor antagonizes the neurotoxic
891 action of capsaicin on primary sensory neurones. *Nature, 301*, 515–517.
892 Pákáski, M., Hugyecz, M., Sántha, P., Jancsó, G., Bjelik, A., Domokos, A., Janka, Z., & Kálmán, J.
893 (2009). Capsaicin promotes the amyloidogenic route of brain amyloid precursor protein
894 processing. *Neurochemistry International, 54*, 426–430.
895 Pan, H. L., Khan, G. M., Alloway, K. D., & Chen, S. R. (2003). Resiniferatoxin induces
896 paradoxical changes in thermal and mechanical sensitivities in rats: Mechanism of action.
897 *The Journal of Neuroscience, 23*, 2911–2919.
898 Park, K. K., & Surh, Y. J. (1997). Effects of capsaicin on chemically-induced two-stage mouse
899 skin carcinogenesis. *Cancer Letters, 114*, 183–184.
900 Pecze, L., Szabó, K., Széll, M., Jósvay, K., Kaszás, K., Kúsz, E., Letoha, T., Prorok, J., Koncz, I.,
901 Tóth, A., Kemény, L., Vizler, C., & Oláh, Z. (2008). Human keratinocytes are vanilloid
902 resistant. *PloS One, 3*, e3419.
903 Phillips, E., Reeve, A., Bevan, S., & McIntyre, P. (2004). Identification of species-specific
904 determinants of the action of the antagonist capsazepine and the agonist PPAHV on TRPV1.
905 *The Journal of Biological Chemistry, 279*, 17165–17172.
906 Pini, A., Baranowski, R., & Lynn, B. (1990). Long-term reduction in the number of C-Fibre
907 Nociceptors following Capsaicin treatment of a cutaneous nerve in adult rats. *The European*
908 *Journal of Neuroscience, 2*, 89–97.
909 Pórszász, R., Szolcsányi, J. (1991–1992). Circulatory and respiratory effects of capsaicin and
910 resiniferatoxin on guinea pigs. *Acta Biochimica Biophysica Hungarica*, *26*, 131–138.
911 Pramanik, K. C., Boreddy, S. R., & Srivastava, S. K. (2011). Role of mitochondrial electron
912 transport chain complexes in capsaicin mediated oxidative stress leading to apoptosis in
913 pancreatic cancer cells. *PloS One, 6*, e20151.
914 Riera, C. E., Menozzi-Smarrito, C., Affolter, M., Michlig, S., Munari, C., Robert, F., Vogel, H.,
915 Simon, S. A., & le Coutre, J. (2009). Compounds from Sichuan and Melegueta peppers
916 activate, covalently and non-covalently, TRPA1 and TRPV1 channels. *British Journal of*
917 *Pharmacology, 157*, 1398–1409.
918 Ritter, S., & Dinh, T. T. (1988). Capsaicin-induced neuronal degeneration: Silver impregnation of
919 cell bodies, axons, and terminals in the central nervous system of the adult rat. *The Journal of*
920 *Comparative Neurology, 271*, 79–90.
921 Roberts, J. C., Davis, J. B., & Benham, C. D. (2004). [3H]Resiniferatoxin autoradiography in the
922 CNS of wild-type and TRPV1 null mice defines TRPV1 (VR-1) protein distribution. *Brain*
923 *Research, 995*, 176–183.
924 Sardar, P., Kumar, A., Bhandari, A., & Goswami, C. (2012). Conservation of tubulin-binding
925 sequences in TRPV1 throughout evolution. *PloS One, 7*, e31448.
926 Sasamura, T., Sasaki, M., Tohda, C., & Kuraishi, Y. (1998). Existence of capsaicin-sensitive
927 glutamatergic terminals in rat hypothalamus. *Neuroreport, 9*, 2045–2048.
928 Sculptoreanu, A., de Groat, W. C., Buffington, C. A., & Birder, L. A. (2005). Abnormal excit-
929 ability in capsaicin-responsive DRG neurons from cats with feline interstitial cystitis. *Exper-*
930 *imental Neurology, 193*, 437–443.
931 Shimomura, Y., Kawada, T., & Suzuki, M. (1989). Capsaicin and its analogs inhibit the activity of
932 NADH-coenzyme Q oxidoreductase of the mitochondrial respiratory chain. *Archives of Bio-*
933 *chemistry and Biophysics, 270*, 573–577.
934 Siemens, J., Zhou, S., Piskorowski, R., Nikai, T., Lumpkin, E. A., Basbaum, A. I., King, D., &
935 Julius, D. (2006). Spider toxins activate the capsaicin receptor to produce inflammatory pain.
936 *Nature, 444*, 208–212.

937 Southall, M. D., Li, T., Gharibova, L. S., Pei, Y., Nicol, G. D., & Travers, J. B. (2003). Activation
938 of epidermal vanilloid receptor-1 induces release of proinflammatory mediators in human
939 keratinocytes. *The Journal of Pharmacology and Experimental Therapeutics, 304*, 217–222.
940 Starowicz, K., Cristino, L., & Di Marzo, V. (2008). TRPV1 receptors in the central nervous
941 system: Potential for previously unforeseen therapeutic applications. *Current Pharmaceutical*
942 *Design, 14*, 42–54.
943 Sugimoto, T., Xiao, C., & Ichikawa, H. (1998). Neonatal primary neuronal death induced by
944 capsaicin and axotomy involves an apoptotic mechanism. *Brain Research, 807*, 147–154.
945 Surh, Y. J. (2002). More than spice: Capsaicin in hot chili peppers makes tumor cells commit
946 suicide. *Journal of the National Cancer Institute, 94*, 1263–1265.
947 Surh, Y. J., Lee, R. C., Park, K. K., Mayne, S. T., Liem, A., & Miller, J. A. (1995).
948 Chemoprotective effects of capsaicin and diallyl sulfide against mutagenesis or tumorigenesis
949 by vinyl carbamate and N-nitrosodimethylamine. *Carcinogenesis, 16*, 2467–2471.
950 Sutton, K. G., Garrett, E. M., Rutter, A. R., Bonnert, T. P., Jarolimek, W., & Seabrook, G. R.
951 (2005). Functional characterisation of the S512Y mutant vanilloid human TRPV1 receptor.
952 *British Journal of Pharmacology, 146*, 702–711.
953 Svichar, N., Kostyuk, P., & Verkhratsky, A. (1997). Mitochondria buffer Ca^{2+} entry but not
954 intracellular Ca^{2+} release in mouse DRG neurones. *Neuroreport, 8*, 3929–3932.
955 Swarnkar, S., Singh, S., Goswami, P., Mathur, R., Patro, I. K., & Nath, C. (2012). Astrocyte
956 activation: A key step in rotenone induced cytotoxicity and DNA damage. *Neurochemical*
957 *Research, 37*, 2178–2189.
958 Szallasi, A., & Blumberg, P. M. (1999). Vanilloid (Capsaicin) receptors and mechanisms. *Phar-*
959 *macological Reviews, 51*, 159–212.
960 Szallasi, A., Goso, C., Blumberg, P. M., & Manzini, S. (1993). Competitive inhibition by
961 capsazepine of [3H]resiniferatoxin binding to central (spinal cord and dorsal root ganglia)
962 and peripheral (urinary bladder and airways) vanilloid (capsaicin) receptors in the rat. *The*
963 *Journal of Pharmacology and Experimental Therapeutics, 267*, 728–733.
964 Szallasi, A., Farkas-Szallasi, T., Tucker, J. B., Lundberg, J. M., Hökfelt, T., & Krause, J. E. (1999).
965 Effects of systemic resiniferatoxin treatment on substance P mRNA in rat dorsal root ganglia
966 and substance P receptor mRNA in the spinal dorsal horn. *Brain Research, 815*, 177–184.
967 Szöke, E., Seress, L., & Szolcsányi, J. (1998). Reevaluation of the effect of neonatal capsaicin
968 treatment on the basis of morphometrical studies. *Neurobiology (Budapest, Hungary), 6*, 477–478.
969 Szöke, E., Seress, L., & Szolcsányi, J. (2002). Neonatal capsaicin treatment results in prolonged
970 mitochondrial damage and delayed cell death of B cells in the rat trigeminal ganglia. *Neuro-*
971 *science, 113*, 925–937.
972 Szolcsányi, J., Joó, F., & Jancsó-Gábor, A. (1971). Mitochondrial changes in preoptic neurons after
973 capsaicin desensitization of the hypothalamic thermodetectors in rats. *Nature, 229*, 116–117.
974 Szolcsányi, J., Jancśo-Gábor, A., & Joo, F. (1975). Functional and fine structural characteristics of
975 the sensory neuron blocking effect of capsaicin. *Naunyn-Schmiedeberg's Archives of Phar-*
976 *macology, 287*, 157–169.
977 Tanaka, T., Kohno, H., Sakata, K., Yamada, Y., Hirose, Y., Sugie, S., & Mori, H. (2002).
978 Modifying effects of dietary capsaicin and rotenone on 4-nitroquinoline 1-oxide-induced rat
979 tongue carcinogenesis. *Carcinogenesis, 23*, 1361–1367.
980 Tender, G. C., Walbridge, S., Olah, Z., Karai, L., Iadarola, M., Oldfield, E. H., & Lonser, R. R.
981 (2005). Selective ablation of nociceptive neurons for elimination of hyperalgesia and neuro-
982 genic inflammation. *Journal of Neurosurgery, 102*, 522–525.
983 Terlau, H., & Olivera, B. M. (2004). Conus venoms: A rich source of novel ion channel-targeted
984 peptides. *Physiological Reviews, 84*, 41–68.
985 Thoennissen, N. H., O'Kelly, J., Lu, D., Iwanski, G. B., La, D. T., Abbassi, S., Leiter, A., Karlan,
986 B., Mehta, R., & Koeffler, H. P. (2010). Capsaicin causes cell-cycle arrest and apoptosis in ER-
987 positive and -negative breast cancer cells by modulating the EGFR/HER-2 pathway. *Onco-*
988 *gene, 29*, 285–296.

989 Tóth, A., Boczán, J., Kedei, N., Lizanecz, E., Bagi, Z., Papp, Z., Edes, I., Csiba, L., & Blumberg,
990 P. M. (2005). Expression and distribution of vanilloid receptor 1 (TRPV1) in the adult rat brain.
991 *Brain Research. Molecular Brain Research, 135*, 162–168.
992 Tóth, B. I., Benko, S., Szöllosi, A. G., Kovács, L., Rajnavölgyi, E., & Bíró, T. (2009). Transient
993 receptor potential vanilloid-1 signaling inhibits differentiation and activation of human den-
994 dritic cells. *FEBS Letters, 583*, 1619–1624.
995 Tsuchiya, H. (2001). Biphasic membrane effects of capsaicin, an active component in *Capsicum*
996 species. *Journal of Ethnopharmacology, 75*, 295–299.
997 Valtschanoff, J. G., Rustioni, A., Guo, A., & Hwang, S. J. (2001). Vanilloid receptor VR1 is both
998 presynaptic and postsynaptic in the superficial laminae of the rat dorsal horn. *The Journal of*
999 *Comparative Neurology, 436*, 225–235.
1000 Vellani, V., Colucci, M., Lattanzi, R., Giannini, E., Negri, L., Melchiorri, P., & McNaughton, P. A.
1001 (2006). Sensitization of transient receptor potential vanilloid 1 by the prokineticin receptor
1002 agonist Bv8. *The Journal of Neuroscience, 26*, 5109–5116.
1003 Verkhratsky, A. J., & Petersen, O. H. (1998). Neuronal calcium stores. *Cell Calcium, 24*, 333–343.
1004 Vlachova, V., Teisinger, J., Susankova, K., Lyfenko, A., Ettrich, R., & Vyklicky, L. (2003).
1005 Functional role of C-terminal cytoplasmic tail of rat vanilloid receptor 1. *The Journal of*
1006 *Neuroscience, 23*, 1340–1350.
1007 Voets, T., Talavera, K., Owsianik, G., & Nilius, B. (2005). Sensing with TRP channels. *Nature*
1008 *Chemical Biology, 1*, 85–92.
1009 Wardle, K. A., Furey, G., & Sanger, G. J. (1996). Pharmacological characterization of the vanilloid
1010 receptor in the rat isolated vas deferens. *The Journal of Pharmacy and Pharmacology, 48*,
1011 285–291.
1012 Welch, J. M., Simon, S. A., & Reinhart, P. H. (2000). The activation mechanism of rat vanilloid
1013 receptor 1 by capsaicin involves the pore domain and differs from the activation by either acid
1014 or heat. *Proceedings of the National Academy of Sciences USA, 97*, 13889–13894.
1015 Winter, J. (1987). Characterization of capsaicin-sensitive neurones in adult rat dorsal root ganglion
1016 cultures. *Neuroscience Letters, 80*, 134–140.
1017 Wolvetang, E. J., Larm, J. A., Moutsoulas, P., & Lawen, A. (1996). Apoptosis induced by
1018 inhibitors of the plasma membrane NADH-oxidase involves Bcl-2 and calcineurin. *Cell*
1019 *Growth & Differentiation, 7*, 1315–1325.
1020 Wong, R., Steenbergen, C., & Murphy, E. (2012). Mitochondrial permeability transition pore and
1021 calcium handling. *Methods in Molecular Biology, 810*, 235–242.
1022 Wood, J. N., Winter, J., James, I. F., Rang, H. P., Yeats, J., & Bevan, S. (1988). Capsaicin-induced
1023 ion fluxes in dorsal root ganglion cells in culture. *The Journal of Neuroscience, 8*, 3208–3320.
1024 Xu, X. J., Farkas-Szallasi, T., Lundberg, J. M., Hökfelt, T., Wiesenfeld-Hallin, Z., & Szallasi, A.
1025 (1997). Effects of the capsaicin analogue resiniferatoxin on spinal nociceptive mechanisms in
1026 the rat: behavioral, electrophysiological and in situ hybridization studies. *Brain Research, 752*,
1027 52–60.
1028 Yagi, T. (1990). Inhibition by capsaicin of NADH-quinone oxidoreductases is correlated with the
1029 presence of energy-coupling site 1 in various organisms. *Archives of Biochemistry and*
1030 *Biophysics, 281*, 305–311.
1031 Zhu, S., Darbon, H., Dyason, K., Verdonck, F., & Tytgat, J. (2003). Evolutionary origin of
1032 inhibitor cystine knot peptides. *The FASEB Journal, 17*, 1765–1767.

Channels

ISSN: 1933-6950 (Print) 1933-6969 (Online) Journal homepage: http://www.tandfonline.com/loi/kchl20

Thermosensitive ion channel TRPV1 is endogenously expressed in the sperm of a fresh water teleost fish (Labeo rohita) and regulates sperm motility

Rakesh Kumar Majhi, Ashutosh Kumar, Manoj Yadav, Nirlipta Swain, Shikha Kumari, Ashish Saha, Avinash Pradhan, Luna Goswami, Somdatta Saha, Luna Samanta, Apratim Maity, Tapas Kumar Nayak, Subhasis Chattopadhyay, Chitra Rajakuberan, Abhishek Kumar & Chandan Goswami

To cite this article: Rakesh Kumar Majhi, Ashutosh Kumar, Manoj Yadav, Nirlipta Swain, Shikha Kumari, Ashish Saha, Avinash Pradhan, Luna Goswami, Somdatta Saha, Luna Samanta, Apratim Maity, Tapas Kumar Nayak, Subhasis Chattopadhyay, Chitra Rajakuberan, Abhishek Kumar & Chandan Goswami (2013) Thermosensitive ion channel TRPV1 is endogenously expressed in the sperm of a fresh water teleost fish (Labeo rohita) and regulates sperm motility, Channels, 7:6, 483-492, DOI: 10.4161/chan.25793

To link to this article: http://dx.doi.org/10.4161/chan.25793

RESEARCH PAPER

Channels 7:6, 483–492; November/December 2013; © 2013 Landes Bioscience

Thermosensitive ion channel TRPV1 is endogenously expressed in the sperm of a fresh water teleost fish (*Labeo rohita*) and regulates sperm motility

Rakesh Kumar Majhi[1,†], Ashutosh Kumar[1,†], Manoj Yadav[1], Nirlipta Swain[1], Shikha Kumari[1], Ashish Saha[2], Avinash Pradhan[2], Luna Goswami[3], Somdatta Saha[3,4], Luna Samanta[4], Apratim Maity[5], Tapas Kumar Nayak[1], Subhasis Chattopadhyay[1], Chitra Rajakuberan[6], Abhishek Kumar[7], and Chandan Goswami[1,*]

[1]National Institute of Science Education and Research; Institute of Physics Campus; Bhubaneswar, India; [2]Central Institute of Freshwater Aquaculture; Bhubaneswar, India; [3]School of Biotechnology; KIIT University; Bhubaneswar, India; [4]Department of Zoology; Ravenshaw University; Cuttack, India; [5]Department of Biochemistry; OVC; Orissa University of Agriculture and Technology; Bhubaneswar, India; [6]San Diego State University; San Diego, CA USA; [7]Department of Genetics & Molecular Biology in Botany; Institute of Botany; Christian-Albrechts-University at Kiel; Kiel, Germany

[†]These authors contributed equally to this work.

Keywords: *Labeo rohita*, TRPV1, teleost fish, Ca^{2+}-signaling, sperm cells, Vertebrate evolution, Ca^{2+} channels, Capsaicin, NADA, sperm motility

Sperm cells exhibit extremely high sensitivity in response to slight changes in temperature, osmotic pressure and/or presence of various chemical stimuli. In most cases throughout the evolution, these physico-chemical stimuli trigger Ca^{2+}-signaling and subsequently alter structure, cellular function, motility and survival of the sperm cells. Few reports have recently demonstrated the presence of Transient Receptor Potential (TRP) channels in the sperm cells from higher eukaryotes, mainly from higher mammals. In this work, we have explored if the sperm cells from lower vertebrates can also have thermo-sensitive TRP channels. In this paper, we demonstrate the endogenous presence of one specific thermo-sensitive ion channel, namely Transient Receptor Potential Vanilloid family member sub type 1 (TRPV1) in the sperm cells collected from fresh water teleost fish, *Labeo rohita*. By using western blot analysis, fluorescence assisted cell sorting (FACS) and confocal microscopy; we confirm the presence of this non-selective cation channel. Activation of TRPV1 by an endogenous activator NADA significantly increases the quality as well as the duration of fish sperm movement. The sperm cell specific expression of TRPV1 matches well with our in silico sequence analysis. The results demonstrate that TRPV1 gene is conserved in various fishes, ranging from 1–3 in copy number, and it originated by fish-specific duplication events within the last 320 million years (MY). To the best of our knowledge, this is the first report demonstrating the presence of any thermo-sensitive TRP channels in the sperm cells of early vertebrates as well as of aquatic animals, which undergo external fertilization in fresh water. This observation may have implications in the aquaculture, breeding of several fresh water and marine fish species and cryopreservation of fish sperms.

Introduction

Continuation of life depends on the reproductive success of individual species. In this context, the fertilization ability of the male gametes, i.e., sperm cells, is important. The spermatozoa of oviparous fishes become motile after being discharged into the aqueous environment while, in viviparous and ovoviviparous fishes, their sperms acquire motility after being discharged into the female genital tract.[1-3] In either case, sperm cells have to locate the female gamete in order to ensure the fertilization. This requires complex tactic yet efficient molecular signaling events that guide the sperm cells movement towards the egg.[4] Ion concentrations, osmolarity and pH of the media into which they are released are crucial for initiation of sperm motility.[5-7] The regulatory mechanisms involved in these functions and the molecules involved in such movements are not well established. So far, it has been established that Ca^{2+}-signaling play important role in such events.[8-12] Though in general this suggests the importance of different Ca^{2+} channels in the context of sperm functions, the molecular identities and nature of the different Ca^{2+} channels involved in such functions are not well understood. Different complex Ca^{2+} signaling events in general are required for the proper functioning and survival of the sperm cells.

*Correspondence to: Chandan Goswami; Email: chandan@niser.ac.in
Submitted: 01/18/2013; Revised: 07/02/2013; Accepted: 07/17/2013
http://dx.doi.org/10.4161/chan.25793

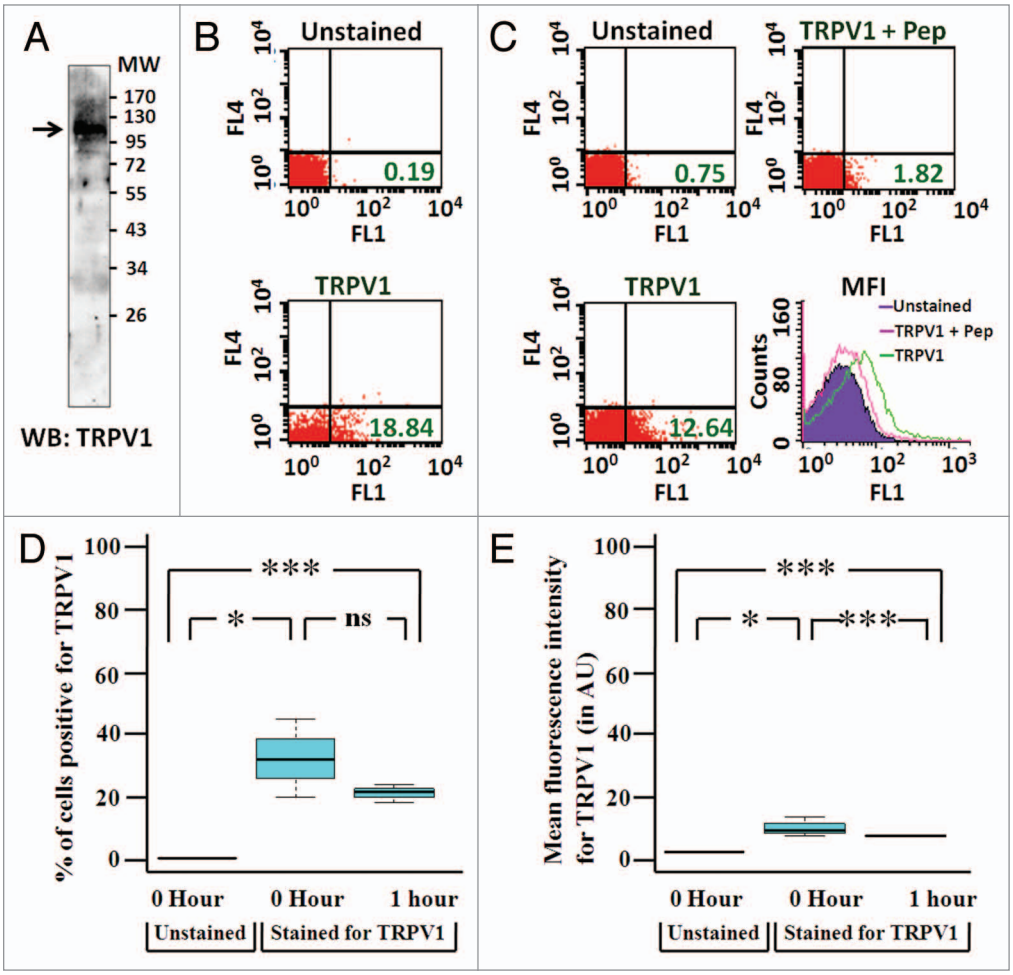

Figure 1. Endogenous expression and immunodetection of TRPV1 channel in fish (*Labeo rohita)* sperm cells. (**A**) western blot analysis of sperm cells by a TRPV1-specific antibody. The arrow indicates a TRPV1-specific band at the position of 95 KDa. (**B**) Fluorescence activated cell sorting analysis of fish sperm cells by a TRPV1 specific antibody. A large number of cells react to an antibody recognizing the N-terminus of TRPV1 (Sigma Aldrich) (lower panel) when compared with the other unstained samples (upper panel). (**C**) Fluorescence activated cell sorting analysis of fish sperm cells by another antibody recognizing the C-terminus of TRPV1 (Alomone) and the respective blocking peptide. A large number of cells react to this TRPV1-specific antibody (lower panel) when compared with the other unstained samples (upper panel, left side) or peptide blocked sample (upper panel, right side). The comparative mean fluorescent intensity is provided in the lower panel (right side). (**D**) Not all sperm cells express TRPV1. This box-plot diagram represents the percentage of sperm cells that reveal TRPV1 staining. After 1 h, less number of cells remains positive for TRPV1. * = Significant, *** = highly significant, ns = non-significant. (**E**) Time-dependent decay of TRPV1 in sperm cells. This box-plot diagram reveals the mean fluorescence intensity (MFI) of TRPV1 present in the sperm population. The MFI-value for TRPV1 reduces after 1 h. *Significant, ***highly significant.

However, the nature and spatio-temporal requirements of the Ca^{2+} signaling is variable and depends largely on several internal and external factors.[13,14] In addition to the internal factors, the Ca^{2+}-signaling experienced by the sperm cells is directly modulated by the environment into which the sperms are released, thus affecting their survival and fertilizing ability. Sperm cells exhibit extreme selectivity and sensitivity towards proper environment, which promotes their survival, whereas slight changes in the environment is detrimental for these cells. For example, sperm cells demonstrate extreme sensitivity for minute changes in pH, temperature, osmolarity of the media and presence of very low level of elements etc.[7-15] The Ca^{2+} channels present in the sperm cells play an important role in these processes.[16] The Ca^{2+} channels present in the sperm cells are potential molecular targets, which respond to several stimuli in order to modulate the intracellular Ca^{2+} levels.[16] Ca^{2+}-signaling also plays an important role in several sperm cell-specific functions such as acrosomal reaction, capacitation, hyper motility etc.[17] Notably, the Ca^{2+}-signaling experienced by the sperm cells is variable and this variability often correlates with species differences, morphology of the sperm cells and the environment where the sperms are released.[4,18]

Recently, a number of studies have demonstrated that Transient Receptor Potential (TRP) family of channels present in neurons can conduct Ca^{2+} influx in response to different physical factors such as temperature, osmotic pressure, pH and light.[19] In addition, these channels can detect a battery of signaling molecules and thus contribute to the chemosensory processes relevant for neuronal guidance and contact formation.[20] As TRP channels act as molecular sensors of physical and chemical factors and are able to conduct Ca^{2+}-influx, we explored if thermosensitive TRP channels, especially the members of TRPV subfamily are present in the sperm cells of early vertebrates. In that context, we explored sperm cells from fresh water teleost fish species, namely *Labeo rohita* (Common name Rahu). Here we report the presence and functional role of TRPV1 in the fish sperm cells.

Results

In order to understand if fish sperm cells contain thermosensitive TRPV channels, we performed western blot analysis of freshly collected sperm cells with a TRPV1-specific antibody (Sigma Aldrich) (**Fig. 1A**). A band specific for TRPV1 at around 95 KDa, the expected size of the TRPV1 was noticed. This indicates the endogenous expression of TRPV1 in fish sperm cells. FACS

analysis was performed to determine the number of fish sperm cells expressing TRPV1 channels. It was noted that in an individual sample, the antibody recognizing N-terminus of TRPV1 (Sigma Aldrich) reacts with nearly 20% sperm cells compared with unstained cells (**Fig. 1B**). To further confirm that the sperm cells indeed express TRPV1 endogenously, another antibody recognizing the C-terminus of TRPV1 (Alomone) was used in presence as well as in absence of a specific blocking peptide (Alomone). Nearly 13% of the sperm cells are detectable with this antibody. However, when the same antibody (Alomone) was used along with a specific blocking peptide, only 1.82% cells were detected (**Fig. 1C**). The mean fluorescence intensity also reduces in presence of this blocking peptide. The comparable immunoreactivities obtained by these 2 different antibodies and effective reduction in the respective immunoreacitivity due to the presence of a blocking peptide show the specificity of the antibodies used and hence strongly support the endogenous expression of TRPV1 in these sperm cells. The FACS analysis also indicates that the endogenous expression of TRPV1 in fish sperm cells is not uniform and a large number of cells express TRPV1 below detection limit or these cells do not express TRPV1 at all. In several cases, time-dependent changes in the protein profiles in sperm cells have been co-related with the sperm functions. Therefore, we compared the endogenous expression of TRPV1 in beginning and after 1 h of incubation in 37°C temperature. To get an estimation of the percentage of cells expressing TRPV1, sperm cells from 3 individual fishes in 2 different time points (0 h and 1 h) were analyzed by FACS. Data showed that only 20–40% cells express TRPV1 in the beginning ($p = 0.01183$; unstained 0 h vs. 0 h sample stained for TRPV1). Interestingly, the expression level reduces slightly with time. After 1 h, approximately 20% cells show detectable TRPV1 indicating a possible time-dependent decay of TRPV1 ($p = 0.0002417$; unstained 0 h vs. 1 h sample stained for TRPV1) (**Fig. 1D**). However, the difference between 0 h and 1 h time points become non-significant (p value = 0.2147). To confirm if TRPV1 really decays with time, the mean fluorescence intensity (MFI) values were measured and compared. This reduction in the number of TRPV1-positive cells also correlates with the reduction in the mean fluorescence intensity of TRPV1 when freshly isolated samples were compared with 1-h-old samples (**Fig. 1E**). Reduction in the MFI-values after 1 h becomes highly significant (p value = 0.000005621; 0 h vs. 1 h sample stained for TRPV1). This indicates that though the number of sperms expressing TRPV1 does not significantly decrease over time, the expression levels may drop down with time.

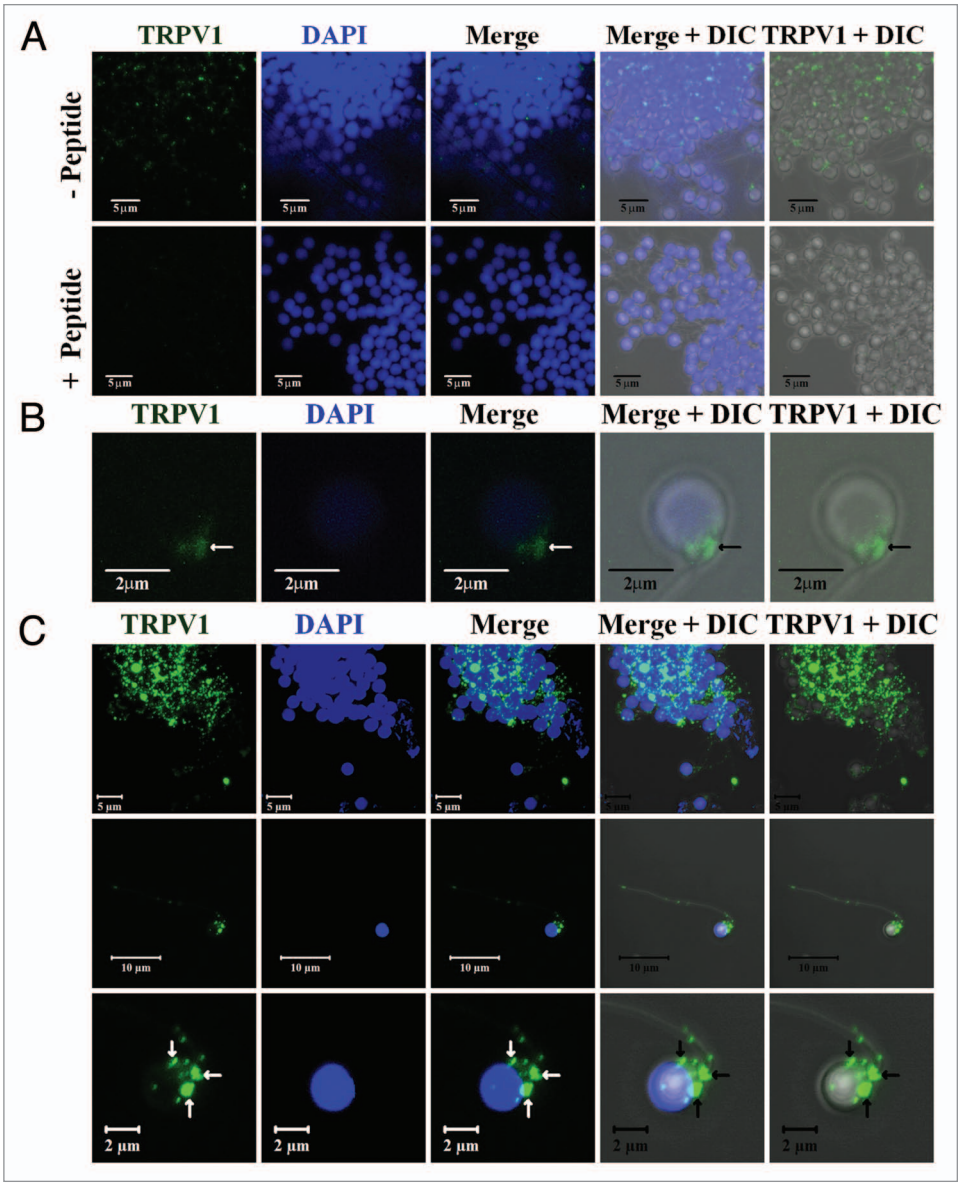

Figure 2. Immunolocalization of TRPV1 channel in *Labeo rohita* sperm cells. (**A**) Shown are the 3D confocal images of clustered sperm cells immunostained with TRPV1-specific antibody either in presence (lower panel) or in absence (upper panel) of a blocking peptide. (**B**) Confocal images depicting an enlarged area of a single sperm cell head region are shown here. The arrows indicate the regions that are enriched with TRPV1. Scale bars are indicated in the respective images. (**C**) Confocal image of sperm cells present in a cluster (upper panel), or an enlarged area of a single sperm cell (middle panel) or a single head region (lower panel) is shown here. The arrows indicate the regions that are enriched with TRPV1. Scale bars are indicated in the respective images.

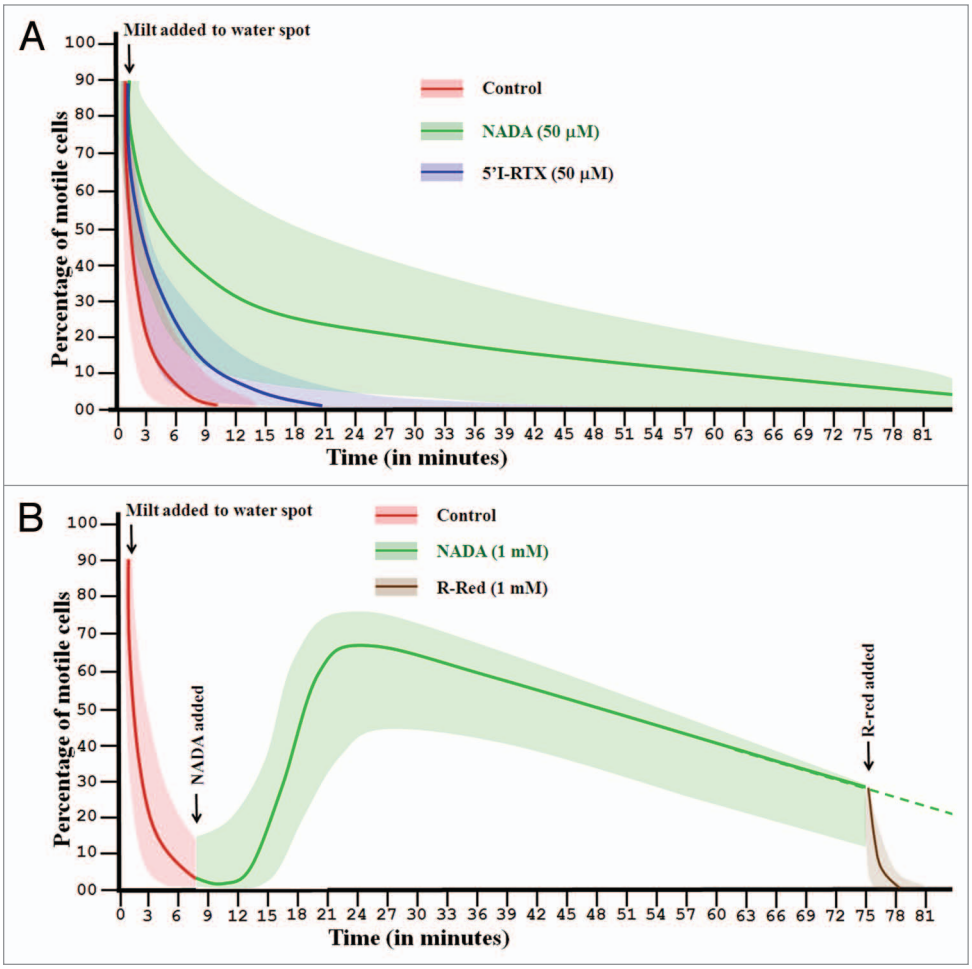

Figure 3. Involvement of TRPV1 in fish sperm motility. The trend of a series of motility experiments with fish sperms are schematically represented here. (**A**) The percentage cell motility of the fish sperm in control conditions (red line and shaded regions) and in presence of NADA (50 μM, indicted by green line and shaded region) or 5′I-RTX (50 μM, indicated by blue line and shaded region) are shown. While the sperm movements in control conditions stop quickly, presence of NADA results in sperm motility for a prolonged time. (**B**) Application of NADA (1mM) in static sperm cells (when cells become static after initial movement), results in further stimulation and sustained movement of the cells for a prolonged time. Addition of Ruthenium-Red (1 mM) results in sharp decline of the motility. For details see **Supplemental Movies**.

To visualize the expression pattern of TRPV1 channels in fish sperms, we performed immunolocalization followed by confocal microscopic analysis of freshly collected sperm cells. When probed with TRPV1 specific antibody (Alomone), we noted the presence of TRPV1 in the sperm cells (**Fig. 2A**, upper panel). This immunoreactivity was abolished when we used a specific blocking peptide (Alomone) suggesting the immunoreactivity was indeed specific for TRPV1 (**Fig. 2A**, lower panel). Notably, TRPV1 specific immunoreactivity was observed primarily in the head and neck regions. Some faint staining was detected in the tail regions too (**Fig. 2B**). To confirm further, we used another antibody specific for TRPV1 (Sigma Aldrich). The second antibody also reveals similar pattern of immunoreactivity in the sperm cells (**Fig. 2C**). In agreement with the FACS data, many of the TRPV1 containing cells reveal differences in the immunoreactivity, both in terms of amount as well as their exact localization. Taken together, these results suggest that fish sperm cells contain TRPV1 endogenously.

Next, we tested the importance of TRPV1 in the sperm functions. For that purpose, we tested the sperm motility and a series of motility experiments were performed. Immediately after coming in contact with water, the initial sperm motility is generally high (approximately 90% or higher percentage of the cells reveal motility in most cases), but it turned out to be variable in individual samples. The initial motility in general reduces with respect to the storage duration also, i.e., the duration of milt stored in 4–8°C after collection. Based on a series of experiments, a general trend becomes prominent (**Fig. 3**). We observed that in control conditions (i.e., no drugs added to the water), these cells move fast for a very short duration (2–5 min only) and afterwards majority of these cells become absolutely static and/or start floating (**Video 1**). In contrast, presence of NADA (50 μM added at the beginning) causes majority of the cells to move for a prolonged time (even more than 60 min in some experiments) (**Video 2**). In the same notion presence of 5′I-RTX (50 μM) results in reduction of sperm movement in the early points (**Video 3**). Similarly, presence of higher concentration of NADA (1 mM added at the beginning) also reveals higher motility, especially in the early time points (data not shown). We also observed that addition of NADA (1mM) after 6–8 min (at a point when sperm cells do not move at all in control conditions) restores the cell movement further (**Video 4**). This NADA-induced movement sustained for a prolonged time and we noted movement till 75 min or more. Addition of Ruthenium-Red (1 mM), a general inhibitor of TRP channels results in sharp decline of sperm movement, even in the NADA-treated samples (**Video 4**). Taken together, these results strongly suggest a functional role of TRPV1 in regulating fish sperm motility.

Next, we attempted to reconstruct the TRPV1 phylogenetic history, especially with respect to fish lineages. For that purpose, we compiled a list of TRPV1 orthologs (**Table 1**) by confirming orthology with help of a standard method of orthology assessment using bi-directional BLAST, assisted by BLAST2GO tool21 with E-value lower than 1e-6. Bayesian

Table 1. List of TRPV1 sequences collected from Ensembl (Release 69, October 2012) and GenBank databases

Sequence name	Species	Accession id	Protein length	E-value	Mean similarity (%)
HsaTRPV1	*Homo sapiens*	ENSP00000382661	839	0	97.00
MmuTRPV1	*Mus_musculus*	ENSMUSP00000099585	839	0	94.95
RnoTRPV1	*Rattus norvegicus*	ENSRNOP00000026493	838	0	94.65
GgaTRPV1	*Gallus gallus*	ENSGALP00000007393	843	0	81.45
MgaTRPV1	*Meleagris gallopavo*	ENSMGAP00000006764	843	0	81.55
TguTRPV1	*Taeniopygia guttata*	ENSTGUP00000007211	844	0	82.20
XtrTRPV1	*Xenopus tropicalis*	ENSXETP00000012743	838	0	77.55
DreTRPV1/2	*Danio rerio*	ENSXETP00000012743	819	0	70.30
LchTRPV1/2	*Latimeria chalumnae*	ENSLACP00000005090*	363	6.73E-136	73.75
TruTRPV1/2a	*Takifugu rubripes*	ENSTRUT00000001736	653	0	72.45
TruTRPV1/2b	*Takifugu rubripes*	ENSTRUP00000011132	684	0	70.20
TniTRPV1/2a	*Tetraodon nigroviridis*	ENSTNIP00000011373	690	0	70.45
TniTRPV1/2b	*Tetraodon nigroviridis*	ENSTNIP00000009206	683	0	70.50
OniTRPV1/2a	*Oreochromis niloticus*	ENSONIP00000016114	775	0	72.95%
OniTRPV1/2b	*Oreochromis niloticus*	ENSONIP00000001735	733	0	67.15
GmoTRPV1/2a	*Gadus morhua*	ENSGMOP00000015245	705	0	67.95
GmoTRPV1/2b	*Gadus morhua*	ENSGMOP00000014152	661	0	69.70
GmoTRPV1/2c	*Gadus morhua*	ENSGMOP00000002023	651	5.76E-159	60.65
XmaTRPV1/2	*Xiphophorus maculatus*	ENSXMAP00000005454	787	0	64.05
GacTRPV1/2	*Gasterosteus aculeatus*	ENSGACP00000026761	739	0	71.90
OlaTRPV1/2	*Oryzias latipes*	ENSORLP00000014367	698	0	70.30
SfoTRPV1/2	*Salvelinus fontinalis*	EV390862.1*$	141	6.22E-35	69.95
OmyTRPV1/2	*Oncorhynchus mykis*	BX884280.3*$	171	8.84E-106	78.65
IpuTRPV1/2	*Ictalurus punctatus*	CF262177.1*$	336	5.73E-137	69.75
SsaTRPV1/2	*Salmo salar*	ACI34236.1$	804	0	72.30
CIN-homolog	*Ciona intestinalis*	XP_002130280$	1150	0	61.40

Orthology of TRPV1 genes are confirmed by bidirectional BLASTP using BLAST2GO tool with E-value lower than $1^{e-6.25}$ Resulting E-value and mean similarity are shown. ENS, Ensembl; $GenBank; *Partial

phylogeny constructs a posterior distribution for a parameter using a phylogenetic tree and a model of evolution, based on the prior for that parameter and the likelihood of the data composed by the multiple alignments. Using this Bayesian phylogenetic method, we reconstructed phylogenetic history of TRPV1 within different vertebrate genomes (**Fig. 4**) from TRPV1 sequences listed in **Table 1**. Tetrapods have single copy of TRPV1 gene. In contrast, fishes demonstrate copy number variation in TRPV1/2 genes with three copies in Atlantic cod, *Gadus morhua* (GmoTRPV1/2a-c) and two copies TRPV1/2a-b in the following 3 fishes: *Takifugu rubripes* (TruTRPV1/2a-b), *Tetraodon nigroviridis* (TniTRPV1/2a-b) and *Oreochromis niloticus* (OniTRPV1/2ab). However, some fishes have single copy only, such as *Danio rerio* (DreTRPV1/2), *Latimeria chalumnae* (LchTRPV1/2), *Xiphophorus maculatus* (XmaTRPV1/2), *Gasterosteus aculeatus* (GacTRPV1/2) and *Oryzias latipes* (OlaTRPV1/2). This suggests that after separation of tetrapods and fishes, some of these teleost fishes had duplication of TRPV1 gene. Absence of duplicated TRPV1/2 genes in *Danio rerio* and *Latimeria chalumnae,* corroborates with the timing of origin of copy number variation which happens within 320 MY after separation of *D. rerio* from other teleost fishes.[22]

Taken together, our work strongly suggests for the sperm-specific expression of the thermosensitive TRPV1 in fresh water living fish (*Labeo rohita*). Such findings may have implications in cryopreservation of fish sperm cells and artificial breeding of common food carps as well as conservation of rare species.

Discussion

Conservation of different domains and motifs in ion channels often correlates with the prime function of respective ion channels. In fact, the conservation of different domains and motifs as well as tissue and cell-specific expression of ion channels are crucial for the survival of any species as these

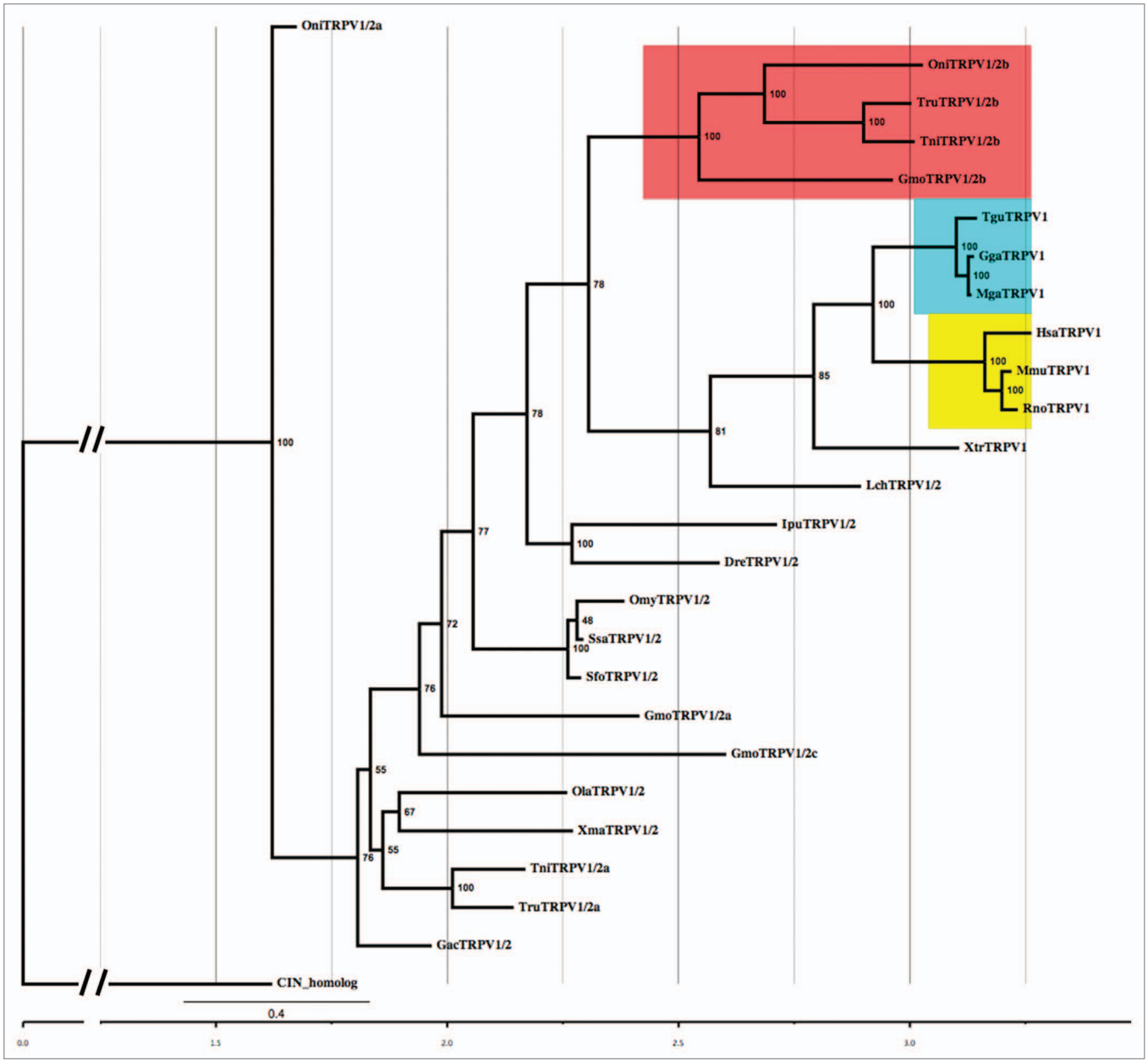

Figure 4. Phylogenetic history of the TRPV1 gene. The Bayesian phylogenetic history demonstrates that there is a single copy of this gene is conserved across different vertebrates with some ray-finned fishes have 2 copies (TRPV1/2a-b). Bayesian phylogenetic tree of TRPV1 proteins from mammals (yellow), birds (cyan), and fishes was generated using Mrbayesversion V3.2.1.[58] Fish-specific TRPV1/2b is marked in red shade. Putative TRPV like gene (GenBank id XP_002130280) from *Ciona intestinalis* served as the out-group in this Bayesian tree. Percentage posterior probabilities are shown at the node of the branches. Has, *Homo sapiens*; Mmu, *Mus musculus*; Rno, *Rattus norvegicus*; Gga, *Gallus gallus*; Mga, *Meleagris gallopavo*; Tgu, *Taeniopygia guttata*; Xtr, *Xenopus tropicalis*; Dre, *Danio rerio*; Lch, *Latimeria chalumnae*; Tru, *Takifugu rubripes*; Tni, *Tetraodon nigroviridis*; Oni, *Oreochromis niloticus*; Gmo, *Gadus morhua*; Xma, *Xiphophorus maculates*; Gac, *Gasterosteus aculeatus;* Ola, Oryzias *latipes*.

aspects are indicative of the selection pressures, and thus, function of the ion channels throughout evolution. Recently, we have reported that TRPV1 is a highly conserved protein throughout the evolution.[23] Endogenous expression and involvement of TRPV1 in the sperm cells from different species is in full agreement with its conservation at the protein as well as in the genome level.

In this work, we have explored the physical and functional presence of thermo-sensitive channel, namely TRPV1 in the sperm cells from teleost fish and demonstrate the endogenous presence as well as importance of TRPV1 in the sperm cells of *Labeo rohita*. The motility experiments with the fish milt also shed light on the general nature of fish sperm motility. The fish milt that we used is mainly a complex suspension of biologically active but uncharacterized lipids. In absence of water, the sperms remain static and start moving vigorously only after encountering with water, though their movement lasts for a very short duration. Though the exact molecular mechanism

is poorly understood, we noted that absolutely metal/ion-free water is extremely lethal to the fish sperm cells as all cells die in double distilled water, whereas in waters with trace of ions (such as pond water or tap water) is suitable. This is in accordance with the requirement of other ions and thus ion channels in the fish sperm motility. This result also fits well with the previous reports demonstrating the endogenous presence of TRP channels in sperm cells from diverse organisms. For example, endogenous expression of TRPV1 in boar spermatozoa has been linked with endocannabinoid and anandamide signaling, which have implications in capacitation and acrosomal reaction.[24,25] In case of human also, endogenous expression of TRPV1 has been detected in sperm and linked with sperm functions. In human sperm cells, both hot and cold-sensitive TRP ion channels are present and regulate several functions related to motility and fertility.[26-28] In boar sperm cells, TRPV1 function is important for fertilization.[29-31] In mouse sperm cells, TRPP2 is present at the anterior sperm head region and it is essential for the zona pellucida induced Ca^{2+} entry into mouse sperm and subsequent acrosomal exocytosis during fertilization.[32] In mouse sperm cells, TRPM8 is involved in the detection of temperature changes and is important for acrosome reaction regulation.[33,34] In the same context, involvement of TRPV6 in male fertility and sterility has been demonstrated.[35,36] Involvement of TRP channels in reproduction may have more important roles and is not limited just to sperm cell survival and movement required for fertilization. TRP channels may even have roles in the spermatogenesis as well, an important aspect which might be evolutionary conserved as well.[37-39] While these reports confirm the endogenous expression and function of TRP channels in the sperm cells of only higher vertebrates, presence of TRP channels in the sperm of any aquatic animals and/or lower vertebrates have not been shown yet. In this work we demonstrated that presence of NADA generally induces a sustained sperm movement (at least for *Labeo rohita*). Interestingly, this NADA-induced sperm movement can be blocked to some extent by 5′-IRTX, a well-established antagonist of mammalian TRPV1. Also we noted that further application of Ruthenium-Red (1 mM) in NADA-treated samples results in sharp decline of the sperm movements suggesting that NADA-induced sperm movements are due to the involvement of TRP channels mainly. However, we noted that application of capsaicin (a very specific agonist of TRPV1 in several species, mainly in mammals) did not alter the motility fish sperms and cells remain mostly non-responsive to capsaicin (data not shown). Though the relative responsiveness of NADA, 5′IRTX and capsaicin to fish sperm indicates the involvement of TRPV1 in fish motility, the species-specificity of these compounds and involvement of other TRP channels cannot be ruled out completely.

Altogether, our results confirm the endogenous expression and functional importance of TRPV1 in the sperms of lower vertebrates, at least in teleost fishes. TRPV1 is present in various teleost fishes with copy numbers ranging from 1–3 (**Table 1**; **Fig. 4**). The copy number variation of TRPV1 gene in teleost fishes originated by duplication events after separation of fishes from last common ancestor of tetrapods and fishes is evident from synteny analysis of TRPV genes.[40] These duplication events are not older than 320 MY, as it happened after separation of *D. rerio* from other teleost fishes.[22]

Recently, presence of TRP channels in the sperm cells have been detected in some lower eukaryotic organisms too. For example, in *C. elegans*, TRP channels are required for sperm-egg interactions during fertilization.[41] Polycystin channels localize to cilia and activate Drosophila sperm cells by mediating Ca^{2+}-influx.[42,43] In Drosophila, a polycystin-2 homolog channel localized in flagella and is required for male fertility.[44] Our results are in full agreement with the previous reports, which demonstrated that temperature is an important regulatory factor for maturation and motility in fish sperm cells.[45-47] Indeed it is known that carp sperms take more time for acquiring motility when incubated in cold water (15°C) vs. warm water (20°C).[47] This thermo sensitivity of sperms could be due to presence of thermosensitive TRP channels in the sperms.

In this work, we demonstrated that a fraction of fish sperm cells express TRPV1 and it localizes mainly in the neck region of the cells. In some cases, TRPV1 localizes in head and tail region also. The differential level of expression and localization of TRPV1 may be a correlative of differential response of sperm cells in response to temperature and other factors. The other functional roles of TRPV1 in fish sperms need to be explored in details.

Materials and Methods

Collection of fish sperm

Male broods of *Labeo rohita* were collected from the experimental pond of Physiology Division, Central Institute of Freshwater Aquaculture (CIFA). Milters were induced with "Ovaprim" at the rate of 0.2–0.3 ml/kg body weight of the fish during peak breeding season (in the time of early August). Milters were stripped into separate plastic tubes held over ice. Extreme care was taken to avoid contamination of water, blood, urine, feces, etc. After that, milt samples were processed for further analysis.

SDS PAGE and western blot analysis

Freshly collected milt was diluted in 1× PBS and quickly centrifuged at 8000 RPM for 5 min in 25°C. After that the pellet fraction was diluted in 1× PBS supplemented with protease inhibitor cocktail (Sigma Aldrich) and sonicated (pulse rate 50Hz for 5 min, 5 s intervals) in ice. 5× Laemmli gel sample buffer was added directly to the sonicated samples. The samples were boiled and subsequently analyzed by 10% sodium dodecyl sulfate PAGE (SDS-PAGE) according to Laemmli.[48] Due to the high lipid and DNA content, the samples were separated by SDS-PAGE for around 12 h in a mini-gel (BioRad). The proteins were electrophoretically transferred to PVDF membrane (Milipore) according to the procedure described elsewhere.[49] After blocking for 1 h in TBST (20 mM Tris [pH 7.4], 0.9% (w/v) NaCl, and 0.1% (v/v) Tween 20) containing 5% (w/v) dry skim milk, the membranes were incubated with mouse monoclonal antibody directed against C-terminus of TRPV1 (Dilution 1:200; Sigma Aldrich) for overnight. After extensive washing in TBST, the membranes were incubated with

horse-radish peroxidase-conjugated secondary antibody raised against mouse (GE Healthcare) for 1 h at room temperature (25°C). Again, the membranes were extensively washed in TBST and bands were visualized on chemi-doc (BioRad) by enhanced chemiluminescence according to the manufacturer's instructions (Thermo scientific).

Immunofluorescence analysis and microscopy

For immunocytochemical analysis, immediately after collection, sperm cells were diluted in PBS and fixed with paraformaldehyde (PFA) (final concentration 2%). After fixing the cells with PFA, the cells were permeabilized with 0.1% Triton X-100 in PBS (5 min). Subsequently, the cells were blocked with 5% bovine serum albumin for 1 h. The primary antibodies were used at the following dilutions: mouse monoclonal anti-TRPV1 (1: 200, Sigma Aldrich), rabbit polyclonal anti-TRPV1 (1: 200, Alomone Lab). In some experiments, blocking peptide [EDAEVFKDSMVPGEK, corresponding to amino acid residues 824–838 of rat TRPV1 (Accession O35433)] was used to confirm the specificity of the immunoreactivity. The blocking peptides were used at 1:1 dilution. The blocking peptides were used against rabbit polyclonal anti-TRPV1 (Alomone Lab).

All primary antibodies were incubated for overnight at 4°C in PBST buffer (PBS supplemented with 0.1% Tween-20). AlexaFluor-488 labeled anti rabbit or anti mouse antibodies (Molecular probes) were used as secondary antibodies and were used at 1:1000 dilutions. All images were taken on a confocal laser-scanning microscope (LSM-780, Zeiss) with a 63X-objective and analyzed with the Zeiss LSM image examiner software and Adobe Photoshop.

Motility assay for fish sperm

Freshly collected water free neat milt from Rohu fishes were collected from the pond and the milt from different individual fishes were brought to lab within 30–40 min. Temperature of the milt was strictly maintained at 15–20°C and subsequently the milt was stored at 4–8°C freezer for a 96 h during which all the motility experiments were done. A spot of 4 µL water was made on microscopic slide (Globe Scientific, 1304) and then a small quantity (0.1–0.2 µl) of Rohu milt was added to the spot. Immediately after adding the milt to the water, a coverslip (Fisher Scientific) was gently placed above the water spot and the sperm movement was visualized/captured by using Olympus (BX51) microscope. The approximate percentage of cell motility was estimated as described previously.[50-53] The movements of rohu spermatozoa were recorded as movies (400-500 frames/minute) for 1 minute. The original movies were processed using Movie-maker software. For modulation of TRPV1, specific activator (NADA, Sigma Aldrich) or inhibitors such as (5′I-RTX, Sigma Aldrich) or RutheniumRed (Sigma Aldrich) at different concentrations was added to the water and these solutions were used for spotting. In some experiments aimed to add activators or inhibitors after a fixed time, the drug containing water solution (5×) was made and 1 µL of this 5× solution was added from the side of the coverslip (after the required time on a control sample). Due to the capillary action, the drug solution added to the side goes inside quickly. For this assay, we used normal tap water as double distilled water turned out to be extremely lethal for the cells.

FACS analysis

Expression of thermo-sensitive TRPV1 channel in fish sperm cells was assessed by Flow cytometry. Single cell suspensions of fish sperm cells were made in presence and absence of TRPV1 specific blocking peptide (EDAEVFKDSMVPGEK, corresponding to amino acid residues 824–838 of rat TRPV1 [Accession O35433]) and used for flow cytometry on a FACS Calibur instrument (BD Biosciences). The cells were washed, blocked (with 5% bovine serum albumin) and incubated with rabbit polyclonal anti-TRPV1 antibodies (1:200, Alomone Lab) or mouse monoclonal anti-TRPV1 (1: 200, Sigma Aldrich) for overnight followed by washing by PBST buffer (PBS supplemented with 0.1% Tween-20). The cells were then incubated with AlexaFluor-488 labeled anti-rabbit or anti-mouse antibodies (1:1000 dilution, Molecular probes) for 1 h. After washing, the cells were re-suspended in PBS supplemented with 2% BSA, 0.1% sodium azide. Unstained cells were used as a negative control. The labeled cells were washed, detected by Flow Cytometry using a FACS Calibur and analyzed by Cell Quest Pro software (BD Biosciences). Around 10,000 cells were analyzed for each sample.

Sequence collection and phylogenetic analyses

TRPV1 sequences were collected using Ensembl[54] from following species: *Latimeria chalumnae, Takifugu rubripes*, *Tetraodon nigroviridis*, *Oreochromis niloticus, Gadus morhua*, *Danio rerio, Gallus gallus*, *Meleagris gallopavo*, *Taeniopygia guttata*, *Xenopus tropicalis, Mus musculus, Rattus norvegicus* and *Homo sapiens*. Furthermore, TRPV1 homologs were collected using GenBank from following species: *Salvelinus fontinalis*, *Oncorhynchus tshawytscha*, *Oncorhynchus mykiss*, *Ictalurus punctatus*, *Salmo salar* and *Ciona intestinalis*. All these sequences were scanned by BLAST tool[55] with E-value lower than 1e-6. Collected sequences were annotated and orthologous status of these sequences were confirmed by using bi-directional blast with the help of BLAST2GO software[21] with E-value lower than 1e-6. Result of this analysis is summarized in **Table 1**. Protein sequence alignment of collected TRPV1 was performed using MUSCLE software.[56,57] Phylogenetic tree was constructed using this protein alignment by the well-accepted and most powerful Bayesian approach (5 runs, until average standard deviation of split frequencies was lower than 0.0098, 25% burn-in-period, WAG matrix-based model in the MrBayes version V3.2.1.[58,59]

Statistical test

The FACS data for 3 individual fishes (n = 3) were imported to "R" software for statistical analysis and graphical representation. Using R, box-plots were generated to represent the percentage of TRPV1 positive cells and their mean fluorescence intensities in arbit unit (au). The Annova test was done for each set of data to check the reliability and significance of the data points. P-values < 0.05 were considered as statistically significant.

Disclosure of Potential Conflicts of Interest

No potential conflicts of interest were disclosed.

Acknowledgments

We thank Mr Vivek Kumar Sahoo and Mr Kishan Kumar Singh for preparation of movies. Funding from NISER and Department of Biotechnology (Govt. India, grant number BT-BRB-TF-2-2011) are acknowledged. The funders had no role in study design, data collection and analysis, decision to publish, or preparation of the manuscript.

Supplemental Material

Supplemental materials may be found here: http://www.landesbioscience.com/journals/channels/article/25793

References

1. Stoss J. Fish gamete preservation and spermatozoan physiology. In: Hoar WS, Randall DJ, Donaldson EM., editors. Fish Physiology, Part B, Behavior and Fertility Control. Academic Press; 1983; 305-350.
2. Billard R. Spermatogenesis and spermatology of some teleost fish species. Reprod Nutr Dev 1986; 2:877e920.
3. Billard R, Cosson MP. The energetics of fish sperm motility. In: Gagnon C, editor. Controls of sperm motility, biological and clinical aspects. Boca Raton, Florida: CRC Press; 1990; 153e73.
4. Chang H, Suarez SS. Rethinking the relationship between hyperactivation and chemotaxis in mammalian sperm. Biol Reprod 2010; 83:507-13; PMID:20463353; http://dx.doi.org/10.1095/biolreprod.109.083113
5. Morisawa M, Suzuki K. Osmolality and potassium ion: their roles in initiation of sperm motility in teleosts. Science 1980; 210:1145-7; PMID:7444445; http://dx.doi.org/10.1126/science.7444445
6. Morisawa M, Suzuki K, Morisawa S. Effects of potassium and osmolality on spermatozoan motility of salmonid fishes. J Exp Biol 1983; 107:105-13; PMID:6421978
7. Le Minh H, Lim HK, Min BH, Park MS, Son MH, Lee JU, Chang YJ. Effects of varying dilutions, pH, temperature and cations on spermatozoa motility in fish Larimichthys polyactis. J Environ Biol 2011; 32:271-6; PMID:22167936
8. Eisenbach M. Mammalian sperm chemotaxis and its association with capacitation. Dev Genet 1999; 25:87-94; PMID:10440842; http://dx.doi.org/10.1002/(SICI)1520-6408(1999)25:2<87::AID-DVG2>3.0.CO;2-4
9. Spehr M, Gisselmann G, Poplawski A, Riffell JA, Wetzel CH, Zimmer RK, Hatt H. Identification of a testicular odorant receptor mediating human sperm chemotaxis. Science 2003; 299:2054-8; PMID:12663925; http://dx.doi.org/10.1126/science.1080376
10. Carlson AE, Westenbroek RE, Quill T, Ren D, Clapham DE, Hille B, Garbers DL, Babcock DF. CatSper1 required for evoked Ca^{2+} entry and control of flagellar function in sperm. Proc Natl Acad Sci U S A 2003; 100:14864-8; PMID:14657352; http://dx.doi.org/10.1073/pnas.2536658100
11. Suarez SS, Ho HC. Hyperactivated motility in sperm. Reprod Domest Anim 2003; 38:119-24; PMID:12654022; http://dx.doi.org/10.1046/j.1439-0531.2003.00397.x
12. Kirkman-Brown JC, Punt EL, Barratt CL, Publicover SJ. Zona pellucida and progesterone-induced Ca2+ signaling and acrosome reaction in human spermatozoa. J Androl 2002; 23:306-15; PMID:12002428
13. Shukla KK, Mahdi AA, Rajender S. Ion channels in sperm physiology and male fertility and infertility. J Androl 2012; 33:777-88; PMID:22441763; http://dx.doi.org/10.2164/jandrol.111.015552
14. Stamboulian S, De Waard M, Villaz M, Arnoult C. Functional interaction between mouse spermatogenic LVA and thapsigargin-modulated calcium channels. Dev Biol 2002; 252:72-83; PMID:12453461; http://dx.doi.org/10.1006/dbio.2002.0844
15. Petrunkina AM, Harrison RA, Ekhlasi-Hundrieser M, Töpfer-Petersen E. Role of volume-stimulated osmolyte and anion channels in volume regulation by mammalian sperm. Mol Hum Reprod 2004; 10:815-23; PMID:15361553; http://dx.doi.org/10.1093/molehr/gah106
16. Darszon A, Nishigaki T, Beltran C, Treviño CL. Calcium channels in the development, maturation, and function of spermatozoa. Physiol Rev 2011; 91:1305-55; PMID:22013213; http://dx.doi.org/10.1152/physrev.00028.2010
17. Wakai T, Vanderheyden V, Fissore RA. Ca^{2+} signaling during mammalian fertilization: requirements, players, and adaptations. Cold Spring Harb Perspect Biol 2011; 3:4; PMID:21441584; http://dx.doi.org/10.1101/cshperspect.a006767
18. Takei GL, Mukai C, Okuno M. Transient Ca^{2+} mobilization caused by osmotic shock initiates salmonid fish sperm motility. J Exp Biol 2012; 215:630-41; PMID:22279070; http://dx.doi.org/10.1242/jeb.063628
19. Venkatachalam K, Montell C. TRP channels. Annu Rev Biochem 2007; 76:387-417; PMID:17579562; http://dx.doi.org/10.1146/annurev.biochem.75.103004.142819
20. Clapham DE. TRP channels as cellular sensors. Nature 2003; 426:517-24; PMID:14654832; http://dx.doi.org/10.1038/nature02196
21. Boryshpolets S, Dzyuba B, Drokin S. Pre-spawning water temperature affects sperm respiration and reactivation parameters in male carps. Fish Physiol Biochem 2009; 35:661-8; PMID:19048380; http://dx.doi.org/10.1007/s10695-008-9292-4
22. Conesa A, Götz S, García-Gómez JM, Terol J, Talón M, Robles M. Blast2GO: a universal tool for annotation, visualization and analysis in functional genomics research. Bioinformatics 2005; 21:3674-6; PMID:16081474; http://dx.doi.org/10.1093/bioinformatics/bti610
23. Kumar A, Bhandari A, Sinha R, Goyal P, Grapputo A. Spliceosomal intron insertions in genome compacted ray-finned fishes as evident from phylogeny of MC receptors, also supported by a few other GPCRs. PLoS One 2011; 6:e22046; PMID:21850219; http://dx.doi.org/10.1371/journal.pone.0022046
24. Sardar P, Kumar A, Bhandari A, Goswami C. Conservation of tubulin-binding sequences in TRPV1 throughout evolution. PLoS One 2012; 7:e31448; PMID:22496727; http://dx.doi.org/10.1371/journal.pone.0031448
25. Maccarrone M, Barboni B, Paradisi A, Bernabò N, Gasperi V, Pistilli MG, Fezza F, Lucidi P, Mattioli M. Characterization of the endocannabinoid system in boar spermatozoa and implications for sperm capacitation and acrosome reaction. J Cell Sci 2005; 118:4393-404; PMID:16144868; http://dx.doi.org/10.1242/jcs.02536
26. Gervasi MG, Osycka-Salut C, Caballero J, Vazquez-Levin M, Pereyra E, Billi S, Franchi A, Perez-Martinez S. Anandamide capacitates bull spermatozoa through CB1 and TRPV1 activation. PLoS One 2011; 6:e16993; PMID:21347292; http://dx.doi.org/10.1371/journal.pone.0016993
27. De Blas GA, Darszon A, Ocampo AY, Serrano CJ, Castellano LE, Hernández-González EO, Chirinos M, Larrea F, Beltrán C, Treviño CL. TRPM8, a versatile channel in human sperm. PLoS One 2009; 4:e6095; PMID:19582168; http://dx.doi.org/10.1371/journal.pone.0006095
28. Francavilla F, Battista N, Barbonetti A, Vassallo MR, Rapino C, Antonangelo C, Pasquariello N, Catanzaro G, Barboni B, Maccarrone M. Characterization of the endocannabinoid system in human spermatozoa and involvement of transient receptor potential vanilloid 1 receptor in their fertilizing ability. Endocrinology 2009; 150:4692-700; PMID:19608651; http://dx.doi.org/10.1210/en.2009-0057
29. Lewis SE, Rapino C, Di Tommaso M, Pucci M, Battista N, Paro R, Simon L, Lutton D, Maccarrone M. Differences in the endocannabinoid system of sperm from fertile and infertile men. PLoS One 2012; 7:e47704; PMID:23082196; http://dx.doi.org/10.1371/journal.pone.0047704
30. Bernabò N, Pistilli MG, Falasca G, Curini V, Garofalo ML, Turriani M, Mattioli M, Barboni B. Role of TRPV1 channels during the acquisition of fertilizing ability in boar spermatozoa. Vet Res Commun 2010; 34(Suppl 1):S5-8; PMID:20437275; http://dx.doi.org/10.1007/s11259-010-9367-4
31. Bernabò N, Pistilli MG, Gloria A, Di Pancrazio C, Falasca G, Barboni B, Mattioli M. Factors affecting TRPV1 receptor immunolocalization in boar spermatozoa capacitated in vitro. Vet Res Commun 2008; 32(Suppl 1):S103-5; PMID:18685993; http://dx.doi.org/10.1007/s11259-008-9106-2
32. Botto L, Bernabò N, Palestini P, Barboni B. Bicarbonate induces membrane reorganization and CBR1 and TRPV1 endocannabinoid receptor migration in lipid microdomains in capacitating boar spermatozoa. J Membr Biol 2010; 238:33-41; PMID:21104238; http://dx.doi.org/10.1007/s00232-010-9316-8
33. Jungnickel MK, Marrero H, Birnbaumer L, Lémos JR, Florman HM. Trp2 regulates entry of Ca^{2+} into mouse sperm triggered by egg ZP3. Nat Cell Biol 2001; 3:499-502; PMID:11331878; http://dx.doi.org/10.1038/35074570
34. Martínez-López P, Treviño CL, de la Vega-Beltrán JL, De Blas G, Monroy E, Beltrán C, Orta G, Gibbs GM, O'Bryan MK, Darszon A. TRPM8 in mouse sperm detects temperature changes and may influence the acrosome reaction. J Cell Physiol 2011; 226:1620-31; PMID:21413020; http://dx.doi.org/10.1002/jcp.22493
35. Gibbs GM, Orta G, Reddy T, Koppers AJ, Martínez-López P, de la Vega-Beltràn JL, Lo JC, Veldhuis N, Jamsai D, McIntyre P, et al. Cysteine-rich secretory protein 4 is an inhibitor of transient receptor potential M8 with a role in establishing sperm function. Proc Natl Acad Sci U S A 2011; 108:7034-9; PMID:21482758; http://dx.doi.org/10.1073/pnas.1015935108
36. Weissgerber P, Kriebs U, Tsvilovskyy V, Olausson J, Kretz O, Stoerger C, Mannebach S, Wissenbach U, Vennekens R, Middendorff R, et al. Excision of Trpv6 gene leads to severe defects in epididymal Ca^{2+} absorption and male fertility much like single D541A pore mutation. J Biol Chem 2012; 287:17930-41; PMID:22427671; http://dx.doi.org/10.1074/jbc.M111.328286
37. Weissgerber P, Kriebs U, Tsvilovskyy V, Olausson J, Kretz O, Stoerger C, Vennekens R, Wissenbach U, Middendorff R, Flockerzi V, et al. Male fertility depends on Ca^{2+} absorption by TRPV6 in epididymal epithelia. Sci Signal 2011; 4:ra27; PMID:21540454; http://dx.doi.org/10.1126/scisignal.2001791

38. Kumar PG, Shoeb M. The role of trp ion channels in testicular function. Adv Exp Med Biol 2011; 704:881-908; PMID:21290332; http://dx.doi.org/10.1007/978-94-007-0265-3_46
39. Li S, Wang X, Ye H, Gao W, Pu X, Yang Z. Distribution profiles of transient receptor potential melastatin – and vanilloid-related channels in rat spermatogenic cells and sperm. Mol Biol Rep 2010; 37:1287-93; PMID:19322679; http://dx.doi.org/10.1007/s11033-009-9503-9
40. Mizrak SC, van Dissel-Emiliani FM. Transient receptor potential vanilloid receptor-1 confers heat resistance to male germ cells. Fertil Steril 2008; 90:1290-3; PMID:18222434; http://dx.doi.org/10.1016/j.fertnstert.2007.10.081
41. Saito S, Fukuta N, Shingai R, Tominaga M. Evolution of vertebrate transient receptor potential vanilloid 3 channels: opposite temperature sensitivity between mammals and western clawed frogs. PLoS Genet 2011; 7:e1002041; PMID:21490957; http://dx.doi.org/10.1371/journal.pgen.1002041
42. Xu XZ, Sternberg PWA. A C. elegans sperm TRP protein required for sperm-egg interactions during fertilization. Cell 2003; 114:285-97; PMID:12914694; http://dx.doi.org/10.1016/S0092-8674(03)00565-8
43. Bae YK, Kim E, L'hernault SW, Barr MM. The CIL-1 PI 5-phosphatase localizes TRP Polycystins to cilia and activates sperm in C. elegans. Curr Biol 2009; 19:1599-607; PMID:19781942; http://dx.doi.org/10.1016/j.cub.2009.08.045
44. Singaravelu G, Chatterjee I, Rahimi S, Druzhinina MK, Kang L, Xu XZ, Singson A. The sperm surface localization of the TRP-3/SPE-41 Ca – permeable channel depends on SPE-38 function in Caenorhabditis elegans. Dev Biol 2012; 365:376-83; PMID:22425620; http://dx.doi.org/10.1016/j.ydbio.2012.02.037
45. Watnick TJ, Jin Y, Matunis E, Kernan MJ, Montell C. A flagellar polycystin-2 homolog required for male fertility in Drosophila. Curr Biol 2003; 13:2179-84; PMID:14680634; http://dx.doi.org/10.1016/j.cub.2003.12.002
46. Alavi SM, Cosson J. Sperm motility in fishes. I. Effects of temperature and pH: a review. Cell Biol Int 2005; 29:101-10; PMID:15774306; http://dx.doi.org/10.1016/j.cellbi.2004.11.021
47. Lahnsteiner F, Mansour N. The effect of temperature on sperm motility and enzymatic activity in brown trout Salmo trutta, burbot Lota lota and grayling Thymallus thymallus. J Fish Biol 2012; 81:197-209; PMID:22747813; http://dx.doi.org/10.1111/j.1095-8649.2012.03323.x
48. Laemmli UK. Cleavage of structural proteins during the assembly of the head of bacteriophage T4. Nature 1970; 227:680-5; PMID:5432063; http://dx.doi.org/10.1038/227680a0
49. Towbin H, Staehelin T, Gordon J. Electrophoretic transfer of proteins from polyacrylamide gels to nitrocellulose sheets: procedure and some applications. Proc Natl Acad Sci U S A 1979; 76:4350-4; PMID:388439; http://dx.doi.org/10.1073/pnas.76.9.4350
50. Perchec G, Jeulin C, Cosson J, André F, Billard R. Relationship between sperm ATP content and motility of carp spermatozoa. J Cell Sci 1995; 108:747-53; PMID:7769016
51. Guthrie HD, Welch GR, Theisen DD, Woods LC 3rd. Effects of hypothermic storage on intracellular calcium, reactive oxygen species formation, mitochondrial function, motility, and plasma membrane integrity in striped bass (Morone saxatilis) sperm. Theriogenology 2011; 75:951-61; PMID:21247623; http://dx.doi.org/10.1016/j.theriogenology.2010.10.037
52. He S, Jenkins-Keeran K, Woods LC 3rd. Activation of sperm motility in striped bass via a cAMP-independent pathway. Theriogenology 2004; 61:1487-98; PMID:15036979; http://dx.doi.org/10.1016/j.theriogenology.2003.08.015
53. Yang H, Tiersch TR. Sperm motility initiation and duration in a euryhaline fish, medaka (Oryzias latipes). Theriogenology 2009; 72:386-92; PMID:19464046; http://dx.doi.org/10.1016/j.theriogenology.2009.03.007
54. Flicek P, Amode MR, Barrell D, Beal K, Brent S, Carvalho-Silva D, Clapham P, Coates G, Fairley S, Fitzgerald S, et al. Ensembl 2012. Nucleic Acids Res 2012; 40(Database issue):D84-90; PMID:22086963; http://dx.doi.org/10.1093/nar/gkr991
55. Altschul SF, Gish W, Miller W, Myers EW, Lipman DJ. Basic local alignment search tool. J Mol Biol 1990; 215:403-10; PMID:2231712
56. Edgar RC. MUSCLE: a multiple sequence alignment method with reduced time and space complexity. BMC Bioinformatics 2004a; 5:113; PMID:15318951; http://dx.doi.org/10.1186/1471-2105-5-113
57. Edgar RC. MUSCLE: multiple sequence alignment with high accuracy and high throughput. Nucleic Acids Res 2004b; 32:1792-7; PMID:15034147; http://dx.doi.org/10.1093/nar/gkh340
58. Ronquist F, Teslenko M, van der Mark P, Ayres DL, Darling A, Höhna S, Larget B, Liu L, Suchard MA, Huelsenbeck JP. MrBayes 3.2: efficient Bayesian phylogenetic inference and model choice across a large model space. Syst Biol 2012; 61:539-42; PMID:22357727; http://dx.doi.org/10.1093/sysbio/sys029
59. Hall BG. Phylogenetic Trees Made Easy: A How To Manual, Fourth Edition, Sinauer Associates, Inc. 2011

General and Comparative Endocrinology 220 (2015) 23–32

Contents lists available at ScienceDirect

General and Comparative Endocrinology

journal homepage: www.elsevier.com/locate/ygcen

Review

Regulation of TRP channels by steroids: Implications in physiology and diseases

Ashutosh Kumar, Shikha Kumari, Rakesh Kumar Majhi, Nirlipta Swain, Manoj Yadav, Chandan Goswami *

School of Biology, National Institute of Science Education and Research, Sachivalaya Marg, Bhubaneswar, Orissa 751005, India

ARTICLE INFO

Article history:
Available online 19 October 2014

Keywords:
TRP channels
Steroids
Non-genomic action of steroids
Ca^{2+}-influx
Expression

ABSTRACT

While effects of different steroids on the gene expression and regulation are well established, it is proven that steroids can also exert rapid non-genomic actions in several tissues and cells. In most cases, these non-genomic rapid effects of steroids are actually due to intracellular mobilization of Ca^{2+}- and other ions suggesting that Ca^{2+} channels are involved in such effects. Transient Receptor Potential (TRP) ion channels or TRPs are the largest group of non-selective and polymodal ion channels which cause Ca^{2+}-influx in response to different physical and chemical stimuli. While non-genomic actions of different steroids on different ion channels have been established to some extent, involvement of TRPs in such functions is largely unexplored. In this review, we critically analyze the literature and summarize how different steroids as well as their metabolic precursors and derivatives can exert non-genomic effects by acting on different TRPs qualitatively and/or quantitatively. Such effects have physiological repercussion on systems such as in sperm cells, immune cells, bone cells, neuronal cells and many others. Different TRPs are also endogenously expressed in diverse steroid-producing tissues and thus may have importance in steroid synthesis as well, a process which is tightly controlled by the intracellular Ca^{2+} concentrations. Tissue and cell-specific expression of TRP channels are also regulated by different steroids. Understanding of the crosstalk between TRP channels and different steroids may have strong significance in physiological, endocrinological and pharmacological context and in future these compounds can also be used as potential biomedicine.

1. Introduction

Steroid actions can be both genomic and non-genomic (i.e., rapid effects produced within minutes and which are independent of transcriptional or translational stimulation). In contrast to the well-established genomic effects, these non-genomic and rapid effects of steroids are poorly understood, although such effects have been noted in several systems including neurons. For example, very rapid effects of several neurosteroids on the neuronal system is well established. Notably, it has been observed that fast and non-genomic actions of steroids are dose-dependent, often reversible, stereo-specific and can be blocked by other signaling compounds suggesting that these steroids initiate specific biological responses through specific signaling cascades (Gu and Moss, 1996; Falkenstein et al., 2000). While a handful of reports suggest that these fast and non-genomic effects of steroids originate at the plasma membrane, the molecular mechanisms and the signaling events are not well understood. The molecular identities of the receptors and ion channels involved in such responses are largely unknown. Nevertheless, identification of molecular candidates involved in rapid steroid signaling events and understanding of the signaling events involved in such processes are important from a physiological, pharmacological and clinical perspective. In this context, Transient Receptor Potential (TRP) ion channels (TRPs) are relevant.

TRPs are a group of non-selective ion channels which mediate the transmembrane flux of Ca^{2+} (and other cations too) down an electrochemical gradient, thereby increasing the intracellular Ca^{2+} and Na^{+} concentration and causing cell depolarization. TRP channels were first discovered in a Drosophila *trp* mutant, which had a modified response to light (Minke, 1977; Montell et al., 1985). Subsequently members of the TRP family have been identified in vertebrates, and other invertebrates and in lower eukaryotes such as yeast and fungi. However, so far TRPs or their exact homologs have not been detected in plants. TRPs are classified on the basis of their sequence homology and by the presence of specific signature domains and motifs such as the TRP-domain, TRP-box motifs, ankyrin repeats, etc. (Clapham, 2003; Nilius and Owsianik, 2011). The primary structure of all TRPs consists of six transmembrane

* Corresponding author.
E-mail address: chandan@niser.ac.in (C. Goswami).

http://dx.doi.org/10.1016/j.ygcen.2014.10.004
0016-6480/

regions with a pore domain between the fifth and sixth transmembrane region and both the N- and C-termini are intracellular. Based on amino acid sequence, homology with other TRP channels, and the presence of specific structural features, the TRPs have been classified into 7 subfamilies, namely, TRPC (Canonical), TRPV (Vanilloid), TRPM (Melastatin), TRPA (Ankyrin), TRPP (Polycystin), TRPML (Mucolipin) and TRPN (No Mechanoreceptor Potential C, NOMPC).

In animals, TRP channels are ubiquitously expressed in almost all cell types and tissues, albeit at different levels. However, involvement of TRP channels in physiological functions and sensory processes are relevant in multi-cellular as well as in unicellular organisms also. Most of the TRPs are selectively activated by specific ligands and are polymodal in nature (Baez-Nieto et al., 2011). TRP channels are regulated by multiple stimuli, both physical and chemical and a few members of TRPs, namely TRPV1, TRPV2, TRPV3, TRPV4, TRPM3, TRPM8, TRPA1 are thermosensitive. In most cases the chemical ligands are hydrophobic in nature and several endogenous hydrophobic compounds (such as different lipids) have been reported to activate or inhibit TRP channels (Holzer, 2011). The complex polymodal regulation of TRP channels by intracellular as well as extracellular components such as, specific lipids, pH, ROS, NO, metal ions, interacting proteins, etc. and the multiple routes of regulation by phosphorylation-dephosphorylation and other post-translational modifications, suggest that these channels integrate multiple signaling events at the plasma membrane. In this context, TRPs have been investigated for rapid signaling mediated by different steroids and may be an important group of molecular targets for the fast and non-genomic actions of different steroids. Reports also suggest that expressions of TRPs are also controlled by different steroids as long-term effects. The crosstalk between steroids and TRPs may have crucial implications in several spheres such as in clinical, pharmacological, endocrinology, food safety, species conservation and several other aspects. The present review will present the importance of TRPs in the signaling of non-genomic responses to different steroids in different systems. In case of multicellular organisms, involvement of TRP channels in neuronal systems and in different sensory processes is a well-studied topic, in this review we will not discuss it in details and this review will mainly summarizes the steroids-TRP crosstalk in the context of non-neuronal systems *per se*.

2. Steroid-mediated regulation (expression) of TRP channels (Long term effects)

Steroid hormones trigger gene expression by directly binding to intracellular steroid receptors which undergo homo- or heterodimerization and bind to specific palindromic hormone response elements (HRE) (Falkenstein et al., 2000). The classical cellular actions of steroids provoke the typical "long-term effects" of steroids that require hours to days and modify gene expression (Gronemeyer, 1992). Indeed, human, rat and mouse genome data suggest that promoter sequences (within 5 kb region) of several TRP genes contain response elements indicative of steroid mediated-transcriptional regulation. For example, the entire TRPM8 gene contains 10 putative androgen responsive elements (one in the promoter region and the remaining 9 in the introns) and dihydrotestosterone (DHT) regulates the transcription of TRPM8 in both smooth muscle and apical epithelial cells of the human prostate (Zhang and Barritt, 2004; Bidaux et al., 2005). Similarly, in cultured bovine aortic endothelial cells (BAECs), β-estradiol causes significant down-regulation of *Trp4* and modest up-regulation of *Trp1a* and *Trp3* expression whereas progesterone and dexamethasone seem to have a stimulatory effect (Chang et al., 1997). Various oestrogens including 17β-estradiol can up-regulate renal TRPV5 mRNA and protein levels as well as duodenal TRPV6 expression in rats (van Abel et al., 2002, 2003). In mice TRPV6 expression was induced after 17β-estradiol treatment (Lee and Jeung, 2007) and in pregnant rat, expression of TRPV6 transcription appeared to be solely controlled by progesterone (Lee et al., 2009). Estrogen in particular has also been shown to induce the expression of TRPV1 channel in rats (Yan et al., 2007). In MCF-7 which is a breast cancer cell line, ERα has been shown to regulate the expression of TRPM8 (Chodon et al., 2010).

Often the expressions of different TRP channels in a given tissue/cell are tightly controlled by the serum levels of different steroid hormones. For example, female sex hormones E2 and P4 alone or in combination can modulate the transcription of *trp* genes involved in physiological functions linked to pregnancy. The uterine expression of TRPV6 during the estrous cycle in rodents is modulated by steroid hormones and TRPV6 transcripts in the rat uterus is highly up-regulated by P4 at diestrus (Kim et al., 2006), while in mouse uterus TRPV6 mRNA is up-regulated by E2 at estrus (Lee and Jeung, 2007). Uterine TRPV6 has increased expression during implantation and just prior to birth while it declines sharply following birth and during lactation, and is mainly regulated by serum concentrations of P4 or E2 in rat and mouse respectively (Lee et al., 2009). In rodents TRPV6 expression in the placenta initially follows the pattern of uterine expression, with an induction in the middle of gestation but not at the end of gestation (Lee and Jeung, 2007). The species-specific regulation of TRPV6 transcription in the uterus and placenta may be a consequence of the uterine calcium ion concentration required for successful implantation of embryo and in rats P4 and PRs are important while in mice E2 and ERs are regulatory (Lee et al., 2009).

Several other TRP channels are also regulated by E2 and P4. For example, both E2 and P4 are involved in the regulation of *trpm2* gene during the oestrous cycle of female rats. Changes in TRPM2 expression in stromal cells of the myometrium and endometrium of mature rats during oestrous and in immature rats after E2 and P4 treatment suggest that E2-induced TRPM2 expression is inhibited by co-treatment with P4 (Ahn et al., 2014). A dramatic increase in the TRPM2 mRNA levels is detected during proestrus, and it drops to the baseline levels at metestrus, and levels are restored at diestrus. Similarly E2 and P4 up-regulated the expression of TRPC1 and enhanced store operated Ca^{2+} influx in cultured hESC (human endometrial stromal cells) (Kawarabayashi et al., 2012). All these effects may be implicated in decidualization, which is an ovarian steroid-induced remodeling/differentiation of the uterus essential for embryo implantation and placentation. In contrast, in human airways, mammary gland epithelial cells and vascular smooth muscle cells TRPV4 is down-regulated by P4 (Jung et al., 2009). Taken together, the results strongly suggest that expression of TRPs in different cells and tissues are tightly regulated by steroids.

3. Expression of TRP channels in specialized steroid-sensitive tissues and cells

Almost all tissues and cells are responsive to different steroids although the response kinetics to specific steroids differs and all cells express different subsets of TRP channels and their spatio-temporal expression and localization pattern differs. In general, such a situation makes it very difficult to dissect out the effect of specific steroids on specific TRP channel. However, the existing literature provides a strong correlation in terms of expression of specific TRPs in certain tissues (and cells) with the sensitive response to specific steroids at very low concentrations. The expression of TRPs in peripheral neurons and central neurons have already been extensively described (Julius, 2013; Talavera et al., 2008; Numazaki and Tominaga, 2004) and so the present review will

focus on TRPs in non-neuronal tissue and their involvement in steroid responsiveness.

3.1. Expression of TRPs in bone cells

It is well established that bone cell function, differentiation and other processes are highly dependent on sex steroids and influenced by the balance between internal as well as external Ca^{2+} concentration, and Ca^{2+} signaling (Karsenty, 2012; Kajiya, 2012). So far a number of TRPs are known to be critically involved in these processes, including intestinal Ca^{2+} absorption (TRPV6), renal calcium re-absorption (TRPV5), osteoclastogenesis (TRPV1, TRPV2, TRPV4, TRPV5), osteoblastogenesis (TRPV1), chondrocyte differentiation/functioning (TRPV4), and bone pain sensation (TRPV1) (Lieben and Carmeliet, 2012). A new splice variant of TRPC1 (termed as TRPC1ε that has its translation start site upstream of a non-AUG site) was identified in early pre-osteoclasts (Ong et al., 2013). Interestingly, phylogenetic analysis indicates that certain TRP channels emerged during vertebrate evolution and this has been associated with their role in the formation and/or regulation of vertebra, i.e. in bone cells. For example, TRPM8 share close relationship with SPP2, a bone morphogen since vertebrate evolution, circa 450 million years (Majhi et al., 2014).

A recent report has demonstrated endogenous expression and the functional repercussion of TRPV1 in osteoclasts (Khan et al., 2012). Human odontoblasts contain functional TRPV1, TRPA1 and TRPM8 channels (El Karim et al., 2011). TRPV4 is expressed in osteoblasts, osteoclasts and synoviocytes and the absence of TRPV4 prevents disuse-induced bone loss (Abed et al., 2009; Masuyama et al., 2008; Mizoguchi et al., 2008; Itoh et al., 2009; Kochukov et al., 2006). TRPV4-mediated Ca^{2+}-influx regulates terminal differentiation of osteoclasts (Masuyama et al., 2008) and TRPV4 activation in osteoclasts increased the number of osteoclasts and their resorption activity and increased bone loss (Masuyama et al., 2012). In articular cartilage, TRPV4 exhibits osmotic sensitivity, controls cellular volume recovery and other physiologic responses to osmotic stress (Phan et al., 2009). In addition, TRPV4 activation promotes chondrogenesis by inducing SOX9 transcription (Muramatsu et al., 2007). Other TRPs detected in the skeletal system include TRPV5 (in human osteoclasts) (Chamoux et al., 2010), TRPM8 in rat synoviocytes and odontoblasts) (Zhu et al., 2014) where it is involved in low-temperature stimulation of the dentin surface together with TRPA1 (Tsumura et al., 2013).

3.2. Expression of TRPs in pancreatic cells

Steroids influence the development, regulation and secretion of hormones from the pancreas (Islam, 2010; Morimoto et al., 2010). So far, at least nine different TRP channels (TRPC1, TRPC4, TRPC6, TRPV1, TRPV5, TRPM2, TRPM3, TRPM4 and TRPM5) that have different functions have been detected in pancreatic β cells (Colsoul et al., 2011; Nilius et al., 2007). For example, TRPM3 is expressed in whole pancreas (Grimm et al., 2003; Fonfria et al., 2006), mouse pancreatic islets and even INS-1 cells (Klose et al., 2011; Wagner et al., 2008). TRPM3 is directly activated by the neurosteroid hormone pregnenolone sulfate (PS). PS increased glucose-induced insulin secretion from pancreatic islets and INS-1E cells, an effect which can be abolished by the selective and potent TRPM3 blocker mefenamic acid (Klose et al., 2011; Wagner et al., 2008). TRPM2 is expressed in insulin secreting cell lines, such as in the rat cell lines CRI-G1 and RIN-5F, and in human and mouse pancreatic islets (Hara et al., 2002; Qian et al., 2002; Inamura et al., 2003; Togashi et al., 2006). TRPM2 has been suggested to contribute to insulin release induced by heat, glucose and incretin hormones (Uchida and Tominaga, 2011; Togashi et al., 2006) and inhibits heat- and exendin-4-evoked insulin release from rat pancreatic islets (Togashi et al., 2008). These functions are specific to TRPM2 as animals lacking this gene (*Trpm2*$^{-/-}$ mouse) have impaired insulin secretion in response to glucose and GLP-1 (Uchida and Tominaga, 2011). TRPM2 has been reported to have an additional role as an intracellular Ca^{2+} release channel in pancreatic beta cells (Lange et al., 2009). In addition, TRPM4 expression and TRPM4-like channel activity is found in the beta cell lines INS-1, HIT-T15, RINm5F, β-TC3 and MIN-6 and the alpha cell line INR1G9 (Cheng et al., 2007; Marigo et al., 2009). Inhibition of TRPM4 decreases the magnitude of the Ca^{2+} signal and insulin release in INS-1 cells (Cheng et al., 2007; Marigo et al., 2009).

3.3. Expression of TRPs in immune cells

Importance of different steroids on immune system is well established. Many processes in the immune response such as macrophage migration, phagocytosis and T-cell activation are dependent on Ca^{2+} and thus Ca^{2+}-channels are important regulators (Vig and Kinet, 2009). Some immune functions are temperature-dependent as well as steroid-sensitive (Knippertz et al., 2011; Hatzfeld-Charbonnier et al., 2007) and theromosensitive TRP channels in these immune cells are important. The expression of the TRPV subfamily is notable and murine dendritic cells express TRPV1 and activation of TRPV1 by capsaicin leads to maturation of dendritic cells (Basu and Srivastava, 2005). TRPV2 mediates the effect of transient heat shock on endocytosis by human monocyte-derived dendritic cells (Szöllősi et al., 2013). TRPV2 also plays a major role in particle binding and phagocytosis in murine peritoneal macrophages (Link et al., 2010). Transcripts for TRPV2, TRPV3 and TRPV4 are found in thymocytes, splenocytes, lymphocytes or purified B-cells and T-cells of C57BL/6 mice (Inada et al., 2006) and TRPV1 and TRPV2 are detected in human PBMCs (Saunders et al., 2007, 2009). Strong and prolonged activation of TRPV1 by capsaicin induces apoptosis in $CD5^{+}$ thymocytes (Amantini et al., 2004) and TRPV6 in Jurkat cells are involved in store operated Ca^{2+}-entry, an essential process involved in T-cell activation (Cui et al., 2002; Yue et al., 2001). Both transcript and proteins of TRPV5 and TRPV6 have been detected in Jurkat and human T-lymphocytes (Vasil'eva et al., 2008). Expressions of TRPC1, TRPC3 and TRPV2 have been implicated in macrophage survival and apoptosis (Berthier et al., 2004; Tano et al., 2011; Yamashiro et al., 2010). TRPC3, TRPC6, TRPV1 have been implicated in monocyte migration (Zhao et al., 2012; Schilling and Eder, 2009), whereas TRPC3, TRPV2 and TRPM8 have been implicated in macrophage migration (Tano et al., 2011; Nagasawa et al., 2007; Nagasawa and Kojima, 2012; Wu et al., 2011). Some TRPC and TRPM subfamily members have also been detected in immune cells and in neutrophils TRPC6 regulates their migration (Damann et al., 2009). Expression of TRPC6 has been detected in human alveolar macrophages, lung tissue macrophages, monocytes and in monocyte-derived macrophages (Finney-Hayward et al., 2010). TRPM4 channel controls monocyte and macrophage, but not neutrophil functions (Serafini et al., 2012). Several members of the TRPC family have also been reported in T-cells (Philipp et al., 2003). In both Jurkat and peripheral blood-derived T-lymphocytes, importance of TRPC1, TRPC3, TRPC6 and TRPM4 have been shown (Gamberucci et al., 2002; Philipp et al., 2003; Wenning et al., 2011; Rao and Kaminski, 2006; Takezawa et al., 2006). Expression and channel function of several TRPs are steroid-dependent, and this may be a mechanism of steroid-mediated changes in immunity and immune suppression.

3.4. Expression of TRP channels in sperm cells

Sperm cells are transcriptionally inactive yet extremely sensitive to different steroids. These sensitivities are mainly due to

the direct regulation of different ion channels by steroids (discussed later). In this context, expression of different TRPs and their homologs are relevant. Indeed several of these channels have been detected in testis and particularly in mature sperm cells. Often these TRPs are localized in very specialized regions of the sperm. During the late 1990s, it was demonstrated that a homolog of the drosophila *Trp* gene, named *bTrp2* is expressed in bovine testis, spleen and liver (Wissenbach et al., 1998). In the testis *bTrp2* mRNA is restricted to spermatocytes suggesting that this channel may be important in sperm cell formation, a sex steroid dependent process.

In human sperm the flagella express TRPC1, TRPC3 and TRPC6 (Castellano et al., 2003) while mouse sperm flagella express TRPC1, TRPC3, TRPC4 and TRPC6 (Trevino et al., 2001). TRPC2 is present in the overlying region of the mouse sperm acrosome (Jungnickel et al., 2001; Trevino et al., 2001) and additional forms of TRP detected in mouse sperm include TRP1 and TRP3 in the flagellum and TRP6 in the postacrosomal region (Trevino et al., 2001). Pharmacologic suppression of TRPC activity impairs the motility of human sperm and this illustrates their importance in sperm function (Castellano et al., 2003). In mature mammalian sperm (such as in boar), TRPV1 has been located in the post acrosomal area and these channels re-localize to the anterior region of the sperm head after capacitation (Bernabò et al., 2010a,b). In this context, it is important to note that steroids like estrogen and progesterone play an important role in the capacitation process (Baldi et al., 2009). Activation of TRPV1 results in an increase in intracellular Ca^{2+} concentrations and these ionic events promote actin cytoskeletal depolymerization and a loss of acrosome structure integrity (Bernabò et al., 2010a). Interestingly, inhibition of actin polymerization and cholesterol depletion prevents this re-localization of TRPV1 during capacitation suggesting that membrane cholesterol controls membrane dynamics of TRPV1 (Bernabò et al., 2010b). The expression of TRPV1 in sperm cells seems to be conserved in all vertebrates ranging from human to fish (Majhi et al., 2013). In addition to TRPV1, the cold-sensitive ion channel TRPM8 has also been detected in human, murine and other vertebrate sperm cells (De Blas et al., 2009; Martínez-López et al., 2011; Majhi et al., 2014). TRPM8 activation by menthol does not alter human sperm motility although it induces acrosome reaction (De Blas et al., 2009). Notably, progesterone and ZP-induced acrosomal reaction can be inhibited in murine but not in human sperm (Martínez-López et al., 2011).

Endogenous expression of TRPs is also detected in invertebrate sperm cells which lack or have impaired steroid biosynthesis pathways. For example, in *Caenorhabditis elegans*; TRPC homolog namely, TRP3 is an important regulator of sperm-egg interactions during fertilization (Xu and Sternberg, 2003). In *Drosophila*, polycystin-2 homolog localizes to the distal tip of the sperm flagella. Mutation in this gene induces infertility as the sperms fail to enter the female sperm storage organs (Watnick et al., 2003). Thus sperm-specific expressions of TRPs and likely responsiveness to different steroids are of evolutionary significance.

4. Non-genomic rapid actions of steroids on TRP channels

Steroids are now recognized to also exert rapid non-genomic effects on tissues and cells and most of these responses are very specific, often stereo-specific, extremely fast and generally reach their maxima within minutes. Since, rapid effects are most likely to be mediated by membrane proteins; this means that ion channels and receptors are prime molecular targets of steroids (Kousteni et al., 2001). Steroids are known to induce sudden increases in intracellular Ca^{2+} concentrations suggesting that these compounds modulate different Ca^{2+} channels and such effects are particularly prominent in neurons and specialized non-neuronal cells such as in sperm cells. Indeed, several neurosteroids and also some non-neuronal steroids can exert an immediate cellular response by directly stimulating ion channels (Chen et al., 2007; Unemoto et al., 2007; Seyrek et al., 2007; Scragg et al., 2007; Harteneck, 2013). However, the mode-of-action of these steroids and their specificities towards different Ca^{2+} channel are not clear. In this context, TRPs are important though the entire range of activity of different steroids against all the TRPs have not yet been investigated. Nonetheless the present literature strongly suggests that TRP channels are both direct and indirect molecular targets of neurosteroids (Nilius and Voets, 2008). A concise summary of such non-genomic effects of these steroids against different TRP channels is listed (Table 1). Different steroids can potentially induce complex conformational changes leading to bidirectional changes such as channel opening or channel closing. Such conformational changes correlate well with different cellular and physiological functions. However, depending on the concentrations and availability, different steroids and/or steroid like molecules can also induce permanent conformational changes in the channels leading to either "constitutively on" or "constitutively off" stages. Such cases generally lead to pathophysiological manifestations. Different steroids and steroid-like molecules therefore seem to modulate TRP channels in a complex manner and modulate intracellular Ca^{2+} levels leading to different cellular responses. Though the exact molecular mechanism may differ for different TRP channels and may also vary from steroids to steroids, a general simplified mechanism can be summarized (Fig. 1).

Glucocorticoids and AEA can activate TRPV1 in a subset of gastric-related preautonomic neurons of the rat hypothalamus and modulate excitatory synaptic input (Boychuk et al., 2013). Similarly, diacylglycerol-sensitive channels, especially TRPC3, TRPC5 and TRPC6 can be inhibited by synthetic and natural steroids as well as structurally related compounds such as norgestimate (Miehe et al., 2012). TRPC5 is inhibited by steroids in a stereo-specific manner (Majeed et al., 2011) and aldosterone induces pro-inflammatory signaling through TRPM7/TRPM7α-kinase and involves the mineralocorticoid receptor (MR) and ROS (Yogi et al., 2013). Norgestimate and progesterone differentially inhibit TRPC-mediated currents and Ca^{2+}-influx in smooth muscles (Miehe et al., 2012) and has been linked with the physiological decrease in uterine contractility and immunosuppression during pregnancy, and has been linked to the high levels of progesterone during gestation. Another example is 17β-estradiol, which can induce Ca^{2+}-influx and activate Ca^{2+}-currents in rat cortical collecting duct cells by acting on TRPV5. This effect can be effectively inhibited by pre-treatment with ruthenium red or by TRPV5-specific siRNA (Irnaten et al., 2009). In a similar manner, Ca^{2+}-entry/signaling by TRPV6 is also sensitive to 17β-estradiol (Irnaten et al., 2008).

Pregnenolone sulfate (PS) has been considered as an endogenous steroid as it has numerous neuropharmacological actions (Lee et al., 2010a). Whole cell patch clump experiments reveal that PS regulates the glutamatergic currents in pre- and post-synapses in isolated dentate gyrus (DG), hilar neurons and these PS-induced currents can be effectively blocked by inhibitors of TRPs (Lee et al., 2010a). Molecular diffusion studies suggest that PS travels a long distance and can act as a modulator of transporters, enzymes and ion channels belonging to the TRPM superfamily, namely to TRPM1 and TRPM3 (Lambert et al., 2011). Among all TRPs, PS activates TRPM3 directly at physiological concentrations and (Wagner et al., 2008) extracellular application activates endogenous mouse TRPM3 present in tissues and cells such as pancreatic β-cells which leads to rapid Ca^{2+}-influx and insulin secretion (Wagner et al., 2008). In a similar study human TRPM3 was activated by PS but not stimulated by progesterone, aldosterone, 17β-oestradiol or by

Table 1
Non-genomic effects through TRP channel.

Steroid	Channels	Effect	References
Progesterone	TRPC3, TRPC4, TRPC5, TRPC6	Channel inhibition	Miehe et al. (2012)
	TRPM3	Channel inhibition	Majeed et al. (2011)
	CatSper2	Rise in intracellular Ca^{2+} causing sperm hyperactivation, acrosome reaction, and potential chemotaxis and thermotaxis towards the egg	Calogero et al. (2000), Lishko et al. (2011), Heath (2011) and Strünker et al. (2011)
Norgestimate	TRPC5, TRPC6, TRPC3	Channel inhibition	Miehe et al. (2012)
Aldosterone	TRPM7	Mg^{2+}-influx and ROS production	Yogi et al. (2013)
17β-estradiol	TRPV5	Ca^{2+}-currents in rat cortical collecting duct cells	Irnaten et al. (2009)
	TRPV6	Rapid Ca^{2+}-influx (within 5 min)	Irnaten et al. (2008)
	TRPM3	Channel inhibition	Majeed et al. (2012)
	TRPV1	Channel inhibition in DRG sensory neurons by a non-classical estrogen-signaling pathway downstream of intracellular ERβ affecting the vanilloid binding site targeted by capsaicin	Xu et al. (2008)
Pregnenolone sulfate	TRPM3	TRPM3 activation cause rapid Ca^{2+}-influx leading to insulin release from mouse pancreatic β cells	Wagner et al. (2008)
	TRPM3	Potentiation of glutamatergic transmission at cerebellar Purkinje neurons from developing rats	Zamudio-Bulcock et al. (2011); Zamudio-Bulcock and Valenzuela (2011)
	TRPV1	Inhibit capsaicin-induced currents rapidly and reversibly	Chen et al. (2004)
	TRPC5	Channel inhibition	Beech (2012)
Dihydrotestosterone	TRPM3	Channel inhibition	Majeed et al. (2011) and Majeed et al. (2012)
Dehydroepiandrosterone (DHEA)	TRPV1	Inhibits the capsaicin-induced current in isolated DRG neurons rapidly and reversibly	Chen et al. (2004)
5-androsten-3α-ol-17-one (3α-DHEA)	TRPV1	Potentiates capsaicin response	Chen et al. (2004)
α-spinasterol	TRPV1	A novel efficacious and safe antagonist of TRPV1 with anti-nociceptive effect, derived from the leaves of the medicinal plant *Vernonia tweedieana* Baker	Trevisan et al. (2012)

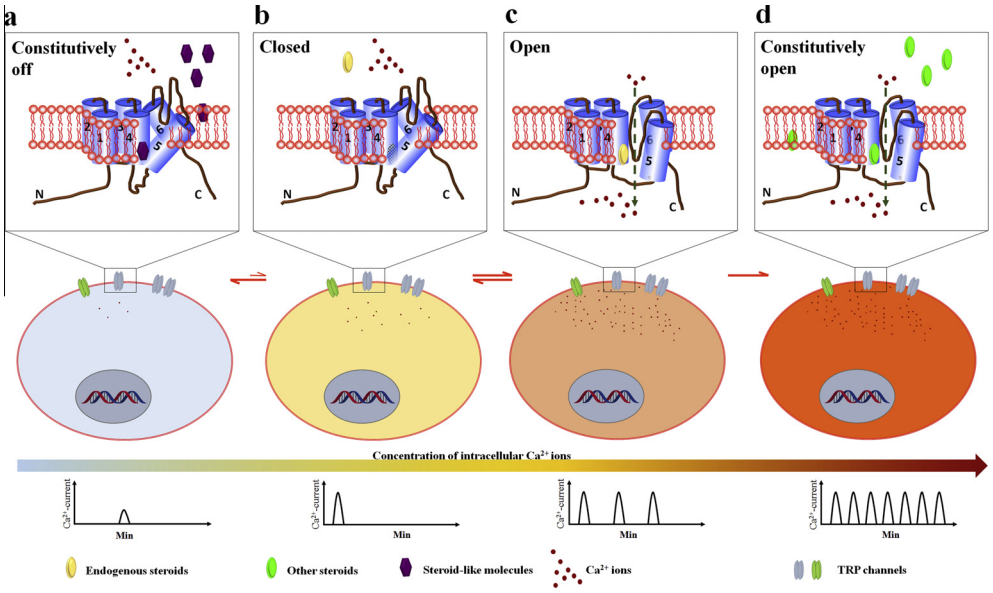

Fig. 1. Non-genomic action of different steroids and steroid-like molecules on TRP channels. The schematic diagram suggests that endogenous steroids readily diffuse to the plasmamembrane and binds to certain steroid-binding pockets (mainly located at the transmembrane and/or loop region) of the TRP channels. Such binding alters the channel conformation resulting in reversible regulation of "on-and-off" mode of TRP channels and thus regulate intracellular concentration of Ca^{2+} ions as well as cellular response leading to physiological functions (described in b–c). However excess steroids as well as different steroid-like molecules bind with different TRP channels with different kinetics leading to irreversible changes such as either constitutive on (described in d) or constitutive off (described in a) mode leading to abnormal intracellular Ca^{2+} and defective cellular functions. Under these scenario, expected Ca^{2+}-currents due to TRP channels are plotted at the bottom.

testosterone (Majeed et al., 2011). In fact, prior application of progesterone at a concentration of 10 nM to 10 μM can inhibit the effect of PS-mediated Ca^{2+}-influx in a dose-dependent manner suggesting that progesterone actually inhibits TRPM3 activity in a Pregnenolone sulfate-independent manner (Majeed et al., 2011).

Compounds with structural similarities to testosterone such as dihydrotestosterone and 17β-oestradiol also inhibit TRPM3 activity but these effects were equivalent to or smaller than those of progesterone (Majeed et al., 2011, 2012). Chen et al. and others have provided useful information regarding the effect as well as the mode of action of different steroids, their intermediates and metabolites on TRPV1 as well as on other TRP channels (Chen et al., 2004; Chen and Wu, 2004). For example, pregnenolone sulfate (PS) acts as an inhibitor of capsaicin induced currents via TRPV1 (Chen and Wu, 2004). Electrophysiology data revels that PS rapidly and reversibly inhibits the capsaicin response in a concentration dependent manner. Progesterone (100 μM) does not exert a significant effect on the capsaicin induced currents via TRPV1. Interestingly, one stereoisomer of DHEA, namely 5-androsten-3α-ol-17-one (3α-DHEA), also fails to inhibit the capsaicin-induced current, and instead potentiates the current. These stereo-specificities indicate that neither a double bond at C-5 nor stereochemistry at C-5 is critical for inhibition of capsaicin-induced currents, whereas addition of a sulfate group at C-3β results in weaker activity. Testosterone produces significantly less inhibition of capsaicin-induced current than DHEA and the female sex steroid hormone 17β-estradiol markedly alters the capsaicin response. While some reports suggest that 17β-estradiol potentiates capsaicin response, other reports suggest that it acts directly on dorsal root ganglion (DRG) sensory neurons and reduces TRPV1 activation by capsaicin (Xu et al., 2008). However, the effect of 17β-estradiol on TRPV1 is probably more complex and likely involves G-protein coupled receptors and atypical PKCs (Goswami et al., 2011). Another study has also confirmed that pregnenolone sulphate, pregnanolone (or its β-sulphated form) and progesterone inhibit TRPC5 activity in HEK293 cells within 1–2 min and that progesterone is a potent and reversible inhibitor (Beech, 2012). 17β-oestradiol has a weak inhibitory effect on TRPC5 activity compared to other inhibitory steroids. The inhibitory concentration of the steroids was within the micro-Molar range, which correlates with normal physiological concentrations.

Compounds isolated from leaves of the medicinal plant *Vernonia tweedieana* that have anti-nociceptive effects, can actually exert antagonistic activity on TRPV1 (Trevisan et al., 2012). The compounds α-spinasterol and stigmasterol present in the dichloromethane fraction, reduce the nociception and edema induced by capsaicin injection. The action of α-spinasterol is most likely via TRPV1 as it affects noxious heat-mediated nociception but does not alter sensitivity to a mechanical stimulus that generally involves TRPV4. Indeed, α-spinasterol displaces [^{3}H]Resiniferatoxin binding to TRPV1 in spinal cord membranes and diminishes Ca^{2+} influx mediated by capsaicin suggesting that it probably competes for the same binding site. Notably, compounds with a similar structure to α-spinasterol such as α-amyrin, β-amyrin and Lupeol fail to affect TRPV1 action. These properties indicate that α-spinasterol is a specific, novel, effective and safe antagonist of TRPV1 with antinociceptive effects.

The steroid-induced Ca^{2+}-influx is not limited to neurons and has also been observed in non-neuronal tissues and cells such as pancreatic cells, immune cells, bone cells as well as cancer cells (Xi et al., 2000). Another example of cells that respond to steroids with a sudden rise in Ca^{2+}-level is sperm characterized by condensed chromatin and minimal transcription and translation suggesting the response is indeed independent of gene transcription (Publicover and Barratt, 2011). Progesterone, a female reproductive steroid hormone causes elevation of intracellular Ca^{2+} leading to sperm hyperactivation, acrosome reaction, and potential chemotaxis and thermotaxis towards the egg (Calogero et al., 2000; Lishko et al., 2011). Progesterone causes this effect by directly activating CatSper2, a close homolog of TRP channels (Heath, 2011; Strünker et al., 2011) and it is pertinent to note that patients lacking CatSper2 activity are infertile (Avidan et al., 2003).

In summary; steroids, their metabolites and precursors as well as other steroid-like molecules can act directly on the TRPs and exert inhibitory or stimulatory effects. However, much better characterization of steroid-TRP interactions are required by systematic exploration of different steroids and TRP family members.

5. Importance of TRP channels in steroid production and secretion

In mammals, steroid production occurs in specialized tissues such as in brain, adrenal glands, gonads (both male and female), and the placenta (Compagnone and Mellon, 2000). In general, Ca^{2+} is required for several steps of steroidogenesis. For example, in Leydig cells, Ca^{2+}-channel blockers inhibit steroidogenesis by reducing the expression of the cholesterol transporting StAR proteins in mitochondria which controls the rate-limiting step of steroidogenesis (Dufau, 1988; Lee et al., 2010b, 2011). Ca^{2+} also plays major regulatory roles in steroidogenesis in general (Cherradi et al., 1998; Cooke, 1999; Davies et al., 1985; Rossier, 2006). In this context, TRPs are relevant for several reasons. First, these channels control total Ca^{2+}-homeostasis by regulating the Ca^{2+} absorption/reabsorption; complex physiological processes which are dependent on endocrine and environmental factors including temperature. Secondly; TRP channels conduct large Ca^{2+}-currents upon activation and induce Ca^{2+}-signaling as well as Ca^{2+}-independent signaling events within the cell. And lastly, TRPs are endogenously expressed in steroid producing cells and can control both steroid production as well as secretion. For example, TRP4 is endogenously expressed in bovine adrenal cortex and specifically in adrenal cells (Philipp et al., 2000). Similarly, the adrenal chromaffin derived cell line, PC12, expresses TRP6 which is involved in diacylglycerol-induced Ca^{2+}-influx (Tesfai et al., 2001). Another steroid producing organ is the testis and so far a battery of TRPs are known to be expressed in testis and also in different cells representing different stages of spermatogenesis indicating that TRPs may have specific role in steroid production and response (reviewed in Kumar and Shoeb, 2011). Similarly, transcripts of TRPV2 and TRPV3 have been reported in mice ovary (Kunert-Keil et al., 2006). TRPV1 is expressed constitutively in rat ovaries and is involved in follicle development (Tutuncu and Özfiliz, 2010). Another steroid producing tissue is the placenta and so far a handful of reports indicate that these are linked to specific physiological functions (Dörr and Fecher-Trost, 2011; Stumpf et al., 2008). In the case of the human placenta, TRPC1, TRPC3, TRPC4, TRPC5 and TRPC6 mRNAs are present during the first and second trimester and at term in the placenta (Sossey-Alaoui et al., 1999). In rat, TRPV1 is expressed during placenta development during pregnancy (Fonseca et al., 2009). The highly Ca^{2+}-selective TRPV5 and TRPV6 are also reported to be expressed in different cells of the placenta (Wissenbach et al., 2001; Bernucci et al., 2006; Stumpf et al., 2008; Moreau et al., 2002a,b; Peng et al., 2003; Lee and Jeung, 2007).

Apart from steroid production, TRPs also regulate steroid secretion (Obukhov and Nowycky, 2002; Iwasaki et al., 2008). This effect is basically due to the regulation of vesicle fusion in response to Ca^{2+}-influx. For example, secretion of testosterone from Leydig cells is a process which is also controlled by Ca^{2+}, mainly by calcium-induced calcium release mechanism (Costa et al., 2010).

6. Conclusion

Steroid-mediated regulation of calcium channels is of physiological significance. For example, dihydrotestosterone affects L-type calcium channels in human ventricular cardiomyocytes (Er et al., 2009). Testosterone increases urinary Ca^{2+} excretion and inhibits expression of renal Ca^{2+} transport proteins, namely TRPV5 and maintains the Ca^{2+} homeostasis (Hsu et al., 2010). In this context, it is interesting that the effects of steroid-induced physiological responses and TRP channels act together and often their effects are overlapping and reveal cross-talk occurs between TRPs and steroid or sterol compounds. In this context, it is important to note that natural and synthetic compounds structurally similar to steroids or have sterol moiety have been termed as "endocrine-disrupters", although their exact mechanisms of actions are unclear (Frye et al., 2012; Testai et al., 2013). The effect of different sterols, steroids, their metabolic intermediates and precursors, and structurally similar compounds on TRP channels strongly suggests that this group of compounds may physically bind to specific regions of TRP channels (most likely in the transmembrane and loop regions) and modulate their functions. A detailed and comparative analysis of the physical interaction, association and dissociation kinetics as well as biological response of these compounds on different TRP channels is required in order to use these compounds as a personalized bio-medicine. However, experimental validation of physical interactions between TRP channels and steroids (also steroid-like molecules), characterization of the binding site/s and subsequent channel modulation is required and will need new experimental and technological approaches. The separation of general homeostatic responses of TRP family members from steroid-specific ones remains a challenge due to difficulties in obtaining an "absolutely steroid-free cell". The generation of reconstituted TRP channels in liposome-based rafts may be a possible solution (Moiseenkova-Bell et al., 2008). *In silico* approach may also minimize the experimental effort and give in-depth theoretical analysis of likely interactions. Recently resolved structures of TRP channels can also be helpful for such *in silico* analysis (Cao et al., 2013; Liao et al., 2013). Never-the-less, advances in understanding of TRP channel-steroid interactions has both basic and clinical implications in the areas of steroid-induced immunosuppression and altered immune functions, steroid-induced osteoporosis (SIOP) and bone remodeling, regulation of pituitary–gonadal axis, reproductive abnormalities, regulation of core body temperature, gender differences in thermoregulation and other sensory processes. Failures/abnormalities in TRP-steroid cross-talk may be behind the development of certain rare diseases and/or syndromes. For example, development of "nephrotic syndrome" characterized by high levels of triglyceride and cholesterol, have been linked with gene variations in TRPC6 (Mir et al., 2012). Similarly, "infantile hypertrophic pyloric stenosis" has been linked to gene variations in TRPC5 and TRPC6 (Everett et al., 2008; Ko et al., 2010). Another example is the disregulation of renal TRPM6/TRPM7 in aldosterone-induced hypertension and kidney damage in hereditary hypomagnesemia (Yogi et al., 2011). Understandings the role of TRPs in these syndromes may give rise to specific treatment policies. (Ciurtin et al., 2010). Indeed, TRPM1 activation by pregnenolone sulfate has also been considered as important for melanocyte function, melanin synthesis, phototransduction, pain modulation, insulin secretion, neuronal development (Harteneck, 2013). Progesterone and TRPs are involved in Ca^{2+} deposition in egg shell which has commercial implication in poultry industry (Bar, 2009). As abnormalities in TRP channel functions and regulation are directly related to development of different diseases and other pathophysiology, these channels are potential pharmacological targets (Kumar et al., 2013). So far a large number of TRP channel-modulatory compounds have been projected and characterized as potential drugs for different pathophysiological conditions (Moran et al., 2011). In this context, understanding of the effect of different steroids and/or steroid-like molecules which can act on specific TRP channels will be of immense interest as potential biomedicines.

Acknowledgments

Intramural support from NISER, Bhubaneswar is acknowledged. AK, SK, RKM, NS, MY and CG wrote the manuscript. The authors declare no conflict of interest.

References

Abed, E. et al., 2009. Expression of transient receptor potential (TRP) channels in human and murine osteoblast-like cells. *Mol. Membr. Biol.* 26, 146–158.
Ahn, C. et al., 2014. Regulation and localization of transient receptor potential melastatin 2 in rat uterus. *Reprod. Sci.* [Epub ahead of print].
Amantini, C. et al., 2004. Distinct thymocyte subsets express the vanilloid receptor VR1 that mediates capsaicin-induced apoptotic cell death. *Cell Death Differ.* 11, 1342–1356.
Avidan, N. et al., 2003. CATSPER2, a human autosomal nonsyndromic male infertility gene. *Eur. J. Hum. Genet.* 11, 497–502.
Baez-Nieto, D. et al., 2011. Thermo-TRP channels: biophysics of polymodal receptors. *Adv. Exp. Med. Biol.* 704, 469–490.
Baldi, E., 2009. Nongenomic activation of spermatozoa by steroid hormones: facts and fictions. *Mol. Cell. Endocrinol.* 308 (1–2), 39–46.
Bar, A., 2009. Calcium transport in strongly calcifying laying birds: mechanisms and regulation. *Comp. Biochem. Physiol. A: Mol. Integr. Physiol.* 152, 447–469.
Basu, S., Srivastava, P., 2005. Immunological role of neuronal receptor vanilloid receptor 1 expressed on dendritic cells. *Proc. Natl. Acad. Sci. U.S.A.* 102, 5120–5125.
Beech, D.J., 2012. Integration of transient receptor potential canonical channels with lipids. *Acta Physiol. (Oxf)* 204, 227–237.
Bernabò, N. et al., 2010a. Role of TRPV1 channels during the acquisition of fertilizing ability in boar spermatozoa. *Vet. Res. Commun.* 34, S5–S8.
Bernabò, N. et al., 2010b. Role of TRPV1 channels in boar spermatozoa acquisition of fertilizing ability. *Mol. Cell. Endocrinol.* 323, 224–231.
Bernucci, L. et al., 2006. Diverse calcium channel types are present in the human placental syncytiotrophoblast basal membrane. *Placenta* 27, 1082–1095.
Berthier, A. et al., 2004. Involvement of a calcium dependent dephosphorylation of BAD associated with the localization of Trpc-1 within lipid rafts in 7-ketocholesterol- induced THP-1 cell apoptosis. *Cell Death Differ.* 11, 897–905.
Bidaux, G. et al., 2005. Evidence for specific TRPM8 expression in human prostate secretory epithelial cells: functional androgen receptor requirement. *Endocr. Relat. Cancer* 12, 367–382.
Boychuk, C.R. et al., 2013. Rapid glucocorticoid-induced activation of TRP and CB1 receptors causes biphasic modulation of glutamate release in gastric-related hypothalamic preautonomic neurons. *Front. Neurosci.* 7, 3.
Calogero, A.E. et al., 2000. Effects of progesterone on sperm function: mechanisms of action. *Hum. Reprod.* 15 (Suppl 1), 28–45.
Cao, E., Liao, M., Cheng, Y., Julius, D., 2013. TRPV1 structures in distinct conformations reveal activation mechanisms. *Nature* 504, 113–118.
Castellano, L.E. et al., 2003. Transient receptor potential (TRPC) channels in human sperm: expression, cellular localization and involvement in the regulation of flagellar motility. *FEBS Lett.* 541, 69–74.
Chamoux, E. et al., 2010. TRPV5 mediates a receptor activator of NF-kappaB (RANK) ligand-induced increase in cytosolic Ca^{2+} in human osteoclasts and down-regulates bone resorption. *J. Biol. Chem.* 285, 25354–25362.
Chen, S.C., Wu, F.S., 2004. Mechanism underlying inhibition of the capsaicin receptor-mediated current by pregnenolone sulfate in rat dorsal root ganglion neurons. *Brain Res.* 1027, 196–200.
Chen, S.C., Chang, T.J., Wu, F.S., 2004. Competitive inhibition of the capsaicin receptor-mediated current by dehydroepiandrosterone in rat dorsal root ganglion neurons. *J. Pharmacol. Exp. Ther.* 311, 529–536.
Chen, X.L. et al., 2007. Testosterone could induce a rapid rise in intracellular free Ca^{2+} concentration through binding to the membrane surface of bone marrow-derived macrophages. *Zhonghua Nan Ke Xue* 13, 784–790.
Chang, A.S. et al., 1997. Concomitant and hormonally regulated expression of trp genes in bovine aortic endothelial cells. *FEBS Lett.* 415, 335–340.
Cheng, H. et al., 2007. TRPM4 controls insulin secretion in pancreatic beta-cells. *Cell Calcium* 41, 51–61.
Cherradi, N., Brandenburger, Y., Capponi, A.M., 1998. Mitochondrial regulation of mineralocorticoid biosynthesis by calcium and the StAR protein. *Eur. J. Endocrinol.* 139, 249–256.
Chodon et al., 2010. Estrogen regulation of TRPM8 expression in breast cancer cells. *BMC Cancer* 10, 212.

Ciurtin, C. et al., 2010. TRPM3 channel stimulated by pregnenolone sulphate in synovial fibroblasts and negatively coupled to hyaluronan. *BMC Musculoskelet. Disord.* 11, 111.

Clapham, D.E., 2003. TRP channels as cellular sensors. *Nature* 426, 517–524.

Colsoul, B., Vennekens, R., Nilius, B., 2011. Transient receptor potential cation channels in pancreatic β cells. *Rev. Physiol. Biochem. Pharmacol.* 161, 87–110.

Compagnone, N.A., Mellon, S.H., 2000. Neurosteroids: biosynthesis and function of these novel neuromodulators. *Front. Neuroendocrinol.* 21, 1–56.

Cooke, B.A., 1999. Signal transduction involving cyclic AMP-dependent and cyclic AMP-independent mechanisms in the control of steroidogenesis. *Mol. Cell. Endocrinol.* 151, 25–35.

Costa, R.R., Varanda, W.A., Franci, C.R., 2010. A calcium-induced calcium release mechanism supports luteinizing hormone-induced testosterone secretion in mouse Leydig cells. *Am. J. Physiol. Cell Physiol.* 299, C316–C323.

Cui, J. et al., 2002. CaT1 contributes to the stores-operated calcium current in Jurkat T-lymphocytes. *J. Biol. Chem.* 277, 47175–47183.

Damann, N. et al., 2009. The calcium-conducting ion channel transient receptor potential canonical 6 is involved in macrophage inflammatory protein-2-induced migration of mouse neutrophils. *Acta Physiol (Oxf).* 195, 3–11.

Davies, E., Kenyon, C.J., Fraser, R., 1985. The role of calcium ions in the mechanism of ACTH stimulation of cortisol synthesis. *Steroids* 45, 551–560.

De Blas, G.A. et al., 2009. TRPM8, a versatile channel in human sperm. *PLoS ONE* 4, e6095.

Dörr, J., Fecher-Trost, C., 2011. TRP channels in female reproductive organs and placenta. *Adv. Exp. Med. Biol.* 704, 909–928.

Dufau, M.L., 1988. Endocrine regulation and communicating functions of the Leydig cell. *Ann. Rev. Physiol.* 50, 483–508.

El Karim, I.A. et al., 2011. Human odontoblasts express functional thermo-sensitive TRP channels: implications for dentin sensitivity. *Pain* 152, 2211–2223.

Er, F. et al., 2009. Impact of dihydrotestosterone on L-type calcium channels in human ventricular cardiomyocytes. *Endocr. Res.* 34, 59–67.

Everett, K.V. et al., 2008. Genome-wide high-density SNP-based linkage analysis of infantile hypertrophic pyloric stenosis identifies loci on chromosomes 11q14-q22 and Xq23. *Am. J. Hum. Genet.* 82, 756–762.

Falkenstein, E. et al., 2000. Multiple actions of steroid hormones–a focus on rapid, nongenomic effects. *Pharmacol. Rev.* 52, 513–556.

Finney-Hayward, T.K. et al., 2010. Expression of transient receptor potential C6 channels in human lung macrophages. *Am. J. Respir. Cell Mol. Biol.* 43, 296–304.

Fonfria, E. et al., 2006. Tissue distribution profiles of the human TRPM cation channel family. *J. Recept. Signal Transduct. Res.* 26, 159–178.

Fonseca, B.M. et al., 2009. Spatio-temporal expression patterns of anandamide-binding receptors in rat implantation sites: evidence for a role of the endocannabinoid system during the period of placental development. *Reprod. Biol. Endocrinol.* 7, 121.

Frye, C.A. et al., 2012. Endocrine disrupters: a review of some sources, effects, and mechanisms of actions on behaviour and neuroendocrine systems. *J. Neuroendocrinol.* 24, 144–159.

Gamberucci, A. et al., 2002. Diacylglycerol activates the influx of extracellular cations in T-lymphocytes independently of intracellular calcium-store depletion and possibly involving endogenous TRP6 gene products. *Biochem. J.* 364, 245–254.

Goswami, C. et al., 2011. Estrogen destabilizes microtubules through an ion-conductivity-independent TRPV1 pathway. *J. Neurochem.* 117, 995–1008.

Grimm, C. et al., 2003. Molecular and functional characterization of the melastatin-related cation channel TRPM3. *J. Biol. Chem.* 278, 21493–21501.

Gronemeyer, H., 1992. Control of transcription activation by steroid hormone receptors. *FASEB J.* 6, 2524–2529.

Gu, Q., Moss, R.L., 1996. 17β-Estradiol potentiates kainate-induced currents via activation of the CAMP cascade. J. Neurosci. 76, 3620–3629.

Hara, Y. et al., 2002. LTRPC2 Ca2+-permeable channel activated by changes in redox status confers susceptibility to cell death. *Mol. Cell* 9, 163–173.

Harteneck, C., 2013. Pregnenolone sulfate: from steroid metabolite to TRP channel ligand. *Molecules* 18, 12012–12028.

Hatzfeld-Charbonnier, A.S. et al., 2007. Influence of heat stress on human monocyte-derived dendritic cell functions with immunotherapeutic potential for antitumor vaccines. *J. Leukoc. Biol.* 81, 1179–1187.

Heath, V., 2011. Reproductive endocrinology: CatSper solves mystery of progesterone action on sperm. *Nat. Rev. Endocrinol.* 7, 316.

Holzer, P., 2011. Transient receptor potential (TRP) channels as drug targets for diseases of the digestive system. *Pharmacol. Ther.* 131, 142–170.

Hsu, Y.J. et al., 2010. Testosterone increases urinary calcium excretion and inhibits expression of renal calcium transport proteins. *Kidney Int.* 77, 601–608.

Inamura, K. et al., 2003. Response to ADP-ribose by activation of TRPM2 in the CRI-G1 insulinoma cell line. *J. Membr. Biol.* 191, 201–207.

Irnaten, M., Blanchard-Gutton, N., Harvey, B.J., 2008. Rapid effects of 17beta-estradiol on epithelial TRPV6 Ca^{2+} channel in human T84 colonic cells. *Cell Calcium* 44, 441–452.

Irnaten, M. et al., 2009. Rapid effects of 17beta-estradiol on TRPV5 epithelial Ca^{2+} channels in rat renal cells. *Steroids* 74, 642–649.

Islam, M.S., 2010. Calcium signaling in the islets. *Adv. Exp. Med. Biol.* 654, 235–259.

Inada, H., Iida, T., Tominaga, M., 2006. Different expression patterns of TRP genes in murine B and T lymphocytes. *Biochem. Biophys. Res. Commun.* 350, 762–767.

Itoh, Y. et al., 2009. An environmental sensor, TRPV4 is a novel regulator of intracellular Ca2+ in human synoviocytes. *Am. J. Physiol. Cell Physiol.* 297, C1082–C1090.

Iwasaki, Y. et al., 2008. TRPA1 agonists–allyl isothiocyanate and cinnamaldehyde–induce adrenaline secretion. *Biosci. Biotechnol. Biochem.* 72, 2608–2614.

Julius, D., 2013. TRP channels and pain. *Annu. Rev. Cell Dev. Biol.* 29, 355–384.

Jung, C. et al., 2009. The progesterone receptor regulates the expression of TRPV4 channel. *Pflugers Arch.* 459, 105–113.

Jungnickel, M.K. et al., 2001. Trp2 regulates entry of Ca^{2+} into mouse sperm triggered by egg ZP3. *Nat. Cell Biol.* 3, 499–502.

Kajiya, H., 2012. Calcium signaling in osteoclast differentiation and bone resorption. *Adv. Exp. Med. Biol.* 740, 917–932.

Karsenty, G., 2012. The mutual dependence between bone and gonads. *J. Endocrinol.* 213, 107–114.

Kawarabayashi, Y. et al., 2012. Critical role of TRPC1-mediated Ca^{2+} entry in decidualization of human endometrial stromal cells. *Mol. Endocrinol.* 26, 846–858.

Khan, K. et al., 2012. [6]-Gingerol induces bone loss in ovary intact adult mice and augments osteoclast function via the transient receptor potential vanilloid 1 channel. *Mol. Nutr. Food Res.* 56, 1860–1873.

Kim, H.J. et al., 2006. Differential expression of uterine calcium transporter 1 and plasma membrane Ca^{2+} ATPase 1b during rat estrous cycle. Am. J. Physiol. Endocrinol. Metab. 291, E234–eE241.

Klose, C. et al., 2011. Fenamates as TRP channel blockers: mefenamic acid selectively blocks TRPM3. *Br. J. Pharmacol.* 162, 1757–1769.

Knippertz, I. et al., 2011. Mild hyperthermia enhances human monocyte-derived dendritic cell functions and offers potential for applications in vaccination strategies. *Int. J. Hyperthermia* 27, 591–603.

Ko, J.S. et al., 2010. A novel DHCR7 mutation in a Smith-Lemli-Opitz syndrome infant presenting with neonatal cholestasis. *J. Korean Med. Sci.* 25, 159–162.

Kochukov, M.Y. et al., 2006. Thermosensitive TRP ion channels mediate cytosolic calcium response in human synoviocytes. *Am. J. Physiol. Cell Physiol.* 291, C424–C432.

Kousteni, S. et al., 2001. Nongenotropic, sex-nonspecific signaling through the estrogen or androgen receptors: dissociation from transcriptional activity. *Cell* 104, 719–730.

Kumar, A., Goswami, L., Goswami, C., 2013. Importance of TRP channels in pain: implications for stress. *Front. Biosci. (Schol. Ed.)* 5, 19–38.

Kumar, P.G., Shoeb, M., 2011. The role of trp ion channels in testicular function. *Adv. Exp. Med. Biol.* 704, 881–908.

Kunert-Keil, C. et al., 2006. Tissue-specific expression of TRP channel genes in the mouse and its variation in three different mouse strains. *BMC Genomics* 7, 159.

Lambert, S. et al., 2011. Transient receptor potential melastatin 1 (TRPM1) is an ion-conducting plasma membrane channel inhibited by zinc ions. *J. Biol. Chem.* 286, 12221–12233.

Lange, I. et al., 2009. TRPM2 functions as a lysosomal Ca^{2+}-release channel in beta cells. *Sci. Signal* 2, ra23.

Lee, G.S., Jeung, E.B., 2007. Uterine TRPV6 expression during the estrous cycle and pregnancy in a mouse model. *Am. J. Physiol. Endocrinol. Metab.* 293, E132–E138.

Lee et al., 2009. Uterine and placental expression of TRPV6 gene is regulated via progesterone receptor- or estrogen receptor-mediated pathways during pregnancy in rodents. *Reprod. Biol. Endocrinol.* 7, 49.

Lee, J.H. et al., 2011. Effects of L- and T-type Ca^{2+} channel blockers on spermatogenesis and steroidogenesis in the prepubertal mouse testis. *J. Assist. Reprod. Genet.* 28, 23–30.

Lee, K.H. et al., 2010a. Pregnenolone sulfate enhances spontaneous glutamate release by inducing presynaptic Ca^{2+}-induced Ca^{2+} release. *Neuroscience* 171, 106–116.

Lee, J.H. et al., 2010b. Inhibitory actions of mibefradil on steroidogenesis in mouse Leydig cells: involvement of Ca^{2+} entry via the T-type Ca^{2+} channel. *Asian J. Androl.* 12, 807–813.

Liao, M., Cao, E., Julius, D., Cheng, Y., 2013. Structure of the TRPV1 ion channel determined by electron cryo-microscopy. *Nature* 504, 107–112.

Lieben, L., Carmeliet, G., 2012. The involvement of TRP channels in bone homeostasis. *Front. Endocrinol. (Lausanne)* 3, 99.

Link, T.M. et al., 2010. TRPV2 has a pivotal role in macrophage particle binding and phagocytosis. *Nat. Immunol.* 11, 232–239.

Lishko, P.V., Botchkina, I.L., Kirichok, Y., 2011. Progesterone activates the principal Ca^{2+} channel of human sperm. *Nature* 471, 387–391.

Majeed, Y. et al., 2011. Stereo-selective inhibition of transient receptor potential TRPC5 cation channels by neuroactive steroids. *Br. J. Pharmacol.* 162, 1509–1520.

Majeed, Y. et al., 2012. Pregnenolone sulphate-independent inhibition of TRPM3 channels by progesterone. *Cell Calcium* 51, 1–11.

Majhi, R.K. et al., 2013. Thermosensitive ion channel TRPV1 is endogenously expressed in the sperm of a fresh water teleost fish (Labeo rohita) and regulates sperm motility. *Channels (Austin)* 7.

Majhi, R.K., 2014. Sperm specific expression of temperature-sensitive ion channel TRPM8 correlates with vertebrate evolution. In: *Peer J. PrePrints* 2, e440v1.

Marigo, V. et al., 2009. TRPM4 impacts on Ca^{2+} signals during agonist-induced insulin secretion in pancreatic beta-cells. *Mol. Cell. Endocrinol.* 299, 194–203.

Martínez-López, P. et al., 2011. TRPM8 in mouse sperm detects temperature changes and may influence the acrosome reaction. *J. Cell. Physiol.* 226, 1620–1631.

Masuyama, R. et al., 2012. Calcium/calmodulin-signaling supports TRPV4 activation in osteoclasts and regulates bone mass. *J. Bone Miner. Res.* 27, 1708–1721.

Masuyama, R. et al., 2008. TRPV4-mediated calcium influx regulates terminal differentiation of osteoclasts. *Cell Metab.* 8, 257–265.

Miehe, S. et al., 2012. Inhibition of diacylglycerol-sensitive TRPC channels by synthetic and natural steroids. *PLoS ONE* 7, e35393.
Minke, B., 1977. Drosophila mutant with a transducer defect. *Biophys. Struct. Mech.* 3, 59–64.
Mir, S. et al., 2012. TRPC6 gene variants in Turkish children with steroid-resistant nephrotic syndrome. *Nephrol. Dial. Transplant.* 27, 205–209.
Mizoguchi, F. et al., 2008. Transient receptor potential vanilloid 4 deficiency suppresses unloading-induced bone loss. *J. Cell. Physiol.* 216, 47–53.
Moiseenkova-Bell, V.Y. et al., 2008. Structure of TRPV1 channel revealed by electron cryomicroscopy. *Proc. Natl. Acad. Sci. U.S.A.* 105, 7451–7455.
Montell, C. et al., 1985. Rescue of the Drosophila phototransduction mutation trp by germline transformation. *Science* 230, 1040–1043.
Moran, M.M. et al., 2011. Transient receptor potential channels as therapeutic targets. *Nat. Rev. Drug Discov.* 10, 601–620.
Moreau, R. et al., 2002a. Calcium uptake and calcium transporter expression by trophoblast cells from human term placenta. *Biochim. Biophys. Acta* 1564, 325–332.
Moreau, R. et al., 2002b. Expression of calcium channels along the differentiation of cultured trophoblast cells from human term placenta. *Biol. Reprod.* 67, 1473–1479.
Morimoto, S. et al., 2010. Sex steroids effects on the endocrine pancreas. *J. Steroid Biochem. Mol. Biol.* 122, 107–113.
Muramatsu, S. et al., 2007. Functional gene screening system identified TRPV4 as a regulator of chondrogenic differentiation. *J. Biol. Chem.* 282, 32158–32167.
Nagasawa, M., Kojima, I., 2012. Translocation of calcium permeable TRPV2 channel to the podosome: Its role in the regulation of podosome assembly. *Cell Calcium* 51, 186–193.
Nagasawa, M. et al., 2007. Chemotactic peptide fMetLeuPhe induces translocation of the TRPV2 channel in macrophages. *J. Cell. Physiol.* 210, 692–702.
Nilius, B. et al., 2007. Transient receptor potential cation channels in disease. *Physiol. Rev.* 87, 165–217.
Nilius, B., Owsianik, G., 2011. The transient receptor potential family of ion channels. *Genome Biol.* 12, 218.
Nilius, B., Voets, T., 2008. A TRP channel-steroid marriage. *Nat. Cell Biol.* 10, 1383–1384.
Numazaki, M., Tominaga, M., 2004. Nociception and TRP Channels. *Curr. Drug Targets CNS Neurol. Disord.* 3, 479–485.
Obukhov, A.G., Nowycky, M.C., 2002. TRPC4 can be activated by G-protein-coupled receptors and provides sufficient Ca^{2+} to trigger exocytosis in neuroendocrine cells. *J. Biol. Chem.* 277, 16172–16178.
Ong, E.C. et al., 2013. A TRPC1 protein-dependent pathway regulates osteoclast formation and function. *J. Biol. Chem.* 288, 22219–22232.
Peng, J.B., Brown, E.M., Hediger, M.A., 2003. Epithelial Ca^{2+} entry channels: transcellular Ca^{2+} transport and beyond. *J. Physiol.* 551, 729–740.
Phan, M.N. et al., 2009. Functional characterization of TRPV4 as an osmotically sensitive ion channel in porcine articular chondrocytes. *Arthritis Rheum.* 60, 3028–3037.
Philipp, S. et al., 2003. TRPC3 mediates T-cell receptor-dependent calcium entry in human T-lymphocytes. *J. Biol. Chem.* 278, 26629–26638.
Philipp, S. et al., 2000. TRP4 (CCE1) protein is part of native calcium release-activated Ca^{2+}-like channels in adrenal cells. *J. Biol. Chem.* 275, 23965–23972.
Publicover, S., Barratt, C., 2011. Reproductive biology: Progesterone's gateway into sperm. *Nature* 471, 313–314.
Qian, F. et al., 2002. TRP genes: candidates for nonselective cation channels and store-operated channels in insulin-secreting cells. *Diabetes* 51 (Suppl 1), S183–S189.
Rao, G.K., Kaminski, N.E., 2006. Induction of intracellular calcium elevation by Delta9-tetrahydrocannabinol in T cells involves TRPC1 channels. *J. Leukoc. Biol.* 79, 202–213.
Rossier, M.F., 2006. T channels and steroid biosynthesis: in search of a link with mitochondria. *Cell Calcium* 40, 155–164.
Saunders, C.I. et al., 2007. Expression of transient receptor potential vanilloid 1 (TRPV1) and 2 (TRPV2) in human peripheral blood. *Mol. Immunol.* 44, 1429–1435.
Saunders, C.I., Fassett, R.G., Geraghty, D.P., 2009. Up-regulation of TRPV1 in mononuclear cells of end-stage kidney disease patients increases susceptibility to N-arachidonoyl-dopamine (NADA)-induced cell death. *Biochim. Biophys. Acta* 1792, 1019–1026.
Schilling, T., Eder, C., 2009. Non-selective cation channel activity is required for lysophosphatidylcholine-induced monocyte migration. *J. Cell. Physiol.* 221, 325–334.
Scragg, J.L., Dallas, M.L., Peers, C., 2007. Molecular requirements for L-type Ca^{2+}-channel blockade by testosterone. *Cell Calcium* 42, 11–15.
Serafini, N. et al., 2012. The TRPM4 channel controls monocyte and macrophage, but not neutrophil, function for survival in sepsis. *J. Immunol.* 189, 3689–3699.
Seyrek, M. et al., 2007. Testosterone relaxes isolated human radial artery by potassium channel opening action. *J. Pharmacol. Sci.* 103, 309–316.
Sossey-Alaoui, K. et al., 1999. Molecular cloning and characterization of TRPC5 (HTRP5), the human homologue of a mouse brain receptor-activated capacitative Ca^{2+} entry channel. *Genomics* 60, 330–340.
Strünker, T. et al., 2011. The CatSper channel mediates progesterone-induced Ca^{2+} influx in human sperm. *Nature* 471, 382–386.
Stumpf, T. et al., 2008. The human TRPV6 channel protein is associated with cyclophilin B in human placenta. *J. Biol. Chem.* 283, 18086–18098.
Szöllősi, A.G. et al., 2013. Transient receptor potential vanilloid-2 mediates the effects of transient heat shock on endocytosis of human monocyte-derived dendritic cells. *FEBS Lett.* 587, 1440–1445.
Takezawa, R. et al., 2006. A pyrazole derivative potently inhibits lymphocyte Ca^{2+} influx and cytokine production by facilitating transient receptor potential melastatin 4 channel activity. *Mol. Pharmacol.* 69, 1413–1420.
Talavera, K., Nilius, B., Voets, T., 2008. Neuronal TRP channels: thermometers, pathfinders and life-savers. *Trends Neurosci.* 31, 287–295.
Tano, J.Y. et al., 2011. Impairment of survival signaling and efferocytosis in TRPC3-deficient macrophages. *Biochem. Biophys. Res. Commun.* 410, 643–647.
Tesfai, Y., Brereton, H.M., Barritt, G.J., 2001. A diacylglycerol-activated Ca^{2+} channel in PC12 cells (an adrenal chromaffin cell line) correlates with expression of the TRP-6 (transient receptor potential) protein. *Biochem. J.* 358, 717–726.
Testai, E. et al., 2013. A plea for risk assessment of endocrine disrupting chemicals. *Toxicology* 314, 51–59.
Togashi, K. et al., 2006. TRPM2 activation by cyclic ADP-ribose at body temperature is involved in insulin secretion. *EMBO J.* 25, 1804–1815.
Togashi, K., Inada, H., Tominaga, M., 2008. Inhibition of the transient receptor potential cation channel TRPM2 by 2-aminoethoxydiphenyl borate (2-APB). *Br. J. Pharmacol.* 153, 1324–1330.
Trevino, C.L. et al., 2001. Identification of mouse trp homologs and lipid rafts from spermatogenic cells and sperm. *FEBS Lett.* 509, 119–125.
Trevisan, G. et al., 2012. Identification of the plant steroid α-spinasterol as a novel transient receptor potential vanilloid 1 antagonist with antinociceptive properties. *J. Pharmacol. Exp. Ther.* 343, 258–269.
Tsumura, M. et al., 2013. Functional expression of TRPM8 and TRPA1 channels in rat odontoblasts. *PLoS ONE* 8, e82233.
Tutuncu, S., Özfiliz, N., 2010. Distribution of the vanilloid (capsaicin) receptor type 1 in the capsaicin treated rat ovaries on different sexual development periods. Revue de Médecine Vétérinaire 6, 272–276.
Uchida, K., Tominaga, M., 2011. The role of thermosensitive TRP (transient receptor potential) channels in insulin secretion. *Endocr. J.* 58, 1021–1028.
Unemoto, T. et al., 2007. Role of BK channels in testosterone-induced relaxation of the aorta in spontaneously hypertensive rats. *Biol. Pharm. Bull.* 30, 1477–1480.
Van Abel, M. et al., 2002. 1,25-Dihydroxyvitamin D3-independent stimulatory effect of estrogen on the expression of ECaC1 in the kidney. *J. Am. Soc. Nephrol.* 13, 2102–2109.
Van Abel, M. et al., 2003. Regulation of the epithelial Ca2+ channels in small intestine as studied by quantitative mRNA detection. *Am. J. Physiol. Gastrointest. Liver Physiol.* 285, G78–G85.
Vasil'eva, I.O. et al., 2008. TRPV5 and TRPV6 calcium channels in human T cells. *Tsitologiia* 50, 953–957.
Vig, M., Kinet, J.P., 2009. Calcium signaling in immune cells. *Nat. Immunol.* 10, 21–27.
Wagner, T.F. et al., 2008. Transient receptor potential M3 channels are ionotropic steroid receptors in pancreatic beta cells. *Nat. Cell Biol.* 10, 1421–1430.
Watnick, T.J. et al., 2003. A flagellar polycystin-2 homolog required for male fertility in Drosophila. *Curr. Biol.* 13, 2179–2184.
Wenning, A.S. et al., 2011. TRP expression pattern and the functional importance of TRPC3 in primary human T-cells. *Biochim. Biophys. Acta* 1813, 412–423.
Wissenbach, U. et al., 2001. Expression of CaT-like, a novel calcium-selective channel, correlates with the malignancy of prostate cancer. *J. Biol. Chem.* 276, 19461–19468.
Wissenbach, U. et al., 1998. Structure and mRNA expression of a bovine trp homologue related to mammalian trp2 transcripts. *FEBS Lett.* 429, 61–66.
Wu, S.N., Wu, P.Y., Tsai, M.L., 2011. Characterization of TRPM8-like channels activated by the cooling agent icilin in the macrophage cell line RAW 264.7. *J. Membr. Biol.* 241, 11–20.
Xi, S.C. et al., 2000. Potential involvement of mt1 receptor and attenuated sex steroid-induced calcium influx in the direct anti-proliferative action of melatonin on androgen-responsive LNCaP human prostate cancer cells. *J. Pineal Res.* 29, 172–183.
Xu, X.Z., Sternberg, P.W., 2003. A *C. elegans* sperm TRP protein required for sperm-egg interactions during fertilization. *Cell* 114, 285–297.
Xu, S. et al., 2008. 17beta-estradiol activates estrogen receptor beta-signalling and inhibits transient receptor potential vanilloid receptor 1 activation by capsaicin in adult rat nociceptor neurons. *Endocrinology* 149, 5540–5548.
Yamashiro, K. et al., 2010. Role of transient receptor potential vanilloid 2 in LPS-induced cytokine production in macrophages. *Biochem. Biophys. Res. Commun.* 398, 284–289.
Yan, T. et al., 2007. Estrogen amplifies pain responses to uterine cervical distension in rats by altering transient receptor potential-1 function. *Anesth. Analg.* 104, 1246–1250.
Yogi, A. et al., 2013. Aldosterone signaling through transient receptor potential melastatin 7 cation channel (TRPM7) and its α-kinase domain. *Cell. Signal.* 25, 2163–2175.
Yogi, A. et al., 2011. Dysregulation of renal transient receptor potential melastatin 6/7 but not paracellin-1 in aldosterone-induced hypertension and kidney damage in a model of hereditary hypomagnesemia. *J. Hypertens.* 29, 1400–1410.
Yue, L. et al., 2001. CaT1 manifests the pore properties of the calcium-release-activated calcium channel. *Nature* 410, 705–709.
Zamudio-Bulcock, P.A. et al., 2011. Activation of steroid-sensitive TRPM3 channels potentiates glutamatergic transmission at cerebellar Purkinje neurons from developing rats. *J. Neurochem.* 119, 474–485.

Zamudio-Bulcock, P.A., Valenzuela, C.F., 2011. Pregnenolone sulfate increases glutamate release at neonatal climbing fiber-to-Purkinje cell synapses. *Neuroscience* 175, 24–36.

Zhang, L., Barritt, G.J., 2004. Evidence that TRPM8 is an androgen-dependent Ca2+channel required for the survival of prostate cancer cells. *Cancer Res.* 64, 8365–8373.

Zhao, Z. et al., 2012. Increased migration of monocytes in essential hypertension is associated with increased transient receptor potential channel canonical type 3 channels. *PLoS ONE* 7, 32628.

Zhu, S. et al., 2014. Involvement of transient receptor potential melastatin-8 (TRPM8) in menthol-induced calcium entry, reactive oxygen species production and cell death in rheumatoid arthritis rat synovial fibroblasts. *Eur. J. Pharmacol.* 725, 1–9.

Biochemical and Biophysical Research Communications 456 (2015) 312–319

Contents lists available at ScienceDirect

Biochemical and Biophysical Research Communications

journal homepage: www.elsevier.com/locate/ybbrc

Influence of membrane cholesterol in the molecular evolution and functional regulation of TRPV4

Shikha Kumari [a,1], Ashutosh Kumar [a,1], Puspendu Sardar [a,1], Manoj Yadav [a], Rakesh Kumar Majhi [a], Abhishek Kumar [b], Chandan Goswami [a,*]

[a] National Institute of Science Education and Research, Bhubaneswar, Orissa, India
[b] Abteilung für Botanische Genetik und Molekularbiologie, Botanisches Institut und Botanischer Garten, Christian-Albrechts-Universität zu Kiel, Kiel, Germany

ARTICLE INFO

Article history:
Received 5 November 2014
Available online 28 November 2014

Keywords:
Gain-of-function mutations
Channelopathy
Steroids
Molecular evolution
CRAC-motif
Pain

ABSTRACT

TRPV4 is involved in several physiological and sensory functions as well as with several diseases and genetic disorders, though the molecular mechanisms for these are unclear. In this work we have analyzed molecular evolution and structure–function relationship of TRPV4 using sequences from different species. TRPV4 has evolved during early vertebrate origin (450 million years). Synteny analysis confirms that TRPV4 has coevolved with two enzymes involved in sterol biosynthesis, namely MVK and GLTP. Cholesterol-recognizing motifs are present within highly conserved TM4–Loop4–TM5 region of TRPV4. TRPV4 is present in lipid raft where it co-localizes with Caveolin1 and Filipin. TM4–Loop4–TM5 region as well as Loop4 alone can physically interact with cholesterol, its precursor mevalonate and derivatives such as stigmasterol and aldosterone. Mobility of TRPV4-GFP depends on membrane cholesterol level. Molecular evolution of TRPV4 shared striking parallelism with the cholesterol bio-synthesis pathways at the genetic, molecular and metabolic levels. We conclude that interaction with sterols and cholesterol-dependent membrane dynamics have influence on TRPV4 function. These results may have importance on TRPV4-medaited cellular functions and pathophysiology.

1. Introduction

TRPs represent a group of non-selective channels that are permeable to different cations. Among all, TRPV4 is unique as it is activated by several physical and chemical stimuli such as temperature, mechanical pressure, osmolarity, infrared, and compounds like vanilloids, 4αPDD, Apigenin, dimethylallyl pyrophosphate and PUFAs [1–4]. A common aspect of TRPV4-specific agonists is their high hydrophobicity, suggesting that these compounds primarily act on the transmembrane regions. Membrane deformation by stretch too causes rapid activation of TRPV4 [5]. All these suggest that TRPV4 function is dependent on the biochemical composition, structure and by the biophysical nature of the membrane. TRPV4 is specifically present in the cholesterol-enriched detergent-resistant membrane fraction (lipid raft) [6]. At the molecular level, TRPV4 forms signaling complex, which includes membranous components and sub-membranous cytoskeleton [7]. Such complexes are critical for proper function and regulation.

TRPV4 is present in several animals and is involved in detection of different physical and chemical stimuli. The primary function of TRPV4 remains conserved across different species. For example, hTRPV4 (but not hTRPV1) can rescue the defects in transduction of osmotic and mechanical stimuli in *osm-9* (but not *ocr-2*) mutants in *Caenorhabditis elegans* and low sequence similarities between hTRPV4 with *osm-9* suggests that smaller regions are sufficient to perform key tasks [8,9]. TRPV4-mediated sensory functions significantly contribute to the natural selection in specific habitats which favor organism's survival as fittest. Therefore, TRPV4 might have influence on the adaptation, speciation and evolution of different species, especially in response to certain selection pressure where the above mentioned sensory processes are involved. Indeed, TRPV4 can regulate certain behaviors that are linked with adaptation [8]. In this work we tested the molecular evolution of TRPV4 *per se*. TRPV4 physically interacts with sterols and some of its functions are dependent on availability of the cholesterol. We demonstrate that molecular evolution of TRPV4 has

* Corresponding author.
E-mail address: chandan@niser.ac.in (C. Goswami).
[1] Equal contributions.

http://dx.doi.org/10.1016/j.bbrc.2014.11.077
0006-291X/

been influenced by the cholesterol-biosynthesis pathway, an unexpected finding that may also explain the molecular mechanism of TRPV4.

2. Materials and methods

2.1. Sequence retrieval and protein sequence analysis

All TRPV4 sequences were retrieved either from Ensembl or NCBI database (provided in Tab:S1). These protein sequences were aligned by using MUSCLE alignment tool with its default parameters within MEGA5 software suite. Histone H4 and Cytochrome C sequences were retrieved from ENSEMBL and NCBI databases as described previously [10].

2.2. Fragmentation of TRPV4 into different domains and motifs

Conservation of different domains and motifs of TRPV4 were analyzed separately (Table 1). In all cases, we used the hTRPV4 sequence (ENSP00000261740) as template. MUSCLE software was used to align and find out the respective regions present in other species. Distance Matrix generation and the statistical tests using "R" software was done as described before [10].

2.3. Phylogenetic analysis

MUSCLE alignment program was used to align the amino acid sequences for the purpose of phylogenetic analysis. The Bayesian phylogenetic tree was constructed by the Bayesian approach (5 runs, 7,500,000 generations, 25% burn-in-period, WAG-matrix-based model in the MrBayes 3.2 program.

2.4. Calculation of evolutionary time

The sequences among different classes were compared and number of changes of amino acids/100 amino acids was calculated by comparing birds with reptiles, fish with reptiles and reptiles with mammals for available TRPV1 and TRPV4 sequences. The hTRPV is considered as the most recent one (considered as 0 MY). The average changes were calculated and radiations of mammalian TRPV4 sequences were plotted against million years.

Table 1
Description of different domains and motifs.

Region	Location (amino acid number)	References
N-terminal	1–470	[9]
C-Terminal	732–871	[9]
Ank-1	149–189	[11,12]
Ank-2	190–236	[11,12]
Ank-3	237–283	[11,12]
Ank-4	284–319	[11,12]
Ank-5	320–368	[11,12]
Ank-6	369–396	[11,12]
TM-1	471–488	[9]
Loop-1	489–512	[9]
TM-2	513–530	[9]
Loop-2	531–550	[9]
TM-3	551–575	[9]
Loop-3	576–579	[9]
TM-4	580–597	[9]
Loop-4	598–614	[9]
Cholesterol binding domain	610–626	[13]
TM-5	615–632	[9]
Loop-5	633–665	[9]
Pore region	666–683	[9]
Loop-6	684–694	[9]
TM-6	695–731	[9]
TRP-box	732–737	[14]
Cam	812–831	[15]

2.5. Synteny analysis

We utilized Ensembl genome browser for building synteny of TRPV4 loci from selected vertebrate genomes. We examined *Xenopus tropicalis* genome using JGI genome browser.

2.6. Cell culture and cholesterol reduction/depletion

F11 cells were grown in Ham's F12 media supplemented with 10% FBS (HiMedia) as described before [7]. For cholesterol depletion/reduction, cells were maintained in serum-free media for 24 h and 1 μM pravastatin (Sigma–Aldrich) was added 12 h before cell fixing by 4% PFA. In certain cases βMCD (5 mM) (Sigma–Aldrich) was added to reduce membrane cholesterol 15 min before fixing or performing FRAP experiments.

2.7. Caveolin1 and Filipin staining

Cells were seeded into a 24 well plate and TRPV4-GFP was expressed as described before [7]. Cells were fixed 36 h after transfection and immunostained with mouse monoclonal anti-Caveolin-1 antibody (Sigma–Aldrich; 1:250) and subsequently with anti-mouse Alexa-fluor-594-conjugated secondary antibody (1:500). For visualization of the cholesterol directly, fixed cells were probed by Flilipin (Sigma–Aldrich). Cells were imaged by confocal microscope (LSM780, Zeiss) with a 63× oil immersion objective (1.4 NA). Images were processed using LSM software (Zeiss) and Adobe Photoshop.

2.8. FRAP

F11 cells were grown on a glass coverslip and hTRPV4-GFP was expressed by transient transfection. Around 36 h after transfection, the cells were used for FRAP experiments. In each case, at least 50 ROI values are measured.

2.9. Cloning of hTRPV4 fragments, protein expression-purification and dot-blot assay

Different regions of hTRPV4 were cloned into the BamHI and SalI site of pGEX-6P1 vector, expressed in *Escherichia coli* by IPTG induction and purified further. The purified proteins were normalized for molar concentrations and used for blot-overlay experiments with mevalonate, cholesterol, stigmasterol and aldosterone (Sigma Aldrich and Avantipolar).

3. Results

3.1. TRPV4 has evolved during Silurian era

We reconstructed the phylogenetic history of vertebrate TRPV4 using Bayesian phylogenetic method (Fig. 1A). TRPV4-mediated functions in *C. elegans* can be rescued by hTRPV4, suggesting that certain functional features of TRPV4 are conserved throughout the evolution [16]. However, hTRPV4 protein shares less identity (~20%) and homology (~36%) with Osm9 (TRPV4 homologue in *C. elegans*). Similarly, NAN (homologue from *Drosophila*) also shares less homology with hTRPV4. Invertebrate homologues show several insertions and deletions (indels) (Fig:S1). In contrast, TRPV4 sequences are well conserved in vertebrates (Fig. 1A). TRPV4 protein from human and zebrafish share 68% identity and 79% homology. Notably, frog genome have six copies (named as TRPV4a–f) sharing more than 70% identity with each other and these paralogs are branched out separately from TRPV4 orthologs (TRPV4a) in Bayesian phylogenic tree (Fig. 1A). Our analysis suggests that

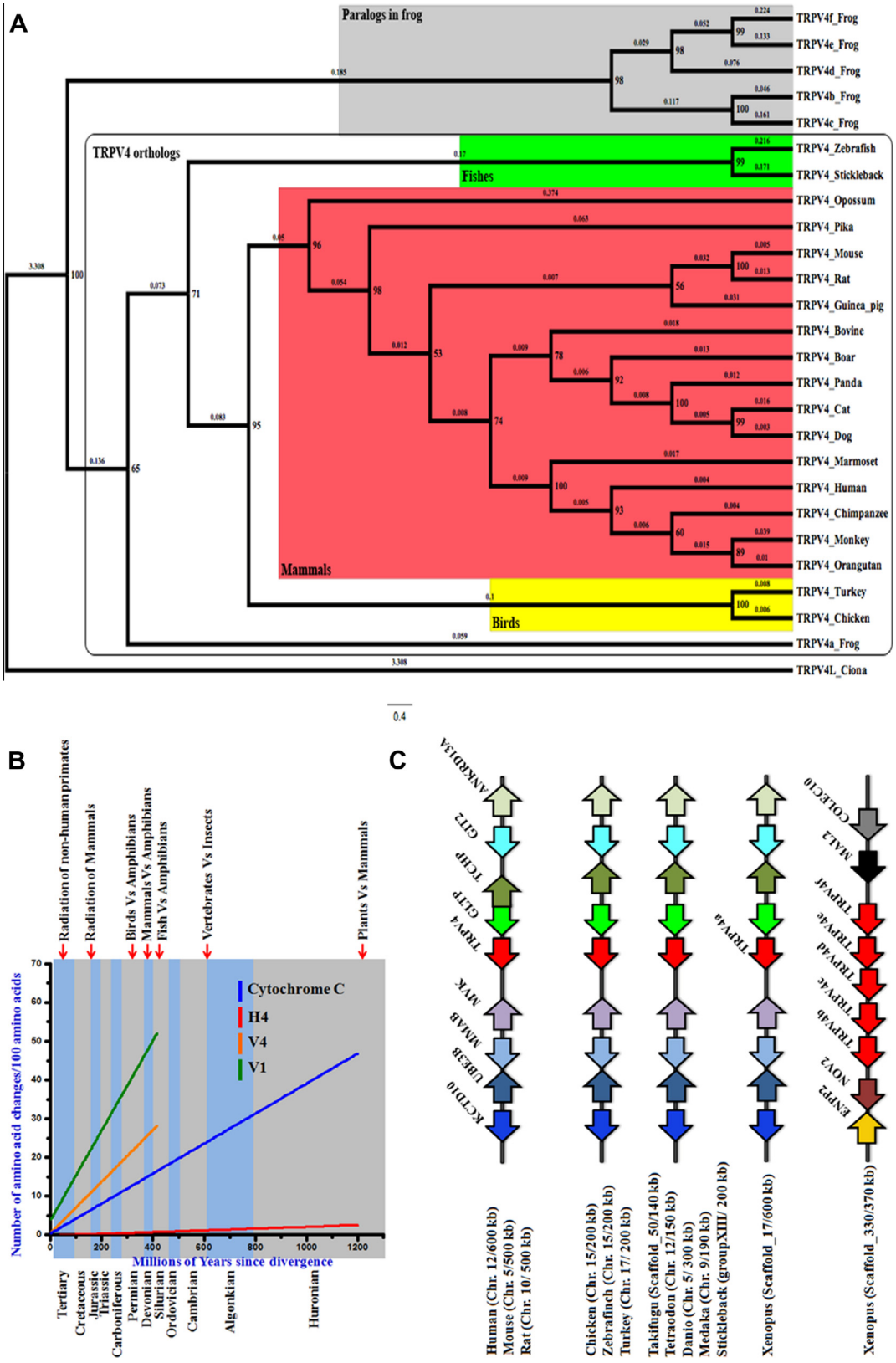

Fig. 1. Molecular evolution of TRPV4. (A) Bayesian phylogenetic tree illustrates six duplicates of TRPV4 in frogs (one ortholog: TRPV4a and five paralogs: TRPV4b–f, indicated in gray) while a single copy is maintained in other vertebrates (mammals: red; birds: yellow, fishes: green). This tree was generated using MrBayes 3.2 and the percentage posterior probabilities are marked at the node of the branches while mean branch length is marked in decimal on the respective branch. Putative TRPV4-like (TRPV4L) gene (gw1.02q.1264.1) from *Ciona intestinalis* served as "out-group-control". (B) Conservation analysis of TRPV4. Histone-H4, Cytochrome-C and TRPV1 were used as controls. (C) Two genes (MVK and GLTP) involved in cholesterol biosynthesis pathway have coevolved with TRPV4. This locus has maintained its organization since development of vertebrates (450 MYA). Another locus in *Xenopus* contains five paralogous TRPV4 originated by tandem duplication. (For interpretation of the references to color in this figure legend, the reader is referred to the web version of this article.)

TRPV4 share high homology and identity during vertebrate evolution.

Next we calculated the changes in the number of amino acids per 100 amino acids in full-length TRPV4 from different species [10]. We excluded the sequences from nematode and insects (~36% and ~33% homology with hTRPV4 respectively) due to low sequence homology. TRPV4 has originated at point of vertebrate emergence; ca 450 MYA (during the transition of Silurian from Devonian era) (Fig. 1B). TRPV4 is less conserved than histone-H4 (highly conserved) and Cytochrome-C (semi-conserved) [10]. Similar comparison indicates that TRPV1 and TRPV4 have been selected via different selection pressure during vertebrate evolution (Fig. 1B) [10].

3.2. TRPV4 and cholesterol biosynthesis pathway have coevolved

We analyzed syntenic organization in different vertebrate genomes. TRPV4 and mevalonate kinase (MVK) genes are clustered into head-to-head orientation flanked by triad of potassium channel tetramerization domain containing 10 (KCTD10), ubiquitin protein ligase E3B (UBE3B) and methylmalonic aciduria (cobalamin deficiency) cblB type (MMAB) on one side and a tetrad of glycolipid transfer protein (GLTP), trichoplein, keratin filament binding (TCHP), G-protein-coupled receptor kinase interacting ArfGAP 2 (GIT2) and ankyrin repeat domain 13A (ANKRD13A) in human (chr12/600 kb) (Fig. 1C). This genomic architecture is conserved in mammals (mouse: chr5/500 kb; rat: chr10/500 kb); in birds (chicken: chr15/200 kb; zebrafinch: chr15/200 kb; turkey: chr17/200 kb); in fishes (*Takifugu*: scaffold_50/140 kb, *Tetraodon*: chr12/150 kb, *Danio*: chr5/300 kb, Medaka: chr9/190 kb, Stickleback: group_XIII/200 kb), in amphibians (*Xenopus*: scaffold_17/600 kb with single TRPV4 i.e. TRPV4a). However, there is another cluster in frogs (scaffold_330/370 kb containing five paralogous (TRPV4b–f), flanked by a diad of ectonucleotide pyrophosphatase/phosphodiesterase 2 (ENPP2) and nephroblastoma overexpressed gene 2 (NOV2) in one side and a diad of T-cell differentiation protein 2 (MAL2) and C-type lectin, collectin sub-family member 10 (COLEC10) on the other side. Noteworthy point of this analysis is that TRPV4 is located between two genes (MVK and GLTP) involved in cholesterol biosynthesis and this synteny is maintained throughout vertebrate evolution (since 450 MY).

3.3. Different regions of TRPV4 have evolved through different selection pressure

To test the conservation of TRPV4 throughout the evolution, we have compared the sequences from different vertebrates and used statistical approach to quantify it. Analysis revealed that TRPV4 is conserved throughout vertebrate evolution ($p \leqslant 0.0001$; 17 species) (Fig. 2A). We compared separately the conservation of different domains, motifs and functional regions present in TRPV4 (Table 1) [9,11–15]. This reveals that functionally and structurally important regions of TRPV4 are conserved, though at different levels (Fig. 2A). Among all, Loop3, TM4, Loop4, TM5 and TRP-box reveal maximum conservation. Among all TM, the TM4 and TM5 are more conserved. The TM4 reveals highest conservation indicating the importance of this region in the channel function. The TM2 is the least conserved indicating that TM4 and TM5 regions are more important for the functional purpose. Among all ankyrin repeat domains, ARD3 is most and ARD1 is least conserved. Our results are in agreement with another report suggesting that the TM regions are conserved [17]. This result fits well with the identification of several deleterious mutations that are located in two regions, namely within the ARD3 and TM4–Loop4–TM5 of hTRPV4 [18]. In this regard, F592L, R594H, F596P, G600W, Y602C, I604M, R616Q, F617L, L618P, V620I, and M625I are important as these mutations cause pathophysiological disorders corroborating the importance of TM4–Loop–TM5 region (where all these mutations are clustered) of TRPV4 [19].

3.4. TM4–Loop4-TM5 of TRPV4 contains cholesterol recognition motifs

Since AA 576–632 is highly conserved in all vertebrates, we explored the significance of this region. As this region mainly represent the membrane-spanning helices and loops, we predicted that this region might be involved in interaction with lipids present in the membrane and/or involved in channel function such as channel gating. Indeed, this region contains sequence (KDLFRFLL, in hTRPV4) that represent a cholesterol-binding CRAC-like motif (L/V-$X_{(1-5)}$-Y-$X_{(1-5)}$-K/R) and spanning through Loop4–TM5 region (Y is replaced by F) [20]. This motif is conserved strictly in all other species including all 6 variants of *Xenopus* TRPV4 and thus suggest for a positive selection (Fig. 2B and C, Fig:S2). The motif present in the TM4-Loop4-TM5 of TRPV4 matches well with the reported CRAC-like motif present in TRPV1 in inverted order [13]. Similarly, there is an inverted CRAC-motif (LTGTYSIMIQK) present in the TM4-Loop4 (upstream of the CRAC-like motif) which is highly conserved in all vertebrates.

3.5. TRPV4 is present in the cholesterol enriched lipid rafts

We expressed hTRPV4-GFP in F11 cells and stained for lipid raft markers. We noted that TRPV4 co-localizes with Caveolin-1 (Fig. 3A). However, after cholesterol depletion by βMCD, or by Pravastatin only (8 h) or by both, Caveolin-1 as well as TRPV4 reveal altered distribution, membrane clustering and much lesser colocalization (not shown). Still, some of the TRPV4 clusters remain intact and colocalized with Caveolin1. This indicates that TRPV4-enriched clusters can retain some cholesterol and resist complete cholesterol depletion in certain patches (data not shown). To confirm these results by another independent manner, we stained hTRPV4-GFP expressing cells with Flilipin, which directly detect cholesterol. We observed colocalization of TRPV4-GFP with Flilipin (Fig. 3B). Similarly, reduction of membrane cholesterol by βMCD and/or by Pravastatin (long-term treatment) results in low or no colocalization at all (Fig. 3B).

3.6. Loop4 alone or along with nearby helices is sufficient for physical interaction with cholesterol, its precursors and derivatives

To test, if the CRAC- and CRAC-like motifs present in the TM4–Loop4–TM5 of TRPV4 indeed interact with cholesterol, we expressed these sequences as different GST-tagged proteins and purified further (Fig. 4A and B). Using blot overlay, we explored if Loop4 alone or in combination with TM4 and/or TM5 can interact with cholesterol. We noted that Loop4 only is sufficient to interact with cholesterol, its precursor (mevalonate) and other cholesterol derivatives (like stigmasterol; steroid hormone aldosterone) (Fig. 4C). Similarly, TM4–Loop4, Loop4–TM5 and TM4–Loop4–TM5 also interact with cholesterol, its precursor, and derivatives though with variable extents. GST-only was used as a negative control which show no or very minimum interactions. This confirms that Loop4 in combination of TM4- and/or TM5 can directly interact with cholesterol, its precursors and derivatives and Loop4 is sufficient for these interactions.

3.7. Membrane mobility of TRPV4 is regulated by cholesterol

Next we performed FRAP in order to visualize the recovery of the hTRPV4-GFP (Fig. 4D). Mobility of TRPV4-GFP is significantly lower (recovers ~30% in 500 s) in control conditions (membrane with cholesterol). When cells were treated with cholesterol

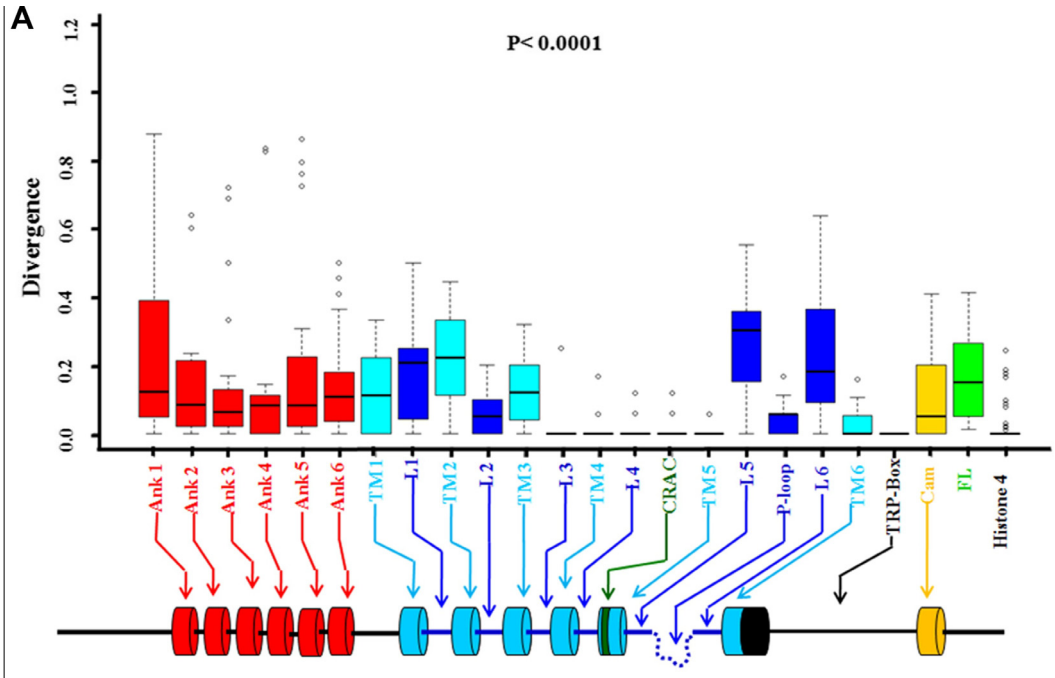

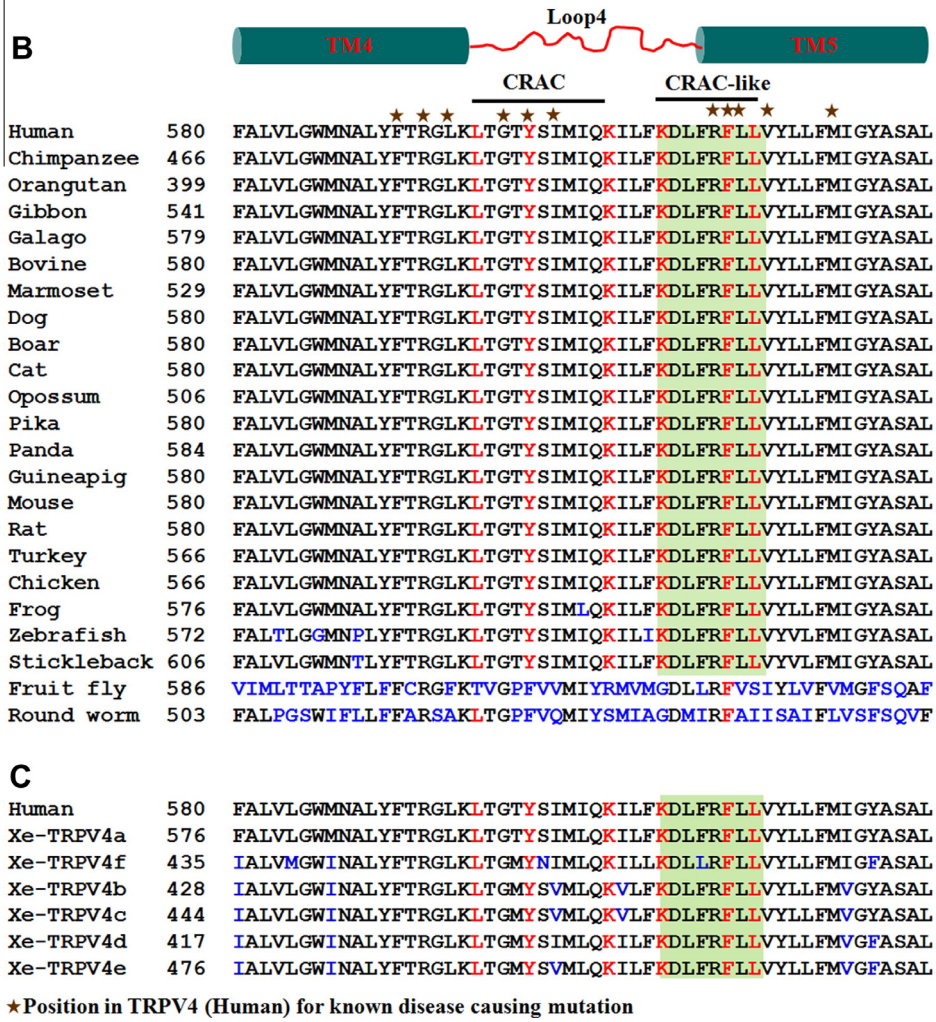

Fig. 2. Conserved domains and motifs including cholesterol interacting sites are present in TRPV4. (A) The lower and higher values indicate more and less conservation respectively. Different domains and motifs of TRPV4 are indicated by different colors. All values are significant ($p < 0.0001$, Kruskal–Wallis test). (B) The CRAC- and "CRAC-like (green shade) motifs present within the TM4-Loop4-TM5 are conserved throughout the vertebrate evolution. (i) The crucial amino acids that form the signature of these two motifs are labeled with red color. The positions of disease causing mutations (∗) and amino acids that differ from hTRPV4 (blue) are indicated. (ii) A similar comparison of *x*TRPV4 sequences with hTRPV4. (For interpretation of the references to color in this figure legend, the reader is referred to the web version of this article.)

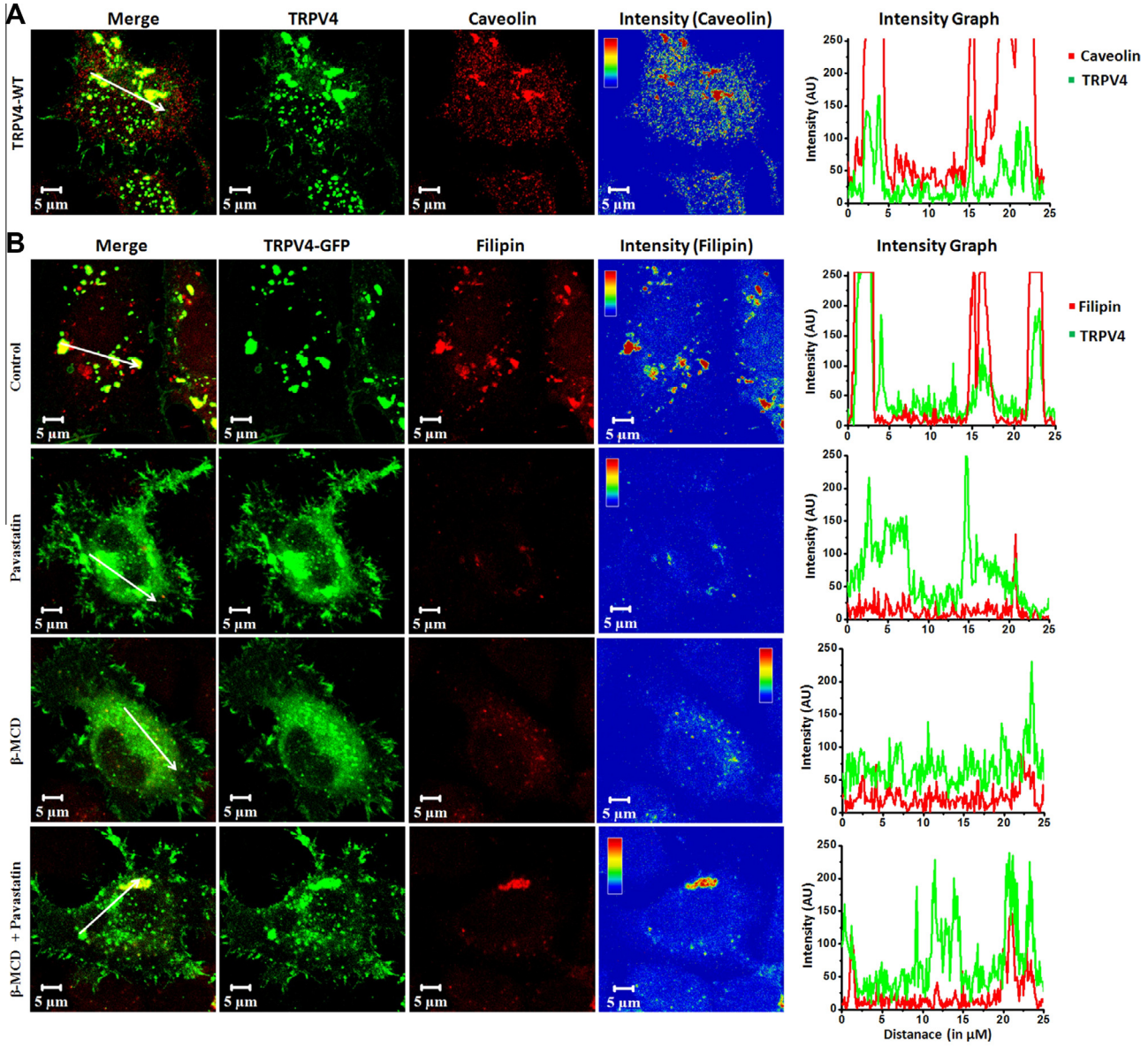

Fig. 3. TRPV4 localizes in cholesterol-enriched membrane microdomains. (A) Confocal images of F11 cells expressing GFP-TRPV4 (green) immunostained for endogenous Caveolin1 (Red). (B) Confocal images of F11 cell expressing GFP-TRPV4 (green) stained with Flilipin (Red). After treating the cells with cholesterol depleting agent βMCD (cholesterol biosynthesis blocker) Pravastatin, or with both. Cells were fixed in control conditions. In each case, the intensity plot is represented (right). (For interpretation of the references to color in this figure legend, the reader is referred to the web version of this article.)

depleting drug Pravastatin or βMCD; the mobility of TRPV4 increases further indicating that that mobility of TRPV4 is dependent on the membrane cholesterol.

4. Discussion

We have combined protein sequence, genomic data, structural information, biochemical and cell-biological experimental results, which demonstrate that TRPV4 is a highly conserved protein and has evolved ~450 MY before when vertebrate evolution started. TRPV4 physically interacts with cholesterol, its precursor molecule mevalonate and some of its derivatives through the Loop4 and nearby helices, a region of TRPV4 which is 100% identical in all vertebrates. In agreement with this physical interaction, in all vertebrates TRPV4 gene is tightly linked with MVK and GLTP, two genes which are involved in the cholesterol-biosynthesis. We show that membrane mobility of TRPV4 depends on the availability of the cholesterol. In vertebrates, TRPV4 seem to be regulated by cholesterol as well as other metabolic components present in the cholesterol biosynthesis pathway. Such molecular interactions of TRPV4 with cholesterol, cholesterol-precursors/derivatives may have importance in the context of several sensory functions which are directly dependent on the TRPV4. Such physical and functional crosstalk may also be relevant for several physiological functions [21]. As TRPV4-mediated sensory and physiological functions can largely influence the adaptation, such functions are crucial determinants of natural selection, speciation and evolution. Therefore, molecular evolution of TRPV4 is guided by availability of membrane cholesterol and its intermediates/derivatives, i.e. metabolites of cholesterol biosynthesis pathway in general which is very much vertebrate-specific.

In this work we demonstrate that Loop3–TM4–Loop4–TM5 region (AA 576–632) of TRPV4 is highly conserved among

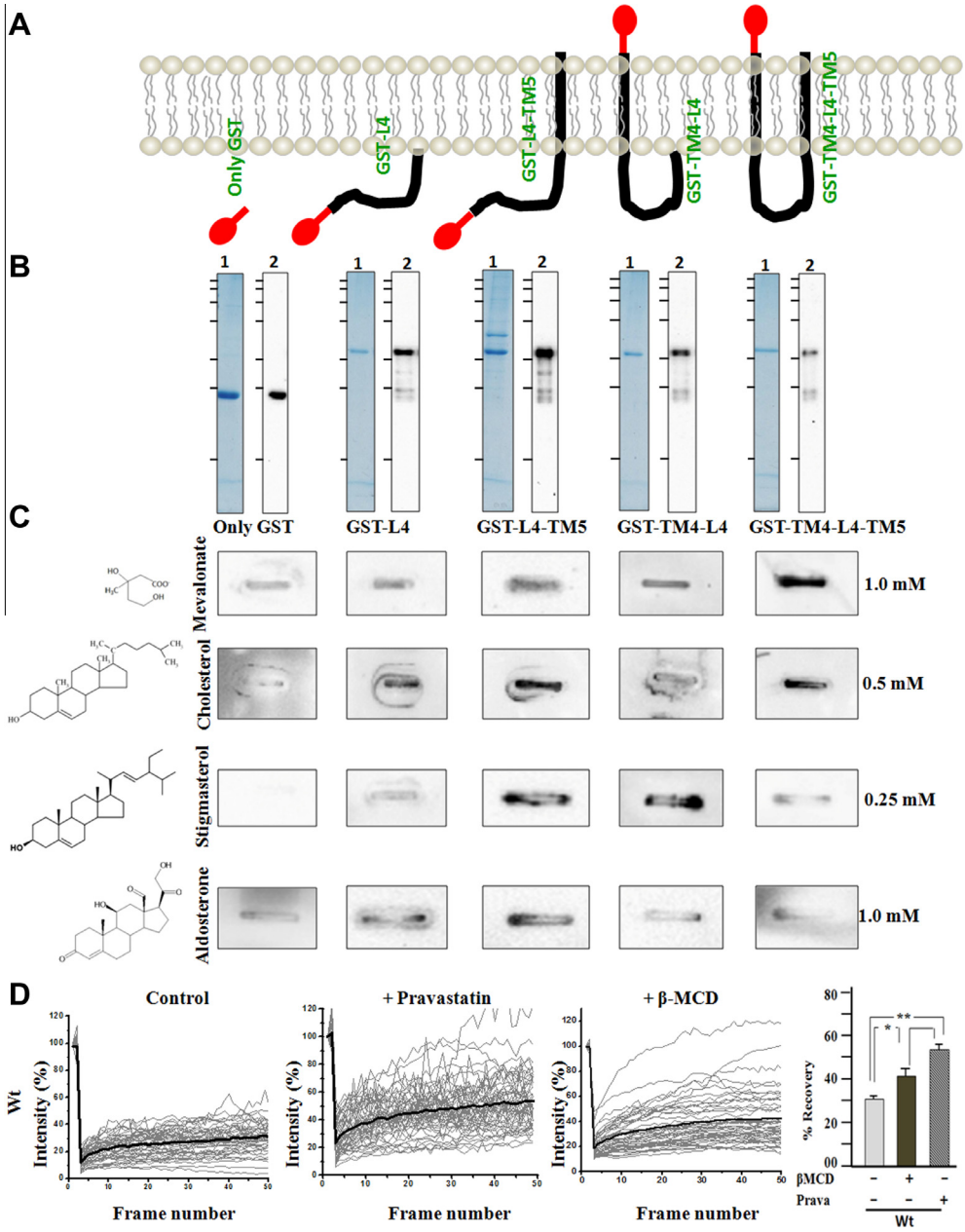

Fig. 4. Physical interaction and functional regulation of TRPV4 by cholesterol. (A) Loop4 alone or in combination with TM4 and/or TM5 is sufficient for physical interaction with cholesterol, its precursor and derivatives. (i) Schematic diagram of the GST-tagged TRPV4-fragments. (ii) SDS–PAGE (1) and Western Blot (2) analysis of purified GST-only, GST–Loop4, GST–Loop4–TM5, GST–TM4–Loop4 and GST–TM4–Loop4–TM5. (iii) The respective blot-overlay of these TRPV4 fragments against mevalonate, cholesterol, stigmasterol and aldosterone are shown. (B) Membrane mobility of TRPV4 depends on the cholesterol. FRAP pattern of cells expressing TRPV4-GFP in control (left), in Pravastatin-treated (middle) and in β-MCD treated conditions (right) are shown. In each case at least 50 ROIs were analyzed (gray lines) and the average value is indicated (bold black line). The fluorescence intensity (in % of the initial conditions) is plotted in *Y*-axis and frame numbers (time interval between each frame is 10 s) are plotted in *X*-axis. Average recovery at the end of 50th frame are shown in bar diagram ($^{*}p < 0.002$; $^{**}p < 0.0001$).

vertebrates and have limited substitutions. Accordingly, different point mutations which are clustered in this region of hTRPV4 are linked with the development of several diseases and pathophysiological situations commonly known as channelopathy [18]. We correlate this conservation as a prerequisite for interaction with cholesterol, its precursors and derivatives. There are several CRAC-motifs present within the N- and C-termini of hTRPV4 and few of these are conserved in most vertebrates (not shown). However, except the TM4–Loop4–TM5 region, we could not find any other CRAC/CRAC-like motif(s) in other TM regions (in hTRPV4). In TRPV1 and TRPV4, the CRAC-motif is 8AA long. Notably, AA 576–632 of TRPV4 is more conserved than that of the cholesterol-binding region of TRPV1 [10]. Even this region is not highly conserved when compared to other TRPVs where this motif is absent (Fig:S3).

The cholesterol interaction seems to be important for "activation/inhibition" of TRPV1/TRPV4 by specific hydrophobic compounds and for "thermo-gating". Indeed, experiments confirmed that TRPV1 function is altered in cholesterol-depleted/saturated membranes [22–23]. Also, cholesterol interaction is needed for temperature-induced activation of TRPV4. For example, when rTRPV4 is expressed in yeast (which cannot synthesize cholesterol); it can be activated by changes in osmolarity but not by temperature [24].

The cross-talk between TRPV4 with sterol compounds is also evident from genomic organization, genetic interaction and

pharmacological evidences. Synteny analysis suggests that TRPV4 share tight linkage with MVK and GLTP, genes involved in cholesterol biosynthesis pathway. Notably this linkage is conserved for 450 MY. In human too, MVK (a key enzyme catalyzing sterol synthesis from mevalonate) gene is tightly linked with TRPV4 (located very closely at 12q24.1) suggesting the dependency and fine regulation of TRPV4 by metabolites of the cholesterol biosynthesis pathway [25]. Common involvement of TRPV4 and sterols in same functions is also prominent from genetic interaction studies. Indeed, mutations in 3β-hydroxysterol Δ14-reductase, (involved in cholesterol biosynthesis pathway) give rise to Greenberg skeletal dysplasia [26]. Similarly, point mutations present in the CRAC-motif region of hTRPV4 give rise to "Skeletal dysplasia" [18].

Non-genomic regulation of TRPs by the metabolites present in the sterol/steroid biosynthesis pathway is important for several physiological, developmental, and endocrinological point of view [21]. For example, while dimethylallyl pyrophosphate activate TRPV4; isopentenyl pyrophosphate inhibits TRPV3 and TRPA1 [3,27,28]. Farnesyl pyrophosphate (FPP; precursor of sterol biosynthesis pathway) activate TRPV3 [27]. While cholesterol inhibits TRPM3, Pregnenolone (cholesterol precursor) can activate it [29,30]. Progesterone (sex hormone) also inhibits TRPM3 [31]. Taken together, results suggest that TRPVs are the molecular targets of cholesterol, its precursors and derivatives, such as steroid hormones. Though the effect of different steroids on TRPV4 has not been fully characterized yet, the crosstalk between TRPV4 and steroid hormones has been established to some extent. For example, progesterone can regulate TRPV4 expression [32]. TRPV4 is essential for mechanosensitivity in the aldosterone-sensitive distal nephron [33]. Steroid hormones also alter the mechanical hyperalgesia where TRPV4 is involved [34–36]. Such aspects may be relevant for vesicular recycling regulated by TRPV channels [37].

Taken together, our results reveal a strong dependency of TRPV4 on sterol molecules indicating that sterol biosynthesis pathway and TRPV4 function may have shared co-evolution. We conclude that TRPV4 structure and function has been determined by the physical interaction with sterol compounds through highly conserved motif sequences and such interactions may have diverse and important physiological functions.

Acknowledgments

We acknowledge Dr. P.V. Alone for GST vector. Funding from NISER and DBT – India (BT-BRB-TF-2-2011) are acknowledged.

Appendix A. Supplementary data

Supplementary data associated with this article can be found, in the online version, at http://dx.doi.org/10.1016/j.bbrc.2014.11.077.

References

[1] X. Gao, L. Wu, R.G. O'Neil, Temperature-modulated diversity of TRPV4 channel gating: activation by physical stresses and phorbol ester derivatives through protein kinase C-dependent and -independent pathways, J. Biol. Chem. 278 (2003) 27129–27137.
[2] X. Ma, D. He, X. Ru, et al., Apigenin, a plant-derived flavone, activates transient receptor potential TRPV4 cation channel, Br. J. Pharmacol. 166 (2011) 349–358.
[3] S. Bang, S. Yoo, T. Yang, et al., Nociceptive and proinflammatory effects of dimethylallyl pyrophosphate via TRPV4 activation, Br. J. Pharmacol. 166 (2012) 1433–1443.
[4] H. Watanabe, J. Vriens, J. Prenen, et al., Anandamide and arachidonic acid use epoxyeicosatrienoic acids to activate TRPV4 channels, Nature 424 (2003) 434–438.
[5] B.D. Matthews, C.K. Thodeti, J.D. Tytell, et al., Ultra-rapid activation of TRPV4 ion channels by mechanical forces applied to cell surface beta1 integrins, Integr. Biol. (Camb.) 2 (2010) 435–442.
[6] F.R. Carreño, L.L. Ji, J.T. Cunningham, Altered central TRPV4 expression and lipid raft association related to inappropriate vasopressin secretion in cirrhotic rats, Am. J. Physiol. Regul. Integr. Comp. Physiol. 296 (2009) R454–R466.
[7] C. Goswami, J. Kuhn, P.A. Heppenstall, et al., Importance of non-selective cation channel TRPV4 interaction with cytoskeleton and their reciprocal regulations in cultured cells, PLoS One 5 (2010) e11654.
[8] W. Liedtke, TRPV4 plays an evolutionary conserved role in the transduction of osmotic and mechanical stimuli in live animals, J. Physiol. 567 (2005) 53–58.
[9] W. Liedtke, Y. Choe, M.A. Martí-Renom, et al., Vanilloid receptor-related osmotically activated channel (VR-OAC), a candidate vertebrate osmoreceptor, Cell 103 (2000) 525–535.
[10] P. Sardar, A. Kumar, A. Bhandari, et al., Conservation of tubulin-binding sequences in TRPV1 throughout evolution, PLoS One 7 (2012) e31448.
[11] C.B. Phelps, R.J. Huang, P.V. Lishko, et al., Structural analyses of the ankyrin repeat domain of TRPV6 and related TRPV ion channels, Biochemistry 47 (2008) 2476–2484.
[12] P.V. Lishko, E. Procko, X. Jin, et al., The ankyrin repeats of TRPV1 bind multiple ligands and modulate channel sensitivity, Neuron 54 (2007) 905–918.
[13] G. Picazo-Juárez, S. Romero-Suárez, A. Nieto-Posadas, et al., Identification of a binding motif in the S5 helix that confers cholesterol sensitivity to the TRPV1 ion channel, J. Biol. Chem. 286 (2011) 24966–24976.
[14] P. Valente, N. García-Sanz, A. Gomis, et al., Identification of molecular determinants of channel gating in the transient receptor potential box of vanilloid receptor I, FASEB J. 22 (2008) 3298–3309.
[15] R. Strotmann, G. Schultz, T.D. Plant, Ca^{2+}-dependent potentiation of the nonselective cation channel TRPV4 is mediated by a C-terminal calmodulin binding site, J. Biol. Chem. 278 (2003) 26541–26549.
[16] W. Liedtke, D.M. Tobin, C.I. Bargmann, et al., Mammalian TRPV4 (VR-OAC) directs behavioural responses to osmotic and mechanical stimuli in *Caenorhabditis elegans*, Proc. Natl. Acad. Sci. U.S.A. 100 (2003) 14531–14536.
[17] P. Doñate-Macián, A. Perálvarez-Marín, Dissecting domain-specific evolutionary pressure profiles of transient receptor potential vanilloid subfamily members 1 to 4, PLoS One 9 (2014) e110715.
[18] P. Verma, A. Kumar, C. Goswami, TRPV4-mediated channelopathies, Channels (Austin) 4 (2010) 319–328.
[19] S.R. Lamandé, Y. Yuan, I.L. Gresshoff, et al., Mutations in TRPV4 cause an inherited arthropathy of hands and feet, Nat. Genet. 43 (2011) 1142–1146.
[20] C.J. Baier, J. Fantini, F.J. Barrantes, Disclosure of cholesterol recognition motifs in transmembrane domains of the human nicotinic acetylcholine receptor, Sci. Rep. 1 (2011) 69.
[21] A. Kumar, S. Kumari, R.K. Majhi, et al., Regulation of TRP channels by steroids: implications in physiology and diseases, Gen. Comp. Endocrinol. (2014), http://dx.doi.org/10.1016/j.ygcen.2014.10.004.
[22] M. Liu, W. Huang, D. Wu, et al., TRPV1, but not P2X, requires cholesterol for its function and membrane expression in rat nociceptors, Eur. J. Neurosci. 24 (2006) 1–6.
[23] E. Szoke, R. Börzsei, D.M. Tóth, et al., Effect of lipid raft disruption on TRPV1 receptor activation of trigeminal sensory neurons and transfected cell line, Eur. J. Pharmacol. 628 (2010) 67–74.
[24] S.H. Loukin, Z. Su, C. Kung, Hypotonic shocks activate rat TRPV4 in yeast in the absence of polyunsaturated fatty acids, FEBS Lett. 583 (2009) 754–758.
[25] I. Buhaescu, H. Izzedine, Mevalonate pathway: a review of clinical and therapeutical implications, Clin. Biochem. 40 (2007) 575–584.
[26] A.M. Bennati, M. Castelli, M.A.D. Fazia, et al., Sterol dependent regulation of human TM7SF2 gene expression: role of the encoded 3beta-hydroxysterol Delta14-reductase in human cholesterol biosynthesis, Biochim. Biophys. Acta 1761 (2006) 677–685.
[27] S. Bang, S. Yoo, T.J. Yang, et al., Farnesyl pyrophosphate is a novel pain-producing molecule via specific activation of TRPV3, J. Biol. Chem. 285 (2010) 19362–19371.
[28] S. Bang, S. Yoo, T.J. Yang, et al., Isopentenyl pyrophosphate is a novel antinociceptive substance that inhibits TRPV3 and TRPA1 ion channels, Pain 152 (2011) 1156–1164.
[29] J. Naylor, J. Li, C.J. Milligan, et al., Pregnenolone sulphate- and cholesterol-regulated TRPM3 channels coupled to vascular smooth muscle secretion and contraction, Circ. Res. 106 (2010) 1507–1515.
[30] T.F. Wagner, S. Loch, S. Lambert, et al., Transient receptor potential M3 channels are ionotropic steroid receptors in pancreatic beta cells, Nat. Cell Biol. 10 (2008) 1421–1430.
[31] Y. Majeed, S. Tumova, B.L. Green, et al., Pregnenolone sulphate-independent inhibition of TRPM3 channels by progesterone, Cell Calcium 51 (2012) 1–11.
[32] C. Jung, C. Fandos, I.M. Lorenzo, et al., The progesterone receptor regulates the expression of TRPV4 channel, Pflugers Arch. 459 (2009) 105–113.
[33] M. Mamenko, O. Zaika, M. Jin, et al., Purinergic activation of Ca^{2+}-permeable TRPV4 channels is essential for mechano-sensitivity in the aldosterone-sensitive distal nephron, PLoS One 6 (2011) e22824.
[34] O.A. Dina, K.O. Aley, W. Isenberg, et al., Sex hormones regulate the contribution of PKCepsilon and PKA signalling in inflammatory pain in the rat, Eur. J. Neurosci. 13 (2001) 2227–2233.
[35] Y. Ji, B. Tang, R.J. Traub, Modulatory effects of estrogen and progesterone on colorectal hyperalgesia in the rat, Pain 117 (2005) 433–442.
[36] W.J. Kowalczyk, M.A. Sullivan, S.M. Evans, et al., Sex differences and hormonal influences on response to mechanical pressure pain in humans, J. Pain 11 (2010) 330–342.
[37] C. Goswami, N. Rademacher, K.H. Smalla, et al., TRPV1 acts as a synaptic protein and regulates vesicle recycling, J. Cell Sci. 123 (2010) 2045–2057.

ANDROLOGY

ISSN: 2047-2919

ANDROLOGY

ORIGINAL ARTICLE

Correspondence:
Chandan Goswami, School of Biological Sciences, National Institute of Science Education and Research, PO: Sainik School, District: Khorda , Bhubaneshwar, Odisha 751005.
India.
E-mail: chandan@niser.ac.in

Keywords:
acrosome, bifurcated nucleus, mitochondria, modified tubulin, spermatozoa, super resolution microscopy

Received: 23-May-2015
Revised: 30-Jul-2015
Accepted: 12-Oct-2015

doi: 10.1111/andr.12130

Light and electron microscopic study of mature spermatozoa from White Pekin duck (*Anas platyrhynchos*): an ultrastructural and molecular analysis

[1]Rakesh Kumar Majhi, [1]Ashutosh Kumar, [1]Manoj Yadav, [2]Pradeep Kumar, [3]Apratim Maity, [2]Sunil C. Giri and [1]Chandan Goswami

[1]School of Biological Sciences, National Institute of Science Education and Research, [2]Central Avian Research Institute, and [3]Department of Biochemistry, OVC, Orissa University of Agriculture and Technology, Bhubaneswar, India

SUMMARY

The morphology, ultrastructure, and functions of mature avian spermatozoa have been of immense commercial and scientific interest for several reasons. This is mainly important in case of birds in poultry production, conservation, and in the use of sperm morphometry as phylogenetic evidence. Avian spermatozoa share complex or no correlation of sperm morphometry with respect to testis and/or body size as described before. In this work, we have isolated mature spermatozoa from White Pekin duck (*Anas platyrhynchos*) by non-invasive methods and performed several immunostaining analysis as well as cytochemical analysis using electron and light microscopes. Here, we report the presence of different post-translationally modified tubulin such as tyrosinated-, detyrosinated-, acetylated-, polyglutamylated-, and glycylated-tubulin in specific regions of the mature spermatozoa. By using field-emission scanning electron microscope, we confirm the presence of acrosome-like structure at the tip of the sperm head. However, this structure remains non-reactive to common lectins such as Peanut Agglutinin (PNA) and cholesterol-sensitive dyes such as Filipin. We report that this acrosomal structure is primarily made of lipid-based structures and is resistant to 0.1% Triton X100. Confocal microscopy and super resolution structured illumination microscopy study indicates that the nucleus is bifurcated at the tip region. By using specific markers, we report that the perforatorium structure present at the tip of the spermatozoa head contains specialized organelles that is similar to atypical mitochondria. We propose that these ultrastructural and molecular parameters can be used as species-specific features. The bifurcated nucleus and presence of atypical mitochondria within this structure may be relevant for the complex mitochondrial inheritance and mitochondrial heteroplasmy observed in case of avian population.

INTRODUCTION

The morphology, ultra structure, and functions of mature male gametes from different species are of immense commercial and scientific interest for several reasons. This is particularly important for avian spermatozoa which have direct implications in poultry production, conservation, and in the use of sperm morphometry as phylogenetic evidences. Current, literature suggests that the avian spermatozoa are highly diverse in morphology, complex in their molecular markers and also in terms of functional regulations. The size of avian spermatozoa is highly variable, ranging from 30 to 300 μm, with little or no correlation between size of the bird and sperm dimensions (McFarlane, 1963; Briskie *et al.*, 1997; Mossman *et al.*, 2009). Generally, avian spermatozoa possess long cylindrical nuclei, whereas the spermatozoa of eutherian mammals have short and flat nuclei (Fawcett, 1970). Certain key differences between passerine and non-passerine birds in spermatozoon structure have also been documented (Breucker, 1982). The spermatozoa of passerine birds are generally spiral-shaped with an external, helically wound undulating membrane and a curved or spiral acrosome without a perforatorium, and a type of wavy membrane which is similar to amphibian spermatozoa (Simões *et al.*, 2012). The spermatozoa of non-passerine birds, like that of galliform, anseriform, and columbiform birds, correspond to the basic type of spermatozoa (relatively simple in morphology, which are plain and elongated) similar to those of reptiles, called sauropsid-type (Humphreys, 1972). These sauropsid spermatozoa are structurally characterized by a small acrosome, perforatorium, well-defined midpiece containing two centrioles and a long and mobile flagellum (Yasuzumi & Sugioka, 1971; Humphreys, 1972; Baccetti *et al.*, 1980).

Recently, the ultrastructural details of the spermatozoa of the domestic duck (*Anas platyrhynchos* sp.) have been described in details (Simões *et al.*, 2012). As reported in this paper, the mature spermatozoa contain a short and tapering head, short midpiece, long principal piece, and a short end-piece. The sperm head revealed a reduced acrosome (formed by a short and tapering cephalic cap) located anteriorly to the nucleus which contains homogenous and moderately electron-dense materials and elliptical mitochondria (Simões *et al.*, 2012). In this work, we have analyzed the morphological, structural, and molecular details of the mature spermatozoa from White Pekin duck *Anas platyrhynchos*. Our work suggests that White Pekin duck spermatozoa has very specific features such as post-translationally modified tubulin at the tail region, a lipid-enriched acrosome-like structure and atypical mitochondria at the tip which can be used as species-specific features.

MATERIALS AND METHODS

Collection of mature spermatozoa from duck

White Pekin ducks (*Anas platyrhynchos*) were maintained in the duck house of Central Avian Research Institute, Bhubaneswar, India and semen collection was performed by trained professionals as per the guidelines of the Institutional animal ethics committee. Mature spermatozoa were collected by manual massage into clean sterile collection vials and were either fixed with 4% paraformaldehyde or incubated at 37 °C immediately after ejaculation. All microscopic analysis was performed at the NISER, Bhubaneswar, India.

Labeling of spermatozoa with JC1, Mitotracker-Red, and Alexafluor 488-conjugated streptavidin

The freshly ejaculated spermatozoa were incubated with mitochondria-specific dye JC1 (5 μM; Life Technologies, Carlsbad, California, USA) at 37 °C for 20 min and imaged under confocal microscope in live condition (Leite *et al.*, 2010). CCCP was purchased from Sigma Aldrich (St Louis, MO, USA) and was used as the un-coupler for mitochondrial oxidative potential. In separate experiments, freshly ejaculated spermatozoa were incubated with Mitotracker-Red (5 μM; Life Technologies) at 37 °C for 20 min and were fixed with 1 : 1 ratio (v/v) of 4% paraformaldehyde for 20 min at room temperature. Mitotracker-Red stained samples were permeabilized with 0.1% Titron-X 100 and blocked with 5% bovine serum albumin (BSA). AF488-labeled streptavidin was incubated with permeabilized spermatozoa for 2 h at room temperature. After washing thrice with PBS-T (Phosphate Buffered Saline with 0.1% Tween20), the samples were stained with DAPI (4',6-diamidino-2-phenylindole) and were stored at 4 °C till further experiments.

Labeling of spermatozoa with lipid-specific dyes

The Paraformaldehyde (PFA) fixed cells were washed thrice with PBS (pH 7.4) by centrifuging at 800 ***g*** for 5 min each time and then incubated with DiI (5 μg/mL final concentration) for 20 min at room temperature (25 °C) to label the lipids. The stained samples were washed thrice with PBS (pH 7.4) by centrifuging at 800 ***g*** for 5 min each time and then visualized under confocal microscope. For the detection of cholesterol present in the sperm cells, Filipin staining was performed (Börnig & Geyer, 1974; Sugii *et al.*, 2003). For Filipin staining, the fixed cells were washed thrice with PBS; background fluorescence was quenched with 1.5 mg/mL glycine in PBS for 30 min, then incubated with Filipin (125 μg/mL) in PBS for 1 h at room temperature (25 °C) and washed three times with PBS to remove excess Filipin. The cells were imaged soon after washing was complete.

Lectin and antibody staining

Paraformaldehyde-fixed spermatozoa were washed thrice with PBS (pH 7.4) by centrifuging at 800 ***g*** for 5 min each time and then incubated with FITC-PNA (purchased from Sigma Aldrich and used at 1 : 200 v/v dilution) for 1 h and washed thrice with PBS to remove un-incorporated FITC-PNA. To stain the modified tubulins, the fixed spermatozoa were washed thrice with PBS (pH 7.4) by centrifuging at 800 g for 5 min each time and then treated with 0.1% Titron-X100 for permeabilization for 5 min. The permeabilized spermatozoa were blocked with 5% BSA for 1 h at room temperature (25 °C). The sperm cells were then incubated overnight with primary antibodies for different modified tubulins: acetylated tubulin (clone 6-11B-1; Sigma-Aldrich); polyglutamylated tubulin (clone B3; Sigma-Aldrich) and tyrosinated tubulin (clone TUB-1A2; Sigma-Aldrich), detyrosinated tubulin (clone GLU; Millipore, Darmstadt, Germany), monoglycylated tubulin (clone TAP 952; Millipore), polyglycylated Tubulin (clone AXO 49; Millipore), and alpha detyrosinated tubulin (Millipore). Following Mouse monoclonal antibodies were used to detect mitochondria of duck spermatozoa: HSP60 antibody (clone NAB11-13; AbCam, Cambridge, UK), Cytochrome C antibody (clone 7H8.2C12; AbCam), ATP5A antibody (clone 7H10BD4F9; AbCam), and Mitofusin2 (Mfn2; AbCam). All these primary antibodies were used at 1 : 500 dilution and incubated overnight at 4 °C in PBS buffer supplemented with 5% BSA in 1 : 1 ratio (v/v). After washing thrice in PBST buffer (PBS supplemented with 0.1% Tween-20), AlexaFluor-488 labeled anti-mouse or anti-rabbit antibodies (Molecular probes) were used as secondary antibodies at 1 : 1000 dilution. All images were taken on a confocal laser-scanning microscope (LSM-780; Zeiss, Goettingen, Germany) with a 63X-objective and analyzed with the Zeiss LSM image examiner software and Adobe Photoshop as described previously (Majhi *et al.*, 2013). Quantification of the length of different parts of the cell was carried out using Zeiss LSM image examiner software. The super resolution images of duck spermatozoa were acquired using super resolution structured illumination microscopy (SR-SIM; Zeiss ELYRA PS.1).

Sample preparation and FE-SEM

The PFA-fixed sperm cells were washed thrice with Milli-Q water and then spotted on aluminum film coated on a glass coverslip. The spots were dried within a desiccator and subsequently imaged on Zeiss field-emission scanning electron microscope (FE-SEM) SIGMA at 15–75 KX magnification and 3 kV EHT (extra-high tension).

Western blot analysis

For western blotting, the fresh semen was collected as mentioned. The freshly collected cells were diluted in 1X-PBS and quickly centrifuged at 800 ***g*** for 5 min in 25 °C. After that the pellet fraction containing sperm cells was directly taken in a sample preparation buffer containing protease inhibitors mixed with 5X-Lammeli buffer. The samples were heated at 95 °C for

5 min and subsequently separated by 10% sodium dodecyl sulfate PAGE (SDS-PAGE) as described before (Laemmli, 1970). Owing to the high lipid and DNA content, the samples were separated by SDS-PAGE for around 12 h in a mini-gel (Bio-Rad, Hercules, California, USA). The proteins were electrophoretically transferred to PVDF (Polyvinylidene fluoride) membrane (Millipore). After blocking for 1 h in TBST [20 mM Tris (pH 7.4), 0.9% (w/v) NaCl, and 0.1% (v/v) Tween 20] containing 5% (w/v) dry skimmed milk, the membranes were incubated with specific antibodies. Mouse monoclonal anti-acetylated tubulin (clone 6-11B-1; Sigma Aldrich), anti-polyglutamylated tubulin (clone B3; Sigma Aldrich), anti-tyrosinated tubulin (clone TUB-1A2; Sigma Aldrich), alpha-detyrosinated tubulin (Millipore) and rabbit polyclonal detyrosinated tubulin (clone GLU; Millipore), monoglycylated tubulin (clone TAP 952; Millipore), and polyglycylated Tubulin (clone AXO 49; Millipore), were used at 1 : 500 dilutions, respectively. After extensive washing in TBST, the membranes were incubated with horse-radish peroxidase-conjugated secondary antibody raised against mouse or rabbit (GE Healthcare, Little Chalfont, UK) for 1 h at room temperature (25 °C). Subsequently the membranes were extensively washed in TBST and immunoreactivities were visualized on chemidoc system (BioRad) by enhanced chemiluminescence according to the manufacturer's instructions (Thermo Scientific, Waltham, Massachusetts, USA).

RESULTS

Morphological details of duck spermatozoa

To resolve the structural and molecular details of the spermatozoa, we performed several Difference Interference Contrast (DIC)-microscopic analysis as well as FE-SEM with the PFA-fixed cells. The DIC-microscopic analysis clearly reveals the presence of an elongated head, short midpiece, and long principal piece as also reported for other avian species (Fig. 1A). The quantitative morphometric analyses (n = 20) reveal that the total length of the spermatozoa is 67.04 ± 2.93 μm. The sperm head is elongated and the size is approximately 13.56 ± 0.67 μm. The principal piece (tail) of White Pekin spermatozoa is also elongated (50.10 ± 2.71 μm) and is at-least three times the length of the head. The midpiece is coiled in shape, is about 3.37 ± 0.25 μm in length and reveals a distinct morphology. To understand the morphological features in more details, we performed FE-SEM analysis which reveals the distinct presence of an elongated head, short midpiece, and long principal piece (Fig. 1B). The midpiece contains on an average 6–12 units of mitochondrial coiling as revealed by the FE-SEM images. FE-SEM images also revealed that the White Pekin sperm head is elongated and cylindrical in shape and ends with a tapering tip (Fig. 1). Notably the FE-SEM images reveal the presence of a prominent cone-like structure resembling perforatorium followed by acrosome-like structure which is present in all the mature sperm head tips (Fig. 1). Interestingly, this acrosome-like structure is not properly visible in DIC images.

Duck sperm head contains bifurcated nucleus and atypical mitochondria at the tip

Although DIC microscopy as well as FE-SEM images revealed that the White Pekin duck sperm head is elongated and cylindrical in shape and ends with a tapering tip (Fig. 1), we aimed to visualize the DNA organization at the sperm head and the organization of the mitochondria in these cells. For that purpose, we labeled the cells with Mitotracker-Red and stained the head with DAPI as well. We analyzed the head portion and in particular the nucleus and the midpiece by laser-based imaging techniques, namely by confocal and SR-SIM (Fig. 2). While confocal microscopy reveals the presence of elongated and cylindrical nucleus within the head, the super resolution microscopy clearly revealed that the nucleus is actually bifurcated at the tip (Fig. 2B Zoom). The midpiece can be labeled with Mitotracker-Red suggesting that this region actually contains functional mitochondria. However, both confocal and SR-SIM images reveal that the Mitotracker-Red labeling can also be observed at the very tip of the sperm head (Fig. 2).

Labeling of these sub-cellular organelles by Mitotracker-Red located at the tip of the sperm nucleus indicates that these structures have high oxidative potential and thus can be mitochondria. The sperm tip also showed staining for other important mitochondrial markers such as Mitochondrial membrane ATP synthase (F1F0 ATP synthase or Complex V, mentioned in this paper as ATP5A) and mitochondrial outer membrane protein Mitofusin2 (Mfn2) (Fig. 3A,B). Surprisingly while ATP5A stained

Figure 1 Unusual structures of mature spermatozoa of White Pekin duck. (A) DIC image of the single sperm cell. Head and midpiece region of the cell in indicated separately. (B–D) Field-emission scanning electron microscopy images of a sperm cell and its enlarged regions demonstrating the structural and morphological details. The mitochondrial region (indicated by arrow in C) and the acrosome-like structure (marked by asterisk in D) are shown in details. The fine tip of the acrosome-like structure is indicted by an arrow (D).

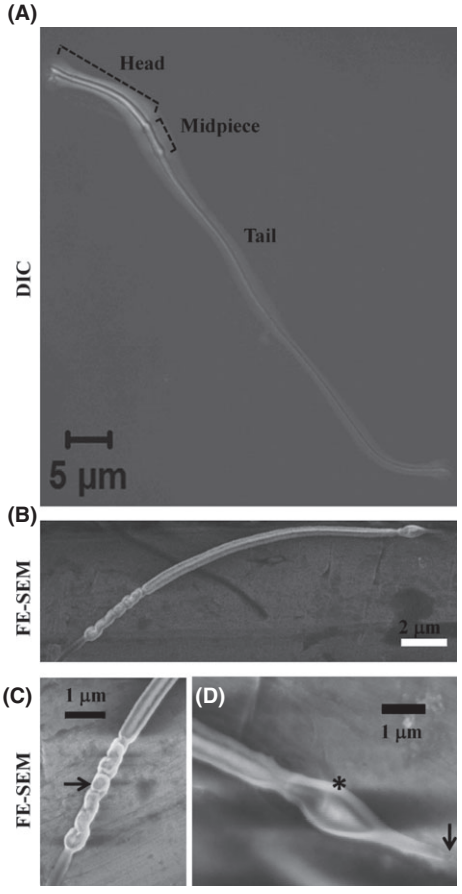

Figure 2 White Pekin duck spermatozoa contains bifurcated nucleus and atypical mitochondria at the tip. (A,B) Confocal image of duck spermatozoa labeled with Mitotracker-Red (red) and DAPI (blue) merged with DIC is shown, scale bar 5 μm. (C,D) Super resolution structured illumination microscopy (SR-SIM) revealed the presence of a bifurcated nucleus in the head and the presence of Mitotracker-Red labeled organelles which are embedded within the bifurcated tip. The asterisk indicates the start of bifurcation and arrow points out to the tip of bifurcated head. The enlarged image of the midpiece region is shown *in set* (scale bar 500 nm).

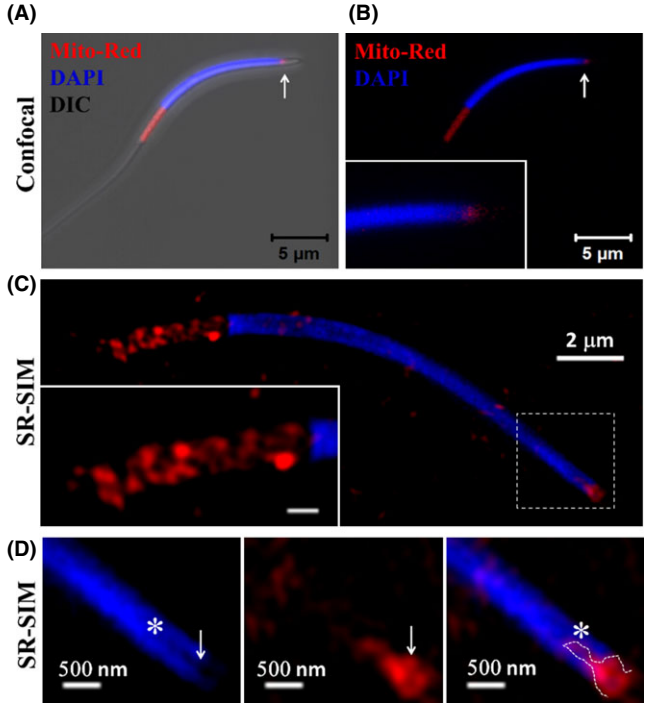

the sperm head region, it did not stain the neck region (Fig. S1a). In a similar manner, Mitofusin2 stains the sperm head and tail, but does not show staining at the neck region which is enriched with mitochondria (Fig. S1b). We confirmed the specificity of these two antibodies against duck spermatozoa by western blot analysis where these two antibodies detect bands at expected sizes (Fig. S1a,b). Another antibody raised against mitochondrial protein, namely anti-HSP60 reveals punctate staining in the head region of the duck spermatozoa, but such staining is absent in the tip as well as in the neck region (Fig. S1c). However, this antibody also detects a specific band of right size in western blot analysis suggesting that HSP60 is not present in the neck regions (Fig. S1c). Another antibody raised against Cytochrome-C does not detect any signal from duck spermatozoa, neither in immunofluorescence analysis not in western blot analysis, most likely because of unmatched epitopes (Fig. S1c). Taken together, results obtained from specific antibodies raised against different mitochondrial proteins strongly suggest the unique distribution of these proteins in the head and absence of these markers in the neck region of the spermatozoa of White Pekin duck. These in general therefore suggest that the distribution of mitochondrial markers in avian spermatozoa is complex and need further in-depth analysis.

In absence of suitable antibodies which can detect mitochondria present in spermatozoa of avian species reliably, we tested indirectly if the tip of the sperm nucleus indeed reveals other mitochondrial properties. To test that, we stained Mitotracker-Red labeled sperm cells with Alexa flour-488 conjugated streptavidin, which binds to biotin (Hollinshead *et al.*, 1997). Indeed, the streptavidin-AF488 diffusely detects the head of spermatozoa and co-localized with the Mitotracker-Red stained regions at the midpiece and also the tip of head (Fig. 3C). To confirm that the tip of White Pekin duck spermatozoa actually contains mitochondria, we stained the freshly collected live spermatozoa with JC-1 dye and imaged the JC1 dye-labeled live spermatozoa under confocal microscope. We noted that JC-1 stained both the midpiece and the tip of the head confirming that the tip actually contains functional mitochondria (Fig. 3E). The JC1 staining was completely diminished (both in tip as well as in neck regions) when live sperm cells were treated with the CCCP, an agent which is known to work as mitochondrial uncoupler (Fig. 3F). Taken together, these results strongly indicate that the tip of the sperm head contains mitochondria with high oxidative potential.

Duck sperm head contains lipid based yet Triton X-100 resistant acrosome-like structures

Acrosomal structures are known to contain several glycoproteins which can be detected by specific lectins. To characterize the nature of the acrosome-like tip of duck spermatozoa in details, we stained it with the conventional acrosome marker namely FITC-PNA (Horrocks *et al.*, 2000; Ashizawa *et al.*, 2006). Although FITC-PNA faithfully stained the acrosome of Bull spermatozoa, it failed to react with the acrosome-like tip of White Pekin duck spermatozoa (Fig. 4). This indicates that the acrosomal tip of White Pekin duck spermatozoa is not enriched with the specific carbohydrates generally observed in almost all mammals.

Next we probed for the enrichment of lipids at the acrosome-like structures by staining the spermatozoa with lipid-sensitive dye DiI. While the entire head of the duck spermatozoa showed DiI labeling, the acrosomal tip displayed a very strong labeling (Fig. 5). Next we tested the biochemical extraction property of this structure against detergents. We noted that this lipid-enriched acrosome-like structure is partially resistant to extraction by ionic detergent such as 0.1% Triton X100 (Fig. 5). As acrosomal regions of mammalian spermatozoa are enriched with cholesterol, we tested the distribution and enrichment of cholesterol in the duck spermatozoa too. For that purpose, we stained the duck spermatozoa with cholesterol sensor dye Filipin, which binds to cholesterol (Börnig & Geyer, 1974). We noted Filipin labeling at the entire head of the duck spermatozoa. However, the tip of duck spermatozoa remained devoid of Filipin staining, indicating that this region is not cholesterol enriched (Fig. 6). Also, we noted that the extraction of cells with 0.1% Triton X100 results in decreased intensity of Filipin staining all over the head regions. However, we also noted that even after 0.1% Triton X100 treatment, the shape of the tip, that is, the acrosome-like structure remains intact (Fig. 6).

Duck spermatozoa contains different post-translationally modified tubulins

To understand the molecular details of the duck spermatozoa, we immunostained the sperm cells with different post-translationally modified tubulins, namely with tyrosinated tubulin, de-tyrosinated tubulin, acetylated tubulin, polyglutamylated tubulin, mono- and polyglycylated tubulin. These post-

Figure 3 White Pekin duck sperm tip contains atypical mitochondria-like organelle. (A) Confocal images of a duck spermatozoa labeled with anti-ATP5A (green) and Mitotracker-Red (Red). The enlarged portion of its head is shown in right side. The tip structure is indicated by an arrow. (B) Confocal images of a duck spermatozoa labeled with anti-Mfn2 (green) and DAPI. The enlarged portion of its head is shown in right side. The staining at tip region is indicated by arrows. (C) Confocal images of the midpiece and head of White Pekin duck spermatozoa stained with Mitotracker-Red (Red) and Alexa flour 488 conjugated streptavidin (Green). DNA-enriched region is counterstained with DAPI (blue). (D) Intensity plot (of the same cell as shown in C) corresponding to white arrow region (shown in right side) is shown. Both Mitotracker-Red and Alexa flour 488 conjugated streptavidin co-localize well at the midpiece and also at the tip of the head. (E) Confocal images of the head portion (upper panel) and the enlarged portion of the tip (lower panel) of the live spermatozoa labeled with JC1 dye (green) are shown. The tip of the sperm head (indicated by blue arrow) revels specific labeling with JC1 dye. (F) Application of CCCP to the live sperm cell results in loss of JC1 dye staining. Intensity of JC1 fluorescence in the presence and absence of CCCP is provided in right side.

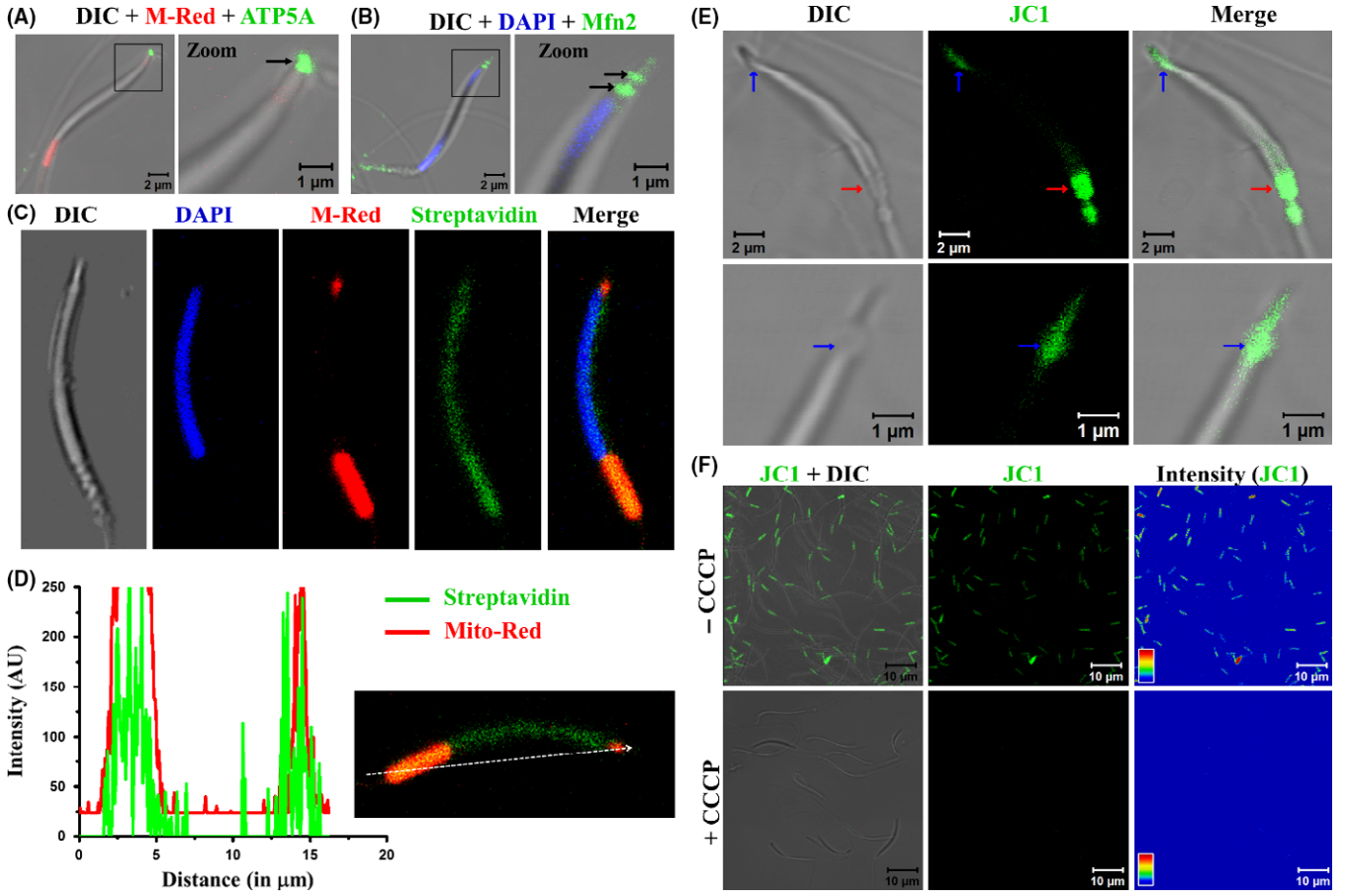

Figure 4 White Pekin duck sperm acrosome-like tip is unreactive to conventional acrosome marker PNA (A). Confocal images of Duck sperm cells stained with the conventional acrosome marker FITC-PNA (green) and counterstained with DAPI (Blue). (B) Enlarged confocal image of FITC-PNA (green) and DAPI (blue) labeled single acrosome-like structure if duck spermatozoa. Scale bar 1 μm. (C) Confocal image of a cluster of mammalian sperm (bovine sperm) cells labeled with FITC-PNA (green) is shown. Scale bar 10 μm.

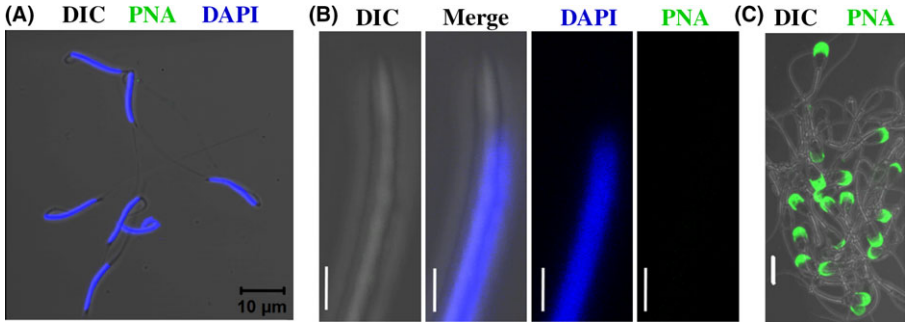

translationally modified tubulins were primarily detected at the tail regions (Fig. 7). By confocal microscopy, we could detect a faint expression of tyrosinated tubulin at the tail region. However, same antibody fails to detect the presence of tyrosinated tubulin in the White Pekin duck spermatozoa extract by western blot analysis (Fig. 7A, lane 1), although the same antibody could detect the tyrosinated tubulin present at the goat brain extract on the same blot (Fig. 7A, lane 2). This in general suggest low abundance of tyrosinated tubulin. Next we probed for detyrosinated tubulin and we have used two different antibodies. Both

Figure 5 Acrosome-like tip of duck spermatozoa is enriched with lipids. Confocal images of White Pekin duck sperm cells stained with DAPI (blue) and lipid-sensitive dye DiI (red). The DiI staining appears to be mildly resistant against 0.1% Triton X-100 extraction. Scale bar 1 μm.

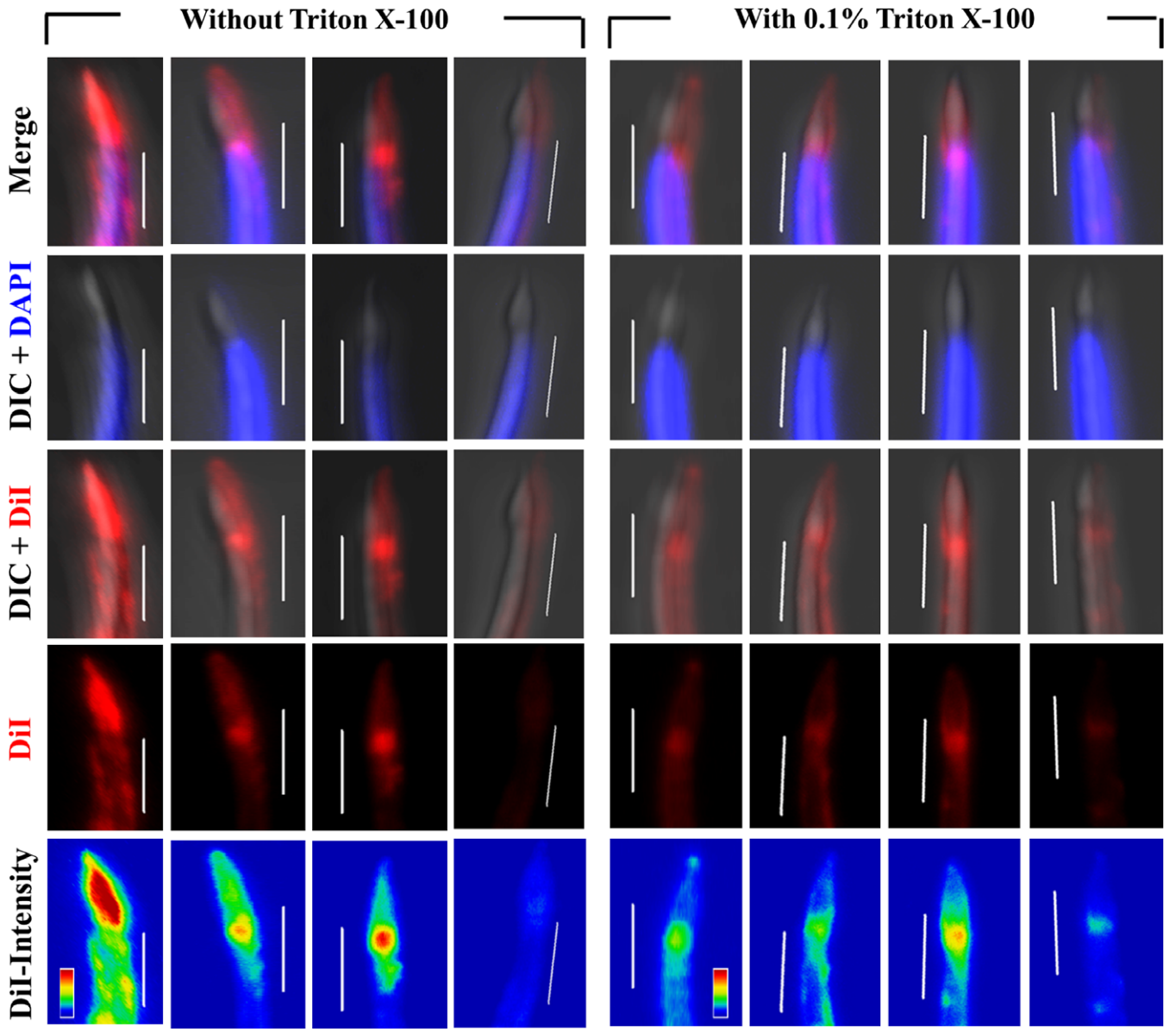

antibodies strongly stained the tail region (Fig. 7B). Western blot analysis also confirms the presence of detyrosinated tubulin in the duck spermatozoa. As tyrosinated tubulin is used as a substrate to form detyrosinated tubulin in a biochemical pathway, the presence of detyrosinated tubulin confirms the presence of tyrosinated tubulin and the existence of the regulatory enzymes as well (MacRae, 1997; Westermann & Weber, 2003). Next, we probed for acetylated tubulin which is present exclusively in the tail and below the midpiece region (Fig. 7C). The presence of acetylated tubulin is also confirmed by western blot analysis. Similarly, polyglutamylated tubulin is present at the tail region and also to some extent in the head region. The midpiece region is exclusively devoid of polyglutamylated tubulin (Fig. 7D). Western blot analysis detect bands at ~55 kD size confirming the presence of polyglutamylated tubulin in duck spermatozoa. Next, we probed for monoglycylated tubulin (detected by TAP952 antibody) and polyglycylated tubulin (detected by AXO49 antibody). Monoglycylated tubulin is exclusively present the tail region and its intensity gradually increased toward the end-tip of the sperm tail (Fig. 7E). Polyglycylated tubulin also shows strong staining in the middle region of sperm tail, but is not enriched at the tail end region (Fig. 7F). The presence of both mono- and polyglycylated tubulin was confirmed by western blot analysis. Taken together our results present morphological and molecular details of the White Pekin duck sperm cells.

DISCUSSION

The morphometry and molecular details of sperm cells of any organism is an indicator of several relevant factors such as reproductive uniqueness, energetics, adaptation, evolution, speciation, population structure, male-female ratio, and other complex behaviors (Korn *et al.*, 2000; Bjork & Pitnick, 2006; Bjork

Figure 6 White Pekin duck sperm head but not the acrosome-like tip structure is enriched with cholesterol. Confocal images of duck sperm cells stained for cholesterol sensing dye Filipin (light blue). Extraction of cells with 0.1% TritonX-100 leads to partial loss of Filipin staining. Notably, the acrosome-like tip structure of duck spermatozoa lacks Filipin staining and remains intact even upon permeabilization by 0.1% Triton X-100. Scale bar 1 μm.

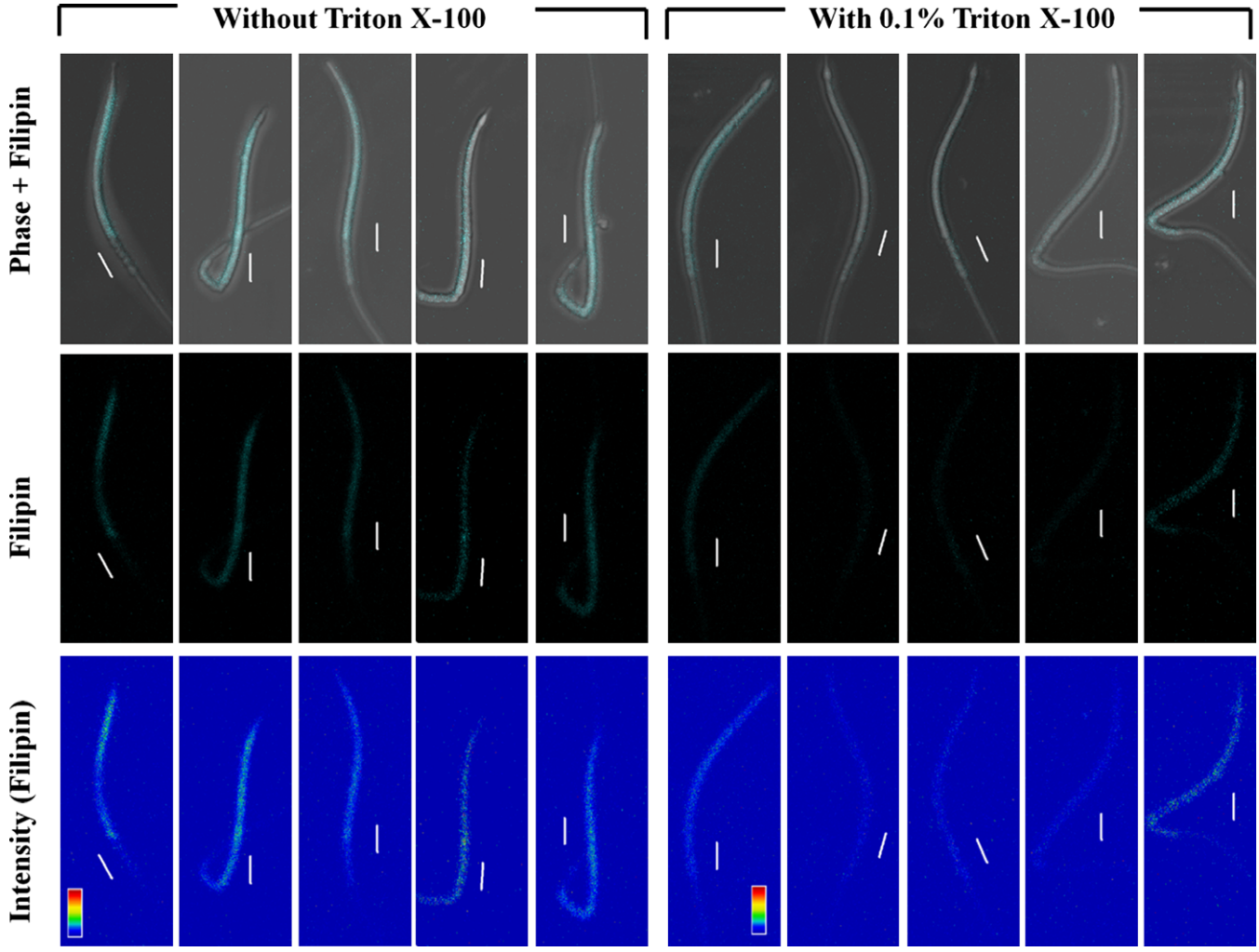

et al., 2007; Immler & Birkhead, 2007; Immler *et al.*, 2007; Lattao *et al.*, 2012; Rowe *et al.*, 2013). In this work, we have performed a series of microscopic and biochemical analysis to elucidate the fine structural and molecular details of the matured haploid male gamete cells obtained from White Pekin duck. These analysis opens up several novel aspects of the sperm cells from this species, such as the presence of a acrosome-like structure at the sperm head, the presence of biforked nucleus, the presence of atypical mitochondria at the head tip and also the presence of different post-translationally modified tubulins. In addition, our studies indicate that the distribution of mitochondrial markers seem to be atypical in avian spermatozoa, an observation that needs further in-depth analysis. We propose that these aspects can also be used as authentic species-specific features.

PNA is a lectin which binds to glycosylated molecules which have the sugar sequence Gal-β(1-3)-GalNAc and is routinely used as an acrosomal marker to detect the acrosome of mammalian spermatozoa (Apostolski *et al.*, 1994). In addition, PNA reactivity has also been reported for certain avian spermatozoa also (Horrocks *et al.*, 2000). In this work, we demonstrated that the white duck sperm cells contain an acrosome-like structure which is visible in FE-SEM images, but not properly visible in DIC. This structure is enriched with lipids, but essentially devoid of cholesterol. This structure does not react also with PNA. Another lectin, IB4 also fails to detect this structure. This structure is likely to be the acrosome, however, it does not match exactly with the typical shape of the acrosome reported from avian species so far (Tingari, 1973; Bakst & Howarth, 1975; Korn *et al.*, 2000).

The typical structure analogous to an acrosomal rod, or perforatorium, has been described for the spermatozoa of many non-passerine birds (Phillips & Asa, 1989; Soley, 1993; Aire, 2003). The perforatorium is a solid, well-defined structure housed inside a posterior nuclear invagination and covered anteriorly by the acrosome. Although the function of the avian perforatorium is not yet understood, it is reported in several birds (Soley, 1993). In this work, we demonstrate that the tip of this perforatorium structure contains some organelles that have properties which are similar to mitochondria. Unlike the spindle-shaped perforatoriums reported in other avian spermatozoa, the structure which we refer as 'atypical mitochondria' starts from the point of nuclear bifurcation and ends at the tip by forming a bulbous structure. This is particularly important as it indicates that these sub-cellular structure located at the

Figure 7 White Pekin duck spermatozoa contains different modified tubulins. (A) A trace amount of Tyrosinated tubulin occurs exclusively in the end portion of the sperm tail. Western blot analyses with this Mouse monoclonal anti-tyrosinated tubulin (Tub 1A2 antibody) is shown in the right side. Goat brain extract (lane 2) contains abundant amount, whereas the duck sperm cell extract (lane 1) has undetectable amount of tyrosinated tubulin. (B) Detyrosinated tubulin is exclusively present in the tail of duck spermatozoa. Western blot analysis with this mouse monoclonal antibody detects a strong band at 55 kDa. (C) A rabbit polyclonal antibody against detyrosinated tubulin (Glu form) also detects detyrosinated tubulin exclusively in the tail and detects a faint band at 55 kDa. (D) Acetylated tubulin occurs exclusively in the tail. (E) Polyglutamylated tubulin is present in the tail as well as in the head regions. (F) Monoglycylated tubulin (detected by TAP952 antibody) occurs exclusively in the end portion of the sperm tail. (G) Polyglycylated tubulin (detected by AXO49 antibody) occurs faintly at the middle region of sperm tail. Western blot analyses of the sperm cell extract (lane 1) against all these specific antibodies are shown in the right side.

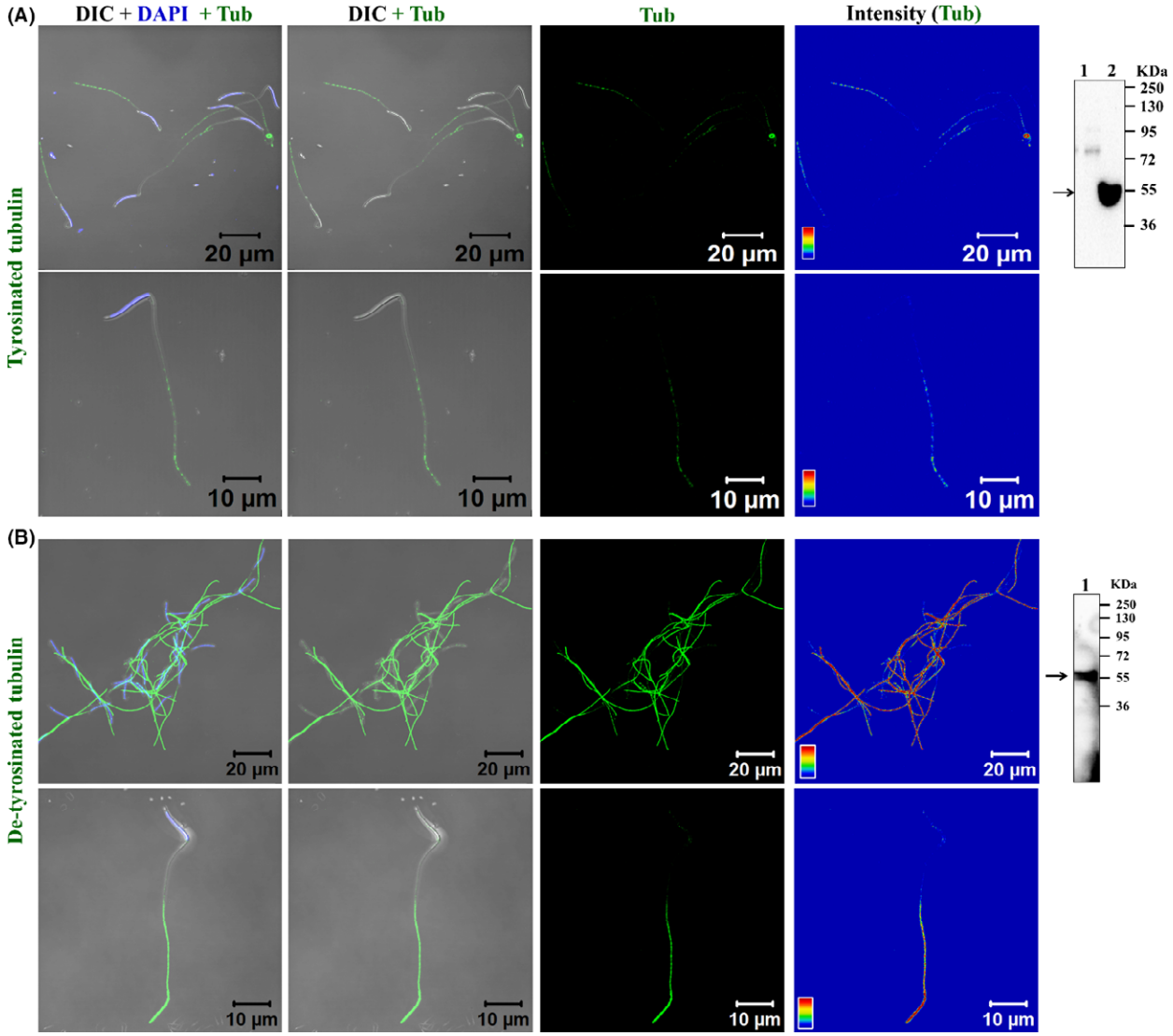

tip has high membrane potential (as indicated by Mitotracker-Red and JC-1 staining), and reactivity to streptavidin, properties which are similar to the mitochondria. Based on these labeling properties, this structure can actually be considered as atypical mitochondria. Our attempts to confirm this structure directly with antibodies developed against conventional mitochondrial markers such as HSP60, Cytochrome-C were unsuccessful as these antibodies were unreactive to duck spermatozoa (failed to detect this tip structure as well as the midpiece of the duck spermatozoa). This could be mostly because of mismatching epitopes as well, because the same antibody detects Cytochrome-C present in the mitochondria of mature murine spermatozoa (Hess *et al.* 1993). However, two other antibodies developed against Mitofusin2 and F1F0 ATP synthase or Complex-V can label the tip structure. The staining patterns of these mitochondrial markers seem to be specific and are indicator of mitochondrial complexity present in duck as well as other mammalian sperm cells. For example, HSP60 has been reported to be present in the mitochondrial region of several mammalian spermatozoa (Volpe *et al.* 2008). However, HSP60 could not be detected in mature mouse spermatozoa (Asquith *et al.* 2004) while it is located exclusively at the acrosomal region of the head in capacitated mouse spermatozoa (Asquith *et al.* 2005). Mitofusin2 has been shown to be present in head and neck of murine spermatozoa (Vadnais *et al.* 2014) and at the neck of boar spermatozoa (Ramió-Lluch *et al.* 2012). ATP5A has been shown to be present in the neck of bull spermatozoa (Yaffe *et al.* 2014). Notably, Mitofusin2 and ATP5A are exclusively absent in

Figure 7 Continued

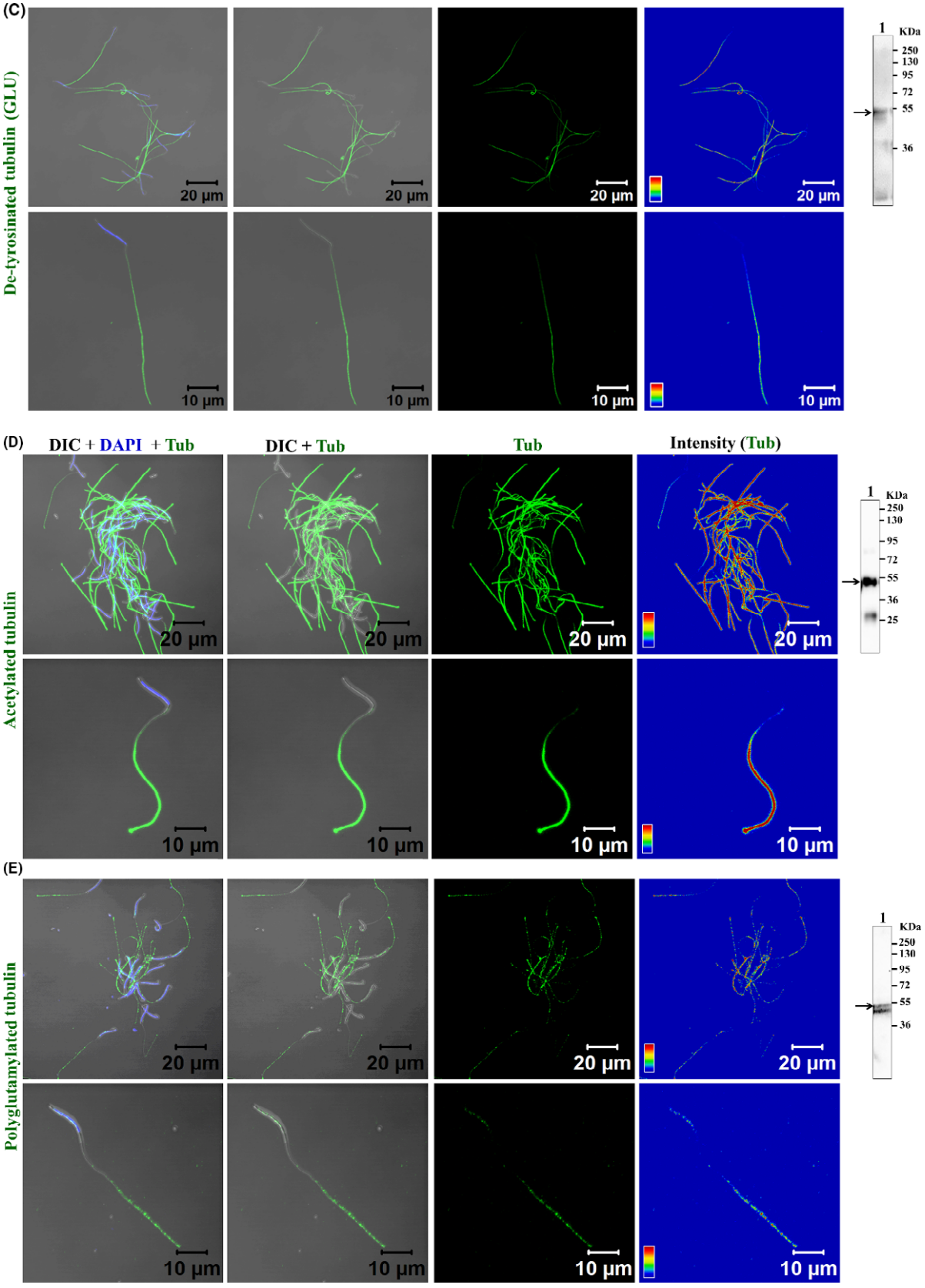

neck mitochondrial region and present in head and tail (as well as tip) of duck spermatozoa. However, the functional implication of these atypical mitochondria located at the head tip is not clear and further in-depth studies are essential. Distribution of mitochondrial markers in avian spermatozoa is also very complex and needs further in-depth analysis.

Figure 7 Continued

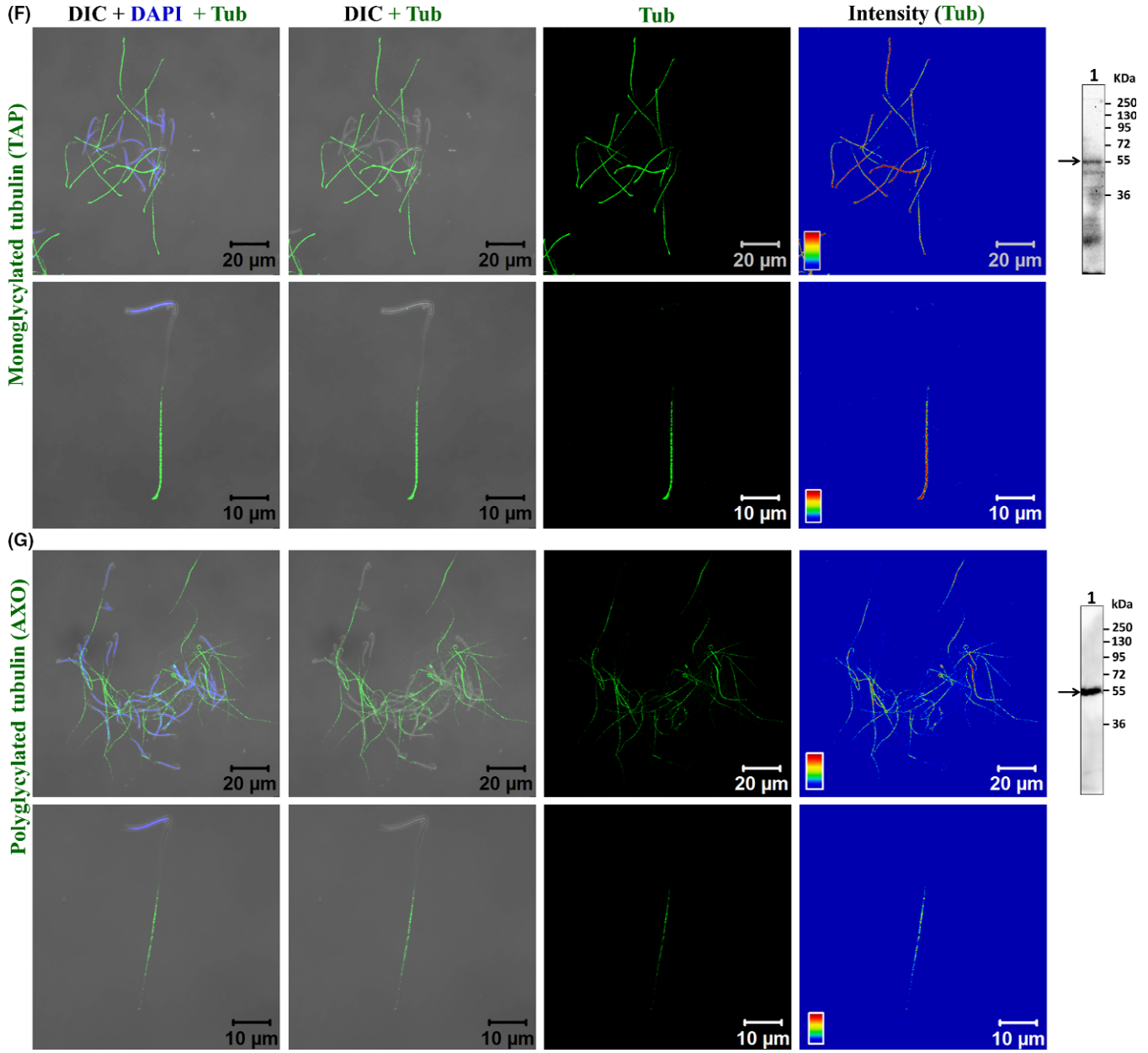

The mitochondria at the midpiece of non-passerine birds also demonstrate a wide variety of shapes (Soley, 1993). In the domestic duck ultrastructure reported recently (Simões *et al.*, 2012), the mitochondria are elliptical and contain a dense matrix and longitudinal cristae. Only 11–12 mitochondria were observed in the domestic duck, which is relatively shorter compared with those of other avian species like quail (Korn *et al.*, 2000; Simões *et al.*, 2012). According to Fawcett (1970), the number of mitochondria in sauropsid spermatozoa indicates the phylogenetic position of the species from which they originated (Fawcett, 1970). We noted that in White Pekin duck, the unit number of mitochondrial coiling is less and varies within 6–12. Although glycolysis is the major source of energy for spermatozoa, according to a general consensus, it is also considered that the number of mitochondria correlates well with the overall energy requirement by the spermatozoa (Piomboni *et al.*, 2012). Therefore, the less number of mitochondrial in duck spermatozoa may indicate that the duck spermatozoa require less energy for flagellar movement compared with other avian species such as Japanese quail during their locomotion in the female reproductive track (Lake *et al.*, 1968; Marquez & Ogasawara, 1975; Thurston & Hess, 1987; Phillips & Asa, 1989; Baccetti *et al.*, 1991; Soley, 1993, 1994; Vernon & Woolley, 1999; Korn *et al.*, 2000).

In this work, we demonstrate that the tip of the nucleus is bifurcated as visualized by DAPI stained using SR-SIM as a technique. The bifurcated nucleus at the sperm tip region is a characteristic feature observed in several non-passerine birds, namely in Fowl, Cock, and Quail (Tingari, 1973; Bakst & Howarth, 1975; Korn *et al.*, 2000). Therefore, the bifurcated nucleus confirms the phylogenetic linkage of this species. However, in past such bifurcations has been detected by analyzing sperm cells by transmission electron microscopy only. This is

the first report demonstrating such ultrastructure by using laser-based technology, namely by SR-SIM.

The presence or absence of different post-translationally modified tubulins is an indicator of several molecular complexities including the cascade of enzymatic activities and the bio-physical properties of the cellular microtubules (Gundersen *et al.*, 1984; Kreis, 1987; Wehland & Weber, 1987; MacRae, 1997; Plessmann & Weber, 1997; Kierszenbaum, 2002; Westermann & Weber, 2003; Hoyle *et al.*, 2008). In this work, we demonstrate that the majority of the sperm cells from White Pekin duck contain different post-translationally modified tubulins, namely acetylated tubulin, polyglutamylated tubulin, and to a lesser extent tyrosinated tubulin. The acetylated tubulin and polyglutamylated tubulin are considered to be a part of stable microtubules (particularly resistant against high concentration of Ca^{2+}, low-temperature, and other destabilizing agents), whereas the tyrosinated tubulin is considered to be the part of dynamic microtubule and susceptible to higher levels of cytosolic Ca^{2+} (Karr *et al.*, 1980; Job *et al.*, 1981; Lieuvin *et al.*, 1994). Therefore, ample staining of sperm cells for acetylated and polyglutamylated tubulin and limited staining for tyrosinated tubulin in general indicates that the mature spermatozoa from White Pekin duck probably experience conditions such as high levels of cytosolic Ca^{2+} which destabilize axonemal microtubules. In this regard, it is important to mention that detyrosination and acetylation of tubulin are important for assembly of sperm tail, whereas polyglutamylation and polyglycylation are important for the propagation of tail wave (Huitorel *et al.*, 2002). Polyglutamylated tubulin has also been shown as important factor for sperm motility (Gagnon *et al.*, 1996).

Our observation, that is, the presence of a bifurcated nucleus and specific positioning of some mitochondrial organelle in the tip head of almost all mature sperm cells suggest a possible mixture of paternal mitochondria to the ova during fertilization. Such a possibility strongly suggests the contribution of mitochondrial genome from paternal side also and possibilities of mitochondrial heteroplasmy in the subsequent generations and essentially in the entire species. Contribution of mitochondria from paternal side, that is, through spermatozoa has also been documented in different species, both in plant kingdom and animal kingdom as well as in several fungal systems. In particular, it has been documented in pine tree, bladder campion plant (*Silene vulgaris*), in lower eukaryotes such as in bees (*Hawaiian hylaeus*, Nesoprosopis), blue mussel (*Mytilus edulis*), European flat oyster (*Ostrea edulis*), mollusks (Ruditapes philippinarum), lower vertebrates such as in fish (*Amia calva*, bowfin; Amiiformes, Amiidae), in frogs (*Hyla cinerea*, green tree frog; Anura, Hylidae, and *Hyla gratiosa*, barking tree frog), in Australian frillneck lizard (*Chlamydosaurus kingie*) (Bermingham *et al.*, 1986; Wu *et al.*, 1998; Cao *et al.*, 2004; Ujvari *et al.*, 2007; Taris *et al.*, 2009; Magnacca & Brown, 2010; Milani *et al.*, 2011). Mitochondrial heteroplasmy has also been reported in higher vertebrates such as in, sheep (*Ovis aries*), non-human primate (*Macaca mulatta*), and also in human (Ankel-Simons & Cummins, 1996; Schwartz & Vissing, 2002; St John & Schatten, 2004; Zhao *et al.*, 2004). Indeed, our observations are in line with these several recent reports which suggest the complexity of the bird mitochondrial genome and/or possible mitochondrial heteroplasmy in several avian species (Mundy *et al.*, 1996; Berlin & Ellegren, 2001; Berlin *et al.*, 2004; Marais, 2007; Hogner *et al.*, 2012). This type of mitochondria at the head tip may also be selected for some special and unconventional purposes such as iron metabolism or contribution of special regulatory RNAs from paternal mitochondria to the ova (Hales, 2010; Kumar *et al.*, 2013). However, such a possibility needs to be verified further by a more direct approach in future. In summary, the detailed morphological and molecular understandings of the spermatozoa of White Pekin duck may have importance in several sectors such as in poultry production, conservation of species by cryopreservation of male gametes, and assessing cytotoxicity against different treatments. Such understandings may also help the artificial insemination program to improve the economically viable breeds for poultry industry as well.

ACKNOWLEDGMENTS

Intramural support from NISER, Bhubaneswar is appreciated. The authors appreciate the Confocal and FE-SEM imaging facility of NISER and thank Nirlipta Swain and Pravakar Mallick (NISER) for helping with FE-SEM imaging. The authors are grateful to Zeiss-India (Bangalore) for extending their SR-SIM imaging facility for this work. We thank Dr. Suryakant Mishra (Director, CARI Regional Centre, Bhubaneswar) for extending his support for this work. Animal facility of CARI, Bhubaneswar is appreciated. We thank Dr. Richa Ricky (IISER, Pune) for providing Alexa-fluor 488 conjugated streptavidin.

REFERENCES

Aire TA. (2003) Ultrastructural study of spermiogenesis in the turkey, *Meleagris gallopavo*. *Br Poult Sci* 44, 674–682.

Ankel-Simons F & Cummins JM. (1996) Misconceptions about mitochondria and mammalian fertilization: implications for theories on human evolution. *Proc Natl Acad Sci U S A* 93, 13859–13863.

Apostolski S, Sadiq SA, Hays A, Corbo M, Suturkova-Milosevic L, Chaliff P, Stefansson K, Lebaron RG, Ruoslahti E, Hays AP & Latov N. (1994) Identification of Gal(beta 1-3)GalNAc bearing glycoproteins at the nodes of Ranvier in peripheral nerve. *J Neurosci Res* 38, 134–141.

Ashizawa K, Wishart GJ, Katayama S, Takano D, Ranasinghe ARAH, Narumi K & Tsuzuki Y. (2006) Regulation of acrosome reaction of fowl spermatozoa: evidence for the involvement of protein kinase C and protein phosphatase-type 1 and/or -type 2A. *Reproduction* 131, 1017–1024.

Asquith KL, Baleato RM, McLaughlin EA, Nixon B & Aitken RJ. (2004) Tyrosine phosphorylation activates surface chaperones facilitating sperm–zona recognition. *J Cell Sci* 117, 3645–3657.

Asquith KL, Harman AJ, McLaughlin EA, Nixon B & Aitken RJ. (2005) Localization and significance of molecular chaperones, heat shock protein 1, and tumor rejection antigen gp96 in the male reproductive tract and during capacitation and acrosome reaction. *Biol Reprod* 72, 328–337.

Baccetti B, Bigliardi E & Burrini AG. (1980) The morphogenesis of vertebrate perforatorium. *J Ultrastruct Res* 71, 272–287.

Baccetti B, Burrini AG & Falchetti E. (1991) Spermatozoa and relationships in Palaeognath birds. *Biol Cell* 71, 209–216.

Bakst MR & Howarth B. (1975) The head, neck and midpiece of cock spermatozoa examined with the transmission electron microscope. *Biol Reprod* 12, 632–640.

Berlin S & Ellegren H. (2001) Evolutionary genetics. Clonal inheritance of avian mitochondrial DNA. *Nature* 413, 37–38.

Berlin S, Smith NG & Ellegren H. (2004) Do avian mitochondria recombine? *J Mol Evol* 58, 163–167.

Bermingham E, Lamb T & Avise JC. (1986) Size polymorphism and heteroplasmy in the mitochondrial DNA of lower vertebrates. *J Hered* 77, 249–252.

Bjork A & Pitnick S. (2006) Intensity of sexual selection along the anisogamy-isogamy continuum. *Nature* 441, 742–745.

Bjork A, Dallai R & Pitnick S. (2007) Adaptive modulation of sperm production rate in *Drosophila bifurca*, a species with giant sperm. *Biol Lett* 3, 517–519.

Börnig H & Geyer G. (1974) Staining of cholesterol with the fluorescent antibiotic 'filipin'. *Acta Histochem* 50, 110–115.

Breucker H. (1982) Seasonal spermatogenesis in the mute swan (*Cygnus olor*). *Anat Embryol Cell Biol* 72, 1–91.

Briskie JV, Montgomerie R & Birkhead TR. (1997) The evolution of sperm size in birds. *Evolution* 51, 937–945.

Cao L, Kenchington E & Zouros E. (2004) Differential segregation patterns of sperm mitochondria in embryos of the blue mussel (*Mytilus edulis*). *Genetics* 166, 883–894.

Fawcett DW. (1970) A comparative view of sperm ultrastructure. *Biol Reprod* 2, 90–127.

Gagnon C, White D, Cosson J, Huitorel P, Eddé B, Desbruyères E, Paturle-Lafanechère L, Multigner L, Job D & Cibert C. (1996) The polyglutamylated lateral chain of alpha-tubulin plays a key role in flagellar motility. *J Cell Sci* 109, 1545–1553.

Gundersen GG, Kalnoski MH & Bulinski JC. (1984) Distinct populations of microtubules: tyrosinated and nontyrosinated alpha tubulin are distributed differently in vivo. *Cell* 38, 779–789.

Hales KG. (2010) Iron testes: sperm mitochondria as a context for dissecting iron metabolism. *BMC Biol* 8, 79.

Hess RA, Miller LA, Kirby JD, Margoliash E & Goldberg E. (1993) Immunoelectron microscopic localization of testicular and somatic cytochromes c in the seminiferous epithelium of the rat. *Biol Reprod* 48, 1299–1308.

Hogner S, Laskemoen T, Lifjeld JT, Porkert J, Kleven O, Albayrak T, Kabasakal B & Johnsen A. (2012) Deep sympatric mitochondrial divergence without reproductive isolation in the common redstart *Phoenicurus phoenicurus*. *Ecol Evol* 2, 2974–2988.

Hollinshead M, Sanderson J & Vaux DJ. (1997) Anti-biotin antibodies offer superior organelle-specific labeling of mitochondria over avidin or streptavidin. *J Histochem Cytochem* 45, 1053–1057.

Horrocks AJ, Stewart S, Jackson L & Wishart GJ. (2000) Induction of acrosomal exocytosis in chicken spermatozoa by inner perivitelline-derived N-linked glycans. *Biochem Biophys Res Commun* 278, 84–89.

Hoyle HD, Turner FR & Raff EC. (2008) Axoneme-dependent tubulin modifications in singlet microtubules of the Drosophila sperm tail. *Cell Motil Cytoskeleton* 65, 295–313.

Huitorel P, White D, Fouquet JP, Kann ML, Cosson J & Gagnon C. (2002) Differential distribution of glutamylated tubulin isoforms along the sea urchin sperm axoneme. *Mol Reprod Dev* 62, 139–148.

Humphreys PN. (1972) Brief observations on the semen and spermatozoa of certain passerine and non-passerine birds. *J Reprod Fertil* 29, 327–336.

Immler S & Birkhead TR. (2007) Sperm competition and sperm midpiece size: no consistent pattern in passerine birds. *Proc Biol Sci* 274, 561–568.

Immler S, Saint-Jalme M, Lesobre L, Sorci G, Roman Y & Birkhead TR. (2007) The evolution of sperm morphometry in pheasants. *J Evol Biol* 20, 1008–1014.

Job D, Fischer EH & Margolis RL. (1981) Rapid disassembly of cold-stable microtubules by calmodulin. *Proc Natl Acad Sci U S A* 78, 4679–4682.

Karr TL, Kristofferson D & Purich DL. (1980) Calcium ion induces endwise depolymerization of bovine brain microtubules. *J Biol Chem* 255, 11853–11856.

Kierszenbaum AL. (2002) Sperm axoneme: a tale of tubulin posttranslation diversity. *Mol Reprod Dev* 62, 1–3.

Korn N, Thurston RJ, Pooser BP & Scott TR. (2000) Ultrastructure of spermatozoa from Japanese quail. *Poult Sci* 79, 407–414.

Kreis TE. (1987) Microtubules containing detyrosinated tubulin are less dynamic. *EMBO J* 6, 2597–2606.

Kumar M, Kumar K, Jain S, Hassan T & Dada R. (2013) Novel insights into the genetic and epigenetic paternal contribution to the human embryo. *Clinics (Sao Paulo)* 68, 5–14.

Laemmli UK. (1970) Cleavage of structural proteins during the assembly of the head of bacteriophage T4. *Nature* 227, 680–685.

Lake PE, Smith W & Young D. (1968) The ultrastructure of the ejaculated fowl spermatozoon. *Exp Physiol* 53, 356–366.

Lattao R, Bonaccorsi S & Gatti M. (2012) Giant meiotic spindles in males from *Drosophila* species with giant sperm tails. *J Cell Sci* 125, 584–588.

Leite TG, do Vale Filho VR, de Arruda RP, de Andrade AF, Emerick LL, Zaffalon FG, Martins JA & de Andrade VJ. (2010) Effects of extender and equilibration time on post-thaw motility and membrane integrity of cryopreserved Gyr bull semen evaluated by CASA and flow cytometry. *Anim Reprod Sci* 120, 31–38.

Lieuvin A, Labbe JC, Doree M & Job D. (1994) Intrinsic microtubule stability in interphase cells. *J Cell Biol* 124, 985–996.

MacRae TH. (1997) Tubulin post-translational modifications – enzymes and their mechanisms of action. *Eur J Biochem* 244, 265–278.

Magnacca KN & Brown MJ. (2010) Mitochondrial heteroplasmy and DNA barcoding in Hawaiian Hylaeus (Nesoprosopis) bees (*Hymenoptera: Colletidae*). *BMC Evol Biol* 10, 174.

Majhi RK, Kumar A, Yadav M, Swain N, Kumari S, Saha A, Pradhan A, Goswami L, Saha S, Samanta L, Maity A, Nayak TK, Chattopadhyay S, Rajakuberan C, Kumar A & Goswami C. (2013) Thermosensitive ion channel TRPV1 is endogenously expressed in the sperm of a fresh water teleost fish (*Labeo rohita*) and regulates sperm motility. *Channels (Austin)* 7, 1–10.

Marais GA. (2007) The Hill-Robertson effects extend from nucleus to mitochondria. *Heredity (Edinb)* 99, 357–358.

Marquez BJ & Ogasawara FX. (1975) Scanning electron microscope studies of turkey semen. *Poult Sci* 54, 1139–1142.

McFarlane RW. (1963) The taxonomic significance of avian sperm. In: *Proceedings of the XIIIth International Ornithological Congress* 11, pp. 91–102.

Milani L, Ghiselli F, Maurizii MG & Passamonti M. (2011) Doubly uniparental inheritance of mitochondria as a model system for studying germ line formation. *PLoS ONE* 6, e28194.

Mossman J, Slate J, Humphries S & Birkhead T. (2009) Sperm morphology and velocity are genetically codetermined in the zebra finch. *Evolution* 63, 2730–2737.

Mundy NI, Winchell CS & Woodruff DS. (1996) Tandem repeats and heteroplasmy in the mitochondrial DNA control region of the loggerhead shrike (*Lanius ludovicianus*). *J Hered* 87, 21–26.

Phillips DM & Asa CS. (1989) Development of spermatozoa in the Rhea. *Anat Rec* 223, 276–282.

Piomboni P, Focarelli R, Stendardi A, Ferramosca A & Zara V. (2012) The role of mitochondria in energy production for human sperm motility. *Int J Androl* 35, 109–124.

Plessmann U & Weber K. (1997) Mammalian sperm tubulin: an exceptionally large number of variants based on several posttranslational modifications. *J Protein Chem* 16, 385–390.

Rowe M, Laskemoen T, Johnsen A & Lifjeld JT. (2013) Evolution of sperm structure and energetics in passerine birds. *Proc Biol Sci.* 280, 20122616. doi:10.1098/rspb.2012.2616.

Ramió-Lluch L, Fernández-Novell JM, Peña A, Bucci D, Rigau T & Rodríguez-Gil JE. (2012) "In vitro" capacitation and subsequent acrosome reaction are related to changes in the expression and location of midpiece actin and mitofusin-2 in boar spermatozoa. *Theriogenology* 77, 979–988.

Schwartz M & Vissing J. (2002) Paternal inheritance of mitochondrial DNA. *N Engl J Med* 347, 576–580.

Simões K, Orsi AM & Artoni SM. (2012) Ultrastructure of the spermatozoa of the domestic duck (*Anas platyrhynchos* sp.). *Anat Histol Embryol* 41, 202–208.

Soley JT. (1993) Ultrastructure of ostrich (*Struthio camelus*) spermatozoa: transmission electron microscopy. *Onderstepoort J Vet Res* 60, 119–130.

Soley JT. (1994) Centriole development and formation of the flagellum during spermiogenesis in the ostrich (*Struthio camelus*). *J Anat* 185, 301–313.

St John JC & Schatten G. (2004) Paternal mitochondrial DNA transmission during nonhuman primate nuclear transfer. *Genetics* 167, 897–905.

Sugii S, Reid PC, Ohgami N, Shimada Y, Maue RA, Ninomiya H, Ohno-Iwashita Y & Chang TY. (2003) Biotinylated theta-toxin derivative as a probe to examine intracellular cholesterol-rich domains in normal and Niemann-Pick type C1 cells. *J Lipid Res* 44, 1033–1041.

Taris N, Boudry P, Bonhomme F, Camara MD & Lapègue S. (2009) Mitochondrial and nuclear DNA analysis of genetic heterogeneity among recruitment cohorts of the European flat oyster *Ostrea edulis*. *Biol Bull* 217, 233–241.

Thurston RJ & Hess RA. (1987) Ultrastructure of spermatozoa from domesticated birds: comparative study of turkey, chicken and guinea fowl. *Scanning Microsc* 1, 1829–1838.

Tingari MD. (1973) Observations on the fine structure of spermatozoa in the testis and excurrent ducts of the male fowl, gallus domesticus. *J Reprod Fertil* 34, 255–265.

Ujvari B, Dowton M & Madsen T. (2007) Mitochondrial DNA recombination in a free-ranging Australian lizard. *Biol Lett* 3, 189–192.

Vadnais ML, Lin AM & Gerton GL. (2014) Mitochondrial fusion protein MFN2 interacts with the mitostatin-related protein MNS1 required for mouse sperm flagellar structure and function. *Cilia* 3, 5. doi: 10.1186/2046-2530-3-5. eCollection 2014.

Vernon GG & Woolley DM. (1999) Three-dimensional motion of avian spermatozoa. *Cell Motil Cytoskeleton* 42, 149–161.

Volpe S, Galeati G, Tamanini C, Mari G, Zambelli D & Spinaci M. (2008) Comparative immunolocalization of heat shock proteins Hsp60, Hsp70, Hsp90 in boar, stallion, dog and cat spermatozoa. *Reprod Domest Anim* 43, 385–392.

Wehland J & Weber K. (1987) Turnover of the carboxy-terminaltyrosine of alpha-tubulin and means of reaching elevated levels of detyrosination in living cells. *J Cell Sci* 88, 185–203.

Westermann S & Weber K. (2003) Post-translational modifications regulate microtubule function. *Nat Rev Mol Cell Biol* 4, 938–947.

Wu J, Krutovskii KV & Strauss SH. (1998) Abundant mitochondrial genome diversity, population differentiation and convergent evolution in pines. *Genetics* 150, 1605–1614.

Yaffe E, Hikri E, Elkis Y, Cohen O, Segal A, Makovski A, Varvak A, Shpungin S & Nir U. (2014) Oncogenic properties of a spermatogenic meiotic variant of fer kinase expressed in somatic cells. *Cancer Res* 74, 6474–6485.

Yasuzumi G & Sugioka T. (1971) Spermatogenesis in animals as revealed by electron microscopy. Microkaryosomes and microtubules appearing during spermatogenesis of the lovebird, Uroloncha striata domestica. *Z Zellforsch Mikrosk Anat* 114, 451–459.

Zhao X, Li N, Guo W, Hu X, Liu Z, Gong G, Wang A, Feng J & Wu C. (2004) Further evidence for paternal inheritance of mitochondrial DNA in the sheep (*Ovis aries*). *Heredity (Edinb)* 93, 399–403.

SUPPORTING INFORMATION

Additional Supporting Information may be found in the online version of this article:

Figure S1. Characterization of uncommon localization of conventional mitochondrial markers in mature duck spermatozoa.

Biochemical and Biophysical Research Communications 473 (2016) 781–788

Contents lists available at ScienceDirect

Biochemical and Biophysical Research Communications

journal homepage: www.elsevier.com/locate/ybbrc

TRPV4 is endogenously expressed in vertebrate spermatozoa and regulates intracellular calcium in human sperm

Ashutosh Kumar [a], Rakesh Kumar Majhi [a, 1], Nirlipta Swain [a, b, 1], S.C. Giri [c], Sujata Kar [d], Luna Samanta [b], Chandan Goswami [a, *]

[a] National Institute of Science Education and Research, Sachivalaya Marg, Bhubaneswar, Orissa, India
[b] Department of Zoology, Ravenshaw University, Cuttack, Orissa, India
[c] Central Avian Research Institute, Bhubaneswar 751003, India
[d] Kar Clinic and Hospital Pvt. Ltd, Bhubaneswar, Orissa, India

ARTICLE INFO

Article history:
Received 5 March 2016
Accepted 17 March 2016
Available online 19 March 2016

Keywords:
Calcium-wave
Sperm
Evolution
TRP channels
TRPV4
Vertebrates

ABSTRACT

Transient Receptor Potential Vanilloid sub-type 4 (TRPV4) is a non-selective cationic channel involved in regulation of temperature, osmolality and different ligand-dependent Ca^{2+}-influx. Recently, we have demonstrated that TRPV4 is conserved in all vertebrates. Now we demonstrate that TRPV4 is endogenously expressed in all vertebrate sperm cells ranging from fish to mammals. In human sperm, TRPV4 is present as N-glycosylated protein and its activation induces Ca^{2+}-influx. Its expression and localization differs in swim-up and swim-down cells suggesting that TRPV4 is an important determining factor for sperm motility. We demonstrate that pharmacological activation or inhibition of TRPV4 regulates Ca^{2+}-wave propagation from head to tail. Such findings may have wide application in male fertility–infertility, contraception and conservation of endangered species as well.

1. Introduction

In case of exogenous fertilization, sperm cells travel a long distance in aqueous media while in case of endogenous fertilization this travel is within the female reproductive tract. In higher mammals, sperm move through mucus, locate the oocyte, penetrate the cumulus and zona-pellucida, and fuse with the plasmalemma to deliver the DNA [1]. Each of these events require sperm to constantly detect appropriate chemical and physical cues (such as temperature, pH gradients) and upon reaching vicinity of the oocyte, undergo capacitation and finally fuse with the oocyte. Timing of each of these responses is crucial and these events must not be activated prematurely and/or inappropriately. Since spermatozoa are transcriptionally and translationally inactive, all cellular activities within it are carried out by the proteins inherited during differentiation and these proteins regulate sperm functions via secondary messengers such as intracellular Ca^{2+} [2,3]. In case of ejaculated spermatozoa, intracellular Ca^{2+} regulates chemotaxis, motility and hyperactivation, acrosomal reaction and is also a major regulator of capacitation [4,5]. Sperm cells also need to sense several physical and chemical cues and re-orient themselves towards the oocyte. The local pH, osmolarity and viscosity of the medium have profound effect on fertilizing ability of sperm [6]. In most vertebrates, "thermotaxis" also serves as conserved sensory and guidance mechanism. In mammalian system, temperature gradient guides sperm from the cooler reservoir site (oviductal isthmus) towards the warmer fertilization site [7]. In fact, rabbit and human spermatozoa have the capacity to sense minute temperature differences (0.5 °C or even lower) during thermotaxis [7].

In mammalian sperm, the signaling events leading to thermotaxis are still unknown. The role of thermosensitive TRP channels in different vertebrates has been investigated recently [8–12]. So far only few reports have shown the presence of different TRPs in sperm from different species. However, the TRPVs are important as these channels are involved in the detection of thermal, chemical, osmotic, voltage and pH conditions in a variety of cells. Based on these criteria, TRPVs are expected to be involved in several of these steps. Indeed, TRPV1 is localized in the post acrosomal region in human spermatozoa while in boar spermatozoa, it is found at the post acrosomal and in midpiece region [9,13]. In fish sperm, TRPV1 is located mainly at the neck region [12]. So far presence of other TRPVs in sperm has not been explored.

* Corresponding author.
E-mail address: chandan@niser.ac.in (C. Goswami).
[1] Equal contribution.

http://dx.doi.org/10.1016/j.bbrc.2016.03.071
0006-291X/

Among all, TRPV4 is uniquely activated at physiological temperature, changes in osmotic pressure, mechanical membrane stress, by the derivatives of phorbol esters and also by some endogenous lipids. Such responsiveness makes TRPV4 as an ideal polymodal receptor which can influence the response of sperm in different environments, irrespective of whether fertilization occurs in water or in aqueous medium. In this work we have explored the presence of TRPV4 in the spermatozoa of different vertebrates and investigated its role in human sperm.

2. Materials and methods

Reagents: Antibodies against TRPV4 and β-tubulin, 4αPDD, RN1734 and Progesterone were purchased from Sigma–Aldrich. Another TRPV4 antibody and its blocking peptide were purchased from Alomone Lab. Anti-Hsp60 antibody was purchased from AbCam. Fluo-4-AM, DAPI, Alexa-488-labelled secondary antibodies were purchased from Invitrogen. HRP-labelled secondary antibody and PVDF-membrane were obtained from Merck Millipore. Sperm wash Media was obtained from SAR Health line Pvt. Ltd.

Collection and isolation of cells from different species: Mature sperm from Rohu (*Labeo rohita)* were collected as described before [12]. Sperm from amphibians and reptiles were obtained from sexually mature common toad (*Duttaphrynus melanostictus*) (n = 3) and house lizard (*Hemidactylus leschenaultii*) (n = 3) as described before [14]. Avian sperm were collected from white pekin duck (*Anas platrhyncos*) (n = 4) and fixed with 4% PFA [15]. Freshly ejaculated sperms were collected from healthy bulls (*Bos indicus*). All experiments were done according to the approval (NISER-IAEC/SBS-AH/07/13/10).

Human spermatozoa were collected (with informed consent and approvals, KHPL-04/2013 and NISER/IEC/2015-11) from healthy proven fertile donors after 3 days of sexual abstinence. After liquefaction, basic semen analysis was done to evaluate sperm parameters and then swim-up (highly motile, termed "Su") and swim-down (nearly immotile, termed "Sd") cells were separated as described before [16]. Either these fractions were treated with drugs or left untreated and then fixed with 4% PFA or were made into gel samples.

Immunofluorescence analysis and microscopy: Immunocytochemical analysis was performed as described previously [12]. Rabbit polyclonal anti-TRPV4 antibody (1:500 dilution, Alomone Lab, or Sigma–Aldrich) were used. Wherever necessary, the antibody was blocked with a specific peptide (CDGHQQGYAPK-WRAEDAPL, corresponding to AA853-871 of rTRPV4, Accession number Q9ERZ8). All images were acquired by a confocal laser-scanning microscope (LSM-780, Zeiss) with a 63X-objective and analyzed (Zeiss LSM image examiner software).

Ca^{2+}-imaging and intensity calculation: Freshly collected sperm were incubated with TRPV4-specific activator/inhibitor for 1 h at 37 °C, followed by incubation with Fluo4-AM (5 μM) for 30 min. Subsequently, ~20 μl sample was dropped onto the live cell chamber and time-series images were acquired. For intensity calculation ImageJ was used, in which multiple image frames wear merged into a single frame and intensity per unit area was calculated.

SDS-PAGE and Western blot analysis: After quantification, equal number of Human spermatozoa were taken from swim-up and swim-down fractions. Gel samples were prepared by boiling the samples for 5 min with Laemmli buffer supplemented with protease inhibitor cocktail (Sigma Aldrich). These samples were separated by 10% SDS-PAGE followed by Western blot analysis as described before [12].

Flow-cytometry: Flow cytometry analysis of 10,000 sperm per sample was performed (FACS Calibur, BD Biosciences) and fluorescence (Alexa Fluor-488) intensities of were analyzed by using Cell Quest Pro software. Mean Fluorescence Intensity (MFI) was analyzed as a numerical value of the TRPV4 expression.

2.1. Deglycosylation of TRPV4 protein with Endoglycosidase-H and N-glycanase

Equal amount of protein lysate of Sd and Su sample was taken for glycosidase treatment as-per manufacturer's instructions (NEB). Briefly, sperm protein lysate were mixed with glycoprotein denaturing buffer (1X) and denaturation was carried out at 100 °C for 5 min. Denatured glycoproteins were chilled in ice for 5 min. Subsequently Glyco buffer (1X) and NP-40 was added. Sample mixture was incubated in presence or absence of Endo-H and PNGase-F at 37 °C for 6 h and separated by one-dimensional SDS-PAGE and probed for TRPV4.

3. Results

3.1. Evolutionary conserved and endogenous expression of TRPV4 in vertebrate spermatozoa

Comparative analysis of the localization pattern of TRPV4 in different regions of spermatozoa (head, neck, tail) was performed for different vertebrate classes. At least one species from five classes of subphylum vertebrata was selected for this study. Spermatozoa were immunostained for TRPV4 and specificity of the TRPV4 antibody was confirmed by pre-incubating the same with blocking peptide.

In the three classes of cold-blooded vertebrates, a distinct difference in localization pattern is observed. While in fish/piscean group (osteichthyes class), TRPV4 is primarily restricted at the tail and neck regions of Rohu (*L. rohita*) sperm (Fig 1a); for reptilian class, TRPV4 is detectable only in the head of (house lizard, *H. leschenaultii*) sperm (Fig 1c). In contrast, in amphibian sperm, TRPV4 expression is present in head, neck and tail regions of Asian common toad (*D. melanostictus*) sperm (Fig 1b). Similar to amphibian spermatozoa, warm-blooded animals also show TRPV4 distribution throughout the sperm. In avian class, TRPV4 expression is although present at all regions, it is primarily restricted in the tail of Duck (*A. platrhyncos*) sperm (Fig 1d). Spermatozoa of bull (*Bos gaourus*) show faint yet distinct expression of TRPV4 in all these regions (Fig 1e).

Furthermore, TRPV4 localization pattern was also studied for spermatozoa of common Indian tree frog (*Polypedates maculatus*), garden lizard (*Calotes versicolor*), chicken (*Gallus gallus domesticus*) and a similar distribution pattern is observed (data not shown). Western blot analysis also confirms the presence of TRPV4 with expected size 98 kDa in Rohu and Duck sperm (Suppl Fig 1). These results suggest that TRPV4 is endogenously present in spermatozoa and such expression is evolutionarily conserved in all vertebrates.

3.2. TRPV4 is expressed in human spermatozoa

We probed for TRPV4 expression in human (*Homo sapiens*) sperm and noted very high level of expression in the head and neck region but faint expression in the tail region (Fig 2a). This staining was completely blocked by pre-incubating this antibody with specific antigenic peptide (Fig 2a). To confirm the expression in human sperm by Western blot analysis, we used two different antibodies raised against the C-terminus of TRPV4. One antibody (Ab1, Sigma–Aldrich) detects a band of 130 kDa (predicted size: 98 kDa) suggesting that in human sperm TRPV4 is subject to post-translational modification (discussed later) (Fig 2b). The second antibody (Ab2, Alomone Labs) detects bands at 130 and 72 kDa and

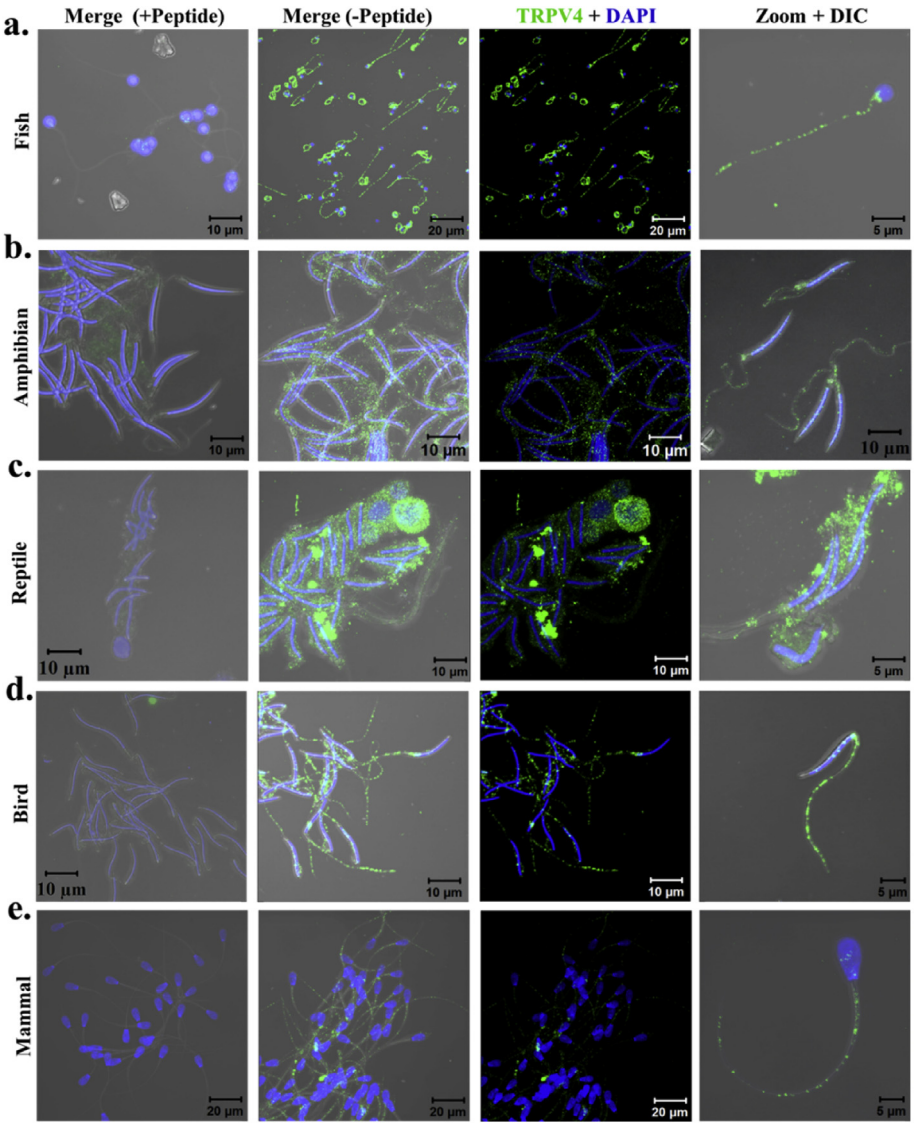

Fig. 1. TRPV4 is endogenously expressed in vertebrate sperm. Confocal images demonstrating the presence of TRPV4 in Piscean (**a**, rohu), amphibian (**b**, common toad), reptilian (**c**, house lizard), avian (**d**, duck) and mammalian (**e**, bovine) sperm are shown. Cells were immunostained for TRPV4-specific antibody in presence (left most column) or absence of a specific blocking peptide. Images of TRPV4 (green) expression and localization in single cell are shown (right panel). (For interpretation of the references to colour in this figure legend, the reader is referred to the web version of this article.)

these signals (Ab1 and Ab2) are blocked by using specific peptide suggesting that these immunoreactivities are specific in nature (Fig 2b). Since the predicted size of TRPV4 is 98 kDa, the higher and lower bands represent post-translational modifications and proteolytically degraded products, respectively (addressed later).

We analyzed the percentage of human spermatozoa expressing TRPV4 by FACS ($n = 6$). Dot plot analysis revealed that all most all spermatozoa (98.98± 0.34%) are $TRPV4^{+}$ (Fig 2c**)**. Upon pre-incubation with a specific blocking peptide, the same antibody detects less than 1% cells as TRPV4+ve, and the mean fluorescence intensity values reduce significantly, confirming the specificity of the TRPV4 antibody in FACS application also (Fig. 2c–e). These experiments confirm the expression of TRPV4 in mature human spermatozoa.

3.3. TRPV4 is differentially expressed and localized in swim-up and swim-down human sperm

To explore if there is any difference in TRPV4 expression in case of immotile and highly motile sperm, we separated the total sperm population into these two fractions, namely swim-up (Su, cells with progressive motility) and swim-down (Sd, cells with mostly impaired motility) samples. In Su cells, TRPV4 is primarily located in the head and faintly in the tail (Fig. 3a–b). However, in Sd cells, TRPV4 is mostly absent in the head region and highly accumulated at the neck regions (Fig. 3a–b).

Western blot analysis was performed using Su and Sd samples obtained from three individuals with proven fertility. The Ab1 detects a distinct band at 130 kDa in Sd fraction of all three donors (Fig 3c). However, the corresponding 130 kDa band is mostly absent or faintly present in Su fraction. Densitometry analysis of the 130 kDa region of all donors revealed nearly 6 fold higher level of TRPV4 in Sd as compared to the Su fraction (Fig 3d**)**. In contrast, several

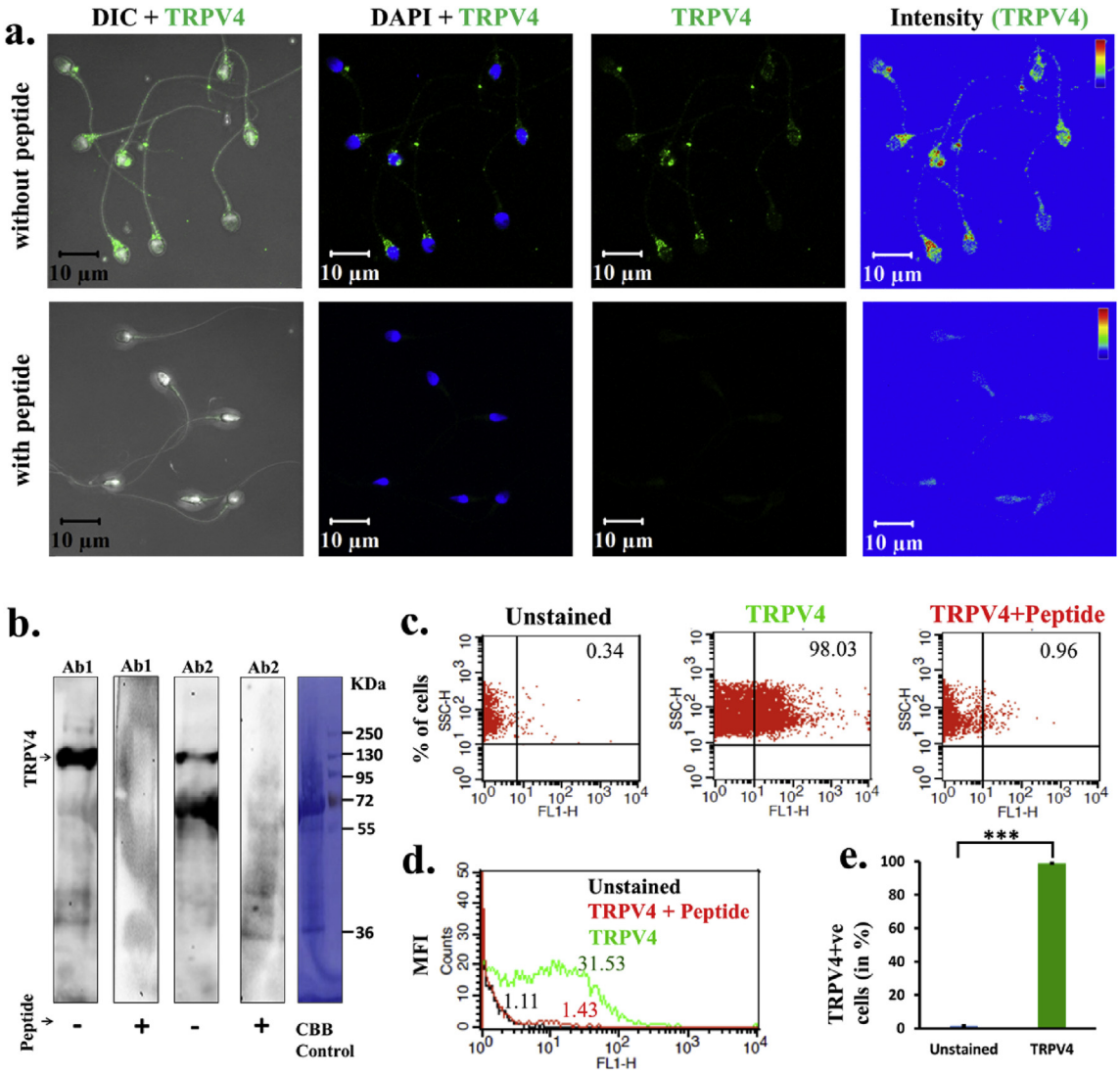

Fig. 2. TRPV4 is endogenously expressed in human sperm. a. Confocal images showing the endogenous expression of TRPV4 (green) in human sperm. TRPV4 is localized in the post acrosomal and neck regions, while faint expression is also present in the acrosomal and tail region (upper panel). TRPV4 signal is abolished upon blocking the primary antibody with its antigenic peptide (lower panel). **b**. Western blot analysis using different antibodies (Ab1 and Ab2) shows TRPV4-specific band at ~130 kDa (indicated by arrow). These TRPV4-specific signals are blocked by specific antigenic peptide. Corresponding Coomassie-stained gel is shown in right side. **c**. Representative dot-plot images from FACS (n = 6) showing the percentage of TRPV4$^+$ cells. Application of blocking peptide reduced this number. **d**. TRPV4 expression is depicted as the MFI values. **e**. About 98.98 ± 0.34% cells are TRPV4$^+$ (FACS, n = 6 individuals). (For interpretation of the references to colour in this figure legend, the reader is referred to the web version of this article.)

smaller fragments of TRPV4 are observed in Su samples. Some of these smaller bands were also observed in Sd samples, but with lesser intensities. This in general suggest for low level of full-length TRPV4 (corresponding to 130 kDa) and more proteolytically-cleaved products in motile sample. Furthermore to analyse the extent of proteolytic activity in Su and Sd samples, we probed the same samples for β-tubulin (abundant in cytoplasm) and Hsp60 (abundant in mitochondria). These Western blot analysis suggests for higher proteolytic activity in cytoplasm and in mitochondria of Su samples as both β-tubulin and Hsp60 levels are low in Su fraction as compared to Sd fraction (Fig 3c).

We analysed the expression of TRPV4 in Su and Sd samples in a more quantitative manner and performed FACS. Nearly 98.98 ± 0.34% and 96.15 ± 2.8% cells are TRPV4$^+$ in Su and Sd samples respectively (data not shown). However, the MFI-values for Su fraction is more (121.56 ± 37.79) compared to the Sd fraction (89.03 ± 23.76) (n = 6) (Fig 3e). Though this difference may suggests for the more TRPV4 in swim-up samples than swim-down sample, the difference turned out to be statistically non-significant (p = 0.105).

3.4. TRPV4 is a glycosylated protein

In human sperm TRPV4 shows higher molecular weight band (~130 kDa) suggesting that it may be glycosylated. To confirm this, enzymatic treatments of the glycan moieties were performed using two different glycosidase: Endoglycosidase-H (Endo-H, cleaves N-linked high mannose-rich oligosaccharides), and Peptide-N-Glycosidase-F (PNGase-F, cleaves both N-linked high mannose-rich oligosaccharides and complex oligosaccharides). Migration of TRPV4 is faster when cell extract was treated with PNGase-F but not with Endo-H. After PNGase-F treatment, the resulting TRPV4 band migrates at expected molecular weight (~98 kDa) (Fig 3f). It suggests that sperm TRPV4 contains complex glycosidic bond with different types of oligosaccharides. As Su sample does not have detectable level of full-length TRPV4, from these experiments

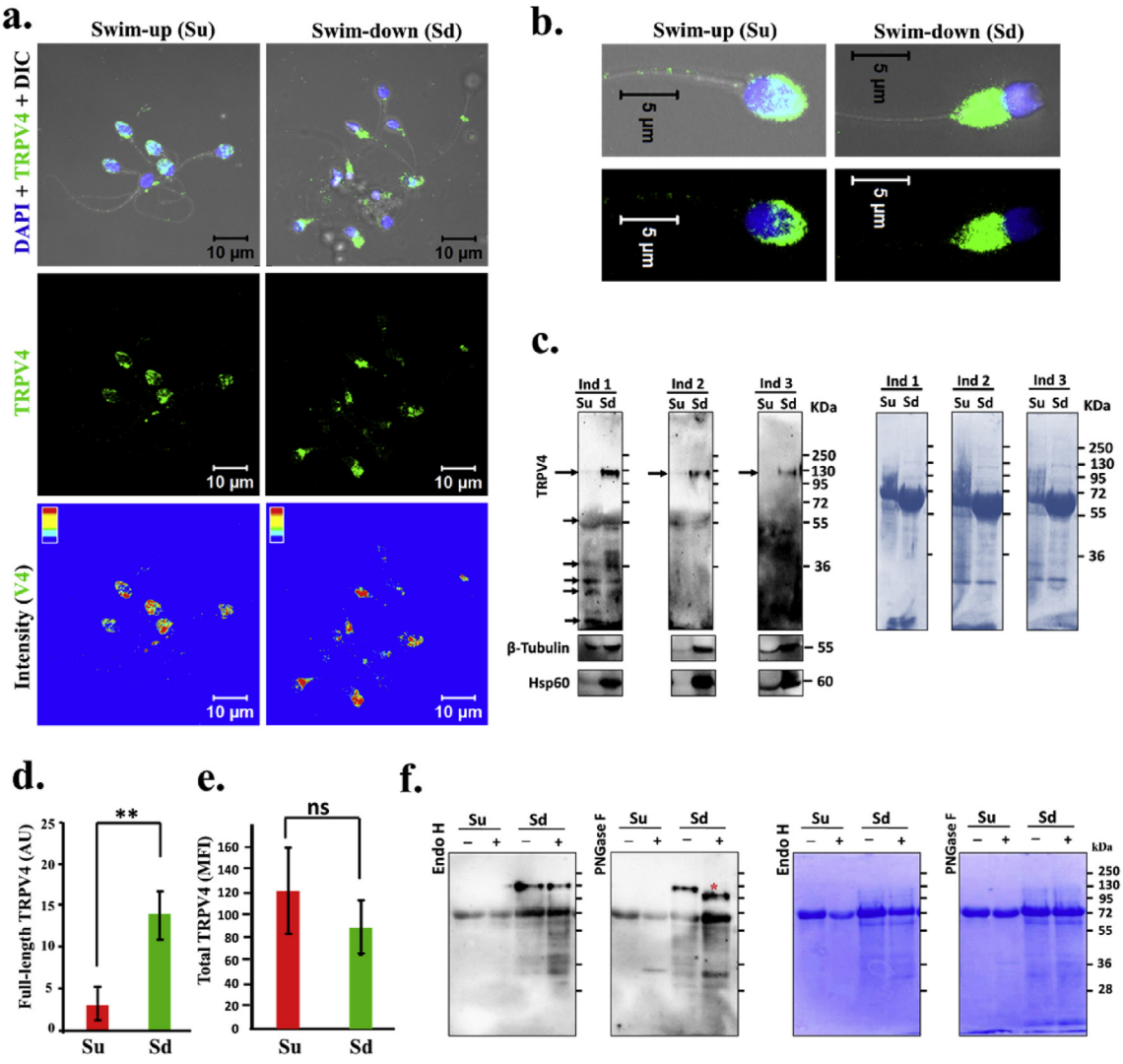

Fig. 3. Swim-up and swim-down fractions of human sperm have different levels of TRPV4. a-b. Cluster (a) and enlarged single cells (b) stained for TRPV4 (green) are shown. Strong signal for TRPV4 is observed throughout the head (primarily in acrosomal region) in the swim-up (Su) fraction. TRPV4 is present in the post-acrosomal and neck regions in the swim-down (Sd) fraction. Faint expression is present in the tail region. **c**. Western blot analysis of Su and Sd fractions (from 3 individuals, Ind 1–3) were probed for TRPV4, β-tubulin and Hsp60. The 130 kDa band (longer arrow) and smaller bands (smaller arrows) represent the full-length (glycosylated) and proteolytically-degraded TRPV4 respectively. The corresponding Coomassie gels are provided at right. The prominent band/s around 70-50 kDa (in Su and Sd fraction) as observed by Coomassie staining represents protein/s present in sperm media. **d**. Densitometry analysis of Western blot signal intensities for 130 kDa band of TRPV4 in Su and Sd fractions ($n = 3$, ANOVA test, $^{**}p$ value < 0.005). **e**. Total TRPV4-specific fluorescence from Su and Sd samples detected as MFI values are shown (ns: non-significant; $n = 6$, ANOVA test, $p = 0.105$). **f**. TRPV4 has complex N-glycosidic linkage and branched complex glycosidic bond, which shows ~30 kDa shift only in presence of PNGase-F (red star). Endo-H treatment does not cause any shift of TRPV4 suggesting that the glycosylated TRPV4 is resistant against Endo-H. The corresponding Coomassie gels are shown in side. (For interpretation of the references to colour in this figure legend, the reader is referred to the web version of this article.)

definitive conclusion cannot be drawn.

3.5. *TRPV4 modulates Ca^{2+}-influx into human sperm*

Ca^{2+}-homeostasis in sperm is precisely regulated by different Voltage Operated Channel (VOC) present in the membrane and by female steroids like progesterone [17]. To evaluate the effect of TRPV4 activator and inhibitor upon the Ca^{2+}-influx, we treated Su and Sd human samples with 4αPDD (5 µM) or RN1734 (10 µM) for 1 h and labeled with Fluo-4-AM and analyzed the intracellular Ca^{2+}-levels. 4αPDD treatment in Su fraction results in increased intracellular Ca^{2+}-levels but inhibition by RN1734 (10 µM) did not decrease the intracellular Ca^{2+}-levels below that of the control conditions (Fig 4a). Notably, in Su fraction, the effect of TRPV4 activation by 4αPDD is comparable to the effect of Progesterone (10 µM), a standard inducer of Ca^{2+}-influx into sperm cells. The above observation is supported by quantification of Fluo4-AM signal intensity per unit area ($n = 4$ individuals), revealing that in Su fraction the effect of 4αPDD and Progesterone is similar (Fig 4b). In Sd fraction, there is no significant difference in basal Ca^{2+}-levels after modulation of TRPV4 by pharmacological agents (Fig 4b).

3.6. *TRPV4 regulates Ca^{2+}-buffering at the mid-piece and Ca^{2+}-wave propagation in tail*

To understand if and how TRPV4 regulates the intracellular Ca^{2+}-waves, we labelled cells with Fluo4-AM and performed live cell imaging followed by manual tracking of Ca^{2+}-wave propagation within single cells (Fig 4c). In progesterone-treated cells, the level of Ca^{2+} is high in the head and neck regions. Progesterone-

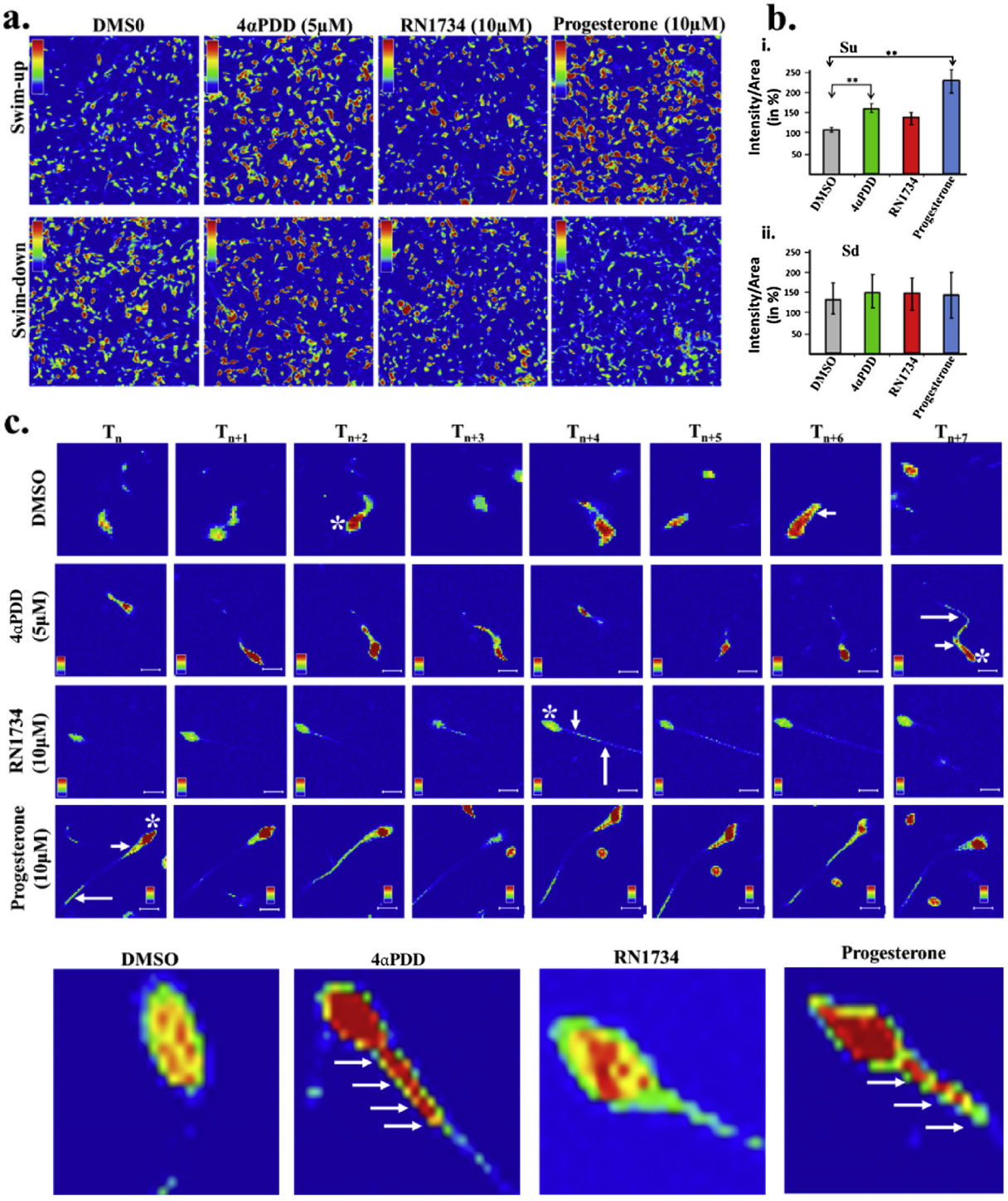

Fig. 4. TRPV4 regulates intracellular Ca^{2+}-levels in human sperm. a. Live cell imaging was performed for Su and Sd fractions pre-treated with TRPV4 activator (4αPDD) or inhibitor (RN1734) or with Progesterone for 1 h and labeled with Fluo-4-AM. The intracellular Ca^{2+}-levels are represented in pseudo color, (red and blue indicating highest and lowest intensity respectively). **b**. Quantification of average fluorescence intensity/area (in arbitrary unit) is shown. In Su sample, 4αPDD and progesterone increases the intracellular Ca^{2+}-levels as comparison to control ($p < 0.05$). In Sd sample, 4αPDD or RN1734 do not alter intracellular Ca^{2+}-levels. ($n = 4$). **c**. Moving sperm (indicated by asterisk, *) was tracked within a fixed time period (T_n to T_{n+7}) and arrows indicate the high-level of Ca^{2+} in neck and tail respectively. Magnified (lower panel) image demonstrating the propagation of Ca^{2+}-waves from head to the tail through the neck. In 4αPDD-treated and progesterone-treated cells, Ca^{2+}-wave propagates through the mitochondrial coiling (green rings, indicated by arrows). High-level of Ca^{2+} (red) in the central stalk region is also visible in this case. In RN1734-treated cells, the Ca^{2+}-waves do not propagate through these regions. The central stalk region reveals mostly moderate-to low-level of Ca^{2+}-flux. (For interpretation of the references to colour in this figure legend, the reader is referred to the web version of this article.)

induced Ca^{2+}-wave originates in the mid-region of sperm head and spreads throughout the neck and then propagates to the tail and mostly covers a large portion of the tail. The Ca^{2+}-wave then subsides and a fresh wave originates in the head. This observation matches with previous reports [18]. In 4αPDD-treated cells, the Ca^{2+}-level is also high in the head and neck regions. The patterns of

4αPDD-mediated waves are visible at the tail and are mostly similar to progesterone-induced waves. Notably, application of RN1734 results in reduction of the intracellular Ca^{2+}-level in the head region. Nevertheless, the Ca^{2+}-wave propagation is observed in the tail region at times, though with less intensity and frequency. Indeed, we observed wavy pattern of intracellular Ca^{2+}-level at the neck regions in case of progesterone- and 4αPDD-induced hyper motile cells (Fig 4c). These results may suggest for a possible Ca^{2+}-buffering activity mediated by TRPV4 at the neck region.

4. Discussion

Sperm cells have highly condensed DNA, no transcriptional activity and negligible translational activity. These cells are motile and show extreme response against number of variable factors such as changes in temperature, pH, osmolality, salts, and compounds at very low concentrations indicating their ability to detect and integrate multiple physical and chemical stimuli precisely [7,19,20]. Notably, sperm cells perform all these tasks by multiple ion channels and receptors regulating complex yet efficient Ca^{2+}-signaling events [21]. We show that TRPV4 is endogenously present in the sperm cells of all vertebrates, ranging from fishes to human. Conserved expression indicates that TRPV4 is probably involved in several of the above mentioned events occurring in sperm cells. We correlate the TRPV4 expression with the ability of sperm to sense optimum temperature, osmolality, and different chemicals and subsequent Ca^{2+}-signaling events.

Different parts of the sperm cell, especially head, neck and tail region are the functionally important areas which regulate different yet specific functions. Sperms head is responsible for acrosomal reaction; neck region contains several mitochondria which continuously supply ATP and also act as the only available organelle for Ca^{2+}-buffering, and tail region is important for motility. In all conditions, Ca^{2+} plays an important role in all physiological conditions. Presence of TRPV4 in the tail of sperm from all vertebrates suggests that it could be a critical regulator of sperm motility. Immunostaining results suggests for the differential localization of TRPV4 in different species. In human sperm, TRPV4 localizes in all the regions and it is significantly enriched in the head region.

In this context, our observation that differential localization of TRPV4 in swim-up and swim-down cells from human sperm is highly indicative. Such differential localizations in these two population correlate well with the better motility regulation by TRPV4. In agreement with that, TRPV4 localization also differs after activation or inhibition by pharmacological agents (data not shown). However our western blot results from these two different fractions indicate that the TRPV4 band at 130 kDa is more abundant in Su sample as compare to Sd sample. On the other hand, the MFI values from FACS data suggest that the total TRPV4 immunoreactivity is more in Su fraction than that of the Sd samples. These in general may suggest that higher level of TRPV4 is present in the Su samples and the same is subjected to more proteolytic degradation, probably due to higher level of Ca^{2+}-influx and Ca^{2+}-dependent proteolytic activation. Western blot analysis of β-tubulin (cytoplasmic) and Hsp60 (mitochondrial) also suggest the same. Western blot results also suggest that in human sperm, TRPV4 migrates at 130 kDa, (higher than the expected size) and therefore suggests for post-translational modification. It is worth mentioning that in other systems too TRPV4 has been reported at higher sizes (~110–120 kDa size) [22,23]. Our results indicate that in human sperm, TRPV4 has branched type of glycosylation, which is sensitive to PNGase-F but resistant to Endo-H glycosidase. It suggests that TRPV4 does not contain any N-glycosidic-linkage or due to the presence of branched oligosaccharides, this glycosidic bond is not freely accessible to the Endo-H.

We confirm that >95% of both Su- and Sd-cells contain TRPV4. The localization of TRPV4 in human sperm also correlates well with the Ca^{2+}-waves observed in these cells. Untreated sperm shows a rhythmic pattern of Ca^{2+}-waves that originates in the head and migrates to the mid-piece. Progesterone-induced Ca^{2+}-waves are initiated in the equatorial segment and then spread throughout the rest of the head and then moves rapidly to the tail [18]. TRPV4 activation-induced Ca^{2+}-wave pattern is similar with the progesterone-evoked Ca^{2+}-waves, while TRPV4 inhibition blocks the Ca^{2+}-wave generation in the sperm head, thereby negligible Ca^{2+}-influx passes to the mid-piece and tail. This indicates that TRPV4 may be involved in the regulation of both Ca^{2+}-wave generation and propagation in human sperm. TRPV4 may also be involved in Ca^{2+}-buffering function at the neck region of sperm cells.

We conclude that TRPV4 is endogenously present in sperm cells of all vertebrates and this is an evolutionary conserved phenomenon since vertebrate evolution. TRPV4 regulates several key functions in human sperm cells, such as Ca^{2+}-levels, Ca^{2+}-wave propagation and motility.

Conflicts of interest

The authors declare that they have no conflict of interests.

Acknowledgments

Support from frozen cattle semen bank (Khapuria, Cuttack), Dr. PK. Mahapatra (RPRC, Bhubaneswar), Dr. P. Routray (CIFA, Bhubaneswar) and lab members is acknowledged. Funding from NISER (XIIth plan, DPR), DST (BL1502) and DBT (BL1501) are acknowledged.

Appendix A. Supplementary data

Supplementary data related to this article can be found at http://dx.doi.org/10.1016/j.bbrc.2016.03.071.

References

[1] M. Yoshida, N. Kawano, K. Yoshida, Control of sperm motility and fertility: diverse factors and common mechanisms, Cell Mol. Life Sci. 65 (2008) 3446–3457.
[2] S. Grunewald, U. Paasch, H.J. Glander, et al., Mature human spermatozoa do not transcribe novel RNA, Androl. 37 (2005) 69–71.
[3] A. Asano, J.L. Nelson, S. Zhang, et al., Characterization of the proteomes associating with three distinct membrane raft sub-types in murine sperm, Proteom. 10 (2010) 3494–3505.
[4] M. Eisenbach, Sperm chemotaxis, Rev. Reprod. 4 (1999) 56–66.
[5] M. Spehr, G. Gisselmann, A. Poplawski, et al., Identification of a testicular odorant receptor mediating human sperm chemotaxis, Sci. 299 (2003) 2054–2058.
[6] A.M. Petrunkina, R.A. Harrison, M. Ekhlasi-Hundrieser, et al., Role of volume-stimulated osmolyte and anion channels in volume regulation by mammalian sperm, Mol. Hum. Reprod. 10 (2004) 815–823.
[7] A. Bahat, I. Tur-Kaspa, A. Gakamsky, et al., Thermotaxis of mammalian sperm cells: a potential navigation mechanism in the female genital tract, Nat. Med. 9 (2003) 149–150.
[8] C. Auzanneau, C. Norez, F. Antigny, et al., Transient receptor potential vanilloid 1 (TRPV1) channels in cultured rat Sertoli cells regulate an acid sensing chloride channel, Biochem. Pharmacol. 75 (2008) 476–483.
[9] N. Bernabo, M.G. Pistilli, M. Mattioli, et al., Role of TRPV1 channels in boar spermatozoa acquisition of fertilizing ability, Mol. Cell Endocrinol. 323 (2010) 224–231.
[10] G.A. De Blas, A. Darszon, A.Y. Ocampo, et al., TRPM8, a versatile channel in human sperm, PLoS One 4 (2009) e6095.
[11] M.G. Gervasi, C. Osycka-Salut, J. Caballero, et al., Anandamide capacitates bull spermatozoa through CB1 and TRPV1 activation, PLoS One 6 (2011) e16993.
[12] R.K. Majhi, A. Kumar, M. Yadav, et al., Thermosensitive ion channel TRPV1 is endogenously expressed in the sperm of a fresh water teleost fish (*Labeo rohita*) and regulates sperm motility, Channels (Austin) 7 (2013) 483–492.

[13] M. Maccarrone, B. Barboni, A. Paradisi, et al., Characterization of the endocannabinoid system in boar spermatozoa and implications for sperm capacitation and acrosome reaction, J. Cell Sci. 118 (2005) 4393–4404.
[14] R.K. Majhi, S. Saha, A. Kumar, et al., Expression of temperature-sensitive ion channel TRPM8 in sperm cells correlates with vertebrate evolution, PeerJ. 3 (2015) e1310.
[15] R.K. Majhi, A. Kumar, M. Yadav, et al., Light and electron microscopic study of mature spermatozoa from White Pekin duck (Anas platyrhynchos): an ultrastructural and molecular analysis, Andrology 4 (2016) 232–244.
[16] T. Jameel, Sperm swim-up: a simple and effective technique of semen processing for intrauterine insemination, J. Pak Med. Assoc. 58 (2008) 71–74.
[17] H.M. Florman, C. Arnoult, I.G. Kazam, et al., A perspective on the control of mammalian fertilization by egg-activated ion channels in sperm: a tale of two channels,, Biol. Reprod. 59 (1998) 12–16.
[18] S. Meizel, K.O. Turner, R. Nuccitelli, Progesterone triggers a wave of increased free calcium during the human sperm acrosome reaction, Dev. Biol. 182 (1997) 67–75.
[19] S. Hamamah, J.L. Gatti, Role of the ionic environment and internal pH on sperm activity, Hum. Reprod. 13 (Suppl 4) (1998) 20–30.
[20] C.H. Yeung, M. Anapolski, M. Depenbusch, et al., Human sperm volume regulation. Response to physiological changes in osmolality, channel blockers and potential sperm osmolytes, Hum. Reprod. 18 (2003) 1029–1036.
[21] W. Alasmari, C.L. Barratt, S.J. Publicover, et al., The clinical significance of calcium-signalling pathways mediating human sperm hyperactivation, Hum. Reprod. 28 (2013) 866–876.
[22] V. Benfenati, M. Caprini, M. Dovizio, et al., An aquaporin-4/transient receptor potential vanilloid 4 (AQP4/TRPV4) complex is essential for cell-volume control in astrocytes, PNAS 108 (2011) 2563–2568.
[23] C.E. Hills, R. Bland, P.E. Squires, Functional expression of TRPV4 channels in human collecting duct cells: implications for secondary hypertension in diabetic nephropathy, Exp. Diabetes Res. (2012) 936518.